



Cancer Risk Coefficients for Environmental Exposure to Radionuclides

Federal Guidance Report No. 13



This report was prepared as an account of work sponsored by agencies of the United States Government. Neither the United States Government nor any agency thereof, nor any of their employees, makes any warranty, express or implied, or assumes any legal liability or responsibility for the accuracy, completeness, or usefulness of any information, apparatus, product, or process disclosed, or represents that its use would not infringe privately owned rights. Reference herein to any specific commercial product, process, or service by trade name, trademark, manufacturer, or otherwise, does not necessarily constitute or imply its endorsement, recommendation, or favoring by the United States Government or any agency thereof.

An electronic document version of this report is available at the US EPA world-wide-web site: <http://www.epa.gov/radiation/federal>. Additional Federal Guidance related information and reports are also available at this site.

This report was prepared for the
Office of Radiation and Indoor Air
U.S. Environmental Protection Agency
Washington, DC 20460
by
Oak Ridge National Laboratory
Oak Ridge, Tennessee 37831

Federal Guidance Report No. 13

**Cancer Risk Coefficients for
Environmental Exposure
to Radionuclides**

Radionuclide-Specific Lifetime Radiogenic Cancer
Risk Coefficients for the U.S. Population, Based on
Age-Dependent Intake, Dosimetry, and Risk Models

Keith F. Eckerman
Richard W. Leggett
Christopher B. Nelson
Jerome S. Puskin
Allan C. B. Richardson

Oak Ridge National Laboratory
Oak Ridge, Tennessee 37831

Office of Radiation and Indoor Air
United States Environmental Protection Agency
Washington, DC 20460

September 1999

PREFACE

The Federal Radiation Council (FRC) was formed in 1959, through Executive Order 10831. A decade later its functions were transferred to the Administrator of the newly formed Environmental Protection Agency (EPA) as part of Reorganization Plan No. 3 of 1970. Under these authorities it is the responsibility of the Administrator to “advise the President with respect to radiation matters, directly or indirectly affecting health, including guidance for all Federal agencies in the formulation of radiation standards and in the establishment and execution of programs of cooperation with States.” The purpose of this guidance to Federal Agencies is to ensure that the regulation of exposure to ionizing radiation is adequately protective, reflects the best available scientific information, and is carried out in a consistent manner.

Since the mid-1980s, EPA has issued a series of Federal guidance documents for the purpose of providing the Federal and State agencies technical information to assist their implementation of radiation protection programs. The first report in this series, Federal Guidance Report No. 10 (EPA, 1984a), presented derived concentrations of radioactivity in air and water corresponding to the limiting annual doses recommended for workers in 1960. That report was superseded in 1988 by Federal Guidance Report No. 11 (EPA, 1988), which provided updated dose coefficients for internal exposure of members of the general public and limiting values of radionuclide intake and air concentrations for implementation of the 1987 Radiation Protection Guidance for Occupational Exposure (EPA, 1987). Federal Guidance Report No. 12 (EPA, 1993) tabulated dose coefficients for external exposure to radionuclides in air, water, and soil.

This report, *Cancer Risk Coefficients for Environmental Exposure to Radionuclides, Federal Guidance Report No. 13*, provides numerical factors for use in estimating the risk of cancer from low-level exposure to radionuclides. A risk coefficient for a radionuclide that exposes persons through a given environmental medium is an estimate of the probability of radiogenic cancer mortality or morbidity per unit activity inhaled or ingested, for internal exposure, or per unit time-integrated activity concentration in air or soil, for external exposure. A risk coefficient may be interpreted either as the average risk per unit exposure for persons exposed throughout life to a constant activity concentration of a radionuclide in an environmental medium, or as the average risk per unit exposure for persons exposed for a brief period to the radionuclide in an environmental medium. The risk coefficients given in this document apply to populations that approximate the age, gender, and mortality experience characterized by the 1989-91 U.S. decennial life tables. These

coefficients are tabulated using the SI unit of activity (becquerel), as are the dose coefficients in Federal Guidance Report No. 11 and Report No. 12.

An interim version of this report was published for public comment in January 1998. That version described the methodology used for derivation of a risk coefficient and provided risk coefficients for exposure to any of approximately 100 important radionuclides through various environmental media. This final version includes the background information given in the interim version, extends the tabulation of risk coefficients to more than 800 radionuclides, and provides additional discussion of the sources and extent of uncertainty in estimates of cancer risk from exposure to radionuclides.

The tabulated risk coefficients are based on state-of-the-art methods and models that take into account age and gender dependence of intake, metabolism, dosimetry, radiogenic risk, and competing causes of death in estimating the risks to health from internal or external exposure to radionuclides. Although many of the biokinetic and dosimetric models used here are updates of models used in Federal Guidance Report No. 11, the present report does not replace either that document or Federal Guidance Report No. 12 or affect their use for radiation protection purposes. The dose coefficients given in Federal Guidance Report No. 11 and Report No. 12 continue to be recommended for determining conformance with the radiation protection guidance to Federal agencies issued by the President and will be updated in the future as warranted. The risk coefficients tabulated in the present report have a different purpose — they are intended for use in assessing risks from radionuclide exposure, in a variety of applications ranging from analyses of specific sites to the general analyses that support rule making. Although the application of these risk coefficients for purposes such as cost/benefit analysis, environmental impact statements (EISs), and environmental assessments (EAs) — especially by Federal agencies — is encouraged to promote consistency in risk assessment, such use is discretionary.

The tabulated risk coefficients are intended mainly for prospective assessments of potential cancer risks from long-term exposure to radionuclides in environmental media. While it is recognized that the tabulations are also likely to be used in retrospective analyses of radiation exposures of populations, it is emphasized that such analyses should be limited to estimation of total or average risks in large populations. The risk coefficients are not intended for application to specific individuals, ages, or genders and should not be used for that purpose. Also, the coefficients are based on radiation risk models developed for application either to low acute doses or low dose rates and should not be applied to accident cases involving high doses and dose rates, either in prospective or retrospective analyses.

Some risk assessment procedures are established as a matter of policy, and additional guidance may be needed before using these risk coefficients in such policy matters. For example, EPA recommends that radiation risk assessments for sites on the National Priorities List under the Comprehensive Environmental Response, Compensation, and Liability Act be performed using the Health Effects Assessment Summary Tables (HEAST), which are periodically updated to reflect new information, such as that contained in this report.

In using Federal Guidance Report No. 13, the cancer risk associated with a radionuclide intake or external exposure is calculated as the product of the appropriate cancer risk coefficient and the corresponding radionuclide intake or exposure. This calculation presumes that risk is directly proportional to intake or exposure, i.e., it follows a linear, no-threshold (LNT) model. Current scientific evidence does not rule out the possibility that the calculated risk at environmental exposure levels may be overestimates or underestimates. However, several recent expert panels (UNSCEAR, 1993, 1994; NRPB, 1993; NCRP, 1997) have concluded that the LNT model is sufficiently consistent with current information on carcinogenic effects of radiation that its use is scientifically justifiable for purposes of estimating risks from low doses of radiation. As a practical matter, the LNT approach is universally used for assessing the risk from environmental exposure to radionuclides as well as other carcinogens. Within the LNT context, sources of uncertainty in the radionuclide cancer risk coefficients are discussed in the report, and judgments of uncertainty in the risk coefficients are given in Chapter 2 for a number of radionuclides. As new scientific evidence becomes available, we shall consider its effect on the information presented in this report and shall update the report as needed.

The risk coefficients were calculated using the DCAL (Dose and Risk Calculation) software, developed at Oak Ridge National Laboratory for the EPA. DCAL is a comprehensive system for calculating dose and risk coefficients using age-dependent models. A manual describing the DCAL software and the quality assurance procedures for this software will be published separately.

This report would not have been possible without the contributions of the many investigators who produced the building blocks that provided the basis for the results presented here. These include: Jerome S. Puskin and Christopher B. Nelson, who assembled the models for age-dependent, organ-specific cancer risks; Richard W. Leggett and Keith F. Eckerman, who developed many of the age-specific biokinetic and dosimetric models published by the International Commission on Radiological Protection and who provided the basis for calculation of doses from internal and external exposure; and Robert Armstrong, who supplied pre-publication values for the 1989-91 U.S. decennial life tables. The major effort required to prepare the report itself was carried out by Keith F. Eckerman, Richard W. Leggett, Christopher B. Nelson, Jerome S. Puskin, and Allan C.B.

Richardson. Preparation of the report was funded by the U.S. Environmental Protection Agency, the U.S. Department of Energy (DOE), and the U.S. Nuclear Regulatory Commission (NRC).

Technical reviews for the draft interim version of the report were contributed by William J. Bair, Bernd Kahn, Charles E. Land, John R. Mauro, and Alan Phipps. Review comments on the interim version (EPA, 1998) were provided by Federal agencies (including NRC and DOE), State agencies, and members of the public. The EPA Science Advisory Board (SAB) formally reviewed and commented on the interim report. This final version of Federal Guidance Report No. 13 reflects consideration of all these comments.

We gratefully acknowledge the work of the authors, the agencies that contributed funding for this work, and the helpful comments of the technical reviewers, the Science Advisory Board, and the public. We would appreciate notice of any errors or suggestions for improvements so that they may be taken into account in future editions. You may address comments to Michael A. Boyd, Radiation Protection Division (6608J), U.S. Environmental Protection Agency, Washington, DC 20460.

Stephen D. Page, Director
Office of Radiation and Indoor Air

CONTENTS

PREFACE	iii
LIST OF TABLES	xi
LIST OF FIGURES	xiii
CHAPTER 1. INTRODUCTION	1
Radionuclides and exposure scenarios addressed	2
Applicability to the current U.S. population	3
Computation of the risk coefficients for internal exposure	4
1. Lifetime risk per unit absorbed dose at each age	4
2. Absorbed dose rates as a function of time post acute intake at each age	5
3. Lifetime cancer risk per unit intake at each age	6
4. Lifetime cancer risk for chronic intake	6
5. Average lifetime cancer risk per unit activity intake	7
Computation of the risk coefficients for external exposure	7
How to apply a risk coefficient	8
Limitations on use of the risk coefficients	9
Uncertainties associated with risk coefficients	10
Software used to compute the risk coefficients	12
Organization of the report	13
CHAPTER 2. TABULATIONS OF RISK COEFFICIENTS	15
Risk coefficients for inhalation	16
Risk coefficients for ingestion	17
Risk coefficients for external exposure	18
Adjustments for current age and gender distributions in the U.S.	19
CHAPTER 3. EXPOSURE SCENARIOS	137
Characteristics of the exposed population	137
Growth of decay chain members	137
Inhalation of radionuclides	138
Intake of radionuclides in food	141
Intake of radionuclides in tap water	142
External exposure to radionuclides in air	143
External exposure to radionuclides in soil	143
CHAPTER 4. BIOKINETIC MODELS FOR RADIONUCLIDES	145
The model of the respiratory tract	145
The model of the gastrointestinal tract	147

Systemic biokinetic models	151
Treatment of decay chain members formed in the body	155
Solution of the biokinetic models	156
CHAPTER 5. DOSIMETRIC MODELS FOR INTERNAL EMITTERS	157
Age-dependent masses of source and target regions	157
Dosimetric quantities	160
Nuclear decay data	161
Specific absorbed fractions for photons	161
Absorbed fractions for beta particles and discrete electrons	163
Absorbed fractions for alpha particles and recoil nuclei	164
Spontaneous fission	165
Computation of <i>SE</i>	165
CHAPTER 6. DOSIMETRIC MODELS FOR EXTERNAL EXPOSURES	167
Interpretation of dose coefficients from Federal Guidance Report No. 12	167
Nuclear data files used	168
Radiations considered	169
Effects of indoor residence	170
CHAPTER 7. RADIOGENIC CANCER RISK MODELS	171
Types of risk projection models	171
Epidemiological studies used in the development of risk models	173
Modification of epidemiological data for application to low doses and dose rates	173
Relative biological effectiveness factors for alpha particles	174
Risk model coefficients for specific organs	174
Association of cancer type with dose location	178
Relation between cancer mortality and morbidity	180
Treatment of discontinuities in risk model coefficients	183
Computation of radionuclide risk coefficients	183
APPENDIX A. MODELS FOR MORTALITY RATES	
FOR ALL CAUSES AND FOR SPECIFIC CANCERS	A-1
APPENDIX B. ADDITIONAL DETAILS OF THE DOSIMETRIC MODELS	B-1
Definitions of special source and target regions	B-1
Age-dependent masses of source and target regions	B-2
Absorbed fractions for radiosensitive tissues in bone	B-2
APPENDIX C. AN ILLUSTRATION OF THE MODELS AND METHODS USED	
TO CALCULATE RISK COEFFICIENTS FOR INTERNAL EXPOSURE	C-1
Gastrointestinal tract model and f_i values	C-1
Respiratory tract model	C-2

Biokinetics of absorbed thorium	C-4
Structure of the systemic biokinetic model for thorium	C-4
Parameter values for the systemic model for thorium	C-6
Predicted differences with age in the systemic biokinetics of thorium	C-8
Treatment of ²³² Th chain members produced in systemic tissues	C-9
Comparison of updated and previous systemic models for thorium	C-11
Conversion of activity to estimates of dose rates to tissues	C-13
<i>SE</i> values	C-13
Use of <i>SE</i> values to calculate dose rates	C-16
Conversion of dose rates to estimates of radiogenic cancers	C-18
Comparison with risk estimates based on effective dose	C-22

APPENDIX D: UNCERTAINTIES IN ESTIMATES OF CANCER RISK

FROM ENVIRONMENTAL EXPOSURE TO RADIONUCLIDES	D-1
Purposes of this appendix	D-1
General sources of uncertainty in biokinetic estimates	D-2
Uncertainties associated with the structure of a biokinetic model	D-2
Types of information used to construct biokinetic models for elements	D-2
Sources of uncertainty in applications of human data	D-3
Uncertainty in interspecies extrapolation of biokinetic data	D-4
Uncertainty in inter-element extrapolation of biokinetic data	D-6
Uncertainty in central estimates stemming from variability in the population	D-7
Examples of data sources for some specific biokinetic models	D-7
Model of the respiratory tract	D-7
Gastrointestinal tract model and f_1 values	D-9
Systemic biokinetic models for parent radionuclides	D-10
Models for radionuclides produced in the body by radioactive decay	D-17
Uncertainties in internal dosimetric models	D-18
Specific energy (<i>SE</i>) for photons	D-18
<i>SEs</i> for beta particles and discrete electrons	D-19
<i>SEs</i> for alpha particles	D-20
Special dosimetric problems presented by walled organs	D-21
Uncertainties in external dosimetric models	D-21
Transport of radiation from the environmental source to humans	D-21
Effects of age and gender	D-23
Uncertainties in risk model coefficients	D-24
Sampling variability	D-24
Diagnostic misclassification	D-24
Errors in dosimetry	D-25
Uncertainties in the effects of radiation at low dose and dose rate	D-26
Uncertainties in the RBE for alpha particles	D-29
Uncertainties in transporting risk estimates across populations	D-30
Uncertainties in age and time dependence of risk per unit dose	D-32

Uncertainties in site-specific cancer morbidity risk estimates	D-33
Imprecision in risk model coefficients as indicated by differences in expert judgments	D-33
Proposed procedure for assigning nominal uncertainty intervals to risk coefficients	D-34
APPENDIX E. ADJUSTMENT OF RISK COEFFICIENTS FOR SHORT-TERM EXPOSURE OF THE CURRENT U.S. POPULATION	E-1
Computation of risk coefficients for the hypothetical current population	E-1
Comparison of coefficients for the current and stationary populations	E-4
APPENDIX F. SAMPLE CALCULATIONS	F-1
APPENDIX G. NUCLEAR DECAY DATA	G-1
GLOSSARY	GL-1
REFERENCES	R-1

LIST OF TABLES

Table	Page
2.1	Mortality and morbidity risk coefficients for inhalation 21
2.2a	Mortality and morbidity risk coefficients for ingestion of tap water and food 83
2.2b	Mortality and morbidity risk coefficients for ingestion of iodine in food, based on usage of cow's milk 105
2.3	Mortality and morbidity risk coefficients for external exposure from environmental media 107
2.4	Uncertainty categories for selected risk coefficients 129
3.1	Age- and gender-specific usage rates of environmental media, for selected ages 139
4.1	Absorption types considered in ICRP Publication 72 for particulate aerosols 148
5.1	Source and target organs used in internal dosimetry methodology 158
7.1	Revised mortality risk model coefficients for cancers other than leukemia, based on the EPA radiation risk methodology 175
7.2	Revised mortality risk model coefficients for leukemia, based on the EPA radiation risk methodology 176
7.3	Age-averaged site-specific cancer mortality risk estimates (cancer deaths per person-Gy) from low-dose, low-LET uniform irradiation of the body 179
7.4	Dose regions associated with cancer types 180
7.5	Lethality data for cancers by site in adults 181
7.6	Age-averaged site-specific cancer morbidity risk estimates (cancer cases per person-Gy) from low-dose, low-LET uniform irradiation of the body 182
A.1	Gender- and age-specific values for the survival function, $S(x)$, and the expected remaining lifetime, $\hat{e}(x)$, used in this report A-2
B.1	Age-specific masses of source and target organs B-3
B.2	Absorbed fractions for alpha and beta emitters in bone B-4
C.1	Age-specific transfer coefficients in the systemic biokinetic model for thorium C-7
C.2	Predictions of 50-y integrated activity of ^{232}Th following injection into blood at age 100 d, 10 y, or 25 y C-9
C.3	Comparison of estimated 50-y integrated activities of ^{232}Th and its decay chain members, assuming independent or shared kinetics of decay chain members, for the case of injection of ^{232}Th into blood of an adult C-12
C.4	Comparison of ICRP's updated and previous models as predictors of 50-y integrated activity after acute intake of ^{232}Th by an adult C-15
C.5	Comparison of cancer mortality risk coefficients with risk estimates based on effective dose, for ingestion or inhalation of ^{232}Th C-24
D.1	Summary of reported data on uptake and retention of iodine by the human thyroid D-14
D.2	Age-averaged site-specific cancer morbidity risk estimates (cancer cases per person-Gy $\times 10^{-2}$) from low-LET uniform irradiation of the body at high dose and dose rate, as estimated by nine experts on health effects of radiation D-34

LIST OF TABLES, continued

Table		Page
E.1	Average daily usage of environmental media by the two hypothetical populations . . .	E-3
E.2	Comparison of risk coefficients for the two hypothetical populations	E-5
G.1	Summary information on the nuclear transformation of radionuclides	G-5

LIST OF FIGURES

Figure	Page
1.1	Components of the risk coefficient computation 4
3.1	Gender-specific survival functions for the stationary population 138
3.2	Age- and gender-specific usage rates used to derive risk coefficients for inhalation, ingestion of water, ingestion of food (energy intake), and ingestion of milk . . 140
4.1	Structure of the ICRP's respiratory tract model 146
4.2	Model of transit of material through the gastrointestinal tract 149
4.3	Structure of the ICRP's biokinetic model for zirconium 152
4.4	Structure of the ICRP's biokinetic model for iodine. 153
4.5	Structure of the ICRP's biokinetic model for iron 154
4.6	The ICRP's generic model structure for calcium-like elements 155
5.1	Illustration of phantoms used to derive age-dependent specific absorbed fractions for photons 162
C.1	Predictions of the ICRP's updated and previous respiratory tract models, for inhalation of ^{232}Th in soluble, moderately soluble, or insoluble 1- μm (AMAD) particles C-3
C.2	The ICRP's generic framework for modeling the systemic biokinetics of a class of bone-surface-seeking elements, including thorium C-5
C.3	Retention of ^{232}Th on trabecular surfaces for three ages at injection, as predicted by the updated model for thorium C-8
C.4	Biokinetic model for thorium given in ICRP Publication 30 C-12
C.5	Comparison of predictions of ICRP's updated and previous systemic biokinetic models for thorium C-14
C.6	Age-specific <i>SE</i> values (high-LET) for ^{232}Th C-15
C.7	Estimated weight of red marrow as a function of age C-16
C.8	Contributions of ^{232}Th in Trabecular Bone Surface, Trabecular Bone Volume, and Red Marrow to the high-LET dose rate to Red Marrow in the adult C-17
C.9	Estimated dose rates to Red Marrow following acute ingestion of ^{232}Th , for three ages at ingestion C-17
C.10	Estimated dose rates to Red Marrow following acute inhalation of moderately soluble ^{232}Th , for three ages at inhalation C-17
C.11	Relative risk functions, $\eta(u, x)$, for leukemia in males for three ages at irradiation . . C-19
C.12	Age- and gender-specific mortality rates for leukemia, based on U.S. data for 1989-91 C-19
C.13	Gender-specific survival functions based on U.S. life tables for 1989-91 C-20
C.14	Gender-specific lifetime risk coefficient (<i>LRC</i>) functions for radiogenic leukemia . . C-20
C.15	Derived gender-specific risk $r_a(x_i)$ of dying from leukemia due to ingestion of 1 Bq of ^{232}Th in food at age x_i C-21

LIST OF FIGURES, continued

Figure		Page
C.16	Derived gender-specific risk $r_a(x_i)$ of dying from leukemia due to inhalation of 1 Bq of ^{232}Th (Type M) at age x_i	C-21
C.17	Gender-weighted average lifetime risk coefficients for ingestion of ^{232}Th in food, using updated and previous biokinetic models for thorium	C-22
C.18	Gender-weighted average lifetime risk coefficients for inhalation of moderately soluble ^{232}Th , using updated and previous biokinetic models for thorium . . .	C-22
D.1	Reported half-times for the short-term retention component for tritium taken in mainly as HTO by adult humans	D-11
D.2	Reported biological half-times for cesium in adult male humans	D-15
D.3	Estimated effects of age on effective dose for photons uniformly distributed in angle	D-23
D.4	Uncertainty distributions assigned to the DDREF in recent reports	D-28
D.5	Comparison of predictions of cancer mortality based on simplistic estimate with risk coefficients for intake of radionuclides in tap water	D-35
E.1	Comparison of gender-specific age-distributions in 1996 U.S. population with hypothetical stationary distributions based on 1989-91 U.S. life table	E-2

CHAPTER 1. INTRODUCTION

Since the mid-1980s, a series of Federal guidance documents has been issued by the Environmental Protection Agency (EPA) for the purpose of providing Federal and State agencies with technical information to assist their implementation of radiation protection programs. Previous reports have dealt with numerical factors, called “dose factors” or “dose coefficients”, for estimating radiation dose due to exposure to radionuclides. The present report is intended as the first of a series of documents that will provide numerical factors, called “risk coefficients”, for estimating risks to health from exposure to radionuclides. These reports will apply state-of-the-art methods and models that take into account age and gender dependence of intake, metabolism, dosimetry, radiogenic risk, and competing causes of death in estimating the risks to health from internal or external exposure to radionuclides. The present report provides tabulations of cancer risk coefficients for internal or external exposure to any of more than 800 radionuclides through various environmental media. Subsequent reports may expand the exposure pathways and health endpoints considered.

The risk coefficients developed in this report apply to an average member of the public, in the sense that estimates of risk are averaged over the age and gender distributions of a hypothetical closed “stationary” population whose survival functions and cancer mortality rates are based on recent data for the U.S. Specifically, the total mortality rates in this population are defined by the 1989-91 U.S. decennial life table (NCHS, 1997), and cancer mortality rates are defined by U.S. cancer mortality data for the same period (NCHS, 1992, 1993a, 1993b). This hypothetical population is referred to as “stationary” because the gender-specific birth rates and survival functions are assumed to remain invariant over time.

For a given radionuclide and exposure mode, both a “mortality risk coefficient” and a “morbidity risk coefficient” are provided. A mortality risk coefficient is an estimate of the risk to an average member of the U.S. population, *per unit activity inhaled or ingested for internal exposures or per unit time-integrated activity concentration in air or soil for external exposures*, of dying from cancer as a result of intake of the radionuclide or external exposure to its emitted radiations. A morbidity risk coefficient is a comparable estimate of the average total risk of experiencing a radiogenic cancer, whether or not the cancer is fatal. The term “risk coefficient” with no modifier should be interpreted throughout this report as “mortality or morbidity risk coefficient”.

It is a common practice to estimate the cancer risk from intake of a radionuclide or external exposure to its emitted radiations as the simple product of a “probability coefficient” and an estimated “effective dose” to a typical adult (see the Glossary for definitions). For example, a

“nominal cancer fatality probability coefficient” of 0.05 Sv^{-1} is given in ICRP Publication 60 (1991) for all cancer types combined. This value is referred to as nominal because of the uncertainties inherent in radiation risk estimates and because it is based on an idealized population receiving a uniform dose over the whole body. It is pointed out by the ICRP (1991) that such a probability coefficient may be a less accurate estimator in situations where the distribution of dose is nonuniform. There are also other situations in which the product of a probability coefficient and the effective dose may not accurately represent the risk implied by current biokinetic, dosimetric, and radiation risk models. For example, such a product may understate the implied risk for intakes of radionuclides for which there is an apparently multiplicative effect during childhood of elevated organ doses and elevated risk per unit dose. Such a product may overstate the risk implied by current models in the case of intake of a long-lived, tenaciously retained radionuclide because much of the dose may be received during late adulthood when there is a relatively high likelihood of dying from a competing cause before a radiogenic cancer can be expressed. Finally, the weighting factors commonly used to calculate effective dose do not reflect the most up-to-date knowledge of the distribution of risk among the organs and tissues of the body.

In contrast to risk estimates based on the product of a probability coefficient and effective dose (for intake by the adult), the risk coefficients tabulated in this document take into account the age dependence of the biological behavior and internal dosimetry of ingested or inhaled radionuclides. Also, compared with risk estimates based on effective dose, the risk coefficients in this document characterize more precisely the implications of age and gender dependence in radiogenic risk models, U.S. cancer mortality rates, and competing risks from non-radiogenic causes of death in the U.S. Finally, these risk coefficients take into account the age and gender dependence in the usage of contaminated environmental media, which is generally not considered in risk estimates based on the simple product of a nominal probability coefficient and an estimated effective dose.

Radionuclides and exposure scenarios addressed

Risk coefficients are provided for the following modes of exposure to a given radionuclide: inhalation of air, ingestion of food, ingestion of tap water, external exposure from submersion in air, external exposure from the ground surface, and external exposure from soil contaminated to an infinite depth.

With a few exceptions described in Chapter 6, the radionuclides addressed in the external exposure scenarios are the same as those considered in Federal Guidance Report No. 12 (EPA,

1993), which tabulates dose coefficients for external exposure to radionuclides in air, water, and soil. Each of the radionuclides considered in the external exposure scenarios either has a half-life of at least 10 min or occurs in the decay chain of such a radionuclide.

With a few exceptions described in Chapter 5, the radionuclides considered in the internal exposure scenarios are the same as those addressed in ICRP Publication 72 (1996), which is a compilation of the ICRP's age-dependent dose coefficients for members of the public from intake of radionuclides. These radionuclides include most but not all of those considered in the external exposure scenarios. Specifically, the radionuclides addressed in the external exposure scenarios but not in the intake scenarios are those with half-lives less than 10 min and radioisotopes of radon or other noble gases. New models and methods for assessing the risk of exposure to radon and its short-lived progeny are under development.

For each of the internal exposure modes, the risk coefficient for a radionuclide includes the contribution to dose from production of decay chain members in the body after intake of the parent radionuclide, regardless of the half-lives of the decay chain members. For both internal and external exposure, a risk coefficient for a given radionuclide is based on the assumption that *this is the only radionuclide present in the environmental medium*. That is, doses due to decay chain members produced in the environment *prior* to intake of, or external exposure to, the radionuclide are *not* considered. However, a separate risk coefficient is provided for each decay chain member of potential dosimetric significance. This allows the user to assess the risks from ingrowth of radionuclides in the environment.

The risk coefficients tabulated in this report are applicable to either chronic or acute exposure to a radionuclide. That is, a risk coefficient may be interpreted either as the average risk per unit exposure to members of a population exposed throughout life to a constant concentration of a radionuclide in an environmental medium, or as the average risk per unit exposure to members of a population acutely exposed to the radionuclide in the environmental medium. For purposes of computing the risk coefficients, it was assumed that the concentration of the radionuclide in the environmental medium remains constant and that all persons in the population are exposed to that environmental medium throughout their lifetimes.

Applicability to the current U.S. population

The risk coefficients are based on exposure of a hypothetical stationary population with survival functions and cancer mortality rates similar to those of the current U.S. population, but with steady-state gender and age distributions based on these survival functions and fixed gender-specific

birth rates. Due to uncertainty in the future composition of the U.S. population, the use of such a stationary population is appropriate for consideration of long-term, chronic exposures. Because the gender-specific age distributions in the current U.S. population differ considerably from those of the hypothetical stationary population, however, the question arises as to the applicability of these risk coefficients to short-term exposures of the U.S. population that might occur in the near future. This question is addressed in Appendix E, where the tabulated risk coefficients are compared with values calculated for short-term exposure of a hypothetical population with the age and gender distributions of the 1996 U.S. population. As is the case for the hypothetical stationary population, total mortality rates in the hypothetical 1996 population during and after exposure are assumed to be those given in the 1989-91 U.S. decennial life table, and cancer mortality rates are taken to be those given by U.S. cancer mortality data for the same period. The comparison reveals only small differences in risk coefficients for the two populations.

Computation of the risk coefficients for internal exposure

A schematic of the method of computation of a risk coefficient is shown in Fig. 1.1 for the case of internal exposure to a radionuclide. The main steps in the computation are shown in the numbered boxes in the figure and are summarized below.

1. Lifetime risk per unit absorbed dose at each age

For each of 14 cancer sites in the body, radiation risk models are used to calculate gender-specific values for the lifetime risk *per unit absorbed dose* received at each age. The age- and gender-specific radiation risk models are described in Chapter 7. These models are taken

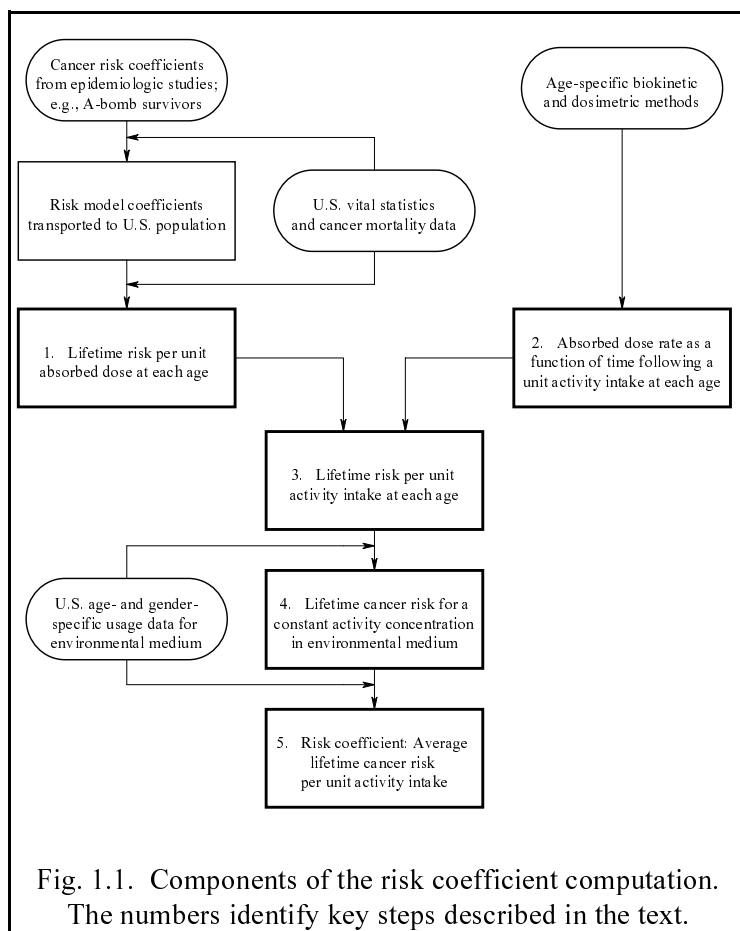


Fig. 1.1. Components of the risk coefficient computation. The numbers identify key steps described in the text.

from a recent EPA report (EPA, 1994) that provides a methodology for calculation of radiogenic cancer risks based on a critical review of data on the Japanese atomic bomb survivors and other study groups and methods of transporting radiation risk estimates across populations. Parameter values given in that EPA report have been modified in some cases to reflect updated vital statistics and cancer mortality data for the U.S. and to achieve greater consistency in the assumptions made in this report for different age groups and genders.

The cancer sites considered are esophagus, stomach, colon, liver, lung, bone, skin, breast, ovary, bladder, kidney, thyroid, red marrow (leukemia), and residual (all remaining cancer sites combined). An absolute risk model is applied to bone, skin, and thyroid; that is, it is assumed for these sites that the radiogenic cancer risk is independent of the baseline cancer mortality rate (the cancer mortality rate for that site in an unexposed population). For the other cancer sites, a relative risk model is used; that is, it is assumed that the likelihood of a radiogenic cancer is proportional to its baseline cancer mortality rate. The baseline cancer mortality rates are calculated from U.S. cancer mortality data for 1989-91 (NCHS, 1992, 1993a, 1993b).

The computation of gender- and cancer site-specific values for the lifetime risk per unit absorbed dose involves an integration over age, beginning at the age at which the dose is received, of the product of the age-specific risk model coefficient (times the baseline mortality rate of the cancer in the case of a relative risk model) and the survival function. The survival function accounts for the possibility that the exposed person may die from a competing cause before a radiogenic cancer is expressed. The computation is described in detail in Chapter 7.

The estimates of lifetime risk per unit absorbed dose are independent of the radionuclide and exposure pathway. They are calculated only once and are used as input for the calculation of each risk coefficient.

2. Absorbed dose rates as a function of time post acute intake at each age

Age-specific biokinetic models are used to calculate the time-dependent inventories of activity in various regions of the body *following acute intake of a unit activity of the radionuclide*. For a given radionuclide and intake mode, this calculation is performed for each of six “basic” ages at intake: infancy (100 days); 1, 5, 10, and 15 years; and maturity (usually 20 years, but 25 years in the biokinetic models for some elements). The biokinetic models used in this document are described in Chapter 4. With a few exceptions described in that chapter, these biokinetic models are the same as those applied by the ICRP in its development of age-specific dose coefficients for

inhalation or ingestion of radionuclides by members of the public (ICRP, 1989, 1993, 1995a, 1995b, 1996).

Age-specific dosimetric models are used to convert the calculated time-dependent regional activities in the body to absorbed dose rates (per unit intake) to radiosensitive tissues as a function of age at intake and time after intake. Absorbed dose rates for intake ages intermediate to the six basic ages at intake (infancy; 1, 5, 10, and 15 years; and maturity) are determined by interpolation. The dosimetric models used in this document are the models used in the ICRP's series of documents on age-specific doses to members of the public from intake of radionuclides (ICRP, 1989, 1993, 1995a, 1995b, 1996). These models are described in Chapter 5.

3. Lifetime cancer risk per unit intake at each age

For each cancer site, the gender-specific values of lifetime risk per unit absorbed dose received at each age (derived in the first step) are used to convert the calculated absorbed dose rates to lifetime cancer risks, for the case of acute intake of one unit of activity at each age x_i . This calculation involves integration over age of the product of the absorbed dose rate at age x for a unit intake at age x_i , the lifetime risk per unit absorbed dose received at age x , and the value of the survival function at age x divided by the value at age x_i . The survival function is used to account for the probability that a person exposed at age x_i is still alive at age x to receive the absorbed dose. It is assumed that the radiation dose is sufficiently low that the survival function is not significantly affected by the number of radiogenic cancer deaths at any age. The calculation is described in Chapter 7.

4. Lifetime cancer risk for chronic intake

The risk coefficients in this document are applicable to either chronic or acute exposures. However, for purposes of computing a risk coefficient, it is assumed that the concentration of the radionuclide in the environmental medium remains constant and that all persons in the population are exposed to that environmental medium throughout their lifetimes.

The usage of environmental media may vary considerably with age and gender. Such variation is taken into account in the calculation of risk coefficients for the internal exposure scenarios. The age- and gender-specific models of usage of environmental media (air, food, or tap water) are described in Chapter 3. Daily ingestion of a given radionuclide in food is assumed to be proportional to age- and gender-specific daily energy intake. For radioisotopes of iodine, alternate

risk coefficients are calculated for food under the assumption that daily ingestion is proportional to age- and gender-specific daily usage of cow's milk. The age- and gender-specific ventilation rates applied here are reference values given by the ICRP. Age- and gender-specific usage rates for tap water, food energy, and cow's milk are average values estimated from recent data for the U.S.

For each cancer site and each gender, the lifetime cancer risk for chronic exposure is obtained by integration over age x of the product of the lifetime cancer risk per unit intake at age x and the expected intake of the environmental medium at age x . The expected intake at a given age is the product of the usage rate of the medium and the value of the survival function at that age.

5. Average lifetime cancer risk per unit activity intake

Because a risk coefficient is the estimated radiogenic cancer risk *per unit activity intake*, the calculated lifetime cancer risk from chronic intake of the environmental medium must be divided by the expected lifetime intake. The expected lifetime intake is given by the integral over age of the product of the usage rate and the survival function.

Therefore, in the calculation of a gender- and cancer site-specific risk coefficient, usage of the environmental medium appears both in the numerator (see Step 4) and the denominator. This makes the risk coefficient independent of the concentration of the radionuclide in the medium and of the population-averaged usage rate of the medium but does not diminish the importance of the usage rate in the derivation of the risk coefficient. For example, the risk coefficient for a given radionuclide in food may differ considerably from the coefficient for the same radionuclide in tap water because the assumed age-specific patterns of consumption are substantially different for food and tap water.

Except for the calculations of the time-dependent organ activities and absorbed dose rates, each of the steps described above is performed separately for each gender and each cancer site. A total risk coefficient is derived by first adding the risk estimates for the different cancer sites in each gender and then calculating a weighted mean of the coefficients for males and females. The weighted mean of coefficients for males and females reflects the gender ratio at birth, the gender-specific risk per unit intake at each age, and the gender-specific survival function at each age.

Computation of the risk coefficients for external exposure

The computation of risk coefficients for external exposure scenarios is similar to that for internal exposure scenarios but involves fewer steps because the absorbed dose rates are taken

directly from Federal Guidance Report No. 12 (EPA, 1993). The methods and models used in that report are summarized in Chapter 6. As in the internal exposure scenarios, it is assumed that the concentration of the radionuclide in the environmental medium remains constant and that all persons in the population are exposed to that environmental medium throughout their lifetimes.

The external dose rates used in the calculation were based on a reference adult, standing outside with no shielding (EPA, 1993). Although there is expected to be some variation with age in organ dose rates from uniform external exposure (usually less than 30%), comprehensive tabulations of age-specific organ dose rates due to external exposure are not yet available. In the present document, the dose rates calculated for the adult are applied to all ages, and no adjustments are made to account for potential reduction in dose rates due to shielding by buildings during time spent indoors.

How to apply a risk coefficient

The risk coefficients in this report may be used to assess *per capita* (population-averaged) risk due to the acute exposure of a population or, equivalently, to assess the risk due to the chronic lifetime exposure of an average individual to a constant environmental concentration. They also may be used to assess the *per capita* lifetime risk in a population from a lifetime exposure to a time varying environmental radionuclide exposure (or intake) rate, using the product of the risk coefficient and the lifetime exposure (or intake) due to that time varying rate.

A risk coefficient, r , is specific to the radionuclide, the environmental medium, and the mode of exposure through that medium. For a given exposure scenario, the computation of lifetime cancer risk, R , associated with intake of, or external exposure to, a given radionuclide involves multiplication of the applicable risk coefficient r by the *per capita* activity intake I or external exposure X . Thus, $R = r \cdot I$ for intake by inhalation or ingestion and $R = r \cdot X$ for external exposure, where I is the activity inhaled or ingested *per capita* and X is the time-integrated activity concentration of the radionuclide in air, on the ground surface, or within the soil.

For external exposure, estimation of the time-integrated activity concentration X requires information on the constant or time-dependent concentration of the radionuclide in the medium and the length of the exposure period. For an internal exposure scenario, estimation of the *per capita* activity intake I of the radionuclide requires the same information, plus an estimate of the average usage rate of the medium by members of the population during the exposure period. The user may apply the *per capita* usage rate of air, food, or tap water given in Chapter 3 (see the “combined lifetime average” usage rates in Table 3.1) or, because the risk coefficients are independent of the

average usage rate of the medium, may apply an average usage rate better suited to the exposure scenario. For example, if the exposure scenario involves acute inhalation of a radionuclide in a rapidly passing cloud, the average inhalation rate in the exposed population during the exposure period may differ from the 24-h average rate given in Chapter 3. However, the assumptions described in Chapter 3 concerning *relative* age- and gender-specific usage of the environmental media are inherent in the risk coefficients for internal exposure and hence cannot be changed by the user.

To ensure consistent risk calculations, the risk coefficients given in this document (Chapter 2) are tabulated to three figures. No indication of the level of uncertainty is intended or should be inferred from this practice. A calculated risk should be rounded appropriately. Appendix F provides sample calculations that illustrate how the tabulated risk coefficients may be applied to different types of exposure.

Limitations on use of the risk coefficients

Analyses involving the risk coefficients tabulated in this report should be limited to estimation of prospective risks in hypothetical or large existing populations, or retrospective analyses of risks to large actual populations. The tabulations are not intended for application to specific individuals and should not be used for that purpose.

In contrast to situations involving representative population samples, the coefficients tabulated in this report may not be appropriate for assessing the risk to an average individual in an *age-specific* cohort due to chronic exposure to an environmental concentration that varies substantially over the life of the cohort. In such special cases, the time-varying environmental concentration must be incorporated explicitly into the calculations described in Chapter 7. Such applications are beyond the scope of this report.

The risk coefficients for external exposure scenarios are based on estimated dose rates for a reference adult male, standing outdoors with no shielding (EPA, 1993). Activity distributions in air, on the ground surface, or in soil are assumed to be of an infinite extent. It is left to the user to decide whether a reduction factor is appropriate for a given application to account for the finite nature of the activity distribution in the environment, shielding by buildings during time spent indoors, or other factors encountered in the real world.

The risk coefficients are based on radiation risk models developed for application either to low doses, defined as acute absorbed doses less than 0.2 Gy, or to low dose rates, defined as dose rates less than 0.1 mGy min⁻¹ (EPA, 1994). The assumption is made that the absorbed dose is

sufficiently low that the survival function is not significantly affected by the number of radiogenic cancer deaths at any age. Thus, these risk coefficients should be applied with care to cases involving large cumulative risks, either in prospective or retrospective analyses.

Uncertainties associated with risk coefficients

The risk coefficients tabulated in this document are derived from models representing characteristics of the U.S. population, the biological behavior of elements in the human body, the doses to radiosensitive tissues from radiation originating either inside the body or in an external medium, and the lifetime cancer risk per unit dose to these tissues. The models representing the U.S. population, including its usage of air, food, and water, are based on reasonably detailed information. The biokinetic, dosimetric, and radiation risk models generally have been derived from much less detailed and sometimes inconsistent data bases and in many cases have substantial uncertainties associated with their predictions. These uncertainties are propagated in the derivation of a risk coefficient, with the result that a risk coefficient is an uncertain representation of the cancer risk per unit intake of, or external exposure to, a radionuclide.

The level of uncertainty associated with a given risk coefficient may vary considerably from one application to another. For example, the uncertainty assigned to an inhalation risk coefficient for a radionuclide may depend strongly on the availability of information on the chemical and physical form of the inhaled radionuclide because the accuracy of the estimated doses to the lungs and other radiosensitive tissues often depends strongly on such information. As a second example, a risk coefficient that is considered to be a reasonably reliable predictor for a relatively high, acute external exposure to a radionuclide may be appreciably less certain for a lower, prolonged exposure due to uncertainty in the shape of the dose-response curve at low dose and dose rate.

On the other hand, each risk coefficient involves important uncertainties, stemming from limitations in the underlying biokinetic, dosimetric, and radiation risk models, that are largely independent of the exposure scenario. For example, there are important gaps in current understanding of the typical biological behavior of many radionuclides. Also, there are substantial uncertainties associated with interpretation of available epidemiological data for radiogenic cancer and extrapolation of that data to other populations and other radiation types, regardless of the assumptions used to extrapolate from high to low dose and dose rate.

In Chapter 2, selected risk coefficients are assigned to “uncertainty categories” that represent different levels of uncertainty associated with estimates of cancer mortality due to intake of, or external exposure to, radionuclides. Essentially, an uncertainty category is intended to reflect the

precision with which an estimate of radiogenic cancer mortality can be made for an ideal population and exposure scenario, assuming that the probability of inducing a radiogenic cancer is proportional to absorbed dose. Thus, an uncertainty category does not reflect uncertainties associated with the use of a linear, no-threshold model for estimating radiogenic cancer at low doses, absorbed dose as a measure of radiogenic cancer risk, or idealized representations of the population and exposure. The selection of an uncertainty category for a given risk coefficient was based on subjective judgments by the authors of this report but was guided by an analysis of the sensitivity of the risk coefficient to major uncertainties in the underlying biokinetic, dosimetric, and radiation risk models.

Appendix D provides a general discussion of current understanding of the biological behavior of radionuclides in the human body, conversion from internally or externally distributed radioactivity to absorbed dose to tissues, and extrapolation from tissue dose to cancer risk. A systematic procedure is proposed for deriving quantitative statements of uncertainty for risk coefficients in the form of “nominal uncertainty intervals”. The term “nominal” is used to reflect the fact that the uncertainty interval for a risk coefficient would be based on a fixed set of typically dominant sources of uncertainty in radiogenic cancer risk estimates, an idealized population and exposure scenario, and the assumption that the probability of inducing a radiogenic cancer is proportional to absorbed dose.

A major source of uncertainty, and controversy, in radiogenic cancer risk estimation is the use of a linear, no-threshold model to calculate risks for low, acute doses or low dose rates. The uncertainty in the cancer risk per unit dose at low dose and dose rate is difficult to quantify and can only be characterized through a broad examination and synthesis of diverse sources of information from molecular, cellular, animal, and human studies.

Arguments for and against the existence of an effective threshold for radiogenic cancer have been made on the basis of epidemiological data, but conclusions appear to depend on the population and cancer type considered and the assumptions underlying the analysis. It is doubtful that human epidemiological data can be used to determine the existence or absence of a threshold for radiogenic cancer, due to the statistical uncertainties inherent in such data. Molecular, cellular, and animal studies can furnish important information but, so far, have not provided definitive evidence regarding the existence of thresholds for radiogenic cancers in man.

Carcinogenesis is understood to be a multistage process in which a single cell gives rise to a tumor, with mutation of DNA required in one or more of the steps leading to malignancy. Since cancer is a common disease, the background rates for each of these steps must be greater than zero, and any filtration mechanism for removing precancerous cells must be imperfect. Traversal of a single ionizing track through a cell appears to be capable of causing DNA damage that cannot always

be faithfully repaired. Until there is more definitive information on the effects of radiation at low doses and dose rates, it seems reasonable to assume that any exposure that increases the rate of mutation of DNA has a nonzero probability of causing cancer (EPA, 1999).

In recent years, various expert panels have concluded that use of a linear, no-threshold model is reasonably consistent with much of the available information on carcinogenic effects of radiation and is scientifically justifiable for purposes of estimating risks from low doses of radiation (UNSCEAR, 1993, 1994; NRPB, 1993; NCRP, 1997). Nevertheless, current scientific evidence does not rule out the possibility that the resulting risk calculated at environmental exposure levels may be substantially over- or underestimated or even that there may be a net beneficial effect of low dose radiation (Luckey, 1990; Jaworowski, 1995; Goldman, 1996). Clearly, further efforts are needed to clarify the dose-response relationship for low dose and dose rates.

Evidence that low dose radiation may induce or activate cellular DNA repair mechanisms through an adaptive response or some stimulatory mechanism has led to speculation that low doses may be protective against cancer. The stimulatory effects seen to date have been short term and may not provide a significant reduction in cancer risk (Puskin, 1997). A detailed review of possible radiation induced adaptive responses can be found in the UNSCEAR (1994) report. At this time, too little is known about the adaptive response to influence EPA's estimates of risk at low doses.

Although the risk coefficients in this document are based on a linear, no-threshold model, their derivation includes a dose and dose-rate effectiveness factor (DDREF) to account for the apparent decrease in cancer risk of low-LET radiation at low dose or dose rate compared with the observed risks due to a much higher acute dose (NCRP, 1980). Reported values of the DDREF generally have been based on comparisons of radiogenic effects at high and moderately low doses or dose rates. Differences in reported DDREFs must be considered when assessing the uncertainty associated with application of a risk coefficient, but consideration of such differences does not address the uncertainty in the linear, no-threshold hypothesis, *per se*.

Software used to compute the risk coefficients

All computations of dose and risk were performed using the DCAL (DOSE CALCULATION) software (Eckerman et al., 1999). DCAL is a comprehensive biokinetics, dosimetry, and risk computational system designed to serve current needs in radiation dosimetry and risk analysis. It performs biokinetic and dosimetric calculations for acute intake of a radionuclide by inhalation, ingestion, or injection into blood at a user-specified age. DCAL couples the generated

absorbed dose rates with radiation risk estimators and mortality data to predict organ-specific risk of radiogenic cancer mortality or morbidity from intake of a radionuclide.

DCAL has been extensively tested and has been compared with several widely used solvers for biokinetic models and systems of differential equations. DCAL was used by a task group of the ICRP to derive or check the dose coefficients given in its series of documents on age-specific doses to members of the public from intake of radionuclides (ICRP, 1989, 1993, 1995a, 1995b, 1996).

Organization of the report

Risk coefficients for intake of, or external exposure to, environmental radionuclides are tabulated in Chapter 2. The tables of risk coefficients are followed by a summary of subjective judgments concerning the extent of uncertainties in risk coefficients for selected radionuclides and exposure modes.

The assumptions and models used to derive the risk coefficients tabulated in Chapter 2 are described in Chapters 3 through 7. The exposure scenarios, including assumptions concerning the vital statistics of the exposed population and the age- and gender-specific usage rates of environmental media by the population, are described in Chapter 3. Biokinetic models, dosimetric models for internal exposure, dosimetric models for external exposure, and radiation risk models are described in Chapters 4, 5, 6, and 7, respectively.

Some additional details concerning the models used in the calculations are given in Appendices A and B. Appendix C provides a detailed illustration of the models and computational steps involved in the derivation of a risk coefficient for ingestion or inhalation of a radionuclide. The sources of uncertainty in the biokinetic, dosimetric, and radiation risk models are discussed in Appendix D. Appendix E compares the tabulated risk coefficients with values calculated for short-term exposure of a non-stationary population with age and gender distributions similar to those of the current U.S. population. Appendix F provides several sample calculations that illustrate how the tabulated risk coefficients may be applied to different types of exposure. Appendix G provides a summary of information on the nuclear decay characteristics of each radionuclide and gives details of its decay chain when indicated. A glossary of terms is provided at the end of the appendices.

CHAPTER 2. TABULATIONS OF RISK COEFFICIENTS

The risk coefficients tabulated here are based on a hypothetical stationary population with total mortality rates defined by the 1989-91 U.S. decennial life table (NCHS, 1997) and cancer mortality rates defined by U.S. cancer mortality data for the same period (NCHS, 1992, 1993a, 1993b). These coefficients may be interpreted in terms of either acute or chronic exposure to environmental radionuclides. That is, a risk coefficient may be interpreted as the risk per unit exposure for a typical person exposed throughout life to a constant concentration of a radionuclide in an environmental medium, or as the average risk per unit exposure to members of a stationary population that experiences an acute exposure to that radionuclide in that environmental medium. Risk coefficients are tabulated for the following modes of exposure:

1. inhalation of a radionuclide in air (Table 2.1);
2. ingestion of a radionuclide in tap water (Table 2.2a);
3. ingestion of a radionuclide in food (Table 2.2a; an alternate set of risk coefficients for radioisotopes of iodine in food is given in Table 2.2b);
4. external exposure to radiation from a radionuclide in air (Table 2.3);
5. external exposure to radiation from a radionuclide on the ground surface (Table 2.3);
6. external exposure to radiation from a radionuclide in soil, assuming contamination to an infinite depth (Table 2.3).

Subjective judgments concerning the extent of the uncertainties associated with selected risk coefficients are summarized in Table 2.4.

A risk coefficient for a given radionuclide is based on the assumption that this is the only radionuclide present in the environmental medium. In particular, growth of chain members *in the environmental medium* is not considered. For each radionuclide addressed, however, a separate risk coefficient is provided for each subsequent member of the chain that is of potential dosimetric significance. Also, in the derivation of risk coefficients for inhalation or ingestion of a radionuclide, ingrowth of chain members *inside the body* is considered.

With a few exceptions described in Chapter 5, the radionuclides addressed in the internal exposure scenarios are the same as those considered in ICRP Publication 72 (1996), which is a compilation of the ICRP's age-dependent dose coefficients for members of the public from intake of radionuclides. With a few exceptions described in Chapter 6, the radionuclides addressed in the external exposure scenarios are the same as those considered in Federal Guidance Report No. 12 (EPA, 1993), which tabulates dose coefficients for external exposure to radionuclides in air, water,

and soil. Some of the radionuclides addressed here may be of little practical importance with regard to radiogenic cancer risk from environmental exposure.

For some of the radionuclides addressed in Table 2.1 (inhalation) or 2.2a (ingestion of tap water or food), the hypothetical radiogenic cancer risk may be of less concern than other potential toxicological hazards. For example, for ingestion of soluble forms of ^{238}U , the possibility of chemically induced damage to the kidneys may be a more important consideration than the hypothetical radiogenic cancer risk (cf. Wrenn et al., 1985). The reference information for assessment of non-radiological risks from intake of radionuclides is beyond the scope of this report.

In a few cases, the half-life of a radionuclide is sufficiently long that the mass intake of the element becomes an important consideration in a prospective risk assessment, in that an extremely small radiogenic cancer risk would result from the mass of the radionuclide that might be inhaled or ingested under any plausible environmental exposure scenario. The mass per unit activity of a radionuclide (kg Bq^{-1}) can be calculated from the expression, $m = 7.56 \times 10^{-20} A T_{1/2}$, where A is the atomic mass number and $T_{1/2}$ is the radionuclide's half-life in years. As an illustration, the radiological half-life of ^{115}In is 5.1×10^{15} y, and the mass per unit activity of ^{115}In is $7.56 \times 10^{-20} \times 115 \times 5.1 \times 10^{15} \text{ kg Bq}^{-1} = 4.4 \times 10^{-2} \text{ kg Bq}^{-1}$; that is, 1 Bq of ^{115}In has a mass of 44 g.

For radioisotopes of elements that are under tight homeostatic control by the human body, the inhalation or ingestion risk coefficients given in this document may not be appropriate for application to some exposure scenarios. For example, the ingestion risk coefficient for ^{40}K would not be appropriate for application to ingestion of ^{40}K in conjunction with an elevated intake of natural potassium. This is because the biokinetic model for potassium used in this document represents the relatively slow removal of potassium (biological half-time of 30 d) that is estimated to occur for typical intakes of potassium, whereas an elevated intake of potassium would result in excretion of a nearly equal mass of natural potassium, and hence of ^{40}K , over a short period.

Risk coefficients for inhalation

Risk coefficients for inhalation of radionuclides in air are given in Table 2.1. These coefficients are expressed as the risk of cancer mortality or morbidity per unit activity intake (Bq^{-1}).

The intake rate of a radionuclide in air is assumed to depend on age and gender. The age- and gender-specific inhalation rates used in this report are given in Chapter 3, Table 3.1.

The form of the inhaled material is classified in terms of the rate of absorption from the lungs to blood, using the classification scheme of ICRP Publication 66 (ICRP, 1994a). Type F, Type M, and Type S represent, respectively, fast, medium, and slow rates of absorption of material inhaled

in particulate form. Material-specific deposition and absorption models are used for vapors and gases (ICRP, 1995b).

ICRP Publication 71 (1995a) critically reviews inhalation data for 31 elements and provides dose coefficients for members of the public for environmentally important radioisotopes of those elements. In that document, inhalation dose coefficients for a radionuclide are provided for all three absorption types, and a default type is recommended for situations where no specific information is available. ICRP Publication 72 (1996), which is a compilation of ingestion and inhalation dose coefficients for members of the public, lists the effective dose coefficients given in ICRP Publication 71 and provides coefficients for 60 additional elements. For each of these 60 elements, attention is restricted in ICRP Publication 72 to those absorption types considered in an earlier document on occupational intakes of radionuclides (ICRP, 1994a). The absorption types addressed in ICRP Publication 72 are summarized in Table 4.1 of this report.

The information underlying the selection of an appropriate absorption type for a radionuclide usually is very limited. In many cases, the selection must be based on occupational rather than environmental experience. Due to the uncertainty in the form of a radionuclide likely to be inhaled by members of the public, inhalation risk coefficients for a radionuclide are provided here for all three absorption types. In cases where a default absorption type is recommended by the ICRP (1995a, 1996), that type is identified in the table of inhalation risk coefficients (Table 2.1).

Inhalation of a radionuclide in the form of a vapor or gas has also been considered for selected cases. In particular, risk coefficients are provided for tritium as a vapor (HTO) or gas (HT), carbon in gaseous form as carbon monoxide (CO) or carbon dioxide (CO₂), sulfur as a vapor (SO₂ or CS₂), nickel as a vapor, ruthenium as a vapor (RuO₄), iodine as a vapor or gas (methyl iodide, CH₃I), tellurium as a vapor, and mercury as a vapor.

Risk coefficients for inhalation of radionuclides in particulate form are based on an assumed activity median aerodynamic diameter (AMAD) of 1 μm. This particle size is recommended by the ICRP for consideration of environmental exposures in the absence of specific information about the physical characteristics of the aerosol (ICRP, 1994a).

Risk coefficients for ingestion

Separate risk coefficients are calculated for ingestion of radionuclides in tap water and ingestion of radionuclides in food. Both sets of coefficients are given in Table 2.2a. These risk coefficients are expressed as the risk of cancer mortality or morbidity per unit activity intake (Bq⁻¹).

The age- and gender-specific usage rates for tap water are given in Chapter 3, Table 3.1. Tap water usage is defined as water drunk directly as a beverage and water added to foods and beverages during preparation. It does not include water that is intrinsic in foods as purchased.

Food usage is defined as the total dietary intake, excluding tap water. The risk coefficients for food in Table 2.2a are based on the assumption that the intake rate of the radionuclide is proportional to food energy usage (kcal d^{-1}). Age- and gender-specific values for daily usage of total food energy are given in Chapter 3, Table 3.1.

The assessment of the intake of a radionuclide in food typically is based on its activity concentration in food (for example, Bq kg^{-1}) and an average usage rate (kg d^{-1}). The relation between food energy usage and food mass usage is discussed in Chapter 3.

The biokinetic model used to derive risk coefficients for ingestion of radiocarbon was based on balance considerations involving daily intake and total-body content of carbon and was designed mainly for dosimetry of ^{14}C -labeled metabolites (ICRP, 1981, 1989). Observations of the short- and intermediate-term behavior of radiocarbon in human subjects and laboratory animals indicate that this model may yield substantial overestimates of tissue doses from ingestion of some commonly encountered forms of radiocarbon. For example, the model may overestimate doses from ingestion of ^{14}C -labeled bicarbonate by an order of magnitude or more.

Table 2.2b gives a second set of risk coefficients for ingestion of radioisotopes of iodine in food, based on the assumption that intake of radioiodine is proportional to intake of milk. Age- and gender-specific values for the assumed daily intake of cow's milk are given in Chapter 3, Table 3.1.

Risk coefficients for external exposure

Risk coefficients are provided in Table 2.3 for each of three external exposure scenarios: external exposure from submersion in contaminated air, external exposure from contamination on the ground surface, and external exposure from soil contaminated to an infinite depth. A risk coefficient for a given radionuclide is expressed as the probability of radiogenic cancer mortality or morbidity per unit time integrated activity concentration in air, on the ground surface, or in soil. The coefficients for submersion in air are given in units of $\text{m}^3 \text{Bq}^{-1} \text{s}^{-1}$, those for exposure to radiation from the ground surface are given in units of $\text{m}^2 \text{Bq}^{-1} \text{s}^{-1}$, and those for exposure to radiation from soil contaminated to an infinite depth are given in units of $\text{kg Bq}^{-1} \text{s}^{-1}$.

The risk coefficients in Table 2.3 are based on external dose rates tabulated in Federal Guidance Report No. 12 (EPA, 1993). Those dose rates were calculated for a reference adult male, standing outdoors with no shielding. Activity distributions in air, on the ground surface, or in soil

were assumed to be of an infinite extent. In this report, no adjustments are made to account for potential differences with age and gender in the external doses received, potential reduction in dose due to shielding by buildings during time spent indoors, or the finite nature of the activity distribution in the environment.

Adjustments for current age and gender distributions in the U.S.

The risk coefficients tabulated in this chapter were developed for a stationary population with gender and age distributions that would eventually occur in a closed population with male-to-female birth ratios indicated by recent U.S. data and with time-invariant survival functions defined by the 1989-91 U.S. decennial life tables. Due to the uncertainty in the future composition of the U.S. population, the use of a stationary population based on recent U.S. vital statistics is judged to be appropriate for consideration of long-term, chronic exposures to the U.S. population. Because the gender-specific age distributions in the current U.S. population differ considerably from those of the hypothetical stationary population, however, the question arises as to the applicability of these risk coefficients to short-term exposures of the U.S. population that might occur in the near future. In Appendix E, risk coefficients for the stationary population are compared with coefficients derived for short-term exposure of a population with gender and age distributions based on the 1996 U.S. population, but with the same survival functions and cancer mortality rates as the stationary population. The comparisons show that the risk coefficients for the stationary population are reasonably good approximations of the corresponding risk coefficients for short-term exposure of the 1996 U.S. population and that, for a given exposure scenario, the ratio of risk coefficients for the two populations varies little from one radionuclide to another. Scaling factors are provided in Appendix E for conversion of risk coefficients for the stationary population to more precise risk coefficients for a hypothetical short-term exposure to the 1996 U.S. population.

Table 2.1. Mortality and morbidity risk coefficients for inhalation.

Explanation of Entries

Risk coefficients for inhalation of radionuclides are expressed as the probability of radiogenic cancer mortality or morbidity per unit intake, where the intake is *averaged over all ages and both genders*. The form of an inhaled radionuclide is classified in terms of the rate of absorption from the lungs to blood, using the classification scheme of ICRP Publication 66 (ICRP, 1994a). For each radionuclide, separate risk coefficients are provided for particulate aerosols of Type F, Type M, and Type S representing, respectively, fast, medium, and slow absorption to blood. For some elements, the ICRP recommends a default absorption type for particulate aerosols when no specific information is available (Table 4.1). A default type for an element is indicated by an asterisk. Risk coefficients are also provided for tritium as a vapor (HTO) or gas (HT), carbon in gaseous form as carbon monoxide (CO) or carbon dioxide (CO₂), sulfur as a vapor (SO₂ or CS₂), nickel as a vapor, ruthenium as a vapor (RuO₄), iodine as a vapor or gas (methyl iodide, CH₃I), tellurium as a vapor, and mercury as a vapor. The f_i (gastrointestinal uptake) values shown are the values for the adult and may differ from the values applied to infants and children (see Chapter 4).

Entries under the heading “Chain” indicate whether the radionuclide is in the same decay chain as other radionuclides addressed in the table (see Appendix G for details concerning decay chains). An entry “Y” (yes) under the subheading “P” (parent) indicates that the radionuclide is the parent of a decay chain containing at least one other radionuclide in the table. An entry “Y” under the subheading “D” (daughter) indicates that the radionuclide is formed in the decay chain of at least one other radionuclide in the table. These entries are included as an aid in the estimation of cancer risk from intake of decay chain members that form in the environment. The risk coefficient for intake of a radionuclide already includes the contribution to dose from production of decay chain members in the body after intake of the parent.

To facilitate application of the risk coefficients, including conversion to other units, the coefficients are tabulated to three figures. No indication of the level of uncertainty is intended or should be inferred from this practice. Calculated risks should be rounded appropriately.

To express a risk coefficient in conventional units (μCi^{-1}), multiply by 3.7×10^4 Bq μCi^{-1} .

To express a risk coefficient in terms of a constant activity concentration in air (Bq m^{-3}), multiply the coefficient by $2.75 \times 10^4 U_A$, where U_A is the lifetime average inhalation rate (for example, $17.8 \text{ m}^3 \text{ d}^{-1}$ in Table 3.1) and 2.75×10^4 d is the average life span. Note that the *relative* age- and gender-specific inhalation rates indicated in Table 3.1 are inherent in the risk coefficient.

Table 2.1. Mortality and morbidity risk coefficients for inhalation.

Nuclide	$T_{1/2}$	Chain P D	AMAD (μm)	Type ^a	f_1	Mortality (Bq^{-1})	Morbidity (Bq^{-1})
Hydrogen (particulate)							
H-3	12.35 y	- -	1.00	F	1.0	3.61E-13	5.28E-13
				*M	0.1	4.58E-12	5.38E-12
				S	0.01	2.12E-11	2.30E-11
Hydrogen (water vapor)							
H-3 _b	12.35 y	- -	-	V	1.0	1.04E-12	1.52E-12
Hydrogen (elemental)							
H-3	12.35 y	- -	-	G	1.0	1.04E-16	1.52E-16
Hydrogen (organic)							
H-3	12.35 y	- -	-	G	1.0	2.37E-12	3.47E-12
Beryllium							
Be-7	53.3 d	- -	1.00	F	0.005	2.17E-12	3.12E-12
				M	0.005	3.68E-12	4.72E-12
				S	0.005	4.60E-12	5.77E-12
Be-10	1.6E6 y	- -	1.00	F	0.005	3.01E-10	3.59E-10
				M	0.005	7.30E-10	8.05E-10
				S	0.005	2.38E-09	2.54E-09
Carbon (particulate)							
C-11	20.38 m	- -	1.00	F	1.0	3.23E-13	3.74E-13
				*M	0.1	6.76E-13	7.52E-13
				S	0.01	7.14E-13	7.92E-13
C-14	5730 y	- -	1.00	F	1.0	1.15E-11	1.68E-11
				*M	0.1	1.76E-10	1.91E-10
				S	0.01	4.29E-10	4.58E-10
Carbon (monoxide)							
C-11	20.38 m	- -	-	G	1.0	8.30E-14	1.22E-13
C-14	5730 y	- -	-	G	1.0	6.14E-14	9.09E-14
Carbon (dioxide)							
C-11	20.38 m	- -	-	G	1.0	1.52E-13	2.23E-13
C-14	5730 y	- -	-	G	1.0	3.68E-13	5.39E-13
Fluorine							
F-18	109.77 m	- -	1.00	F	1.0	7.78E-13	9.11E-13
				M	1.0	2.78E-12	3.04E-12
				S	1.0	3.00E-12	3.28E-12
Sodium							
Na-22	2.602 y	- -	1.00	F	1.0	7.21E-11	1.05E-10
				M	1.0	8.28E-10	9.46E-10
				S	1.0	2.31E-09	2.63E-09
Na-24	15.00 h	- -	1.00	F	1.0	8.94E-12	1.28E-11
				M	1.0	2.59E-11	3.05E-11
				S	1.0	2.79E-11	3.25E-11

Table 2.1, continued

Nuclide	T _{1/2}	Chain		AMAD (μm)	Type ^a f ₁	Mortality (Bq ⁻¹)	Morbidity (Bq ⁻¹)
		P	D				
Magnesium							
Mg-28	20.91 h	-	-	1.00	F 0.5	4.21E-11	6.95E-11
					M 0.5	9.94E-11	1.39E-10
					S 0.5	1.06E-10	1.47E-10
Aluminum							
Al-26	7.16E5 y	-	-	1.00	F 0.01	7.49E-10	1.08E-09
					M 0.01	1.58E-09	1.87E-09
					S 0.01	7.03E-09	7.85E-09
Silicon							
Si-31	157.3 m	-	-	1.00	F 0.01	1.94E-12	3.03E-12
					M 0.01	5.82E-12	7.71E-12
					S 0.01	6.24E-12	8.23E-12
Si-32	450 y	Y	-	1.00	F 0.01	2.50E-10	3.83E-10
					M 0.01	1.41E-09	1.55E-09
					S 0.01	7.48E-09	7.91E-09
Phosphorus							
P-32	14.29 d	-	Y	1.00	F 0.8	5.88E-11	8.00E-11
					M 0.8	2.93E-10	3.29E-10
					S 0.8	3.39E-10	3.77E-10
P-33	25.4 d	-	-	1.00	F 0.8	6.12E-12	8.91E-12
					M 0.8	1.28E-10	1.38E-10
					S 0.8	1.55E-10	1.65E-10
Sulfur (inorganic)							
S-35	87.44 d	-	-	1.00	F 0.8	3.93E-12	6.28E-12
					*M 0.1	1.25E-10	1.36E-10
					S 0.01	1.63E-10	1.77E-10
Sulfur (dioxide)							
S-35	87.44 d	-	-	-	V 0.8	8.63E-12	1.34E-11
Sulfur (carbon disulfide)							
S-35	87.44 d	-	-	-	V 0.8	5.30E-11	7.85E-11
Chlorine							
Cl-36	3.01E5 y	-	-	1.00	F 1.0	2.37E-11	3.58E-11
					M 1.0	6.32E-10	6.76E-10
					S 1.0	2.58E-09	2.73E-09
Cl-38	37.21 m	-	-	1.00	F 1.0	1.06E-12	1.28E-12
					M 1.0	2.29E-12	2.54E-12
					S 1.0	2.42E-12	2.68E-12
Cl-39	55.6 m	Y	-	1.00	F 1.0	9.16E-13	1.13E-12
					M 1.0	2.26E-12	2.53E-12
					S 1.0	2.41E-12	2.68E-12

Table 2.1, continued

Nuclide	$T_{1/2}$	Chain		AMAD (μm)	Type ^a	f_1	Mortality (Bq^{-1})	Morbidity (Bq^{-1})
		P	D					
Potassium								
K-40	1.28E9 y	-	-	1.00	F	1.0	1.77E-10	2.78E-10
					M	1.0	1.20E-09	1.35E-09
					S	1.0	5.61E-09	6.01E-09
K-42	12.36 h	-	-	1.00	F	1.0	8.00E-12	1.17E-11
					M	1.0	2.74E-11	3.13E-11
					S	1.0	2.96E-11	3.36E-11
K-43	22.6 h	-	-	1.00	F	1.0	5.66E-12	8.34E-12
					M	1.0	2.41E-11	2.74E-11
					S	1.0	2.62E-11	2.96E-11
K-44	22.13 m	-	-	1.00	F	1.0	7.72E-13	9.15E-13
					M	1.0	1.43E-12	1.59E-12
					S	1.0	1.51E-12	1.66E-12
K-45	20 m	Y	-	1.00	F	1.0	5.34E-13	6.30E-13
					M	1.0	1.00E-12	1.11E-12
					S	1.0	1.06E-12	1.17E-12
Calcium								
Ca-41	1.4E5 y	-	-	1.00	F	0.3	6.98E-12	7.42E-12
					*M	0.1	5.13E-12	5.64E-12
					S	0.01	1.27E-11	1.37E-11
Ca-45	163 d	-	Y	1.00	F	0.3	2.68E-11	3.23E-11
					*M	0.1	2.35E-10	2.54E-10
					S	0.01	3.22E-10	3.47E-10
Ca-47	4.53 d	Y	-	1.00	F	0.3	3.44E-11	5.37E-11
					*M	0.1	1.73E-10	2.13E-10
					S	0.01	1.96E-10	2.40E-10
Scandium								
Sc-43	3.891 h	-	-	1.00	F	0.0001	2.59E-12	4.05E-12
					M	0.0001	7.14E-12	9.70E-12
					S	0.0001	7.65E-12	1.03E-11
Sc-44	3.927 h	-	Y	1.00	F	0.0001	4.82E-12	7.60E-12
					M	0.0001	1.16E-11	1.64E-11
					S	0.0001	1.24E-11	1.74E-11
Sc-44m	58.6 h	Y	-	1.00	F	0.0001	5.03E-11	7.95E-11
					M	0.0001	1.25E-10	1.77E-10
					S	0.0001	1.35E-10	1.88E-10
Sc-46	83.83 d	-	-	1.00	F	0.0001	3.78E-10	5.12E-10
					M	0.0001	4.91E-10	5.83E-10
					S	0.0001	5.79E-10	6.68E-10
Sc-47	3.351 d	-	Y	1.00	F	0.0001	1.13E-11	1.80E-11
					M	0.0001	6.09E-11	7.51E-11
					S	0.0001	6.74E-11	8.25E-11

Table 2.1, continued

Nuclide	$T_{1/2}$	Chain		AMAD (μm)	Type ^a	f_1	Mortality (Bq^{-1})	Morbidity (Bq^{-1})
		P	D					
Scandium, continued								
Sc-48	43.7 h	-	-	1.00	F	0.0001	3.13E-11	4.83E-11
						0.0001	7.32E-11	1.01E-10
						0.0001	7.83E-11	1.07E-10
Sc-49	57.4 m	-	-	1.00	F	0.0001	8.74E-13	1.15E-12
						0.0001	2.29E-12	2.72E-12
						0.0001	2.45E-12	2.89E-12
Titanium								
Ti-44	47.3 y	Y	-	1.00	F	0.01	3.69E-09	5.43E-09
						0.01	2.96E-09	3.79E-09
						0.01	8.31E-09	9.22E-09
Ti-45	3.08 h	-	-	1.00	F	0.01	2.05E-12	3.19E-12
						0.01	5.86E-12	7.83E-12
						0.01	6.29E-12	8.34E-12
Vanadium								
V-47	32.6 m	-	-	1.00	F	0.01	7.04E-13	9.11E-13
						0.01	1.40E-12	1.61E-12
						0.01	1.48E-12	1.69E-12
V-48	16.238 d	-	Y	1.00	F	0.01	5.37E-11	8.53E-11
						0.01	2.02E-10	2.51E-10
						0.01	2.32E-10	2.84E-10
V-49	330 d	-	Y	1.00	F	0.01	1.42E-12	1.98E-12
						0.01	3.27E-12	3.96E-12
						0.01	6.78E-12	7.63E-12
Chromium								
Cr-48	22.96 h	Y	-	1.00	F	0.1	5.09E-12	8.04E-12
						0.1	1.44E-11	1.83E-11
						0.1	1.62E-11	2.03E-11
Cr-49	42.09 m	Y	-	1.00	F	0.1	7.02E-13	9.05E-13
						0.1	1.62E-12	1.89E-12
						0.1	1.72E-12	1.99E-12
Cr-51	27.704 d	-	Y	1.00	F	0.1	1.38E-12	2.22E-12
						0.1	2.98E-12	3.98E-12
						0.1	3.46E-12	4.50E-12
Manganese								
Mn-51	46.2 m	Y	-	1.00	F	0.1	9.54E-13	1.24E-12
						0.1	2.18E-12	2.58E-12
						0.1	2.31E-12	2.73E-12
Mn-52	5.591 d	-	Y	1.00	F	0.1	4.84E-11	7.22E-11
						0.1	8.96E-11	1.19E-10
						0.1	9.58E-11	1.26E-10

Table 2.1, continued

Nuclide	$T_{1/2}$	Chain		AMAD (μm)	Type ^a f_1	Mortality (Bq^{-1})	Morbidity (Bq^{-1})
		P	D				
Manganese, continued							
Mn-52m	21.1 m	Y	Y	1.00	F 0.1	6.64E-13	8.06E-13
					M 0.1	1.20E-12	1.37E-12
					S 0.1	1.26E-12	1.43E-12
Mn-53	3.7E6 y	-	-	1.00	F 0.1	1.65E-12	2.34E-12
					M 0.1	4.95E-12	5.87E-12
					S 0.1	2.43E-11	2.62E-11
Mn-54	312.5 d	-	-	1.00	F 0.1	5.33E-11	7.55E-11
					M 0.1	1.26E-10	1.59E-10
					S 0.1	2.67E-10	3.26E-10
Mn-56	2.5785 h	-	-	1.00	F 0.1	3.32E-12	5.09E-12
					M 0.1	8.22E-12	1.12E-11
					S 0.1	8.76E-12	1.18E-11
Iron							
Fe-52	8.275 h	Y	-	1.00	F 0.1	2.48E-11	3.72E-11
					*M 0.1	4.97E-11	7.37E-11
					S 0.01	5.40E-11	8.09E-11
Fe-55	2.7 y	-	Y	1.00	F 0.1	3.30E-11	4.00E-11
					*M 0.1	1.81E-11	2.16E-11
					S 0.01	1.59E-11	1.75E-11
Fe-59	44.529 d	-	-	1.00	F 0.1	1.53E-10	2.15E-10
					*M 0.1	3.08E-10	3.60E-10
					S 0.01	3.48E-10	3.97E-10
Fe-60	1E5 y	Y	-	1.00	F 0.1	7.82E-09	1.00E-08
					*M 0.1	3.96E-09	4.97E-09
					S 0.01	2.29E-09	2.63E-09
Cobalt							
Co-55	17.54 h	Y	-	1.00	F 0.1	1.46E-11	2.47E-11
					*M 0.1	3.81E-11	5.59E-11
					S 0.01	4.21E-11	6.19E-11
Co-56	78.76 d	-	Y	1.00	F 0.1	1.11E-10	1.67E-10
					*M 0.1	4.07E-10	5.01E-10
					S 0.01	5.74E-10	6.91E-10
Co-57	270.9 d	-	Y	1.00	F 0.1	1.25E-11	1.88E-11
					*M 0.1	4.75E-11	5.65E-11
					S 0.01	8.74E-11	1.01E-10
Co-58	70.80 d	-	Y	1.00	F 0.1	3.12E-11	4.70E-11
					*M 0.1	1.34E-10	1.62E-10
					S 0.01	1.81E-10	2.15E-10
Co-58m	9.15 h	Y	-	1.00	F 0.1	4.67E-13	7.74E-13
					*M 0.1	1.32E-12	1.86E-12
					S 0.01	1.64E-12	2.26E-12

Table 2.1, continued

Nuclide	$T_{1/2}$	Chain		AMAD (μm)	Type ^a	f_1	Mortality (Bq^{-1})	Morbidity (Bq^{-1})
		P	D					
Cobalt, continued								
Co-60 ^b	5.271 y	-	Y	1.00	F	0.1	3.16E-10	4.62E-10
					*M	0.1	8.02E-10	9.68E-10
					S	0.01	2.32E-09	2.72E-09
Co-60m	10.47 m	Y	Y	1.00	F	0.1	5.42E-14	5.87E-14
					*M	0.1	1.00E-13	1.07E-13
					S	0.01	1.11E-13	1.18E-13
Co-61	1.65 h	-	-	1.00	F	0.1	9.99E-13	1.44E-12
					*M	0.1	3.15E-12	3.86E-12
					S	0.01	3.41E-12	4.16E-12
Co-62m	13.91 m	-	-	1.00	F	0.1	4.66E-13	5.55E-13
					*M	0.1	7.61E-13	8.57E-13
					S	0.01	7.94E-13	8.91E-13
Nickel (particulate)								
Ni-56	6.10 d	Y	-	1.00	F	0.05	2.37E-11	3.63E-11
					*M	0.05	5.98E-11	7.78E-11
					S	0.01	7.52E-11	9.54E-11
Ni-57	36.08 h	Y	-	1.00	F	0.05	1.20E-11	2.02E-11
					*M	0.05	3.40E-11	4.80E-11
					S	0.01	3.72E-11	5.24E-11
Ni-59	7.5E4 y	-	-	1.00	F	0.05	1.05E-11	1.55E-11
					*M	0.05	9.73E-12	1.26E-11
					S	0.01	3.16E-11	3.43E-11
Ni-63	96 y	-	-	1.00	F	0.05	2.52E-11	3.72E-11
					*M	0.05	3.67E-11	4.43E-11
					S	0.01	9.34E-11	1.01E-10
Ni-65	2.520 h	-	-	1.00	F	0.05	2.40E-12	3.85E-12
					*M	0.05	6.14E-12	8.19E-12
					S	0.01	6.59E-12	8.74E-12
Ni-66	54.6 h	-	-	1.00	F	0.05	5.09E-11	9.03E-11
					*M	0.05	1.71E-10	2.43E-10
					S	0.01	1.89E-10	2.67E-10
Nickel (vapor)								
Ni-56	6.10 d	Y	-	-	V	0.05	7.87E-11	1.14E-10
Ni-57	36.08 h	Y	-	-	V	0.05	3.03E-11	3.97E-11
Ni-59	7.5E4 y	-	-	-	V	0.05	4.57E-11	6.51E-11
Ni-63	96 y	-	-	-	V	0.05	1.09E-10	1.56E-10
Ni-65	2.520 h	-	-	-	V	0.05	1.72E-11	1.91E-11
Ni-66	54.6 h	-	-	-	V	0.05	9.35E-11	1.24E-10
Copper								
Cu-60	23.2 m	-	-	1.00	F	0.5	7.19E-13	8.96E-13
					M	0.5	1.29E-12	1.50E-12
					S	0.5	1.35E-12	1.56E-12

Table 2.1, continued

Nuclide	$T_{1/2}$	Chain		AMAD (μm)	Type ^a f_1	Mortality (Bq^{-1})	Morbidity (Bq^{-1})
		P	D				
Copper, continued							
Cu-61	3.408 h	-	-	1.00	F 0.5	1.67E-12	2.55E-12
					M 0.5	4.70E-12	6.12E-12
					S 0.5	5.03E-12	6.51E-12
Cu-64	12.701 h	-	-	1.00	F 0.5	2.11E-12	3.39E-12
					M 0.5	8.59E-12	1.09E-11
					S 0.5	9.33E-12	1.17E-11
Cu-67	61.86 h	-	-	1.00	F 0.5	7.86E-12	1.26E-11
					M 0.5	4.93E-11	5.77E-11
					S 0.5	5.45E-11	6.34E-11
Zinc							
Zn-62	9.26 h	Y	-	1.00	F 0.5	1.47E-11	2.42E-11
					*M 0.1	4.71E-11	7.15E-11
					S 0.01	5.22E-11	7.95E-11
Zn-63	38.1 m	-	-	1.00	F 0.5	7.94E-13	1.00E-12
					*M 0.1	1.75E-12	2.04E-12
					S 0.01	1.86E-12	2.16E-12
Zn-65	243.9 d	-	Y	1.00	F 0.5	1.41E-10	2.05E-10
					*M 0.1	1.20E-10	1.57E-10
					S 0.01	1.66E-10	2.02E-10
Zn-69	57 m	-	Y	1.00	F 0.5	4.33E-13	5.35E-13
					*M 0.1	1.46E-12	1.65E-12
					S 0.01	1.57E-12	1.78E-12
Zn-69m	13.76 h	Y	-	1.00	F 0.5	5.60E-12	9.25E-12
					*M 0.1	2.45E-11	3.45E-11
					S 0.01	2.73E-11	3.86E-11
Zn-71m	3.92 h	-	-	1.00	F 0.5	3.37E-12	5.18E-12
					*M 0.1	1.04E-11	1.44E-11
					S 0.01	1.13E-11	1.57E-11
Zn-72	46.5 h	Y	-	1.00	F 0.5	3.10E-11	4.84E-11
					*M 0.1	1.11E-10	1.48E-10
					S 0.01	1.23E-10	1.65E-10
Gallium							
Ga-65	15.2 m	Y	-	1.00	F 0.001	3.91E-13	4.55E-13
					M 0.001	6.92E-13	7.68E-13
					S 0.001	7.29E-13	8.06E-13
Ga-66	9.40 h	-	Y	1.00	F 0.001	1.81E-11	3.04E-11
					M 0.001	3.82E-11	5.89E-11
					S 0.001	4.04E-11	6.21E-11
Ga-67	78.26 h	-	Y	1.00	F 0.001	4.17E-12	6.84E-12
					M 0.001	2.13E-11	2.58E-11
					S 0.001	2.35E-11	2.83E-11

Table 2.1, continued

Nuclide	$T_{1/2}$	Chain		AMAD (μm)	Type ^a	f_1	Mortality (Bq^{-1})	Morbidity (Bq^{-1})
		P	D					
Gallium, continued								
Ga-68	68.0 m	-	Y	1.00	F	0.001	1.14E-12	1.58E-12
						0.001	2.80E-12	3.45E-12
						0.001	2.98E-12	3.66E-12
Ga-70	21.15 m	-	-	1.00	F	0.001	3.43E-13	3.94E-13
						0.001	7.22E-13	7.88E-13
						0.001	7.64E-13	8.31E-13
Ga-72	14.1 h	-	Y	1.00	F	0.001	1.72E-11	2.86E-11
						0.001	3.99E-11	5.87E-11
						0.001	4.25E-11	6.21E-11
Ga-73	4.91 h	-	-	1.00	F	0.001	3.95E-12	6.46E-12
						0.001	1.21E-11	1.66E-11
						0.001	1.30E-11	1.77E-11
Germanium								
Ge-66	2.27 h	Y	-	1.00	F	1.0	2.33E-12	3.80E-12
						1.0	5.46E-12	6.77E-12
						1.0	5.81E-12	7.11E-12
Ge-67	18.7 m	Y	-	1.00	F	1.0	5.97E-13	7.08E-13
						1.0	1.12E-12	1.24E-12
						1.0	1.18E-12	1.30E-12
Ge-68	288 d	Y	-	1.00	F	1.0	4.41E-11	7.80E-11
						1.0	1.21E-09	1.32E-09
						1.0	2.70E-09	2.91E-09
Ge-69	39.05 h	-	Y	1.00	F	1.0	6.39E-12	1.07E-11
						1.0	1.95E-11	2.38E-11
						1.0	2.10E-11	2.53E-11
Ge-71	11.8 d	-	Y	1.00	F	1.0	4.01E-13	7.13E-13
						1.0	1.12E-12	1.40E-12
						1.0	1.25E-12	1.53E-12
Ge-75	82.78 m	-	-	1.00	F	1.0	6.03E-13	7.72E-13
						1.0	2.08E-12	2.28E-12
						1.0	2.24E-12	2.44E-12
Ge-77	11.30 h	Y	-	1.00	F	1.0	7.56E-12	1.25E-11
						1.0	2.63E-11	3.10E-11
						1.0	2.85E-11	3.32E-11
Ge-78	87 m	Y	-	1.00	F	1.0	1.93E-12	2.87E-12
						1.0	5.81E-12	6.71E-12
						1.0	6.24E-12	7.13E-12
Arsenic								
As-69	15.2 m	Y	-	1.00	F	0.5	5.73E-13	7.18E-13
						0.5	1.01E-12	1.16E-12
						0.5	1.06E-12	1.21E-12

Table 2.1, continued

Nuclide	$T_{1/2}$	Chain		AMAD (μm)	Type ^a f_1	Mortality (Bq^{-1})	Morbidity (Bq^{-1})
		P	D				
Arsenic, continued							
As-70	52.6 m	-	Y	1.00	F 0.5	1.56E-12	2.16E-12
					M 0.5	3.00E-12	3.70E-12
					S 0.5	3.16E-12	3.87E-12
As-71	64.8 h	Y	-	1.00	F 0.5	1.12E-11	1.91E-11
					M 0.5	3.18E-11	4.10E-11
					S 0.5	3.44E-11	4.38E-11
As-72	26.0 h	-	Y	1.00	F 0.5	4.33E-11	7.52E-11
					M 0.5	8.00E-11	1.16E-10
					S 0.5	8.42E-11	1.21E-10
As-73	80.30 d	-	Y	1.00	F 0.5	8.86E-12	1.54E-11
					M 0.5	9.36E-11	1.05E-10
					S 0.5	1.23E-10	1.35E-10
As-74	17.76 d	-	-	1.00	F 0.5	3.82E-11	6.49E-11
					M 0.5	1.92E-10	2.28E-10
					S 0.5	2.24E-10	2.61E-10
As-76	26.32 h	-	-	1.00	F 0.5	4.00E-11	7.03E-11
					M 0.5	7.72E-11	1.12E-10
					S 0.5	8.15E-11	1.16E-10
As-77	38.8 h	-	Y	1.00	F 0.5	1.08E-11	1.90E-11
					M 0.5	3.75E-11	4.75E-11
					S 0.5	4.07E-11	5.08E-11
As-78	90.7 m	-	Y	1.00	F 0.5	2.70E-12	4.02E-12
					M 0.5	5.71E-12	7.27E-12
					S 0.5	6.04E-12	7.63E-12
Selenium							
Se-70	41.0 m	Y	-	1.00	*F 0.8	1.45E-12	1.99E-12
					M 0.1	3.78E-12	4.81E-12
					S 0.01	4.03E-12	5.12E-12
Se-73	7.15 h	Y	Y	1.00	*F 0.8	3.61E-12	5.38E-12
					M 0.1	1.47E-11	2.09E-11
					S 0.01	1.62E-11	2.30E-11
Se-73m	39 m	Y	-	1.00	*F 0.8	3.95E-13	5.56E-13
					M 0.1	1.38E-12	1.88E-12
					S 0.01	1.51E-12	2.06E-12
Se-75	119.8 d	-	Y	1.00	*F 0.8	7.18E-11	1.02E-10
					M 0.1	8.90E-11	1.09E-10
					S 0.01	1.15E-10	1.35E-10
Se-79	65000 y	-	-	1.00	*F 0.8	6.30E-11	8.99E-11
					M 0.1	2.25E-10	2.50E-10
					S 0.01	5.05E-10	5.39E-10

Table 2.1, continued

Nuclide	T _{1/2}	Chain		AMAD (μm)	Type ^a	f ₁	Mortality (Bq ⁻¹)	Morbidity (Bq ⁻¹)
		P	D					
Selenium, continued								
Se-81	18.5 m	-	Y	1.00	*F	0.8	3.04E-13	3.44E-13
					M	0.1	6.17E-13	6.69E-13
					S	0.01	6.51E-13	7.05E-13
Se-81m	57.25 m	Y	-	1.00	*F	0.8	7.46E-13	9.56E-13
					M	0.1	3.08E-12	3.57E-12
					S	0.01	3.34E-12	3.86E-12
Se-83	22.5 m	Y	-	1.00	*F	0.8	5.82E-13	7.34E-13
					M	0.1	1.53E-12	1.83E-12
					S	0.01	1.64E-12	1.95E-12
Bromine								
Br-74	25.3 m	-	-	1.00	F	1.0	8.42E-13	1.03E-12
					M	1.0	1.53E-12	1.74E-12
					S	1.0	1.60E-12	1.82E-12
Br-74m	41.5 m	-	-	1.00	F	1.0	1.36E-12	1.70E-12
					M	1.0	2.74E-12	3.12E-12
					S	1.0	2.90E-12	3.28E-12
Br-75	98 m	Y	-	1.00	F	1.0	9.72E-13	1.26E-12
					M	1.0	2.70E-12	3.05E-12
					S	1.0	2.91E-12	3.27E-12
Br-76	16.2 h	-	-	1.00	F	1.0	1.00E-11	1.50E-11
					M	1.0	2.46E-11	2.97E-11
					S	1.0	2.63E-11	3.14E-11
Br-77	56 h	-	-	1.00	F	1.0	2.23E-12	3.36E-12
					M	1.0	4.39E-12	5.57E-12
					S	1.0	4.67E-12	5.85E-12
Br-80	17.4 m	-	Y	1.00	F	1.0	2.51E-13	2.88E-13
					M	1.0	4.46E-13	4.86E-13
					S	1.0	4.68E-13	5.07E-13
Br-80m	4.42 h	Y	-	1.00	F	1.0	1.70E-12	2.40E-12
					M	1.0	5.80E-12	6.57E-12
					S	1.0	6.25E-12	7.03E-12
Br-82	35.30 h	-	-	1.00	F	1.0	1.27E-11	1.91E-11
					M	1.0	3.76E-11	4.48E-11
					S	1.0	4.06E-11	4.79E-11
Br-83	2.39 h	-	Y	1.00	F	1.0	6.18E-13	7.69E-13
					M	1.0	3.03E-12	3.27E-12
					S	1.0	3.29E-12	3.55E-12
Br-84	31.80 m	-	-	1.00	F	1.0	8.41E-13	1.01E-12
					M	1.0	1.75E-12	1.94E-12
					S	1.0	1.84E-12	2.04E-12

Table 2.1, continued

Nuclide	$T_{1/2}$	Chain		AMAD (μm)	Type ^a	f_1	Mortality (Bq^{-1})	Morbidity (Bq^{-1})
		P	D					
Rubidium								
Rb-79	22.9 m	-	-	1.00	F	1.0	5.48E-13	6.41E-13
					M	1.0	1.11E-12	1.22E-12
					S	1.0	1.17E-12	1.28E-12
Rb-81	4.58 h	-	Y	1.00	F	1.0	9.32E-13	1.25E-12
					M	1.0	4.10E-12	4.56E-12
					S	1.0	4.45E-12	4.93E-12
Rb-81m	32 m	Y	-	1.00	F	1.0	2.48E-13	2.98E-13
					M	1.0	9.79E-13	1.06E-12
					S	1.0	1.06E-12	1.15E-12
Rb-82m	6.2 h	-	-	1.00	F	1.0	2.57E-12	3.64E-12
					M	1.0	5.07E-12	6.27E-12
					S	1.0	5.34E-12	6.57E-12
Rb-83	86.2 d	-	Y	1.00	F	1.0	4.27E-11	6.26E-11
					M	1.0	9.02E-11	1.16E-10
					S	1.0	1.19E-10	1.48E-10
Rb-84	32.77 d	-	-	1.00	F	1.0	6.59E-11	9.69E-11
					M	1.0	1.79E-10	2.16E-10
					S	1.0	2.12E-10	2.51E-10
Rb-86	18.66 d	-	-	1.00	F	1.0	7.29E-11	1.08E-10
					M	1.0	3.46E-10	3.89E-10
					S	1.0	4.06E-10	4.50E-10
Rb-87	4.7E10 y	-	Y	1.00	F	1.0	3.89E-11	5.78E-11
					M	1.0	4.07E-10	4.45E-10
					S	1.0	1.09E-09	1.17E-09
Rb-88	17.8 m	-	-	1.00	F	1.0	7.45E-13	8.58E-13
					M	1.0	1.33E-12	1.45E-12
					S	1.0	1.40E-12	1.52E-12
Rb-89	15.2 m	Y	-	1.00	F	1.0	4.78E-13	5.64E-13
					M	1.0	8.96E-13	9.95E-13
					S	1.0	9.66E-13	1.07E-12
Strontium								
Sr-80	100 m	-	-	1.00	F	0.3	4.02E-12	6.02E-12
					*M	0.1	9.13E-12	1.22E-11
					S	0.01	9.76E-12	1.30E-11
Sr-81	25.5 m	Y	-	1.00	F	0.3	8.18E-13	1.07E-12
					*M	0.1	1.81E-12	2.18E-12
					S	0.01	1.93E-12	2.32E-12
Sr-82	25.0 d	-	-	1.00	F	0.3	1.68E-10	2.53E-10
					*M	0.1	8.24E-10	9.97E-10
					S	0.01	9.97E-10	1.19E-09

Table 2.1, continued

Nuclide	$T_{1/2}$	Chain		AMAD (μm)	Type ^a f_1	Mortality (Bq^{-1})	Morbidity (Bq^{-1})
		P	D				
Strontium, continued							
Sr-83	32.4 h	Y	-	1.00	F 0.3	8.19E-12	1.32E-11
					*M 0.1	2.39E-11	3.40E-11
					S 0.01	2.67E-11	3.81E-11
Sr-85	64.84 d	-	Y	1.00	F 0.3	2.78E-11	3.97E-11
					*M 0.1	5.55E-11	6.93E-11
					S 0.01	7.17E-11	8.73E-11
Sr-85m	69.5 m	Y	-	1.00	F 0.3	8.95E-14	1.27E-13
					*M 0.1	1.75E-13	2.25E-13
					S 0.01	1.94E-13	2.47E-13
Sr-87m	2.805 h	Y	-	1.00	F 0.3	4.15E-13	6.31E-13
					*M 0.1	1.15E-12	1.52E-12
					S 0.01	1.24E-12	1.64E-12
Sr-89	50.5 d	-	Y	1.00	F 0.3	7.60E-11	1.08E-10
					*M 0.1	5.52E-10	6.32E-10
					S 0.01	7.22E-10	8.17E-10
Sr-90 ^b	29.12 y	Y	-	1.00	F 0.3	1.08E-09	1.17E-09
					*M 0.1	2.65E-09	2.84E-09
					S 0.01	1.08E-08	1.15E-08
Sr-91	9.5 h	Y	-	1.00	F 0.3	1.00E-11	1.65E-11
					*M 0.1	3.22E-11	4.59E-11
					S 0.01	3.65E-11	5.18E-11
Sr-92	2.71 h	Y	-	1.00	F 0.3	6.61E-12	1.11E-11
					*M 0.1	1.89E-11	2.79E-11
					S 0.01	2.08E-11	3.07E-11
Yttrium							
Y-86	14.74 h	-	Y	1.00	F 0.0001	1.49E-11	2.41E-11
					M 0.0001	2.71E-11	4.08E-11
					S 0.0001	2.85E-11	4.27E-11
Y-86m	48 m	Y	-	1.00	F 0.0001	8.70E-13	1.40E-12
					M 0.0001	1.61E-12	2.40E-12
					S 0.0001	1.70E-12	2.51E-12
Y-87	80.3 h	Y	-	1.00	F 0.0001	1.21E-11	1.90E-11
					M 0.0001	2.76E-11	3.78E-11
					S 0.0001	2.96E-11	4.02E-11
Y-88	106.64 d	-	Y	1.00	F 0.0001	4.00E-10	5.50E-10
					M 0.0001	3.16E-10	4.05E-10
					S 0.0001	3.73E-10	4.60E-10
Y-90	64.0 h	-	Y	1.00	F 0.0001	5.77E-11	9.65E-11
					M 0.0001	1.48E-10	2.13E-10
					S 0.0001	1.60E-10	2.27E-10

Table 2.1, continued

Nuclide	$T_{1/2}$	Chain		AMAD (μm)	Type ^a f_1	Mortality (Bq^{-1})	Morbidity (Bq^{-1})
		P	D				
Yttrium, continued							
Y-90m	3.19 h	Y	-	1.00	F 0.0001	3.44E-12	5.67E-12
					M 0.0001	8.53E-12	1.22E-11
					S 0.0001	9.16E-12	1.30E-11
Y-91	58.51 d	-	Y	1.00	F 0.0001	1.98E-10	2.44E-10
					M 0.0001	6.25E-10	7.15E-10
					S 0.0001	8.05E-10	9.07E-10
Y-91m	49.71 m	Y	Y	1.00	F 0.0001	2.37E-13	3.12E-13
					M 0.0001	5.77E-13	6.90E-13
					S 0.0001	6.93E-13	8.14E-13
Y-92	3.54 h	-	Y	1.00	F 0.0001	7.66E-12	1.26E-11
					M 0.0001	1.65E-11	2.39E-11
					S 0.0001	1.75E-11	2.52E-11
Y-93	10.1 h	Y	-	1.00	F 0.0001	2.07E-11	3.56E-11
					M 0.0001	4.42E-11	6.78E-11
					S 0.0001	4.69E-11	7.13E-11
Y-94	19.1 m	-	-	1.00	F 0.0001	7.20E-13	8.60E-13
					M 0.0001	1.28E-12	1.43E-12
					S 0.0001	1.34E-12	1.49E-12
Y-95	10.7 m	Y	-	1.00	F 0.0001	4.31E-13	4.97E-13
					M 0.0001	6.85E-13	7.51E-13
					S 0.0001	7.22E-13	7.89E-13
Zirconium							
Zr-86	16.5 h	Y	-	1.00	F 0.002	1.37E-11	2.21E-11
					*M 0.002	2.82E-11	4.22E-11
					S 0.002	2.99E-11	4.45E-11
Zr-88	83.4 d	Y	Y	1.00	F 0.002	1.94E-10	2.63E-10
					*M 0.002	1.94E-10	2.42E-10
					S 0.002	3.04E-10	3.65E-10
Zr-89	78.43 h	-	Y	1.00	F 0.002	1.55E-11	2.43E-11
					*M 0.002	3.77E-11	5.18E-11
					S 0.002	4.05E-11	5.52E-11
Zr-93	1.53E6 y	Y	Y	1.00	F 0.002	3.81E-10	4.11E-10
					*M 0.002	1.81E-10	1.97E-10
					S 0.002	1.53E-10	1.64E-10
Zr-95	63.98 d	Y	Y	1.00	F 0.002	1.33E-10	1.77E-10
					*M 0.002	3.92E-10	4.47E-10
					S 0.002	5.06E-10	5.70E-10
Zr-97	16.90 h	Y	-	1.00	F 0.002	3.29E-11	5.57E-11
					*M 0.002	8.76E-11	1.30E-10
					S 0.002	9.37E-11	1.38E-10

Table 2.1, continued

Nuclide	$T_{1/2}$	Chain		AMAD (μm)	Type ^a f_1	Mortality (Bq^{-1})	Morbidity (Bq^{-1})
		P	D				
Niobium							
Nb-88	14.3 m	Y	-	1.00	F 0.01	6.54E-13	7.84E-13
					*M 0.01	1.07E-12	1.22E-12
					S 0.01	1.13E-12	1.28E-12
Nb-89b	122 m	Y	-	1.00	F 0.01	3.46E-12	5.26E-12
					*M 0.01	8.03E-12	1.10E-11
					S 0.01	8.55E-12	1.16E-11
Nb-89a	66 m	Y	-	1.00	F 0.01	1.64E-12	2.31E-12
					*M 0.01	3.71E-12	4.71E-12
					S 0.01	3.95E-12	4.98E-12
Nb-90	14.60 h	-	Y	1.00	F 0.01	1.85E-11	2.97E-11
					*M 0.01	4.21E-11	6.14E-11
					S 0.01	4.47E-11	6.49E-11
Nb-93m	13.6 y	-	Y	1.00	F 0.01	1.38E-11	1.91E-11
					*M 0.01	4.49E-11	5.14E-11
					S 0.01	1.42E-10	1.53E-10
Nb-94	2.03E4 y	-	-	1.00	F 0.01	3.89E-10	5.42E-10
					*M 0.01	8.66E-10	1.02E-09
					S 0.01	3.20E-09	3.64E-09
Nb-95	35.15 d	-	Y	1.00	F 0.01	3.55E-11	5.12E-11
					*M 0.01	1.26E-10	1.47E-10
					S 0.01	1.50E-10	1.74E-10
Nb-95m	86.6 h	Y	Y	1.00	F 0.01	1.47E-11	2.31E-11
					*M 0.01	7.23E-11	8.84E-11
					S 0.01	8.13E-11	9.84E-11
Nb-96	23.35 h	-	-	1.00	F 0.01	1.71E-11	2.74E-11
					*M 0.01	4.38E-11	6.16E-11
					S 0.01	4.69E-11	6.55E-11
Nb-97	72.1 m	-	Y	1.00	F 0.01	8.52E-13	1.16E-12
					*M 0.01	2.39E-12	2.88E-12
					S 0.01	2.56E-12	3.07E-12
Nb-98	51.5 m	-	-	1.00	F 0.01	1.24E-12	1.66E-12
					*M 0.01	2.73E-12	3.32E-12
					S 0.01	2.89E-12	3.50E-12
Molybdenum							
Mo-90	5.67 h	Y	-	1.00	F 0.8	6.09E-12	9.03E-12
					*M 0.1	2.37E-11	3.36E-11
					S 0.01	2.61E-11	3.71E-11
Mo-93	3.5E3 y	Y	Y	1.00	F 0.8	2.96E-11	3.29E-11
					*M 0.1	3.11E-11	3.43E-11
					S 0.01	1.45E-10	1.55E-10

Table 2.1, continued

Nuclide	$T_{1/2}$	Chain		AMAD (μm)	Type ^a f_1	Mortality (Bq^{-1})	Morbidity (Bq^{-1})
		P	D				
Molybdenum, continued							
Mo-93m	6.85 h	Y	-	1.00	F 0.8	2.81E-12	4.09E-12
					*M 0.1	8.33E-12	1.17E-11
					S 0.01	9.04E-12	1.27E-11
Mo-99	66.0 h	Y	-	1.00	F 0.8	1.44E-11	2.15E-11
					*M 0.1	8.75E-11	1.16E-10
					S 0.01	9.80E-11	1.30E-10
Mo-101	14.62 m	Y	-	1.00	F 0.8	4.94E-13	5.78E-13
					*M 0.1	1.05E-12	1.17E-12
					S 0.01	1.12E-12	1.23E-12
Technetium							
Tc-93	2.75 h	Y	Y	1.00	F 0.8	7.65E-13	1.28E-12
					*M 0.1	1.17E-12	1.72E-12
					S 0.01	1.22E-12	1.77E-12
Tc-93m	43.5 m	Y	-	1.00	F 0.8	3.70E-13	6.18E-13
					*M 0.1	6.43E-13	8.58E-13
					S 0.01	6.75E-13	8.87E-13
Tc-94	293 m	-	-	1.00	F 0.8	2.96E-12	5.17E-12
					*M 0.1	5.14E-12	7.58E-12
					S 0.01	5.42E-12	7.91E-12
Tc-94m	52 m	-	Y	1.00	F 0.8	1.33E-12	2.51E-12
					*M 0.1	2.21E-12	2.78E-12
					S 0.01	2.31E-12	2.81E-12
Tc-95	20.0 h	-	Y	1.00	F 0.8	2.97E-12	5.00E-12
					*M 0.1	4.66E-12	7.10E-12
					S 0.01	4.91E-12	7.43E-12
Tc-95m	61 d	Y	-	1.00	F 0.8	1.35E-11	2.16E-11
					*M 0.1	7.51E-11	9.20E-11
					S 0.01	1.03E-10	1.24E-10
Tc-96	4.28 d	-	Y	1.00	F 0.8	2.22E-11	3.58E-11
					*M 0.1	3.80E-11	5.41E-11
					S 0.01	4.03E-11	5.68E-11
Tc-96m	51.5 m	Y	-	1.00	F 0.8	2.30E-13	3.84E-13
					*M 0.1	4.03E-13	5.55E-13
					S 0.01	4.27E-13	5.80E-13
Tc-97	2.6E6 y	-	Y	1.00	F 0.8	1.89E-12	3.16E-12
					*M 0.1	2.06E-11	2.30E-11
					S 0.01	1.22E-10	1.30E-10
Tc-97m	87 d	Y	Y	1.00	F 0.8	1.57E-11	2.67E-11
					*M 0.1	2.78E-10	3.03E-10
					S 0.01	3.59E-10	3.88E-10

Table 2.1, continued

Nuclide	$T_{1/2}$	Chain		AMAD (μm)	Type ^a f_1	Mortality (Bq^{-1})	Morbidity (Bq^{-1})
		P	D				
Technetium, continued							
Tc-98	4.2E6 y	-	-	1.00	F 0.8	5.18E-11	8.44E-11
					*M 0.1	7.12E-10	8.14E-10
					S 0.01	2.97E-09	3.36E-09
Tc-99	2.13E5 y	-	Y	1.00	F 0.8	1.86E-11	3.14E-11
					*M 0.1	3.49E-10	3.81E-10
					S 0.01	9.67E-10	1.03E-09
Tc-99m	6.02 h	Y	Y	1.00	F 0.8	3.63E-13	6.90E-13
					*M 0.1	1.20E-12	1.54E-12
					S 0.01	1.29E-12	1.64E-12
Tc-101	14.2 m	-	Y	1.00	F 0.8	2.66E-13	3.49E-13
					*M 0.1	4.56E-13	4.99E-13
					S 0.01	4.76E-13	5.16E-13
Tc-104	18.2 m	-	-	1.00	F 0.8	8.28E-13	1.25E-12
					*M 0.1	1.26E-12	1.44E-12
					S 0.01	1.31E-12	1.46E-12
Ruthenium (particulate)							
Ru-94	51.8 m	Y	-	1.00	F 0.05	1.06E-12	1.65E-12
					*M 0.05	2.48E-12	3.32E-12
					S 0.01	2.64E-12	3.53E-12
Ru-97	2.9 d	Y	-	1.00	F 0.05	2.71E-12	4.39E-12
					*M 0.05	6.61E-12	9.08E-12
					S 0.01	7.17E-12	9.79E-12
Ru-103	39.28 d	Y	-	1.00	F 0.05	3.28E-11	5.12E-11
					*M 0.05	2.12E-10	2.41E-10
					S 0.01	2.59E-10	2.90E-10
Ru-105	4.44 h	Y	-	1.00	F 0.05	4.01E-12	6.61E-12
					*M 0.05	1.30E-11	1.75E-11
					S 0.01	1.41E-11	1.89E-11
Ru-106	368.2 d	-	-	1.00	F 0.05	6.13E-10	9.41E-10
					*M 0.05	2.42E-09	2.77E-09
					S 0.01	5.56E-09	6.02E-09
Ruthenium (vapor)							
Ru-94	51.8 m	Y	-	-	V 0.05	3.77E-12	5.95E-12
Ru-97	2.9 d	Y	-	-	V 0.05	8.79E-12	1.47E-11
Ru-103	39.28 d	Y	-	-	V 0.05	8.72E-11	1.40E-10
Ru-105 _b	4.44 h	Y	-	-	V 0.05	1.47E-11	2.52E-11
Ru-106 _b	368.2 d	-	-	-	V 0.05	1.49E-09	2.33E-09
Rhodium							
Rh-99m	4.7 h	-	-	1.00	F 0.05	8.91E-13	1.41E-12
					M 0.05	1.80E-12	2.57E-12
					S 0.05	1.91E-12	2.70E-12

Table 2.1, continued

Nuclide	$T_{1/2}$	Chain		AMAD (μm)	Type ^a	f_1	Mortality (Bq^{-1})	Morbidity (Bq^{-1})
		P	D					
Rhodium, continued								
Rh-99	16 d	-	-	1.00	F	0.05	1.84E-11	2.90E-11
						0.05	6.64E-11	7.99E-11
						0.05	7.60E-11	9.00E-11
Rh-100	20.8 h	-	Y	1.00	F	0.05	1.05E-11	1.70E-11
						0.05	1.78E-11	2.70E-11
						0.05	1.87E-11	2.81E-11
Rh-101	3.2 y	-	Y	1.00	F	0.05	8.30E-11	1.23E-10
						0.05	1.87E-10	2.21E-10
						0.05	4.34E-10	4.90E-10
Rh-101m	4.34 d	Y	Y	1.00	F	0.05	4.81E-12	7.78E-12
						0.05	1.39E-11	1.79E-11
						0.05	1.52E-11	1.93E-11
Rh-102	2.9 y	-	Y	1.00	F	0.05	4.19E-10	6.16E-10
						0.05	5.06E-10	6.57E-10
						0.05	1.34E-09	1.62E-09
Rh-102m	207 d	Y	-	1.00	F	0.05	1.04E-10	1.60E-10
						0.05	3.50E-10	4.09E-10
						0.05	6.17E-10	6.91E-10
Rh-103m	56.12 m	-	Y	1.00	F	0.05	5.86E-14	7.35E-14
						0.05	2.05E-13	2.30E-13
						0.05	2.21E-13	2.47E-13
Rh-105	35.36 h	-	Y	1.00	F	0.05	7.18E-12	1.24E-11
						0.05	3.09E-11	3.98E-11
						0.05	3.37E-11	4.30E-11
Rh-106m	132 m	-	-	1.00	F	0.05	2.19E-12	3.29E-12
						0.05	5.30E-12	6.92E-12
						0.05	5.64E-12	7.32E-12
Rh-107	21.7 m	Y	-	1.00	F	0.05	3.13E-13	3.62E-13
						0.05	6.74E-13	7.38E-13
						0.05	7.13E-13	7.79E-13
Palladium								
Pd-100	3.63 d	Y	-	1.00	F	0.005	3.10E-11	4.71E-11
						0.005	6.03E-11	7.94E-11
						0.005	6.44E-11	8.39E-11
Pd-101	8.27 h	Y	-	1.00	F	0.005	1.72E-12	2.78E-12
						0.005	3.57E-12	5.04E-12
						0.005	3.80E-12	5.32E-12
Pd-103	16.96 d	Y	Y	1.00	F	0.005	6.36E-12	1.05E-11
						0.005	3.56E-11	4.19E-11
						0.005	4.13E-11	4.79E-11

Table 2.1, continued

Nuclide	$T_{1/2}$	Chain		AMAD (μm)	Type ^a	f_1	Mortality (Bq^{-1})	Morbidity (Bq^{-1})
		P	D					
Palladium, continued								
Pd-107	6.5E6 y	-	Y	1.00	F	0.005	1.63E-12	2.64E-12
					M	0.005	8.56E-12	1.01E-11
					S	0.005	4.22E-11	4.56E-11
Pd-109	13.427 h	-	-	1.00	F	0.005	1.09E-11	1.87E-11
					M	0.005	3.45E-11	4.69E-11
					S	0.005	3.72E-11	5.00E-11
Silver								
Ag-102	12.9 m	-	-	1.00	F	0.05	3.89E-13	4.68E-13
					*M	0.05	6.06E-13	6.93E-13
					S	0.01	6.30E-13	7.18E-13
Ag-103	65.7 m	Y	-	1.00	F	0.05	5.30E-13	7.27E-13
					*M	0.05	1.34E-12	1.64E-12
					S	0.01	1.44E-12	1.75E-12
Ag-104	69.2 m	-	Y	1.00	F	0.05	7.32E-13	1.04E-12
					*M	0.05	1.27E-12	1.69E-12
					S	0.01	1.33E-12	1.77E-12
Ag-104m	33.5 m	Y	-	1.00	F	0.05	5.60E-13	7.37E-13
					*M	0.05	1.09E-12	1.33E-12
					S	0.01	1.15E-12	1.40E-12
Ag-105	41.0 d	-	-	1.00	F	0.05	3.91E-11	5.55E-11
					*M	0.05	6.20E-11	7.66E-11
					S	0.01	7.10E-11	8.55E-11
Ag-106	23.96 m	-	-	1.00	F	0.05	3.28E-13	3.95E-13
					*M	0.05	6.49E-13	7.34E-13
					S	0.01	6.85E-13	7.71E-13
Ag-106m	8.41 d	-	-	1.00	F	0.05	6.07E-11	8.78E-11
					*M	0.05	7.04E-11	9.58E-11
					S	0.01	7.17E-11	9.67E-11
Ag-108m	127 y	-	-	1.00	F	0.05	4.09E-10	5.68E-10
					*M	0.05	5.82E-10	7.21E-10
					S	0.01	2.42E-09	2.82E-09
Ag-110m	249.9 d	-	-	1.00	F	0.05	3.90E-10	5.47E-10
					*M	0.05	6.22E-10	7.65E-10
					S	0.01	1.03E-09	1.22E-09
Ag-111	7.45 d	-	-	1.00	F	0.05	3.46E-11	5.63E-11
					*M	0.05	1.45E-10	1.80E-10
					S	0.01	1.63E-10	2.00E-10
Ag-112	3.12 h	-	-	1.00	F	0.05	5.63E-12	8.99E-12
					*M	0.05	1.38E-11	1.96E-11
					S	0.01	1.48E-11	2.10E-11

Table 2.1, continued

Nuclide	T _{1/2}	Chain		AMAD (μm)	Type ^a	f ₁	Mortality (Bq ⁻¹)	Morbidity (Bq ⁻¹)
		P	D					
Silver, continued								
Ag-115	20.0 m	Y	-	1.00	F	0.05	6.68E-13	8.65E-13
					*M	0.05	1.54E-12	1.84E-12
					S	0.01	1.65E-12	1.97E-12
Cadmium								
Cd-104	57.7 m	Y	-	1.00	F	0.05	7.31E-13	1.09E-12
					M	0.05	1.46E-12	1.97E-12
					S	0.05	1.54E-12	2.07E-12
Cd-107	6.49 h	-	-	1.00	F	0.05	1.08E-12	1.71E-12
					M	0.05	6.39E-12	7.72E-12
					S	0.05	6.99E-12	8.39E-12
Cd-109	464 d	-	Y	1.00	F	0.05	2.83E-10	3.99E-10
					M	0.05	4.12E-10	4.78E-10
					S	0.05	5.44E-10	5.91E-10
Cd-113	9.3E15 y	-	-	1.00	F	0.05	2.18E-09	3.03E-09
					M	0.05	1.22E-09	1.60E-09
					S	0.05	1.11E-09	1.25E-09
Cd-113m	13.6 y	-	-	1.00	F	0.05	2.51E-09	3.52E-09
					M	0.05	1.52E-09	1.97E-09
					S	0.05	1.76E-09	1.95E-09
Cd-115	53.46 h	Y	Y	1.00	F	0.05	2.69E-11	4.47E-11
					M	0.05	9.69E-11	1.29E-10
					S	0.05	1.06E-10	1.39E-10
Cd-115m	44.6 d	Y	Y	1.00	F	0.05	2.10E-10	3.09E-10
					M	0.05	5.66E-10	6.62E-10
					S	0.05	6.93E-10	7.90E-10
Cd-117	2.49 h	Y	-	1.00	F	0.05	4.03E-12	6.48E-12
					M	0.05	1.22E-11	1.65E-11
					S	0.05	1.31E-11	1.76E-11
Cd-117m	3.36 h	Y	-	1.00	F	0.05	4.09E-12	6.42E-12
					M	0.05	1.26E-11	1.66E-11
					S	0.05	1.35E-11	1.77E-11
Indium								
In-109	4.2 h	Y	-	1.00	F	0.02	1.07E-12	1.57E-12
					M	0.02	2.20E-12	2.99E-12
					S	0.02	2.36E-12	3.18E-12
In-110b	4.9 h	-	-	1.00	F	0.02	3.10E-12	4.73E-12
					M	0.02	4.79E-12	7.16E-12
					S	0.02	4.98E-12	7.42E-12
In-110a	69.1 m	-	Y	1.00	F	0.02	1.15E-12	1.59E-12
					M	0.02	2.51E-12	3.16E-12
					S	0.02	2.66E-12	3.33E-12

Table 2.1, continued

Nuclide	$T_{1/2}$	Chain		AMAD (μm)	Type ^a	f_1	Mortality (Bq^{-1})	Morbidity (Bq^{-1})
		P	D					
Indium, continued								
In-111	2.83 d	-	Y	1.00	F	0.02	6.65E-12	9.95E-12
						0.02	1.66E-11	2.17E-11
						0.02	1.78E-11	2.32E-11
In-112	14.4 m	-	-	1.00	F	0.02	1.46E-13	1.64E-13
						0.02	2.75E-13	2.98E-13
						0.02	2.89E-13	3.13E-13
In-113m	1.658 h	-	Y	1.00	F	0.02	3.88E-13	5.46E-13
						0.02	1.13E-12	1.40E-12
						0.02	1.22E-12	1.49E-12
In-114m	49.51 d	-	-	1.00	F	0.02	5.52E-10	6.67E-10
						0.02	6.84E-10	8.10E-10
						0.02	7.57E-10	8.84E-10
In-115	5.1E15 y	-	Y	1.00	F	0.02	9.85E-09	1.09E-08
						0.02	4.29E-09	4.74E-09
						0.02	2.07E-09	2.23E-09
In-115m	4.486 h	Y	Y	1.00	F	0.02	1.36E-12	2.12E-12
						0.02	4.37E-12	5.80E-12
						0.02	4.71E-12	6.20E-12
In-116m	54.15 m	-	-	1.00	F	0.02	8.37E-13	1.11E-12
						0.02	1.97E-12	2.37E-12
						0.02	2.09E-12	2.51E-12
In-117	43.8 m	Y	Y	1.00	F	0.02	4.72E-13	5.81E-13
						0.02	1.34E-12	1.51E-12
						0.02	1.44E-12	1.61E-12
In-117m	116.5 m	Y	Y	1.00	F	0.02	1.55E-12	2.29E-12
						0.02	4.98E-12	6.29E-12
						0.02	5.35E-12	6.73E-12
In-119m	18.0 m	Y	-	1.00	F	0.02	4.38E-13	5.03E-13
						0.02	8.25E-13	9.02E-13
						0.02	8.68E-13	9.47E-13
Tin								
Sn-110	4.0 h	Y	-	1.00	F	0.02	6.50E-12	1.12E-11
						0.02	1.20E-11	1.81E-11
						0.02	1.26E-11	1.89E-11
Sn-111	35.3 m	Y	-	1.00	F	0.02	2.90E-13	3.95E-13
						0.02	6.39E-13	7.65E-13
						0.02	6.79E-13	8.07E-13
Sn-113	115.1 d	Y	-	1.00	F	0.02	4.17E-11	6.36E-11
						0.02	2.36E-10	2.71E-10
						0.02	3.50E-10	3.92E-10

Table 2.1, continued

Nuclide	$T_{1/2}$	Chain		AMAD (μm)	Type ^a	f_1	Mortality (Bq^{-1})	Morbidity (Bq^{-1})
		P	D					
Tin, continued								
Sn-117m	13.61 d	-	Y	1.00	F	0.02	2.27E-11	3.66E-11
						0.02	2.12E-10	2.39E-10
						0.02	2.46E-10	2.75E-10
Sn-119m	293.0 d	-	Y	1.00	F	0.02	2.20E-11	3.28E-11
						0.02	1.91E-10	2.11E-10
						0.02	2.97E-10	3.22E-10
Sn-121	27.06 h	-	Y	1.00	F	0.02	5.35E-12	9.28E-12
						0.02	2.18E-11	2.76E-11
						0.02	2.37E-11	2.97E-11
Sn-121m	55 y	Y	-	1.00	F	0.02	5.25E-11	7.30E-11
						0.02	3.81E-10	4.16E-10
						0.02	1.10E-09	1.17E-09
Sn-123	129.2 d	-	-	1.00	F	0.02	1.01E-10	1.58E-10
						0.02	7.25E-10	8.19E-10
						0.02	1.14E-09	1.25E-09
Sn-123m	40.08 m	-	-	1.00	F	0.02	5.25E-13	6.60E-13
						0.02	1.35E-12	1.52E-12
						0.02	1.45E-12	1.61E-12
Sn-125	9.64 d	Y	-	1.00	F	0.02	9.11E-11	1.51E-10
						0.02	2.97E-10	3.81E-10
						0.02	3.37E-10	4.24E-10
Sn-126	1.0E5 y	Y	-	1.00	F	0.02	7.23E-10	1.02E-09
						0.02	2.34E-09	2.69E-09
						0.02	1.02E-08	1.11E-08
Sn-127	2.10 h	Y	-	1.00	F	0.02	3.44E-12	5.48E-12
						0.02	9.18E-12	1.19E-11
						0.02	9.90E-12	1.27E-11
Sn-128	59.1 m	Y	-	1.00	F	0.02	2.10E-12	3.01E-12
						0.02	5.07E-12	6.18E-12
						0.02	5.40E-12	6.52E-12
Antimony								
Sb-115	31.8 m	-	-	1.00	F	0.1	2.70E-13	3.45E-13
						0.01	5.36E-13	6.30E-13
						0.01	5.65E-13	6.61E-13
Sb-116	15.8 m	-	Y	1.00	F	0.1	2.71E-13	3.33E-13
						0.01	4.41E-13	5.09E-13
						0.01	4.59E-13	5.29E-13
Sb-116m	60.3 m	-	-	1.00	F	0.1	8.84E-13	1.22E-12
						0.01	1.92E-12	2.38E-12
						0.01	2.03E-12	2.51E-12

Table 2.1, continued

Nuclide	$T_{1/2}$	Chain		AMAD (μm)	Type ^a f_1	Mortality (Bq^{-1})	Morbidity (Bq^{-1})
		P	D				
Antimony, continued							
Sb-117	2.80 h	-	-	1.00	F 0.1	2.63E-13	3.94E-13
					*M 0.01	8.76E-13	1.10E-12
					S 0.01	9.43E-13	1.17E-12
Sb-118m	5.00 h	-	-	1.00	F 0.1	2.72E-12	4.25E-12
					*M 0.01	4.84E-12	7.14E-12
					S 0.01	5.07E-12	7.44E-12
Sb-119	38.1 h	-	-	1.00	F 0.1	1.41E-12	2.41E-12
					*M 0.01	2.95E-12	4.69E-12
					S 0.01	3.12E-12	4.93E-12
Sb-120b	5.76 d	-	-	1.00	F 0.1	2.46E-11	3.82E-11
					*M 0.01	6.78E-11	8.91E-11
					S 0.01	7.41E-11	9.64E-11
Sb-120a	15.89 m	-	-	1.00	F 0.1	1.54E-13	1.80E-13
					*M 0.01	2.74E-13	3.04E-13
					S 0.01	2.87E-13	3.18E-13
Sb-122	2.70 d	-	-	1.00	F 0.1	3.34E-11	5.64E-11
					*M 0.01	1.06E-10	1.48E-10
					S 0.01	1.15E-10	1.58E-10
Sb-124	60.20 d	-	Y	1.00	F 0.1	8.55E-11	1.30E-10
					*M 0.01	5.65E-10	6.58E-10
					S 0.01	7.54E-10	8.65E-10
Sb-124n	20.2 m	Y	-	1.00	F 0.1	1.01E-13	1.28E-13
					*M 0.01	2.72E-13	3.12E-13
					S 0.01	3.16E-13	3.60E-13
Sb-125 ^b	2.77 y	Y	-	1.00	F 0.1	7.52E-11	1.04E-10
					*M 0.01	3.99E-10	4.49E-10
					S 0.01	9.74E-10	1.08E-09
Sb-126	12.4 d	-	Y	1.00	F 0.1	5.90E-11	9.26E-11
					*M 0.01	2.51E-10	3.10E-10
					S 0.01	2.85E-10	3.49E-10
Sb-126m	19.0 m	Y	Y	1.00	F 0.1	3.99E-13	4.83E-13
					*M 0.01	7.53E-13	8.54E-13
					S 0.01	7.94E-13	8.97E-13
Sb-127	3.85 d	Y	Y	1.00	F 0.1	3.50E-11	5.83E-11
					*M 0.01	1.60E-10	2.03E-10
					S 0.01	1.77E-10	2.23E-10
Sb-128b	9.01 h	-	-	1.00	F 0.1	1.11E-11	1.82E-11
					*M 0.01	2.68E-11	3.89E-11
					S 0.01	2.85E-11	4.11E-11
Sb-128a	10.4 m	-	Y	1.00	F 0.1	3.32E-13	3.85E-13
					*M 0.01	5.14E-13	5.72E-13
					S 0.01	5.34E-13	5.92E-13

Table 2.1, continued

Nuclide	$T_{1/2}$	Chain		AMAD (μm)	Type ^a f_1	Mortality (Bq^{-1})	Morbidity (Bq^{-1})
		P	D				
Antimony, continued							
Sb-129	4.32 h	Y	-	1.00	F 0.1	6.54E-12	1.08E-11
					*M 0.01	1.86E-11	2.60E-11
					S 0.01	2.00E-11	2.78E-11
Sb-130	40 m	-	-	1.00	F 0.1	1.06E-12	1.38E-12
					*M 0.01	2.20E-12	2.63E-12
					S 0.01	2.33E-12	2.77E-12
Sb-131	23 m	Y	-	1.00	F 0.1	9.24E-13	2.41E-12
					*M 0.01	2.11E-12	2.63E-12
					S 0.01	2.25E-12	2.60E-12
Tellurium (particulate)							
Te-116	2.49 h	Y	-	1.00	F 0.3	2.44E-12	3.83E-12
					*M 0.1	6.41E-12	8.66E-12
					S 0.01	6.93E-12	9.34E-12
Te-121	17 d	-	Y	1.00	F 0.3	1.22E-11	1.86E-11
					*M 0.1	2.69E-11	3.52E-11
					S 0.01	3.02E-11	3.88E-11
Te-121m	154 d	Y	-	1.00	F 0.3	9.62E-11	1.32E-10
					*M 0.1	3.43E-10	3.88E-10
					S 0.01	4.91E-10	5.48E-10
Te-123	1E13 y	-	Y	1.00	F 0.3	9.22E-11	1.05E-10
					*M 0.1	5.97E-11	6.77E-11
					S 0.01	1.27E-10	1.39E-10
Te-123m	119.7 d	Y	Y	1.00	F 0.3	4.48E-11	6.25E-11
					*M 0.1	3.34E-10	3.67E-10
					S 0.01	4.41E-10	4.80E-10
Te-125m	58 d	-	Y	1.00	F 0.3	2.54E-11	3.87E-11
					*M 0.1	2.88E-10	3.16E-10
					S 0.01	3.61E-10	3.92E-10
Te-127	9.35 h	-	Y	1.00	F 0.3	2.98E-12	5.08E-12
					*M 0.1	1.24E-11	1.65E-11
					S 0.01	1.37E-11	1.83E-11
Te-127m	109 d	Y	Y	1.00	F 0.3	8.65E-11	1.20E-10
					*M 0.1	6.34E-10	6.97E-10
					S 0.01	8.60E-10	9.34E-10
Te-129	69.6 m	Y	Y	1.00	F 0.3	7.77E-13	1.06E-12
					*M 0.1	2.26E-12	2.69E-12
					S 0.01	2.43E-12	2.88E-12
Te-129m	33.6 d	Y	Y	1.00	F 0.3	9.13E-11	1.50E-10
					*M 0.1	5.83E-10	6.72E-10
					S 0.01	7.15E-10	8.11E-10

Table 2.1, continued

Nuclide	T _{1/2}	Chain		AMAD (μm)	Type ^a f ₁	Mortality (Bq ⁻¹)	Morbidity (Bq ⁻¹)
		P	D				
Tellurium (particulate), continued							
Te-131	25.0 m	Y	Y	1.00	F 0.3	6.60E-13	2.25E-12
					*M 0.1	1.34E-12	1.73E-12
					S 0.01	1.42E-12	1.60E-12
Te-131m	30 h	Y	Y	1.00	F 0.3	2.52E-11	9.95E-11
					*M 0.1	7.77E-11	1.14E-10
					S 0.01	8.56E-11	1.13E-10
Te-132	78.2 h	Y	-	1.00	F 0.3	6.08E-11	2.19E-10
					*M 0.1	1.74E-10	2.52E-10
					S 0.01	1.91E-10	2.54E-10
Te-133	12.45 m	Y	Y	1.00	F 0.3	5.07E-13	2.05E-12
					*M 0.1	9.31E-13	1.33E-12
					S 0.01	9.81E-13	1.23E-12
Te-133m	55.4 m	Y	-	1.00	F 0.3	2.19E-12	9.06E-12
					*M 0.1	4.91E-12	7.14E-12
					S 0.01	5.24E-12	6.80E-12
Te-134	41.8 m	Y	-	1.00	F 0.3	1.31E-12	2.95E-12
					*M 0.1	3.43E-12	4.33E-12
					S 0.01	3.66E-12	4.49E-12
Tellurium (vapor)							
Te-116	2.49 h	Y	-	-	V 0.3	5.12E-12	7.47E-12
Te-121	17 d	-	Y	-	V 0.3	3.26E-11	4.91E-11
Te-121m	154 d	Y	-	-	V 0.3	2.86E-10	3.87E-10
Te-123	1E13 y	-	Y	-	V 0.3	2.81E-10	3.21E-10
Te-123m	119.7 d	Y	Y	-	V 0.3	1.28E-10	1.75E-10
Te-125m	58 d	-	Y	-	V 0.3	6.89E-11	1.02E-10
Te-127	9.35 h	-	Y	-	V 0.3	6.00E-12	9.25E-12
Te-127m	109 d	Y	Y	-	V 0.3	2.43E-10	3.28E-10
Te-129	69.6 m	Y	Y	-	V 0.3	2.52E-12	3.06E-12
Te-129m	33.6 d	Y	Y	-	V 0.3	2.29E-10	3.66E-10
Te-131	25.0 m	Y	Y	-	V 0.3	2.49E-12	6.62E-12
Te-131m	30 h	Y	Y	-	V 0.3	5.52E-11	2.59E-10
Te-132	78.2 h	Y	-	-	V 0.3	1.40E-10	5.78E-10
Te-133	12.45 m	Y	Y	-	V 0.3	1.84E-12	5.83E-12
Te-133m	55.4 m	Y	-	-	V 0.3	6.02E-12	2.37E-11
Te-134	41.8 m	Y	-	-	V 0.3	4.21E-12	8.47E-12
Iodine (particulate)							
I-120	81.0 m	-	-	1.00	*F 1.0	2.92E-12	1.05E-11
					M 0.1	5.82E-12	8.17E-12
					S 0.01	6.11E-12	7.94E-12
I-120m	53 m	-	-	1.00	*F 1.0	2.10E-12	5.36E-12
					M 0.1	3.94E-12	5.19E-12
					S 0.01	4.13E-12	5.18E-12

Table 2.1, continued

Nuclide	$T_{1/2}$	Chain		AMAD (μm)	Type ^a f_1	Mortality (Bq^{-1})	Morbidity (Bq^{-1})
		P	D				
Iodine (particulate), continued							
I-121	2.12 h	Y	-	1.00	*F 1.0	5.43E-13	2.65E-12
					M 0.1	1.24E-12	1.85E-12
					S 0.01	1.32E-12	1.71E-12
I-123	13.2 h	Y	-	1.00	*F 1.0	1.13E-12	8.18E-12
					M 0.1	3.81E-12	5.83E-12
					S 0.01	4.14E-12	5.51E-12
I-124	4.18 d	-	-	1.00	*F 1.0	5.12E-11	4.77E-10
					M 0.1	6.04E-11	1.39E-10
					S 0.01	6.16E-11	8.76E-11
I-125	60.14 d	-	Y	1.00	*F 1.0	2.97E-11	2.87E-10
					M 0.1	2.91E-11	8.71E-11
					S 0.01	3.24E-11	4.04E-11
I-126	13.02 d	-	-	1.00	*F 1.0	1.04E-10	1.00E-09
					M 0.1	1.20E-10	2.81E-10
					S 0.01	1.23E-10	1.54E-10
I-128	24.99 m	-	-	1.00	*F 1.0	4.59E-13	8.21E-13
					M 0.1	9.11E-13	1.03E-12
					S 0.01	9.61E-13	1.06E-12
I-129	1.57E7 y	-	Y	1.00	*F 1.0	1.68E-10	1.64E-09
					M 0.1	2.60E-10	7.64E-10
					S 0.01	5.96E-10	6.91E-10
I-130	12.36 h	-	-	1.00	*F 1.0	1.04E-11	7.47E-11
					M 0.1	2.67E-11	4.48E-11
					S 0.01	2.87E-11	4.09E-11
I-131	8.04 d	-	Y	1.00	*F 1.0	5.55E-11	5.27E-10
					M 0.1	1.29E-10	2.20E-10
					S 0.01	1.40E-10	1.69E-10
I-132	2.30 h	-	Y	1.00	*F 1.0	2.46E-12	1.01E-11
					M 0.1	6.09E-12	8.72E-12
					S 0.01	6.49E-12	8.58E-12
I-132m	83.6 m	Y	-	1.00	*F 1.0	1.56E-12	7.31E-12
					M 0.1	4.24E-12	6.88E-12
					S 0.01	4.54E-12	6.82E-12
I-133	20.8 h	-	Y	1.00	*F 1.0	1.93E-11	1.69E-10
					M 0.1	4.02E-11	7.48E-11
					S 0.01	4.29E-11	6.21E-11
I-134	52.6 m	-	Y	1.00	*F 1.0	1.15E-12	2.77E-12
					M 0.1	2.47E-12	3.12E-12
					S 0.01	2.61E-12	3.16E-12
I-135	6.61 h	Y	-	1.00	*F 1.0	5.56E-12	3.63E-11
					M 0.1	1.47E-11	2.37E-11
					S 0.01	1.58E-11	2.22E-11

Table 2.1, continued

Nuclide	T _{1/2}	Chain		AMAD (μm)	Type ^a f ₁	Mortality (Bq ⁻¹)	Morbidity (Bq ⁻¹)
		P	D				
Iodine (vapor)							
I-120	81.0 m	-	-	-	V 1.0	1.02E-11	3.01E-11
I-120m	53 m	-	-	-	V 1.0	8.05E-12	1.67E-11
I-121	2.12 h	Y	-	-	V 1.0	2.52E-12	8.05E-12
I-123	13.2 h	Y	-	-	V 1.0	4.00E-12	2.22E-11
I-124	4.18 d	-	-	-	V 1.0	1.32E-10	1.23E-09
I-125	60.14 d	-	Y	-	V 1.0	7.75E-11	7.48E-10
I-126	13.02 d	-	-	-	V 1.0	2.70E-10	2.59E-09
I-128	24.99 m	-	-	-	V 1.0	4.56E-12	5.69E-12
I-129	1.57E7 y	-	Y	-	V 1.0	4.42E-10	4.32E-09
I-130	12.36 h	-	-	-	V 1.0	3.15E-11	1.97E-10
I-131 ^b	8.04 d	-	Y	-	V 1.0	1.48E-10	1.36E-09
I-132	2.30 h	-	Y	-	V 1.0	1.12E-11	3.12E-11
I-132m	83.6 m	Y	-	-	V 1.0	8.67E-12	2.37E-11
I-133	20.8 h	-	Y	-	V 1.0	5.46E-11	4.39E-10
I-134	52.6 m	-	Y	-	V 1.0	7.41E-12	1.19E-11
I-135	6.61 h	Y	-	-	V 1.0	1.93E-11	9.86E-11
Iodine (methyl iodide)							
I-120	81.0 m	-	-	-	V 1.0	4.41E-12	2.26E-11
I-120m	53 m	-	-	-	V 1.0	2.77E-12	1.09E-11
I-121	2.12 h	Y	-	-	V 1.0	8.84E-13	5.41E-12
I-123	13.2 h	Y	-	-	V 1.0	2.08E-12	1.65E-11
I-124	4.18 d	-	-	-	V 1.0	1.02E-10	9.56E-10
I-125	60.14 d	-	Y	-	V 1.0	6.03E-11	5.83E-10
I-126	13.02 d	-	-	-	V 1.0	2.08E-10	2.02E-09
I-128	24.99 m	-	-	-	V 1.0	3.69E-13	1.44E-12
I-129	1.57E7 y	-	Y	-	V 1.0	3.43E-10	3.36E-09
I-130	12.36 h	-	-	-	V 1.0	1.93E-11	1.51E-10
I-131	8.04 d	-	Y	-	V 1.0	1.10E-10	1.06E-09
I-132	2.30 h	-	Y	-	V 1.0	3.88E-12	2.09E-11
I-132m	83.6 m	Y	-	-	V 1.0	2.40E-12	1.43E-11
I-133	20.8 h	-	Y	-	V 1.0	3.76E-11	3.41E-10
I-134	52.6 m	-	Y	-	V 1.0	1.38E-12	5.40E-12
I-135	6.61 h	Y	-	-	V 1.0	1.01E-11	7.42E-11
Cesium							
Cs-125	45 m	Y	-	1.00	*F 1.0	3.61E-13	4.44E-13
					M 0.1	9.26E-13	1.10E-12
					S 0.01	9.85E-13	1.16E-12
Cs-127	6.25 h	-	-	1.00	*F 1.0	4.73E-13	6.68E-13
					M 0.1	1.94E-12	2.71E-12
					S 0.01	2.11E-12	2.96E-12

Table 2.1, continued

Nuclide	$T_{1/2}$	Chain		AMAD (μm)	Type ^a f_1	Mortality (Bq^{-1})	Morbidity (Bq^{-1})
		P	D				
Cesium, continued							
Cs-129	32.06 h	-	-	1.00	*F 1.0	1.37E-12	2.01E-12
					M 0.1	4.37E-12	6.42E-12
					S 0.01	4.78E-12	7.05E-12
Cs-130	29.9 m	-	-	1.00	*F 1.0	2.82E-13	3.36E-13
					M 0.1	6.25E-13	7.15E-13
					S 0.01	6.61E-13	7.54E-13
Cs-131	9.69 d	-	Y	1.00	*F 1.0	1.36E-12	2.03E-12
					M 0.1	3.43E-12	4.59E-12
					S 0.01	3.78E-12	5.04E-12
Cs-132	6.475 d	-	-	1.00	*F 1.0	1.09E-11	1.60E-11
					M 0.1	1.90E-11	2.58E-11
					S 0.01	2.02E-11	2.73E-11
Cs-134	2.062 y	-	Y	1.00	*F 1.0	3.05E-10	4.45E-10
					M 0.1	7.05E-10	8.36E-10
					S 0.01	1.66E-09	1.89E-09
Cs-134m	2.90 h	Y	-	1.00	*F 1.0	4.41E-13	5.38E-13
					M 0.1	3.65E-12	4.21E-12
					S 0.01	4.15E-12	4.78E-12
Cs-135	2.3E6 y	-	Y	1.00	*F 1.0	3.40E-11	5.03E-11
					M 0.1	2.58E-10	2.82E-10
					S 0.01	6.30E-10	6.72E-10
Cs-135m	53 m	Y	-	1.00	*F 1.0	2.63E-13	3.56E-13
					M 0.1	4.91E-13	6.57E-13
					S 0.01	5.14E-13	6.85E-13
Cs-136	13.1 d	-	-	1.00	*F 1.0	6.39E-11	9.44E-11
					M 0.1	2.12E-10	2.54E-10
					S 0.01	2.40E-10	2.83E-10
Cs-137 ^b	30.0 y	-	-	1.00	*F 1.0	2.19E-10	3.21E-10
					M 0.1	7.81E-10	8.91E-10
					S 0.01	2.77E-09	3.03E-09
Cs-138	32.2 m	-	-	1.00	*F 1.0	8.94E-13	1.08E-12
					M 0.1	1.93E-12	2.25E-12
					S 0.01	2.04E-12	2.37E-12
Barium							
Ba-126	96.5 m	-	-	1.00	F 0.2	4.61E-12	7.39E-12
					*M 0.1	7.06E-12	9.42E-12
					S 0.01	7.35E-12	9.69E-12
Ba-128	2.43 d	-	-	1.00	F 0.2	7.15E-11	1.25E-10
					*M 0.1	1.33E-10	1.95E-10
					S 0.01	1.43E-10	2.08E-10

Table 2.1, continued

Nuclide	$T_{1/2}$	Chain		AMAD (μm)	Type ^a f_1	Mortality (Bq^{-1})	Morbidity (Bq^{-1})
		P	D				
Barium, continued							
Ba-131	11.8 d	Y	Y	1.00	F 0.2	1.33E-11	2.17E-11
					*M 0.1	6.68E-11	7.87E-11
					S 0.01	7.63E-11	8.89E-11
Ba-131m	14.6 m	Y	-	1.00	F 0.2	1.90E-13	2.17E-13
					*M 0.1	4.23E-13	4.57E-13
					S 0.01	4.52E-13	4.87E-13
Ba-133	10.74 y	-	Y	1.00	F 0.2	1.23E-10	1.69E-10
					*M 0.1	2.67E-10	3.14E-10
					S 0.01	7.74E-10	8.78E-10
Ba-133m	38.9 h	Y	-	1.00	F 0.2	1.43E-11	2.51E-11
					*M 0.1	4.17E-11	5.51E-11
					S 0.01	4.57E-11	6.00E-11
Ba-135m	28.7 h	-	-	1.00	F 0.2	1.12E-11	1.96E-11
					*M 0.1	3.27E-11	4.34E-11
					S 0.01	3.57E-11	4.71E-11
Ba-139	82.7 m	-	-	1.00	F 0.2	2.17E-12	3.39E-12
					*M 0.1	3.84E-12	4.83E-12
					S 0.01	4.03E-12	5.00E-12
Ba-140	12.74 d	Y	-	1.00	F 0.2	1.02E-10	1.70E-10
					*M 0.1	4.61E-10	5.48E-10
					S 0.01	5.30E-10	6.20E-10
Ba-141	18.27 m	Y	-	1.00	F 0.2	1.17E-12	1.77E-12
					*M 0.1	2.03E-12	2.62E-12
					S 0.01	2.15E-12	2.75E-12
Ba-142	10.6 m	Y	-	1.00	F 0.2	6.09E-13	8.70E-13
					*M 0.1	9.95E-13	1.23E-12
					S 0.01	1.04E-12	1.27E-12
Lanthanum							
La-131	59 m	Y	-	1.00	F 0.0005	4.89E-13	6.57E-13
					M 0.0005	1.24E-12	1.48E-12
					S 0.0005	1.33E-12	1.59E-12
La-132	4.8 h	-	-	1.00	F 0.0005	5.32E-12	8.51E-12
					M 0.0005	1.14E-11	1.69E-11
					S 0.0005	1.21E-11	1.78E-11
La-135	19.5 h	-	Y	1.00	F 0.0005	4.51E-13	7.25E-13
					M 0.0005	8.74E-13	1.36E-12
					S 0.0005	9.22E-13	1.43E-12
La-137	6E4 y	-	Y	1.00	F 0.0005	3.11E-10	3.77E-10
					M 0.0005	1.35E-10	1.62E-10
					S 0.0005	1.27E-10	1.42E-10

Table 2.1, continued

Nuclide	$T_{1/2}$	Chain		AMAD (μm)	Type ^a f_1	Mortality (Bq^{-1})	Morbidity (Bq^{-1})
		P	D				
Lanthanum, continued							
La-138	1.35E11 y	-	-	1.00	F 0.0005	6.35E-09	8.24E-09
					M 0.0005	2.65E-09	3.39E-09
					S 0.0005	1.77E-09	2.10E-09
La-140	40.272 h	-	Y	1.00	F 0.0005	3.67E-11	5.83E-11
					M 0.0005	8.98E-11	1.29E-10
					S 0.0005	9.61E-11	1.37E-10
La-141	3.93 h	Y	Y	1.00	F 0.0005	5.16E-12	8.30E-12
					M 0.0005	1.43E-11	2.01E-11
					S 0.0005	1.55E-11	2.16E-11
La-142	92.5 m	-	Y	1.00	F 0.0005	2.17E-12	3.14E-12
					M 0.0005	5.05E-12	6.54E-12
					S 0.0005	5.36E-12	6.92E-12
La-143	14.23 m	Y	-	1.00	F 0.0005	5.76E-13	7.26E-13
					M 0.0005	1.28E-12	1.53E-12
					S 0.0005	1.36E-12	1.63E-12
Cerium							
Ce-134	72.0 h	-	-	1.00	F 0.0005	5.05E-11	8.02E-11
					*M 0.0005	1.31E-10	1.88E-10
					S 0.0005	1.41E-10	2.01E-10
Ce-135	17.6 h	Y	-	1.00	F 0.0005	1.23E-11	1.97E-11
					*M 0.0005	3.42E-11	4.74E-11
					S 0.0005	3.67E-11	5.06E-11
Ce-137	9.0 h	Y	Y	1.00	F 0.0005	3.56E-13	5.86E-13
					*M 0.0005	6.94E-13	1.11E-12
					S 0.0005	7.32E-13	1.17E-12
Ce-137m	34.4 h	Y	-	1.00	F 0.0005	9.43E-12	1.55E-11
					*M 0.0005	3.97E-11	5.24E-11
					S 0.0005	4.33E-11	5.67E-11
Ce-139	137.66 d	-	Y	1.00	F 0.0005	8.83E-11	1.14E-10
					*M 0.0005	1.34E-10	1.53E-10
					S 0.0005	1.67E-10	1.86E-10
Ce-141	32.501 d	-	Y	1.00	F 0.0005	4.93E-11	6.41E-11
					*M 0.0005	2.76E-10	3.07E-10
					S 0.0005	3.30E-10	3.64E-10
Ce-143	33.0 h	Y	Y	1.00	F 0.0005	2.14E-11	3.41E-11
					*M 0.0005	7.50E-11	1.01E-10
					S 0.0005	8.24E-11	1.10E-10
Ce-144	284.3 d	Y	-	1.00	F 0.0005	1.95E-09	2.26E-09
					*M 0.0005	2.65E-09	2.96E-09
					S 0.0005	4.49E-09	4.87E-09

Table 2.1, continued

Nuclide	$T_{1/2}$	Chain		AMAD (μm)	Type ^a	f_1	Mortality (Bq^{-1})	Morbidity (Bq^{-1})
		P	D					
Praseodymium								
Pr-136	13.1 m	-	Y	1.00	F	0.0005	3.14E-13	3.75E-13
						0.0005	4.95E-13	5.61E-13
						0.0005	5.15E-13	5.82E-13
Pr-137	76.6 m	Y	-	1.00	F	0.0005	4.87E-13	7.04E-13
						0.0005	1.09E-12	1.42E-12
						0.0005	1.16E-12	1.50E-12
Pr-138m	2.1 h	-	-	1.00	F	0.0005	1.67E-12	2.49E-12
						0.0005	3.35E-12	4.55E-12
						0.0005	3.54E-12	4.77E-12
Pr-139	4.51 h	Y	Y	1.00	F	0.0005	5.69E-13	8.73E-13
						0.0005	1.27E-12	1.75E-12
						0.0005	1.39E-12	1.88E-12
Pr-142	19.13 h	-	Y	1.00	F	0.0005	2.28E-11	3.87E-11
						0.0005	5.71E-11	8.60E-11
						0.0005	6.10E-11	9.13E-11
Pr-142m	14.6 m	Y	-	1.00	F	0.0005	2.90E-13	4.95E-13
						0.0005	7.30E-13	1.10E-12
						0.0005	7.80E-13	1.17E-12
Pr-143	13.56 d	-	Y	1.00	F	0.0005	3.86E-11	5.48E-11
						0.0005	1.96E-10	2.32E-10
						0.0005	2.24E-10	2.63E-10
Pr-144	17.28 m	-	Y	1.00	F	0.0005	4.60E-13	5.30E-13
						0.0005	8.45E-13	9.24E-13
						0.0005	8.87E-13	9.68E-13
Pr-145	5.98 h	-	-	1.00	F	0.0005	6.22E-12	1.04E-11
						0.0005	1.62E-11	2.36E-11
						0.0005	1.74E-11	2.50E-11
Pr-147	13.6 m	Y	-	1.00	F	0.0005	4.04E-13	4.69E-13
						0.0005	8.21E-13	9.11E-13
						0.0005	8.76E-13	9.70E-13
Neodymium								
Nd-136	50.65 m	Y	-	1.00	F	0.0005	1.18E-12	1.64E-12
						0.0005	2.78E-12	3.43E-12
						0.0005	2.96E-12	3.63E-12
Nd-138	5.04 h	-	-	1.00	F	0.0005	9.55E-12	1.58E-11
						0.0005	2.12E-11	3.18E-11
						0.0005	2.25E-11	3.36E-11
Nd-139	29.7 m	Y	Y	1.00	F	0.0005	2.35E-13	3.12E-13
						0.0005	4.94E-13	6.05E-13
						0.0005	5.27E-13	6.41E-13

Table 2.1, continued

Nuclide	$T_{1/2}$	Chain		AMAD (μm)	Type ^a f_1	Mortality (Bq^{-1})	Morbidity (Bq^{-1})
		P	D				
Neodymium, continued							
Nd-139m	5.5 h	Y	-	1.00	F 0.0005	3.84E-12	6.04E-12
					M 0.0005	9.07E-12	1.27E-11
					S 0.0005	9.70E-12	1.34E-11
Nd-141	2.49 h	-	Y	1.00	F 0.0005	1.10E-13	1.67E-13
					M 0.0005	2.53E-13	3.42E-13
					S 0.0005	2.68E-13	3.62E-13
Nd-147	10.98 d	Y	Y	1.00	F 0.0005	3.76E-11	5.24E-11
					M 0.0005	1.90E-10	2.24E-10
					S 0.0005	2.18E-10	2.53E-10
Nd-149	1.73 h	Y	-	1.00	F 0.0005	1.93E-12	2.89E-12
					M 0.0005	6.30E-12	8.02E-12
					S 0.0005	6.80E-12	8.61E-12
Nd-151	12.44 m	Y	-	1.00	F 0.0005	3.96E-13	4.99E-13
					M 0.0005	8.36E-13	1.00E-12
					S 0.0005	8.86E-13	1.06E-12
Promethium							
Pm-141	20.90 m	Y	Y	1.00	F 0.0005	3.45E-13	4.21E-13
					M 0.0005	6.44E-13	7.36E-13
					S 0.0005	6.77E-13	7.70E-13
Pm-143	265 d	-	Y	1.00	F 0.0005	1.86E-10	2.45E-10
					M 0.0005	1.07E-10	1.35E-10
					S 0.0005	1.21E-10	1.45E-10
Pm-144	363 d	-	Y	1.00	F 0.0005	1.13E-09	1.49E-09
					M 0.0005	5.82E-10	7.46E-10
					S 0.0005	6.19E-10	7.47E-10
Pm-145	17.7 y	-	Y	1.00	F 0.0005	2.97E-10	3.47E-10
					M 0.0005	1.48E-10	1.70E-10
					S 0.0005	1.60E-10	1.78E-10
Pm-146	2020 d	Y	-	1.00	F 0.0005	2.23E-09	2.79E-09
					M 0.0005	1.14E-09	1.38E-09
					S 0.0005	1.29E-09	1.46E-09
Pm-147	2.6234 y	Y	Y	1.00	F 0.0005	2.28E-10	2.46E-10
					M 0.0005	2.90E-10	3.13E-10
					S 0.0005	4.06E-10	4.34E-10
Pm-148	5.37 d	-	Y	1.00	F 0.0005	6.50E-11	9.92E-11
					M 0.0005	1.96E-10	2.62E-10
					S 0.0005	2.15E-10	2.84E-10
Pm-148m	41.3 d	Y	-	1.00	F 0.0005	2.47E-10	3.26E-10
					M 0.0005	4.30E-10	5.04E-10
					S 0.0005	4.98E-10	5.74E-10

Table 2.1, continued

Nuclide	$T_{1/2}$	Chain		AMAD (μm)	Type ^a	f_1	Mortality (Bq^{-1})	Morbidity (Bq^{-1})
		P	D					
Promethium, continued								
Pm-149	53.08 h	-	Y	1.00	F	0.0005	1.92E-11	3.15E-11
						0.0005	6.75E-11	9.16E-11
						0.0005	7.34E-11	9.89E-11
Pm-150	2.68 h	-	-	1.00	F	0.0005	3.54E-12	5.50E-12
						0.0005	8.67E-12	1.18E-11
						0.0005	9.24E-12	1.25E-11
Pm-151	28.40 h	Y	Y	1.00	F	0.0005	1.31E-11	2.16E-11
						0.0005	4.34E-11	5.94E-11
						0.0005	4.69E-11	6.38E-11
Samarium								
Sm-141	10.2 m	Y	Y	1.00	F	0.0005	3.68E-13	4.47E-13
						0.0005	6.62E-13	7.54E-13
						0.0005	6.94E-13	7.88E-13
Sm-141m	22.6 m	Y	-	1.00	F	0.0005	6.95E-13	8.95E-13
						0.0005	1.44E-12	1.70E-12
						0.0005	1.53E-12	1.79E-12
Sm-142	72.49 m	-	-	1.00	F	0.0005	2.03E-12	2.88E-12
						0.0005	4.54E-12	5.77E-12
						0.0005	4.82E-12	6.09E-12
Sm-145	340 d	Y	Y	1.00	F	0.0005	1.35E-10	1.61E-10
						0.0005	1.05E-10	1.22E-10
						0.0005	1.38E-10	1.55E-10
Sm-146	1.03E8 y	-	Y	1.00	F	0.0005	3.37E-07	3.76E-07
						0.0005	1.95E-07	2.13E-07
						0.0005	2.73E-07	2.88E-07
Sm-147	1.06E11 y	-	Y	1.00	F	0.0005	3.06E-07	3.41E-07
						0.0005	1.69E-07	1.86E-07
						0.0005	2.38E-07	2.51E-07
Sm-151	90 y	-	Y	1.00	F	0.0005	2.31E-10	2.48E-10
						0.0005	1.23E-10	1.32E-10
						0.0005	1.23E-10	1.32E-10
Sm-153	46.7 h	-	-	1.00	F	0.0005	1.42E-11	2.32E-11
						0.0005	6.14E-11	7.96E-11
						0.0005	6.71E-11	8.63E-11
Sm-155	22.1 m	Y	-	1.00	F	0.0005	3.61E-13	4.15E-13
						0.0005	7.79E-13	8.50E-13
						0.0005	8.25E-13	8.99E-13
Sm-156	9.4 h	Y	-	1.00	F	0.0005	5.98E-12	9.13E-12
						0.0005	2.05E-11	2.62E-11
						0.0005	2.26E-11	2.86E-11

Table 2.1, continued

Nuclide	$T_{1/2}$	Chain		AMAD (μm)	Type ^a	f_1	Mortality (Bq^{-1})	Morbidity (Bq^{-1})		
		P	D							
Europium										
Eu-145	5.94 d	Y	Y	1.00	F	0.0005	2.72E-11	3.87E-11		
							M	0.0005	3.60E-11	4.89E-11
							S	0.0005	3.81E-11	5.13E-11
Eu-146	4.61 d	Y	Y	1.00	F	0.0005	3.66E-11	5.32E-11		
							M	0.0005	5.02E-11	7.01E-11
							S	0.0005	5.22E-11	7.25E-11
Eu-147	24 d	Y	Y	1.00	F	0.0005	3.56E-11	4.84E-11		
							M	0.0005	8.92E-11	1.04E-10
							S	0.0005	1.02E-10	1.18E-10
Eu-148	54.5 d	Y	-	1.00	F	0.0005	2.51E-10	3.38E-10		
							M	0.0005	2.11E-10	2.68E-10
							S	0.0005	2.29E-10	2.83E-10
Eu-149	93.1 d	-	Y	1.00	F	0.0005	2.14E-11	2.73E-11		
							M	0.0005	2.40E-11	2.89E-11
							S	0.0005	2.93E-11	3.43E-11
Eu-150b	34.2 y	-	-	1.00	F	0.0005	5.56E-09	7.14E-09		
							M	0.0005	2.38E-09	3.02E-09
							S	0.0005	2.03E-09	2.41E-09
Eu-150a	12.62 h	-	-	1.00	F	0.0005	6.59E-12	1.12E-11		
							M	0.0005	1.96E-11	2.78E-11
							S	0.0005	2.11E-11	2.96E-11
Eu-152	13.33 y	Y	-	1.00	F	0.0005	4.12E-09	5.14E-09		
							M	0.0005	2.02E-09	2.46E-09
							S	0.0005	2.15E-09	2.45E-09
Eu-152m	9.32 h	Y	-	1.00	F	0.0005	8.32E-12	1.40E-11		
							M	0.0005	2.06E-11	3.04E-11
							S	0.0005	2.20E-11	3.22E-11
Eu-154	8.8 y	-	-	1.00	F	0.0005	4.69E-09	5.71E-09		
							M	0.0005	2.65E-09	3.12E-09
							S	0.0005	3.43E-09	3.81E-09
Eu-155	4.96 y	-	Y	1.00	F	0.0005	4.48E-10	5.15E-10		
							M	0.0005	3.59E-10	4.01E-10
							S	0.0005	4.67E-10	5.08E-10
Eu-156	15.19 d	-	Y	1.00	F	0.0005	9.98E-11	1.40E-10		
							M	0.0005	3.07E-10	3.70E-10
							S	0.0005	3.48E-10	4.15E-10
Eu-157	15.15 h	-	-	1.00	F	0.0005	1.05E-11	1.76E-11		
							M	0.0005	2.96E-11	4.23E-11
							S	0.0005	3.18E-11	4.50E-11
Eu-158	45.9 m	-	-	1.00	F	0.0005	1.07E-12	1.38E-12		
							M	0.0005	2.54E-12	2.97E-12
							S	0.0005	2.70E-12	3.14E-12

Table 2.1, continued

Nuclide	$T_{1/2}$	Chain		AMAD (μm)	Type ^a	f_1	Mortality (Bq^{-1})	Morbidity (Bq^{-1})
		P	D					
Gadolinium								
Gd-145	22.9 m	Y	-	1.00	F	0.0005	4.87E-13	6.25E-13
						0.0005	8.22E-13	9.80E-13
						0.0005	8.62E-13	1.02E-12
Gd-146	48.3 d	Y	-	1.00	F	0.0005	2.83E-10	3.75E-10
						0.0005	5.32E-10	6.13E-10
						0.0005	6.30E-10	7.15E-10
Gd-147	38.1 h	Y	Y	1.00	F	0.0005	1.27E-11	1.94E-11
						0.0005	2.66E-11	3.62E-11
						0.0005	2.87E-11	3.86E-11
Gd-148	93 y	-	-	1.00	F	0.0005	2.99E-07	3.41E-07
						0.0005	2.39E-07	2.61E-07
						0.0005	3.92E-07	4.13E-07
Gd-149	9.4 d	Y	Y	1.00	F	0.0005	1.80E-11	2.58E-11
						0.0005	6.28E-11	7.47E-11
						0.0005	7.08E-11	8.33E-11
Gd-151	120 d	Y	Y	1.00	F	0.0005	3.85E-11	4.73E-11
						0.0005	6.90E-11	7.89E-11
						0.0005	8.88E-11	9.97E-11
Gd-152	1.08E14 y	-	Y	1.00	F	0.0005	2.16E-07	2.46E-07
						0.0005	1.30E-07	1.44E-07
						0.0005	2.20E-07	2.32E-07
Gd-153	242 d	-	Y	1.00	F	0.0005	1.03E-10	1.25E-10
						0.0005	1.57E-10	1.77E-10
						0.0005	2.09E-10	2.32E-10
Gd-159	18.56 h	-	-	1.00	F	0.0005	9.31E-12	1.59E-11
						0.0005	2.83E-11	3.94E-11
						0.0005	3.04E-11	4.21E-11
Terbium								
Tb-147	1.65 h	Y	-	1.00	F	0.0005	2.17E-12	3.26E-12
						0.0005	4.58E-12	6.11E-12
						0.0005	4.87E-12	6.45E-12
Tb-149	4.15 h	Y	-	1.00	F	0.0005	3.45E-11	4.22E-11
						0.0005	4.20E-10	4.45E-10
						0.0005	4.63E-10	4.90E-10
Tb-150	3.27 h	-	-	1.00	F	0.0005	3.61E-12	5.77E-12
						0.0005	7.30E-12	1.05E-11
						0.0005	7.71E-12	1.10E-11
Tb-151	17.6 h	Y	-	1.00	F	0.0005	5.68E-12	9.04E-12
						0.0005	1.56E-11	2.09E-11
						0.0005	1.68E-11	2.24E-11

Table 2.1, continued

Nuclide	T _{1/2}	Chain		AMAD (μm)	Type ^a f ₁	Mortality (Bq ⁻¹)	Morbidity (Bq ⁻¹)
		P	D				
Terbium, continued							
Tb-153	2.34 d	Y	-	1.00	F 0.0005	5.94E-12	9.11E-12
					M 0.0005	1.70E-11	2.21E-11
					S 0.0005	1.89E-11	2.42E-11
Tb-154	21.4 h	-	-	1.00	F 0.0005	1.06E-11	1.67E-11
					M 0.0005	2.16E-11	3.07E-11
					S 0.0005	2.29E-11	3.23E-11
Tb-155	5.32 d	-	Y	1.00	F 0.0005	5.34E-12	8.13E-12
					M 0.0005	1.96E-11	2.43E-11
					S 0.0005	2.17E-11	2.66E-11
Tb-156	5.34 d	-	Y	1.00	F 0.0005	3.30E-11	4.90E-11
					M 0.0005	9.08E-11	1.14E-10
					S 0.0005	9.91E-11	1.23E-10
Tb-156m	24.4 h	Y	-	1.00	F 0.0005	6.17E-12	9.09E-12
					M 0.0005	1.87E-11	2.29E-11
					S 0.0005	2.05E-11	2.49E-11
Tb-156n	5.0 h	Y	-	1.00	F 0.0005	2.07E-12	3.12E-12
					M 0.0005	8.45E-12	1.02E-11
					S 0.0005	9.23E-12	1.11E-11
Tb-157	150 y	-	Y	1.00	F 0.0005	7.82E-11	8.65E-11
					M 0.0005	3.55E-11	3.95E-11
					S 0.0005	3.68E-11	4.02E-11
Tb-158	150 y	-	-	1.00	F 0.0005	3.77E-09	4.63E-09
					M 0.0005	1.87E-09	2.24E-09
					S 0.0005	2.00E-09	2.26E-09
Tb-160	72.3 d	-	-	1.00	F 0.0005	2.39E-10	3.07E-10
					M 0.0005	5.83E-10	6.63E-10
					S 0.0005	7.23E-10	8.11E-10
Tb-161	6.91 d	-	-	1.00	F 0.0005	1.99E-11	3.06E-11
					M 0.0005	1.15E-10	1.36E-10
					S 0.0005	1.29E-10	1.52E-10
Dysprosium							
Dy-155	10.0 h	Y	Y	1.00	F 0.0005	2.06E-12	3.29E-12
					M 0.0005	4.78E-12	6.62E-12
					S 0.0005	5.12E-12	7.03E-12
Dy-157	8.1 h	Y	Y	1.00	F 0.0005	8.54E-13	1.37E-12
					M 0.0005	1.52E-12	2.25E-12
					S 0.0005	1.59E-12	2.35E-12
Dy-159	144.4 d	-	Y	1.00	F 0.0005	2.16E-11	2.70E-11
					M 0.0005	2.93E-11	3.45E-11
					S 0.0005	3.94E-11	4.52E-11

Table 2.1, continued

Nuclide	$T_{1/2}$	Chain		AMAD (μm)	Type ^a	f_1	Mortality (Bq^{-1})	Morbidity (Bq^{-1})
		P	D					
Dysprosium, continued								
Dy-165	2.334 h	-	-	1.00	F	0.0005	1.52E-12	2.35E-12
						0.0005	4.45E-12	5.68E-12
						0.0005	4.77E-12	6.05E-12
Dy-166	81.6 h	Y	-	1.00	F	0.0005	4.37E-11	6.89E-11
						0.0005	1.80E-10	2.26E-10
						0.0005	1.99E-10	2.47E-10
Holmium								
Ho-155	48 m	Y	-	1.00	F	0.0005	5.52E-13	7.73E-13
						0.0005	1.15E-12	1.43E-12
						0.0005	1.21E-12	1.51E-12
Ho-157	12.6 m	Y	-	1.00	F	0.0005	9.92E-14	1.26E-13
						0.0005	1.65E-13	1.99E-13
						0.0005	1.72E-13	2.07E-13
Ho-159	33 m	Y	-	1.00	F	0.0005	1.33E-13	1.68E-13
						0.0005	2.88E-13	3.29E-13
						0.0005	3.05E-13	3.47E-13
Ho-161	2.5 h	-	Y	1.00	F	0.0005	1.92E-13	2.94E-13
						0.0005	3.91E-13	5.34E-13
						0.0005	4.12E-13	5.60E-13
Ho-162	15 m	-	Y	1.00	F	0.0005	6.79E-14	7.64E-14
						0.0005	1.34E-13	1.46E-13
						0.0005	1.42E-13	1.53E-13
Ho-162m	68 m	Y	-	1.00	F	0.0005	4.02E-13	5.50E-13
						0.0005	1.18E-12	1.40E-12
						0.0005	1.27E-12	1.49E-12
Ho-164	29 m	-	Y	1.00	F	0.0005	1.59E-13	1.84E-13
						0.0005	4.10E-13	4.46E-13
						0.0005	4.38E-13	4.75E-13
Ho-164m	37.5 m	Y	-	1.00	F	0.0005	2.41E-13	3.14E-13
						0.0005	8.33E-13	9.41E-13
						0.0005	8.98E-13	1.01E-12
Ho-166	26.80 h	-	Y	1.00	F	0.0005	3.79E-11	6.07E-11
						0.0005	7.14E-11	1.04E-10
						0.0005	7.53E-11	1.09E-10
Ho-166m	1.20E3 y	-	-	1.00	F	0.0005	1.56E-08	2.06E-08
						0.0005	6.42E-09	8.34E-09
						0.0005	3.53E-09	4.15E-09
Ho-167	3.1 h	-	-	1.00	F	0.0005	1.53E-12	2.30E-12
						0.0005	4.89E-12	6.09E-12
						0.0005	5.26E-12	6.51E-12

Table 2.1, continued

Nuclide	$T_{1/2}$	Chain		AMAD (μm)	Type ^a f_1	Mortality (Bq^{-1})	Morbidity (Bq^{-1})
		P	D				
Erbium							
Er-161	3.24 h	Y	-	1.00	F 0.0005	1.17E-12	1.84E-12
					M 0.0005	2.62E-12	3.62E-12
					S 0.0005	2.78E-12	3.81E-12
Er-165	10.36 h	-	-	1.00	F 0.0005	2.88E-13	4.80E-13
					M 0.0005	5.54E-13	8.46E-13
					S 0.0005	5.83E-13	8.87E-13
Er-169	9.3 d	-	-	1.00	F 0.0005	1.17E-11	1.77E-11
					M 0.0005	9.08E-11	1.04E-10
					S 0.0005	1.04E-10	1.18E-10
Er-171	7.52 h	Y	-	1.00	F 0.0005	6.30E-12	1.05E-11
					M 0.0005	1.86E-11	2.54E-11
					S 0.0005	2.00E-11	2.71E-11
Er-172	49.3 h	Y	-	1.00	F 0.0005	2.52E-11	3.94E-11
					M 0.0005	1.03E-10	1.28E-10
					S 0.0005	1.13E-10	1.40E-10
Thulium							
Tm-162	21.7 m	-	Y	1.00	F 0.0005	3.42E-13	4.21E-13
					M 0.0005	6.42E-13	7.36E-13
					S 0.0005	6.75E-13	7.70E-13
Tm-166	7.70 h	-	Y	1.00	F 0.0005	4.11E-12	6.56E-12
					M 0.0005	1.01E-11	1.39E-11
					S 0.0005	1.08E-11	1.47E-11
Tm-167	9.24 d	-	Y	1.00	F 0.0005	1.75E-11	2.60E-11
					M 0.0005	1.01E-10	1.18E-10
					S 0.0005	1.15E-10	1.33E-10
Tm-170	128.6 d	-	-	1.00	F 0.0005	2.20E-10	2.54E-10
					M 0.0005	5.92E-10	6.57E-10
					S 0.0005	8.21E-10	8.99E-10
Tm-171	1.92 y	-	Y	1.00	F 0.0005	7.51E-11	8.53E-11
					M 0.0005	8.14E-11	9.00E-11
					S 0.0005	1.09E-10	1.18E-10
Tm-172	63.6 h	-	Y	1.00	F 0.0005	3.57E-11	5.86E-11
					M 0.0005	1.12E-10	1.52E-10
					S 0.0005	1.22E-10	1.63E-10
Tm-173	8.24 h	-	-	1.00	F 0.0005	5.23E-12	8.74E-12
					M 0.0005	1.51E-11	2.09E-11
					S 0.0005	1.62E-11	2.23E-11
Tm-175	15.2 m	Y	-	1.00	F 0.0005	3.70E-13	4.38E-13
					M 0.0005	7.86E-13	8.81E-13
					S 0.0005	8.35E-13	9.33E-13

Table 2.1, continued

Nuclide	$T_{1/2}$	Chain		AMAD (μm)	Type ^a	f_1	Mortality (Bq^{-1})	Morbidity (Bq^{-1})
		P	D					
Ytterbium								
Yb-162	18.9 m	Y	-	1.00	F	0.0005	2.84E-13	3.80E-13
						0.0005	6.53E-13	7.68E-13
						0.0005	6.93E-13	8.11E-13
Yb-166	56.7 h	Y	-	1.00	F	0.0005	1.98E-11	3.21E-11
						0.0005	5.52E-11	7.31E-11
						0.0005	5.97E-11	7.82E-11
Yb-167	17.5 m	Y	-	1.00	F	0.0005	1.41E-13	1.71E-13
						0.0005	3.83E-13	4.28E-13
						0.0005	4.15E-13	4.62E-13
Yb-169	32.01 d	-	Y	1.00	F	0.0005	3.91E-11	5.42E-11
						0.0005	2.18E-10	2.47E-10
						0.0005	2.61E-10	2.92E-10
Yb-175	4.19 d	-	Y	1.00	F	0.0005	1.12E-11	1.85E-11
						0.0005	6.02E-11	7.26E-11
						0.0005	6.68E-11	7.98E-11
Yb-177	1.9 h	Y	-	1.00	F	0.0005	1.46E-12	2.23E-12
						0.0005	4.67E-12	5.75E-12
						0.0005	5.06E-12	6.18E-12
Yb-178	74 m	Y	-	1.00	F	0.0005	1.65E-12	2.51E-12
						0.0005	4.92E-12	6.04E-12
						0.0005	5.28E-12	6.43E-12
Lutetium								
Lu-169	34.06 h	Y	-	1.00	F	0.0005	9.19E-12	1.44E-11
						0.0005	2.51E-11	3.27E-11
						0.0005	2.79E-11	3.59E-11
Lu-170	2.00 d	-	Y	1.00	F	0.0005	1.85E-11	2.95E-11
						0.0005	4.17E-11	5.76E-11
						0.0005	4.46E-11	6.09E-11
Lu-171	8.22 d	-	-	1.00	F	0.0005	1.97E-11	2.98E-11
						0.0005	7.01E-11	8.59E-11
						0.0005	7.81E-11	9.46E-11
Lu-172	6.70 d	-	Y	1.00	F	0.0005	3.45E-11	5.25E-11
						0.0005	1.21E-10	1.49E-10
						0.0005	1.34E-10	1.63E-10
Lu-173	1.37 y	-	Y	1.00	F	0.0005	1.38E-10	1.69E-10
						0.0005	1.41E-10	1.63E-10
						0.0005	2.09E-10	2.35E-10
Lu-174	3.31 y	-	Y	1.00	F	0.0005	2.62E-10	3.14E-10
						0.0005	2.41E-10	2.74E-10
						0.0005	3.46E-10	3.84E-10

Table 2.1, continued

Nuclide	$T_{1/2}$	Chain		AMAD (μm)	Type ^a	f_1	Mortality (Bq^{-1})	Morbidity (Bq^{-1})
		P	D					
Lutetium, continued								
Lu-174m	142 d	Y	-	1.00	F	0.0005	1.20E-10	1.42E-10
						0.0005	2.83E-10	3.14E-10
						0.0005	3.73E-10	4.09E-10
Lu-176	3.60E10 y	-	-	1.00	F	0.0005	4.12E-09	4.74E-09
						0.0005	2.51E-09	2.83E-09
						0.0005	3.48E-09	3.80E-09
Lu-176m	3.68 h	-	-	1.00	F	0.0005	2.98E-12	4.86E-12
						0.0005	8.77E-12	1.15E-11
						0.0005	9.42E-12	1.23E-11
Lu-177	6.71 d	-	Y	1.00	F	0.0005	1.51E-11	2.37E-11
						0.0005	9.63E-11	1.13E-10
						0.0005	1.08E-10	1.26E-10
Lu-177m	160.9 d	Y	-	1.00	F	0.0005	4.04E-10	5.04E-10
						0.0005	1.05E-09	1.17E-09
						0.0005	1.40E-09	1.54E-09
Lu-178	28.4 m	-	Y	1.00	F	0.0005	5.49E-13	6.62E-13
						0.0005	1.22E-12	1.36E-12
						0.0005	1.30E-12	1.43E-12
Lu-178m	22.7 m	-	-	1.00	F	0.0005	6.10E-13	7.13E-13
						0.0005	1.36E-12	1.49E-12
						0.0005	1.44E-12	1.58E-12
Lu-179	4.59 h	-	-	1.00	F	0.0005	3.72E-12	6.20E-12
						0.0005	9.52E-12	1.31E-11
						0.0005	1.02E-11	1.39E-11
Hafnium								
Hf-170	16.01 h	Y	-	1.00	F	0.002	8.84E-12	1.41E-11
						0.002	2.39E-11	3.23E-11
						0.002	2.57E-11	3.44E-11
Hf-172	1.87 y	Y	Y	1.00	F	0.002	1.47E-09	1.87E-09
						0.002	1.27E-09	1.50E-09
						0.002	2.00E-09	2.28E-09
Hf-173	24.0 h	Y	Y	1.00	F	0.002	3.75E-12	5.98E-12
						0.002	1.21E-11	1.60E-11
						0.002	1.32E-11	1.73E-11
Hf-175	70 d	-	Y	1.00	F	0.002	4.34E-11	5.86E-11
						0.002	9.84E-11	1.16E-10
						0.002	1.25E-10	1.45E-10
Hf-177m	51.4 m	-	-	1.00	F	0.002	1.37E-12	1.71E-12
						0.002	4.32E-12	4.89E-12
						0.002	4.65E-12	5.24E-12

Table 2.1, continued

Nuclide	$T_{1/2}$	Chain		AMAD (μm)	Type ^a	f_1	Mortality (Bq^{-1})	Morbidity (Bq^{-1})	
		P	D						
Hafnium, continued									
Hf-178m	31 y	-	-	1.00	F	0.002	8.12E-09	1.00E-08	
						M	0.002	4.35E-09	5.21E-09
						S	0.002	5.17E-09	5.88E-09
Hf-179m	25.1 d	-	-	1.00	F	0.002	6.49E-11	9.26E-11	
						M	0.002	3.26E-10	3.72E-10
						S	0.002	3.84E-10	4.34E-10
Hf-180m	5.5 h	-	-	1.00	F	0.002	2.42E-12	3.78E-12	
						M	0.002	8.71E-12	1.12E-11
						S	0.002	9.41E-12	1.20E-11
Hf-181	42.4 d	-	-	1.00	F	0.002	7.85E-11	1.07E-10	
						M	0.002	4.26E-10	4.77E-10
						S	0.002	5.19E-10	5.75E-10
Hf-182	9E6 y	Y	Y	1.00	F	0.002	7.72E-09	9.22E-09	
						M	0.002	3.50E-09	4.12E-09
						S	0.002	3.74E-09	4.19E-09
Hf-182m	61.5 m	Y	-	1.00	F	0.002	7.42E-13	9.45E-13	
						M	0.002	2.48E-12	2.82E-12
						S	0.002	2.71E-12	3.06E-12
Hf-183	64 m	Y	-	1.00	F	0.002	1.06E-12	1.49E-12	
						M	0.002	3.74E-12	4.46E-12
						S	0.002	4.07E-12	4.83E-12
Hf-184	4.12 h	Y	-	1.00	F	0.002	8.12E-12	1.34E-11	
						M	0.002	2.73E-11	3.72E-11
						S	0.002	2.95E-11	3.99E-11
Tantalum									
Ta-172	36.8 m	Y	-	1.00	F	0.001	6.64E-13	8.33E-13	
						M	0.001	1.57E-12	1.80E-12
						S	0.001	1.70E-12	1.95E-12
Ta-173	3.65 h	Y	-	1.00	F	0.001	2.79E-12	4.46E-12	
						M	0.001	8.32E-12	1.12E-11
						S	0.001	8.96E-12	1.20E-11
Ta-174	1.2 h	-	-	1.00	F	0.001	7.68E-13	1.03E-12	
						M	0.001	2.37E-12	2.80E-12
						S	0.001	2.55E-12	2.99E-12
Ta-175	10.5 h	Y	-	1.00	F	0.001	3.11E-12	4.95E-12	
						M	0.001	7.95E-12	1.10E-11
						S	0.001	8.63E-12	1.18E-11
Ta-176	8.08 h	-	Y	1.00	F	0.001	4.38E-12	6.95E-12	
						M	0.001	1.10E-11	1.52E-11
						S	0.001	1.17E-11	1.61E-11

Table 2.1, continued

Nuclide	$T_{1/2}$	Chain		AMAD (μm)	Type ^a	f_1	Mortality (Bq^{-1})	Morbidity (Bq^{-1})
		P	D					
Tantalum, continued								
Ta-177	56.6 h	-	Y	1.00	F	0.001	2.09E-12	3.43E-12
						0.001	8.74E-12	1.11E-11
						0.001	9.57E-12	1.20E-11
Ta-178b	2.2 h	-	-	1.00	F	0.001	1.06E-12	1.53E-12
						0.001	3.72E-12	4.52E-12
						0.001	4.01E-12	4.85E-12
Ta-179	664.9 d	-	Y	1.00	F	0.001	7.78E-12	1.15E-11
						0.001	1.94E-11	2.34E-11
						0.001	4.85E-11	5.55E-11
Ta-180	1.0E13 y	-	-	1.00	F	0.001	1.19E-10	1.75E-10
						0.001	5.49E-10	6.23E-10
						0.001	1.76E-09	1.96E-09
Ta-180m	8.1 h	-	-	1.00	F	0.001	8.61E-13	1.41E-12
						0.001	3.60E-12	4.66E-12
						0.001	3.91E-12	5.02E-12
Ta-182	115.0 d	-	Y	1.00	F	0.001	1.38E-10	2.06E-10
						0.001	6.59E-10	7.49E-10
						0.001	9.05E-10	1.01E-09
Ta-182m	15.84 m	Y	-	1.00	F	0.001	3.52E-13	3.89E-13
						0.001	7.93E-13	8.51E-13
						0.001	8.59E-13	9.21E-13
Ta-183	5.1 d	-	Y	1.00	F	0.001	3.28E-11	5.36E-11
						0.001	1.79E-10	2.16E-10
						0.001	2.00E-10	2.38E-10
Ta-184	8.7 h	-	Y	1.00	F	0.001	1.02E-11	1.68E-11
						0.001	3.19E-11	4.38E-11
						0.001	3.43E-11	4.68E-11
Ta-185	49 m	Y	-	1.00	F	0.001	8.72E-13	1.09E-12
						0.001	2.61E-12	2.97E-12
						0.001	2.83E-12	3.20E-12
Ta-186	10.5 m	-	-	1.00	F	0.001	3.94E-13	4.46E-13
						0.001	6.39E-13	7.00E-13
						0.001	6.66E-13	7.28E-13
Tungsten								
W-176	2.3 h	Y	-	1.00	F	0.3	1.99E-12	3.34E-12
						0.3	4.14E-12	5.60E-12
						0.3	4.38E-12	5.86E-12
W-177	135 m	Y	Y	1.00	F	0.3	1.03E-12	1.62E-12
						0.3	2.58E-12	3.24E-12
						0.3	2.76E-12	3.42E-12

Table 2.1, continued

Nuclide	$T_{1/2}$	Chain		AMAD (μm)	Type ^a f_1	Mortality (Bq^{-1})	Morbidity (Bq^{-1})
		P	D				
Tungsten, continued							
W-178	21.7 d	-	Y	1.00	F 0.3	5.93E-12	1.04E-11
					M 0.3	5.74E-11	6.53E-11
					S 0.3	6.80E-11	7.66E-11
W-179	37.5 m	Y	-	1.00	F 0.3	3.57E-14	4.94E-14
					M 0.3	6.05E-14	7.34E-14
					S 0.3	6.44E-14	7.73E-14
W-181	121.2 d	-	Y	1.00	F 0.3	2.14E-12	3.65E-12
					M 0.3	1.58E-11	1.88E-11
					S 0.3	2.47E-11	2.88E-11
W-185	75.1 d	-	Y	1.00	F 0.3	1.43E-11	2.53E-11
					M 0.3	2.60E-10	2.85E-10
					S 0.3	3.40E-10	3.68E-10
W-187	23.9 h	Y	-	1.00	F 0.3	1.69E-11	2.99E-11
					M 0.3	3.82E-11	5.19E-11
					S 0.3	4.07E-11	5.45E-11
W-188	69.4 d	Y	-	1.00	F 0.3	7.02E-11	1.25E-10
					M 0.3	9.86E-10	1.10E-09
					S 0.3	1.37E-09	1.50E-09
Rhenium							
Re-177	14.0 m	Y	-	1.00	F 0.8	3.49E-13	5.14E-13
					M 0.8	6.86E-13	8.03E-13
					S 0.8	7.24E-13	8.35E-13
Re-178	13.2 m	Y	-	1.00	F 0.8	3.35E-13	4.39E-13
					M 0.8	5.66E-13	6.31E-13
					S 0.8	5.94E-13	6.54E-13
Re-181	20 h	Y	Y	1.00	F 0.8	7.69E-12	1.45E-11
					M 0.8	1.57E-11	2.15E-11
					S 0.8	1.67E-11	2.24E-11
Re-182b	64.0 h	-	-	1.00	F 0.8	3.06E-11	5.37E-11
					M 0.8	9.73E-11	1.20E-10
					S 0.8	1.06E-10	1.28E-10
Re-182a	12.7 h	-	Y	1.00	F 0.8	4.85E-12	8.94E-12
					M 0.8	1.13E-11	1.49E-11
					S 0.8	1.21E-11	1.56E-11
Re-184	38.0 d	-	Y	1.00	F 0.8	2.21E-11	3.61E-11
					M 0.8	1.57E-10	1.82E-10
					S 0.8	1.94E-10	2.23E-10
Re-184m	165 d	Y	-	1.00	F 0.8	3.41E-11	5.65E-11
					M 0.8	5.49E-10	6.11E-10
					S 0.8	8.56E-10	9.48E-10

Table 2.1, continued

Nuclide	$T_{1/2}$	Chain		AMAD (μm)	Type ^a f_1	Mortality (Bq^{-1})	Morbidity (Bq^{-1})
		P	D				
Rhenium, continued							
Re-186	90.64 h	-	Y	1.00	F 0.8	3.28E-11	6.03E-11
					M 0.8	9.07E-11	1.15E-10
					S 0.8	9.85E-11	1.22E-10
Re-186m	2.0E5 y	Y	-	1.00	F 0.8	5.45E-11	8.73E-11
					M 0.8	1.04E-09	1.13E-09
					S 0.8	4.23E-09	4.49E-09
Re-187	5E10 y	-	Y	1.00	F 0.8	1.20E-13	2.04E-13
					M 0.8	5.71E-13	6.78E-13
					S 0.8	2.96E-12	3.19E-12
Re-188	16.98 h	-	Y	1.00	F 0.8	2.41E-11	4.98E-11
					M 0.8	4.02E-11	6.01E-11
					S 0.8	4.20E-11	6.12E-11
Re-188m	18.6 m	Y	-	1.00	F 0.8	5.58E-13	1.06E-12
					M 0.8	9.82E-13	1.37E-12
					S 0.8	1.03E-12	1.41E-12
Re-189	24.3 h	Y	-	1.00	F 0.8	1.49E-11	2.96E-11
					M 0.8	3.47E-11	4.68E-11
					S 0.8	3.70E-11	4.88E-11
Osmium							
Os-180	22 m	-	-	1.00	F 0.01	2.61E-13	3.19E-13
					M 0.01	5.93E-13	6.70E-13
					S 0.01	6.30E-13	7.08E-13
Os-181	105 m	Y	-	1.00	F 0.01	1.40E-12	2.18E-12
					M 0.01	3.78E-12	4.96E-12
					S 0.01	4.05E-12	5.27E-12
Os-182	22 h	Y	Y	1.00	F 0.01	9.93E-12	1.63E-11
					M 0.01	2.70E-11	3.67E-11
					S 0.01	2.90E-11	3.91E-11
Os-185	94 d	-	Y	1.00	F 0.01	7.91E-11	1.13E-10
					M 0.01	1.06E-10	1.32E-10
					S 0.01	1.38E-10	1.66E-10
Os-189m	6.0 h	-	Y	1.00	F 0.01	2.88E-13	4.95E-13
					M 0.01	5.67E-13	8.86E-13
					S 0.01	5.97E-13	9.29E-13
Os-191	15.4 d	-	Y	1.00	F 0.01	2.01E-11	3.21E-11
					M 0.01	1.47E-10	1.68E-10
					S 0.01	1.71E-10	1.92E-10
Os-191m	13.03 h	Y	-	1.00	F 0.01	2.17E-12	3.62E-12
					M 0.01	1.30E-11	1.55E-11
					S 0.01	1.45E-11	1.72E-11

Table 2.1, continued

Nuclide	$T_{1/2}$	Chain		AMAD (μm)	Type ^a	f_1	Mortality (Bq^{-1})	Morbidity (Bq^{-1})
		P	D					
Osmium, continued								
Os-193	30.0 h	-	-	1.00	F	0.01	1.57E-11	2.72E-11
						0.01	4.95E-11	6.84E-11
						0.01	5.35E-11	7.32E-11
Os-194	6.0 y	Y	-	1.00	F	0.01	6.09E-10	8.77E-10
						0.01	1.79E-09	2.02E-09
						0.01	6.45E-09	6.88E-09
Iridium								
Ir-182	15 m	Y	-	1.00	F	0.01	5.63E-13	7.10E-13
						0.01	1.10E-12	1.30E-12
						0.01	1.16E-12	1.36E-12
Ir-184	3.02 h	-	-	1.00	F	0.01	2.46E-12	3.81E-12
						0.01	6.40E-12	8.41E-12
						0.01	6.84E-12	8.92E-12
Ir-185	14.0 h	Y	-	1.00	F	0.01	4.81E-12	7.90E-12
						0.01	1.35E-11	1.82E-11
						0.01	1.46E-11	1.96E-11
Ir-186a	15.8 h	-	-	1.00	F	0.01	7.73E-12	1.26E-11
						0.01	1.96E-11	2.70E-11
						0.01	2.09E-11	2.86E-11
Ir-186b	1.75 h	-	Y	1.00	F	0.01	8.54E-13	1.25E-12
						0.01	2.26E-12	2.83E-12
						0.01	2.41E-12	3.01E-12
Ir-187	10.5 h	-	-	1.00	F	0.01	1.94E-12	3.20E-12
						0.01	5.33E-12	7.31E-12
						0.01	5.71E-12	7.77E-12
Ir-188	41.5 h	-	Y	1.00	F	0.01	1.15E-11	1.84E-11
						0.01	2.57E-11	3.53E-11
						0.01	2.74E-11	3.73E-11
Ir-189	13.3 d	Y	Y	1.00	F	0.01	8.92E-12	1.41E-11
						0.01	4.78E-11	5.58E-11
						0.01	5.47E-11	6.31E-11
Ir-190	12.1 d	-	Y	1.00	F	0.01	4.89E-11	7.43E-11
						0.01	1.80E-10	2.13E-10
						0.01	2.03E-10	2.38E-10
Ir-190n	3.1 h	Y	-	1.00	F	0.01	1.70E-12	2.61E-12
						0.01	4.13E-12	5.47E-12
						0.01	4.41E-12	5.79E-12
Ir-190m	1.2 h	Y	Y	1.00	F	0.01	2.31E-13	3.49E-13
						0.01	7.92E-13	9.47E-13
						0.01	8.91E-13	1.05E-12

Table 2.1, continued

Nuclide	$T_{1/2}$	Chain		AMAD (μm)	Type ^a	f_1	Mortality (Bq^{-1})	Morbidity (Bq^{-1})
		P	D					
Iridium, continued								
Ir-192	74.02 d	-	Y	1.00	F	0.01	1.31E-10	1.93E-10
						0.01	4.52E-10	5.18E-10
						0.01	5.80E-10	6.52E-10
Ir-192m	241. y	Y	-	1.00	F	0.01	3.24E-10	4.57E-10
						0.01	4.50E-10	5.41E-10
						0.01	2.49E-09	2.77E-09
Ir-194	19.15 h	-	Y	1.00	F	0.01	2.45E-11	4.28E-11
						0.01	5.77E-11	8.69E-11
						0.01	6.14E-11	9.18E-11
Ir-194m	171 d	-	-	1.00	F	0.01	3.92E-10	5.62E-10
						0.01	7.51E-10	8.92E-10
						0.01	1.08E-09	1.24E-09
Ir-195	2.5 h	-	Y	1.00	F	0.01	1.44E-12	2.21E-12
						0.01	4.80E-12	6.03E-12
						0.01	5.18E-12	6.45E-12
Ir-195m	3.8 h	Y	-	1.00	F	0.01	3.45E-12	5.54E-12
						0.01	1.17E-11	1.50E-11
						0.01	1.26E-11	1.61E-11
Platinum								
Pt-186	2.0 h	Y	-	1.00	F	0.01	1.38E-12	2.23E-12
						0.01	3.28E-12	4.53E-12
						0.01	3.49E-12	4.79E-12
Pt-188	10.2 d	Y	-	1.00	F	0.01	3.19E-11	5.09E-11
						0.01	1.50E-10	1.76E-10
						0.01	1.71E-10	1.98E-10
Pt-189	10.87 h	Y	-	1.00	F	0.01	2.16E-12	3.58E-12
						0.01	6.79E-12	8.94E-12
						0.01	7.41E-12	9.64E-12
Pt-191	2.8 d	-	-	1.00	F	0.01	7.49E-12	1.25E-11
						0.01	2.38E-11	3.08E-11
						0.01	2.59E-11	3.31E-11
Pt-193	50 y	-	Y	1.00	F	0.01	1.86E-12	3.01E-12
						0.01	9.56E-12	1.11E-11
						0.01	4.95E-11	5.31E-11
Pt-193m	4.33 d	Y	-	1.00	F	0.01	1.22E-11	2.09E-11
						0.01	7.92E-11	9.33E-11
						0.01	8.84E-11	1.03E-10
Pt-195m	4.02 d	-	-	1.00	F	0.01	1.66E-11	2.84E-11
						0.01	9.49E-11	1.13E-10
						0.01	1.05E-10	1.25E-10

Table 2.1, continued

Nuclide	$T_{1/2}$	Chain		AMAD (μm)	Type ^a	f_1	Mortality (Bq^{-1})	Morbidity (Bq^{-1})
		P	D					
Platinum, continued								
Pt-197	18.3 h	-	Y	1.00	F	0.01	8.19E-12	1.41E-11
						0.01	3.13E-11	4.09E-11
						0.01	3.39E-11	4.40E-11
Pt-197m	94.4 m	Y	-	1.00	F	0.01	1.50E-12	2.34E-12
						0.01	5.52E-12	6.88E-12
						0.01	5.98E-12	7.38E-12
Pt-199	30.8 m	Y	-	1.00	F	0.01	5.24E-13	6.70E-13
						0.01	1.51E-12	1.71E-12
						0.01	1.62E-12	1.84E-12
Pt-200	12.5 h	Y	-	1.00	F	0.01	2.30E-11	4.01E-11
						0.01	6.01E-11	8.66E-11
						0.01	6.43E-11	9.18E-11
Gold								
Au-193	17.65 h	Y	Y	1.00	F	0.1	2.06E-12	3.47E-12
						0.1	8.75E-12	1.14E-11
						0.1	9.52E-12	1.23E-11
Au-194	39.5 h	-	Y	1.00	F	0.1	5.93E-12	9.63E-12
						0.1	1.41E-11	2.02E-11
						0.1	1.51E-11	2.14E-11
Au-195	183 d	-	Y	1.00	F	0.1	4.70E-12	7.97E-12
						0.1	9.91E-11	1.11E-10
						0.1	1.58E-10	1.75E-10
Au-198	2.696 d	-	Y	1.00	F	0.1	1.70E-11	2.93E-11
						0.1	7.52E-11	9.89E-11
						0.1	8.25E-11	1.08E-10
Au-198m	2.30 d	Y	-	1.00	F	0.1	2.15E-11	3.66E-11
						0.1	1.58E-10	1.91E-10
						0.1	1.76E-10	2.10E-10
Au-199	3.139 d	-	Y	1.00	F	0.1	7.53E-12	1.29E-11
						0.1	6.42E-11	7.63E-11
						0.1	7.15E-11	8.44E-11
Au-200	48.4 m	-	Y	1.00	F	0.1	7.58E-13	9.91E-13
						0.1	1.87E-12	2.18E-12
						0.1	1.99E-12	2.31E-12
Au-200m	18.7 h	Y	-	1.00	F	0.1	1.58E-11	2.65E-11
						0.1	5.17E-11	7.09E-11
						0.1	5.58E-11	7.60E-11
Au-201	26.4 m	-	-	1.00	F	0.1	3.27E-13	3.83E-13
						0.1	7.70E-13	8.42E-13
						0.1	8.19E-13	8.92E-13

Table 2.1, continued

Nuclide	T _{1/2}	Chain		AMAD (μm)	Type ^a	f ₁	Mortality (Bq ⁻¹)	Morbidity (Bq ⁻¹)
		P	D					
Mercury (inorganic particulate)								
Hg-193	3.5 h	Y	Y	1.00	F	0.02	1.30E-12	2.07E-12
						0.02	5.41E-12	6.85E-12
						0.02	5.87E-12	7.39E-12
Hg-193m	11.1 h	Y	-	1.00	F	0.02	5.97E-12	9.87E-12
						0.02	1.85E-11	2.54E-11
						0.02	2.00E-11	2.71E-11
Hg-194	260 y	Y	Y	1.00	F	0.02	4.21E-10	6.07E-10
						0.02	4.14E-10	5.28E-10
						0.02	1.49E-09	1.73E-09
Hg-195	9.9 h	Y	Y	1.00	F	0.02	1.53E-12	2.51E-12
						0.02	5.87E-12	7.67E-12
						0.02	6.45E-12	8.35E-12
Hg-195m	41.6 h	Y	-	1.00	F	0.02	1.05E-11	1.77E-11
						0.02	4.97E-11	6.29E-11
						0.02	5.49E-11	6.88E-11
Hg-197	64.1 h	-	Y	1.00	F	0.02	4.63E-12	7.78E-12
						0.02	2.79E-11	3.39E-11
						0.02	3.08E-11	3.72E-11
Hg-197m	23.8 h	Y	-	1.00	F	0.02	8.54E-12	1.45E-11
						0.02	4.97E-11	6.16E-11
						0.02	5.46E-11	6.71E-11
Hg-199m	42.6 m	-	-	1.00	F	0.02	4.97E-13	5.93E-13
						0.02	1.55E-12	1.71E-12
						0.02	1.66E-12	1.83E-12
Hg-203	46.60 d	-	-	1.00	F	0.02	3.35E-11	5.24E-11
						0.02	2.08E-10	2.34E-10
						0.02	2.56E-10	2.83E-10
Mercury (organic particulate)								
Hg-193	3.5 h	Y	Y	1.00	F	0.4	1.08E-12	1.67E-12
						0.4	5.02E-12	6.14E-12
						0.4	5.47E-12	6.64E-12
Hg-193m	11.1 h	Y	-	1.00	F	0.4	4.69E-12	7.58E-12
						0.4	1.63E-11	2.14E-11
						0.4	1.77E-11	2.29E-11
Hg-194	260 y	Y	Y	1.00	F	0.4	5.04E-10	7.28E-10
						0.4	5.88E-10	7.78E-10
						0.4	1.70E-09	2.04E-09
Hg-195	9.9 h	Y	Y	1.00	F	0.4	1.24E-12	1.99E-12
						0.4	5.35E-12	6.71E-12
						0.4	5.91E-12	7.35E-12

Table 2.1, continued

Nuclide	T _{1/2}	Chain		AMAD (μm)	Type ^a f ₁	Mortality (Bq ⁻¹)	Morbidity (Bq ⁻¹)
		P	D				
Mercury (organic particulate), continued							
Hg-195m	41.6 h	Y	-	1.00	F 0.4	8.10E-12	1.33E-11
					M 0.4	4.57E-11	5.54E-11
					S 0.4	5.07E-11	6.09E-11
Hg-197	64.1 h	-	Y	1.00	F 0.4	3.56E-12	5.82E-12
					M 0.4	2.62E-11	3.07E-11
					S 0.4	2.91E-11	3.38E-11
Hg-197m	23.8 h	Y	-	1.00	F 0.4	6.39E-12	1.05E-11
					M 0.4	4.60E-11	5.47E-11
					S 0.4	5.08E-11	5.99E-11
Hg-199m	42.6 m	-	-	1.00	F 0.4	4.93E-13	5.85E-13
					M 0.4	1.54E-12	1.70E-12
					S 0.4	1.66E-12	1.82E-12
Hg-203	46.60 d	-	-	1.00	F 0.4	3.80E-11	5.81E-11
					M 0.4	2.14E-10	2.42E-10
					S 0.4	2.62E-10	2.91E-10
Mercury (vapor)							
Hg-193	3.5 h	Y	Y	-	V 1.0	9.70E-11	1.02E-10
Hg-193m	11.1 h	Y	-	-	V 1.0	2.64E-10	2.79E-10
Hg-194	260 y	Y	Y	-	V 1.0	1.41E-09	1.95E-09
Hg-195	9.9 h	Y	Y	-	V 1.0	1.21E-10	1.28E-10
Hg-195m	41.6 h	Y	-	-	V 1.0	6.96E-10	7.36E-10
Hg-197	64.1 h	-	Y	-	V 1.0	3.71E-10	3.92E-10
Hg-197m	23.8 h	Y	-	-	V 1.0	4.92E-10	5.19E-10
Hg-199m	42.6 m	-	-	-	V 1.0	1.51E-11	1.59E-11
Hg-203	46.60 d	-	-	-	V 1.0	5.94E-10	6.61E-10
Thallium							
Tl-194	33 m	Y	-	1.00	F 1.0	1.06E-13	1.38E-13
					M 1.0	1.76E-13	2.13E-13
					S 1.0	1.84E-13	2.21E-13
Tl-194m	32.8 m	Y	-	1.00	F 1.0	5.50E-13	6.75E-13
					M 1.0	1.19E-12	1.35E-12
					S 1.0	1.26E-12	1.42E-12
Tl-195	1.16 h	Y	Y	1.00	F 1.0	4.13E-13	5.63E-13
					M 1.0	1.17E-12	1.35E-12
					S 1.0	1.27E-12	1.45E-12
Tl-197	2.84 h	Y	-	1.00	F 1.0	4.57E-13	6.47E-13
					M 1.0	2.24E-12	2.50E-12
					S 1.0	2.46E-12	2.72E-12
Tl-198	5.3 h	-	Y	1.00	F 1.0	1.49E-12	2.14E-12
					M 1.0	2.49E-12	3.17E-12
					S 1.0	2.60E-12	3.29E-12

Table 2.1, continued

Nuclide	$T_{1/2}$	Chain		AMAD (μm)	Type ^a f_1	Mortality (Bq^{-1})	Morbidity (Bq^{-1})
		P	D				
Thallium, continued							
Tl-198m	1.87 h	Y	-	1.00	F 1.0	9.92E-13	1.33E-12
					M 1.0	3.03E-12	3.45E-12
					S 1.0	3.26E-12	3.69E-12
Tl-199	7.42 h	-	Y	1.00	F 1.0	5.51E-13	7.81E-13
					M 1.0	2.62E-12	2.93E-12
					S 1.0	2.85E-12	3.17E-12
Tl-200	26.1 h	-	Y	1.00	F 1.0	4.57E-12	6.82E-12
					M 1.0	8.24E-12	1.05E-11
					S 1.0	8.68E-12	1.10E-11
Tl-201	3.044 d	-	Y	1.00	F 1.0	2.55E-12	4.02E-12
					M 1.0	1.50E-11	1.69E-11
					S 1.0	1.66E-11	1.85E-11
Tl-202	12.23 d	-	Y	1.00	F 1.0	1.08E-11	1.66E-11
					M 1.0	2.64E-11	3.32E-11
					S 1.0	2.94E-11	3.63E-11
Tl-204	3.779 y	-	-	1.00	F 1.0	3.99E-11	6.62E-11
					M 1.0	5.60E-10	6.13E-10
					S 1.0	1.53E-09	1.64E-09
Lead							
Pb-195m	15.8 m	Y	-	1.00	F 0.2	4.82E-13	5.79E-13
					*M 0.1	1.04E-12	1.18E-12
					S 0.01	1.11E-12	1.25E-12
Pb-198	2.4 h	Y	-	1.00	F 0.2	1.24E-12	1.84E-12
					*M 0.1	2.94E-12	3.87E-12
					S 0.01	3.15E-12	4.14E-12
Pb-199	90 m	Y	-	1.00	F 0.2	6.42E-13	9.36E-13
					*M 0.1	1.57E-12	2.01E-12
					S 0.01	1.68E-12	2.14E-12
Pb-200	21.5 h	Y	Y	1.00	F 0.2	6.82E-12	1.06E-11
					*M 0.1	2.41E-11	3.14E-11
					S 0.01	2.64E-11	3.45E-11
Pb-201	9.4 h	Y	Y	1.00	F 0.2	2.27E-12	3.55E-12
					*M 0.1	7.01E-12	9.47E-12
					S 0.01	7.70E-12	1.04E-11
Pb-202	3E5 y	Y	Y	1.00	F 0.2	4.73E-10	6.23E-10
					*M 0.1	3.08E-10	3.86E-10
					S 0.01	7.70E-10	8.91E-10
Pb-202m	3.62 h	Y	Y	1.00	F 0.2	1.82E-12	2.71E-12
					*M 0.1	4.56E-12	6.08E-12
					S 0.01	4.92E-12	6.55E-12

Table 2.1, continued

Nuclide	$T_{1/2}$	Chain		AMAD (μm)	Type ^a	f_1	Mortality (Bq^{-1})	Morbidity (Bq^{-1})
		P	D					
Lead, continued								
Pb-203	52.05 h	-	Y	1.00	F	0.2	4.26E-12	6.69E-12
					*M	0.1	1.55E-11	2.04E-11
					S	0.01	1.72E-11	2.26E-11
Pb-205	1.43E7 y	-	Y	1.00	F	0.2	1.31E-11	1.53E-11
					*M	0.1	1.54E-11	1.74E-11
					S	0.01	5.96E-11	6.37E-11
Pb-209	3.253 h	-	Y	1.00	F	0.2	8.81E-13	1.31E-12
					*M	0.1	4.18E-12	5.13E-12
					S	0.01	4.58E-12	5.62E-12
Pb-210	22.3 y	Y	Y	1.00	F	0.2	1.82E-08	2.47E-08
					*M	0.1	6.84E-08	7.48E-08
					S	0.01	4.06E-07	4.28E-07
Pb-211	36.1 m	-	Y	1.00	F	0.2	2.08E-10	2.24E-10
					*M	0.1	9.51E-10	1.00E-09
					S	0.01	1.03E-09	1.09E-09
Pb-212	10.64 h	Y	Y	1.00	F	0.2	3.83E-10	5.42E-10
					*M	0.1	1.48E-08	1.56E-08
					S	0.01	1.64E-08	1.73E-08
Pb-214	26.8 m	Y	Y	1.00	F	0.2	1.13E-10	1.24E-10
					*M	0.1	9.31E-10	9.81E-10
					S	0.01	1.02E-09	1.08E-09
Bismuth								
Bi-200	36.4 m	Y	-	1.00	F	0.05	8.60E-13	1.31E-12
					M	0.05	1.60E-12	2.04E-12
					S	0.05	1.68E-12	2.12E-12
Bi-201	108 m	Y	-	1.00	F	0.05	2.15E-12	3.48E-12
					M	0.05	3.81E-12	5.14E-12
					S	0.05	4.00E-12	5.33E-12
Bi-202	1.67 h	Y	-	1.00	F	0.05	1.50E-12	2.30E-12
					M	0.05	2.25E-12	3.02E-12
					S	0.05	2.33E-12	3.09E-12
Bi-203	11.76 h	Y	Y	1.00	F	0.05	8.98E-12	1.49E-11
					M	0.05	1.54E-11	2.22E-11
					S	0.05	1.62E-11	2.30E-11
Bi-205	15.31 d	Y	Y	1.00	F	0.05	2.03E-11	3.32E-11
					M	0.05	6.75E-11	8.77E-11
					S	0.05	7.73E-11	9.89E-11
Bi-206	6.243 d	-	-	1.00	F	0.05	4.21E-11	7.00E-11
					M	0.05	1.22E-10	1.58E-10
					S	0.05	1.34E-10	1.71E-10

Table 2.1, continued

Nuclide	T _{1/2}	Chain		AMAD (μm)	Type ^a f ₁	Mortality (Bq ⁻¹)	Morbidity (Bq ⁻¹)
		P	D				
Bismuth, continued							
Bi-207	38 y	-	Y	1.00	F 0.05	3.35E-11	5.62E-11
					M 0.05	4.82E-10	5.68E-10
					S 0.05	2.60E-09	2.97E-09
Bi-210	5.012 d	Y	Y	1.00	F 0.05	5.85E-11	9.92E-11
					M 0.05	8.10E-09	8.56E-09
					S 0.05	1.16E-08	1.23E-08
Bi-210m	3.0E6 y	-	-	1.00	F 0.05	1.61E-09	2.43E-09
					M 0.05	3.00E-07	3.17E-07
					S 0.05	7.50E-07	7.90E-07
Bi-212	60.55 m	-	Y	1.00	F 0.05	3.71E-10	4.06E-10
					M 0.05	1.99E-09	2.10E-09
					S 0.05	2.17E-09	2.28E-09
Bi-213	45.65 m	Y	Y	1.00	F 0.05	3.95E-10	4.28E-10
					M 0.05	1.75E-09	1.85E-09
					S 0.05	1.90E-09	2.01E-09
Bi-214	19.9 m	Y	Y	1.00	F 0.05	2.86E-10	3.05E-10
					M 0.05	7.45E-10	7.84E-10
					S 0.05	7.96E-10	8.38E-10
Polonium							
Po-203	36.7 m	Y	-	1.00	F 0.1	7.71E-13	1.10E-12
					*M 0.1	1.60E-12	2.09E-12
					S 0.01	1.72E-12	2.24E-12
Po-205	1.80 h	Y	-	1.00	F 0.1	1.27E-12	1.76E-12
					*M 0.1	3.97E-12	4.66E-12
					S 0.01	4.28E-12	5.00E-12
Po-207	350 m	Y	Y	1.00	F 0.1	2.00E-12	3.08E-12
					*M 0.1	3.71E-12	5.37E-12
					S 0.01	4.03E-12	5.83E-12
Po-210	138.38 d	-	Y	1.00	F 0.1	1.97E-08	2.69E-08
					*M 0.1	2.76E-07	2.93E-07
					S 0.01	3.71E-07	3.91E-07
Astatine							
At-207	1.80 h	Y	-	1.00	F 1.0	2.63E-11	3.02E-11
					M 1.0	1.98E-10	2.10E-10
					S 1.0	2.17E-10	2.30E-10
At-211	7.214 h	Y	-	1.00	F 1.0	5.79E-10	7.28E-10
					M 1.0	9.11E-09	9.67E-09
					S 1.0	1.01E-08	1.07E-08
Francium							
Fr-222	14.4 m	Y	Y	1.00	F 1.0	6.14E-10	6.54E-10
					M 1.0	1.42E-09	1.50E-09
					S 1.0	1.51E-09	1.59E-09

Table 2.1, continued

Nuclide	T _{1/2}	Chain		AMAD (μm)	Type ^a	f ₁	Mortality (Bq ⁻¹)	Morbidity (Bq ⁻¹)
		P	D					
Francium, continued								
Fr-223	21.8 m	Y	Y	1.00	F	1.0	5.52E-11	8.26E-11
					M	1.0	8.81E-10	9.46E-10
					S	1.0	1.02E-09	1.09E-09
Radium								
Ra-223	11.434 d	Y	Y	1.00	F	0.2	3.91E-09	5.40E-09
					*M	0.1	6.42E-07	6.76E-07
					S	0.01	7.50E-07	7.90E-07
Ra-224	3.66 d	Y	Y	1.00	F	0.2	2.60E-09	3.61E-09
					*M	0.1	2.56E-07	2.70E-07
					S	0.01	2.90E-07	3.06E-07
Ra-225	14.8 d	Y	Y	1.00	F	0.2	2.43E-09	3.33E-09
					*M	0.1	5.39E-07	5.67E-07
					S	0.01	6.70E-07	7.05E-07
Ra-226 ^b	1600 y	Y	Y	1.00	F	0.2	8.11E-09	1.14E-08
					*M	0.1	2.93E-07	3.10E-07
					S	0.01	7.23E-07	7.61E-07
Ra-227	42.2 m	Y	-	1.00	F	0.2	5.12E-12	6.92E-12
					*M	0.1	7.41E-12	8.47E-12
					S	0.01	1.55E-11	1.65E-11
Ra-228	5.75 y	Y	Y	1.00	F	0.2	2.34E-08	3.28E-08
					*M	0.1	1.26E-07	1.40E-07
					S	0.01	1.12E-06	1.18E-06
Actinium								
Ac-224	2.9 h	Y	Y	1.00	F	0.0005	2.43E-10	2.90E-10
					M	0.0005	9.21E-09	9.71E-09
					S	0.0005	1.04E-08	1.10E-08
Ac-225	10.0 d	Y	Y	1.00	F	0.0005	1.90E-08	2.29E-08
					M	0.0005	6.32E-07	6.66E-07
					S	0.0005	7.34E-07	7.73E-07
Ac-226	29 h	Y	Y	1.00	F	0.0005	2.39E-09	3.03E-09
					M	0.0005	9.97E-08	1.05E-07
					S	0.0005	1.11E-07	1.17E-07
Ac-227	21.773 y	Y	Y	1.00	F	0.0005	2.21E-06	2.71E-06
					M	0.0005	1.92E-06	2.16E-06
					S	0.0005	3.82E-06	4.04E-06
Ac-228	6.13 h	Y	Y	1.00	F	0.0005	2.45E-10	3.04E-10
					M	0.0005	7.60E-10	8.22E-10
					S	0.0005	1.25E-09	1.33E-09
Thorium								
Th-226	30.9 m	Y	Y	1.00	F	0.0005	1.03E-09	1.10E-09
					M	0.0005	3.70E-09	3.90E-09
					*S	0.0005	3.99E-09	4.21E-09

Table 2.1, continued

Nuclide	$T_{1/2}$	Chain		AMAD (μm)	Type ^a f_1	Mortality (Bq^{-1})	Morbidity (Bq^{-1})
		P	D				
Thorium, continued							
Th-227	18.718 d	Y	Y	1.00	F 0.0005	1.20E-08	1.63E-08
					M 0.0005	7.23E-07	7.62E-07
					*S 0.0005	9.00E-07	9.48E-07
Th-228	1.9131 y	Y	Y	1.00	F 0.0005	4.25E-07	5.86E-07
					M 0.0005	2.03E-06	2.18E-06
					*S 0.0005	3.40E-06	3.58E-06
Th-229	7340 y	Y	Y	1.00	F 0.0005	2.04E-06	2.70E-06
					M 0.0005	2.07E-06	2.39E-06
					*S 0.0005	4.47E-06	4.73E-06
Th-230	7.7E4 y	Y	Y	1.00	F 0.0005	6.70E-07	9.20E-07
					M 0.0005	5.28E-07	6.36E-07
					*S 0.0005	7.23E-07	7.70E-07
Th-231	25.52 h	Y	Y	1.00	F 0.0005	6.00E-12	9.96E-12
					M 0.0005	2.95E-11	3.78E-11
					*S 0.0005	3.23E-11	4.10E-11
Th-232 ^b	1.41E10 y	Y	Y	1.00	F 0.0005	8.09E-07	1.12E-06
					M 0.0005	5.18E-07	6.45E-07
					*S 0.0005	1.10E-06	1.17E-06
Th-234	24.10 d	Y	Y	1.00	F 0.0005	1.73E-10	2.25E-10
					M 0.0005	6.06E-10	7.16E-10
					*S 0.0005	7.11E-10	8.31E-10
Protactinium							
Pa-227	38.3 m	Y	-	1.00	F 0.0005	1.02E-09	1.10E-09
					M 0.0005	4.98E-09	5.25E-09
					S 0.0005	5.44E-09	5.73E-09
Pa-228	22 h	Y	-	1.00	F 0.0005	5.78E-10	7.99E-10
					M 0.0005	4.01E-09	4.29E-09
					S 0.0005	5.96E-09	6.29E-09
Pa-230	17.4 d	Y	-	1.00	F 0.0005	1.24E-09	1.77E-09
					M 0.0005	5.13E-08	5.41E-08
					S 0.0005	6.63E-08	6.98E-08
Pa-231	3.276E4 y	Y	Y	1.00	F 0.0005	1.52E-06	2.06E-06
					M 0.0005	8.83E-07	1.10E-06
					S 0.0005	1.15E-06	1.23E-06
Pa-232	1.31 d	Y	-	1.00	F 0.0005	2.38E-11	3.60E-11
					M 0.0005	6.70E-11	8.23E-11
					S 0.0005	1.64E-10	1.84E-10
Pa-233	27.0 d	Y	Y	1.00	F 0.0005	5.54E-11	7.28E-11
					M 0.0005	2.92E-10	3.27E-10
					S 0.0005	3.45E-10	3.84E-10

Table 2.1, continued

Nuclide	T _{1/2}	Chain		AMAD (μm)	Type ^a	f ₁	Mortality (Bq ⁻¹)	Morbidity (Bq ⁻¹)
		P	D					
Protactinium, continued								
Pa-234	6.70 h	Y	Y	1.00	F	0.0005	7.80E-12	1.25E-11
						0.0005	2.80E-11	3.67E-11
						0.0005	3.02E-11	3.94E-11
Uranium								
U-230	20.8 d	Y	Y	1.00	F	0.02	9.88E-09	1.46E-08
						*M 0.02	1.17E-06	1.23E-06
						S 0.002	1.40E-06	1.48E-06
U-231	4.2 d	Y	Y	1.00	F	0.02	5.01E-12	8.45E-12
						*M 0.02	4.09E-11	4.86E-11
						S 0.002	4.70E-11	5.54E-11
U-232	72 y	Y	Y	1.00	F	0.02	7.11E-08	9.96E-08
						*M 0.02	4.86E-07	5.26E-07
						S 0.002	2.37E-06	2.50E-06
U-233	1.585E5 y	Y	Y	1.00	F	0.02	1.23E-08	1.74E-08
						*M 0.02	2.96E-07	3.13E-07
						S 0.002	7.27E-07	7.65E-07
U-234 ^a	2.445E5 y	Y	Y	1.00	F	0.02	1.20E-08	1.70E-08
						*M 0.02	2.90E-07	3.08E-07
						S 0.002	7.14E-07	7.51E-07
U-235	703.8E6 y	Y	Y	1.00	F	0.02	1.12E-08	1.59E-08
						*M 0.02	2.57E-07	2.73E-07
						S 0.002	6.42E-07	6.77E-07
U-236	2.3415E7 y	Y	Y	1.00	F	0.02	1.13E-08	1.61E-08
						*M 0.02	2.68E-07	2.83E-07
						S 0.002	6.63E-07	6.98E-07
U-237	6.75 d	Y	Y	1.00	F	0.02	1.38E-11	2.33E-11
						*M 0.02	1.50E-10	1.74E-10
						S 0.002	1.71E-10	1.97E-10
U-238	4.468E9 y	Y	Y	1.00	F	0.02	1.09E-08	1.54E-08
						*M 0.02	2.38E-07	2.52E-07
						S 0.002	6.07E-07	6.39E-07
U-239	23.54 m	Y	-	1.00	F	0.02	4.44E-13	5.93E-13
						*M 0.02	1.33E-12	1.54E-12
						S 0.002	1.43E-12	1.65E-12
U-240	14.1 h	Y	Y	1.00	F	0.02	1.76E-11	3.08E-11
						*M 0.02	5.60E-11	7.99E-11
						S 0.002	6.07E-11	8.62E-11
Neptunium								
Np-232	14.7 m	Y	-	1.00	F	0.0005	9.05E-13	1.21E-12
						*M 0.0005	7.09E-13	8.58E-13
						S 0.0005	1.24E-12	1.34E-12

Table 2.1, continued

Nuclide	$T_{1/2}$	Chain		AMAD (μm)	Type ^a	f_1	Mortality (Bq^{-1})	Morbidity (Bq^{-1})
		P	D					
Neptunium, continued								
Np-233	36.2 m	Y	Y	1.00	F	0.0005	2.72E-14	3.54E-14
					*M	0.0005	5.67E-14	6.72E-14
					S	0.0005	6.01E-14	7.08E-14
Np-234	4.4 d	Y	Y	1.00	F	0.0005	1.75E-11	2.66E-11
					*M	0.0005	3.64E-11	5.04E-11
					S	0.0005	3.90E-11	5.36E-11
Np-235	396.1 d	Y	Y	1.00	F	0.0005	2.16E-11	2.50E-11
					*M	0.0005	2.78E-11	3.11E-11
					S	0.0005	4.84E-11	5.25E-11
Np-236a	115E3 y	Y	-	1.00	F	0.0005	4.61E-08	6.33E-08
					*M	0.0005	1.97E-08	2.64E-08
					S	0.0005	3.06E-08	3.30E-08
Np-236b	22.5 h	Y	Y	1.00	F	0.0005	7.71E-11	1.04E-10
					*M	0.0005	1.97E-10	2.18E-10
					S	0.0005	3.28E-10	3.49E-10
Np-237	2.14E6 y	Y	Y	1.00	F	0.0005	3.48E-07	4.72E-07
					*M	0.0005	4.18E-07	4.79E-07
					S	0.0005	7.32E-07	7.75E-07
Np-238	2.117 d	Y	Y	1.00	F	0.0005	3.97E-11	5.83E-11
					*M	0.0005	8.86E-11	1.13E-10
					S	0.0005	1.19E-10	1.43E-10
Np-239	2.355 d	Y	Y	1.00	F	0.0005	1.48E-11	2.44E-11
					*M	0.0005	8.75E-11	1.08E-10
					S	0.0005	9.66E-11	1.18E-10
Np-240	65 m	Y	-	1.00	F	0.0005	1.36E-12	1.75E-12
					*M	0.0005	4.62E-12	5.27E-12
					S	0.0005	4.99E-12	5.66E-12
Plutonium								
Pu-234	8.8 h	Y	Y	1.00	F	0.0005	7.77E-11	9.91E-11
					*M	0.0005	1.75E-09	1.85E-09
					S	0.00001	2.05E-09	2.16E-09
Pu-235	25.3 m	Y	-	1.00	F	0.0005	2.85E-14	3.49E-14
					*M	0.0005	5.67E-14	6.47E-14
					S	0.00001	6.06E-14	6.88E-14
Pu-236	2.851 y	Y	Y	1.00	F	0.0005	4.92E-07	5.91E-07
					*M	0.0005	5.60E-07	6.16E-07
					S	0.00001	7.56E-07	7.99E-07
Pu-237	45.3 d	Y	Y	1.00	F	0.0005	1.23E-11	1.61E-11
					*M	0.0005	2.99E-11	3.43E-11
					S	0.00001	3.58E-11	4.03E-11

Table 2.1, continued

Nuclide	$T_{1/2}$	Chain		AMAD (μm)	Type ^a	f_1	Mortality (Bq^{-1})	Morbidity (Bq^{-1})	
		P	D						
Plutonium, continued									
Pu-238	87.74 y	Y	Y	1.00	F	0.0005	1.19E-06	1.41E-06	
						*M	0.0005	8.04E-07	9.07E-07
						S	0.00001	9.06E-07	9.60E-07
Pu-239 ^b	24065 y	Y	Y	1.00	F	0.0005	1.26E-06	1.49E-06	
						*M	0.0005	7.94E-07	8.99E-07
						S	0.00001	8.45E-07	8.96E-07
Pu-240	6537 y	Y	Y	1.00	F	0.0005	1.26E-06	1.50E-06	
						*M	0.0005	7.95E-07	9.00E-07
						S	0.00001	8.47E-07	8.98E-07
Pu-241	14.4 y	Y	Y	1.00	F	0.0005	1.98E-08	2.34E-08	
						*M	0.0005	7.67E-09	9.02E-09
						S	0.00001	3.51E-09	3.82E-09
Pu-242	3.763E5 y	Y	Y	1.00	F	0.0005	1.19E-06	1.42E-06	
						*M	0.0005	7.46E-07	8.46E-07
						S	0.00001	7.88E-07	8.36E-07
Pu-243	4.956 h	Y	Y	1.00	F	0.0005	1.49E-12	2.33E-12	
						*M	0.0005	6.31E-12	7.94E-12
						S	0.00001	6.85E-12	8.57E-12
Pu-245	10.5 h	Y	-	1.00	F	0.0005	1.16E-11	1.97E-11	
						*M	0.0005	4.06E-11	5.59E-11
						S	0.00001	4.38E-11	6.00E-11
Pu-246	10.85 d	Y	Y	1.00	F	0.0005	1.12E-10	1.58E-10	
						*M	0.0005	3.87E-10	4.68E-10
						S	0.00001	4.35E-10	5.20E-10
Americium									
Am-237	73.0 m	Y	-	1.00	F	0.0005	3.69E-13	4.70E-13	
						*M	0.0005	1.38E-12	1.56E-12
						S	0.0005	1.50E-12	1.68E-12
Am-238	98 m	Y	Y	1.00	F	0.0005	1.98E-12	2.59E-12	
						*M	0.0005	2.11E-12	2.57E-12
						S	0.0005	2.69E-12	3.07E-12
Am-239	11.9 h	Y	-	1.00	F	0.0005	4.00E-12	6.50E-12	
						*M	0.0005	1.77E-11	2.27E-11
						S	0.0005	1.92E-11	2.45E-11
Am-240	50.8 h	Y	-	1.00	F	0.0005	1.19E-11	1.80E-11	
						*M	0.0005	2.83E-11	3.82E-11
						S	0.0005	3.05E-11	4.08E-11
Am-241	432.2 y	Y	Y	1.00	F	0.0005	7.98E-07	1.02E-06	
						*M	0.0005	6.59E-07	7.60E-07
						S	0.0005	9.04E-07	9.58E-07

Table 2.1, continued

Nuclide	$T_{1/2}$	Chain		AMAD (μm)	Type ^a f_1	Mortality (Bq^{-1})	Morbidity (Bq^{-1})
		P	D				
Americium, continued							
Am-242	16.02 h	Y	Y	1.00	F 0.0005	1.99E-10	2.37E-10
					*M 0.0005	1.28E-09	1.36E-09
					S 0.0005	1.72E-09	1.81E-09
Am-242m	152 y	Y	-	1.00	F 0.0005	7.26E-07	9.30E-07
					*M 0.0005	3.41E-07	4.21E-07
					S 0.0005	4.76E-07	5.08E-07
Am-243	7380 y	Y	Y	1.00	F 0.0005	7.88E-07	1.00E-06
					*M 0.0005	6.33E-07	7.31E-07
					S 0.0005	8.58E-07	9.11E-07
Am-244	10.1 h	Y	-	1.00	F 0.0005	4.35E-11	5.72E-11
					*M 0.0005	6.97E-11	8.34E-11
					S 0.0005	9.14E-11	1.04E-10
Am-244m	26 m	Y	-	1.00	F 0.0005	1.91E-12	2.36E-12
					*M 0.0005	2.48E-12	2.76E-12
					S 0.0005	3.34E-12	3.56E-12
Am-245	2.05 h	Y	Y	1.00	F 0.0005	9.20E-13	1.30E-12
					*M 0.0005	3.52E-12	4.21E-12
					S 0.0005	3.81E-12	4.54E-12
Am-246	39 m	Y	-	1.00	F 0.0005	1.08E-12	1.28E-12
					*M 0.0005	3.23E-12	3.55E-12
					S 0.0005	3.47E-12	3.80E-12
Am-246m	25.0 m	Y	Y	1.00	F 0.0005	4.55E-13	5.46E-13
					*M 0.0005	9.52E-13	1.07E-12
					S 0.0005	1.01E-12	1.12E-12
Curium							
Cm-238	2.4 h	Y	-	1.00	F 0.0005	3.61E-11	4.06E-11
					*M 0.0005	3.45E-10	3.65E-10
					S 0.0005	3.80E-10	4.01E-10
Cm-240	27 d	Y	Y	1.00	F 0.0005	1.96E-08	2.37E-08
					*M 0.0005	2.44E-07	2.57E-07
					S 0.0005	2.97E-07	3.13E-07
Cm-241	32.8 d	Y	-	1.00	F 0.0005	3.55E-10	4.44E-10
					*M 0.0005	2.56E-09	2.73E-09
					S 0.0005	3.12E-09	3.31E-09
Cm-242	162.8 d	Y	Y	1.00	F 0.0005	5.77E-08	6.80E-08
					*M 0.0005	3.84E-07	4.07E-07
					S 0.0005	5.15E-07	5.42E-07
Cm-243	28.5 y	Y	-	1.00	F 0.0005	6.50E-07	8.18E-07
					*M 0.0005	6.43E-07	7.27E-07
					S 0.0005	9.38E-07	9.93E-07

Table 2.1, continued

Nuclide	$T_{1/2}$	Chain		AMAD (μm)	Type ^a	f_1	Mortality (Bq^{-1})	Morbidity (Bq^{-1})
		P	D					
Curium, continued								
Cm-244	18.11 y	Y	Y	1.00	F	0.0005	5.68E-07	7.11E-07
					*M	0.0005	6.10E-07	6.84E-07
					S	0.0005	9.09E-07	9.61E-07
Cm-245	8500 y	Y	Y	1.00	F	0.0005	8.05E-07	1.03E-06
					*M	0.0005	6.49E-07	7.50E-07
					S	0.0005	8.80E-07	9.33E-07
Cm-246	4730 y	Y	Y	1.00	F	0.0005	7.97E-07	1.02E-06
					*M	0.0005	6.47E-07	7.48E-07
					S	0.0005	8.81E-07	9.35E-07
Cm-247	1.56E7 y	Y	Y	1.00	F	0.0005	7.40E-07	9.43E-07
					*M	0.0005	5.83E-07	6.75E-07
					S	0.0005	7.86E-07	8.34E-07
Cm-249	64.15 m	Y	Y	1.00	F	0.0005	7.43E-13	9.51E-13
					*M	0.0005	1.71E-12	1.96E-12
					S	0.0005	1.87E-12	2.11E-12
Berkelium								
Bk-245	4.94 d	Y	-	1.00	F	0.0005	1.79E-11	2.60E-11
					M	0.0005	1.74E-10	1.95E-10
					S	0.0005	1.96E-10	2.18E-10
Bk-246	1.83 d	Y	-	1.00	F	0.0005	9.78E-12	1.47E-11
					M	0.0005	1.75E-11	2.50E-11
					S	0.0005	1.86E-11	2.63E-11
Bk-247	1380 y	Y	Y	1.00	F	0.0005	1.07E-06	1.29E-06
					M	0.0005	7.75E-07	8.80E-07
					S	0.0005	9.47E-07	1.00E-06
Bk-249	320 d	Y	Y	1.00	F	0.0005	2.58E-09	3.13E-09
					M	0.0005	1.17E-09	1.39E-09
					S	0.0005	1.27E-09	1.35E-09
Bk-250	3.222 h	Y	Y	1.00	F	0.0005	1.91E-11	2.36E-11
					M	0.0005	2.42E-11	2.79E-11
					S	0.0005	3.28E-11	3.61E-11
Californium								
Cf-244	19.4 m	Y	-	1.00	F	0.0005	2.55E-10	2.72E-10
					M	0.0005	7.60E-10	8.01E-10
					S	0.0005	8.30E-10	8.74E-10
Cf-246	35.7 h	Y	-	1.00	F	0.0005	1.32E-09	1.60E-09
					M	0.0005	3.76E-08	3.96E-08
					S	0.0005	4.28E-08	4.51E-08
Cf-248	333.5 d	Y	Y	1.00	F	0.0005	1.19E-07	1.42E-07
					M	0.0005	4.58E-07	4.88E-07
					S	0.0005	6.57E-07	6.92E-07

Table 2.1, continued

Nuclide	$T_{1/2}$	Chain		AMAD (μm)	Type ^a	f_1	Mortality (Bq^{-1})	Morbidity (Bq^{-1})	
		P	D						
Californium, continued									
Cf-249	350.6 y	Y	Y	1.00	F	0.0005	1.08E-06	1.31E-06	
							M	8.10E-07	9.18E-07
							S	1.00E-06	1.06E-06
Cf-250	13.08 y	Y	Y	1.00	F	0.0005	6.11E-07	7.34E-07	
							M	6.52E-07	7.20E-07
							S	9.42E-07	9.95E-07
Cf-251	898 y	Y	Y	1.00	F	0.0005	1.10E-06	1.33E-06	
							M	8.10E-07	9.18E-07
							S	9.95E-07	1.05E-06
Cf-253	17.81 d	Y	Y	1.00	F	0.0005	5.48E-09	6.50E-09	
							M	1.08E-07	1.14E-07
							S	1.39E-07	1.46E-07
Einsteinium									
Es-250	2.1 h	Y	-	1.00	F	0.0005	1.14E-11	1.38E-11	
							M	1.23E-11	1.37E-11
							S	1.77E-11	1.88E-11
Es-251	33 h	Y	-	1.00	F	0.0005	1.14E-11	1.51E-11	
							M	1.61E-10	1.73E-10
							S	1.79E-10	1.92E-10
Es-253	20.47 d	Y	Y	1.00	F	0.0005	6.77E-09	8.08E-09	
							M	2.27E-07	2.39E-07
							S	2.70E-07	2.85E-07
Es-254	275.7 d	Y	Y	1.00	F	0.0005	1.09E-07	1.30E-07	
							M	4.70E-07	5.00E-07
							S	6.65E-07	7.00E-07
Es-254m	39.3 h	Y	-	1.00	F	0.0005	8.64E-10	1.09E-09	
							M	3.92E-08	4.14E-08
							S	4.40E-08	4.64E-08
Fermium									
Fm-252	22.7 h	Y	-	1.00	F	0.0005	1.08E-09	1.31E-09	
							M	2.64E-08	2.79E-08
							S	2.98E-08	3.14E-08
Fm-253	3.00 d	Y	-	1.00	F	0.0005	9.90E-10	1.18E-09	
							M	3.28E-08	3.46E-08
							S	3.93E-08	4.13E-08
Fm-254	3.240 h	Y	Y	1.00	F	0.0005	4.35E-10	4.91E-10	
							M	5.06E-09	5.34E-09
							S	5.58E-09	5.88E-09
Fm-255	20.07 h	Y	-	1.00	F	0.0005	7.11E-10	8.60E-10	
							M	2.26E-08	2.39E-08
							S	2.51E-08	2.65E-08

Table 2.1, continued

Nuclide	T _{1/2}	Chain		AMAD (μm)	Type ^a	f ₁	Mortality (Bq ⁻¹)	Morbidity (Bq ⁻¹)
		P	D					
Fermium, continued								
Fm-257	100.5 d	Y	Y	1.00	F	0.0005	5.95E-08	7.06E-08
					M	0.0005	5.21E-07	5.51E-07
					S	0.0005	7.14E-07	7.51E-07
Mendelevium								
Md-257	5.2 h	Y	-	1.00	F	0.0005	1.67E-10	1.97E-10
					M	0.0005	1.97E-09	2.08E-09
					S	0.0005	2.46E-09	2.59E-09
Md-258	55 d	Y	-	1.00	F	0.0005	3.98E-08	4.73E-08
					M	0.0005	4.29E-07	4.53E-07
					S	0.0005	5.55E-07	5.84E-07

^aAn asterisk indicates the default absorption type recommended by the ICRP for environmental exposure to particulate forms of the element (see Table 4.1).

^bThe uncertainty in the risk coefficient for a form of this radionuclide is addressed in Table 2.4.

Table 2.2a. Mortality and morbidity risk coefficients for ingestion of tap water and food.

Explanation of Entries

Risk coefficients for ingestion of radionuclides in tap water or food are expressed as the probability of radiogenic cancer mortality or morbidity per unit intake, where the intake is *averaged over all ages and both genders*. A risk coefficient for ingestion applies to all forms of the radionuclide, except that separate risk coefficients are given for ^3H as tritiated water and organically bound tritium, and for inorganic and organic forms of radioisotopes of sulfur, mercury, and polonium. The indicated f_I values apply to the adult and, as explained in Chapter 4, may differ from values for infants and children.

The entries under the heading “Chain” indicate whether the radionuclide is in the same decay chain as other radionuclides addressed in the table (see Appendix G for details concerning decay chains). An entry “Y” (yes) under the subheading “P” (parent) indicates that the radionuclide is the parent of a decay chain containing at least one other radionuclide in the table. An entry “Y” under the subheading “D” (daughter) indicates that the radionuclide is formed in the decay chain of at least one other radionuclide in the table. These entries are included as an aid in the estimation of cancer risk from intake of decay chain members that form in the environment. The risk coefficient for intake of a radionuclide already includes the contribution to dose from production of decay chain members in the body after intake of the parent.

To facilitate application of the risk coefficients, including conversion to other units, the coefficients are tabulated to three decimal places. No indication of the level of uncertainty is intended or should be inferred from this practice. A calculated risk should be rounded appropriately.

To express a risk coefficient in conventional units (μCi^{-1}), multiply by $3.7 \times 10^4 \text{ Bq } \mu\text{Ci}^{-1}$.

To express a risk coefficient for intake of tap water in terms of a constant activity concentration in tap water (Bq L^{-1}), multiply the coefficient by $2.75 \times 10^4 U_W$, where U_W is the lifetime average rate of ingestion of tap water (for example, 1.11 L d^{-1} in Table 3.1) and $2.75 \times 10^4 \text{ d}$ is the average life span. To express a risk coefficient for intake of food in terms of a constant activity concentration in food (Bq kg^{-1}), multiply by $2.75 \times 10^4 U_F$, where U_F is the lifetime average intake rate of food in terms of mass (for example, 1.2 kg d^{-1} , suggested in Chapter 3), and $2.75 \times 10^4 \text{ d}$ is the average life span. To express a risk coefficient in terms of activity per unit energy (Bq kcal^{-1}), multiply by $2.75 \times 10^4 U_E$, where U_E is the lifetime average intake rate of food energy (for example, 2048 kcal d^{-1} in Table 3.1). Note that the *relative* age- and gender-specific intake rates of tap water or food indicated in Table 3.1 are inherent in the risk coefficients.

Table 2.2a. Mortality and morbidity risk coefficients for ingestion of water and food.

Nuclide	$T_{1/2}$	Chain			Tap Water Intakes		Dietary Intakes	
		P	D	f_1	Mortality (Bq ⁻¹)	Morbidity (Bq ⁻¹)	Mortality (Bq ⁻¹)	Morbidity (Bq ⁻¹)
Hydrogen (tritiated water)								
H-3 ^a	12.35 y	-	-	1.0	9.44E-13	1.37E-12	1.20E-12	1.76E-12
Hydrogen (organically bound)								
H-3	12.35 y	-	-	1.0	2.09E-12	3.03E-12	2.66E-12	3.89E-12
Beryllium								
Be-7	53.3 d	-	-	0.005	1.39E-12	2.34E-12	1.91E-12	3.25E-12
Be-10	1.6E6 y	-	-	0.005	1.07E-10	1.90E-10	1.56E-10	2.77E-10
Carbon								
C-11	20.38 m	-	-	1.0	9.34E-13	1.10E-12	1.27E-12	1.51E-12
C-14 ^b	5730 y	-	-	1.0	2.89E-11	4.20E-11	3.68E-11	5.40E-11
Fluorine								
F-18	109.77 m	-	-	1.0	2.20E-12	2.63E-12	2.91E-12	3.50E-12
Sodium								
Na-22	2.602 y	-	-	1.0	1.80E-10	2.60E-10	2.34E-10	3.41E-10
Na-24	15.00 h	-	-	1.0	2.35E-11	3.33E-11	3.12E-11	4.45E-11
Magnesium								
Mg-28	20.91 h	Y	-	0.5	1.77E-10	3.07E-10	2.56E-10	4.46E-10
Aluminum								
Al-26	7.16E5 y	-	-	0.01	2.68E-10	4.67E-10	3.83E-10	6.72E-10
Silicon								
Si-31	157.3 m	-	-	0.01	1.05E-11	1.75E-11	1.52E-11	2.54E-11
Si-32	450 y	Y	-	0.01	5.28E-11	9.31E-11	7.65E-11	1.35E-10
Phosphorus								
P-32	14.29 d	-	Y	0.8	1.68E-10	2.42E-10	2.25E-10	3.32E-10
P-33	25.4 d	-	-	0.8	1.73E-11	2.65E-11	2.37E-11	3.68E-11
Sulfur (inorganic)								
S-35	87.44 d	-	-	1.0	8.87E-12	1.39E-11	1.21E-11	1.90E-11
Sulfur (organic)								
S-35	87.44 d	-	-	1.0	4.99E-11	7.36E-11	6.72E-11	1.00E-10
Chlorine								
Cl-36	3.01E5 y	-	-	1.0	5.94E-11	8.92E-11	7.93E-11	1.20E-10
Cl-38	37.21 m	-	-	1.0	4.45E-12	5.21E-12	6.09E-12	7.13E-12
Cl-39	55.6 m	Y	-	1.0	3.42E-12	4.11E-12	4.66E-12	5.61E-12
Potassium								
K-40	1.28E9 y	-	-	1.0	4.30E-10	6.68E-10	5.89E-10	9.26E-10
K-42	12.36 h	-	-	1.0	2.40E-11	3.41E-11	3.28E-11	4.70E-11
K-43	22.6 h	-	-	1.0	1.45E-11	2.13E-11	1.96E-11	2.89E-11
K-44	22.13 m	-	-	1.0	3.23E-12	3.76E-12	4.42E-12	5.15E-12
K-45	20 m	Y	-	1.0	2.08E-12	2.42E-12	2.84E-12	3.31E-12

Table 2.2a, continued

Nuclide	T _{1/2}	Chain			Tap Water Intakes		Dietary Intakes	
		P	D	f ₁	Mortality (Bq ⁻¹)	Morbidity (Bq ⁻¹)	Mortality (Bq ⁻¹)	Morbidity (Bq ⁻¹)
Calcium								
Ca-41	1.4E5 y	-	-	0.3	8.58E-12	9.55E-12	1.04E-11	1.18E-11
Ca-45	163 d	-	Y	0.3	4.74E-11	6.68E-11	6.27E-11	9.10E-11
Ca-47	4.53 d	Y	-	0.3	1.19E-10	2.04E-10	1.69E-10	2.92E-10
Scandium								
Sc-43	3.891 h	-	-	0.0001	1.31E-11	2.21E-11	1.87E-11	3.18E-11
Sc-44	3.927 h	-	Y	0.0001	2.50E-11	4.22E-11	3.58E-11	6.09E-11
Sc-44m	58.6 h	Y	-	0.0001	2.09E-10	3.74E-10	3.03E-10	5.44E-10
Sc-46	83.83 d	-	-	0.0001	9.59E-11	1.68E-10	1.36E-10	2.40E-10
Sc-47	3.351 d	-	Y	0.0001	5.24E-11	9.44E-11	7.67E-11	1.38E-10
Sc-48	43.7 h	-	-	0.0001	1.13E-10	1.98E-10	1.62E-10	2.84E-10
Sc-49	57.4 m	-	-	0.0001	3.96E-12	5.54E-12	5.59E-12	7.89E-12
Titanium								
Ti-44	47.3 y	Y	-	0.01	4.11E-10	6.93E-10	5.78E-10	9.84E-10
Ti-45	3.08 h	-	-	0.01	1.05E-11	1.74E-11	1.50E-11	2.52E-11
Vanadium								
V-47	32.6 m	-	-	0.01	2.65E-12	3.38E-12	3.67E-12	4.71E-12
V-48	16.238 d	-	Y	0.01	1.27E-10	2.22E-10	1.80E-10	3.16E-10
V-49	330 d	-	Y	0.01	1.83E-12	3.30E-12	2.68E-12	4.83E-12
Chromium								
Cr-48	22.96 h	Y	-	0.1	1.18E-11	2.01E-11	1.65E-11	2.83E-11
Cr-49	42.09 m	Y	-	0.1	2.72E-12	3.64E-12	3.79E-12	5.10E-12
Cr-51	27.704 d	-	Y	0.1	2.87E-12	5.01E-12	4.10E-12	7.19E-12
Manganese								
Mn-51	46.2 m	Y	-	0.1	4.20E-12	5.66E-12	5.86E-12	7.97E-12
Mn-52	5.591 d	-	Y	0.1	1.04E-10	1.74E-10	1.44E-10	2.45E-10
Mn-52m	21.1 m	Y	Y	0.1	2.79E-12	3.42E-12	3.84E-12	4.73E-12
Mn-53	3.7E6 y	-	-	0.1	2.46E-12	4.21E-12	3.52E-12	6.07E-12
Mn-54	312.5 d	-	-	0.1	3.94E-11	6.16E-11	5.30E-11	8.40E-11
Mn-56	2.5785 h	-	-	0.1	1.70E-11	2.78E-11	2.44E-11	4.01E-11
Iron								
Fe-52	8.275 h	Y	-	0.1	1.10E-10	1.91E-10	1.59E-10	2.78E-10
Fe-55	2.7 y	-	Y	0.1	1.81E-11	2.33E-11	2.39E-11	3.14E-11
Fe-59	44.529 d	-	-	0.1	1.36E-10	2.13E-10	1.91E-10	3.01E-10
Fe-60	1E5 y	Y	-	0.1	3.75E-09	4.86E-09	4.94E-09	6.47E-09
Cobalt								
Co-55	17.54 h	Y	-	0.1	7.16E-11	1.25E-10	1.03E-10	1.81E-10
Co-56	78.76 d	-	Y	0.1	1.67E-10	2.74E-10	2.35E-10	3.87E-10
Co-57	270.9 d	-	Y	0.1	1.70E-11	2.81E-11	2.43E-11	4.03E-11
Co-58	70.80 d	-	Y	0.1	4.85E-11	7.97E-11	6.82E-11	1.13E-10
Co-58m	9.15 h	Y	-	0.1	1.94E-12	3.40E-12	2.82E-12	4.95E-12

Table 2.2a, continued

Nuclide	T _{1/2}	Chain			Tap Water Intakes		Dietary Intakes	
		P	D	f ₁	Mortality (Bq ⁻¹)	Morbidity (Bq ⁻¹)	Mortality (Bq ⁻¹)	Morbidity (Bq ⁻¹)
Cobalt, continued								
Co-60 ^a	5.271 y	-	Y	0.1	2.75E-10	4.25E-10	3.88E-10	6.03E-10
Co-60m	10.47 m	Y	Y	0.1	6.30E-14	7.19E-14	8.67E-14	9.90E-14
Co-61	1.65 h	-	-	0.1	4.26E-12	6.56E-12	6.08E-12	9.42E-12
Co-62m	13.91 m	-	-	0.1	1.87E-12	2.23E-12	2.56E-12	3.06E-12
Nickel								
Ni-56	6.10 d	Y	-	0.05	4.54E-11	7.66E-11	6.29E-11	1.07E-10
Ni-57	36.08 h	Y	-	0.05	6.01E-11	1.05E-10	8.58E-11	1.50E-10
Ni-59	7.5E4 y	-	-	0.05	4.44E-12	7.41E-12	6.26E-12	1.05E-11
Ni-63	96 y	-	-	0.05	1.08E-11	1.81E-11	1.53E-11	2.57E-11
Ni-65	2.520 h	-	-	0.05	1.15E-11	1.88E-11	1.65E-11	2.73E-11
Ni-66	54.6 h	Y	-	0.05	3.00E-10	5.41E-10	4.40E-10	7.95E-10
Copper								
Cu-60	23.2 m	-	-	0.5	2.95E-12	3.70E-12	4.04E-12	5.10E-12
Cu-61	3.408 h	-	-	0.5	7.74E-12	1.25E-11	1.11E-11	1.81E-11
Cu-64	12.701 h	-	-	0.5	1.00E-11	1.73E-11	1.45E-11	2.52E-11
Cu-67	61.86 h	-	-	0.5	3.04E-11	5.25E-11	4.41E-11	7.65E-11
Zinc								
Zn-62	9.26 h	Y	-	0.5	7.77E-11	1.34E-10	1.13E-10	1.96E-10
Zn-63	38.1 m	-	-	0.5	3.38E-12	4.36E-12	4.70E-12	6.10E-12
Zn-65	243.9 d	-	Y	0.5	2.16E-10	3.15E-10	2.82E-10	4.15E-10
Zn-69	57 m	-	Y	0.5	1.43E-12	1.95E-12	2.02E-12	2.78E-12
Zn-69m	13.76 h	Y	-	0.5	2.88E-11	5.04E-11	4.19E-11	7.37E-11
Zn-71m	3.92 h	-	-	0.5	1.60E-11	2.61E-11	2.29E-11	3.77E-11
Zn-72	46.5 h	Y	-	0.5	1.05E-10	1.78E-10	1.50E-10	2.55E-10
Gallium								
Ga-65	15.2 m	Y	-	0.001	1.44E-12	1.71E-12	1.98E-12	2.36E-12
Ga-66	9.40 h	-	Y	0.001	9.84E-11	1.73E-10	1.43E-10	2.52E-10
Ga-67	78.26 h	-	Y	0.001	1.58E-11	2.81E-11	2.28E-11	4.08E-11
Ga-68	68.0 m	-	Y	0.001	5.25E-12	7.64E-12	7.40E-12	1.09E-11
Ga-70	21.15 m	-	-	0.001	1.19E-12	1.41E-12	1.64E-12	1.95E-12
Ga-72	14.1 h	-	Y	0.001	8.58E-11	1.51E-10	1.24E-10	2.18E-10
Ga-73	4.91 h	-	-	0.001	2.16E-11	3.76E-11	3.15E-11	5.48E-11
Germanium								
Ge-66	2.27 h	Y	-	1.0	6.21E-12	9.99E-12	8.25E-12	1.32E-11
Ge-67	18.7 m	Y	-	1.0	2.46E-12	2.86E-12	3.36E-12	3.91E-12
Ge-68	288 d	Y	-	1.0	1.07E-10	1.88E-10	1.51E-10	2.67E-10
Ge-69	39.05 h	-	Y	1.0	1.60E-11	2.66E-11	2.19E-11	3.65E-11
Ge-71	11.8 d	-	Y	1.0	9.94E-13	1.75E-12	1.41E-12	2.48E-12
Ge-75	82.78 m	-	-	1.0	1.87E-12	2.34E-12	2.53E-12	3.15E-12
Ge-77	11.30 h	Y	-	1.0	2.03E-11	3.30E-11	2.75E-11	4.46E-11
Ge-78	87 m	Y	-	1.0	5.79E-12	8.34E-12	7.62E-12	1.09E-11

Table 2.2a, continued

Nuclide	T _{1/2}	Chain			Tap Water Intakes		Dietary Intakes	
		P	D	f ₁	Mortality (Bq ⁻¹)	Morbidity (Bq ⁻¹)	Mortality (Bq ⁻¹)	Morbidity (Bq ⁻¹)
Arsenic								
As-69	15.2 m	Y	-	0.5	2.29E-12	2.83E-12	3.16E-12	3.94E-12
As-70	52.6 m	-	Y	0.5	6.27E-12	8.66E-12	8.69E-12	1.21E-11
As-71	64.8 h	Y	-	0.5	3.54E-11	6.15E-11	5.08E-11	8.88E-11
As-72	26.0 h	-	Y	0.5	1.56E-10	2.75E-10	2.27E-10	4.01E-10
As-73	80.30 d	-	Y	0.5	2.39E-11	4.22E-11	3.48E-11	6.16E-11
As-74	17.76 d	-	-	0.5	1.04E-10	1.81E-10	1.50E-10	2.62E-10
As-76	26.32 h	-	-	0.5	1.47E-10	2.61E-10	2.15E-10	3.83E-10
As-77	38.8 h	-	Y	0.5	3.80E-11	6.76E-11	5.56E-11	9.93E-11
As-78	90.7 m	-	Y	0.5	1.15E-11	1.71E-11	1.63E-11	2.44E-11
Selenium								
Se-70	41.0 m	Y	-	0.8	5.70E-12	7.97E-12	7.91E-12	1.11E-11
Se-73	7.15 h	Y	Y	0.8	1.37E-11	2.15E-11	1.92E-11	3.06E-11
Se-73m	39 m	Y	-	0.8	1.53E-12	2.24E-12	2.14E-12	3.16E-12
Se-75	119.8 d	-	Y	0.8	1.56E-10	2.20E-10	2.04E-10	2.91E-10
Se-79	65000 y	-	-	0.8	1.38E-10	1.97E-10	1.82E-10	2.62E-10
Se-81	18.5 m	-	Y	0.8	9.99E-13	1.16E-12	1.38E-12	1.60E-12
Se-81m	57.25 m	Y	-	0.8	2.55E-12	3.52E-12	3.59E-12	5.00E-12
Se-83	22.5 m	Y	-	0.8	2.12E-12	2.77E-12	2.93E-12	3.86E-12
Bromine								
Br-74	25.3 m	-	-	1.0	3.40E-12	4.06E-12	4.63E-12	5.54E-12
Br-74m	41.5 m	-	-	1.0	5.54E-12	6.66E-12	7.55E-12	9.09E-12
Br-75	98 m	Y	-	1.0	3.38E-12	4.23E-12	4.60E-12	5.77E-12
Br-76	16.2 h	-	-	1.0	2.67E-11	3.91E-11	3.60E-11	5.33E-11
Br-77	56 h	-	-	1.0	5.45E-12	8.14E-12	7.23E-12	1.09E-11
Br-80	17.4 m	-	Y	1.0	1.12E-12	1.27E-12	1.54E-12	1.75E-12
Br-80m	4.42 h	Y	-	1.0	5.65E-12	7.63E-12	7.74E-12	1.05E-11
Br-82	35.30 h	-	-	1.0	3.10E-11	4.62E-11	4.13E-11	6.21E-11
Br-83	2.39 h	Y	Y	1.0	1.83E-12	2.28E-12	2.51E-12	3.13E-12
Br-84	31.80 m	-	-	1.0	3.41E-12	3.99E-12	4.66E-12	5.47E-12
Rubidium								
Rb-79	22.9 m	Y	-	1.0	1.93E-12	2.26E-12	2.64E-12	3.09E-12
Rb-81	4.58 h	Y	Y	1.0	2.61E-12	3.47E-12	3.52E-12	4.71E-12
Rb-81m	32 m	Y	-	1.0	4.33E-13	5.55E-13	5.87E-13	7.56E-13
Rb-82m	6.2 h	-	-	1.0	6.82E-12	9.48E-12	9.03E-12	1.27E-11
Rb-83	86.2 d	Y	Y	1.0	1.06E-10	1.54E-10	1.39E-10	2.03E-10
Rb-84	32.77 d	-	-	1.0	1.64E-10	2.38E-10	2.15E-10	3.17E-10
Rb-86	18.66 d	-	-	1.0	1.82E-10	2.67E-10	2.44E-10	3.63E-10
Rb-87	4.7E10 y	-	Y	1.0	9.54E-11	1.41E-10	1.28E-10	1.91E-10
Rb-88	17.8 m	-	-	1.0	3.33E-12	3.78E-12	4.56E-12	5.19E-12
Rb-89	15.2 m	Y	-	1.0	1.82E-12	2.13E-12	2.49E-12	2.92E-12

Table 2.2a, continued

Nuclide	T _{1/2}	Chain			Tap Water Intakes		Dietary Intakes	
		P	D	f ₁	Mortality (Bq ⁻¹)	Morbidity (Bq ⁻¹)	Mortality (Bq ⁻¹)	Morbidity (Bq ⁻¹)
Strontium								
Sr-80	100 m	Y	-	0.3	1.92E-11	2.94E-11	2.73E-11	4.20E-11
Sr-81	25.5 m	Y	-	0.3	3.44E-12	4.61E-12	4.79E-12	6.45E-12
Sr-82	25.0 d	Y	-	0.3	5.02E-10	8.45E-10	7.13E-10	1.21E-09
Sr-83	32.4 h	Y	-	0.3	3.46E-11	5.98E-11	4.94E-11	8.58E-11
Sr-85	64.84 d	-	Y	0.3	4.09E-11	6.12E-11	5.56E-11	8.41E-11
Sr-85m	69.5 m	Y	-	0.3	3.09E-13	4.51E-13	4.23E-13	6.23E-13
Sr-87m	2.805 h	Y	Y	0.3	1.79E-12	2.88E-12	2.53E-12	4.09E-12
Sr-89 _a	50.5 d	-	Y	0.3	2.10E-10	3.47E-10	2.97E-10	4.96E-10
Sr-90 _a	29.12 y	Y	-	0.3	1.34E-09	1.51E-09	1.62E-09	1.86E-09
Sr-91	9.5 h	Y	-	0.3	5.02E-11	8.71E-11	7.24E-11	1.26E-10
Sr-92	2.71 h	Y	-	0.3	3.46E-11	6.07E-11	5.01E-11	8.81E-11
Yttrium								
Y-86	14.74 h	-	Y	0.0001	6.34E-11	1.10E-10	9.02E-11	1.57E-10
Y-86m	48 m	Y	-	0.0001	3.69E-12	6.34E-12	5.24E-12	9.06E-12
Y-87	80.3 h	Y	-	0.0001	3.94E-11	6.96E-11	5.65E-11	1.00E-10
Y-88	106.64 d	-	Y	0.0001	6.68E-11	1.13E-10	9.26E-11	1.58E-10
Y-90	64.0 h	-	Y	0.0001	2.70E-10	4.88E-10	3.96E-10	7.16E-10
Y-90m	3.19 h	Y	-	0.0001	1.57E-11	2.80E-11	2.29E-11	4.09E-11
Y-91	58.51 d	-	Y	0.0001	2.39E-10	4.33E-10	3.51E-10	6.36E-10
Y-91m	49.71 m	Y	Y	0.0001	6.29E-13	9.50E-13	8.77E-13	1.34E-12
Y-92	3.54 h	-	Y	0.0001	3.92E-11	6.69E-11	5.70E-11	9.77E-11
Y-93	10.1 h	Y	-	0.0001	1.09E-10	1.94E-10	1.60E-10	2.85E-10
Y-94	19.1 m	-	-	0.0001	3.13E-12	3.71E-12	4.31E-12	5.13E-12
Y-95	10.7 m	Y	-	0.0001	1.71E-12	1.96E-12	2.35E-12	2.70E-12
Zirconium								
Zr-86	16.5 h	Y	-	0.01	5.93E-11	1.04E-10	8.47E-11	1.50E-10
Zr-88	83.4 d	Y	Y	0.01	2.61E-11	4.26E-11	3.57E-11	5.90E-11
Zr-89	78.43 h	-	Y	0.01	5.54E-11	9.72E-11	7.93E-11	1.40E-10
Zr-93	1.53E6 y	Y	Y	0.01	2.26E-11	3.01E-11	2.83E-11	3.90E-11
Zr-95	63.98 d	Y	Y	0.01	7.09E-11	1.24E-10	1.01E-10	1.78E-10
Zr-97	16.90 h	Y	-	0.01	1.89E-10	3.38E-10	2.76E-10	4.95E-10
Niobium								
Nb-88	14.3 m	Y	-	0.01	2.53E-12	3.06E-12	3.46E-12	4.20E-12
Nb-89b	122 m	Y	-	0.01	1.75E-11	2.82E-11	2.50E-11	4.07E-11
Nb-89a	66 m	Y	-	0.01	7.28E-12	1.08E-11	1.02E-11	1.53E-11
Nb-90	14.60 h	-	Y	0.01	8.86E-11	1.54E-10	1.27E-10	2.22E-10
Nb-93m	13.6 y	-	Y	0.01	1.21E-11	2.17E-11	1.77E-11	3.17E-11
Nb-94	2.03E4 y	-	-	0.01	1.22E-10	2.10E-10	1.73E-10	3.01E-10
Nb-95	35.15 d	-	Y	0.01	3.81E-11	6.63E-11	5.41E-11	9.45E-11
Nb-95m	86.6 h	Y	Y	0.01	5.49E-11	9.88E-11	8.03E-11	1.45E-10
Nb-96	23.35 h	-	-	0.01	7.80E-11	1.36E-10	1.12E-10	1.96E-10
Nb-97	72.1 m	-	Y	0.01	3.60E-12	5.29E-12	5.08E-12	7.53E-12
Nb-98	51.5 m	-	-	0.01	5.44E-12	7.56E-12	7.58E-12	1.06E-11

Table 2.2a, continued

Nuclide	T _{1/2}	Chain			Tap Water Intakes		Dietary Intakes	
		P	D	f ₁	Mortality (Bq ⁻¹)	Morbidity (Bq ⁻¹)	Mortality (Bq ⁻¹)	Morbidity (Bq ⁻¹)
Molybdenum								
Mo-90	5.67 h	Y	-	1.0	1.27E-11	1.78E-11	1.67E-11	2.36E-11
Mo-93	3.5E3 y	Y	Y	1.0	8.21E-11	9.06E-11	1.01E-10	1.13E-10
Mo-93m	6.85 h	Y	-	1.0	6.28E-12	8.66E-12	8.29E-12	1.15E-11
Mo-99	66.0 h	Y	-	1.0	3.12E-11	4.33E-11	4.06E-11	5.71E-11
Mo-101	14.62 m	Y	-	1.0	1.60E-12	1.86E-12	2.18E-12	2.55E-12
Technetium								
Tc-93	2.75 h	Y	Y	0.5	2.71E-12	4.29E-12	3.72E-12	5.94E-12
Tc-93m	43.5 m	Y	-	0.5	1.21E-12	1.84E-12	1.67E-12	2.55E-12
Tc-94	293 m	-	-	0.5	1.04E-11	1.72E-11	1.44E-11	2.40E-11
Tc-94m	52 m	-	Y	0.5	4.47E-12	6.39E-12	6.23E-12	8.98E-12
Tc-95	20.0 h	-	Y	0.5	9.25E-12	1.56E-11	1.28E-11	2.17E-11
Tc-95m	61 d	Y	-	0.5	2.96E-11	4.87E-11	4.09E-11	6.79E-11
Tc-96	4.28 d	-	Y	0.5	5.59E-11	9.23E-11	7.66E-11	1.28E-10
Tc-96m	51.5 m	Y	-	0.5	6.07E-13	9.70E-13	8.37E-13	1.35E-12
Tc-97	2.6E6 y	-	Y	0.5	4.25E-12	7.31E-12	6.09E-12	1.05E-11
Tc-97m	87 d	Y	Y	0.5	3.67E-11	6.42E-11	5.30E-11	9.31E-11
Tc-98	4.2E6 y	-	-	0.5	1.14E-10	1.92E-10	1.61E-10	2.73E-10
Tc-99	2.13E5 y	-	Y	0.5	4.28E-11	7.44E-11	6.17E-11	1.08E-10
Tc-99m	6.02 h	Y	Y	0.5	1.22E-12	2.15E-12	1.73E-12	3.07E-12
Tc-101	14.2 m	-	Y	0.5	7.07E-13	8.28E-13	9.72E-13	1.14E-12
Tc-104	18.2 m	-	-	0.5	3.09E-12	3.72E-12	4.25E-12	5.14E-12
Ruthenium								
Ru-94	51.8 m	Y	-	0.05	5.17E-12	8.27E-12	7.35E-12	1.18E-11
Ru-97	2.9 d	Y	-	0.05	9.85E-12	1.72E-11	1.40E-11	2.45E-11
Ru-103	39.28 d	Y	-	0.05	5.88E-11	1.04E-10	8.48E-11	1.50E-10
Ru-105	4.44 h	Y	-	0.05	2.10E-11	3.64E-11	3.05E-11	5.30E-11
Ru-106 ^a	368.2 d	Y	-	0.05	6.45E-10	1.14E-09	9.35E-10	1.65E-09
Rhodium								
Rh-99	16 d	-	-	0.05	3.44E-11	5.97E-11	4.88E-11	8.52E-11
Rh-99m	4.7 h	-	-	0.05	3.94E-12	6.54E-12	5.54E-12	9.25E-12
Rh-100	20.8 h	-	Y	0.05	4.20E-11	7.17E-11	5.91E-11	1.01E-10
Rh-101	3.2 y	-	Y	0.05	3.52E-11	5.80E-11	4.89E-11	8.13E-11
Rh-101m	4.34 d	Y	Y	0.05	1.46E-11	2.54E-11	2.07E-11	3.63E-11
Rh-102	2.9 y	-	Y	0.05	1.33E-10	2.08E-10	1.78E-10	2.82E-10
Rh-102m	207 d	Y	-	0.05	9.42E-11	1.64E-10	1.35E-10	2.36E-10
Rh-103m	56.12 m	-	Y	0.05	1.82E-13	2.54E-13	2.57E-13	3.61E-13
Rh-105	35.36 h	-	Y	0.05	3.52E-11	6.33E-11	5.16E-11	9.27E-11
Rh-106m	132 m	-	-	0.05	9.31E-12	1.48E-11	1.31E-11	2.09E-11
Rh-107	21.7 m	Y	-	0.05	9.42E-13	1.13E-12	1.30E-12	1.57E-12

Table 2.2a, continued

Nuclide	T _{1/2}	Chain			Tap Water Intakes		Dietary Intakes	
		P	D	f ₁	Mortality (Bq ⁻¹)	Morbidity (Bq ⁻¹)	Mortality (Bq ⁻¹)	Morbidity (Bq ⁻¹)
Palladium								
Pd-100	3.63 d	Y	-	0.005	6.21E-11	1.09E-10	8.83E-11	1.56E-10
Pd-101	8.27 h	Y	-	0.005	6.59E-12	1.14E-11	9.44E-12	1.64E-11
Pd-103	16.96 d	Y	Y	0.005	1.87E-11	3.38E-11	2.74E-11	4.96E-11
Pd-107	6.5E6 y	-	Y	0.005	3.74E-12	6.77E-12	5.49E-12	9.93E-12
Pd-109	13.427 h	-	-	0.005	5.28E-11	9.46E-11	7.74E-11	1.39E-10
Silver								
Ag-102	12.9 m	-	-	0.05	1.62E-12	1.96E-12	2.21E-12	2.69E-12
Ag-103	65.7 m	Y	-	0.05	2.21E-12	3.23E-12	3.11E-12	4.56E-12
Ag-104	69.2 m	-	Y	0.05	3.03E-12	4.47E-12	4.17E-12	6.19E-12
Ag-104m	33.5 m	Y	-	0.05	2.42E-12	3.26E-12	3.35E-12	4.55E-12
Ag-105	41.0 d	-	-	0.05	2.88E-11	4.79E-11	4.02E-11	6.73E-11
Ag-106	23.96 m	-	-	0.05	1.30E-12	1.60E-12	1.80E-12	2.22E-12
Ag-106m	8.41 d	-	-	0.05	7.82E-11	1.30E-10	1.08E-10	1.82E-10
Ag-108m	127 y	Y	-	0.05	1.42E-10	2.20E-10	1.92E-10	3.03E-10
Ag-110m	249.9 d	Y	-	0.05	1.68E-10	2.67E-10	2.30E-10	3.71E-10
Ag-111	7.45 d	-	-	0.05	1.24E-10	2.22E-10	1.81E-10	3.26E-10
Ag-112	3.12 h	-	-	0.05	3.20E-11	5.39E-11	4.64E-11	7.84E-11
Ag-115	20.0 m	Y	-	0.05	2.78E-12	3.78E-12	3.90E-12	5.34E-12
Cadmium								
Cd-104	57.7 m	Y	-	0.05	2.93E-12	4.65E-12	4.08E-12	6.52E-12
Cd-107	6.49 h	-	-	0.05	5.39E-12	9.46E-12	7.86E-12	1.38E-11
Cd-109	464 d	-	Y	0.05	8.65E-11	1.35E-10	1.14E-10	1.81E-10
Cd-113	9.3E15 y	-	-	0.05	4.34E-10	6.17E-10	5.48E-10	7.85E-10
Cd-113m	13.6 y	-	-	0.05	5.36E-10	7.77E-10	6.72E-10	9.84E-10
Cd-115	53.46 h	Y	Y	0.05	1.30E-10	2.34E-10	1.90E-10	3.42E-10
Cd-115m	44.6 d	Y	Y	0.05	2.62E-10	4.60E-10	3.76E-10	6.64E-10
Cd-117	2.49 h	Y	-	0.05	2.16E-11	3.70E-11	3.12E-11	5.37E-11
Cd-117m	3.36 h	Y	-	0.05	1.96E-11	3.31E-11	2.80E-11	4.75E-11
Indium								
In-109	4.2 h	Y	-	0.02	4.02E-12	6.66E-12	5.67E-12	9.47E-12
In-110b	4.9 h	-	-	0.02	1.26E-11	2.05E-11	1.74E-11	2.85E-11
In-110a	69.1 m	-	Y	0.02	5.20E-12	7.59E-12	7.30E-12	1.08E-11
In-111	2.83 d	-	Y	0.02	1.99E-11	3.48E-11	2.84E-11	5.00E-11
In-112	14.4 m	-	-	0.02	3.87E-13	4.55E-13	5.32E-13	6.27E-13
In-113m	1.658 h	-	Y	0.02	1.65E-12	2.56E-12	2.34E-12	3.66E-12
In-114m	49.51 d	Y	-	0.02	3.85E-10	6.70E-10	5.55E-10	9.73E-10
In-115	5.1E15 y	-	Y	0.02	7.87E-10	9.13E-10	9.94E-10	1.17E-09
In-115m	4.486 h	Y	Y	0.02	6.90E-12	1.19E-11	1.00E-11	1.73E-11
In-116m	54.15 m	-	-	0.02	3.09E-12	4.38E-12	4.27E-12	6.11E-12

Table 2.2a, continued

Nuclide	T _{1/2}	Chain			Tap Water Intakes		Dietary Intakes	
		P	D	f ₁	Mortality (Bq ⁻¹)	Morbidity (Bq ⁻¹)	Mortality (Bq ⁻¹)	Morbidity (Bq ⁻¹)
Indium, continued								
In-117	43.8 m	Y	Y	0.02	1.40E-12	1.90E-12	1.95E-12	2.66E-12
In-117m	116.5 m	Y	Y	0.02	7.40E-12	1.20E-11	1.06E-11	1.74E-11
In-119m	18.0 m	Y	-	0.02	1.75E-12	2.04E-12	2.41E-12	2.82E-12
Tin								
Sn-110	4.0 h	Y	-	0.02	2.87E-11	5.05E-11	4.16E-11	7.33E-11
Sn-111	35.3 m	Y	-	0.02	1.08E-12	1.49E-12	1.50E-12	2.08E-12
Sn-113	115.1 d	Y	-	0.02	6.56E-11	1.17E-10	9.54E-11	1.71E-10
Sn-117m	13.61 d	-	Y	0.02	6.59E-11	1.18E-10	9.63E-11	1.73E-10
Sn-119m	293.0 d	-	Y	0.02	3.33E-11	5.98E-11	4.87E-11	8.75E-11
Sn-121	27.06 h	-	Y	0.02	2.25E-11	4.05E-11	3.30E-11	5.95E-11
Sn-121m	55 y	Y	-	0.02	3.58E-11	6.33E-11	5.19E-11	9.21E-11
Sn-123	129.2 d	-	-	0.02	2.10E-10	3.78E-10	3.07E-10	5.53E-10
Sn-123m	40.08 m	-	-	0.02	1.65E-12	2.15E-12	2.31E-12	3.03E-12
Sn-125	9.64 d	Y	-	0.02	3.01E-10	5.43E-10	4.41E-10	7.96E-10
Sn-126	1.0E5 y	Y	-	0.02	3.96E-10	6.91E-10	5.69E-10	9.98E-10
Sn-127	2.10 h	Y	-	0.02	1.35E-11	2.23E-11	1.94E-11	3.22E-11
Sn-128	59.1 m	Y	-	0.02	7.97E-12	1.17E-11	1.12E-11	1.66E-11
Antimony								
Sb-115	31.8 m	-	-	0.1	1.06E-12	1.39E-12	1.46E-12	1.92E-12
Sb-116	15.8 m	-	Y	0.1	1.09E-12	1.34E-12	1.49E-12	1.84E-12
Sb-116m	60.3 m	-	-	0.1	3.29E-12	4.77E-12	4.53E-12	6.62E-12
Sb-117	2.80 h	-	-	0.1	1.10E-12	1.78E-12	1.55E-12	2.55E-12
Sb-118m	5.00 h	-	-	0.1	1.16E-11	1.89E-11	1.61E-11	2.65E-11
Sb-119	38.1 h	-	-	0.1	7.21E-12	1.29E-11	1.05E-11	1.88E-11
Sb-120b	5.76 d	-	-	0.1	7.04E-11	1.20E-10	9.83E-11	1.68E-10
Sb-120a	15.89 m	-	-	0.1	5.62E-13	6.70E-13	7.73E-13	9.23E-13
Sb-122	2.70 d	-	-	0.1	1.60E-10	2.87E-10	2.34E-10	4.20E-10
Sb-124	60.20 d	-	Y	0.1	2.00E-10	3.48E-10	2.86E-10	5.01E-10
Sb-124 _n	20.2 m	Y	-	0.1	3.48E-13	4.51E-13	4.80E-13	6.26E-13
Sb-125 _a	2.77 y	Y	Y	0.1	7.27E-11	1.18E-10	1.01E-10	1.66E-10
Sb-126	12.4 d	-	Y	0.1	1.72E-10	3.00E-10	2.46E-10	4.29E-10
Sb-126m	19.0 m	Y	Y	0.1	1.46E-12	1.80E-12	2.01E-12	2.49E-12
Sb-127	3.85 d	Y	Y	0.1	1.52E-10	2.72E-10	2.22E-10	3.97E-10
Sb-128b	9.01 h	-	-	0.1	5.41E-11	9.33E-11	7.74E-11	1.34E-10
Sb-128a	10.4 m	-	Y	0.1	1.27E-12	1.49E-12	1.73E-12	2.04E-12
Sb-129	4.32 h	Y	-	0.1	3.41E-11	5.93E-11	4.95E-11	8.62E-11
Sb-130	40 m	-	-	0.1	4.15E-12	5.59E-12	5.73E-12	7.78E-12
Sb-131	23 m	Y	-	0.1	3.28E-12	6.91E-12	4.56E-12	9.71E-12

Table 2.2a, continued

Nuclide	T _{1/2}	Chain			Tap Water Intakes		Dietary Intakes	
		P	D	f ₁	Mortality (Bq ⁻¹)	Morbidity (Bq ⁻¹)	Mortality (Bq ⁻¹)	Morbidity (Bq ⁻¹)
Tellurium								
Te-116	2.49 h	Y	-	0.3	1.11E-11	1.82E-11	1.58E-11	2.60E-11
Te-121	17 d	-	Y	0.3	2.43E-11	3.94E-11	3.30E-11	5.43E-11
Te-121m	154 d	Y	-	0.3	1.20E-10	1.73E-10	1.56E-10	2.30E-10
Te-123	1E13 y	-	Y	0.3	9.59E-11	1.11E-10	1.18E-10	1.38E-10
Te-123m	119.7 d	Y	Y	0.3	7.28E-11	1.12E-10	9.72E-11	1.53E-10
Te-125m	58 d	-	Y	0.3	5.42E-11	8.99E-11	7.51E-11	1.27E-10
Te-127	9.35 h	-	Y	0.3	1.54E-11	2.71E-11	2.25E-11	3.99E-11
Te-127m	109 d	Y	Y	0.3	1.51E-10	2.33E-10	2.03E-10	3.23E-10
Te-129	69.6 m	Y	Y	0.3	3.21E-12	4.62E-12	4.55E-12	6.60E-12
Te-129m	33.6 d	Y	Y	0.3	2.39E-10	4.14E-10	3.39E-10	5.95E-10
Te-131	25.0 m	Y	Y	0.3	2.08E-12	5.86E-12	2.89E-12	8.25E-12
Te-131m	30 h	Y	Y	0.3	9.04E-11	2.23E-10	1.30E-10	3.21E-10
Te-132	78.2 h	Y	-	0.3	1.94E-10	4.60E-10	2.78E-10	6.60E-10
Te-133	12.45 m	Y	Y	0.3	1.60E-12	5.20E-12	2.22E-12	7.37E-12
Te-133m	55.4 m	Y	-	0.3	7.62E-12	2.36E-11	1.07E-11	3.36E-11
Te-134	41.8 m	Y	-	0.3	4.29E-12	8.13E-12	5.90E-12	1.13E-11
Iodine								
I-120	81.0 m	-	-	1.0	9.51E-12	2.44E-11	1.28E-11	3.38E-11
I-120m	53 m	-	-	1.0	7.36E-12	1.36E-11	9.94E-12	1.87E-11
I-121	2.12 h	Y	-	1.0	1.46E-12	6.14E-12	1.97E-12	8.45E-12
I-123	13.2 h	Y	-	1.0	2.70E-12	1.88E-11	3.72E-12	2.66E-11
I-124	4.18 d	-	-	1.0	1.21E-10	1.12E-09	1.71E-10	1.58E-09
I-125	60.14 d	-	Y	1.0	7.14E-11	6.87E-10	9.64E-11	9.28E-10
I-126	13.02 d	-	-	1.0	2.45E-10	2.36E-09	3.44E-10	3.31E-09
I-128	24.99 m	-	-	1.0	1.58E-12	2.20E-12	2.16E-12	3.03E-12
I-129	1.57E7 y	-	Y	1.0	4.07E-10	3.99E-09	5.31E-10	5.21E-09
I-130	12.36 h	-	-	1.0	2.53E-11	1.72E-10	3.47E-11	2.44E-10
I-131 ^a	8.04 d	Y	Y	1.0	1.31E-10	1.23E-09	1.85E-10	1.75E-09
I-132	2.30 h	-	Y	1.0	6.87E-12	2.28E-11	9.21E-12	3.17E-11
I-132m	83.6 m	Y	-	1.0	3.79E-12	1.65E-11	5.19E-12	2.34E-11
I-133	20.8 h	Y	Y	1.0	4.63E-11	3.90E-10	6.51E-11	5.58E-10
I-134	52.6 m	-	Y	1.0	3.68E-12	6.76E-12	4.97E-12	9.28E-12
I-135	6.61 h	Y	-	1.0	1.39E-11	8.24E-11	1.90E-11	1.17E-10
Cesium								
Cs-125	45 m	Y	-	1.0	1.35E-12	1.61E-12	1.84E-12	2.21E-12
Cs-127	6.25 h	Y	-	1.0	1.27E-12	1.76E-12	1.69E-12	2.36E-12
Cs-129	32.06 h	-	-	1.0	3.44E-12	5.00E-12	4.56E-12	6.69E-12
Cs-130	29.9 m	-	-	1.0	1.09E-12	1.28E-12	1.49E-12	1.75E-12
Cs-131	9.69 d	-	Y	1.0	3.40E-12	5.02E-12	4.51E-12	6.73E-12

Table 2.2a, continued

Nuclide	T _{1/2}	Chain			Tap Water Intakes		Dietary Intakes	
		P	D	f ₁	Mortality (Bq ⁻¹)	Morbidity (Bq ⁻¹)	Mortality (Bq ⁻¹)	Morbidity (Bq ⁻¹)
Cesium, continued								
Cs-132	6.475 d	-	-	1.0	2.70E-11	3.95E-11	3.51E-11	5.17E-11
Cs-134	2.062 y	-	Y	1.0	7.91E-10	1.14E-09	9.57E-10	1.39E-09
Cs-134m	2.90 h	Y	-	1.0	8.65E-13	1.12E-12	1.16E-12	1.50E-12
Cs-135	2.3E6 y	-	Y	1.0	8.72E-11	1.28E-10	1.07E-10	1.59E-10
Cs-135m	53 m	Y	-	1.0	9.36E-13	1.22E-12	1.26E-12	1.64E-12
Cs-136	13.1 d	-	-	1.0	1.60E-10	2.34E-10	2.05E-10	3.04E-10
Cs-137 ^a	30.0 y	Y	-	1.0	5.66E-10	8.22E-10	6.88E-10	1.01E-09
Cs-138	32.2 m	-	-	1.0	3.61E-12	4.26E-12	4.93E-12	5.83E-12
Barium								
Ba-126	96.5 m	Y	-	0.2	1.49E-11	2.30E-11	2.13E-11	3.31E-11
Ba-128	2.43 d	Y	-	0.2	2.31E-10	4.12E-10	3.38E-10	6.04E-10
Ba-131	11.8 d	Y	Y	0.2	3.15E-11	5.41E-11	4.50E-11	7.76E-11
Ba-131m	14.6 m	Y	-	0.2	2.01E-13	2.50E-13	2.78E-13	3.48E-13
Ba-133	10.74 y	-	Y	0.2	1.27E-10	1.84E-10	1.73E-10	2.55E-10
Ba-133m	38.9 h	Y	-	0.2	4.82E-11	8.62E-11	7.06E-11	1.26E-10
Ba-135m	28.7 h	-	-	0.2	3.87E-11	6.91E-11	5.66E-11	1.01E-10
Ba-139	82.7 m	-	-	0.2	6.67E-12	9.99E-12	9.51E-12	1.44E-11
Ba-140	12.74 d	Y	-	0.2	2.30E-10	4.03E-10	3.34E-10	5.86E-10
Ba-141	18.27 m	Y	-	0.2	3.86E-12	5.78E-12	5.50E-12	8.30E-12
Ba-142	10.6 m	Y	-	0.2	1.75E-12	2.51E-12	2.46E-12	3.54E-12
Lanthanum								
La-131	59 m	Y	-	0.0005	1.74E-12	2.52E-12	2.43E-12	3.55E-12
La-132	4.8 h	-	-	0.0005	2.82E-11	4.82E-11	4.05E-11	6.96E-11
La-135	19.5 h	-	Y	0.0005	2.23E-12	3.94E-12	3.22E-12	5.70E-12
La-137	6E4 y	-	Y	0.0005	5.46E-12	9.40E-12	7.79E-12	1.35E-11
La-138	1.35E11 y	-	-	0.0005	5.82E-11	9.55E-11	8.05E-11	1.34E-10
La-140	40.272 h	-	Y	0.0005	1.67E-10	2.96E-10	2.41E-10	4.30E-10
La-141	3.93 h	Y	Y	0.0005	2.95E-11	5.07E-11	4.29E-11	7.41E-11
La-142	92.5 m	-	Y	0.0005	1.02E-11	1.56E-11	1.44E-11	2.22E-11
La-143	14.23 m	Y	-	0.0005	2.53E-12	3.41E-12	3.56E-12	4.82E-12
Cerium								
Ce-134	72.0 h	Y	-	0.0005	2.39E-10	4.31E-10	3.50E-10	6.31E-10
Ce-135	17.6 h	Y	-	0.0005	5.86E-11	1.03E-10	8.41E-11	1.48E-10
Ce-137	9.0 h	Y	Y	0.0005	2.02E-12	3.55E-12	2.92E-12	5.15E-12
Ce-137m	34.4 h	Y	-	0.0005	5.20E-11	9.37E-11	7.62E-11	1.37E-10
Ce-139	137.66 d	-	Y	0.0005	2.05E-11	3.65E-11	2.96E-11	5.28E-11
Ce-141	32.501 d	-	Y	0.0005	6.93E-11	1.25E-10	1.02E-10	1.83E-10
Ce-143	33.0 h	Y	Y	0.0005	1.07E-10	1.92E-10	1.56E-10	2.81E-10
Ce-144	284.3 d	Y	-	0.0005	5.27E-10	9.52E-10	7.73E-10	1.40E-09

Table 2.2a, continued

Nuclide	T _{1/2}	Chain			Tap Water Intakes		Dietary Intakes	
		P	D	f ₁	Mortality (Bq ⁻¹)	Morbidity (Bq ⁻¹)	Mortality (Bq ⁻¹)	Morbidity (Bq ⁻¹)
Praseodymium								
Pr-136	13.1 m	-	Y	0.0005	1.33E-12	1.59E-12	1.81E-12	2.18E-12
Pr-137	76.6 m	Y	-	0.0005	2.21E-12	3.38E-12	3.13E-12	4.82E-12
Pr-138m	2.1 h	-	-	0.0005	7.17E-12	1.13E-11	1.00E-11	1.60E-11
Pr-139	4.51 h	Y	Y	0.0005	2.32E-12	3.96E-12	3.34E-12	5.73E-12
Pr-142	19.13 h	-	Y	0.0005	1.29E-10	2.32E-10	1.90E-10	3.41E-10
Pr-142m	14.6 m	Y	-	0.0005	1.66E-12	2.98E-12	2.43E-12	4.38E-12
Pr-143	13.56 d	-	Y	0.0005	1.18E-10	2.14E-10	1.73E-10	3.14E-10
Pr-144	17.28 m	-	Y	0.0005	1.88E-12	2.19E-12	2.60E-12	3.03E-12
Pr-145	5.98 h	-	-	0.0005	3.53E-11	6.20E-11	5.15E-11	9.08E-11
Pr-147	13.6 m	Y	-	0.0005	1.30E-12	1.58E-12	1.79E-12	2.19E-12
Neodymium								
Nd-136	50.65 m	Y	-	0.0005	5.02E-12	7.31E-12	7.03E-12	1.03E-11
Nd-138	5.04 h	Y	-	0.0005	5.31E-11	9.24E-11	7.72E-11	1.35E-10
Nd-139	29.7 m	Y	Y	0.0005	9.51E-13	1.34E-12	1.33E-12	1.88E-12
Nd-139m	5.5 h	Y	-	0.0005	1.72E-11	2.93E-11	2.45E-11	4.21E-11
Nd-141	2.49 h	-	Y	0.0005	5.14E-13	8.35E-13	7.31E-13	1.19E-12
Nd-147	10.98 d	Y	Y	0.0005	1.04E-10	1.88E-10	1.53E-10	2.76E-10
Nd-149	1.73 h	Y	-	0.0005	8.90E-12	1.47E-11	1.29E-11	2.14E-11
Nd-151	12.44 m	Y	-	0.0005	1.43E-12	1.99E-12	2.01E-12	2.81E-12
Promethium								
Pm-141	20.90 m	Y	Y	0.0005	1.46E-12	1.80E-12	2.02E-12	2.50E-12
Pm-143	265 d	-	Y	0.0005	1.37E-11	2.36E-11	1.93E-11	3.34E-11
Pm-144	363 d	-	Y	0.0005	5.32E-11	9.02E-11	7.40E-11	1.26E-10
Pm-145	17.7 y	-	Y	0.0005	8.63E-12	1.51E-11	1.24E-11	2.18E-11
Pm-146	2020 d	Y	-	0.0005	6.49E-11	1.13E-10	9.25E-11	1.62E-10
Pm-147	2.6234 y	Y	Y	0.0005	2.55E-11	4.57E-11	3.72E-11	6.70E-11
Pm-148	5.37 d	-	Y	0.0005	2.58E-10	4.65E-10	3.77E-10	6.80E-10
Pm-148m	41.3 d	Y	-	0.0005	1.23E-10	2.16E-10	1.76E-10	3.10E-10
Pm-149	53.08 h	-	Y	0.0005	9.95E-11	1.80E-10	1.46E-10	2.64E-10
Pm-150	2.68 h	-	-	0.0005	1.77E-11	2.92E-11	2.54E-11	4.22E-11
Pm-151	28.40 h	Y	Y	0.0005	6.78E-11	1.22E-10	9.90E-11	1.78E-10
Samarium								
Sm-141	10.2 m	Y	Y	0.0005	1.57E-12	1.92E-12	2.16E-12	2.65E-12
Sm-141m	22.6 m	Y	-	0.0005	2.88E-12	3.79E-12	3.99E-12	5.28E-12
Sm-142	72.49 m	Y	-	0.0005	9.86E-12	1.45E-11	1.40E-11	2.08E-11
Sm-145	340 d	Y	Y	0.0005	1.77E-11	3.16E-11	2.57E-11	4.60E-11
Sm-146	1.03E8 y	-	Y	0.0005	8.69E-10	1.11E-09	1.09E-09	1.42E-09
Sm-147	1.06E11 y	-	Y	0.0005	7.89E-10	1.01E-09	9.89E-10	1.29E-09
Sm-151	90 y	-	Y	0.0005	8.46E-12	1.50E-11	1.23E-11	2.18E-11

Table 2.2a, continued

Nuclide	T _{1/2}	Chain			Tap Water Intakes		Dietary Intakes	
		P	D	f ₁	Mortality (Bq ⁻¹)	Morbidity (Bq ⁻¹)	Mortality (Bq ⁻¹)	Morbidity (Bq ⁻¹)
Samarium, continued								
Sm-153	46.7 h	-	-	0.0005	7.25E-11	1.31E-10	1.06E-10	1.92E-10
Sm-155	22.1 m	Y	-	0.0005	1.12E-12	1.34E-12	1.55E-12	1.86E-12
Sm-156	9.4 h	Y	-	0.0005	2.26E-11	4.02E-11	3.30E-11	5.88E-11
Europium								
Eu-145	5.94 d	Y	Y	0.0005	4.29E-11	7.38E-11	6.02E-11	1.04E-10
Eu-146	4.61 d	Y	Y	0.0005	7.15E-11	1.23E-10	1.00E-10	1.73E-10
Eu-147	24 d	Y	Y	0.0005	3.11E-11	5.47E-11	4.45E-11	7.85E-11
Eu-148	54.5 d	Y	-	0.0005	6.80E-11	1.16E-10	9.49E-11	1.63E-10
Eu-149	93.1 d	-	Y	0.0005	7.80E-12	1.39E-11	1.12E-11	2.00E-11
Eu-150b	34.2 y	-	-	0.0005	7.03E-11	1.17E-10	9.76E-11	1.64E-10
Eu-150a	12.62 h	-	-	0.0005	3.60E-11	6.44E-11	5.28E-11	9.45E-11
Eu-152	13.33 y	Y	-	0.0005	9.50E-11	1.64E-10	1.35E-10	2.35E-10
Eu-152m	9.32 h	Y	-	0.0005	4.53E-11	8.05E-11	6.62E-11	1.18E-10
Eu-154	8.8 y	-	-	0.0005	1.59E-10	2.79E-10	2.29E-10	4.03E-10
Eu-155	4.96 y	-	Y	0.0005	2.88E-11	5.13E-11	4.19E-11	7.48E-11
Eu-156	15.19 d	-	Y	0.0005	1.91E-10	3.42E-10	2.77E-10	4.97E-10
Eu-157	15.15 h	-	-	0.0005	5.59E-11	9.99E-11	8.17E-11	1.46E-10
Eu-158	45.9 m	-	-	0.0005	4.28E-12	5.78E-12	5.98E-12	8.14E-12
Gadolinium								
Gd-145	22.9 m	Y	-	0.0005	1.87E-12	2.41E-12	2.57E-12	3.33E-12
Gd-146	48.3 d	Y	-	0.0005	7.64E-11	1.36E-10	1.10E-10	1.97E-10
Gd-147	38.1 h	Y	Y	0.0005	3.84E-11	6.65E-11	5.43E-11	9.46E-11
Gd-148	93 y	-	-	0.0005	8.53E-10	1.14E-09	1.08E-09	1.49E-09
Gd-149	9.4 d	Y	Y	0.0005	3.40E-11	6.02E-11	4.89E-11	8.69E-11
Gd-151	120 d	Y	Y	0.0005	1.71E-11	3.07E-11	2.49E-11	4.47E-11
Gd-152	1.08E14 y	-	Y	0.0005	6.03E-10	8.02E-10	7.64E-10	1.04E-09
Gd-153	242 d	-	Y	0.0005	2.31E-11	4.12E-11	3.35E-11	6.00E-11
Gd-159	18.56 h	-	-	0.0005	4.80E-11	8.62E-11	7.04E-11	1.26E-10
Terbium								
Tb-147	1.65 h	Y	-	0.0005	9.08E-12	1.44E-11	1.29E-11	2.05E-11
Tb-149	4.15 h	Y	-	0.0005	1.73E-11	2.92E-11	2.47E-11	4.21E-11
Tb-150	3.27 h	-	-	0.0005	1.75E-11	2.92E-11	2.51E-11	4.21E-11
Tb-151	17.6 h	Y	-	0.0005	2.31E-11	4.02E-11	3.30E-11	5.76E-11
Tb-153	2.34 d	Y	-	0.0005	1.96E-11	3.47E-11	2.83E-11	5.03E-11
Tb-154	21.4 h	-	-	0.0005	4.04E-11	6.94E-11	5.70E-11	9.85E-11
Tb-155	5.32 d	-	Y	0.0005	1.64E-11	2.91E-11	2.37E-11	4.22E-11
Tb-156	5.34 d	-	Y	0.0005	7.69E-11	1.34E-10	1.09E-10	1.92E-10
Tb-156m	24.4 h	Y	-	0.0005	1.29E-11	2.28E-11	1.85E-11	3.29E-11
Tb-156n	5.0 h	Y	-	0.0005	6.21E-12	1.09E-11	8.97E-12	1.58E-11
Tb-157	150 y	-	Y	0.0005	2.84E-12	5.02E-12	4.12E-12	7.31E-12

Table 2.2a, continued

Nuclide	T _{1/2}	Chain			Tap Water Intakes		Dietary Intakes	
		P	D	f ₁	Mortality (Bq ⁻¹)	Morbidity (Bq ⁻¹)	Mortality (Bq ⁻¹)	Morbidity (Bq ⁻¹)
Terbium, continued								
Tb-158	150 y	-	-	0.0005	7.67E-11	1.32E-10	1.09E-10	1.89E-10
Tb-160	72.3 d	-	-	0.0005	1.32E-10	2.35E-10	1.91E-10	3.42E-10
Tb-161	6.91 d	-	-	0.0005	7.16E-11	1.29E-10	1.05E-10	1.90E-10
Dysprosium								
Dy-155	10.0 h	Y	Y	0.0005	8.25E-12	1.42E-11	1.17E-11	2.02E-11
Dy-157	8.1 h	Y	Y	0.0005	3.62E-12	6.11E-12	5.09E-12	8.65E-12
Dy-159	144.4 d	-	Y	0.0005	8.05E-12	1.43E-11	1.16E-11	2.08E-11
Dy-165	2.334 h	-	-	0.0005	6.83E-12	1.12E-11	9.87E-12	1.63E-11
Dy-166	81.6 h	Y	-	0.0005	1.66E-10	3.01E-10	2.43E-10	4.41E-10
Holmium								
Ho-155	48 m	Y	-	0.0005	1.91E-12	2.85E-12	2.68E-12	4.04E-12
Ho-157	12.6 m	Y	-	0.0005	3.01E-13	4.15E-13	4.15E-13	5.76E-13
Ho-159	33 m	Y	-	0.0005	3.58E-13	4.80E-13	4.92E-13	6.64E-13
Ho-161	2.5 h	-	Y	0.0005	8.20E-13	1.34E-12	1.17E-12	1.93E-12
Ho-162	15 m	-	Y	0.0005	1.33E-13	1.61E-13	1.82E-13	2.21E-13
Ho-162m	68 m	Y	-	0.0005	1.36E-12	2.02E-12	1.90E-12	2.84E-12
Ho-164	29 m	-	Y	0.0005	3.83E-13	4.74E-13	5.32E-13	6.62E-13
Ho-164m	37.5 m	Y	-	0.0005	7.95E-13	1.12E-12	1.12E-12	1.59E-12
Ho-166	26.80 h	-	Y	0.0005	1.38E-10	2.49E-10	2.03E-10	3.65E-10
Ho-166m	1.20E3 y	-	-	0.0005	1.31E-10	2.17E-10	1.84E-10	3.07E-10
Ho-167	3.1 h	-	-	0.0005	5.88E-12	9.83E-12	8.46E-12	1.42E-11
Erbium								
Er-161	3.24 h	Y	-	0.0005	5.11E-12	8.52E-12	7.24E-12	1.22E-11
Er-165	10.36 h	-	-	0.0005	1.39E-12	2.42E-12	2.00E-12	3.50E-12
Er-169	9.3 d	-	-	0.0005	3.78E-11	6.84E-11	5.55E-11	1.00E-10
Er-171	7.52 h	Y	-	0.0005	3.11E-11	5.47E-11	4.52E-11	7.99E-11
Er-172	49.3 h	Y	-	0.0005	9.03E-11	1.62E-10	1.32E-10	2.37E-10
Thulium								
Tm-162	21.7 m	-	Y	0.0005	1.21E-12	1.53E-12	1.66E-12	2.10E-12
Tm-166	7.70 h	-	Y	0.0005	1.78E-11	3.03E-11	2.52E-11	4.31E-11
Tm-167	9.24 d	-	Y	0.0005	5.19E-11	9.35E-11	7.59E-11	1.37E-10
Tm-170	128.6 d	-	-	0.0005	1.34E-10	2.41E-10	1.96E-10	3.54E-10
Tm-171	1.92 y	-	Y	0.0005	1.05E-11	1.89E-11	1.54E-11	2.77E-11
Tm-172	63.6 h	-	Y	0.0005	1.61E-10	2.91E-10	2.36E-10	4.25E-10
Tm-173	8.24 h	-	-	0.0005	2.65E-11	4.66E-11	3.85E-11	6.81E-11
Tm-175	15.2 m	Y	-	0.0005	1.12E-12	1.41E-12	1.55E-12	1.96E-12
Ytterbium								
Yb-162	18.9 m	Y	-	0.0005	1.04E-12	1.41E-12	1.44E-12	1.97E-12
Yb-166	56.7 h	Y	-	0.0005	6.69E-11	1.18E-10	9.57E-11	1.70E-10
Yb-167	17.5 m	Y	-	0.0005	3.11E-13	4.21E-13	4.32E-13	5.90E-13
Yb-169	32.01 d	-	Y	0.0005	6.05E-11	1.08E-10	8.78E-11	1.58E-10

Table 2.2a, continued

Nuclide	T _{1/2}	Chain			Tap Water Intakes		Dietary Intakes	
		P	D	f ₁	Mortality (Bq ⁻¹)	Morbidity (Bq ⁻¹)	Mortality (Bq ⁻¹)	Morbidity (Bq ⁻¹)
Ytterbium, continued								
Yb-175	4.19 d	-	Y	0.0005	4.30E-11	7.76E-11	6.30E-11	1.14E-10
Yb-177	1.9 h	Y	-	0.0005	5.80E-12	9.36E-12	8.34E-12	1.36E-11
Yb-178	74 m	Y	-	0.0005	6.57E-12	1.05E-11	9.45E-12	1.51E-11
Lutetium								
Lu-169	34.06 h	Y	-	0.0005	3.01E-11	5.24E-11	4.28E-11	7.48E-11
Lu-170	2.00 d	-	Y	0.0005	6.45E-11	1.12E-10	9.12E-11	1.59E-10
Lu-171	8.22 d	-	-	0.0005	5.00E-11	8.84E-11	7.19E-11	1.27E-10
Lu-172	6.70 d	-	Y	0.0005	8.65E-11	1.51E-10	1.23E-10	2.17E-10
Lu-173	1.37 y	-	Y	0.0005	2.06E-11	3.66E-11	2.97E-11	5.30E-11
Lu-174m	142 d	Y	-	0.0005	5.07E-11	9.14E-11	7.42E-11	1.34E-10
Lu-174	3.31 y	-	Y	0.0005	2.23E-11	3.95E-11	3.22E-11	5.74E-11
Lu-176	3.60E10 y	-	-	0.0005	1.42E-10	2.51E-10	2.06E-10	3.64E-10
Lu-176m	3.68 h	-	-	0.0005	1.35E-11	2.31E-11	1.96E-11	3.37E-11
Lu-177	6.71 d	-	Y	0.0005	5.27E-11	9.53E-11	7.73E-11	1.40E-10
Lu-177m	160.9 d	Y	-	0.0005	1.42E-10	2.53E-10	2.05E-10	3.67E-10
Lu-178	28.4 m	-	Y	0.0005	1.90E-12	2.33E-12	2.63E-12	3.25E-12
Lu-178m	22.7 m	-	-	0.0005	1.56E-12	1.92E-12	2.14E-12	2.66E-12
Lu-179	4.59 h	-	-	0.0005	1.75E-11	3.04E-11	2.55E-11	4.44E-11
Hafnium								
Hf-170	16.01 h	Y	-	0.002	3.37E-11	5.91E-11	4.82E-11	8.48E-11
Hf-172	1.87 y	Y	Y	0.002	7.83E-11	1.34E-10	1.11E-10	1.93E-10
Hf-173	24.0 h	Y	Y	0.002	1.63E-11	2.87E-11	2.34E-11	4.12E-11
Hf-175	70 d	-	Y	0.002	3.01E-11	5.30E-11	4.31E-11	7.64E-11
Hf-177m	51.4 m	-	-	0.002	3.88E-12	5.44E-12	5.38E-12	7.60E-12
Hf-178m	31 y	-	-	0.002	2.51E-10	4.09E-10	3.48E-10	5.75E-10
Hf-179m	25.1 d	-	-	0.002	9.96E-11	1.77E-10	1.44E-10	2.57E-10
Hf-180m	5.5 h	-	-	0.002	1.14E-11	1.94E-11	1.62E-11	2.78E-11
Hf-181	42.4 d	-	-	0.002	9.62E-11	1.72E-10	1.40E-10	2.50E-10
Hf-182	9E6 y	Y	Y	0.002	1.01E-10	1.45E-10	1.34E-10	1.96E-10
Hf-182m	61.5 m	Y	-	0.002	2.09E-12	3.01E-12	2.91E-12	4.24E-12
Hf-183	64 m	Y	-	0.002	4.22E-12	6.46E-12	5.99E-12	9.25E-12
Hf-184	4.12 h	Y	-	0.002	4.45E-11	7.86E-11	6.47E-11	1.15E-10
Tantalum								
Ta-172	36.8 m	Y	-	0.001	2.33E-12	3.08E-12	3.22E-12	4.30E-12
Ta-173	3.65 h	Y	-	0.001	1.43E-11	2.44E-11	2.06E-11	3.54E-11
Ta-174	1.2 h	-	-	0.001	2.97E-12	4.38E-12	4.19E-12	6.22E-12
Ta-175	10.5 h	Y	-	0.001	1.37E-11	2.35E-11	1.94E-11	3.35E-11
Ta-176	8.08 h	-	Y	0.001	1.99E-11	3.38E-11	2.81E-11	4.80E-11
Ta-177	56.6 h	-	Y	0.001	8.93E-12	1.59E-11	1.30E-11	2.32E-11
Ta-178b	2.2 h	-	-	0.001	4.22E-12	6.72E-12	5.95E-12	9.55E-12
Ta-179	664.9 d	-	Y	0.001	5.22E-12	9.30E-12	7.54E-12	1.35E-11

Table 2.2a, continued

Nuclide	T _{1/2}	Chain			Tap Water Intakes		Dietary Intakes	
		P	D	f ₁	Mortality (Bq ⁻¹)	Morbidity (Bq ⁻¹)	Mortality (Bq ⁻¹)	Morbidity (Bq ⁻¹)
Tantalum, continued								
Ta-180	1.0E13 y	-	-	0.001	6.76E-11	1.20E-10	9.77E-11	1.74E-10
Ta-180m	8.1 h	-	-	0.001	4.64E-12	8.18E-12	6.76E-12	1.19E-11
Ta-182	115.0 d	-	Y	0.001	1.21E-10	2.15E-10	1.75E-10	3.11E-10
Ta-182m	15.84 m	Y	-	0.001	4.50E-13	5.39E-13	6.19E-13	7.45E-13
Ta-183	5.1 d	-	Y	0.001	1.25E-10	2.25E-10	1.82E-10	3.29E-10
Ta-184	8.7 h	-	Y	0.001	5.44E-11	9.54E-11	7.88E-11	1.38E-10
Ta-185	49 m	Y	-	0.001	3.12E-12	4.24E-12	4.38E-12	6.01E-12
Ta-186	10.5 m	-	-	0.001	1.27E-12	1.49E-12	1.74E-12	2.04E-12
Tungsten								
W-176	2.3 h	Y	-	0.3	6.55E-12	1.11E-11	9.28E-12	1.59E-11
W-177	135 m	Y	Y	0.3	3.39E-12	5.42E-12	4.77E-12	7.68E-12
W-178	21.7 d	Y	Y	0.3	1.83E-11	3.26E-11	2.65E-11	4.73E-11
W-179	37.5 m	Y	-	0.3	1.47E-13	1.95E-13	2.04E-13	2.72E-13
W-181	121.2 d	-	Y	0.3	6.07E-12	1.07E-11	8.72E-12	1.54E-11
W-185	75.1 d	-	Y	0.3	4.40E-11	7.91E-11	6.43E-11	1.16E-10
W-187	23.9 h	Y	-	0.3	5.57E-11	9.92E-11	8.11E-11	1.45E-10
W-188	69.4 d	Y	-	0.3	2.10E-10	3.78E-10	3.07E-10	5.53E-10
Rhenium								
Re-177	14.0 m	Y	-	0.8	8.94E-13	1.23E-12	1.23E-12	1.71E-12
Re-178	13.2 m	Y	-	0.8	9.58E-13	1.15E-12	1.31E-12	1.58E-12
Re-181	20 h	Y	Y	0.8	2.07E-11	3.81E-11	2.91E-11	5.40E-11
Re-182b	64.0 h	-	-	0.8	7.68E-11	1.34E-10	1.07E-10	1.89E-10
Re-182a	12.7 h	-	Y	0.8	1.31E-11	2.35E-11	1.82E-11	3.30E-11
Re-184	38.0 d	-	Y	0.8	5.20E-11	8.54E-11	7.18E-11	1.19E-10
Re-184m	165 d	Y	-	0.8	7.95E-11	1.32E-10	1.12E-10	1.88E-10
Re-186	90.64 h	-	Y	0.8	8.27E-11	1.51E-10	1.18E-10	2.17E-10
Re-186m	2.0E5 y	Y	-	0.8	1.23E-10	1.98E-10	1.74E-10	2.83E-10
Re-187	5E10 y	-	Y	0.8	2.84E-13	4.83E-13	4.04E-13	6.92E-13
Re-188	16.98 h	-	Y	0.8	6.77E-11	1.32E-10	9.68E-11	1.91E-10
Re-188m	18.6 m	Y	-	0.8	1.43E-12	2.68E-12	2.04E-12	3.84E-12
Re-189	24.3 h	Y	-	0.8	4.03E-11	7.74E-11	5.76E-11	1.11E-10
Osmium								
Os-180	22 m	Y	-	0.01	7.60E-13	9.81E-13	1.04E-12	1.35E-12
Os-181	105 m	Y	-	0.01	5.75E-12	9.57E-12	8.17E-12	1.37E-11
Os-182	22 h	Y	Y	0.01	3.97E-11	7.00E-11	5.69E-11	1.01E-10
Os-185	94 d	-	Y	0.01	3.05E-11	5.19E-11	4.27E-11	7.31E-11
Os-189m	6.0 h	-	Y	0.01	1.57E-12	2.76E-12	2.30E-12	4.05E-12
Os-191	15.4 d	-	Y	0.01	5.46E-11	9.83E-11	7.99E-11	1.44E-10
Os-191m	13.03 h	Y	-	0.01	9.20E-12	1.65E-11	1.35E-11	2.42E-11
Os-193	30.0 h	-	-	0.01	7.94E-11	1.43E-10	1.16E-10	2.10E-10
Os-194	6.0 y	Y	-	0.01	2.33E-10	4.14E-10	3.38E-10	6.03E-10

Table 2.2a, continued

Nuclide	T _{1/2}	Chain			Tap Water Intakes		Dietary Intakes	
		P	D	f ₁	Mortality (Bq ⁻¹)	Morbidity (Bq ⁻¹)	Mortality (Bq ⁻¹)	Morbidity (Bq ⁻¹)
Iridium								
Ir-182	15 m	Y	-	0.01	2.05E-12	2.69E-12	2.84E-12	3.75E-12
Ir-184	3.02 h	-	-	0.01	1.06E-11	1.74E-11	1.50E-11	2.49E-11
Ir-185	14.0 h	Y	-	0.01	2.03E-11	3.56E-11	2.92E-11	5.16E-11
Ir-186a	15.8 h	-	-	0.01	3.26E-11	5.63E-11	4.63E-11	8.05E-11
Ir-186b	1.75 h	-	Y	0.01	3.48E-12	5.41E-12	4.90E-12	7.68E-12
Ir-187	10.5 h	-	-	0.01	8.96E-12	1.56E-11	1.29E-11	2.25E-11
Ir-188	41.5 h	-	Y	0.01	3.94E-11	6.81E-11	5.57E-11	9.68E-11
Ir-189	13.3 d	Y	Y	0.01	2.28E-11	4.09E-11	3.32E-11	5.97E-11
Ir-190	12.1 d	-	Y	0.01	8.71E-11	1.53E-10	1.24E-10	2.19E-10
Ir-190n	3.1 h	Y	-	0.01	7.04E-12	1.15E-11	9.91E-12	1.63E-11
Ir-190m	1.2 h	Y	Y	0.01	5.14E-13	8.57E-13	7.34E-13	1.23E-12
Ir-192	74.02 d	-	Y	0.01	1.12E-10	1.99E-10	1.62E-10	2.89E-10
Ir-192m	241. y	Y	-	0.01	1.76E-11	2.65E-11	2.34E-11	3.56E-11
Ir-194	19.15 h	-	Y	0.01	1.30E-10	2.33E-10	1.90E-10	3.41E-10
Ir-194m	171 d	-	-	0.01	1.39E-10	2.40E-10	1.97E-10	3.41E-10
Ir-195	2.5 h	-	Y	0.01	6.48E-12	1.07E-11	9.37E-12	1.56E-11
Ir-195m	3.8 h	Y	-	0.01	1.63E-11	2.79E-11	2.36E-11	4.06E-11
Platinum								
Pt-186	2.0 h	Y	-	0.01	6.28E-12	1.06E-11	8.95E-12	1.52E-11
Pt-188	10.2 d	Y	-	0.01	5.76E-11	1.02E-10	8.29E-11	1.47E-10
Pt-189	10.87 h	Y	-	0.01	9.15E-12	1.60E-11	1.32E-11	2.31E-11
Pt-191	2.8 d	-	-	0.01	2.67E-11	4.75E-11	3.86E-11	6.88E-11
Pt-193	50 y	-	Y	0.01	3.16E-12	5.70E-12	4.63E-12	8.36E-12
Pt-193m	4.33 d	Y	-	0.01	4.54E-11	8.20E-11	6.66E-11	1.20E-10
Pt-195m	4.02 d	-	-	0.01	6.18E-11	1.11E-10	9.05E-11	1.63E-10
Pt-197	18.3 h	-	Y	0.01	3.94E-11	7.08E-11	5.78E-11	1.04E-10
Pt-197m	94.4 m	Y	-	0.01	6.40E-12	1.08E-11	9.27E-12	1.57E-11
Pt-199	30.8 m	Y	-	0.01	1.77E-12	2.39E-12	2.48E-12	3.37E-12
Pt-200	12.5 h	Y	-	0.01	1.16E-10	2.09E-10	1.70E-10	3.06E-10
Gold								
Au-193	17.65 h	Y	Y	0.1	1.13E-11	1.99E-11	1.63E-11	2.90E-11
Au-194	39.5 h	-	Y	0.1	2.61E-11	4.49E-11	3.68E-11	6.38E-11
Au-195	183 d	-	Y	0.1	2.27E-11	4.06E-11	3.30E-11	5.92E-11
Au-198	2.696 d	-	Y	0.1	9.48E-11	1.70E-10	1.38E-10	2.48E-10
Au-198m	2.30 d	Y	-	0.1	1.12E-10	2.01E-10	1.63E-10	2.93E-10
Au-199	3.139 d	-	Y	0.1	4.18E-11	7.51E-11	6.11E-11	1.10E-10
Au-200	48.4 m	-	Y	0.1	3.11E-12	4.20E-12	4.36E-12	5.94E-12
Au-200m	18.7 h	Y	-	0.1	8.37E-11	1.47E-10	1.21E-10	2.13E-10
Au-201	26.4 m	-	-	0.1	9.64E-13	1.17E-12	1.34E-12	1.63E-12

Table 2.2a, continued

Nuclide	T _{1/2}	Chain			Tap Water Intakes		Dietary Intakes	
		P	D	f ₁	Mortality (Bq ⁻¹)	Morbidity (Bq ⁻¹)	Mortality (Bq ⁻¹)	Morbidity (Bq ⁻¹)
Mercury (inorganic)								
Hg-193	3.5 h	Y	Y	0.02	6.44E-12	1.11E-11	9.31E-12	1.62E-11
Hg-193m	11.1 h	Y	-	0.02	3.03E-11	5.32E-11	4.36E-11	7.68E-11
Hg-194	260 y	Y	Y	0.02	4.98E-11	7.80E-11	6.74E-11	1.07E-10
Hg-195	9.9 h	Y	Y	0.02	7.81E-12	1.37E-11	1.13E-11	1.99E-11
Hg-195m	41.6 h	Y	-	0.02	5.07E-11	9.09E-11	7.39E-11	1.33E-10
Hg-197	64.1 h	-	Y	0.02	2.15E-11	3.86E-11	3.14E-11	5.65E-11
Hg-197m	23.8 h	Y	-	0.02	4.51E-11	8.10E-11	6.60E-11	1.19E-10
Hg-199m	42.6 m	-	-	0.02	1.37E-12	1.81E-12	1.91E-12	2.55E-12
Hg-203	46.60 d	-	-	0.02	4.67E-11	8.32E-11	6.78E-11	1.21E-10
Mercury (methyl)								
Hg-193	3.5 h	Y	Y	1.0	1.56E-12	2.10E-12	2.11E-12	2.86E-12
Hg-193m	11.1 h	Y	-	1.0	6.74E-12	9.61E-12	8.97E-12	1.29E-11
Hg-194	260 y	Y	Y	1.0	1.52E-09	2.18E-09	1.98E-09	2.87E-09
Hg-195	9.9 h	Y	Y	1.0	1.77E-12	2.50E-12	2.38E-12	3.37E-12
Hg-195m	41.6 h	Y	-	1.0	1.19E-11	1.76E-11	1.59E-11	2.37E-11
Hg-197	64.1 h	-	Y	1.0	5.37E-12	7.96E-12	7.19E-12	1.07E-11
Hg-197m	23.8 h	Y	-	1.0	7.69E-12	1.12E-11	1.03E-11	1.52E-11
Hg-199m	42.6 m	-	-	1.0	1.09E-12	1.28E-12	1.49E-12	1.75E-12
Hg-203	46.60 d	-	-	1.0	1.03E-10	1.54E-10	1.37E-10	2.06E-10
Mercury (organic)								
Hg-193	3.5 h	Y	Y	0.4	4.93E-12	8.33E-12	7.13E-12	1.21E-11
Hg-193m	11.1 h	Y	-	0.4	2.20E-11	3.78E-11	3.16E-11	5.46E-11
Hg-194	260 y	Y	Y	0.4	6.29E-10	9.07E-10	8.22E-10	1.19E-09
Hg-195	9.9 h	Y	Y	0.4	5.80E-12	9.98E-12	8.39E-12	1.45E-11
Hg-195m	41.6 h	Y	-	0.4	3.60E-11	6.32E-11	5.23E-11	9.21E-11
Hg-197	64.1 h	-	Y	0.4	1.54E-11	2.70E-11	2.24E-11	3.94E-11
Hg-197m	23.8 h	Y	-	0.4	3.14E-11	5.54E-11	4.59E-11	8.12E-11
Hg-199m	42.6 m	-	-	0.4	1.34E-12	1.75E-12	1.87E-12	2.47E-12
Hg-203	46.60 d	-	-	0.4	6.95E-11	1.12E-10	9.58E-11	1.56E-10
Thallium								
Tl-194	33 m	Y	-	1.0	3.85E-13	4.89E-13	5.18E-13	6.62E-13
Tl-194m	32.8 m	Y	-	1.0	1.72E-12	2.11E-12	2.33E-12	2.87E-12
Tl-195	1.16 h	Y	Y	1.0	1.32E-12	1.73E-12	1.78E-12	2.35E-12
Tl-197	2.84 h	Y	-	1.0	1.21E-12	1.69E-12	1.64E-12	2.31E-12
Tl-198	5.3 h	-	Y	1.0	3.96E-12	5.56E-12	5.26E-12	7.43E-12
Tl-198m	1.87 h	Y	-	1.0	2.64E-12	3.51E-12	3.55E-12	4.74E-12
Tl-199	7.42 h	-	Y	1.0	1.41E-12	1.99E-12	1.90E-12	2.70E-12
Tl-200	26.1 h	-	Y	1.0	1.12E-11	1.66E-11	1.49E-11	2.22E-11
Tl-201	3.044 d	-	Y	1.0	6.22E-12	9.76E-12	8.52E-12	1.35E-11
Tl-202	12.23 d	-	Y	1.0	2.64E-11	4.03E-11	3.52E-11	5.43E-11
Tl-204	3.779 y	-	-	1.0	9.58E-11	1.58E-10	1.34E-10	2.23E-10

Table 2.2a, continued

Nuclide	T _{1/2}	Chain			Tap Water Intakes		Dietary Intakes	
		P	D	f ₁	Mortality (Bq ⁻¹)	Morbidity (Bq ⁻¹)	Mortality (Bq ⁻¹)	Morbidity (Bq ⁻¹)
Lead								
Pb-195m	15.8 m	Y	-	0.2	1.15E-12	1.48E-12	1.57E-12	2.04E-12
Pb-198	2.4 h	Y	-	0.2	4.40E-12	7.03E-12	6.09E-12	9.80E-12
Pb-199	90 m	Y	-	0.2	2.52E-12	3.83E-12	3.47E-12	5.33E-12
Pb-200	21.5 h	Y	Y	0.2	2.49E-11	4.26E-11	3.52E-11	6.05E-11
Pb-201	9.4 h	Y	Y	0.2	9.51E-12	1.60E-11	1.34E-11	2.26E-11
Pb-202	3E5 y	Y	Y	0.2	4.51E-10	5.99E-10	5.90E-10	7.93E-10
Pb-202m	3.62 h	Y	Y	0.2	7.11E-12	1.13E-11	9.83E-12	1.58E-11
Pb-203	52.05 h	-	Y	0.2	1.61E-11	2.77E-11	2.29E-11	3.95E-11
Pb-205	1.43E7 y	-	Y	0.2	1.37E-11	1.71E-11	1.73E-11	2.23E-11
Pb-209	3.253 h	-	Y	0.2	3.92E-12	6.51E-12	5.64E-12	9.43E-12
Pb-210	22.3 y	Y	Y	0.2	1.75E-08	2.38E-08	2.31E-08	3.18E-08
Pb-211	36.1 m	Y	Y	0.2	8.39E-12	1.11E-11	1.17E-11	1.57E-11
Pb-212	10.64 h	Y	Y	0.2	4.22E-10	6.76E-10	5.95E-10	9.58E-10
Pb-214	26.8 m	Y	Y	0.2	6.82E-12	9.31E-12	9.51E-12	1.31E-11
Bismuth								
Bi-200	36.4 m	Y	-	0.05	2.73E-12	4.10E-12	3.80E-12	5.75E-12
Bi-201	108 m	Y	-	0.05	7.03E-12	1.14E-11	9.96E-12	1.63E-11
Bi-202	1.67 h	Y	-	0.05	4.67E-12	7.15E-12	6.46E-12	9.97E-12
Bi-203	11.76 h	Y	Y	0.05	3.04E-11	5.19E-11	4.29E-11	7.37E-11
Bi-205	15.31 d	Y	Y	0.05	5.22E-11	8.96E-11	7.32E-11	1.26E-10
Bi-206	6.243 d	-	-	0.05	1.21E-10	2.09E-10	1.71E-10	2.97E-10
Bi-207	38 y	-	Y	0.05	8.76E-11	1.53E-10	1.25E-10	2.20E-10
Bi-210	5.012 d	Y	Y	0.05	1.34E-10	2.41E-10	1.95E-10	3.52E-10
Bi-210m	3.0E6 y	Y	-	0.05	8.63E-10	1.49E-09	1.21E-09	2.10E-09
Bi-212	60.55 m	Y	Y	0.05	1.35E-11	1.92E-11	1.88E-11	2.70E-11
Bi-213	45.65 m	Y	Y	0.05	9.85E-12	1.38E-11	1.38E-11	1.94E-11
Bi-214	19.9 m	Y	Y	0.05	4.34E-12	5.19E-12	5.98E-12	7.17E-12
Polonium (organic)								
Po-203	36.7 m	Y	-	0.5	2.45E-12	3.63E-12	3.38E-12	5.07E-12
Po-205	1.80 h	Y	-	0.5	3.15E-12	4.71E-12	4.32E-12	6.51E-12
Po-207	350 m	Y	Y	0.5	6.66E-12	1.07E-11	9.27E-12	1.50E-11
Po-210	138.38 d	-	Y	0.5	3.53E-08	4.79E-08	4.44E-08	6.09E-08
Polonium (inorganic)								
Po-203	36.7 m	Y	-	0.1	2.84E-12	4.40E-12	3.95E-12	6.17E-12
Po-205	1.80 h	Y	-	0.1	3.17E-12	4.90E-12	4.38E-12	6.84E-12
Po-207	350 m	Y	-	0.1	8.45E-12	1.40E-11	1.19E-11	1.98E-11
Po-210	138.38 d	-	-	0.1	7.40E-09	1.02E-08	9.38E-09	1.31E-08
Astatine								
At-207	1.80 h	Y	-	1.0	1.29E-11	1.88E-11	1.75E-11	2.57E-11
At-211	7.214 h	Y	-	1.0	6.10E-10	9.10E-10	8.32E-10	1.25E-09

Table 2.2a, continued

Nuclide	T _{1/2}	Chain			Tap Water Intakes		Dietary Intakes	
		P	D	f ₁	Mortality (Bq ⁻¹)	Morbidity (Bq ⁻¹)	Mortality (Bq ⁻¹)	Morbidity (Bq ⁻¹)
Francium								
Fr-222	14.4 m	Y	Y	1.0	2.85E-11	4.00E-11	3.88E-11	5.47E-11
Fr-223	21.8 m	Y	Y	1.0	1.32E-10	1.97E-10	1.80E-10	2.71E-10
Radium								
Ra-223	11.434 d	Y	Y	0.2	4.00E-09	6.44E-09	5.63E-09	9.15E-09
Ra-224	3.66 d	Y	Y	0.2	2.74E-09	4.50E-09	3.88E-09	6.42E-09
Ra-225	14.8 d	Y	Y	0.2	2.20E-09	3.09E-09	2.93E-09	4.15E-09
Ra-226 ^a	1600 y	Y	Y	0.2	7.17E-09	1.04E-08	9.56E-09	1.39E-08
Ra-227	42.2 m	Y	-	0.2	2.15E-12	2.85E-12	2.96E-12	3.95E-12
Ra-228	5.75 y	Y	Y	0.2	2.00E-08	2.81E-08	2.74E-08	3.86E-08
Actinium								
Ac-224	2.9 h	Y	Y	0.0005	9.02E-11	1.51E-10	1.28E-10	2.17E-10
Ac-225	10.0 d	Y	Y	0.0005	2.94E-09	5.10E-09	4.20E-09	7.33E-09
Ac-226	29 h	Y	Y	0.0005	1.03E-09	1.87E-09	1.52E-09	2.74E-09
Ac-227	21.773 y	Y	Y	0.0005	4.43E-09	5.43E-09	5.34E-09	6.63E-09
Ac-228	6.13 h	Y	Y	0.0005	3.10E-11	5.38E-11	4.49E-11	7.82E-11
Thorium								
Th-226	30.9 m	Y	Y	0.0005	1.45E-11	1.80E-11	2.02E-11	2.52E-11
Th-227	18.718 d	Y	Y	0.0005	7.21E-10	1.28E-09	1.05E-09	1.87E-09
Th-228	1.9131 y	Y	Y	0.0005	1.82E-09	2.90E-09	2.46E-09	3.99E-09
Th-229	7340 y	Y	Y	0.0005	4.39E-09	6.05E-09	5.65E-09	7.85E-09
Th-230	7.7E4 y	Y	Y	0.0005	1.67E-09	2.46E-09	2.16E-09	3.22E-09
Th-231	25.52 h	Y	Y	0.0005	3.31E-11	5.96E-11	4.86E-11	8.75E-11
Th-232 ^a	1.41E10 y	Y	Y	0.0005	1.87E-09	2.73E-09	2.45E-09	3.60E-09
Th-234	24.10 d	Y	Y	0.0005	3.46E-10	6.25E-10	5.07E-10	9.18E-10
Protactinium								
Pa-227	38.3 m	Y	-	0.0005	2.00E-11	2.62E-11	2.81E-11	3.70E-11
Pa-228	22 h	Y	-	0.0005	5.53E-11	9.72E-11	7.96E-11	1.40E-10
Pa-230	17.4 d	Y	-	0.0005	5.79E-11	1.02E-10	8.29E-11	1.46E-10
Pa-231	3.276E4 y	Y	Y	0.0005	3.30E-09	4.67E-09	4.29E-09	6.11E-09
Pa-232	1.31 d	Y	-	0.0005	5.32E-11	9.41E-11	7.68E-11	1.36E-10
Pa-233	27.0 d	Y	Y	0.0005	8.34E-11	1.50E-10	1.22E-10	2.20E-10
Pa-234	6.70 h	Y	Y	0.0005	4.00E-11	6.93E-11	5.77E-11	1.00E-10
Uranium								
U-230	20.8 d	Y	Y	0.02	3.24E-09	5.65E-09	4.59E-09	8.05E-09
U-231	4.2 d	Y	Y	0.02	2.63E-11	4.73E-11	3.84E-11	6.91E-11
U-232	72 y	Y	Y	0.02	5.52E-09	7.88E-09	7.22E-09	1.04E-08
U-233	1.585E5 y	Y	Y	0.02	1.26E-09	1.94E-09	1.69E-09	2.62E-09
U-234 ^a	2.445E5 y	Y	Y	0.02	1.24E-09	1.91E-09	1.66E-09	2.58E-09
U-235	703.8E6 y	Y	Y	0.02	1.21E-09	1.88E-09	1.62E-09	2.55E-09
U-236	2.3415E7 y	Y	Y	0.02	1.17E-09	1.81E-09	1.57E-09	2.44E-09
U-237	6.75 d	Y	Y	0.02	7.31E-11	1.32E-10	1.07E-10	1.93E-10

Table 2.2a, continued

Nuclide	T _{1/2}	Chain			Tap Water Intakes		Dietary Intakes	
		P	D	f ₁	Mortality (Bq ⁻¹)	Morbidity (Bq ⁻¹)	Mortality (Bq ⁻¹)	Morbidity (Bq ⁻¹)
Uranium, continued								
U-238	4.468E9 y	Y	Y	0.02	1.13E-09	1.73E-09	1.51E-09	2.34E-09
U-239	23.54 m	Y	-	0.02	1.40E-12	2.00E-12	1.98E-12	2.86E-12
U-240	14.1 h	Y	Y	0.02	1.06E-10	1.90E-10	1.55E-10	2.79E-10
Neptunium								
Np-232	14.7 m	Y	-	0.0005	4.21E-13	5.33E-13	5.73E-13	7.29E-13
Np-233	36.2 m	Y	Y	0.0005	1.01E-13	1.36E-13	1.39E-13	1.89E-13
Np-234	4.4 d	Y	Y	0.0005	5.27E-11	9.19E-11	7.49E-11	1.31E-10
Np-235	396.1 d	Y	Y	0.0005	5.18E-12	9.34E-12	7.59E-12	1.37E-11
Np-236a	115E3 y	Y	-	0.0005	1.78E-10	2.83E-10	2.42E-10	3.90E-10
Np-236b	22.5 h	Y	Y	0.0005	1.68E-11	3.01E-11	2.46E-11	4.41E-11
Np-237	2.14E6 y	Y	Y	0.0005	1.10E-09	1.67E-09	1.44E-09	2.24E-09
Np-238	2.117 d	Y	Y	0.0005	8.14E-11	1.46E-10	1.19E-10	2.13E-10
Np-239	2.355 d	Y	Y	0.0005	7.70E-11	1.39E-10	1.13E-10	2.03E-10
Np-240	65 m	Y	-	0.0005	4.18E-12	6.04E-12	5.86E-12	8.55E-12
Plutonium								
Pu-234	8.8 h	Y	Y	0.0005	1.31E-11	2.32E-11	1.90E-11	3.37E-11
Pu-235	25.3 m	Y	-	0.0005	9.16E-14	1.18E-13	1.26E-13	1.63E-13
Pu-236	2.851 y	Y	Y	0.0005	1.44E-09	2.02E-09	1.87E-09	2.68E-09
Pu-237	45.3 d	Y	Y	0.0005	8.73E-12	1.56E-11	1.27E-11	2.27E-11
Pu-238	87.74 y	Y	Y	0.0005	2.75E-09	3.55E-09	3.50E-09	4.58E-09
Pu-239 ^a	24065 y	Y	Y	0.0005	2.85E-09	3.64E-09	3.63E-09	4.70E-09
Pu-240	6537 y	Y	Y	0.0005	2.85E-09	3.65E-09	3.63E-09	4.71E-09
Pu-241	14.4 y	Y	Y	0.0005	3.94E-11	4.77E-11	5.07E-11	6.17E-11
Pu-242	3.763E5 y	Y	Y	0.0005	2.71E-09	3.46E-09	3.45E-09	4.47E-09
Pu-243	4.956 h	Y	Y	0.0005	7.33E-12	1.28E-11	1.07E-11	1.87E-11
Pu-245	10.5 h	Y	-	0.0005	6.75E-11	1.21E-10	9.87E-11	1.77E-10
Pu-246	10.85 d	Y	Y	0.0005	2.60E-10	4.68E-10	3.80E-10	6.84E-10
Americium								
Am-237	73.0 m	Y	-	0.0005	9.26E-13	1.37E-12	1.30E-12	1.94E-12
Am-238	98 m	Y	Y	0.0005	1.70E-12	2.60E-12	2.36E-12	3.64E-12
Am-239	11.9 h	Y	-	0.0005	2.10E-11	3.73E-11	3.06E-11	5.44E-11
Am-240	50.8 h	Y	-	0.0005	4.00E-11	6.99E-11	5.71E-11	1.00E-10
Am-241	432.2 y	Y	Y	0.0005	2.01E-09	2.81E-09	2.56E-09	3.63E-09
Am-242	16.02 h	Y	Y	0.0005	2.71E-11	4.83E-11	3.96E-11	7.08E-11
Am-242m	152 y	Y	-	0.0005	1.47E-09	1.91E-09	1.80E-09	2.37E-09
Am-243	7380 y	Y	Y	0.0005	2.00E-09	2.79E-09	2.54E-09	3.61E-09
Am-244	10.1 h	Y	-	0.0005	3.86E-11	6.80E-11	5.60E-11	9.89E-11
Am-244m	26 m	Y	-	0.0005	1.14E-12	1.38E-12	1.58E-12	1.92E-12
Am-245	2.05 h	Y	Y	0.0005	3.73E-12	6.01E-12	5.37E-12	8.71E-12
Am-246	39 m	Y	-	0.0005	2.54E-12	3.33E-12	3.53E-12	4.67E-12
Am-246m	25.0 m	Y	Y	0.0005	1.43E-12	1.78E-12	1.97E-12	2.46E-12

Table 2.2a, continued

Nuclide	T _{1/2}	Chain			Tap Water Intakes		Dietary Intakes	
		P	D	f ₁	Mortality (Bq ⁻¹)	Morbidity (Bq ⁻¹)	Mortality (Bq ⁻¹)	Morbidity (Bq ⁻¹)
Curium								
Cm-238	2.4 h	Y	-	0.0005	5.28E-12	8.86E-12	7.55E-12	1.27E-11
Cm-240	27 d	Y	Y	0.0005	5.34E-10	9.42E-10	7.71E-10	1.37E-09
Cm-241	32.8 d	Y	-	0.0005	7.33E-11	1.31E-10	1.06E-10	1.90E-10
Cm-242	162.8 d	Y	Y	0.0005	6.15E-10	1.04E-09	8.65E-10	1.48E-09
Cm-243	28.5 y	Y	-	0.0005	1.81E-09	2.56E-09	2.30E-09	3.33E-09
Cm-244	18.11 y	Y	Y	0.0005	1.59E-09	2.26E-09	2.02E-09	2.93E-09
Cm-245	8500 y	Y	Y	0.0005	2.02E-09	2.82E-09	2.57E-09	3.64E-09
Cm-246	4730 y	Y	Y	0.0005	1.98E-09	2.76E-09	2.51E-09	3.55E-09
Cm-247	1.56E7 y	Y	Y	0.0005	1.92E-09	2.69E-09	2.44E-09	3.50E-09
Cm-249	64.15 m	Y	Y	0.0005	1.59E-12	2.27E-12	2.25E-12	3.25E-12
Berkelium								
Bk-245	4.94 d	Y	-	0.0005	5.16E-11	9.27E-11	7.53E-11	1.35E-10
Bk-246	1.83 d	Y	-	0.0005	3.13E-11	5.44E-11	4.45E-11	7.78E-11
Bk-247	1380 y	Y	Y	0.0005	2.54E-09	3.36E-09	3.22E-09	4.32E-09
Bk-249	320 d	Y	Y	0.0005	1.82E-11	3.00E-11	2.55E-11	4.25E-11
Bk-250	3.222 h	Y	Y	0.0005	9.20E-12	1.53E-11	1.32E-11	2.21E-11
Californium								
Cf-244	19.4 m	Y	-	0.0005	2.75E-12	3.37E-12	3.81E-12	4.71E-12
Cf-246	35.7 h	Y	-	0.0005	3.16E-10	5.69E-10	4.63E-10	8.35E-10
Cf-248	333.5 d	Y	Y	0.0005	7.47E-10	1.20E-09	1.03E-09	1.68E-09
Cf-249	350.6 y	Y	Y	0.0005	2.60E-09	3.44E-09	3.28E-09	4.41E-09
Cf-250	13.08 y	Y	Y	0.0005	1.70E-09	2.33E-09	2.15E-09	3.02E-09
Cf-251	898 y	Y	Y	0.0005	2.67E-09	3.56E-09	3.40E-09	4.59E-09
Cf-253	17.81 d	Y	Y	0.0005	6.73E-11	1.15E-10	9.56E-11	1.65E-10
Einsteinium								
Es-250	2.1 h	Y	-	0.0005	1.03E-12	1.61E-12	1.43E-12	2.26E-12
Es-251	33 h	Y	-	0.0005	1.54E-11	2.75E-11	2.24E-11	4.02E-11
Es-253	20.47 d	Y	Y	0.0005	5.25E-10	9.42E-10	7.67E-10	1.38E-09
Es-254	275.7 d	Y	Y	0.0005	9.01E-10	1.49E-09	1.26E-09	2.11E-09
Es-254m	39.3 h	Y	-	0.0005	4.08E-10	7.37E-10	5.97E-10	1.08E-09
Fermium								
Fm-252	22.7 h	Y	-	0.0005	2.55E-10	4.58E-10	3.73E-10	6.71E-10
Fm-253	3.00 d	Y	-	0.0005	7.74E-11	1.39E-10	1.13E-10	2.03E-10
Fm-254	3.240 h	Y	Y	0.0005	3.42E-11	5.80E-11	4.97E-11	8.47E-11
Fm-255	20.07 h	Y	-	0.0005	2.49E-10	4.47E-10	3.65E-10	6.55E-10
Fm-257	100.5 d	Y	Y	0.0005	6.98E-10	1.19E-09	9.89E-10	1.70E-09
Mendelevium								
Md-257	5.2 h	Y	-	0.0005	9.18E-12	1.59E-11	1.33E-11	2.32E-11
Md-258	55 d	Y	-	0.0005	6.76E-10	1.17E-09	9.69E-10	1.69E-09

^aThe uncertainty in the risk coefficient for this radionuclide is addressed in Table 2.4.

^bRisk coefficients are based on a biokinetic model designed mainly for ¹⁴C-labeled metabolites and may substantially overestimate risk from ingestion of some forms of ¹⁴C (see p. 18).

Table 2.2b. Mortality and morbidity risk coefficients for ingestion of iodine in food, based on usage of cow's milk.

Explanation of Entries

This table provides additional risk coefficients for intake of radioisotopes of iodine in diet. In this tabulation, the rate of intake of a radioisotope of iodine is assumed to be proportional to the ingestion rate of cow's milk.

Risk coefficients for ingestion of radioisotopes of iodine in cow's milk are expressed as the probability of radiogenic cancer mortality or morbidity per unit intake, where the intake is *averaged over all ages and both genders*.

To facilitate application of the risk coefficients, including conversion to other units, the coefficients are tabulated to three decimal places. No indication of the level of uncertainty is intended or should be inferred from this practice. A calculated risk should be rounded appropriately.

To express a risk coefficient in conventional units (μCi^{-1}), multiply by $3.7 \times 10^4 \text{ Bq } \mu\text{Ci}^{-1}$.

To express a risk coefficient in terms of a constant activity concentration in milk (Bq L^{-1}), multiply the coefficient by $2.75 \times 10^4 U_M$, where U_M is the lifetime average rate of ingestion of milk (for example, 0.243 L d^{-1} in Table 3.1) and $2.75 \times 10^4 \text{ d}$ is the average life span. Note that the *relative* age- and gender-specific energy intake rates specified in Table 3.1 are inherent in the risk coefficient.

Table 2.2b. Mortality and morbidity risk coefficients for ingestion of iodine in food, based on usage of cow's milk.

Isotope	T _{1/2}	f ₁	Mortality (Bq ⁻¹)	Morbidity (Bq ⁻¹)
I-120	81.0 m	1.0E+00	2.29E-11	6.66E-11
I-120m	53 m	1.0E+00	1.73E-11	3.50E-11
I-121	2.12 h	1.0E+00	3.51E-12	1.63E-11
I-123	13.2 h	1.0E+00	7.27E-12	5.53E-11
I-124	4.18 d	1.0E+00	3.51E-10	3.29E-09
I-125	60.14 d	1.0E+00	1.76E-10	1.70E-09
I-126	13.02 d	1.0E+00	6.92E-10	6.70E-09
I-128	24.99 m	1.0E+00	3.83E-12	5.57E-12
I-129	1.57E7 y	1.0E+00	8.86E-10	8.69E-09
I-130	12.36 h	1.0E+00	6.77E-11	5.08E-10
I-131 ^a	8.04 d	1.0E+00	3.78E-10	3.61E-09
I-132	2.30 h	1.0E+00	1.65E-11	6.33E-11
I-132m	83.6 m	1.0E+00	9.74E-12	4.82E-11
I-133	20.8 h	1.0E+00	1.34E-10	1.19E-09
I-134	52.6 m	1.0E+00	8.64E-12	1.74E-11
I-135	6.61 h	1.0E+00	3.63E-11	2.43E-10

^aThe uncertainty in the risk coefficient for this radionuclide is addressed in Table 2.4.

**Table 2.3. Mortality and morbidity risk coefficients
for external exposure from environmental media.**

Explanation of Entries

Risk coefficients are provided for each of three external exposure scenarios: submersion in contaminated air, exposure from contamination on the ground surface, and exposure from soil contaminated to an infinite depth. It is assumed that the contaminated ground surface is an infinite plane and the contaminated air or soil occupies an infinite half-space. Risk coefficients are expressed as the probability of radiogenic cancer mortality or morbidity per unit time-integrated activity concentration in air, on the ground surface, or in soil. These risk coefficients are based on the dosimetric data of Federal Guidance Report No. 12 (EPA, 1993).

A risk coefficient for a radionuclide *does not include any contribution to dose from chain members that form in the environmental medium*. To allow the user to assess the risks from ingrowth of radionuclides, a separate risk coefficient is provided for each decay chain member of potential dosimetric significance, and entries are provided under the heading “Chain” to indicate whether a radionuclide is in the same chain as other radionuclides listed in the table. An entry “Y” (yes) under the subheading “P” (parent) indicates that the radionuclide is the parent of a decay chain containing at least one other radionuclide in the table, and “Y” under the subheading “D” (daughter) indicates that the radionuclide is in the decay chain of at least one other radionuclide in the table.

To facilitate application of the risk coefficients, including conversion to other units, the coefficients are tabulated to three decimal places. No indication of the level of uncertainty is intended or should be inferred from this practice. A calculated risk should be rounded appropriately.

To express a risk coefficient in terms of a constant activity concentration of the radionuclide in the environmental medium, multiply the coefficient by 2.37×10^9 s.

To express a risk coefficient in conventional units of activity, multiply the coefficient by 3.7×10^4 Bq μ Ci⁻¹.

To express a risk coefficient in time units of year (y), multiply the coefficient by 3.16×10^7 s y⁻¹.

To express a risk coefficient for submersion in volume units of cm³, multiply the coefficient by 1×10^6 cm³ m⁻³.

To express a risk coefficient for ground plane in area units of cm², multiply the coefficient by 1×10^4 cm² m⁻².

To express a risk coefficient for soil in mass units of g, multiply the coefficient by 1×10^3 g kg⁻¹.

**Table 2.3. Mortality and morbidity risk coefficients
for external exposure from environmental media.**

Nuclide	T _{1/2}	Chain P D	Mortality			Morbidity			
			Submersion (m ³ /Bq-s)	Ground Plane (m ² /Bq-s)	Soil (kg/Bq-s)	Submersion (m ³ /Bq-s)	Ground Plane (m ² /Bq-s)	Soil (kg/Bq-s)	
Hydrogen									
H-3 ^a	12.35 y	- -	0.00	0.00	0.00	0.00	0.00	0.00	0.00
Beryllium									
Be-7	53.3 d	- -	1.19E-16	2.58E-18	1.24E-16	1.76E-16	3.80E-18	1.82E-16	
Be-10	1.6E6 y	- -	1.78E-18	4.81E-20	4.32E-19	2.02E-18	5.70E-20	6.36E-19	
Carbon									
C-11	20.38 m	- -	2.48E-15	5.37E-17	2.59E-15	3.65E-15	7.90E-17	3.81E-15	
C-14	5730 y	- -	3.23E-20	5.30E-22	4.46E-21	3.66E-20	8.24E-22	6.71E-21	
Nitrogen									
N-13	9.965 m	- -	2.48E-15	5.39E-17	2.59E-15	3.65E-15	7.92E-17	3.81E-15	
Oxygen									
O-15	122.24 s	- -	2.49E-15	5.44E-17	2.60E-15	3.66E-15	7.98E-17	3.82E-15	
Fluorine									
F-18	109.77 m	- -	2.48E-15	5.36E-17	2.60E-15	3.65E-15	7.89E-17	3.81E-15	
Neon									
Ne-19	17.22 s	- -	2.49E-15	5.48E-17	2.61E-15	3.67E-15	8.03E-17	3.83E-15	
Sodium									
Na-22	2.602 y	- -	5.57E-15	1.12E-16	6.02E-15	8.19E-15	1.66E-16	8.84E-15	
Na-24	15.00 h	- -	1.15E-14	1.96E-16	1.28E-14	1.70E-14	2.88E-16	1.88E-14	
Magnesium									
Mg-28	20.91 h	Y -	3.50E-15	6.93E-17	3.83E-15	5.15E-15	1.02E-16	5.62E-15	
Aluminum									
Al-26	7.16E5 y	- -	7.06E-15	1.34E-16	7.73E-15	1.04E-14	1.97E-16	1.14E-14	
Al-28	2.240 m	- Y	4.88E-15	8.88E-17	5.43E-15	7.17E-15	1.30E-16	7.98E-15	
Silicon									
Si-31	157.3 m	- -	9.45E-18	8.32E-19	6.62E-18	1.22E-17	9.03E-19	9.47E-18	
Si-32	450 y	Y -	1.02E-19	1.10E-21	1.25E-20	1.13E-19	1.68E-21	1.87E-20	
Phosphorus									
P-30	2.499 m	- -	2.51E-15	5.55E-17	2.62E-15	3.69E-15	8.11E-17	3.85E-15	
P-32	14.29 d	- Y	9.11E-18	9.63E-19	5.74E-18	1.14E-17	1.03E-18	8.06E-18	
P-33	25.4 d	- -	1.70E-19	1.63E-21	2.14E-20	1.86E-19	2.49E-21	3.19E-20	
Sulfur									
S-35	87.44 d	- -	3.79E-20	5.60E-22	5.00E-21	4.27E-20	8.68E-22	7.51E-21	
Chlorine									
Cl-36	3.01E5 y	- -	2.50E-18	1.37E-19	1.02E-18	3.00E-18	1.52E-19	1.49E-18	
Cl-38	37.21 m	- -	4.15E-15	7.40E-17	4.62E-15	6.10E-15	1.08E-16	6.79E-15	
Cl-39	55.6 m	Y -	3.78E-15	7.35E-17	4.14E-15	5.56E-15	1.08E-16	6.07E-15	
Argon									
Ar-37	35.02 d	- -	0.00	0.00	0.00	0.00	0.00	0.00	
Ar-39	269 y	- Y	1.46E-18	3.67E-20	3.46E-19	1.66E-18	4.39E-20	5.09E-19	
Ar-41	1.827 h	- -	3.38E-15	6.54E-17	3.73E-15	4.96E-15	9.60E-17	5.47E-15	
Potassium									
K-38	7.636 m	- -	8.55E-15	1.58E-16	9.37E-15	1.26E-14	2.32E-16	1.38E-14	
K-40	1.28E9 y	- -	4.23E-16	8.50E-18	4.66E-16	6.20E-16	1.22E-17	6.83E-16	

Table 2.3, continued

Nuclide	T _{1/2}	Chain P D		Mortality			Morbidity		
				Submersion (m ³ /Bq-s)	Ground		Submersion (m ³ /Bq-s)	Ground	
					Plane (m ² /Bq-s)	Soil (kg/Bq-s)		Plane (m ² /Bq-s)	Soil (kg/Bq-s)
Potassium, continued									
K-42	12.36 h	-	-	7.72E-16	1.57E-17	8.50E-16	1.13E-15	2.25E-17	1.25E-15
K-43	22.6 h	-	-	2.36E-15	5.08E-17	2.47E-15	3.48E-15	7.47E-17	3.62E-15
K-44	22.13 m	-	-	6.27E-15	1.12E-16	6.92E-15	9.21E-15	1.63E-16	1.02E-14
K-45	20 m	Y	-	5.06E-15	9.25E-17	5.56E-15	7.44E-15	1.35E-16	8.16E-15
Calcium									
Ca-41	1.4E5 y	-	-	0.00	0.00	0.00	0.00	0.00	0.00
Ca-45	163 d	-	Y	1.79E-19	1.69E-21	2.28E-20	1.97E-19	2.59E-21	3.39E-20
Ca-47	4.53 d	Y	-	2.78E-15	5.41E-17	3.06E-15	4.09E-15	7.95E-17	4.49E-15
Ca-49	8.716 m	Y	-	9.23E-15	1.44E-16	1.02E-14	1.36E-14	2.11E-16	1.50E-14
Scandium									
Sc-43	3.891 h	-	-	2.65E-15	5.75E-17	2.75E-15	3.90E-15	8.46E-17	4.05E-15
Sc-44	3.927 h	-	Y	5.39E-15	1.11E-16	5.80E-15	7.93E-15	1.63E-16	8.52E-15
Sc-44m	58.6 h	Y	-	6.73E-16	1.43E-17	6.68E-16	9.91E-16	2.11E-17	9.81E-16
Sc-46	83.83 d	-	-	5.14E-15	1.03E-16	5.62E-15	7.56E-15	1.52E-16	8.25E-15
Sc-47	3.351 d	-	Y	2.46E-16	5.39E-18	2.11E-16	3.63E-16	7.92E-18	3.10E-16
Sc-48	43.7 h	-	-	8.66E-15	1.71E-16	9.50E-15	1.27E-14	2.52E-16	1.39E-14
Sc-49	57.4 m	-	Y	1.48E-17	1.22E-18	1.15E-17	1.93E-17	1.33E-18	1.63E-17
Titanium									
Ti-44	47.3 y	Y	-	2.40E-16	6.27E-18	1.39E-16	3.57E-16	9.26E-18	2.05E-16
Ti-45	3.08 h	-	-	2.11E-15	4.59E-17	2.21E-15	3.11E-15	6.75E-17	3.25E-15
Vanadium									
V-47	32.6 m	-	-	2.43E-15	5.32E-17	2.54E-15	3.57E-15	7.79E-17	3.73E-15
V-48	16.238 d	-	Y	7.49E-15	1.49E-16	8.16E-15	1.10E-14	2.19E-16	1.20E-14
V-49	330 d	-	Y	0.00	0.00	0.00	0.00	0.00	0.00
Chromium									
Cr-48	22.96 h	Y	-	1.01E-15	2.20E-17	9.44E-16	1.49E-15	3.24E-17	1.39E-15
Cr-49	42.09 m	Y	-	2.53E-15	5.55E-17	2.58E-15	3.72E-15	8.15E-17	3.79E-15
Cr-51	27.704 d	-	Y	7.49E-17	1.62E-18	7.45E-17	1.10E-16	2.39E-18	1.09E-16
Manganese									
Mn-51	46.2 m	Y	-	2.44E-15	5.35E-17	2.55E-15	3.58E-15	7.83E-17	3.74E-15
Mn-52	5.591 d	-	Y	8.89E-15	1.77E-16	9.72E-15	1.31E-14	2.60E-16	1.43E-14
Mn-52m	21.1 m	Y	Y	6.19E-15	1.24E-16	6.72E-15	9.10E-15	1.82E-16	9.86E-15
Mn-53	3.7E6 y	-	-	0.00	0.00	0.00	0.00	0.00	0.00
Mn-54	312.5 d	-	-	2.10E-15	4.34E-17	2.27E-15	3.08E-15	6.39E-17	3.33E-15
Mn-56	2.5785 h	-	-	4.48E-15	8.59E-17	4.93E-15	6.58E-15	1.26E-16	7.23E-15
Iron									
Fe-52	8.275 h	Y	-	1.77E-15	3.84E-17	1.79E-15	2.61E-15	5.65E-17	2.63E-15
Fe-55	2.7 y	-	Y	0.00	0.00	0.00	0.00	0.00	0.00
Fe-59	44.529 d	-	-	3.09E-15	6.05E-17	3.40E-15	4.54E-15	8.90E-17	4.99E-15
Fe-60	1E5 y	Y	-	2.32E-20	4.79E-22	3.62E-21	2.70E-20	7.48E-22	5.46E-21
Cobalt									
Co-55	17.54 h	Y	-	5.01E-15	1.04E-16	5.38E-15	7.37E-15	1.52E-16	7.89E-15
Co-56	78.76 d	-	Y	9.55E-15	1.77E-16	1.05E-14	1.40E-14	2.61E-16	1.54E-14
Co-57	270.9 d	-	Y	2.63E-16	5.86E-18	2.07E-16	3.89E-16	8.63E-18	3.04E-16
Co-58	70.80 d	-	Y	2.43E-15	5.07E-17	2.62E-15	3.58E-15	7.46E-17	3.84E-15

Table 2.3, continued

Nuclide	T _{1/2}	Chain P D	Mortality			Morbidity		
			Submersion (m ³ /Bq-s)	Ground		Submersion (m ³ /Bq-s)	Ground	
				Plane (m ² /Bq-s)	Soil (kg/Bq-s)		Plane (m ² /Bq-s)	Soil (kg/Bq-s)
Cobalt, continued								
Co-58 ^m	9.15 h	Y -	2.25E-21	2.35E-22	5.21E-22	3.80E-21	3.83E-22	8.59E-22
Co-60 ^a	5.271 y	- Y	6.55E-15	1.27E-16	7.23E-15	9.63E-15	1.87E-16	1.06E-14
Co-60m	10.47 m	Y Y	1.08E-17	2.30E-19	1.08E-17	1.59E-17	3.37E-19	1.59E-17
Co-61	1.65 h	- -	1.84E-16	4.89E-18	1.44E-16	2.72E-16	7.00E-18	2.12E-16
Co-62m	13.91 m	- -	7.15E-15	1.37E-16	7.89E-15	1.05E-14	2.01E-16	1.16E-14
Nickel								
Ni-56	6.10 d	Y -	4.27E-15	8.85E-17	4.51E-15	6.29E-15	1.30E-16	6.63E-15
Ni-57	36.08 h	Y Y	5.03E-15	9.67E-17	5.50E-15	7.39E-15	1.42E-16	8.08E-15
Ni-59	7.5E4 y	- -	0.00	0.00	0.00	0.00	0.00	0.00
Ni-63	96 y	- -	0.00	0.00	0.00	0.00	0.00	0.00
Ni-65	2.520 h	- -	1.45E-15	2.84E-17	1.60E-15	2.14E-15	4.15E-17	2.35E-15
Ni-66	54.6 h	Y -	1.24E-19	1.25E-21	1.54E-20	1.37E-19	1.92E-21	2.29E-20
Copper								
Cu-60	23.2 m	- -	1.03E-14	1.96E-16	1.12E-14	1.51E-14	2.88E-16	1.65E-14
Cu-61	3.408 h	- -	2.02E-15	4.35E-17	2.12E-15	2.97E-15	6.39E-17	3.11E-15
Cu-62	9.74 m	- Y	2.47E-15	5.45E-17	2.58E-15	3.63E-15	7.96E-17	3.79E-15
Cu-64	12.701 h	- -	4.62E-16	9.92E-18	4.84E-16	6.79E-16	1.46E-17	7.11E-16
Cu-66	5.10 m	- Y	2.36E-16	5.86E-18	2.53E-16	3.44E-16	8.07E-18	3.70E-16
Cu-67	61.86 h	- -	2.59E-16	5.71E-18	2.23E-16	3.82E-16	8.40E-18	3.28E-16
Zinc								
Zn-62	9.26 h	Y -	1.04E-15	2.26E-17	1.09E-15	1.54E-15	3.34E-17	1.60E-15
Zn-63	38.1 m	- -	2.70E-15	5.87E-17	2.84E-15	3.97E-15	8.60E-17	4.17E-15
Zn-65	243.9 d	- Y	1.50E-15	2.97E-17	1.64E-15	2.20E-15	4.37E-17	2.41E-15
Zn-69	57 m	- Y	2.77E-18	2.34E-19	9.94E-19	3.25E-18	2.49E-19	1.43E-18
Zn-69m	13.76 h	Y -	1.00E-15	2.18E-17	1.03E-15	1.48E-15	3.20E-17	1.52E-15
Zn-71m	3.92 h	- -	3.80E-15	8.16E-17	3.99E-15	5.59E-15	1.20E-16	5.86E-15
Zn-72	46.5 h	Y -	3.27E-16	7.23E-18	2.72E-16	4.84E-16	1.06E-17	4.01E-16
Gallium								
Ga-65	15.2 m	Y -	2.85E-15	6.21E-17	2.94E-15	4.20E-15	9.10E-17	4.32E-15
Ga-66	9.40 h	- Y	6.75E-15	1.21E-16	7.37E-15	9.92E-15	1.77E-16	1.08E-14
Ga-67	78.26 h	- Y	3.47E-16	7.69E-18	3.12E-16	5.13E-16	1.13E-17	4.59E-16
Ga-68	68.0 m	- Y	2.32E-15	5.07E-17	2.43E-15	3.42E-15	7.43E-17	3.57E-15
Ga-70	21.15 m	- -	2.74E-17	1.26E-18	2.58E-17	3.85E-17	1.51E-18	3.76E-17
Ga-72	14.1 h	- Y	7.23E-15	1.35E-16	7.94E-15	1.06E-14	1.98E-16	1.17E-14
Ga-73	4.91 h	- -	7.39E-16	1.64E-17	7.30E-16	1.09E-15	2.40E-17	1.07E-15
Germanium								
Ge-66	2.27 h	Y -	1.63E-15	3.52E-17	1.66E-15	2.40E-15	5.19E-17	2.45E-15
Ge-67	18.7 m	Y -	3.48E-15	7.44E-17	3.63E-15	5.12E-15	1.09E-16	5.34E-15
Ge-68	288 d	Y -	3.00E-21	9.59E-22	2.58E-22	4.89E-21	1.44E-21	4.02E-22
Ge-69	39.05 h	- Y	2.18E-15	4.52E-17	2.34E-15	3.21E-15	6.65E-17	3.44E-15
Ge-71	11.8 d	- Y	3.04E-21	9.71E-22	2.60E-22	4.96E-21	1.46E-21	4.06E-22
Ge-75	82.78 m	- -	8.51E-17	2.19E-18	8.03E-17	1.24E-16	3.04E-18	1.18E-16
Ge-77	11.30 h	Y -	2.70E-15	5.66E-17	2.81E-15	3.97E-15	8.30E-17	4.13E-15
Ge-78	87 m	Y -	6.59E-16	1.43E-17	6.43E-16	9.71E-16	2.11E-17	9.45E-16

Table 2.3, continued

Nuclide	T _{1/2}	Mortality					Morbidity		
		Chain P D	Submersion (m ³ /Bq-s)	Ground Plane		Soil (kg/Bq-s)	Submersion (m ³ /Bq-s)	Ground Plane	
				(m ² /Bq-s)	(kg/Bq-s)			(m ² /Bq-s)	(kg/Bq-s)
Arsenic									
As-69	15.2 m	Y -	2.48E-15	5.47E-17	2.58E-15	3.64E-15	8.00E-17	3.79E-15	
As-70	52.6 m	- Y	1.05E-14	2.10E-16	1.15E-14	1.55E-14	3.08E-16	1.68E-14	
As-71	64.8 h	Y -	1.37E-15	2.94E-17	1.38E-15	2.02E-15	4.33E-17	2.03E-15	
As-72	26.0 h	- Y	4.49E-15	9.44E-17	4.79E-15	6.60E-15	1.38E-16	7.03E-15	
As-73	80.30 d	- Y	7.57E-18	2.58E-19	3.32E-18	1.14E-17	3.83E-19	4.95E-18	
As-74	17.76 d	- -	1.85E-15	3.99E-17	1.96E-15	2.72E-15	5.86E-17	2.87E-15	
As-76	26.32 h	- -	1.10E-15	2.37E-17	1.17E-15	1.61E-15	3.43E-17	1.72E-15	
As-77	38.8 h	- Y	2.24E-17	5.22E-19	2.09E-17	3.25E-17	7.43E-19	3.07E-17	
As-78	90.7 m	- Y	3.27E-15	6.54E-17	3.57E-15	4.81E-15	9.56E-17	5.23E-15	
Selenium									
Se-70	41.0 m	Y -	2.38E-15	5.22E-17	2.45E-15	3.50E-15	7.66E-17	3.61E-15	
Se-73	7.15 h	Y Y	2.58E-15	5.67E-17	2.63E-15	3.81E-15	8.33E-17	3.87E-15	
Se-73m	39 m	Y -	5.91E-16	1.29E-17	6.17E-16	8.69E-16	1.89E-17	9.06E-16	
Se-75	119.8 d	- Y	9.02E-16	1.97E-17	8.41E-16	1.33E-15	2.89E-17	1.24E-15	
Se-77m	17.45 s	- -	1.93E-16	4.22E-18	1.66E-16	2.84E-16	6.21E-18	2.44E-16	
Se-79	65000 y	- -	4.80E-20	6.94E-22	6.25E-21	5.39E-20	1.08E-21	9.40E-21	
Se-81	18.5 m	- Y	2.99E-17	1.29E-18	2.75E-17	4.23E-17	1.57E-18	4.01E-17	
Se-81m	57.25 m	Y -	2.85E-17	6.64E-19	2.07E-17	4.22E-17	9.80E-19	3.05E-17	
Se-83	22.5 m	Y -	6.24E-15	1.24E-16	6.74E-15	9.18E-15	1.82E-16	9.89E-15	
Bromine									
Br-74	25.3 m	- Y	1.25E-14	2.19E-16	1.36E-14	1.84E-14	3.21E-16	1.99E-14	
Br-74m	41.5 m	- -	1.08E-14	2.05E-16	1.17E-14	1.58E-14	3.01E-16	1.71E-14	
Br-75	98 m	Y -	2.94E-15	6.38E-17	3.04E-15	4.33E-15	9.37E-17	4.46E-15	
Br-76	16.2 h	- Y	6.95E-15	1.32E-16	7.54E-15	1.02E-14	1.93E-16	1.11E-14	
Br-77	56 h	- Y	7.60E-16	1.63E-17	7.81E-16	1.12E-15	2.41E-17	1.15E-15	
Br-80	17.4 m	- Y	1.97E-16	4.45E-18	2.07E-16	2.89E-16	6.44E-18	3.04E-16	
Br-80m	4.42 h	Y -	1.04E-17	5.94E-19	3.33E-18	1.63E-17	9.09E-19	5.10E-18	
Br-82	35.30 h	- -	6.67E-15	1.36E-16	7.22E-15	9.81E-15	2.01E-16	1.06E-14	
Br-83	2.39 h	Y Y	2.10E-17	6.32E-19	2.02E-17	3.01E-17	8.34E-19	2.96E-17	
Br-84	31.80 m	- -	4.95E-15	8.75E-17	5.45E-15	7.27E-15	1.28E-16	8.01E-15	
Krypton									
Kr-74	11.50 m	Y -	2.81E-15	6.16E-17	2.86E-15	4.13E-15	9.03E-17	4.20E-15	
Kr-76	14.8 h	Y -	1.01E-15	2.20E-17	1.01E-15	1.49E-15	3.24E-17	1.48E-15	
Kr-77	74.7 m	Y Y	2.43E-15	5.34E-17	2.46E-15	3.58E-15	7.83E-17	3.61E-15	
Kr-79	35.04 h	- Y	6.09E-16	1.31E-17	6.29E-16	8.97E-16	1.92E-17	9.24E-16	
Kr-81	2.1E5 y	- Y	1.32E-17	3.06E-19	1.27E-17	1.94E-17	4.54E-19	1.87E-17	
Kr-81m	13 s	Y -	2.97E-16	6.45E-18	2.68E-16	4.38E-16	9.49E-18	3.94E-16	
Kr-83m	1.83 h	- Y	4.44E-20	1.07E-20	6.99E-21	7.61E-20	1.76E-20	1.15E-20	
Kr-85	10.72 y	- Y	7.23E-18	2.15E-19	6.15E-18	1.00E-17	2.79E-19	9.02E-18	
Kr-85m	4.48 h	Y -	3.61E-16	8.00E-18	3.18E-16	5.33E-16	1.17E-17	4.68E-16	
Kr-87	76.3 m	Y -	2.15E-15	4.06E-17	2.34E-15	3.16E-15	5.92E-17	3.43E-15	
Kr-88	2.84 h	Y -	5.37E-15	9.45E-17	5.94E-15	7.89E-15	1.39E-16	8.72E-15	

Table 2.3, continued

Nuclide	T _{1/2}	Mortality					Morbidity		
		Chain P D	Submersion (m ³ /Bq-s)	Ground		Soil (kg/Bq-s)	Submersion (m ³ /Bq-s)	Ground	
				Plane (m ² /Bq-s)	Plane (m ² /Bq-s)			Plane (m ² /Bq-s)	Soil (kg/Bq-s)
Rubidium									
Rb-79	22.9 m	Y -	3.29E-15	7.16E-17	3.41E-15	4.84E-15	1.05E-16	5.01E-15	
Rb-80	34 s	- Y	3.09E-15	6.80E-17	3.24E-15	4.54E-15	9.95E-17	4.76E-15	
Rb-81	4.58 h	Y Y	1.48E-15	3.21E-17	1.51E-15	2.18E-15	4.73E-17	2.22E-15	
Rb-81m	32 m	Y -	8.33E-18	2.35E-19	5.28E-18	1.24E-17	3.53E-19	7.78E-18	
Rb-82	1.3 m	- Y	2.69E-15	5.91E-17	2.83E-15	3.96E-15	8.64E-17	4.15E-15	
Rb-82m	6.2 h	- -	7.34E-15	1.50E-16	7.92E-15	1.08E-14	2.21E-16	1.16E-14	
Rb-83	86.2 d	Y Y	1.21E-15	2.60E-17	1.27E-15	1.78E-15	3.83E-17	1.87E-15	
Rb-84	32.77 d	- -	2.28E-15	4.76E-17	2.46E-15	3.36E-15	7.00E-17	3.61E-15	
Rb-86	18.66 d	- -	2.52E-16	5.75E-18	2.73E-16	3.69E-16	8.10E-18	4.00E-16	
Rb-87	4.7E10 y	- Y	3.87E-19	3.36E-21	5.25E-20	4.25E-19	5.11E-21	7.80E-20	
Rb-88	17.8 m	- Y	1.77E-15	3.37E-17	1.96E-15	2.60E-15	4.88E-17	2.88E-15	
Rb-89	15.2 m	Y -	5.55E-15	1.04E-16	6.11E-15	8.15E-15	1.53E-16	8.97E-15	
Strontium									
Sr-80	100 m	Y -	1.81E-19	4.78E-20	2.54E-20	3.19E-19	8.00E-20	4.35E-20	
Sr-81	25.5 m	Y -	3.37E-15	7.34E-17	3.48E-15	4.96E-15	1.08E-16	5.11E-15	
Sr-82	25.0 d	Y -	1.78E-19	4.70E-20	2.50E-20	3.13E-19	7.86E-20	4.28E-20	
Sr-83	32.4 h	Y -	1.97E-15	4.11E-17	2.10E-15	2.89E-15	6.05E-17	3.08E-15	
Sr-85	64.84 d	- Y	1.22E-15	2.64E-17	1.28E-15	1.80E-15	3.89E-17	1.88E-15	
Sr-85m	69.5 m	Y -	5.10E-16	1.10E-17	4.78E-16	7.53E-16	1.62E-17	7.03E-16	
Sr-87m	2.805 h	Y Y	7.64E-16	1.66E-17	7.77E-16	1.13E-15	2.44E-17	1.14E-15	
Sr-89	50.5 d	- Y	7.30E-18	7.72E-19	4.37E-18	9.04E-18	8.25E-19	6.16E-18	
Sr-90 ^a	29.12 y	Y -	1.24E-18	2.60E-20	2.80E-19	1.40E-18	3.20E-20	4.13E-19	
Sr-91	9.5 h	Y -	1.78E-15	3.69E-17	1.93E-15	2.61E-15	5.39E-17	2.83E-15	
Sr-92	2.71 h	Y -	3.53E-15	6.75E-17	3.91E-15	5.19E-15	9.92E-17	5.73E-15	
Yttrium									
Y-86	14.74 h	- Y	9.27E-15	1.82E-16	1.01E-14	1.36E-14	2.68E-16	1.48E-14	
Y-86m	48 m	Y -	5.16E-16	1.11E-17	4.87E-16	7.61E-16	1.64E-17	7.15E-16	
Y-87	80.3 h	Y -	1.08E-15	2.35E-17	1.13E-15	1.60E-15	3.47E-17	1.66E-15	
Y-88	106.64 d	- Y	7.17E-15	1.33E-16	7.94E-15	1.05E-14	1.96E-16	1.17E-14	
Y-90 ^a	64.0 h	- Y	1.53E-17	1.31E-18	1.16E-17	1.96E-17	1.43E-18	1.64E-17	
Y-90m	3.19 h	Y -	1.50E-15	3.25E-17	1.50E-15	2.21E-15	4.78E-17	2.21E-15	
Y-91	58.51 d	- Y	1.69E-17	9.84E-19	1.48E-17	2.31E-17	1.12E-18	2.15E-17	
Y-91m	49.71 m	Y Y	1.29E-15	2.78E-17	1.37E-15	1.90E-15	4.09E-17	2.00E-15	
Y-92	3.54 h	- Y	6.78E-16	1.49E-17	7.35E-16	9.93E-16	2.13E-17	1.08E-15	
Y-93	10.1 h	Y -	2.55E-16	6.08E-18	2.69E-16	3.71E-16	8.37E-18	3.94E-16	
Y-94	19.1 m	- -	2.91E-15	5.89E-17	3.18E-15	4.28E-15	8.60E-17	4.67E-15	
Y-95	10.7 m	Y -	2.53E-15	4.45E-17	2.80E-15	3.72E-15	6.49E-17	4.11E-15	
Zirconium									
Zr-86	16.5 h	Y -	6.29E-16	1.38E-17	6.06E-16	9.28E-16	2.04E-17	8.91E-16	
Zr-88	83.4 d	Y Y	9.41E-16	2.05E-17	9.60E-16	1.39E-15	3.03E-17	1.41E-15	
Zr-89	78.43 h	- Y	2.91E-15	6.02E-17	3.14E-15	4.28E-15	8.86E-17	4.61E-15	
Zr-93	1.53E6 y	Y Y	0.00	0.00	0.00	0.00	0.00	0.00	
Zr-95	63.98 d	Y Y	1.84E-15	3.85E-17	1.98E-15	2.71E-15	5.68E-17	2.91E-15	
Zr-97	16.90 h	Y -	4.68E-16	1.01E-17	5.03E-16	6.87E-16	1.45E-17	7.38E-16	

Table 2.3, continued

Nuclide	T _{1/2}	Mortality					Morbidity		
		Chain P D	Submersion (m ³ /Bq-s)	Ground Plane		Soil (kg/Bq-s)	Submersion (m ³ /Bq-s)	Ground Plane	
				(m ² /Bq-s)	(kg/Bq-s)			(m ² /Bq-s)	(kg/Bq-s)
Niobium									
Nb-88	14.3 m	Y -	1.03E-14	2.15E-16	1.11E-14	1.52E-14	3.16E-16	1.62E-14	
Nb-89b	122 m	Y -	3.60E-15	7.16E-17	3.88E-15	5.30E-15	1.05E-16	5.69E-15	
Nb-89a	66 m	Y -	4.70E-15	1.02E-16	4.94E-15	6.91E-15	1.49E-16	7.26E-15	
Nb-90	14.60 h	- Y	1.13E-14	2.07E-16	1.24E-14	1.66E-14	3.05E-16	1.82E-14	
Nb-93m	13.6 y	- Y	1.07E-19	2.08E-20	1.89E-20	1.92E-19	3.55E-20	3.28E-20	
Nb-94	2.03E4 y	- -	3.94E-15	8.18E-17	4.25E-15	5.79E-15	1.21E-16	6.24E-15	
Nb-95	35.15 d	- Y	1.91E-15	3.99E-17	2.06E-15	2.81E-15	5.88E-17	3.02E-15	
Nb-95m	86.6 h	Y Y	1.44E-16	3.17E-18	1.35E-16	2.12E-16	4.68E-18	1.99E-16	
Nb-96	23.35 h	- -	6.23E-15	1.28E-16	6.72E-15	9.16E-15	1.89E-16	9.86E-15	
Nb-97	72.1 m	- Y	1.62E-15	3.48E-17	1.73E-15	2.39E-15	5.10E-17	2.54E-15	
Nb-97m	60 s	Y Y	1.81E-15	3.80E-17	1.95E-15	2.67E-15	5.60E-17	2.86E-15	
Nb-98	51.5 m	- -	6.21E-15	1.26E-16	6.75E-15	9.13E-15	1.85E-16	9.90E-15	
Molybdenum									
Mo-90	5.67 h	Y -	1.97E-15	4.19E-17	1.99E-15	2.90E-15	6.17E-17	2.92E-15	
Mo-93	3.5E3 y	Y Y	6.06E-19	1.18E-19	1.07E-19	1.09E-18	2.02E-19	1.86E-19	
Mo-93m	6.85 h	Y -	5.83E-15	1.14E-16	6.36E-15	8.57E-15	1.67E-16	9.34E-15	
Mo-99	66.0 h	Y -	3.71E-16	8.16E-18	3.87E-16	5.45E-16	1.18E-17	5.69E-16	
Mo-101	14.62 m	Y -	3.55E-15	6.97E-17	3.87E-15	5.22E-15	1.02E-16	5.67E-15	
Technetium									
Tc-93	2.75 h	Y Y	3.85E-15	7.26E-17	4.26E-15	5.65E-15	1.07E-16	6.26E-15	
Tc-93m	43.5 m	Y -	1.95E-15	3.48E-17	2.11E-15	2.86E-15	5.12E-17	3.10E-15	
Tc-94	293 m	- -	6.66E-15	1.38E-16	7.20E-15	9.80E-15	2.04E-16	1.06E-14	
Tc-94m	52 m	- Y	4.72E-15	9.62E-17	5.08E-15	6.94E-15	1.41E-16	7.45E-15	
Tc-95	20.0 h	- Y	1.96E-15	4.10E-17	2.12E-15	2.89E-15	6.04E-17	3.11E-15	
Tc-95m	61 d	Y -	1.63E-15	3.45E-17	1.71E-15	2.40E-15	5.08E-17	2.51E-15	
Tc-96	4.28 d	- Y	6.26E-15	1.30E-16	6.78E-15	9.22E-15	1.91E-16	9.96E-15	
Tc-96m	51.5 m	Y -	1.14E-16	2.40E-18	1.24E-16	1.68E-16	3.55E-18	1.82E-16	
Tc-97	2.6E6 y	- Y	7.89E-19	1.41E-19	1.45E-19	1.42E-18	2.42E-19	2.52E-19	
Tc-97m	87 d	Y Y	1.43E-18	1.43E-19	5.80E-19	2.34E-18	2.41E-19	8.93E-19	
Tc-98	4.2E6 y	- -	3.50E-15	7.38E-17	3.76E-15	5.15E-15	1.09E-16	5.52E-15	
Tc-99	2.13E5 y	- Y	3.38E-19	2.98E-21	4.69E-20	3.72E-19	4.53E-21	6.97E-20	
Tc-99m	6.02 h	Y Y	2.79E-16	6.15E-18	2.29E-16	4.12E-16	9.06E-18	3.37E-16	
Tc-101	14.2 m	- Y	8.02E-16	1.78E-17	7.97E-16	1.18E-15	2.59E-17	1.17E-15	
Tc-104	18.2 m	- -	5.24E-15	1.01E-16	5.69E-15	7.71E-15	1.48E-16	8.35E-15	
Ruthenium									
Ru-94	51.8 m	Y -	1.28E-15	2.73E-17	1.35E-15	1.89E-15	4.02E-17	1.98E-15	
Ru-97	2.9 d	Y -	5.33E-16	1.17E-17	5.03E-16	7.86E-16	1.72E-17	7.39E-16	
Ru-103	39.28 d	Y -	1.14E-15	2.45E-17	1.19E-15	1.67E-15	3.61E-17	1.75E-15	
Ru-105	4.44 h	Y -	1.94E-15	4.12E-17	2.05E-15	2.85E-15	6.06E-17	3.01E-15	
Ru-106 ^a	368.2 d	Y -	0.00	0.00	0.00	0.00	0.00	0.00	
Rhodium									
Rh-99	16 d	- -	1.43E-15	3.07E-17	1.46E-15	2.10E-15	4.53E-17	2.14E-15	
Rh-99m	4.7 h	- -	1.67E-15	3.49E-17	1.76E-15	2.46E-15	5.14E-17	2.59E-15	
Rh-100	20.8 h	- Y	7.33E-15	1.37E-16	8.05E-15	1.08E-14	2.01E-16	1.18E-14	

Table 2.3, continued

Nuclide	T _{1/2}	Chain P D		Mortality			Morbidity		
				Submersion (m ³ /Bq-s)	Ground Plane		Submersion (m ³ /Bq-s)	Ground Plane	
					(m ² /Bq-s)	Soil (kg/Bq-s)		(m ² /Bq-s)	Soil (kg/Bq-s)
Rhodium, continued									
Rh-101	3.2 y	-	Y	5.80E-16	1.29E-17	5.15E-16	8.57E-16	1.90E-17	7.57E-16
Rh-101m	4.34 d	Y	Y	7.00E-16	1.53E-17	6.94E-16	1.03E-15	2.26E-17	1.02E-15
Rh-102	2.9 y	-	Y	5.30E-15	1.11E-16	5.67E-15	7.79E-15	1.63E-16	8.33E-15
Rh-102m	207 d	Y	-	1.17E-15	2.52E-17	1.23E-15	1.72E-15	3.71E-17	1.81E-15
Rh-103m	56.12 m	-	Y	2.17E-19	2.85E-20	4.75E-20	3.78E-19	4.79E-20	7.97E-20
Rh-105	35.36 h	-	Y	1.85E-16	4.02E-18	1.84E-16	2.73E-16	5.91E-18	2.70E-16
Rh-106 ^a	29.9 s	-	Y	5.36E-16	1.26E-17	5.64E-16	7.85E-16	1.80E-17	8.27E-16
Rh-106m	132 m	-	-	7.40E-15	1.50E-16	7.98E-15	1.09E-14	2.21E-16	1.17E-14
Rh-107	21.7 m	Y	-	7.50E-16	1.66E-17	7.46E-16	1.10E-15	2.42E-17	1.10E-15
Palladium									
Pd-100	3.63 d	Y	-	2.04E-16	5.38E-18	1.29E-16	3.04E-16	8.02E-18	1.90E-16
Pd-101	8.27 h	Y	-	7.70E-16	1.66E-17	8.06E-16	1.13E-15	2.45E-17	1.18E-15
Pd-103	16.96 d	Y	Y	1.97E-18	2.46E-19	6.11E-19	3.39E-18	4.15E-19	9.82E-19
Pd-107	6.5E6 y	-	Y	0.00	0.00	0.00	0.00	0.00	0.00
Pd-109	13.427 h	-	-	1.25E-17	6.64E-19	7.40E-18	1.78E-17	8.75E-19	1.09E-17
Silver									
Ag-102	12.9 m	-	-	8.63E-15	1.71E-16	9.33E-15	1.27E-14	2.52E-16	1.37E-14
Ag-103	65.7 m	Y	-	1.86E-15	3.93E-17	1.94E-15	2.74E-15	5.78E-17	2.85E-15
Ag-104	69.2 m	-	Y	6.76E-15	1.38E-16	7.31E-15	9.95E-15	2.03E-16	1.07E-14
Ag-104m	33.5 m	Y	-	2.99E-15	6.01E-17	3.21E-15	4.40E-15	8.83E-17	4.71E-15
Ag-105	41.0 d	-	-	1.23E-15	2.66E-17	1.25E-15	1.81E-15	3.92E-17	1.84E-15
Ag-106	23.96 m	-	-	1.72E-15	3.77E-17	1.80E-15	2.53E-15	5.53E-17	2.64E-15
Ag-106m	8.41 d	-	-	7.09E-15	1.45E-16	7.64E-15	1.04E-14	2.13E-16	1.12E-14
Ag-108	2.37 m	-	Y	5.06E-17	1.74E-18	5.01E-17	7.27E-17	2.23E-18	7.33E-17
Ag-108m	127 y	Y	-	3.96E-15	8.44E-17	4.19E-15	5.82E-15	1.24E-16	6.15E-15
Ag-109m	39.6 s	-	-	7.59E-18	3.07E-19	4.42E-18	1.16E-17	4.83E-19	6.56E-18
Ag-110	24.6 s	-	Y	9.81E-17	3.27E-18	9.97E-17	1.41E-16	4.22E-18	1.45E-16
Ag-110m	249.9 d	Y	-	6.97E-15	1.42E-16	7.57E-15	1.03E-14	2.09E-16	1.11E-14
Ag-111	7.45 d	-	-	6.59E-17	1.67E-18	6.38E-17	9.61E-17	2.33E-18	9.37E-17
Ag-112	3.12 h	-	-	1.73E-15	3.52E-17	1.88E-15	2.55E-15	5.12E-17	2.77E-15
Ag-115	20.0 m	Y	-	1.87E-15	3.65E-17	2.01E-15	2.75E-15	5.32E-17	2.95E-15
Cadmium									
Cd-104	57.7 m	Y	-	5.65E-16	1.26E-17	5.66E-16	8.33E-16	1.86E-17	8.31E-16
Cd-107	6.49 h	-	-	2.53E-17	9.56E-19	2.02E-17	3.84E-17	1.50E-18	2.98E-17
Cd-109	464 d	-	Y	1.01E-17	6.08E-19	4.96E-18	1.59E-17	9.84E-19	7.48E-18
Cd-113	9.3E15 y	-	-	2.99E-19	2.67E-21	4.24E-20	3.29E-19	4.06E-21	6.30E-20
Cd-113m	13.6 y	-	-	1.14E-18	2.65E-20	2.59E-19	1.29E-18	3.21E-20	3.81E-19
Cd-115	53.46 h	Y	Y	5.65E-16	1.24E-17	5.89E-16	8.31E-16	1.81E-17	8.65E-16
Cd-115m	44.6 d	Y	Y	6.39E-17	1.93E-18	6.61E-17	9.22E-17	2.52E-18	9.68E-17
Cd-117	2.49 h	Y	-	2.81E-15	5.54E-17	3.05E-15	4.14E-15	8.13E-17	4.48E-15
Cd-117m	3.36 h	Y	-	5.45E-15	1.02E-16	6.01E-15	8.02E-15	1.50E-16	8.83E-15
Indium									
In-109	4.2 h	Y	-	1.62E-15	3.39E-17	1.69E-15	2.39E-15	5.00E-17	2.48E-15
In-110b	4.9 h	-	-	7.61E-15	1.58E-16	8.24E-15	1.12E-14	2.32E-16	1.21E-14

Table 2.3, continued

Nuclide	T _{1/2}	Mortality					Morbidity		
		Chain		Submersion (m ³ /Bq-s)	Ground Plane		Submersion (m ³ /Bq-s)	Ground Plane	
		P	D		(m ² /Bq-s)	Soil (kg/Bq-s)		(m ² /Bq-s)	Soil (kg/Bq-s)
Indium, continued									
In-110a	69.1 m	-	Y	3.90E-15	8.08E-17	4.16E-15	5.74E-15	1.19E-16	6.11E-15
In-111	2.83 d	-	Y	9.01E-16	1.99E-17	8.30E-16	1.33E-15	2.93E-17	1.22E-15
In-112	14.4 m	-	-	6.40E-16	1.40E-17	6.71E-16	9.42E-16	2.06E-17	9.85E-16
In-113m	1.658 h	-	Y	6.05E-16	1.32E-17	6.15E-16	8.91E-16	1.95E-17	9.03E-16
In-114	71.9 s	-	Y	7.46E-18	1.44E-19	7.90E-18	1.09E-17	2.11E-19	1.16E-17
In-114m	49.51 d	Y	-	2.08E-16	4.60E-18	2.08E-16	3.07E-16	6.81E-18	3.06E-16
In-115	5.1E15 y	-	Y	8.07E-19	9.47E-21	1.57E-19	9.02E-19	1.32E-20	2.31E-19
In-115m	4.486 h	Y	Y	3.67E-16	8.10E-18	3.65E-16	5.41E-16	1.20E-17	5.37E-16
In-116m	54.15 m	-	-	6.48E-15	1.25E-16	7.13E-15	9.53E-15	1.84E-16	1.05E-14
In-117	43.8 m	Y	Y	1.66E-15	3.59E-17	1.69E-15	2.44E-15	5.28E-17	2.48E-15
In-117m	116.5 m	Y	Y	2.07E-16	4.96E-18	1.95E-16	3.05E-16	7.14E-18	2.87E-16
In-119	2.4 m	Y	Y	1.92E-15	4.08E-17	2.06E-15	2.82E-15	5.97E-17	3.03E-15
In-119m	18.0 m	Y	-	3.68E-17	1.92E-18	3.34E-17	5.11E-17	2.30E-18	4.82E-17
Tin									
Sn-110	4.0 h	Y	-	6.74E-16	1.49E-17	6.57E-16	9.94E-16	2.21E-17	9.66E-16
Sn-111	35.3 m	Y	-	1.25E-15	2.62E-17	1.33E-15	1.84E-15	3.85E-17	1.96E-15
Sn-113	115.1 d	Y	-	1.52E-17	6.61E-19	1.17E-17	2.32E-17	1.04E-18	1.73E-17
Sn-117m	13.61 d	-	Y	3.22E-16	7.39E-18	2.73E-16	4.77E-16	1.09E-17	4.02E-16
Sn-121	27.06 h	-	Y	4.68E-19	4.16E-21	7.50E-20	5.17E-19	6.29E-21	1.11E-19
Sn-121m	55 y	Y	-	1.83E-18	1.39E-19	4.79E-19	2.92E-18	2.21E-19	7.58E-19
Sn-119m	293.0 d	-	Y	2.64E-18	2.67E-19	6.30E-19	4.44E-18	4.34E-19	1.03E-18
Sn-123	129.2 d	-	-	2.37E-17	1.01E-18	2.27E-17	3.34E-17	1.21E-18	3.32E-17
Sn-123m	40.08 m	-	-	3.15E-16	7.37E-18	2.69E-16	4.64E-16	1.06E-17	3.96E-16
Sn-125	9.64 d	Y	-	8.23E-16	1.70E-17	8.96E-16	1.21E-15	2.46E-17	1.31E-15
Sn-126	1.0E5 y	Y	-	9.25E-17	2.46E-18	5.78E-17	1.38E-16	3.66E-18	8.53E-17
Sn-127	2.10 h	Y	-	4.96E-15	9.72E-17	5.40E-15	7.29E-15	1.43E-16	7.92E-15
Sn-128	59.1 m	Y	-	1.49E-15	3.34E-17	1.52E-15	2.20E-15	4.94E-17	2.24E-15
Antimony									
Sb-115	31.8 m	-	-	2.19E-15	4.74E-17	2.29E-15	3.22E-15	6.98E-17	3.36E-15
Sb-116	15.8 m	-	Y	5.60E-15	1.09E-16	6.11E-15	8.22E-15	1.61E-16	8.97E-15
Sb-116m	60.3 m	-	-	7.94E-15	1.60E-16	8.59E-15	1.17E-14	2.36E-16	1.26E-14
Sb-117	2.80 h	-	-	3.81E-16	8.70E-18	3.37E-16	5.63E-16	1.29E-17	4.95E-16
Sb-118m	5.00 h	-	-	6.54E-15	1.31E-16	7.10E-15	9.62E-15	1.93E-16	1.04E-14
Sb-119	38.1 h	-	-	5.66E-18	5.61E-19	1.35E-18	9.47E-18	9.12E-19	2.21E-18
Sb-120b	5.76 d	-	-	6.22E-15	1.25E-16	6.69E-15	9.16E-15	1.84E-16	9.82E-15
Sb-120a	15.89 m	-	-	1.08E-15	2.37E-17	1.13E-15	1.59E-15	3.49E-17	1.66E-15
Sb-122	2.70 d	-	-	1.09E-15	2.38E-17	1.15E-15	1.60E-15	3.47E-17	1.69E-15
Sb-124	60.20 d	-	Y	4.74E-15	9.22E-17	5.18E-15	6.97E-15	1.35E-16	7.61E-15
Sb-124n	20.2 m	Y	-	1.73E-20	1.80E-21	4.04E-21	2.93E-20	2.93E-21	6.65E-21
Sb-124m	93 s	Y	Y	8.62E-16	1.85E-17	9.14E-16	1.27E-15	2.72E-17	1.34E-15
Sb-125 ^a	2.77 y	Y	Y	1.02E-15	2.22E-17	1.06E-15	1.50E-15	3.27E-17	1.55E-15
Sb-126	12.4 d	-	Y	7.00E-15	1.48E-16	7.47E-15	1.03E-14	2.18E-16	1.10E-14
Sb-126m	19.0 m	Y	Y	3.81E-15	8.16E-17	4.05E-15	5.61E-15	1.20E-16	5.94E-15
Sb-127	3.85 d	Y	Y	1.69E-15	3.61E-17	1.79E-15	2.49E-15	5.31E-17	2.63E-15

Table 2.3, continued

Nuclide	T _{1/2}	Chain P D		Mortality			Morbidity		
				Submersion (m ³ /Bq-s)	Ground		Submersion (m ³ /Bq-s)	Ground	
					Plane (m ² /Bq-s)	Soil (kg/Bq-s)		Plane (m ² /Bq-s)	Soil (kg/Bq-s)
Antimony, continued									
Sb-128b	9.01 h	-	-	7.68E-15	1.61E-16	8.21E-15	1.13E-14	2.37E-16	1.20E-14
Sb-128a	10.4 m	-	Y	4.94E-15	1.05E-16	5.26E-15	7.27E-15	1.53E-16	7.73E-15
Sb-129	4.32 h	Y	-	3.68E-15	7.40E-17	4.00E-15	5.41E-15	1.09E-16	5.87E-15
Sb-130	40 m	-	-	8.19E-15	1.69E-16	8.78E-15	1.20E-14	2.49E-16	1.29E-14
Sb-131	23 m	Y	-	4.85E-15	9.50E-17	5.30E-15	7.13E-15	1.40E-16	7.78E-15
Tellurium									
Te-116	2.49 h	Y	-	1.02E-16	2.92E-18	7.78E-17	1.52E-16	4.40E-18	1.15E-16
Te-121	17 d	-	Y	1.36E-15	2.97E-17	1.44E-15	2.01E-15	4.38E-17	2.11E-15
Te-121m	154 d	Y	-	4.83E-16	1.06E-17	4.57E-16	7.12E-16	1.57E-17	6.71E-16
Te-123m	119.7 d	Y	Y	3.08E-16	7.04E-18	2.61E-16	4.55E-16	1.04E-17	3.84E-16
Te-123	1E13 y	-	Y	5.84E-18	5.31E-19	1.45E-18	9.64E-18	8.53E-19	2.34E-18
Te-125m	58 d	-	Y	1.32E-17	1.04E-18	3.77E-18	2.14E-17	1.65E-18	5.95E-18
Te-127	9.35 h	-	Y	1.32E-17	3.22E-19	1.22E-17	1.89E-17	4.50E-19	1.80E-17
Te-127m	109 d	Y	Y	4.49E-18	3.30E-19	1.51E-18	7.18E-18	5.21E-19	2.34E-18
Te-129	69.6 m	Y	Y	1.41E-16	3.63E-18	1.43E-16	2.06E-16	5.10E-18	2.10E-16
Te-129m	33.6 d	Y	Y	7.83E-17	2.03E-18	8.05E-17	1.15E-16	2.91E-18	1.18E-16
Te-131	25.0 m	Y	Y	1.03E-15	2.24E-17	1.04E-15	1.51E-15	3.26E-17	1.53E-15
Te-131m	30 h	Y	Y	3.59E-15	7.31E-17	3.86E-15	5.28E-15	1.08E-16	5.66E-15
Te-132	78.2 h	Y	-	4.97E-16	1.13E-17	4.57E-16	7.35E-16	1.68E-17	6.71E-16
Te-133	12.45 m	Y	Y	2.35E-15	4.86E-17	2.50E-15	3.46E-15	7.11E-17	3.67E-15
Te-133m	55.4 m	Y	-	5.88E-15	1.19E-16	6.35E-15	8.64E-15	1.75E-16	9.32E-15
Te-134	41.8 m	Y	-	2.14E-15	4.58E-17	2.21E-15	3.15E-15	6.74E-17	3.24E-15
Iodine									
I-120	81.0 m	-	Y	7.15E-15	1.38E-16	7.74E-15	1.05E-14	2.03E-16	1.14E-14
I-120m	53 m	-	-	1.37E-14	2.70E-16	1.48E-14	2.01E-14	3.97E-16	2.18E-14
I-121	2.12 h	Y	Y	9.62E-16	2.11E-17	9.54E-16	1.42E-15	3.12E-17	1.40E-15
I-122	3.62 m	-	Y	2.32E-15	5.07E-17	2.43E-15	3.41E-15	7.43E-17	3.57E-15
I-123	13.2 h	Y	Y	3.44E-16	8.04E-18	2.97E-16	5.09E-16	1.19E-17	4.37E-16
I-124	4.18 d	-	-	2.76E-15	5.60E-17	2.98E-15	4.06E-15	8.24E-17	4.37E-15
I-125	60.14 d	-	Y	1.48E-17	1.22E-18	3.89E-18	2.41E-17	1.94E-18	6.20E-18
I-126	13.02 d	-	-	1.09E-15	2.36E-17	1.15E-15	1.61E-15	3.47E-17	1.68E-15
I-128	24.99 m	-	-	2.14E-16	5.45E-18	2.18E-16	3.13E-16	7.63E-18	3.20E-16
I-129	1.57E7 y	-	Y	1.17E-17	8.05E-19	3.34E-18	1.85E-17	1.26E-18	5.22E-18
I-130	12.36 h	-	-	5.29E-15	1.12E-16	5.64E-15	7.78E-15	1.64E-16	8.28E-15
I-131 ^a	8.04 d	Y	Y	9.14E-16	1.98E-17	9.28E-16	1.35E-15	2.92E-17	1.36E-15
I-132	2.30 h	-	Y	5.73E-15	1.19E-16	6.18E-15	8.43E-15	1.75E-16	9.08E-15
I-132m	83.6 m	Y	-	7.73E-16	1.66E-17	8.15E-16	1.14E-15	2.45E-17	1.20E-15
I-133	20.8 h	Y	Y	1.50E-15	3.21E-17	1.58E-15	2.20E-15	4.71E-17	2.33E-15
I-134	52.6 m	-	Y	6.68E-15	1.36E-16	7.25E-15	9.83E-15	2.00E-16	1.06E-14
I-135	6.61 h	Y	-	4.15E-15	7.96E-17	4.57E-15	6.10E-15	1.17E-16	6.71E-15
Xenon									
Xe-120	40 m	Y	-	9.69E-16	2.15E-17	9.91E-16	1.43E-15	3.17E-17	1.46E-15
Xe-121	40.1 m	Y	-	4.73E-15	9.04E-17	5.09E-15	6.95E-15	1.33E-16	7.48E-15
Xe-122	20.1 h	Y	-	1.16E-16	3.03E-18	1.07E-16	1.72E-16	4.54E-18	1.57E-16

Table 2.3, continued

Nuclide	T _{1/2}	Mortality					Morbidity		
		Chain		Submersion (m ³ /Bq-s)	Ground Plane (m ² /Bq-s)	Soil (kg/Bq-s)	Submersion (m ³ /Bq-s)	Ground Plane (m ² /Bq-s)	Soil (kg/Bq-s)
		P	D						
Xenon, continued									
Xe-123	2.08 h	Y	-	1.53E-15	3.20E-17	1.59E-15	2.26E-15	4.71E-17	2.33E-15
Xe-125	17.0 h	Y	Y	5.79E-16	1.31E-17	5.46E-16	8.56E-16	1.94E-17	8.03E-16
Xe-127	36.41 d	-	Y	6.01E-16	1.37E-17	5.54E-16	8.88E-16	2.02E-17	8.15E-16
Xe-129m	8.0 d	-	-	4.06E-17	1.82E-18	2.44E-17	6.19E-17	2.80E-18	3.64E-17
Xe-131m	11.9 d	-	Y	1.47E-17	6.88E-19	8.11E-18	2.24E-17	1.06E-18	1.21E-17
Xe-133	5.245 d	-	Y	6.59E-17	1.96E-18	3.83E-17	9.86E-17	2.93E-18	5.67E-17
Xe-133m	2.188 d	Y	Y	6.30E-17	1.74E-18	5.38E-17	9.34E-17	2.61E-18	7.92E-17
Xe-135	9.09 h	Y	Y	5.87E-16	1.29E-17	5.66E-16	8.65E-16	1.89E-17	8.31E-16
Xe-135m	15.29 m	Y	Y	1.03E-15	2.24E-17	1.09E-15	1.52E-15	3.30E-17	1.59E-15
Xe-138	14.17 m	Y	-	3.01E-15	5.61E-17	3.28E-15	4.42E-15	8.22E-17	4.81E-15
Cesium									
Cs-125	45 m	Y	-	1.63E-15	3.55E-17	1.70E-15	2.40E-15	5.22E-17	2.50E-15
Cs-126	1.64 m	-	Y	2.66E-15	5.87E-17	2.77E-15	3.91E-15	8.59E-17	4.06E-15
Cs-127	6.25 h	Y	-	9.64E-16	2.13E-17	9.81E-16	1.42E-15	3.15E-17	1.44E-15
Cs-128	3.9 m	-	Y	2.19E-15	4.81E-17	2.29E-15	3.22E-15	7.04E-17	3.36E-15
Cs-129	32.06 h	-	-	6.09E-16	1.40E-17	6.11E-16	9.00E-16	2.07E-17	8.98E-16
Cs-130	29.9 m	-	-	1.24E-15	2.73E-17	1.30E-15	1.82E-15	4.00E-17	1.90E-15
Cs-131	9.69 d	-	Y	9.73E-18	7.24E-19	2.67E-18	1.56E-17	1.14E-18	4.20E-18
Cs-132	6.475 d	-	-	1.70E-15	3.64E-17	1.81E-15	2.50E-15	5.36E-17	2.66E-15
Cs-134	2.062 y	-	Y	3.86E-15	8.11E-17	4.14E-15	5.68E-15	1.19E-16	6.08E-15
Cs-134m	2.90 h	Y	-	4.00E-17	1.11E-18	2.92E-17	5.97E-17	1.67E-18	4.30E-17
Cs-135	2.3E6 y	-	Y	1.12E-19	1.18E-21	1.35E-20	1.23E-19	1.81E-21	2.02E-20
Cs-135m	53 m	Y	-	3.97E-15	8.25E-17	4.30E-15	5.84E-15	1.21E-16	6.31E-15
Cs-136	13.1 d	-	-	5.44E-15	1.11E-16	5.86E-15	8.01E-15	1.64E-16	8.60E-15
Cs-137 ^a	30.0 y	Y	-	1.20E-18	3.96E-20	3.14E-19	1.37E-18	4.57E-20	4.56E-19
Cs-138	32.2 m	-	Y	6.31E-15	1.19E-16	6.93E-15	9.27E-15	1.75E-16	1.02E-14
Barium									
Ba-126	96.5 m	Y	-	3.44E-16	8.00E-18	3.39E-16	5.08E-16	1.18E-17	4.99E-16
Ba-128	2.43 d	Y	-	1.34E-16	3.45E-18	1.22E-16	1.99E-16	5.15E-18	1.80E-16
Ba-131	11.8 d	Y	Y	1.04E-15	2.31E-17	1.04E-15	1.53E-15	3.41E-17	1.52E-15
Ba-131m	14.6 m	Y	-	1.37E-16	3.46E-18	9.70E-17	2.03E-16	5.13E-18	1.43E-16
Ba-133	10.74 y	-	Y	8.70E-16	1.99E-17	8.37E-16	1.28E-15	2.95E-17	1.23E-15
Ba-133m	38.9 h	Y	-	1.25E-16	3.09E-18	1.14E-16	1.85E-16	4.59E-18	1.68E-16
Ba-135m ^a	28.7 h	-	-	1.10E-16	2.76E-18	9.90E-17	1.62E-16	4.12E-18	1.46E-16
Ba-137m ^a	2.552 m	-	Y	1.47E-15	3.12E-17	1.57E-15	2.16E-15	4.60E-17	2.30E-15
Ba-139	82.7 m	-	-	1.10E-16	3.36E-18	9.65E-17	1.60E-16	4.47E-18	1.41E-16
Ba-140	12.74 d	Y	-	4.32E-16	9.57E-18	4.44E-16	6.36E-16	1.40E-17	6.52E-16
Ba-141	18.27 m	Y	-	2.12E-15	4.43E-17	2.21E-15	3.12E-15	6.47E-17	3.25E-15
Ba-142	10.6 m	Y	-	2.64E-15	5.39E-17	2.83E-15	3.88E-15	7.92E-17	4.15E-15
Lanthanum									
La-131	59 m	Y	-	1.57E-15	3.46E-17	1.60E-15	2.32E-15	5.09E-17	2.36E-15
La-132	4.8 h	-	-	5.16E-15	1.02E-16	5.55E-15	7.59E-15	1.50E-16	8.15E-15
La-134	6.67 m	-	Y	1.70E-15	3.73E-17	1.78E-15	2.50E-15	5.46E-17	2.61E-15
La-135	19.5 h	-	Y	3.84E-17	1.41E-18	3.02E-17	5.80E-17	2.14E-18	4.46E-17

Table 2.3, continued

Nuclide	T _{1/2}	Chain		Mortality			Morbidity		
				Submersion	Ground		Submersion	Ground	
					(m ³ /Bq-s)	Plane		Soil	(m ³ /Bq-s)
P	D	(m ³ /Bq-s)	(m ² /Bq-s)	(kg/Bq-s)	(m ³ /Bq-s)	(m ² /Bq-s)	(kg/Bq-s)		
Lanthanum, continued									
La-137	6E4 y	-	Y	1.27E-17	8.28E-19	3.71E-18	2.01E-17	1.28E-18	5.78E-18
La-138	1.35E11 y	-	-	3.22E-15	6.22E-17	3.54E-15	4.73E-15	9.15E-17	5.20E-15
La-140	40.272 h	-	Y	6.10E-15	1.17E-16	6.70E-15	8.96E-15	1.71E-16	9.83E-15
La-141	3.93 h	Y	Y	1.30E-16	3.50E-18	1.39E-16	1.88E-16	4.64E-18	2.03E-16
La-142	92.5 m	-	Y	7.58E-15	1.34E-16	8.38E-15	1.11E-14	1.96E-16	1.23E-14
La-143	14.23 m	Y	-	2.77E-16	6.52E-18	2.99E-16	4.04E-16	8.97E-18	4.38E-16
Cerium									
Ce-134	72.0 h	Y	-	1.51E-17	9.26E-19	4.56E-18	2.38E-17	1.43E-18	7.06E-18
Ce-135	17.6 h	Y	-	4.32E-15	9.25E-17	4.52E-15	6.36E-15	1.36E-16	6.63E-15
Ce-137	9.0 h	Y	Y	3.57E-17	1.38E-18	2.57E-17	5.40E-17	2.09E-18	3.82E-17
Ce-137m	34.4 h	Y	-	9.18E-17	2.40E-18	8.04E-17	1.36E-16	3.58E-18	1.18E-16
Ce-139	137.66 d	-	Y	3.15E-16	7.52E-18	2.64E-16	4.66E-16	1.11E-17	3.89E-16
Ce-141	32.501 d	-	Y	1.62E-16	3.69E-18	1.32E-16	2.39E-16	5.44E-18	1.94E-16
Ce-143	33.0 h	Y	Y	6.40E-16	1.46E-17	6.36E-16	9.43E-16	2.14E-17	9.34E-16
Ce-144	284.3 d	Y	-	3.90E-17	9.61E-19	2.92E-17	5.78E-17	1.42E-18	4.30E-17
Praseodymium									
Pr-136	13.1 m	-	Y	5.31E-15	1.08E-16	5.68E-15	7.81E-15	1.59E-16	8.34E-15
Pr-137	76.6 m	Y	-	1.19E-15	2.60E-17	1.25E-15	1.75E-15	3.82E-17	1.83E-15
Pr-138	1.45 m	-	Y	1.99E-15	4.40E-17	2.09E-15	2.93E-15	6.43E-17	3.06E-15
Pr-138m	2.1 h	-	-	6.18E-15	1.28E-16	6.62E-15	9.09E-15	1.88E-16	9.72E-15
Pr-139	4.51 h	Y	Y	2.55E-16	5.99E-18	2.57E-16	3.76E-16	8.86E-18	3.78E-16
Pr-142	19.13 h	-	Y	1.70E-16	4.01E-18	1.84E-16	2.47E-16	5.47E-18	2.69E-16
Pr-142m	14.6 m	Y	-	0.00	0.00	0.00	0.00	0.00	0.00
Pr-143	13.56 d	-	Y	2.70E-18	2.31E-19	9.72E-19	3.16E-18	2.46E-19	1.40E-18
Pr-144	17.28 m	-	Y	1.09E-16	3.27E-18	1.14E-16	1.56E-16	4.22E-18	1.66E-16
Pr-144m	7.2 m	Y	Y	1.01E-17	4.75E-19	4.99E-18	1.56E-17	7.23E-19	7.48E-18
Pr-145	5.98 h	-	-	4.15E-17	1.60E-18	4.08E-17	5.91E-17	1.99E-18	5.95E-17
Pr-147	13.6 m	Y	-	2.11E-15	4.50E-17	2.21E-15	3.10E-15	6.58E-17	3.24E-15
Neodymium									
Nd-136	50.65 m	Y	-	6.16E-16	1.44E-17	5.89E-16	9.10E-16	2.13E-17	8.66E-16
Nd-138	5.04 h	Y	-	5.32E-17	1.81E-18	3.89E-17	8.00E-17	2.72E-18	5.76E-17
Nd-139	29.7 m	Y	Y	9.58E-16	2.10E-17	1.00E-15	1.41E-15	3.09E-17	1.47E-15
Nd-139m	5.5 h	Y	-	3.89E-15	8.04E-17	4.16E-15	5.73E-15	1.18E-16	6.11E-15
Nd-141	2.49 h	-	Y	1.37E-16	3.49E-18	1.33E-16	2.04E-16	5.19E-18	1.95E-16
Nd-141m	62.4 s	Y	Y	1.89E-15	3.97E-17	2.03E-15	2.78E-15	5.84E-17	2.98E-15
Nd-147	10.98 d	Y	Y	3.01E-16	7.07E-18	2.84E-16	4.44E-16	1.04E-17	4.17E-16
Nd-149	1.73 h	Y	-	8.94E-16	2.00E-17	8.72E-16	1.32E-15	2.93E-17	1.28E-15
Nd-151	12.44 m	Y	-	2.28E-15	4.75E-17	2.39E-15	3.35E-15	6.95E-17	3.51E-15
Promethium									
Pm-141	20.90 m	Y	Y	1.84E-15	3.92E-17	1.94E-15	2.70E-15	5.74E-17	2.85E-15
Pm-142	40.5 s	-	Y	2.14E-15	4.70E-17	2.25E-15	3.15E-15	6.87E-17	3.31E-15
Pm-143	265 d	-	Y	7.33E-16	1.60E-17	7.73E-16	1.08E-15	2.37E-17	1.14E-15
Pm-144	363 d	-	Y	3.79E-15	8.13E-17	4.02E-15	5.58E-15	1.20E-16	5.91E-15
Pm-145	17.7 y	-	Y	2.50E-17	1.20E-18	9.11E-18	3.86E-17	1.82E-18	1.38E-17

Table 2.3, continued

Nuclide	T _{1/2}	Chain P D		Mortality			Morbidity		
				Submersion (m ³ /Bq-s)	Ground		Submersion (m ³ /Bq-s)	Ground	
					Plane (m ² /Bq-s)	Soil (kg/Bq-s)		Plane (m ² /Bq-s)	Soil (kg/Bq-s)
Promethium, continued									
Pm-146	2020 d	Y	-	1.82E-15	3.91E-17	1.92E-15	2.68E-15	5.76E-17	2.82E-15
Pm-147	2.6234 y	Y	Y	1.09E-19	1.26E-21	1.85E-20	1.23E-19	1.93E-21	2.75E-20
Pm-148	5.37 d	-	Y	1.50E-15	3.02E-17	1.63E-15	2.20E-15	4.40E-17	2.40E-15
Pm-148m	41.3 d	Y	-	4.93E-15	1.04E-16	5.24E-15	7.25E-15	1.54E-16	7.69E-15
Pm-149	53.08 h	-	Y	2.89E-17	8.86E-19	2.69E-17	4.16E-17	1.17E-18	3.94E-17
Pm-150	2.68 h	-	-	3.70E-15	7.34E-17	4.01E-15	5.44E-15	1.08E-16	5.88E-15
Pm-151	28.40 h	Y	Y	7.49E-16	1.65E-17	7.44E-16	1.10E-15	2.43E-17	1.09E-15
Samarium									
Sm-141	10.2 m	Y	Y	3.51E-15	7.30E-17	3.73E-15	5.16E-15	1.07E-16	5.47E-15
Sm-141m	22.6 m	Y	-	4.95E-15	1.02E-16	5.27E-15	7.29E-15	1.50E-16	7.74E-15
Sm-142	72.49 m	Y	-	1.82E-16	4.55E-18	1.74E-16	2.69E-16	6.75E-18	2.56E-16
Sm-145	340 d	Y	Y	5.81E-17	2.59E-18	2.17E-17	8.90E-17	3.92E-18	3.28E-17
Sm-146	1.03E8 y	-	Y	0.00	0.00	0.00	0.00	0.00	0.00
Sm-147	1.06E11 y	-	Y	0.00	0.00	0.00	0.00	0.00	0.00
Sm-151	90 y	-	Y	8.65E-22	1.14E-22	1.81E-22	1.52E-21	1.92E-22	3.08E-22
Sm-153	46.7 h	-	-	9.90E-17	2.85E-18	6.17E-17	1.47E-16	4.20E-18	9.11E-17
Sm-155	22.1 m	Y	-	2.18E-16	5.64E-18	1.64E-16	3.21E-16	8.03E-18	2.41E-16
Sm-156	9.4 h	Y	-	2.58E-16	5.90E-18	2.21E-16	3.82E-16	8.69E-18	3.25E-16
Europium									
Eu-145	5.94 d	Y	Y	3.72E-15	7.37E-17	4.05E-15	5.48E-15	1.08E-16	5.95E-15
Eu-146	4.61 d	Y	Y	6.29E-15	1.29E-16	6.78E-15	9.25E-15	1.89E-16	9.95E-15
Eu-147	24 d	Y	Y	1.16E-15	2.50E-17	1.19E-15	1.71E-15	3.69E-17	1.75E-15
Eu-148	54.5 d	Y	-	5.38E-15	1.12E-16	5.74E-15	7.92E-15	1.66E-16	8.43E-15
Eu-149	93.1 d	-	Y	1.01E-16	2.87E-18	8.27E-17	1.50E-16	4.27E-18	1.22E-16
Eu-150b	34.2 y	-	-	3.62E-15	7.72E-17	3.78E-15	5.33E-15	1.14E-16	5.56E-15
Eu-150a	12.62 h	-	-	1.12E-16	2.64E-18	1.14E-16	1.65E-16	3.78E-18	1.67E-16
Eu-152	13.33 y	Y	-	2.89E-15	5.86E-17	3.09E-15	4.25E-15	8.63E-17	4.54E-15
Eu-152m	9.32 h	Y	-	7.27E-16	1.57E-17	7.74E-16	1.07E-15	2.29E-17	1.14E-15
Eu-154	8.8 y	-	-	3.15E-15	6.35E-17	3.40E-15	4.63E-15	9.34E-17	4.99E-15
Eu-155	4.96 y	-	Y	1.10E-16	2.81E-18	7.22E-17	1.64E-16	4.15E-18	1.06E-16
Eu-156	15.19 d	-	Y	3.51E-15	6.68E-17	3.86E-15	5.16E-15	9.81E-17	5.67E-15
Eu-157	15.15 h	-	-	5.76E-16	1.35E-17	5.59E-16	8.49E-16	1.98E-17	8.22E-16
Eu-158	45.9 m	-	-	2.72E-15	5.51E-17	2.95E-15	3.99E-15	8.06E-17	4.33E-15
Gadolinium									
Gd-145	22.9 m	Y	-	5.99E-15	1.13E-16	6.57E-15	8.80E-15	1.65E-16	9.64E-15
Gd-146	48.3 d	Y	-	4.46E-16	1.15E-17	3.23E-16	6.63E-16	1.71E-17	4.76E-16
Gd-147	38.1 h	Y	Y	3.26E-15	6.86E-17	3.43E-15	4.81E-15	1.01E-16	5.03E-15
Gd-148	93 y	-	-	0.00	0.00	0.00	0.00	0.00	0.00
Gd-149	9.4 d	Y	Y	9.44E-16	2.11E-17	9.23E-16	1.39E-15	3.12E-17	1.36E-15
Gd-151	120 d	Y	Y	9.56E-17	2.81E-18	6.95E-17	1.43E-16	4.19E-18	1.03E-16
Gd-152	1.08E14 y	-	Y	0.00	0.00	0.00	0.00	0.00	0.00
Gd-153	242 d	-	Y	1.57E-16	4.65E-18	9.37E-17	2.34E-16	6.92E-18	1.39E-16
Gd-159	18.56 h	-	-	1.08E-16	2.69E-18	1.01E-16	1.59E-16	3.90E-18	1.49E-16

Table 2.3, continued

Nuclide	T _{1/2}	Mortality					Morbidity		
		Chain		Ground		Soil	Ground		Soil
		P	D	Submersion	Plane		Submersion	Plane	
(m ³ /Bq-s)	(m ² /Bq-s)	(kg/Bq-s)	(m ³ /Bq-s)	(m ² /Bq-s)	(kg/Bq-s)				
Terbium									
Tb-147	1.65 h	Y	-	3.98E-15	8.25E-17	4.26E-15	5.85E-15	1.21E-16	6.25E-15
Tb-149	4.15 h	Y	-	4.12E-15	8.16E-17	4.43E-15	6.06E-15	1.20E-16	6.51E-15
Tb-150	3.27 h	-	-	4.24E-15	8.65E-17	4.55E-15	6.23E-15	1.27E-16	6.67E-15
Tb-151	17.6 h	Y	-	2.10E-15	4.55E-17	2.13E-15	3.09E-15	6.71E-17	3.13E-15
Tb-153	2.34 d	Y	-	4.70E-16	1.11E-17	4.21E-16	6.96E-16	1.64E-17	6.20E-16
Tb-154	21.4 h	-	-	6.30E-15	1.15E-16	6.91E-15	9.26E-15	1.68E-16	1.01E-14
Tb-155	5.32 d	-	Y	2.51E-16	6.50E-18	1.89E-16	3.73E-16	9.63E-18	2.79E-16
Tb-156	5.34 d	-	Y	4.57E-15	9.26E-17	4.88E-15	6.73E-15	1.36E-16	7.17E-15
Tb-156m	24.4 h	Y	-	3.01E-17	1.10E-18	1.24E-17	4.55E-17	1.63E-18	1.85E-17
Tb-156n	5.0 h	Y	-	4.71E-18	1.57E-19	2.34E-18	7.07E-18	2.34E-19	3.48E-18
Tb-157	150 y	-	Y	2.50E-18	1.05E-19	9.30E-19	3.81E-18	1.58E-19	1.40E-18
Tb-158	150 y	-	-	1.95E-15	4.07E-17	2.08E-15	2.88E-15	6.00E-17	3.06E-15
Tb-160	72.3 d	-	-	2.84E-15	5.77E-17	3.05E-15	4.17E-15	8.49E-17	4.48E-15
Tb-161	6.91 d	-	-	4.12E-17	1.42E-18	1.98E-17	6.18E-17	2.12E-18	2.95E-17
Dysprosium									
Dy-155	10.0 h	Y	Y	1.39E-15	2.92E-17	1.42E-15	2.05E-15	4.31E-17	2.09E-15
Dy-157	8.1 h	Y	Y	7.97E-16	1.80E-17	7.70E-16	1.18E-15	2.66E-17	1.13E-15
Dy-159	144.4 d	-	Y	4.70E-17	1.87E-18	1.82E-17	7.14E-17	2.80E-18	2.73E-17
Dy-165	2.334 h	-	-	6.08E-17	1.79E-18	5.54E-17	8.86E-17	2.44E-18	8.13E-17
Dy-166	81.6 h	Y	-	5.95E-17	1.78E-18	3.49E-17	8.89E-17	2.65E-18	5.16E-17
Holmium									
Ho-155	48 m	Y	-	8.88E-16	2.00E-17	8.87E-16	1.31E-15	2.94E-17	1.30E-15
Ho-157	12.6 m	Y	-	1.10E-15	2.47E-17	1.07E-15	1.62E-15	3.65E-17	1.58E-15
Ho-159	33 m	Y	-	7.62E-16	1.78E-17	6.73E-16	1.13E-15	2.63E-17	9.90E-16
Ho-161	2.5 h	-	Y	6.78E-17	2.48E-18	3.17E-17	1.03E-16	3.72E-18	4.73E-17
Ho-162	15 m	-	Y	3.60E-16	8.17E-18	3.51E-16	5.31E-16	1.21E-17	5.16E-16
Ho-162m	68 m	Y	-	1.38E-15	2.88E-17	1.44E-15	2.04E-15	4.25E-17	2.11E-15
Ho-164m	37.5 m	Y	-	5.09E-17	1.91E-18	2.08E-17	7.71E-17	2.85E-18	3.11E-17
Ho-164	29 m	-	Y	3.62E-17	1.35E-18	1.59E-17	5.43E-17	1.97E-18	2.38E-17
Ho-166	26.80 h	-	Y	7.39E-17	2.29E-18	6.89E-17	1.07E-16	3.01E-18	1.01E-16
Ho-166m	1.20E3 y	-	-	4.28E-15	9.04E-17	4.49E-15	6.30E-15	1.33E-16	6.59E-15
Ho-167	3.1 h	-	-	8.56E-16	1.88E-17	8.45E-16	1.26E-15	2.77E-17	1.24E-15
Erbium									
Er-161	3.24 h	Y	-	2.25E-15	4.67E-17	2.39E-15	3.31E-15	6.88E-17	3.50E-15
Er-165	10.36 h	-	-	4.30E-17	1.59E-18	1.75E-17	6.51E-17	2.38E-18	2.61E-17
Er-169	9.3 d	-	-	3.53E-19	3.14E-21	5.25E-20	3.89E-19	4.76E-21	7.79E-20
Er-171	7.52 h	Y	-	8.74E-16	1.96E-17	8.31E-16	1.29E-15	2.88E-17	1.22E-15
Er-172	49.3 h	Y	-	1.24E-15	2.71E-17	1.28E-15	1.83E-15	3.99E-17	1.88E-15
Thulium									
Tm-162	21.7 m	-	Y	4.67E-15	8.84E-17	5.07E-15	6.87E-15	1.30E-16	7.44E-15
Tm-166	7.70 h	-	Y	4.83E-15	9.34E-17	5.24E-15	7.10E-15	1.37E-16	7.69E-15
Tm-167	9.24 d	-	Y	2.81E-16	6.94E-18	2.31E-16	4.17E-16	1.03E-17	3.40E-16
Tm-170	128.6 d	-	-	1.13E-17	4.83E-19	5.86E-18	1.61E-17	6.14E-19	8.62E-18
Tm-171	1.92 y	-	Y	8.71E-19	2.82E-20	4.01E-19	1.31E-18	4.18E-20	5.97E-19

Table 2.3, continued

Nuclide	T _{1/2}	Chain P D		Mortality			Morbidity		
				Submersion (m ³ /Bq-s)	Ground Plane		Submersion (m ³ /Bq-s)	Ground Plane	
					(m ² /Bq-s)	Soil (kg/Bq-s)		(m ² /Bq-s)	Soil (kg/Bq-s)
Thulium, continued									
Tm-172	63.6 h	-	Y	1.25E-15	2.45E-17	1.37E-15	1.84E-15	3.58E-17	2.01E-15
Tm-173	8.24 h	-	-	9.27E-16	2.04E-17	9.43E-16	1.36E-15	2.99E-17	1.39E-15
Tm-175	15.2 m	Y	-	2.62E-15	5.49E-17	2.79E-15	3.85E-15	8.07E-17	4.09E-15
Ytterbium									
Yb-162	18.9 m	Y	-	2.56E-16	6.41E-18	1.89E-16	3.80E-16	9.48E-18	2.79E-16
Yb-166	56.7 h	Y	-	1.16E-16	3.76E-18	5.45E-17	1.74E-16	5.59E-18	8.10E-17
Yb-167	17.5 m	Y	-	4.93E-16	1.25E-17	3.61E-16	7.32E-16	1.84E-17	5.32E-16
Yb-169	32.01 d	-	Y	5.88E-16	1.47E-17	4.51E-16	8.72E-16	2.17E-17	6.64E-16
Yb-175	4.19 d	-	Y	9.24E-17	2.04E-18	8.98E-17	1.36E-16	3.00E-18	1.32E-16
Yb-177	1.9 h	Y	-	4.70E-16	9.97E-18	4.87E-16	6.91E-16	1.45E-17	7.15E-16
Yb-178	74 m	Y	-	8.40E-17	1.85E-18	8.38E-17	1.23E-16	2.71E-18	1.23E-16
Lutetium									
Lu-169	34.06 h	Y	-	2.60E-15	5.22E-17	2.76E-15	3.82E-15	7.69E-17	4.05E-15
Lu-170	2.00 d	-	Y	6.69E-15	1.21E-16	7.35E-15	9.83E-15	1.78E-16	1.08E-14
Lu-171	8.22 d	-	-	1.63E-15	3.55E-17	1.69E-15	2.41E-15	5.23E-17	2.48E-15
Lu-172	6.70 d	-	Y	4.73E-15	9.63E-17	5.07E-15	6.96E-15	1.42E-16	7.45E-15
Lu-173	1.37 y	-	Y	2.29E-16	6.07E-18	1.69E-16	3.40E-16	8.97E-18	2.50E-16
Lu-174	3.31 y	-	Y	2.64E-16	6.00E-18	2.49E-16	3.91E-16	8.85E-18	3.65E-16
Lu-174m	142 d	Y	-	9.30E-17	2.74E-18	5.72E-17	1.39E-16	4.06E-18	8.46E-17
Lu-176	3.60E10 y	-	-	1.13E-15	2.49E-17	1.07E-15	1.67E-15	3.66E-17	1.57E-15
Lu-176m	3.68 h	-	-	2.82E-17	1.12E-18	1.62E-17	4.08E-17	1.45E-18	2.38E-17
Lu-177	6.71 d	-	Y	7.75E-17	1.73E-18	6.63E-17	1.14E-16	2.55E-18	9.75E-17
Lu-177m	160.9 d	Y	-	2.27E-15	5.05E-17	2.12E-15	3.35E-15	7.44E-17	3.11E-15
Lu-178	28.4 m	-	Y	3.69E-16	7.99E-18	3.95E-16	5.41E-16	1.14E-17	5.79E-16
Lu-178m	22.7 m	-	-	2.58E-15	5.70E-17	2.48E-15	3.80E-15	8.38E-17	3.65E-15
Lu-179	4.59 h	-	-	7.66E-17	2.09E-18	6.94E-17	1.12E-16	2.86E-18	1.02E-16
Hafnium									
Hf-170	16.01 h	Y	-	1.23E-15	2.77E-17	1.19E-15	1.82E-15	4.08E-17	1.75E-15
Hf-172	1.87 y	Y	Y	1.71E-16	5.06E-18	9.41E-17	2.55E-16	7.51E-18	1.39E-16
Hf-173	24.0 h	Y	Y	8.87E-16	2.01E-17	7.83E-16	1.31E-15	2.97E-17	1.15E-15
Hf-175	70 d	-	Y	8.27E-16	1.87E-17	7.91E-16	1.22E-15	2.75E-17	1.16E-15
Hf-177m	51.4 m	-	-	5.21E-15	1.14E-16	5.00E-15	7.68E-15	1.69E-16	7.35E-15
Hf-178m	31 y	-	-	5.56E-15	1.21E-16	5.58E-15	8.20E-15	1.79E-16	8.20E-15
Hf-179m	25.1 d	-	-	2.07E-15	4.58E-17	1.99E-15	3.05E-15	6.75E-17	2.93E-15
Hf-180m	5.5 h	-	-	2.34E-15	5.16E-17	2.29E-15	3.45E-15	7.60E-17	3.37E-15
Hf-181	42.4 d	-	-	1.31E-15	2.86E-17	1.31E-15	1.93E-15	4.21E-17	1.92E-15
Hf-182	9E6 y	Y	Y	5.57E-16	1.22E-17	5.30E-16	8.22E-16	1.79E-17	7.79E-16
Hf-182m	61.5 m	Y	-	2.21E-15	4.78E-17	2.23E-15	3.26E-15	7.04E-17	3.28E-15
Hf-183	64 m	Y	-	1.84E-15	3.93E-17	1.93E-15	2.71E-15	5.77E-17	2.83E-15
Hf-184	4.12 h	Y	-	5.52E-16	1.25E-17	5.03E-16	8.14E-16	1.84E-17	7.40E-16
Tantalum									
Ta-172	36.8 m	Y	-	3.87E-15	7.92E-17	4.10E-15	5.70E-15	1.16E-16	6.03E-15
Ta-173	3.65 h	Y	-	1.37E-15	2.99E-17	1.39E-15	2.02E-15	4.39E-17	2.04E-15
Ta-174	1.2 h	-	-	1.48E-15	3.21E-17	1.48E-15	2.18E-15	4.72E-17	2.18E-15

Table 2.3, continued

Nuclide	T _{1/2}	Mortality					Morbidity		
		Chain		Submersion (m ³ /Bq-s)	Ground Plane		Submersion (m ³ /Bq-s)	Ground Plane	
		P	D		(m ² /Bq-s)	Soil (kg/Bq-s)		(m ² /Bq-s)	Soil (kg/Bq-s)
Tantalum, continued									
Ta-175	10.5 h	Y	-	2.32E-15	4.65E-17	2.43E-15	3.41E-15	6.84E-17	3.56E-15
Ta-176	8.08 h	-	Y	5.66E-15	1.06E-16	6.19E-15	8.32E-15	1.56E-16	9.09E-15
Ta-177	56.6 h	-	Y	1.10E-16	3.05E-18	6.99E-17	1.64E-16	4.52E-18	1.03E-16
Ta-178b	2.2 h	-	-	2.32E-15	5.18E-17	2.20E-15	3.43E-15	7.63E-17	3.24E-15
Ta-178a	9.31 m	-	Y	2.19E-16	5.12E-18	1.92E-16	3.24E-16	7.55E-18	2.82E-16
Ta-179	664.9 d	-	Y	4.46E-17	1.40E-18	2.09E-17	6.69E-17	2.08E-18	3.10E-17
Ta-180	1.0E13 y	-	-	1.26E-15	2.82E-17	1.18E-15	1.86E-15	4.15E-17	1.74E-15
Ta-180m	8.1 h	-	-	7.08E-17	2.15E-18	3.54E-17	1.06E-16	3.18E-18	5.25E-17
Ta-182	115.0 d	-	Y	3.28E-15	6.56E-17	3.52E-15	4.83E-15	9.64E-17	5.17E-15
Ta-182m	15.84 m	Y	-	5.23E-16	1.21E-17	4.29E-16	7.74E-16	1.79E-17	6.32E-16
Ta-183	5.1 d	-	Y	6.27E-16	1.44E-17	5.47E-16	9.26E-16	2.12E-17	8.05E-16
Ta-184	8.7 h	-	Y	3.94E-15	8.35E-17	4.09E-15	5.80E-15	1.23E-16	6.01E-15
Ta-185	49 m	Y	-	4.20E-16	1.03E-17	3.63E-16	6.18E-16	1.48E-17	5.34E-16
Ta-186	10.5 m	-	-	3.79E-15	8.18E-17	3.90E-15	5.58E-15	1.20E-16	5.73E-15
Tungsten									
W-176	2.3 h	Y	-	3.06E-16	8.10E-18	1.86E-16	4.55E-16	1.20E-17	2.74E-16
W-177	135 m	Y	Y	2.12E-15	4.56E-17	2.12E-15	3.12E-15	6.71E-17	3.11E-15
W-178	21.7 d	Y	Y	1.90E-17	5.83E-19	9.17E-18	2.85E-17	8.64E-19	1.36E-17
W-179	37.5 m	Y	-	7.37E-17	2.47E-18	3.46E-17	1.11E-16	3.68E-18	5.15E-17
W-181	121.2 d	-	Y	5.78E-17	1.77E-18	2.80E-17	8.66E-17	2.62E-18	4.16E-17
W-185	75.1 d	-	Y	6.81E-19	7.95E-21	1.69E-19	7.96E-19	1.19E-20	2.50E-19
W-187	23.9 h	Y	-	1.15E-15	2.49E-17	1.19E-15	1.70E-15	3.66E-17	1.75E-15
W-188	69.4 d	Y	-	4.66E-18	9.87E-20	4.09E-18	6.75E-18	1.45E-19	6.01E-18
Rhenium									
Re-177	14.0 m	Y	-	1.49E-15	3.12E-17	1.53E-15	2.20E-15	4.58E-17	2.24E-15
Re-178	13.2 m	Y	-	3.13E-15	6.07E-17	3.29E-15	4.60E-15	8.91E-17	4.84E-15
Re-180	2.43 m	-	Y	2.91E-15	6.09E-17	3.08E-15	4.28E-15	8.97E-17	4.53E-15
Re-181	20 h	Y	Y	1.83E-15	3.93E-17	1.85E-15	2.69E-15	5.79E-17	2.72E-15
Re-182b	64.0 h	-	-	4.63E-15	9.48E-17	4.79E-15	6.82E-15	1.39E-16	7.04E-15
Re-182a	12.7 h	-	Y	2.95E-15	5.93E-17	3.14E-15	4.34E-15	8.72E-17	4.60E-15
Re-184	38.0 d	-	Y	2.18E-15	4.57E-17	2.30E-15	3.20E-15	6.73E-17	3.37E-15
Re-184m	165 d	Y	-	9.00E-16	1.95E-17	8.83E-16	1.33E-15	2.87E-17	1.30E-15
Re-186m	2.0E5 y	Y	-	2.05E-17	6.45E-19	1.01E-17	3.08E-17	9.58E-19	1.50E-17
Re-186	90.64 h	-	Y	4.41E-17	1.26E-18	3.20E-17	6.44E-17	1.74E-18	4.70E-17
Re-187	5E10 y	-	Y	0.00	0.00	0.00	0.00	0.00	0.00
Re-188	16.98 h	-	Y	1.47E-16	3.96E-18	1.39E-16	2.14E-16	5.41E-18	2.04E-16
Re-188m	18.6 m	Y	-	1.30E-16	3.54E-18	7.44E-17	1.94E-16	5.23E-18	1.10E-16
Re-189	24.3 h	Y	-	1.57E-16	3.67E-18	1.41E-16	2.31E-16	5.31E-18	2.07E-16
Osmium									
Os-180	22 m	Y	-	9.99E-17	2.78E-18	6.28E-17	1.49E-16	4.12E-18	9.28E-17
Os-181	105 m	Y	-	3.02E-15	6.18E-17	3.16E-15	4.44E-15	9.10E-17	4.63E-15
Os-182	22 h	Y	Y	9.87E-16	2.20E-17	9.55E-16	1.46E-15	3.25E-17	1.40E-15
Os-185	94 d	-	Y	1.73E-15	3.72E-17	1.81E-15	2.55E-15	5.47E-17	2.66E-15
Os-189m	6.0 h	-	Y	3.94E-21	1.21E-21	3.85E-22	6.54E-21	1.88E-21	6.17E-22

Table 2.3, continued

Nuclide	T _{1/2}	Mortality				Morbidity			
		Chain		Ground		Ground		Soil	
		P	D	Submersion (m ³ /Bq-s)	Plane (m ² /Bq-s)	Soil (kg/Bq-s)	Submersion (m ³ /Bq-s)	Plane (m ² /Bq-s)	Soil (kg/Bq-s)
Osmium, continued									
Os-190m	9.9 m	-	-	3.82E-15	8.24E-17	3.94E-15	5.63E-15	1.21E-16	5.79E-15
Os-191	15.4 d	-	Y	1.44E-16	3.58E-18	9.62E-17	2.13E-16	5.28E-18	1.42E-16
Os-191m	13.03 h	Y	-	1.16E-17	3.32E-19	6.04E-18	1.73E-17	4.91E-19	8.95E-18
Os-193	30.0 h	-	-	1.68E-16	4.00E-18	1.56E-16	2.47E-16	5.77E-18	2.30E-16
Os-194	6.0 y	Y	-	1.01E-18	4.42E-20	3.73E-19	1.54E-18	6.66E-20	5.63E-19
Iridium									
Ir-182	15 m	Y	-	3.28E-15	6.99E-17	3.41E-15	4.83E-15	1.03E-16	5.01E-15
Ir-184	3.02 h	-	-	4.78E-15	9.68E-17	5.05E-15	7.04E-15	1.42E-16	7.42E-15
Ir-185	14.0 h	Y	-	1.50E-15	2.92E-17	1.57E-15	2.21E-15	4.29E-17	2.30E-15
Ir-186a	15.8 h	-	-	4.11E-15	8.28E-17	4.32E-15	6.04E-15	1.22E-16	6.34E-15
Ir-186b	1.75 h	-	Y	2.36E-15	4.94E-17	2.46E-15	3.47E-15	7.26E-17	3.61E-15
Ir-187	10.5 h	-	-	8.34E-16	1.83E-17	8.30E-16	1.23E-15	2.69E-17	1.22E-15
Ir-188	41.5 h	-	Y	4.14E-15	7.81E-17	4.48E-15	6.10E-15	1.15E-16	6.58E-15
Ir-189	13.3 d	Y	Y	1.43E-16	3.69E-18	9.83E-17	2.13E-16	5.45E-18	1.45E-16
Ir-190	12.1 d	-	Y	3.43E-15	7.43E-17	3.49E-15	5.06E-15	1.09E-16	5.13E-15
Ir-190n	3.1 h	Y	-	3.70E-15	8.03E-17	3.78E-15	5.45E-15	1.18E-16	5.55E-15
Ir-190m	1.2 h	Y	Y	4.54E-21	1.39E-21	4.58E-22	7.61E-21	2.18E-21	7.44E-22
Ir-191m	4.94 s	-	-	1.36E-16	3.36E-18	9.18E-17	2.02E-16	4.96E-18	1.35E-16
Ir-192	74.02 d	-	Y	1.96E-15	4.24E-17	1.98E-15	2.88E-15	6.24E-17	2.91E-15
Ir-192m	241. y	Y	-	3.65E-16	7.98E-18	3.14E-16	5.39E-16	1.17E-17	4.62E-16
Ir-194	19.15 h	-	Y	2.34E-16	5.76E-18	2.38E-16	3.42E-16	8.05E-18	3.50E-16
Ir-194m	171 d	-	-	5.67E-15	1.22E-16	5.89E-15	8.34E-15	1.79E-16	8.66E-15
Ir-195	2.5 h	-	Y	1.04E-16	2.88E-18	6.48E-17	1.54E-16	4.13E-18	9.55E-17
Ir-195m	3.8 h	Y	-	9.51E-16	2.12E-17	9.17E-16	1.40E-15	3.12E-17	1.35E-15
Platinum									
Pt-186	2.0 h	Y	-	1.78E-15	3.82E-17	1.87E-15	2.63E-15	5.63E-17	2.74E-15
Pt-188	10.2 d	Y	-	4.18E-16	9.77E-18	3.51E-16	6.18E-16	1.44E-17	5.16E-16
Pt-189	10.87 h	Y	-	7.21E-16	1.61E-17	6.79E-16	1.06E-15	2.38E-17	9.98E-16
Pt-191	2.8 d	-	-	6.43E-16	1.50E-17	5.70E-16	9.50E-16	2.21E-17	8.38E-16
Pt-193	50 y	-	Y	1.36E-20	4.09E-21	1.45E-21	2.30E-20	6.48E-21	2.38E-21
Pt-193m	4.33 d	Y	-	1.80E-17	4.86E-19	9.77E-18	2.68E-17	7.18E-19	1.44E-17
Pt-195m	4.02 d	-	-	1.24E-16	3.25E-18	7.34E-17	1.84E-16	4.81E-18	1.08E-16
Pt-197	18.3 h	-	Y	4.68E-17	1.15E-18	3.27E-17	6.90E-17	1.68E-18	4.82E-17
Pt-197m	94.4 m	Y	-	1.66E-16	3.90E-18	1.39E-16	2.45E-16	5.75E-18	2.04E-16
Pt-199	30.8 m	Y	-	4.93E-16	1.11E-17	5.06E-16	7.25E-16	1.61E-17	7.44E-16
Pt-200	12.5 h	Y	-	1.19E-16	2.83E-18	9.16E-17	1.75E-16	4.16E-18	1.35E-16
Gold									
Au-193	17.65 h	Y	Y	3.17E-16	7.59E-18	2.50E-16	4.69E-16	1.12E-17	3.68E-16
Au-194	39.5 h	-	Y	2.71E-15	5.34E-17	2.88E-15	3.99E-15	7.85E-17	4.22E-15
Au-195	183 d	-	Y	1.39E-16	3.71E-18	8.01E-17	2.07E-16	5.47E-18	1.18E-16
Au-195m	30.5 s	Y	-	4.57E-16	1.00E-17	4.30E-16	6.74E-16	1.48E-17	6.31E-16
Au-198	2.696 d	-	Y	9.75E-16	2.13E-17	9.96E-16	1.43E-15	3.13E-17	1.46E-15
Au-198m	2.30 d	Y	-	1.27E-15	2.84E-17	1.10E-15	1.88E-15	4.18E-17	1.62E-15
Au-199	3.139 d	-	Y	1.94E-16	4.32E-18	1.62E-16	2.86E-16	6.36E-18	2.39E-16

Table 2.3, continued

Nuclide	T _{1/2}	Mortality					Morbidity			
		Chain	P	D	Ground			Submersion	Ground	
					Submersion	Plane	Soil		Plane	Soil
				(m ³ /Bq-s)	(m ² /Bq-s)	(kg/Bq-s)	(m ³ /Bq-s)	(m ² /Bq-s)	(kg/Bq-s)	
Gold, continued										
Au-200	48.4 m	-	Y	7.05E-16	1.49E-17	7.59E-16	1.04E-15	2.15E-17	1.11E-15	
Au-200m	18.7 h	Y	-	5.07E-15	1.08E-16	5.27E-15	7.46E-15	1.59E-16	7.74E-15	
Au-201	26.4 m	-	-	1.31E-16	3.19E-18	1.33E-16	1.92E-16	4.52E-18	1.96E-16	
Mercury										
Hg-193	3.5 h	Y	Y	4.04E-16	9.58E-18	3.23E-16	5.98E-16	1.41E-17	4.75E-16	
Hg-193m	11.1 h	Y	-	2.55E-15	5.29E-17	2.65E-15	3.76E-15	7.78E-17	3.89E-15	
Hg-194	260 y	Y	Y	2.18E-20	6.30E-21	2.58E-21	3.74E-20	1.02E-20	4.32E-21	
Hg-195	9.9 h	Y	Y	4.50E-16	9.98E-18	4.28E-16	6.65E-16	1.47E-17	6.29E-16	
Hg-195m	41.6 h	Y	-	4.71E-16	1.05E-17	4.47E-16	6.95E-16	1.54E-17	6.58E-16	
Hg-197	64.1 h	-	Y	1.15E-16	3.05E-18	6.63E-17	1.72E-16	4.50E-18	9.79E-17	
Hg-197m	23.8 h	Y	-	1.88E-16	4.36E-18	1.45E-16	2.79E-16	6.43E-18	2.14E-16	
Hg-199m	42.6 m	-	-	3.98E-16	9.03E-18	3.36E-16	5.88E-16	1.33E-17	4.94E-16	
Hg-203	46.60 d	-	-	5.57E-16	1.21E-17	5.37E-16	8.22E-16	1.79E-17	7.89E-16	
Thallium										
Tl-194	33 m	Y	-	1.86E-15	4.01E-17	1.90E-15	2.73E-15	5.91E-17	2.78E-15	
Tl-194m	32.8 m	Y	-	5.62E-15	1.21E-16	5.87E-15	8.27E-15	1.77E-16	8.62E-15	
Tl-195	1.16 h	Y	Y	3.27E-15	6.33E-17	3.52E-15	4.81E-15	9.31E-17	5.16E-15	
Tl-197	2.84 h	Y	-	9.62E-16	2.05E-17	9.57E-16	1.42E-15	3.01E-17	1.41E-15	
Tl-198	5.3 h	-	Y	5.21E-15	1.00E-16	5.64E-15	7.66E-15	1.47E-16	8.28E-15	
Tl-198m	1.87 h	Y	-	2.86E-15	6.18E-17	2.94E-15	4.21E-15	9.10E-17	4.32E-15	
Tl-199	7.42 h	-	Y	5.47E-16	1.23E-17	4.99E-16	8.07E-16	1.81E-17	7.33E-16	
Tl-200	26.1 h	-	Y	3.27E-15	6.67E-17	3.46E-15	4.81E-15	9.81E-17	5.08E-15	
Tl-201	3.044 d	-	Y	1.68E-16	4.23E-18	1.09E-16	2.50E-16	6.24E-18	1.61E-16	
Tl-202	12.23 d	-	Y	1.08E-15	2.40E-17	1.07E-15	1.60E-15	3.53E-17	1.57E-15	
Tl-204	3.779 y	-	-	3.66E-18	1.64E-19	1.61E-18	4.85E-18	1.97E-19	2.36E-18	
Tl-206	4.20 m	-	Y	6.47E-18	6.82E-19	3.68E-18	7.98E-18	7.28E-19	5.18E-18	
Tl-207	4.77 m	-	Y	1.11E-17	7.10E-19	8.95E-18	1.49E-17	8.01E-19	1.30E-17	
Tl-208 ^a	3.07 m	-	Y	9.33E-15	1.62E-16	1.03E-14	1.37E-14	2.37E-16	1.51E-14	
Tl-209	2.20 m	Y	Y	5.30E-15	1.03E-16	5.74E-15	7.79E-15	1.50E-16	8.42E-15	
Lead										
Pb-195m	15.8 m	Y	-	3.88E-15	8.24E-17	4.03E-15	5.71E-15	1.21E-16	5.91E-15	
Pb-198	2.4 h	Y	-	1.00E-15	2.21E-17	9.49E-16	1.47E-15	3.25E-17	1.39E-15	
Pb-199	90 m	Y	-	3.75E-15	7.44E-17	4.00E-15	5.51E-15	1.10E-16	5.88E-15	
Pb-200	21.5 h	Y	Y	4.31E-16	9.99E-18	3.48E-16	6.37E-16	1.47E-17	5.11E-16	
Pb-201	9.4 h	Y	Y	1.82E-15	3.87E-17	1.85E-15	2.68E-15	5.69E-17	2.72E-15	
Pb-202	3E5 y	Y	Y	1.60E-20	4.88E-21	1.63E-21	2.68E-20	7.64E-21	2.65E-21	
Pb-202m	3.62 h	Y	Y	5.08E-15	1.06E-16	5.44E-15	7.48E-15	1.56E-16	7.98E-15	
Pb-203	52.05 h	-	Y	6.93E-16	1.55E-17	6.33E-16	1.02E-15	2.29E-17	9.31E-16	
Pb-205	1.43E7 y	-	Y	1.77E-20	5.37E-21	1.84E-21	2.97E-20	8.41E-21	3.00E-21	
Pb-209	3.253 h	-	Y	1.29E-18	4.21E-20	3.13E-19	1.46E-18	4.85E-20	4.60E-19	
Pb-210	22.3 y	Y	Y	2.11E-18	9.43E-20	8.06E-19	3.22E-18	1.43E-19	1.21E-18	
Pb-211	36.1 m	Y	Y	1.29E-16	3.15E-18	1.34E-16	1.89E-16	4.42E-18	1.96E-16	
Pb-212	10.64 h	Y	Y	3.31E-16	7.35E-18	2.97E-16	4.89E-16	1.08E-17	4.36E-16	
Pb-214 ^a	26.8 m	Y	Y	5.85E-16	1.28E-17	5.72E-16	8.62E-16	1.89E-17	8.41E-16	

Table 2.3, continued

Nuclide	T _{1/2}	Mortality					Morbidity		
		Chain P D	Submersion (m ³ /Bq-s)	Ground Plane		Soil (kg/Bq-s)	Submersion (m ³ /Bq-s)	Ground Plane	
				(m ² /Bq-s)	(kg/Bq-s)			(m ² /Bq-s)	(kg/Bq-s)
Bismuth									
Bi-200	36.4 m	Y -	5.87E-15	1.23E-16	6.17E-15	8.65E-15	1.82E-16	9.06E-15	
Bi-201	108 m	Y -	3.32E-15	6.90E-17	3.53E-15	4.88E-15	1.01E-16	5.18E-15	
Bi-202	1.67 h	Y -	6.79E-15	1.39E-16	7.25E-15	9.99E-15	2.05E-16	1.06E-14	
Bi-203	11.76 h	Y Y	6.20E-15	1.20E-16	6.76E-15	9.12E-15	1.76E-16	9.92E-15	
Bi-205	15.31 d	Y Y	4.39E-15	8.46E-17	4.78E-15	6.46E-15	1.24E-16	7.01E-15	
Bi-206	6.243 d	- -	8.27E-15	1.68E-16	8.87E-15	1.22E-14	2.47E-16	1.30E-14	
Bi-207	38 y	- Y	3.85E-15	7.90E-17	4.13E-15	5.67E-15	1.16E-16	6.06E-15	
Bi-210	5.012 d	Y Y	3.79E-18	3.89E-19	1.66E-18	4.52E-18	4.13E-19	2.36E-18	
Bi-210m	3.0E6 y	Y -	6.04E-16	1.31E-17	5.87E-16	8.90E-16	1.93E-17	8.62E-16	
Bi-211	2.14 m	Y Y	1.10E-16	2.41E-18	1.10E-16	1.62E-16	3.54E-18	1.61E-16	
Bi-212	60.55 m	Y Y	4.78E-16	1.01E-17	5.18E-16	7.02E-16	1.46E-17	7.60E-16	
Bi-213	45.65 m	Y Y	3.24E-16	7.38E-18	3.30E-16	4.75E-16	1.07E-17	4.84E-16	
Bi-214 ^a	19.9 m	Y Y	3.98E-15	7.65E-17	4.37E-15	5.85E-15	1.12E-16	6.41E-15	
Polonium									
Po-203	36.7 m	Y -	4.16E-15	8.36E-17	4.46E-15	6.12E-15	1.23E-16	6.55E-15	
Po-205	1.80 h	Y -	4.00E-15	8.04E-17	4.29E-15	5.88E-15	1.18E-16	6.30E-15	
Po-207	350 m	Y Y	3.33E-15	6.81E-17	3.55E-15	4.89E-15	1.00E-16	5.21E-15	
Po-210	138.38 d	- Y	2.13E-20	4.43E-22	2.30E-20	3.13E-20	6.52E-22	3.38E-20	
Po-211	0.516 s	- Y	1.95E-17	4.06E-19	2.09E-17	2.86E-17	5.98E-19	3.07E-17	
Po-212	0.305 us	- Y	0.00	0.00	0.00	0.00	0.00	0.00	
Po-213	4.2 us	Y Y	0.00	0.00	0.00	0.00	0.00	0.00	
Po-214	164.3 us	Y Y	2.09E-19	4.34E-21	2.26E-19	3.07E-19	6.39E-21	3.31E-19	
Po-215	0.001780 s	Y Y	4.24E-19	9.21E-21	4.36E-19	6.24E-19	1.36E-20	6.41E-19	
Po-216	0.15 s	Y Y	4.24E-20	8.82E-22	4.59E-20	6.24E-20	1.30E-21	6.74E-20	
Po-218	3.05 m	Y Y	2.30E-20	4.74E-22	2.48E-20	3.38E-20	6.99E-22	3.65E-20	
Astatine									
At-207	1.80 h	Y -	3.34E-15	6.71E-17	3.56E-15	4.91E-15	9.88E-17	5.23E-15	
At-211	7.214 h	Y -	7.12E-17	1.76E-18	4.61E-17	1.06E-16	2.60E-18	6.80E-17	
At-215	0.10 ms	Y Y	4.62E-19	1.00E-20	4.72E-19	6.81E-19	1.48E-20	6.93E-19	
At-216	0.30 ms	Y Y	2.78E-18	6.86E-20	1.79E-18	4.13E-18	1.01E-19	2.64E-18	
At-217	0.0323 s	Y Y	7.43E-19	1.60E-20	7.66E-19	1.09E-18	2.35E-20	1.13E-18	
At-218	2 s	Y Y	4.74E-18	1.73E-19	2.05E-18	7.14E-18	2.59E-19	3.06E-18	
Radon									
Rn-218	35 ms	Y Y	1.86E-18	3.96E-20	1.97E-18	2.73E-18	5.83E-20	2.90E-18	
Rn-219	3.96 s	Y Y	1.33E-16	2.89E-18	1.31E-16	1.96E-16	4.25E-18	1.93E-16	
Rn-220	55.6 s	Y Y	9.40E-19	2.02E-20	9.91E-19	1.38E-18	2.97E-20	1.46E-18	
Rn-222	3.8235 d	Y Y	9.67E-19	2.09E-20	1.01E-18	1.42E-18	3.08E-20	1.49E-18	
Francium									
Fr-219	21 ms	Y Y	8.29E-18	1.80E-19	8.35E-18	1.22E-17	2.66E-19	1.23E-17	
Fr-220	27.4 s	Y Y	2.32E-17	5.27E-19	1.89E-17	3.43E-17	7.77E-19	2.78E-17	
Fr-221	4.8 m	Y Y	7.08E-17	1.55E-18	6.48E-17	1.04E-16	2.28E-18	9.53E-17	
Fr-222	14.4 m	Y Y	1.03E-17	1.00E-18	6.94E-18	1.29E-17	1.08E-18	9.75E-18	
Fr-223	21.8 m	Y Y	1.06E-16	2.94E-18	8.16E-17	1.57E-16	4.23E-18	1.20E-16	

Table 2.3, continued

Nuclide	T _{1/2}	Chain		Mortality			Morbidity		
				Submersion	Ground		Submersion	Ground	
					(m ³ /Bq-s)	Plane		Soil	Plane
P	D	(m ³ /Bq-s)	(m ² /Bq-s)	(kg/Bq-s)	(m ³ /Bq-s)	(m ² /Bq-s)	(kg/Bq-s)		
Radium									
Ra-222	38.0 s	Y	Y	2.18E-17	4.73E-19	2.17E-17	3.21E-17	6.97E-19	3.18E-17
Ra-223	11.434 d	Y	Y	2.91E-16	6.55E-18	2.53E-16	4.30E-16	9.64E-18	3.72E-16
Ra-224	3.66 d	Y	Y	2.30E-17	5.00E-19	2.17E-17	3.40E-17	7.35E-19	3.19E-17
Ra-225	14.8 d	Y	Y	9.98E-18	4.84E-19	3.33E-18	1.53E-17	7.35E-19	5.06E-18
Ra-226 ^a	1600 y	Y	Y	1.51E-17	3.32E-19	1.33E-17	2.23E-17	4.89E-19	1.96E-17
Ra-227	42.2 m	Y	-	3.69E-16	8.45E-18	3.63E-16	5.43E-16	1.23E-17	5.33E-16
Ra-228	5.75 y	Y	Y	0.00	0.00	0.00	0.00	0.00	0.00
Actinium									
Ac-223	2.2 m	Y	Y	1.00E-17	2.32E-19	9.08E-18	1.48E-17	3.43E-19	1.33E-17
Ac-224	2.9 h	Y	Y	4.25E-16	9.58E-18	3.52E-16	6.28E-16	1.41E-17	5.19E-16
Ac-225	10.0 d	Y	Y	3.35E-17	7.82E-19	2.62E-17	4.96E-17	1.16E-18	3.85E-17
Ac-226	29 h	Y	Y	2.92E-16	6.57E-18	2.60E-16	4.30E-16	9.59E-18	3.82E-16
Ac-227	21.773 y	Y	Y	2.67E-19	6.91E-21	2.02E-19	3.96E-19	1.04E-20	2.98E-19
Ac-228 ^a	6.13 h	Y	Y	2.45E-15	4.99E-17	2.64E-15	3.61E-15	7.33E-17	3.88E-15
Thorium									
Th-226	30.9 m	Y	Y	1.69E-17	3.86E-19	1.38E-17	2.50E-17	5.70E-19	2.02E-17
Th-227	18.718 d	Y	Y	2.37E-16	5.30E-18	2.20E-16	3.50E-16	7.81E-18	3.24E-16
Th-228	1.9131 y	Y	Y	4.24E-18	1.07E-19	3.25E-18	6.29E-18	1.60E-19	4.79E-18
Th-229	7340 y	Y	Y	1.76E-16	4.17E-18	1.31E-16	2.61E-16	6.16E-18	1.93E-16
Th-230	7.7E4 y	Y	Y	7.46E-19	2.69E-20	4.74E-19	1.12E-18	4.17E-20	7.01E-19
Th-231	25.52 h	Y	Y	2.25E-17	7.05E-19	1.42E-17	3.36E-17	1.08E-18	2.10E-17
Th-232 ^a	1.41E10 y	Y	Y	3.51E-19	1.73E-20	1.97E-19	5.35E-19	2.74E-20	2.93E-19
Th-234	24.10 d	Y	Y	1.50E-17	3.86E-19	9.52E-18	2.23E-17	5.74E-19	1.40E-17
Protactinium									
Pa-227	38.3 m	Y	-	3.82E-17	9.50E-19	2.54E-17	5.67E-17	1.41E-18	3.74E-17
Pa-228	22 h	Y	-	2.82E-15	5.75E-17	2.98E-15	4.15E-15	8.47E-17	4.37E-15
Pa-230	17.4 d	Y	-	1.59E-15	3.31E-17	1.67E-15	2.34E-15	4.88E-17	2.45E-15
Pa-231	3.276E4 y	Y	Y	8.41E-17	1.96E-18	8.09E-17	1.24E-16	2.92E-18	1.19E-16
Pa-232	1.31 d	Y	-	2.33E-15	4.82E-17	2.50E-15	3.43E-15	7.10E-17	3.67E-15
Pa-233	27.0 d	Y	Y	4.58E-16	1.01E-17	4.32E-16	6.75E-16	1.49E-17	6.36E-16
Pa-234	6.70 h	Y	Y	4.77E-15	9.81E-17	5.08E-15	7.02E-15	1.44E-16	7.46E-15
Pa-234m	1.17 m	Y	Y	4.17E-17	1.73E-18	4.04E-17	5.88E-17	2.11E-18	5.88E-17
Uranium									
U-230	20.8 d	Y	Y	2.36E-18	7.04E-20	1.78E-18	3.51E-18	1.08E-19	2.63E-18
U-231	4.2 d	Y	Y	1.33E-16	3.29E-18	9.32E-17	1.98E-16	4.89E-18	1.37E-16
U-232	72 y	Y	Y	5.66E-19	2.97E-20	3.45E-19	8.67E-19	4.78E-20	5.12E-19
U-233	1.585E5 y	Y	Y	7.24E-19	2.51E-20	5.70E-19	1.09E-18	3.91E-20	8.41E-19
U-234 ^a	2.445E5 y	Y	Y	2.79E-19	2.01E-20	1.44E-19	4.37E-19	3.29E-20	2.16E-19
U-235	703.8E6 y	Y	Y	3.45E-16	7.60E-18	3.02E-16	5.09E-16	1.12E-17	4.44E-16
U-236	2.3415E7 y	Y	Y	1.66E-19	1.65E-20	7.03E-20	2.67E-19	2.73E-20	1.07E-19
U-237	6.75 d	Y	Y	2.77E-16	6.54E-18	2.19E-16	4.11E-16	9.67E-18	3.22E-16
U-238	4.468E9 y	Y	Y	9.95E-20	1.34E-20	2.70E-20	1.66E-19	2.25E-20	4.27E-20
U-239	23.54 m	Y	-	1.01E-16	2.83E-18	7.05E-17	1.48E-16	4.01E-18	1.04E-16
U-240	14.1 h	Y	Y	1.53E-18	1.10E-19	4.07E-19	2.29E-18	1.81E-19	6.28E-19

Table 2.3, continued

Nuclide	T _{1/2}	Mortality					Morbidity		
		Chain P D		Ground			Ground		
				Submersion (m ³ /Bq-s)	Plane (m ² /Bq-s)	Soil (kg/Bq-s)	Submersion (m ³ /Bq-s)	Plane (m ² /Bq-s)	Soil (kg/Bq-s)
Neptunium									
Np-232	14.7 m	Y	-	2.93E-15	6.14E-17	3.07E-15	4.32E-15	9.05E-17	4.50E-15
Np-233	36.2 m	Y	Y	1.78E-16	4.14E-18	1.33E-16	2.63E-16	6.11E-18	1.96E-16
Np-234	4.4 d	Y	Y	3.77E-15	7.17E-17	4.12E-15	5.54E-15	1.05E-16	6.05E-15
Np-235	396.1 d	Y	Y	2.01E-18	1.04E-19	1.22E-18	3.09E-18	1.69E-19	1.82E-18
Np-236a	115E3 y	Y	-	2.48E-16	5.81E-18	1.89E-16	3.67E-16	8.62E-18	2.78E-16
Np-236b	22.5 h	Y	Y	9.99E-17	2.31E-18	7.81E-17	1.48E-16	3.41E-18	1.15E-16
Np-237	2.14E6 y	Y	Y	4.56E-17	1.24E-18	3.11E-17	6.79E-17	1.86E-18	4.59E-17
Np-238	2.117 d	Y	Y	1.40E-15	2.84E-17	1.52E-15	2.06E-15	4.18E-17	2.24E-15
Np-239	2.355 d	Y	Y	3.67E-16	8.24E-18	3.15E-16	5.42E-16	1.22E-17	4.63E-16
Np-240	65 m	Y	-	3.20E-15	6.71E-17	3.38E-15	4.72E-15	9.88E-17	4.97E-15
Np-240m	7.4 m	Y	Y	8.28E-16	1.80E-17	8.82E-16	1.22E-15	2.62E-17	1.29E-15
Plutonium									
Pu-234	8.8 h	Y	Y	1.30E-16	3.05E-18	9.39E-17	1.93E-16	4.51E-18	1.38E-16
Pu-235	25.3 m	Y	-	1.81E-16	4.23E-18	1.38E-16	2.69E-16	6.25E-18	2.03E-16
Pu-236	2.851 y	Y	Y	1.87E-19	2.33E-20	6.56E-20	3.13E-19	3.92E-20	1.02E-19
Pu-237	45.3 d	Y	Y	9.19E-17	2.21E-18	6.54E-17	1.36E-16	3.28E-18	9.63E-17
Pu-238	87.74 y	Y	Y	1.34E-19	1.95E-20	3.88E-20	2.28E-19	3.30E-20	6.18E-20
Pu-239 ^a	24065 y	Y	Y	1.65E-19	9.99E-21	1.15E-19	2.56E-19	1.63E-20	1.71E-19
Pu-240	6537 y	Y	Y	1.31E-19	1.88E-20	3.76E-20	2.24E-19	3.17E-20	5.98E-20
Pu-241	14.4 y	Y	Y	3.29E-21	8.44E-23	2.39E-21	4.89E-21	1.27E-22	3.52E-21
Pu-242	3.763E5 y	Y	Y	1.12E-19	1.57E-20	3.38E-20	1.91E-19	2.64E-20	5.35E-20
Pu-243	4.956 h	Y	Y	4.70E-17	1.16E-18	3.20E-17	6.95E-17	1.71E-18	4.71E-17
Pu-245	10.5 h	Y	-	1.00E-15	2.15E-17	1.03E-15	1.48E-15	3.15E-17	1.52E-15
Pu-246	10.85 d	Y	Y	2.83E-16	6.56E-18	2.35E-16	4.18E-16	9.69E-18	3.46E-16
Americium									
Am-237	73.0 m	Y	-	8.34E-16	1.83E-17	7.87E-16	1.23E-15	2.70E-17	1.16E-15
Am-238	98 m	Y	Y	2.21E-15	4.51E-17	2.34E-15	3.25E-15	6.65E-17	3.44E-15
Am-239	11.9 h	Y	-	4.89E-16	1.11E-17	4.03E-16	7.23E-16	1.64E-17	5.92E-16
Am-240	50.8 h	Y	-	2.55E-15	5.23E-17	2.74E-15	3.76E-15	7.70E-17	4.02E-15
Am-241	432.2 y	Y	Y	3.33E-17	1.11E-18	1.59E-17	5.00E-17	1.68E-18	2.36E-17
Am-242	16.02 h	Y	Y	2.86E-17	7.23E-19	2.02E-17	4.22E-17	1.07E-18	2.98E-17
Am-242m	152 y	Y	-	1.12E-18	7.80E-20	5.97E-19	1.77E-18	1.28E-19	8.96E-19
Am-243	7380 y	Y	Y	9.45E-17	2.51E-18	5.49E-17	1.41E-16	3.71E-18	8.11E-17
Am-244	10.1 h	Y	-	1.96E-15	4.12E-17	2.09E-15	2.89E-15	6.07E-17	3.07E-15
Am-244m	26 m	Y	-	5.81E-18	6.32E-19	3.09E-18	7.16E-18	6.85E-19	4.36E-18
Am-245	2.05 h	Y	Y	7.12E-17	1.69E-18	6.07E-17	1.05E-16	2.43E-18	8.92E-17
Am-246	39 m	Y	-	1.65E-15	3.56E-17	1.71E-15	2.43E-15	5.23E-17	2.51E-15
Am-246m	25.0 m	Y	Y	2.59E-15	5.26E-17	2.82E-15	3.81E-15	7.72E-17	4.14E-15
Curium									
Cm-238	2.4 h	Y	-	1.50E-16	3.47E-18	1.10E-16	2.22E-16	5.13E-18	1.63E-16
Cm-240	27 d	Y	Y	1.51E-19	2.40E-20	3.17E-20	2.64E-19	4.06E-20	5.30E-20
Cm-241	32.8 d	Y	-	1.14E-15	2.51E-17	1.13E-15	1.68E-15	3.71E-17	1.66E-15
Cm-242	162.8 d	Y	Y	1.50E-19	2.20E-20	4.10E-20	2.59E-19	3.71E-20	6.62E-20

Table 2.3, continued

Nuclide	T _{1/2}	Chain		Mortality			Morbidity		
				Submersion	Ground		Submersion	Ground	
					(m ³ /Bq-s)	Plane		Soil	Plane
P	D	(m ³ /Bq-s)	(m ² /Bq-s)	(kg/Bq-s)	(m ³ /Bq-s)	(m ² /Bq-s)	(kg/Bq-s)		
Curium, continued									
Cm-243	28.5 y	Y	-	2.81E-16	6.31E-18	2.44E-16	4.16E-16	9.31E-18	3.59E-16
Cm-244	18.11 y	Y	Y	1.22E-19	2.00E-20	2.46E-20	2.15E-19	3.39E-20	4.15E-20
Cm-245	8500 y	Y	Y	1.83E-16	4.25E-18	1.39E-16	2.71E-16	6.29E-18	2.04E-16
Cm-246	4730 y	Y	Y	1.12E-19	1.79E-20	2.33E-20	1.97E-19	3.03E-20	3.91E-20
Cm-247	1.56E7 y	Y	Y	7.50E-16	1.63E-17	7.62E-16	1.11E-15	2.41E-17	1.12E-15
Cm-249	64.15 m	Y	Y	4.88E-17	1.16E-18	4.96E-17	7.11E-17	1.65E-18	7.29E-17
Berkelium									
Bk-245	4.94 d	Y	-	4.92E-16	1.11E-17	4.12E-16	7.26E-16	1.63E-17	6.07E-16
Bk-246	1.83 d	Y	-	2.34E-15	4.85E-17	2.48E-15	3.44E-15	7.14E-17	3.64E-15
Bk-247	1380 y	Y	Y	2.22E-16	5.06E-18	1.80E-16	3.28E-16	7.47E-18	2.65E-16
Bk-249	320 d	Y	Y	6.89E-21	2.13E-22	1.49E-21	8.48E-21	3.35E-22	2.25E-21
Bk-250	3.222 h	Y	Y	2.26E-15	4.57E-17	2.46E-15	3.32E-15	6.71E-17	3.62E-15
Californium									
Cf-244	19.4 m	Y	-	1.69E-19	2.58E-20	3.45E-20	2.98E-19	4.36E-20	5.85E-20
Cf-246	35.7 h	Y	-	1.51E-19	1.84E-20	5.03E-20	2.56E-19	3.09E-20	7.92E-20
Cf-248	333.5 d	Y	Y	1.16E-19	1.76E-20	2.39E-20	2.04E-19	2.97E-20	4.05E-20
Cf-249	350.6 y	Y	Y	7.87E-16	1.72E-17	7.93E-16	1.16E-15	2.53E-17	1.17E-15
Cf-250	13.08 y	Y	Y	1.11E-19	1.67E-20	2.27E-20	1.94E-19	2.83E-20	3.84E-20
Cf-251	898 y	Y	Y	2.64E-16	6.00E-18	2.19E-16	3.90E-16	8.87E-18	3.22E-16
Cf-253	17.81 d	Y	Y	2.07E-19	2.21E-21	2.79E-20	2.29E-19	3.42E-21	4.16E-20
Einsteinium									
Es-250	2.1 h	Y	-	9.58E-16	1.99E-17	9.87E-16	1.41E-15	2.92E-17	1.45E-15
Es-251	33 h	Y	-	1.92E-16	4.43E-18	1.48E-16	2.84E-16	6.55E-18	2.18E-16
Es-253	20.47 d	Y	Y	8.20E-19	2.80E-20	7.28E-19	1.23E-18	4.37E-20	1.07E-18
Es-254	275.7 d	Y	Y	7.53E-18	3.72E-19	4.92E-18	1.16E-17	5.95E-19	7.32E-18
Es-254m	39.3 h	Y	-	1.15E-15	2.45E-17	1.22E-15	1.69E-15	3.60E-17	1.80E-15
Fermium									
Fm-252	22.7 h	Y	-	1.24E-19	1.74E-20	2.59E-20	2.16E-19	2.92E-20	4.36E-20
Fm-253	3.00 d	Y	-	1.65E-16	3.78E-18	1.31E-16	2.44E-16	5.59E-18	1.92E-16
Fm-254	3.240 h	Y	Y	1.88E-19	1.97E-20	6.72E-20	3.14E-19	3.29E-20	1.05E-19
Fm-255	20.07 h	Y	-	4.11E-18	2.31E-19	2.21E-18	6.36E-18	3.72E-19	3.30E-18
Fm-257	100.5 d	Y	Y	2.19E-16	5.02E-18	1.78E-16	3.24E-16	7.43E-18	2.62E-16
Mendelevium									
Md-257	5.2 h	Y	-	2.41E-16	5.42E-18	2.11E-16	3.56E-16	8.01E-18	3.10E-16
Md-258	55 d	Y	-	1.70E-18	1.18E-19	7.36E-19	2.69E-18	1.92E-19	1.12E-18

^aThe uncertainty in the risk coefficient for this radionuclide in soil is addressed in Table 2.4.

Table 2.4. Uncertainty categories for selected risk coefficients.

Explanation of entries

This table gives subjective judgments concerning the precision with which risk coefficients for selected radionuclides are determined by current information on the biological behavior of radionuclides in the human body, conversion from internally or externally distributed radioactivity to absorbed doses to tissues, and extrapolation from tissue dose to cancer risk. These judgments were made by the authors of this report and were based on the results of a sensitivity analysis in which various combinations of substantially different but equally plausible biokinetic and dosimetric models and radiation risk model coefficients were used to generate alternative risk coefficients. The analysis did not include consideration of uncertainties associated with the use of a linear, no-threshold model for estimating radiogenic cancer at low doses, absorbed dose as a measure of radiogenic cancer risk, or idealized representations of the population and exposure.

Judgments are given in terms of relatively broad, semi-quantitative “uncertainty categories” identified by letters A-E, with Category A representing the most narrowly determined risk coefficients, Category E representing the least well characterized coefficients, and Categories B, C, and D representing intermediate, declining levels of uncertainty. The uncertainty in a risk coefficient was first characterized in terms of reasonable lower and upper bounds, X and Y, as judged from the results of the sensitivity analysis. The values X and Y were then used to assign the risk coefficient to one of the five categories A-E as indicated by the following table:

Uncertainty category	Definition ^a
A	$Y/X < 15$
B	$Y/X \sim 25$
C	$Y/X \sim 50$
D	$Y/X \sim 100$
E	$Y/X > 150$

^aA derived value Y/X in the range 15-35, 35-65, or 65-150 was considered to be approximately 25, 50, or 100, respectively.

Category A is intended to represent those cases in which the risk coefficient is “established” within a factor of 4, in the sense that application of any reasonable alternative biokinetic and dosimetric models, risk model coefficients (based on a linear, no-threshold model), dose and dose rate effectiveness factor (DDREF), and relative radiobiological effectiveness (RBE) for alpha particles would be expected to change the risk coefficient by less than a factor of 4. Categories B, C, and D are intended to represent cases in which the risk coefficient is established within a factor of roughly 5, 7, and 10, respectively. Category E is intended to represent cases in which the risk coefficient could change by more than a factor of 10 if plausible alternative models were used in the derivation. The factors 4, 5, 7, and 10 indicated above are rounded square roots of the values 15, 25, 50, and 100 shown in the second column of the table. The interpretation is that all values in the interval from X to Y are within a factor of roughly $(Y/X)^{1/2}$ of the risk coefficient, provided the risk coefficient is near the geometric mean of X and Y. Although a risk coefficient is not always centrally located in its assigned uncertainty interval, either as a geometric mean or an arithmetic mean, this provides a convenient, concise, uniform way of summarizing the authors’ subjective judgments.

For purposes of the sensitivity analysis, it was necessary to make general assumptions concerning the type of information that may be available for assessment of a given exposure. For consideration of risk coefficients for ingestion, it was assumed that the radionuclide is known to be incorporated in food. For consideration of risk coefficients for inhalation of particulates, it was assumed that the particle size is known to be approximately 1 μm (AMAD) and that the absorption type indicated in the table is known in the sense that there is sufficient general information on the form of the inhaled radionuclide to establish with reasonable confidence that this is the most nearly accurate absorption type (see Appendix D). For example, it may be known that the radionuclide is in a readily soluble form indicative of “Type F” material or a highly insoluble form indicative of “Type S” material. It was considered in the analysis, however, that a given absorption type is intended to represent a relatively wide range of absorption rates (ICRP, 1995b) and that the actual absorption rate could be substantially different from the baseline parameter values specified by the ICRP for that absorption type. For consideration of inhaled gases or vapors, it was assumed that deposition is complete and that absorption to blood is rapid and complete.

The last column of Table 2.4 summarizes the authors’ conclusions regarding the relative contributions of various sources to the uncertainty in the risk coefficient. In this column, the term “Biokinetics” refers to the biological behavior of the parent radionuclide and any radioactive progeny in the human body after acute deposition in the stomach or respiratory tract; “Dosimetry” refers to conversion of activity distributed in the human body or the environment (in the case of external

exposure) to absorbed dose to tissues; “Deposition” refers to fractional deposition of inhaled material in the respiratory tract; and “Risk model” refers to the risk model as described in Chapter 7, including the risk model coefficients (RMCs), DDREF for low-LET radiation, and RBE for high-LET radiation. The absence of one of the four main sources (Biokinetics, Dosimetry, Deposition, or Risk model) indicates that the source was judged to be only a minor contributor to the uncertainty in the risk coefficient, or was not applicable to the given coefficient (such as Deposition for an ingested radionuclide or Biokinetics for external exposure). Although some of the sources of uncertainty addressed here are assumed to be independent of the radionuclide (e.g., fractional deposition in the respiratory tract), the relative contributions of these sources to the total uncertainty may change from one radionuclide to another due to differences in radionuclide-dependent uncertainties such as biokinetic or dosimetric estimates.

In the last column of the table, the notation “S1 ~ S2” for sources of uncertainty S1 and S2 (for example, “Risk model ~ Biokinetics”) indicates that S1 and S2 contribute comparably to the total uncertainty, and “S1 > S2” indicates that S1 is a more important contributor than S2. “Dominant sites” refers to a small number of cancer sites that dominate the projected cancer risk as well as the uncertainty in that projection for the given radionuclide and exposure mode. The notation “C1 >> C2” for dominant cancer sites C1 and C2 indicates that C1 is projected to be a considerably more important cancer site than C2 under most plausible alternative models. The abbreviations RW, MW, and NW in parentheses following an organ indicate that the risk model coefficient for that organ is judged to be reasonably well established, moderately well established, or not well established, respectively.

Table 2.4. Uncertainty categories for selected risk coefficients.

Case	Category	Main sources of uncertainty and comments
Inhalation^a:		
H-3 (HTO vapor)	A	Risk model > Biokinetics. Rapid and nearly complete absorption expected. Absorbed tritium known to be fairly uniformly distributed. Systemic biokinetics well understood except for long-term component that contributes little to dose. Projected cancer risk distributed over several tissues with risk model coefficients (RMCs) having varying degrees of uncertainty.
Co-60, Type M	C	Biokinetics ~ Risk model > Deposition. Dominant sites are lung (MW) >> colon (MW). Lung dose varies considerably as absorption rate varies within the range associated with Type M. Typical GI uptake moderately well established. Whole-body retention of absorbed cobalt reasonably well known but distribution less well characterized.
Sr-90, Type M	D	Biokinetics ~ Risk model > Deposition. Dominant sites are lung (MW) >> leukemia (RW). Lung dose varies widely as absorption rate varies within the range associated with Type M. GI uptake and skeletal biokinetics reasonably well characterized. Potential migration of ⁹⁰ Y introduces some uncertainty.
Ru-106, Type M	D	Biokinetics ~ Risk model > Deposition. Dominant sites are lung (MW) >> colon (MW). Lung dose varies considerably as absorption rate varies within the range associated with Type M. GI uptake and systemic biokinetics understood only broadly, but risk estimate relatively insensitive to associated uncertainties.
Sb-125, Type M	D	Biokinetics ~ Risk model > Deposition. Dominant sites are lung (MW) >> colon (MW). Lung dose varies considerably as absorption rate varies within the range associated with Type M. GI uptake and systemic biokinetics not well established, but risk estimate relatively insensitive to associated uncertainties.
I-131 (Vapor)	C	Risk model > Biokinetics. Rapid and nearly complete absorption expected. Dominant site is thyroid (NW). Typical thyroidal uptake and half-time cannot be closely determined due to scatter in reported data. Risk estimate insensitive to half-time in thyroid but sensitive to fractional uptake by thyroid.
Cs-137, Type F	B	Risk model ~ Biokinetics > Deposition. Data indicate high absorption and fairly uniform distribution of absorbed cesium. Systemic biokinetics of cesium well established by data for man, but potentially rapid migration of ^{137m} Ba from ¹³⁷ Cs yields moderate uncertainty in dose to some tissues. No dominant cancer sites.
Ra-226, Type M	E	Risk model > Biokinetics > Deposition. Dominant site is lung (MW). GI uptake and systemic biokinetics of radium reasonably well understood. Risk estimate moderately sensitive to uncertainties in behavior of chain members produced in the body.

Table 2.4, continued

Case	Category	Main sources of uncertainty and comments
Inhalation, continued		
Th-232, Type S	D	Risk model > Biokinetics > Deposition. Dominant site is lung (MW). Lung dose sensitive to uncertainty in risk apportionment factors for lung regions. Lung dose varies moderately as absorption rate varies within the range associated with Type S. Risk estimate insensitive to uncertainties in biokinetics, dose, RMCs for systemic tissues.
U-234, Type M	D	Risk model > Biokinetics > Deposition. Dominant site is lung (MW). Lung dose varies widely as absorption rate varies within the range associated with Type M. Risk estimate not highly sensitive to uncertainties in biokinetics, dose, RMCs for systemic tissues.
Pu-239, Type M	C	Risk model > Deposition > Biokinetics. Dominant sites are lung (MW) ~ liver (NW) > bone (NW). Lung dose varies widely as absorption rate varies within the range associated with Type M. Initial distribution between liver and skeleton is uncertain but has little effect on risk estimate. Long-term systemic distribution and retention reasonably well established. Residence time on bone surfaces known within broad bounds.
Ingestion:		
H-3 (HTO)	A	Risk model > Biokinetics > Dosimetry. Known that GI uptake is virtually complete and absorbed activity is fairly uniformly distributed. Systemic biokinetics well understood except for long-term component that contributes little to dose. Dosimetry for colon as target and colon contents as source not well established. No dominant cancer sites.
Co-60	B	Biokinetics ~ Risk model. Dominant site is colon (MW) due to dose from unabsorbed activity. Typical GI uptake moderately well established. Whole-body retention reasonably well known but distribution less well characterized. Biokinetics of ingested environmental forms may differ from forms used in biokinetic studies.
Sr-90	B	Biokinetics ~ Risk model. Dominant sites are leukemia (RW) >> colon (MW). GI uptake and skeletal biokinetics reasonably well characterized. Some information available on migration of ⁹⁰ Y from ⁹⁰ Sr; risk estimate for leukemia relatively insensitive to remaining uncertainties concerning ⁹⁰ Y.
Ru-106	B	Risk model > Biokinetics. Dominant site is colon (MW) due to dose from unabsorbed activity. GI uptake and systemic biokinetics of ¹⁰⁶ Ru- ¹⁰⁶ Rh known only broadly, but risk estimate relatively insensitive to associated uncertainties.

Table 2.4, continued

Case	Category	Main sources of uncertainty and comments
Ingestion, continued		
Sb-125	B	Risk model > Dosimetry > Biokinetics. Dominant sites are colon (MW) >> leukemia (RW). Dosimetry for colon as target and colon contents as source not well established. GI uptake and systemic biokinetics poorly established, but risk estimate relatively insensitive to associated uncertainties.
I-131	C	Risk model > Biokinetics. Dominant site is thyroid (NW). Typical thyroidal uptake and half-time cannot be closely determined due to scatter in reported data. Risk estimate insensitive to half-time in thyroid but sensitive to fractional uptake by thyroid.
Cs-137	A	Risk model > Biokinetics. Known that GI uptake virtually complete and absorbed cesium fairly uniformly distributed. Systemic biokinetics of cesium well established, but potentially rapid migration of ^{137m} Ba from ¹³⁷ Cs yields moderate uncertainty in dose to some tissues. No dominant cancer sites.
Ra-226	C	Risk model > Biokinetics > Dosimetry. Dominant sites are bone (NW) ~ colon (MW). GI uptake and systemic biokinetics of radium reasonably well understood. Risk estimate moderately sensitive to uncertainties regarding migration of chain members from parent. Dosimetry for colon as target and colon contents as source not well established for this chain.
Th-232	E	Risk model > Biokinetics > Dosimetry. Dominant sites are bone (NW) ~ colon (MW) > liver (NW). Typical GI uptake apparently low but not known with much precision. Systemic biokinetics of parent reasonably well understood but dose arises mainly from ingrowing chain members, whose behavior is only broadly understood. Dosimetry for colon as target and colon contents as source not well established for this chain.
U-234	C	Risk model > Biokinetics ~ Dosimetry. Dominant sites are colon (MW) > kidney (NW). GI uptake moderately well established. Short-term systemic biokinetics understood but less known about long-term retention in skeleton and soft tissues. Dosimetry for colon as target and colon contents as source not well established.
Pu-239	E	Risk model > Biokinetics ~ Dosimetry. Dominant sites are liver (NW) > colon (MW) ~ bone (NW). Typical GI uptake known to be low but not determined with much precision. Initial distribution between liver and skeleton uncertain but has little effect on risk estimate. Long-term distribution reasonably well established. Residence time on bone surfaces known only within broad bounds. Dosimetry for colon as target and colon contents as source not well established.

Table 2.4, continued

Case	Category	Main sources of uncertainty and comments
External exposure (Soil)^b		
H-3	N/A ^c	
Co-60	A	Risk model > Dosimetry. Beta emitter – $E_{\beta}^{\max} = 1.55$ MeV, mean photon energy 1.25 MeV – kerma constant ^d = $8.50E-17$ Gy m ² (Bq-s) ⁻¹ . All tissues receive similar absorbed doses. No dominant sites.
Sr-90	E	Dosimetry > Risk model. Beta emitter – $E_{\beta}^{\max} = 0.546$ MeV, tissue absorbed dose excluding skin ranges over a factor of 6. No dominant sites. Uncertainty in bremsstrahlung yield and in transport of, and dose from, low energy photons.
(Y-90)	E	Dosimetry > Risk model. No dominant sites. Beta emitter – $E_{\beta}^{\max} = 2.28$ MeV, tissue absorbed dose (excluding skin) range over a factor of 3. Uncertainty in bremsstrahlung yield and in transport of, and dose from, low energy photons.
Ru-106 ^e	N/A ^c	
(Rh-106)	B	Risk model ~ Dosimetry. Beta emitter – $E_{\beta}^{\max} = 3.54$ MeV, mean photon energy 0.60 MeV – kerma constant = $7.62E-18$ Gy m ² (Bq-s) ⁻¹ . All tissues except skin receive similar absorbed doses. No dominant sites. Uncertainty in transport of, and dose from, low energy photons.
Sb-125	A	Risk model > Dosimetry. Beta emitter – $E_{\beta}^{\max} = 0.622$ MeV, mean photon energy 0.46 MeV – kerma constant = $1.89E-17$ Gy m ² (Bq-s) ⁻¹ . All tissues receive similar absorbed doses. No dominant sites.
I-131	A	Risk model > Dosimetry. Beta emitter – $E_{\beta}^{\max} = 0.807$ MeV, mean photon energy 0.38 MeV – kerma constant = $1.45E-17$ Gy m ² (Bq-s) ⁻¹ . All tissues receive similar absorbed doses. No dominant sites.
Cs-137 ^e	E	Dosimetry > Risk model. No dominant sites. Beta emitter – $E_{\beta}^{\max} = 1.17$ MeV, tissue absorbed doses excluding skin range over a factor of 4. Uncertainty in bremsstrahlung yield and in transport of, and dose from, low energy photons.
(Ba-137m)	A	Risk model > Dosimetry. Isomeric transition, mean photon energy 0.66 MeV – kerma constant = $2.26E-17$ Gy m ² (Bq-s) ⁻¹ . All tissues receive similar absorbed doses. No dominant sites.
Ra-226 ^e	C	Dosimetry ~ Risk model. Alpha emitter, mean photon energy 0.18 MeV – kerma constant = $4.65E-19$ Gy m ² (Bq-s) ⁻¹ . Tissue absorbed doses range over a factor of 3. No dominant sites. Uncertainty in transport of, and dose from, low energy photons.
(Pb-214)	A	Risk model > Dosimetry. Beta emitter – $E_{\beta}^{\max} = 1.02$ MeV, mean photon energy 0.33 MeV – kerma constant = $1.42E-17$ Gy m ² (Bq-s) ⁻¹ . All tissues receive similar absorbed doses. No dominant sites.

Table 2.4, continued

Case	Category	Main sources of uncertainty and comments
External exposure, continued		
(Bi-214)	A	Risk model > Dosimetry. Beta emitter – $E_{\beta}^{\max} = 3.27$ MeV, mean photon energy 1.12 MeV – kerma constant = $5.07E-17$ Gy m ² (Bq-s) ⁻¹ . All tissues receive similar absorbed doses. No dominant sites.
Th-232 ^e	D	Dosimetry > Risk model. Alpha emitter, mean photon energy 0.07 keV – kerma constant = $2.24E-18$ Gy m ² (Bq-s) ⁻¹ . Tissue absorbed doses range over a factor of 3. No dominant sites. Uncertainty in transport of, and dose from, low energy photons.
(Ac-228)	A	Risk model > Dosimetry. Beta emitter – $E_{\beta}^{\max} = 2.08$ MeV, mean photon energy 0.77 MeV – kerma constant = $4.46E-17$ Gy m ² (Bq-s) ⁻¹ . All tissues receive similar absorbed doses. No dominant sites.
(Tl-208)	A	Risk model > Dosimetry. Beta emitter – $E_{\beta}^{\max} = 1.79$ MeV, mean photon energy 1.46 MeV – kerma constant = $1.03E-16$ Gy m ² (Bq-s) ⁻¹ . All tissues receive similar absorbed doses. No dominant sites.
U-234	D	Dosimetry > Risk model. No dominant sites. Alpha emitter, mean photon energy 0.08 MeV – kerma constant = $2.63E-18$ Gy m ² (Bq-s) ⁻¹ . Tissue absorbed doses range over a factor > 10. Uncertainty in transport of, and dose from, low energy photons.
Pu-239	E	Dosimetry > Risk model. No dominant sites. Alpha emitter, mean photon energy 0.016 MeV – kerma constant = $9.37E-19$ Gy m ² (Bq-s) ⁻¹ . Tissue absorbed doses range over a factor > 10. Uncertainty in transport of, and dose from, low energy photons.

^aThe absorption type addressed for a given radionuclide in particulate form is the default type recommended in ICRP Publication 72 (1996).

^bFor external exposure, the radionuclides in parentheses following the parent radionuclide Sr-90, Ru-106, Cs-137, Ra-226, or Th-232 are the most important radioactive progeny of that parent radionuclide present in the environment at secular equilibrium.

^cCategories A-E are based on quotients of maximum and minimum plausible values and are not applicable (N/A) to radionuclides for which estimated external dose (EPA, 1993) is zero.

^dShort for air kerma-rate constant (see Glossary).

^eIn most situations, the cancer risk from external exposure to this radionuclide is likely to be negligible compared with the risk from external exposure to its radioactive progeny.

CHAPTER 3. EXPOSURE SCENARIOS

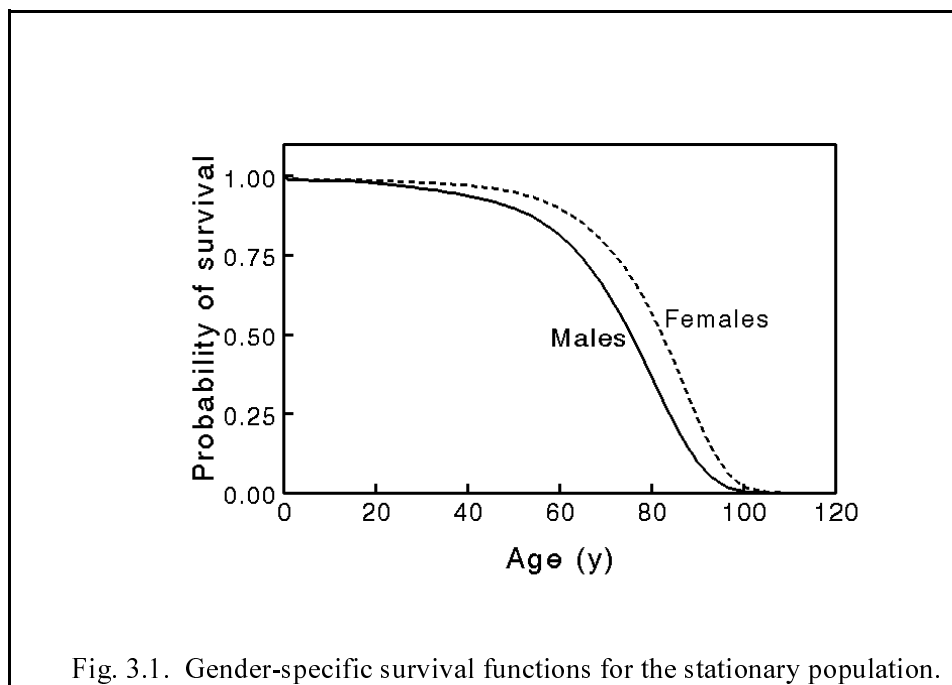
The risk coefficients developed in this report are gender-averaged values based on biokinetic, dosimetric, and radiation risk models that represent typical or “reference” male and female members of the U.S. population, from infancy through old age. Although the coefficients may be interpreted in terms of either acute or chronic exposure, computations are based on the assumption that these persons are exposed throughout life, beginning at birth, to a constant concentration of a radionuclide in a given environmental medium. *In utero* exposures are not considered in this document.

Characteristics of the exposed population

The physical characteristics of the reference male and reference female at different ages are described in reports by Cristy and Eckerman (1987, 1993). The vital statistics for these reference persons are based on the 1989-91 U.S. decennial life table (NCHS, 1997) and U.S. cancer mortality data for the same period (NCHS, 1992, 1993a, 1993b). That is, it is assumed that the exposed male and female are subject to the risk of dying from a competing cause (any cause other than a cancer produced by the radiation exposure hypothesized here) indicated by the 1989-91 U.S. decennial life table and are subject to the risk of experiencing or dying from cancer at a specific site indicated by U.S. cancer mortality data for the same period. Gender-specific survival functions (fractions of live-born individuals surviving to different ages) for the stationary population are shown in Fig. 3.1. Methods of extending or smoothing the U.S. vital statistics for use in this report are described in Appendix A.

Growth of decay chain members

For each of the internal exposure scenarios, the risk coefficient for a radionuclide includes the contribution to dose from production of decay chain members in the body after intake of the parent radionuclide. However, for either an internal or external exposure scenario, the risk coefficient for a given radionuclide is based on the assumption that this is the only radionuclide present in the environmental medium. Growth of chain members in the environment is not considered because this would require the assumption of a temporal pattern of contamination and environmental behavior of decay chain members and thus would limit the applicability of the risk coefficients. For each radionuclide addressed in this report, however, a separate risk coefficient is



provided for any subsequent chain member that is of potential dosimetric significance. This enables the user to assess the risks from ingrowth of radionuclides in the environment.

Inhalation of radionuclides

Risk coefficients (Bq^{-1}) for inhalation of radionuclides in air are expressed as risk of cancer mortality or morbidity per unit activity intake. The age- and gender-specific inhalation rates used in this report (Table 3.1, Fig. 3.2) are taken from ICRP Publication 66 (1994a). These inhalation rates are based on breathing rates measured during periods of rest, light activity, or heavy activity. The average 24-h ventilation rate is estimated as a time-weighted average of ventilation rates for rest periods and periods of light and heavy activity.

Recently, Layton (1993) proposed a different approach for the estimation of average inhalation rates at different ages. Estimates are based on typical oxygen consumption associated with energy expenditure and are derived using the equation $V_E = E \times H \times VQ$, where V_E is the ventilation rate (L min^{-1}), E is the average rate of energy expenditure ($\text{kilojoules min}^{-1}$), H is the volume of oxygen (at standard temperature and pressure) consumed in the production of 1 kilojoule

Table 3.1. Age- and gender-specific usage rates of environmental media, for selected ages.^a

Age (y)	Air ^b (m ³ d ⁻¹)		Tap water ^c (L d ⁻¹)		Food energy ^d (kcal d ⁻¹)		Cow's milk ^e (L d ⁻¹)	
	M	F	M	F	M	F	M	F
0	2.9	2.9	0.191	0.188	478	470	0.339	0.350
1	5.2	5.2	0.223	0.216	791	752	0.349	0.358
5	8.8	8.8	0.542	0.499	1566	1431	0.413	0.409
10	15.3	15.3	0.725	0.649	1919	1684	0.486	0.428
15	20.1	15.7	0.900	0.712	2425	1828	0.519	0.356
20	22.2	17.7	1.137	0.754	2952	1927	0.414	0.249
50	22.2	17.7	1.643	1.119	2570	1758	0.192	0.139
75	22.2	17.7	1.564	1.179	1990	1508	0.192	0.139
Lifetime average	19.2	16.5	1.29	0.93	2418	1695	0.282	0.207
Combined lifetime average ^f	17.8		1.11		2048 ^g		0.243	

^aAll values are based on estimated averages for the U.S. population for the indicated age. Ages refer to birthdays; e.g., age 5 y indicates the fifth birthday. Data reported for age intervals were converted to point estimates by preserving the total intake in each interval using a cubic spline fitting method (Fritsch and Carlson, 1980). Fitted curves were smoothed using a 3-point moving average. The listed usage rates are the values used in the calculation and are generally more precise than the data would support.

^bFrom Tables B.16A and B.16B of ICRP Publication 66, 1994a.

^cBased on survey data of the U.S. Department of Agriculture (Ershow and Cantor, 1989). Includes drinking water, water added to beverages, and water added to foods during preparation, but not water intrinsic in food as purchased.

^dBased on data from the Third National Health and Nutrition Examination Survey (McDowell et al., 1994).

^eUsed in one of two scenarios for ingestion of radioisotopes of iodine in diet. The other scenario assumes that iodine intake is proportional to food energy usage. Milk usage is based on data from EPA report 520/1-84-021 (1984b).

^fBased on the male-to-female ratio at birth, the gender-specific survival function, and the gender-specific usage function.

^gFor a typical U.S. diet, equivalent to a lifetime average intake of about 1.2 kg food d⁻¹ (see text).

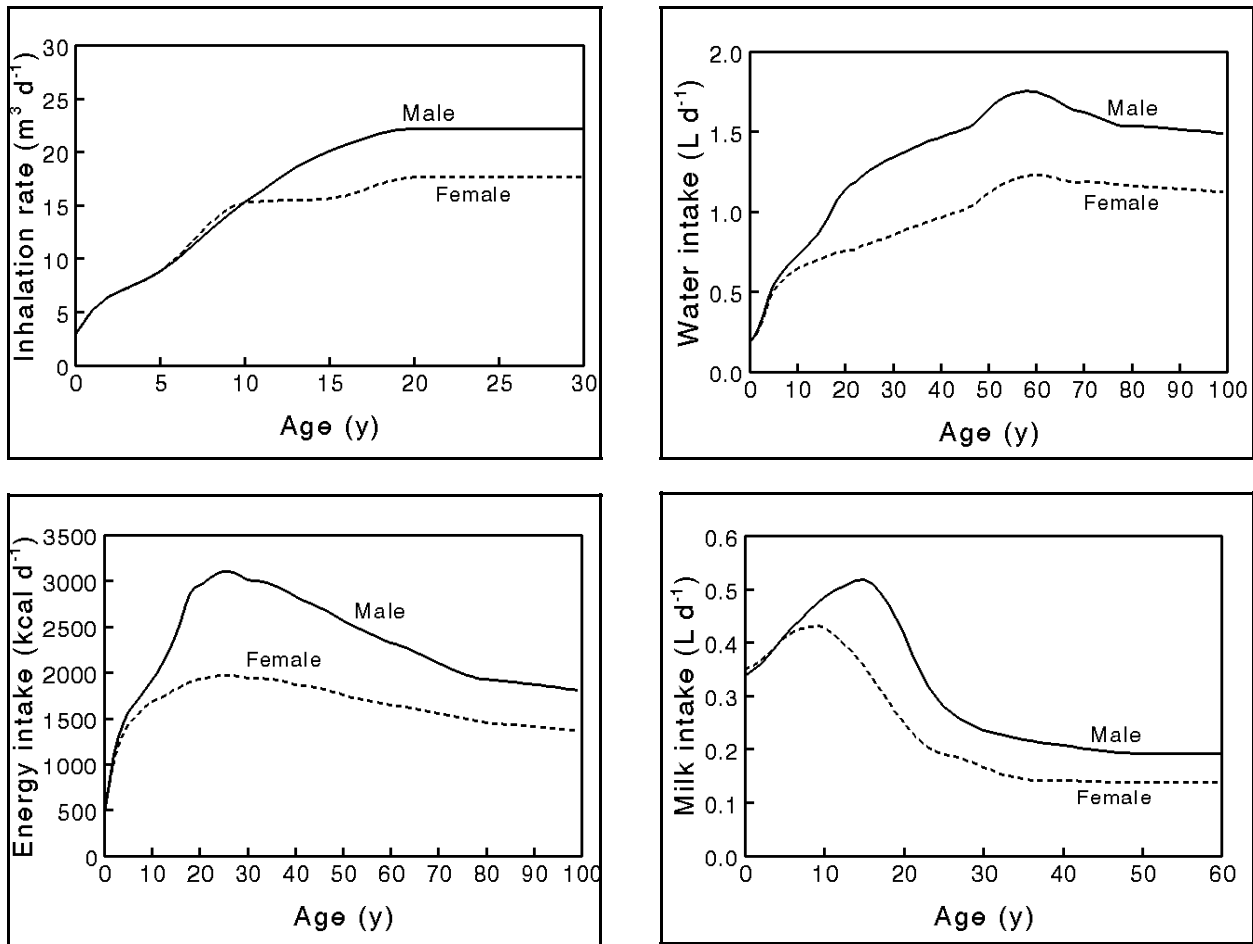


Fig. 3.2. Age- and gender-specific usage rates used to derive risk coefficients for inhalation, ingestion of water, ingestion of food (energy intake), and ingestion of milk.

of energy, and VQ is the ventilatory equivalent (ratio of ventilation rate to oxygen uptake rate). The value H has been determined within narrow bounds, and the average daily energy expenditure E at a given age in the U.S. population can be estimated reasonably well on the basis of data from food consumption surveys when biases in the data are taken into account. The main uncertainty in this method lies in the ventilatory equivalent, VQ . Layton concluded that VQ is nearly independent of the ventilation rate and proposed the value $VQ = 27$ for all ages and activity levels and for both genders. This value is based on data for adult humans (almost all male subjects, a large portion of which were highly trained athletes) and data from two studies on newborns. Little information is available for adult females, but results of a study on children of age 7-17 y (Zapletal et al., 1987) give

a mean value for VQ of about 36 and suggest a slight increase with age, from about 35 at age 7 y to about 37 at age 17 y. Because reliable age- and gender-dependent central values for VQ have not been established, the ICRP's recommended age- and gender-specific inhalation rates, rather than rates derived from Layton's method, are applied in the present study.¹

Risk coefficients for inhalation are based on an activity median aerodynamic diameter (AMAD) of 1 μm . This particle size is recommended by the ICRP for consideration of environmental exposures in the absence of specific information about the physical characteristics of the aerosol (ICRP, 1994a).

The form of the inhaled material is classified in terms of the rate of absorption from the lungs to blood, using the classification scheme of ICRP Publication 66 (ICRP, 1994a). Type F, Type M, and Type S represent fast, medium, and slow rates, respectively, of absorption of material inhaled in particulate form. Although the ICRP recommends default absorption types of many of the radionuclides considered in this document, the information underlying the selection of an absorption type is often very limited and in many cases reflects occupational rather than environmental experience. Due to the uncertainties in the form of a radionuclide likely to be inhaled by members of the public, risk coefficients for inhalation of a radionuclide in particulate form are derived for all three absorption types.

Inhalation of a radionuclide in the form of a vapor or gas is also considered for selected cases. In particular, risk coefficients are provided for inhalation of tritium as a vapor (HTO) or gas (HT), carbon in gaseous form as carbon monoxide (CO) or carbon dioxide (CO₂), sulfur as a vapor (SO₂ or CS₂), nickel as a vapor, ruthenium as a vapor (RuO₄), iodine as a vapor or gas (methyl iodide, CH₃I), tellurium as a vapor, and mercury as a vapor. Material-specific deposition and absorption models are used for vapors and gases (ICRP, 1995b).

Intake of radionuclides in food

Risk coefficients (Bq^{-1}) for ingestion of radionuclides in food are expressed as risk of cancer mortality or morbidity per unit activity intake. The intake rate of a radionuclide in food is assumed to be proportional to food energy usage (kcal per day). Age- and gender-specific values for food

¹The problem also arises that fractional deposition in different regions of the respiratory tract depends on the tidal volume and respiratory frequency associated with the various daily activities (ICRP, 1994a). Layton's method does not address these individual components of the inhalation rate, and it is not evident how these two parameters should be adjusted for application of Layton's estimates of daily air intake.

energy usage (Table 3.1) are based on data from the Third National Health and Nutrition Examination Survey (NHANES III), Phase 1, 1989-91 (McDowell et al., 1994).

Food usage is usually expressed in terms of mass rather than energy. Based on a 1994-95 food-intake survey by the U.S. Department of Agriculture, the lifetime average intake rate of food is approximately 1.2 kg per day (Wilson et al., 1997). This value and the lifetime average energy intake of 2048 kcal per day given in Table 3.1 imply an average energy density for the U.S. diet of about 1700 kcal per kg food.

For radioiodine, a second set of risk coefficients is derived under the assumption that the intake rate is proportional to usage of cow's milk, typically the dominant source of radioiodine in diet (UNSCEAR, 1982). Age- and gender-specific values for average daily usage of cow's milk (Table 3.1) are based on data tabulated by the EPA (EPA, 1984b).

For ^3H in diet, separate risk coefficients are given for tritiated water and organically bound tritium because different systemic biokinetic models are applied to these different forms of ^3H . Similarly, separate risk coefficients are given for inorganic and organic forms of radioisotopes of sulfur, mercury, and polonium because different systemic biokinetic models and/or f_i values are used for the different forms.

Intake of radionuclides in tap water

Risk coefficients (Bq^{-1}) for ingestion of radionuclides in tap water are expressed as risk of cancer mortality or morbidity per unit activity intake. Age-specific usage rates for tap water (Table 3.1) are based on results of the 1977-1978 Nationwide Food Consumption Survey of the U.S. Department of Agriculture as analyzed by Ershow and Cantor (1989). The data for usage of tap water in Table 3.1 include drinking water, water added to beverages, and water added to foods during preparation but do not include usage of water intrinsic in food as purchased. The reported data for tap water usage (Ershow and Cantor, 1989) were not divided by gender. Gender-specific values were derived by assuming (before the intake rate curves were smoothed) that the male-to-female intake rate ratio at a given age is the same as that observed for food energy intake (McDowell et al., 1994).

As is the case for intake in food, separate risk coefficients for tap water usage are given for tritiated water and organically bound tritium, and for inorganic and organic forms of radioisotopes of sulfur, mercury, and polonium.

External exposure to radionuclides in air

Risk coefficients ($\text{m}^3 \text{Bq}^{-1} \text{s}^{-1}$) for submersion are expressed as risk of cancer mortality or morbidity per unit integrated exposure to a radionuclide in air. The external dose rates used in the calculations (EPA, 1993) were calculated for a reference adult male, standing outdoors with no shielding. No adjustments are made in this exposure scenario to account for potential differences with age and gender in the external doses received or for potential reduction in dose due to shielding by buildings during time spent indoors.

External exposure to radionuclides in soil

Risk coefficients are tabulated for two different scenarios for exposure to contaminated soil: (1) external exposure to radiations from the ground surface, and (2) external exposure to radiations from soil contaminated to an infinite depth. In both cases the contamination is assumed to be of infinite lateral extent. The risk coefficients are expressed as risk of cancer mortality or morbidity per unit integrated exposure to a radionuclide. The units are $\text{m}^2 \text{Bq}^{-1} \text{s}^{-1}$ for contaminated ground surface and $\text{kg Bq}^{-1} \text{s}^{-1}$ for soil contaminated to an infinite depth.

The tabulations of dose coefficients in Federal Guidance Report No. 12 (EPA, 1993) for cases of external exposure to radiations from contaminated soil were calculated for a reference adult standing on the contaminated soil. No adjustments are made in this exposure scenario to account for potential differences with age in the external doses received or for potential reduction in dose due to shielding by buildings during time spent indoors.

Recommendations concerning cleanup of contaminated soil are sometimes based on the radionuclide concentration in soil to a depth of 15 cm (NRC, 1977). As indicated by the tabulations of dose coefficients in Federal Guidance Report No. 12, dose rates from soil contaminated to a depth of 15 cm generally differ by only 0-20% from dose rates from soil contaminated to an infinite depth (that is, to several meters below the surface) due to shielding provided by the top 15 cm of soil against radiations emitted at lower depths (EPA, 1993). Because risk coefficients for external exposure to soil contaminated to 15 cm would differ only slightly from those for contamination to an infinite depth, it would not be useful to provide tabulations of risk coefficients for both situations.

CHAPTER 4. BIOKINETIC MODELS FOR RADIONUCLIDES

In the dose-computation scheme of the ICRP, information on the behavior of radionuclides in the body is condensed into three main types of biokinetic models: a respiratory tract model, a gastrointestinal tract model, and element-specific systemic models. The generic respiratory tract model is used to describe the deposition and retention of inhaled material in the respiratory tract and its subsequent clearance to blood or to the gastrointestinal tract. The generic gastrointestinal tract model is used to describe the movement of swallowed or endogenously secreted material through the stomach and intestines, and, together with element-specific gastrointestinal absorption fractions (f_I values), to describe the rate and extent of absorption of radionuclides from the small intestine to blood. Element-specific systemic biokinetic models are used to describe the time-dependent distribution and excretion of radionuclides after their absorption into blood.

The model of the respiratory tract

The ICRP recently introduced a new respiratory tract model that involves considerably greater detail and physiological realism than previous models of the respiratory system (ICRP, 1994a). The model structure is shown in Fig. 4.1. The model divides the respiratory system into extrathoracic (*ET*) and thoracic regions. The airways of the *ET* region are further divided into two categories: the anterior nasal passages, in which deposits are removed by extrinsic means such as nose blowing, and the posterior nasal passages including the nasopharynx, oropharynx, and the larynx, from which deposits are swallowed. The airways of the thorax include the bronchi (compartments labeled BB_i), bronchioles (compartments labeled bb_i), and alveolar region (compartments labeled AI_i). Material deposited in the thoracic airways may be cleared into blood by absorption, to the GI tract by mechanical processes (that is, transported upward and swallowed), and to the regional lymph nodes via lymphatic channels.

The number of compartments in each region was chosen to allow duplication of the different kinetic phases observed in humans or laboratory animals. In Fig. 4.1, particle transport rates shown beside the arrows are reference values in units of d^{-1} . For example, particle transport from bb_1 to BB_1 is assumed to occur at a fractional rate of $2 d^{-1}$, and particle transport from ET_2 to the gastrointestinal tract is assumed to occur at a fractional rate of $100 d^{-1}$.

For an inhaled compound, the mechanical clearances of particles indicated in Fig. 4.1 are in addition to dissolution rates and absorption to blood, which depend on the element and the chemical

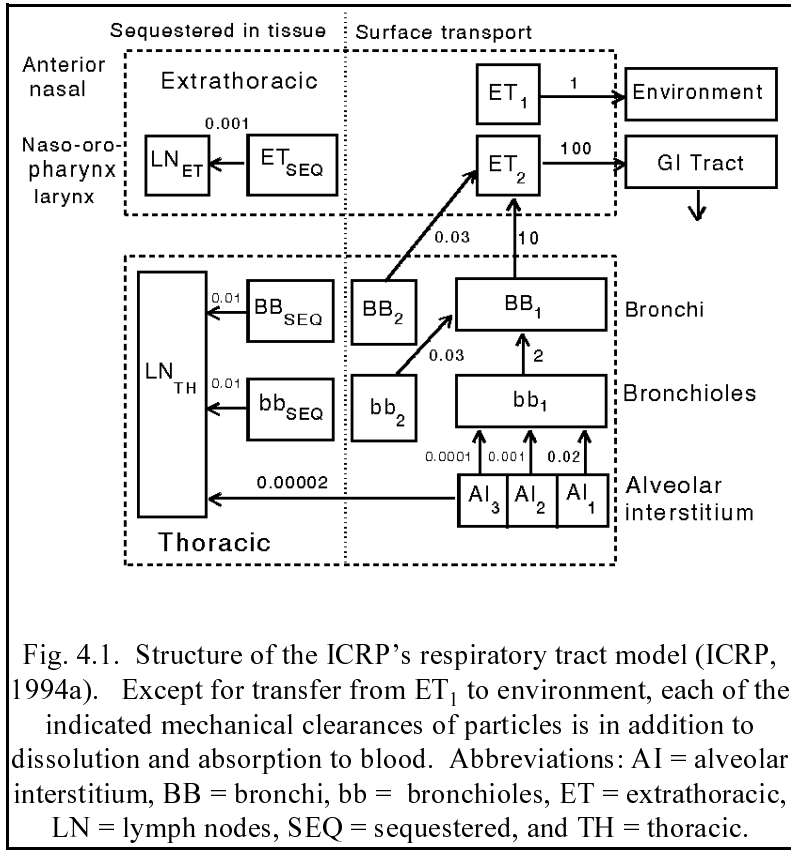


Fig. 4.1. Structure of the ICRP's respiratory tract model (ICRP, 1994a). Except for transfer from ET₁ to environment, each of the indicated mechanical clearances of particles is in addition to dissolution and absorption to blood. Abbreviations: AI = alveolar interstitium, BB = bronchi, bb = bronchioles, ET = extrathoracic, LN = lymph nodes, SEQ = sequestered, and TH = thoracic.

and physical form in which it is inhaled. Although the model permits consideration of compound-specific dissolution rates, a particulate is generally assigned to one of three default absorption types: Type F (fast dissolution and a high level of absorption to blood), Type M (an intermediate rate of dissolution and an intermediate level of absorption to blood), and Type S (slow dissolution and a low level of absorption to blood). The fractional rate of absorption (d^{-1}) assigned to the default types are

$$\begin{aligned}
 \text{Type F: } & 100 , \\
 \text{Type M: } & 10.0 e^{-100 t} + 5.0 \times 10^{-3} e^{-0.005 t} , \\
 \text{Type S: } & 0.1 e^{-100 t} + 1.0 \times 10^{-4} e^{-0.0001 t} ,
 \end{aligned}$$

where t is time (days) since deposition.

The absorption types for particulate forms of an element considered in the ICRP's compilation of dose coefficients for members of the public (ICRP, 1996) are listed in Table 4.1. For each of the 31 elements that were critically reviewed with regard to forms likely to be inhaled by members of the public (ICRP, 1995a), the ICRP recommended a default absorption type for application when no specific information is available. The default types are identified in Table 4.1.

The information underlying the selection of an absorption type is often very limited. In many cases, selection must be based on occupational rather than environmental experience. Due to the uncertainties in the form of a radionuclide likely to be inhaled by members of the public, risk coefficients for inhalation of particulate aerosols are provided in the present document for all three absorption types. Where appropriate, risk coefficients are also provided for inhalation of radionuclides in the form of a gas or vapor.

The model of the gastrointestinal tract

The model of the gastrointestinal (GI) tract applied in this report was originally developed for application to occupational intakes of radionuclides (ICRP, 1979) but has also been applied to environmental intakes of radionuclides by members of the public (ICRP, 1989, 1993, 1995a, 1995b). The model, shown in Fig. 4.2, divides the GI tract into four segments or compartments: *stomach (St)*, *small intestine (SI)*, *upper large intestine (ULI)*, and *lower large intestine (LLI)*, and depicts first-order transfer of material from one segment to the next. Material is assumed to transfer from *St* to *SI* at the fractional rate of 24 d^{-1} , from *SI* to *ULI* at 6 d^{-1} , from *ULI* to *LLI* at 1.8 d^{-1} , and from *LLI* to the compartment *Feces* at 1 d^{-1} .

Absorption of ingested material to blood generally is assumed to occur only in *SI*. Absorption to blood is described in terms of a fraction f_i . In the absence of radioactive decay, the fraction f_i of ingested material moves from *SI* to *BLOOD* and the fraction $1-f_i$ moves from *SI* to *ULI* and eventually is excreted in feces. The transfer coefficient from *SI* to *BLOOD* is $6f_i / (1-f_i) \text{ d}^{-1}$.

With two modifications explained below (see the discussions regarding chromium and polonium), the f_i values used in this report are those applied in ICRP Publication 72 (1996), which is a compilation of the ICRP's ingestion and inhalation dose coefficients for members of the public. Values for the adult are given in Chapter 2, in the tabulations of risk coefficients for inhalation (Tables 2.1) and ingestion of tap water or food (Table 2.2a). Modifications of the f_i values for adults for application to infants and (in some cases) children are summarized below.

For 31 of the elements considered in this report, f_i values for ingestion were developed specifically for members of the public, as described in the ICRP's series of documents on doses to

Table 4.1. Absorption types considered in ICRP Publication 72 (1996) for particulate aerosols.

Element	Lung absorption type(s) ^a	Element	Lung absorption type(s) ^a	Element	Lung absorption type(s) ^a
Hydrogen	F, M ^b , S	Zirconium	F, M ^b , S	Lutetium ^c	M, S
Beryllium ^c	M, S	Niobium	F, M ^b , S	Hafnium ^c	F, M
Carbon	F, M ^b , S	Molybdenum	F, M ^b , S	Tantalum ^c	M, S
Fluorine ^c	F, M, S	Technetium	F, M ^b , S	Tungsten ^c	F
Sodium ^c	F	Ruthenium	F, M ^b , S	Rhenium ^c	F, M
Magnesium ^c	F, M	Rhodium ^c	F, M, S	Osmium ^c	F, M, S
Aluminum ^c	F, M	Palladium ^c	F, M, S	Iridium ^c	F, M, S
Silicon ^c	F, M, S	Silver	F, M ^b , S	Platinum ^c	F
Phosphorous ^c	F, M	Cadmium ^c	F, M, S	Gold ^c	F, M, S
Sulfur	F, M ^b , S	Indium ^c	F, M	Mercury ^c	F, M
Chlorine ^c	F, M	Tin ^c	F, M	Thallium ^c	F
Potassium ^c	F	Antimony	F, M ^b , S	Lead	F, M ^b , S
Calcium	F, M ^b , S	Tellurium	F, M ^b , S	Bismuth ^c	F, M
Scandium ^c	S	Iodine	F ^b , M, S	Polonium	F, M ^b , S
Titanium ^c	F, M, S	Cesium	F ^b , M, S	Astatine ^c	F, M
Vanadium ^c	F, M	Barium	F, M ^b , S	Francium ^c	F
Chromium ^c	F, M, S	Lanthanum ^c	F, M	Radium	F, M ^b , S
Manganese ^c	F, M	Cerium	F, M ^b , S	Actinium ^c	F, M, S
Iron	F, M ^b , S	Praseodymium ^c	M, S	Thorium	F, M, S ^b
Cobalt	F, M ^b , S	Neodymium ^c	M, S	Protactinium ^c	M, S
Nickel	F, M ^b , S	Promethium ^c	M, S	Uranium	F, M ^b , S
Copper ^c	F, M, S	Samarium ^c	M	Neptunium	F, M ^b , S
Zinc	F, M ^b , S	Europium ^c	M	Plutonium	F, M ^b , S
Gallium ^c	F, M	Gadolinium ^c	F, M	Americium	F, M ^b , S
Germanium ^c	F, M	Terbium ^c	M	Curium	F, M ^b , S
Arsenic ^c	M	Dysprosium ^c	M	Berkelium ^c	M
Selenium	F ^b , M, S	Holmium ^c	M	Californium ^c	M
Bromine ^c	F, M	Erbium ^c	M	Einsteinium ^c	M
Rubidium ^c	F	Thulium ^c	M	Fermium ^c	M
Strontium	F, M ^b , S	Ytterbium ^c	M, S	Mendelevium ^c	M
Yttrium ^c	M, S				

^aAbsorption types defined in ICRP Publication 66 (1994a); F is fast, M is moderate, and S is slow absorption.

^bRecommended default absorption type when no specific information is available (ICRP, 1995b, 1996).

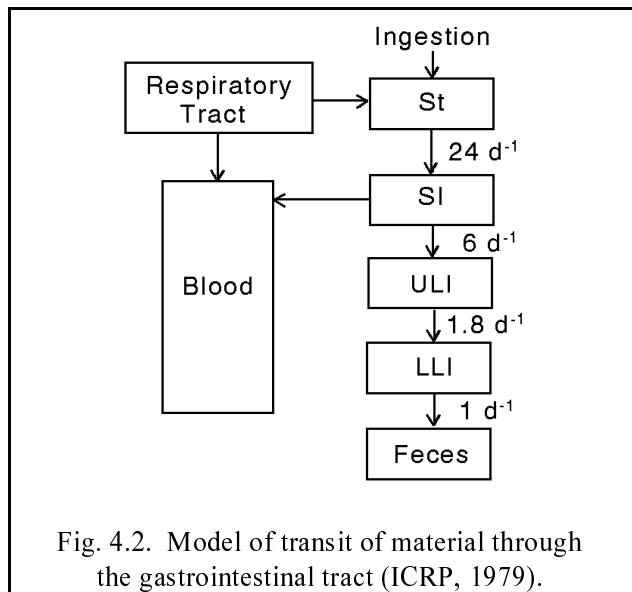
^cInhalation data for this element were not critically reviewed in the ICRP document on inhalation dose coefficients for members of the public (ICRP, 1995b). The listed absorption types are based on lung clearance categories assigned in earlier ICRP documents on occupational exposure.

members of the public from intake of radionuclides (ICRP, 1989, 1993, 1995a, 1995b). These elements are hydrogen, carbon, sulfur, calcium, iron, cobalt, nickel, zinc, selenium, strontium, zirconium, niobium, molybdenum, technetium, ruthenium, silver, antimony, tellurium, iodine, cesium, barium, cerium, lead, polonium, radium, thorium, uranium, neptunium, plutonium, americium, and curium. For most of these elements, the following rules were applied by the ICRP in the assignment of age-specific f_i values, based on patterns of changes with age indicated by the collective experimental and environmental data:

- (1) The f_i value for adults is assigned to ages ≥ 1 y.
- (2) If f_i for adults is ≤ 0.001 , then f_i for infants is 10 times the value for adults.
- (3) If f_i for adults is in the range 0.01-0.5, then f_i for infants is 2 times the value for adults.
- (4) If f_i for adults is greater than 0.5, then complete absorption is assumed for the infant.

These rules were not applied by the ICRP to ingested calcium, iron, cobalt, strontium, barium, lead, or radium (ICRP 1993, 1995a, 1995b). For these seven elements, separate f_i values were assigned to infants, children of ages 1-15 y, and adults, respectively, based on indications that gastrointestinal absorption of these elements is elevated in young children and adolescents as well as infants. For calcium and strontium, the f_i values applied to these three age groups are 0.6, 0.4, and 0.3, respectively; for barium and radium, the values are 0.6, 0.3, and 0.2, respectively; for iron, the values are 0.6, 0.2, and 0.1, respectively; for cobalt, the values are 0.6, 0.3, and 0.1, respectively; and for lead, the values are 0.6, 0.4, and 0.2, respectively.

For elements not addressed in the ICRP's series of documents on doses to members of the public, the f_i values for ingestion by the adult used in ICRP Publication 72 (1996) and in the present document were taken from ICRP Publication 30 (1979, 1980, 1981) and ICRP Publication 68 (1994b) on occupational exposures. The f_i values for the adult were extended to other age groups using Rules (1)-(4) given above, with three exceptions: for palladium, values of 0.005 and 0.05 are applied to the adult and infant, respectively; for beryllium, values of 0.005 and 0.02 are applied to



the adult and infant, respectively; and for hafnium, values of 0.002 and 0.02 are applied to the adult and infant, respectively (ICRP Publication 72, 1996).

In ICRP Publication 72, two different sets of age-dependent f_i values are considered for radioisotopes of chromium. Because chromium is not addressed in the ICRP documents on intake of radionuclides by members of the public, f_i values for ingestion of chromium by the adult were carried over from ICRP documents on occupational intakes and extended to younger age groups using the rules listed above. The different f_i values for the adult, 0.1 and 0.01, reflect expected differences in absorption of hexavalent compounds and trivalent compounds, respectively, of chromium encountered in the work place. The present document considers only the set of age-specific f_i values from ICRP Publication 72 that applies to hexavalent chromium because this seems appropriate for consideration of environmental chromium.

The set of age-specific f_i values for polonium used in ICRP Publication 72 is taken from ICRP Publication 67 (1993) on environmental intake of radionuclides by members of the public and is based on data for ingestion of organically bound polonium. The authors of ICRP Publication 67 point out that gastrointestinal absorption of inorganic forms of polonium appears to be much lower than that of polonium that is biologically incorporated into food. Because there are situations in which environmental polonium seems more likely to be in inorganic than organic form (for example, in tap water), separate sets of age-specific f_i values for inorganic and organic polonium are considered in this report. For polonium ingested in inorganic form, the f_i value for the adult is taken as 0.1 (ICRP 1979, 1994b). Based on Rules (1)-(4) listed above, this value is applied to ages ≥ 1 y, and the value 0.2 is applied to infants.

In the calculation of doses from inhalation of radionuclides, allowance is made for the absorption of material passing through the gastrointestinal tract after clearance from the respiratory tract. However, it is considered that radionuclides cleared from the respiratory tract may typically be present as minor constituents of the inhaled particles and that absorption from the gastrointestinal tract may depend on dissolution of the particle matrix as well as the elemental form of the radionuclide (ICRP 1996). In ICRP Publication 72 and hence in the present document, the element-specific f_i values applied to ingestion generally are applied to inhalation of Type F compounds; the most important exception is polonium, for which an f_i value of 0.5 is applied to ingestion in food and a value of 0.1 is applied to polonium inhaled as a Type F compound (in ICRP Publication 72 as well as in the present report). For inhaled material of Type M or S, a default f_i value of 0.1 or 0.01, respectively, is applied unless a lower f_i value for that absorption type, or a more soluble type, was used in the ICRP's most recent document on occupational exposures (ICRP Publication 68, 1994b). In the latter case, the lower f_i value is applied.

The f_i values as well as other biokinetic parameter values for “infant” apply to ages 0-100 days. Biokinetic parameter values are assumed to vary with age up to age 20 y for some elements (e.g., iron, cesium, and iodine) and up to age 25 y for others (e.g., calcium, radium, and plutonium) and to be constant thereafter. Parameter values for ages not explicitly addressed in a biokinetic model are determined by linear interpolation with age between parameter values for the nearest ages.

Systemic biokinetic models

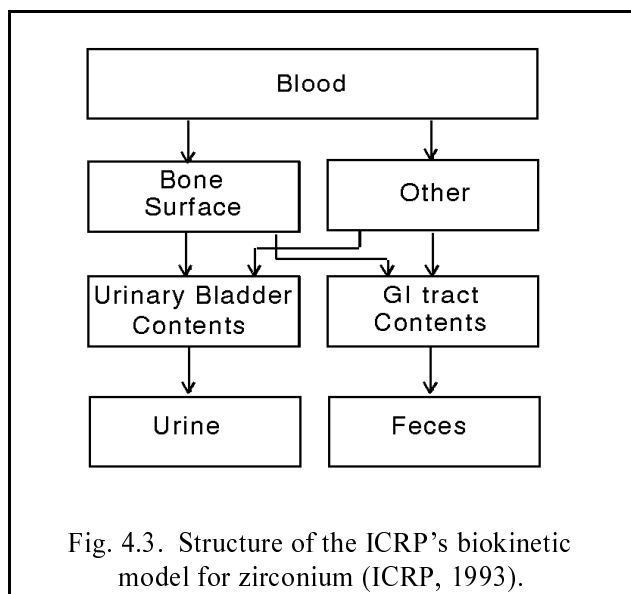
With two exceptions described below, the systemic biokinetic models used in this report are those applied in ICRP Publication 72 (1996). The systemic biokinetic models for 31 of the elements considered here were developed specifically for members of the public and, in many cases, involve parameter values that vary with age (ICRP, 1989, 1993, 1995a, 1995b). The models for the remaining elements were originally intended for application to adults exposed in the work place (ICRP, 1989, 1993, 1995a, 1995b) but are applied in ICRP Publication 72 and in the present report to all age groups. The 31 elements for which systemic biokinetic models were developed specifically for members of the public are listed above in the discussion of f_i values.

In ICRP Publication 72 (1996), a generic model structure (see Appendix C of this report) was applied to the “plutonium-like” or “bone-surface-seeking” actinide elements thorium, neptunium, plutonium, americium, and curium. This model structure, introduced in ICRP Publication 67 (1993), describes a gradual translocation of activity from bone surface to bone volume and marrow as a result of bone restructuring, and it explicitly depicts recycling of activity that returns to blood from bone and soft tissues. By contrast, the models applied in ICRP Publication 72 (1996) to other bone-surface seeking actinide elements (ICRP 1979, 1980, 1981) assign all skeletal activity to bone surface and depict one-directional flow of material from blood to organs to excreta. In this report, the generic model structure introduced in ICRP Publication 67 is extended to the actinide elements actinium and protactinium. Specifically, parameter values for americium are assigned to actinium and parameter values for thorium are assigned to protactinium, due mainly to similarities in the biokinetics of these element pairs in laboratory animals (Durbin, 1960; Taylor, 1970; Ralston et al., 1985). External measurements as well as bioassay measurements on a worker accidentally exposed to isotopes of actinium and protactinium also provide some support for the models selected here for these two elements (Newton and Brown, 1974).

The above discussion regarding models for actinide elements illustrates two different types of systemic biokinetic models currently applied by the ICRP. These are referred to here as “retention models” and “physiologically based models”.

A retention model is not intended to depict actual paths of movement of a radionuclide in the body. Rather, it is a mathematically convenient representation of the estimated inventories of the radionuclide in its major repositories as a function of time after its initial entry into blood. The initial distribution of activity leaving blood is represented by compartment-specific deposition fractions, and subsequent time-dependent inventories in the compartments are described in terms of compartment-specific biological removal half-times. Material leaving a tissue compartment is assumed either to move directly to excretion or to move to excretion via an excretion pathway such as the contents of the urinary bladder or the gastrointestinal tract.

An example of the type of retention models used by the ICRP is the model for zirconium originally described in ICRP Publication 30 (1979) and updated in ICRP Publications 56 (1989) and 67 (1993). The structure of this model is shown in Fig. 4.3. Parameter values were based largely on observations of the behavior of zirconium in rats and mice. For all age groups, 50% of zirconium leaving blood is assumed to deposit on bone surfaces and the remainder is assumed to be uniformly distributed in the rest of the body, referred to as *Other*. For the adult, zirconium is assumed to be removed to excretion with a biological half-time of 10,000 days.

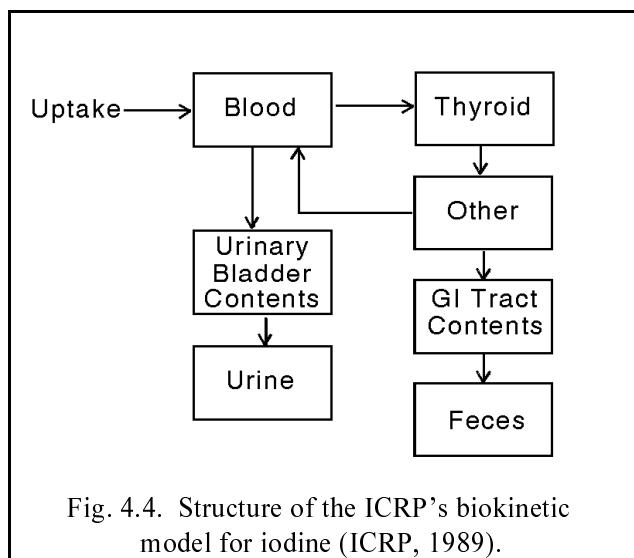


In the absence of age-specific data on zirconium in humans, the removal half-time from bone in children is assumed to be proportional to the bone turnover rate, which is considerably greater in children than in adults; for example, a removal half-time from bone to excretion pathways of 1000 days is applied to the 10-year-old child. For all age groups, zirconium is assumed to be removed from *Other* to excretion pathways with a biological half-time of 7 days. Of zirconium going to excreta, five-sixths is assigned to the urinary bladder contents and one-sixth is assigned to the contents of the upper large intestine. Generic models are used to describe removal from the contents of the urinary bladder and the gastrointestinal tract to excretion (ICRP, 1993).

In the ICRP's documents on age-dependent dosimetry (ICRP, 1989, 1993, 1995a, 1995b, 1996), physiologically based models were used for radioisotopes of calcium, iron, strontium, iodine, barium, lead, radium, thorium, uranium, neptunium, plutonium, americium, and curium. The model

frameworks applied to these elements depict loss of material by specific excretion pathways, feedback of material from organs to blood plasma, and certain physiological processes that are known to influence the distribution and translocation of the elements in the body. Clearly, the degree of biological realism incorporated into each of the models is limited by practical considerations regarding the amount and quality of information available to determine actual paths of movement and parameter values for specific elements.

The model for iodine (Fig. 4.4) is essentially the same as that used in ICRP Publication 30 (1979), except that parameter values were extended to pre-adult ages. The model structure is relatively simple compared with the other physiologically based models used in the ICRP Publication 56 series. According to this model, iodine entering blood is taken up by the thyroid or excreted in urine. It leaves the thyroid in organic form and is metabolized by the tissues in the rest of the body. A portion of iodine leaving these tissues is excreted in feces and the remainder is returned to blood in inorganic form and behaves the same as the original input to blood.



The model structure for iron is shown in Fig. 4.5. The model describes three main aspects of iron metabolism: (1) the hemoglobin cycle, including uptake of transferrin-bound iron by the erythroid marrow for incorporation into hemoglobin, subsequent appearance of iron in red blood cells, uptake of old and damaged red blood cells by the reticuloendothelial system, and eventual return of iron to plasma; (2) removal of transferrin-bound iron from plasma to the extravascular spaces and return to plasma via the lymphatic system; and (3) uptake and retention of iron by the parenchymal tissues. The soft tissues include a pool of extravascular iron that exchanges rapidly with plasma iron. Storage iron is divided among liver, spleen, red marrow, and other soft tissues. Destruction of red blood cells is viewed as occurring in the red marrow. The liver is viewed as consisting of two pools: a transit pool representing parenchymal tissues that exchange iron with plasma, and a storage pool associated with the reticuloendothelial system. Excretion of iron is depicted as occurring through exfoliation of skin, losses of plasma iron in urine, and leakage of red blood cells into the intestines and subsequent removal in feces.

The ICRP's physiologically based models for bone-seeking elements were developed within one of two generic model frameworks (Leggett 1992a, 1992b; ICRP, 1993), one designed for application to a class of "calcium-like" or bone-volume-seeking elements such as strontium, radium, and lead (Fig. 4.6), and, as described earlier, the other designed for application to a class of "plutonium-like" or bone-surface-seeking elements such as americium, neptunium, and thorium (see Appendix C). In contrast to the treatment of bone-seeking radionuclides in ICRP Publication 30 (1979), the new bone models account for the facts that bone-surface seekers are buried to a large extent in bone volume, bone-volume seekers may have a significant residence time on bone surfaces, and elements from both groups may be recycled to tissues to a significant extent after removal from their initial repositories to blood plasma. The physiologically based systemic biokinetic model for thorium, which is typical of bone-surface seekers, is described in detail in Appendix C.

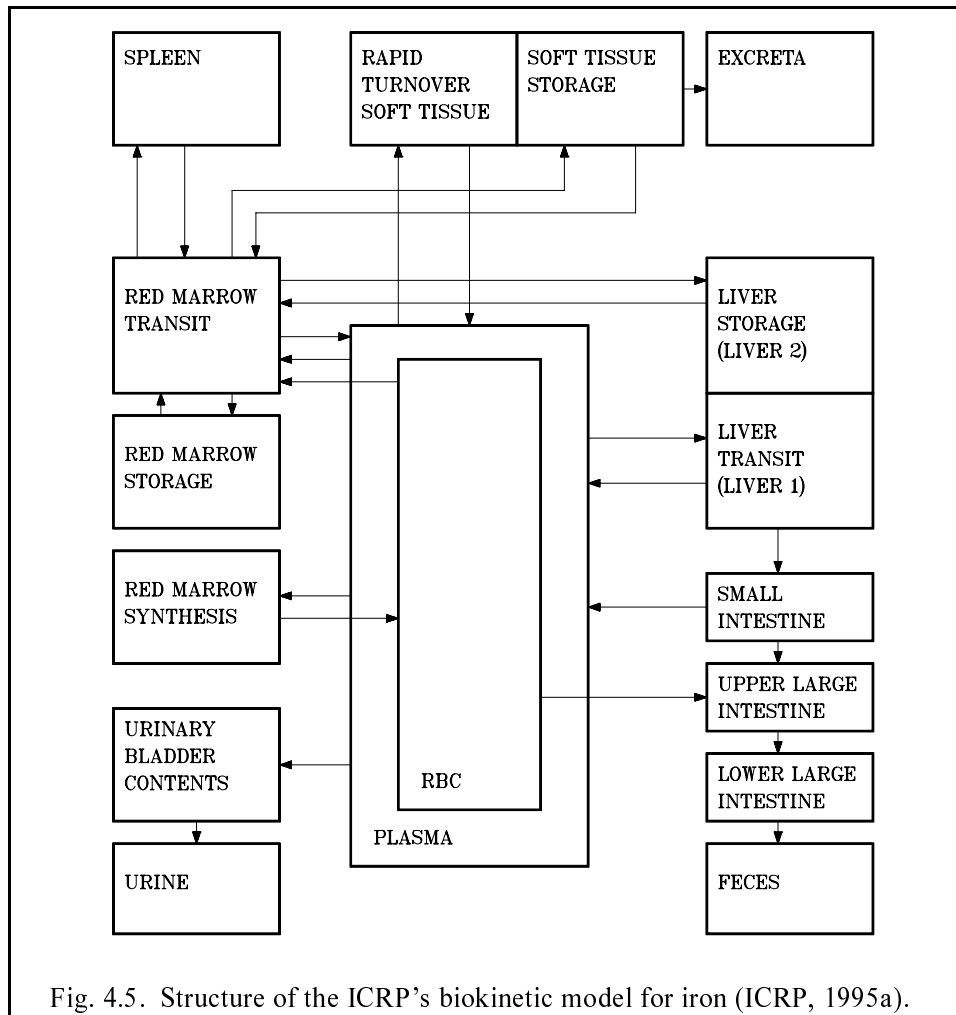
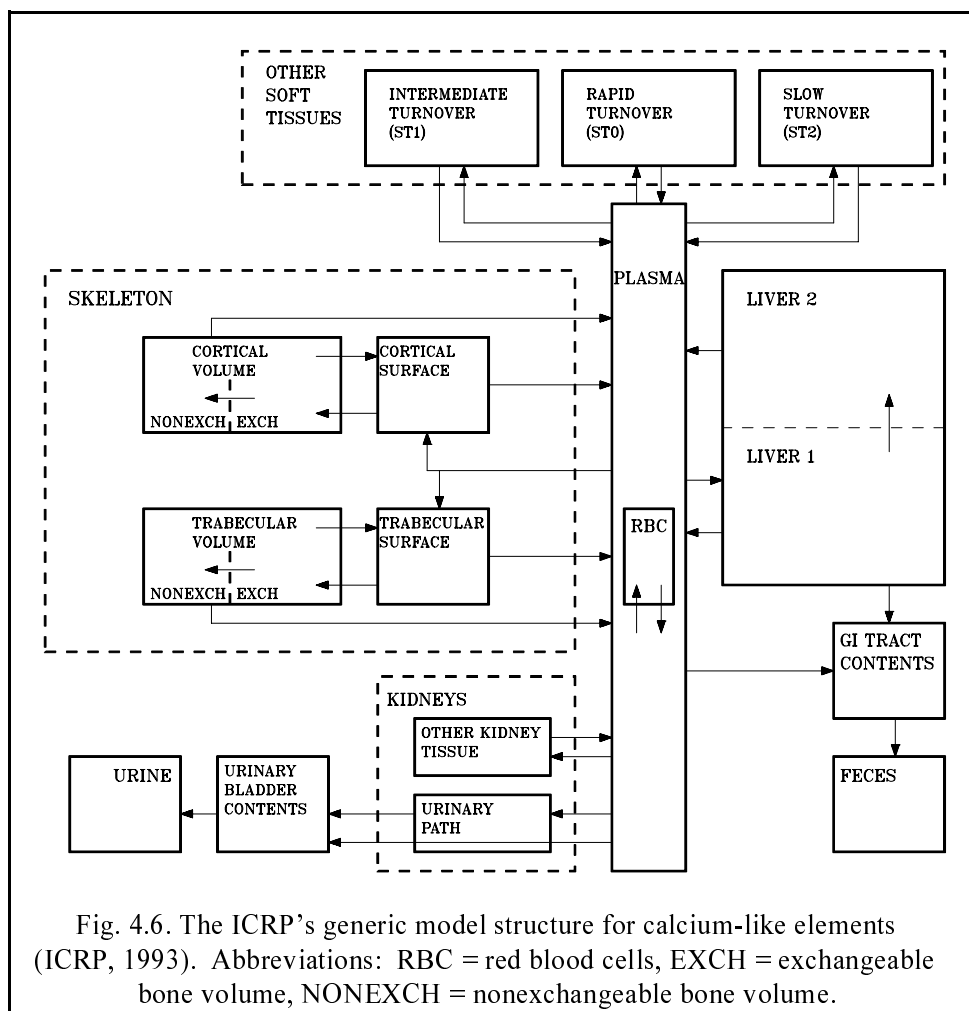


Fig. 4.5. Structure of the ICRP's biokinetic model for iron (ICRP, 1995a).

Treatment of decay chain members formed in the body

Assumptions concerning the behavior of decay chain members formed *in vivo* are consistent with those used in the ICRP's series on age-dependent doses from intake of radionuclides (ICRP, 1989, 1993, 1995a, 1995b, 1996) or, for elements not addressed in that document, assumptions used in ICRP Publication 30 (1979, 1980, 1981, 1988). In most cases, decay chain members produced *in vivo* are assigned the systemic biokinetic model of the parent (that is, the radionuclide taken into the body). However, the following exceptions are made:

1. Iodine produced from decay of tellurium is assumed to be translocated at a fractional rate of 1000 d^{-1} to the transfer compartment in inorganic form and then to follow the same kinetics as iodine introduced into the transfer compartment as a parent radionuclide.



2. If the parent is an isotope of lead, radium, actinium, thorium, protactinium, or uranium, then a radionuclide other than a noble gas formed in soft tissues or on bone surfaces is assigned the characteristic biokinetics of that radionuclide. That is, a radionuclide born either in soft tissues or on bone surfaces is assumed to have the same biokinetics as if the radionuclide had been taken in as a parent radionuclide. A radionuclide other than a noble gas formed in bone volume is assigned the biokinetics of the parent. Noble gases produced in soft tissues and bone surfaces are assumed to migrate from the body with a transfer coefficient of 100 d^{-1} . Noble gases produced in exchangeable and non-exchangeable bone volume are assumed to migrate from the body at rates of 1.5 d^{-1} and 0.36 d^{-1} , respectively.

Appendix C describes in detail the treatment of decay chain members produced in the body after absorption of the parent radionuclide, ^{232}Th , to blood.

Radionuclides produced in the respiratory tract are assumed to have the same kinetics as the parent radionuclide while in the respiratory tract. The rate of dissolution of the carrier of the radionuclide is assumed to control the rate of migration of inhaled radionuclides and their radioactive progeny. An exception is made for ^{222}Rn , which is assumed to escape from the body at a fractional rate of 100 d^{-1} after its production in any segment of the respiratory tract.

Chain members produced in, or migrating to, the gastrointestinal tract after intake of the parent radionuclide are assigned the gastrointestinal absorption fraction (f_I) of the parent in most cases. For consistency with the treatment of the systemic biokinetics of radionuclides formed *in vivo*, exceptions are made if the parent radionuclide is an isotope of lead, radium, actinium, thorium, protactinium, or uranium. In these cases, fractional absorption of a chain member produced *in vivo* is assumed to be the same as if that chain member had been taken in as a parent radionuclide.

Solution of the biokinetic models

The solver used in the DCAL computational system (Eckerman et al., 1999) to track the time-dependent distribution of activity of the parent and the decay chain members in the body is described by Leggett et al. (1993).

CHAPTER 5. DOSIMETRIC MODELS FOR INTERNAL EMITTERS

The dosimetric methodology used in this report is that of the ICRP and is generally consistent with the schema of the Medical Internal Radiation Dose Committee (MIRD) of the U.S. Society of Nuclear Medicine (Loevinger et al., 1988). The methodology considers two sets of anatomical regions within the body. A set of “source regions” is used to specify the location of radioactivity within the body. A set of “target regions” consists of those organs and tissues for which the radiation dose may be calculated.

Both the ICRP and MIRD consider the mean absorbed dose to a target region as the fundamental dosimetric quantity. The principal biological effect of interest in radiation protection, cancer induction, is cellular in origin, and the mean dose in a target is relevant to the extent that dose is representative of the dose to the cells at risk. The cells at risk are assumed to be uniformly distributed in the target region. Thus, the mean dose is assumed to be the relevant quantity.

The source regions selected for a given application consist of explicitly identified anatomical regions and an implicit region, referred to as *Other*, defined as the complement of the set of explicitly identified regions. The radioactivity in each source region is assumed to be uniformly distributed. For most regions the distribution is by volume, but for mineral bone regions and the airways of the respiratory tract the distribution may be by surface area. For all target regions, the relevant quantity is the mean energy absorbed in the target volume averaged over the mass of the target.

A full list of source and target regions currently used by the ICRP is given in Table 5.1. The names of most source or target regions adequately identify the associated organs or tissues of the body, but additional explanation is needed for some regions, such as *Body Tissues*, *Other*, and *Bone Surface*. These and other special source and target regions are defined in Appendix B.

The esophagus is a radiosensitive tissue but has not yet been incorporated explicitly into the mathematical phantom used for internal dosimetric calculations. At present, the dose calculated for the target region *Thymus* is used as a surrogate for the dose to the esophagus.

Age-dependent masses of source and target regions

With the exception of *Urinary Bladder Contents*, masses of source and target regions in children are taken from the phantom series of Cristy and Eckerman (1987), and values for the adult

Table 5.1. Source and target organs used in internal dosimetry methodology.

Organ or Tissue	Source Region	Target Region
Adrenals	Yes	Yes
Blood	Yes	No
Brain	Yes	Yes
Breasts	Yes	Yes
Gall Bladder Contents	Yes	No
Gall Bladder Wall	Yes	Yes
Heart Contents	Yes	No
Heart Wall	Yes	Yes
Kidneys	Yes	Yes
Liver	Yes	Yes
Muscle	Yes	Yes
Ovaries	Yes	Yes
Pancreas	Yes	Yes
Skin	Yes	Yes
Spleen	Yes	Yes
Testes	Yes	Yes
Thymus	Yes	Yes
Thyroid	Yes	Yes
Urinary Bladder Contents	Yes	No
Urinary Bladder Wall	Yes	Yes
Uterus	Yes	Yes
Body Tissues	Yes	No
Soft Tissues of Body Tissues	Yes	No
Other	Yes	No

Table 5.1, continued

Organ or Tissue	Source Region	Target Region
Skeleton:		
Bone Surface	No	Yes
Cortical Bone Surface	Yes	No
Cortical Bone Volume	Yes	No
Trabecular Bone Surface	Yes	No
Trabecular Bone Volume	Yes	No
Red Marrow	Yes	Yes
Gastrointestinal Tract:		
Stomach Contents	Yes	No
Stomach Wall	Yes	Yes
Small Intestine Contents	Yes	No
Small Intestine Wall	Yes	Yes
Upper Large Intestine Contents	Yes	No
Upper Large Intestine Wall	Yes	Yes
Lower Large Intestine Contents	Yes	No
Lower Large Intestine Wall	Yes	Yes
Respiratory Tract:		
Extrathoracic Region 1 – Surface	Yes	No
Extrathoracic Region 1 – Basal Cells	No	Yes
Extrathoracic Region 2 – Surface	Yes	No
Extrathoracic Region 2 – Bound	Yes	No
Extrathoracic Region 2 – Sequestered	Yes	No
Extrathoracic Region 2 – Basal Cells	No	Yes
Lymph Nodes – Extrathoracic Region	Yes	Yes
Bronchial Region – Gel (Fast Mucus)	Yes	No
Bronchial Region – Sol (Slow Mucus)	Yes	No
Bronchial Region – Bound	Yes	No
Bronchial Region – Sequestered	Yes	No
Bronchial Region – Basal Cells	No	Yes
Bronchial Region – Secretory Cells	No	Yes
Bronchial Region – Secretory Cells	Yes	No
Bronchiolar Region – Gel (Fast Mucus)	Yes	No
Bronchiolar Region – Sol (Slow Mucus)	Yes	No
Bronchiolar Region – Bound	Yes	No
Bronchiolar Region – Sequestered	Yes	No
Bronchiolar Region – Basal Cells	No	Yes
Bronchiolar Region – Secretory Cells	No	Yes
Bronchiolar Region – Secretory Cells	Yes	Yes
Alveolar-Interstitial Region	Yes	Yes
Lymph Nodes – Thoracic Region	Yes	Yes

male are taken from the Reference Man document (ICRP Publication 23, 1975). Masses of *Urinary Bladder Contents* are based on data assembled for the revision of Reference Man and are intended to represent the contents of the bladder averaged over the filling and voiding cycles (Cristy and Eckerman, 1993).

For the adult female, regional masses are mostly reference values from ICRP Publication 23 (1975) but, where none are given, are scaled from those for the reference adult male. Masses for the target region *Bone Surface* or for source regions within mineral bone of the adult female are taken as 75% of the values for males. For *Urinary Bladder Contents* and *Urinary Bladder Wall*, values for the 15-y-old male are applied to the adult female.

Age-specific masses of source and target regions are listed in Appendix B.

Dosimetric quantities

The mean energy absorbed in the target region depends on the nature of the radiations emitted in the source regions, the spatial relationships between the source and target regions, and the nature of the tissues between the regions. The details of these considerations are embodied in a radionuclide-specific coefficient called the specific energy or *SE*.

For any radionuclide, source organ *S*, and target organ *T*, the specific energy at age *t* is defined as

$$SE(T \leftarrow S; t) = \frac{1}{M_T(t)} \sum_i Y_i E_i AF_i(T \leftarrow S; t) , \quad (5.1)$$

where Y_i is the yield of radiations of type *i* per nuclear transformation, E_i is the average or unique energy of radiation type *i*, $AF_i(T \leftarrow S; t)$ is the fraction of energy emitted in source region *S* that is absorbed within target region *T* at age *t*, and $M_T(t)$ is the mass of target region *T* at age *t*. The age dependence in *SE* arises from the age dependence of the absorbed fraction and the mass of the target region. The quantity $AF_i(T \leftarrow S; t)$ is called the absorbed fraction (*AF*), and when divided by the mass of the target region, M_T , is called the specific absorbed fraction (*SAF*).

Whether one is interested in equivalent dose to a region, effective dose, or assessment of risk, the basic quantity to be computed is the absorbed dose rate at various times. The dose rate in target region *T* includes contributions from each radionuclide in the body and from each region in which radionuclides are present. The absorbed dose rate at age *t* in region *T* of an individual of age t_0 at the time of intake, $\dot{D}_T(t, t_0)$, can be expressed as

$$\dot{D}_T(t, t_0) = c \sum_S \sum_j q_{S,j}(t) SE(T \leftarrow S; t)_j, \quad (5.2)$$

where $q_{S,j}(t)$ is the activity of radionuclide j present in source region S at age t , $SE(T \leftarrow S; t)_j$ is the specific energy deposited in target region T per nuclear transformation of radionuclide j in source region S at age t , and c is any numerical constant required by the units of q and SE .

The following shorthand terminology is sometimes used: "photons" for x radiation, gamma radiation, and annihilation quanta; "electrons" for β^+ particles, β^- particles, internal conversion electrons, and Auger electrons; and "alphas" for alpha particles and alpha recoil nuclei.

Nuclear decay data

In Eq. 5.1, there are two terms from the nuclear decay data: Y_i is the yield of radiations of type i per nuclear transformation, and E_i is the average or unique energy of radiation type i . The radiations that contribute the overwhelming majority of the energy per nuclear transformation are tabulated in ICRP Publication 38 (1983) and in a MIRD publication (Weber et al., 1989).

The decay data files in the DCAL computational system include the beta spectra (Eckerman et al., 1994). The beta spectra files are used in the dosimetry for the ICRP's new respiratory tract model. For other organs, only the average energy of each beta transition is used.

The nuclear decay data files include the kinetic energies of each emitted alpha particle but not the corresponding kinetic energies of the recoiling nucleus. The recoil energy E_r for an alpha transition is computed as

$$E_r = \frac{4.0026 E_\alpha}{A - 4}, \quad (5.3)$$

where E_α is the kinetic energy of the alpha particle, A is the mass number of the nuclide, and 4.0026 is the atomic mass of an alpha particle.

Specific absorbed fractions for photons

Photon *SAFs* are derived from radiation transport calculations in anthropomorphic phantoms representing newborn, 1 y, 5 y, 10 y, 15-y-old male, and adult male (with breasts, ovaries, and uterus

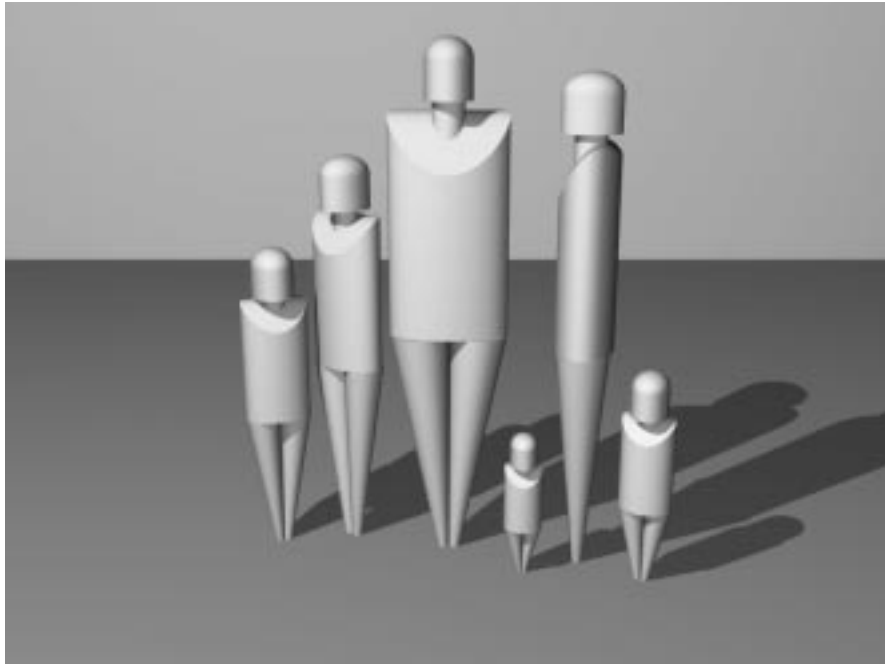


Fig. 5.1. Illustration of phantoms used to derive age-dependent specific absorbed fractions for photons.

added). These phantoms are illustrated in Fig. 5.1. In this report, the specific absorbed fractions for the adult male are also applied to the adult female.

The specific absorbed fractions are tabulated for 12 energies between 10 keV and 4 MeV. *SAFs* at intermediate energies are calculated by interpolating linearly between energies. Photons of energy below 10 keV are treated as nonpenetrating radiations for most regions and are considered to be absorbed in the source region. For bone dosimetry and for sources in the contents of walled organs (e.g., stomach), the dosimetry for photons is analogous to that described below for electrons.

The most commonly applied method of computing specific absorbed fractions for photon emissions is the Monte Carlo method, which is a computer simulation of photon interactions within target organs after emission from a source organ. This method is carried out for all combinations of source and target organs and for several photon energies. The body is represented by an idealized phantom in which the internal organs are assigned masses, shapes, positions, and attenuation coefficients based on their chemical composition. Hypothetical interactions of numerous photons emanating in randomly chosen directions from points in the source organ are recorded as the photon travels through tissues and escapes from the body or loses its energy. This approach can result in significant statistical errors in situations where few interactions are expected to occur, such as cases

involving low initial energies or target organs that are relatively small or remote from important sources of activity.

An alternate method of estimating specific absorbed fractions for photon emissions involves integration of a point-source kernel $\phi(x)$, where x is the distance from the point source. The function ϕ is composed of inverse-square and exponential attenuation factors that reflect the loss of energy from photon interactions and a buildup factor that reflects the contribution of scattered photons to dose. The point-source kernel method technically is valid only for a homogeneous, unbounded medium and may involve substantial errors (a factor of two or more) in cases involving significant variations in composition or density of body tissue or smaller errors (up to about 10%) in cases where target organs or important sources of activity lie near a boundary of the body.

Maximal differences between the Monte Carlo and classical point-kernel method are expected to occur for widely separated organ pairs and for large coefficients of variation for the Monte Carlo estimates. A comparison of the two methods was made for such situations in phantoms representing children of ages 1-15 y (Cristy and Eckerman, 1987). The results of this comparison indicate that the two approaches agree within a factor of two at all energies and within about 20% at energies greater than 500 keV. The largest differences between the methods occur at very low energies (10 keV or less) and at energies near 100 keV. The disagreement at 10 keV or less probably results from some combination of poor statistics for the Monte Carlo values and poor data underlying the point-source kernel at these energies. The disagreement at energy levels near 100 keV probably is due largely to the inability of the point-source kernel method to account properly for the effects of scattering. Comparisons of the Monte Carlo and point-kernel methods have been used to determine correction factors for values generated by the point-kernel method (Cristy and Eckerman, 1987). It appears that errors in estimates of photon absorbed fractions can be minimized in most situations by applying a weighted average of the specific absorbed fraction $SAF(T,S)$ and the reciprocal $SAF(T,S)$ produced by the Monte Carlo method. In cases where the Monte Carlo values are statistically unreliable, however, a better estimate may be obtained by applying the corrected point-kernel method.

Absorbed fractions for beta particles and discrete electrons

The kinetic energy of beta particles or discrete electrons is assumed to be absorbed entirely in the source region, except when the source is in the contents of a walled organ or in certain regions of the respiratory tract or skeleton. Thus, for solid regions,

$$AF(T \leftarrow S; t) = \begin{cases} 1, & \text{if } T=S \\ 0, & \text{if } T \neq S \text{ and } S \neq BT \\ M_T / M_{BT}, & \text{if } S=BT \end{cases} \quad (5.4)$$

where *BT* (*Body Tissues*) indicates the systemic tissues of the body. If the source region is *Body Tissues* of mass M_{BT} , then the fraction of the activity in *Body Tissues* present in the target region is M_T/M_{BT} , to which an absorbed fraction of 1 is applied.

For contents of walled organs, it is assumed that the dose to the wall is the dose at the surface of a half-space, or half the equilibrium dose to the contents. Thus, the specific absorbed fraction is

$$SAF(\text{wall} \leftarrow \text{cont}; t) = 0.5 / M_{\text{cont}} \quad (5.5)$$

where M_{cont} is the mass of the contents of the walled organ.

In the respiratory tract, there are narrow layers of radiosensitive basal and secretory cells in the epithelium. These are irradiated to some extent by beta particles and discrete electrons emanating from nearby "source organs", including the gel layer, the sol layer, and other identified compartments within the epithelium.

The skeleton is generally represented as a uniform mixture of its component tissues: cortical bone, trabecular bone, fatty marrow, red marrow, and connective tissues. Tissues of interest for dosimetric purposes are the red marrow, which lies within the generally tiny cavities of trabecular bone, and osteogenic cells adjacent to the surfaces of both cortical and trabecular bone. For the red marrow the pertinent dose is assumed to be the average dose to the marrow space within trabecular bone. For the osteogenic tissue, the ICRP recommends that the equivalent dose be calculated as an average over tissues up to a distance of 10 μm from the relevant bone surface.

Appendix B lists absorbed fractions for beta emitters for cases in which the source organ and target organ are both in bone (ICRP, 1979). The values are assumed to be independent of age.

Absorbed fractions for alpha particles and recoil nuclei

For alpha particles and alpha recoil nuclei, the radiation is assumed to be absorbed entirely in the source region, except when the source is in part of the skeleton or when the source is in the contents of a walled organ. Equation 5.4 applies to all solid regions.

The assumptions of ICRP Publication 30 (1979, 1980, 1981) are applied to contents of walled organs. That is, for application to alpha particles, the right side of Eq. 5.5 is multiplied by 0.01 to

account for the reduced alpha dose to radiosensitive cells in the wall, and an absorbed fraction of zero is applied to alpha recoil nuclei. The value 0.01 is not based on calculations of energy deposition but is a cautiously high value based on comparative studies of radiogenic effects from alpha and beta emitters in the gastrointestinal tracts of rats.

If an alpha emitter is uniformly distributed on the surface of trabecular bone then, by simple geometric considerations, the absorbed fraction in the marrow space is one half. Lacking information on the location of the hematopoietic stem cells, the ICRP assumes that the cells are uniformly distributed within the marrow space.

For an alpha emitter uniformly distributed in the mineral of trabecular bone, the absorbed fraction in the red marrow depends on the energy of the alpha particle. Calculations for alpha emitters ranging in energy from 5 to 8 MeV indicate that the absorbed fraction in the marrow space ranges between 0.041 and 0.087, which bracket the value of 0.05 recommended by the ICRP.

For an alpha emitter uniformly distributed in bone mineral, estimates of the absorbed fraction in bone surface ranges from less than 0.02 to more than 0.03, depending on the energy of the alpha particle. The nominal value recommended by the ICRP is 0.025.

Appendix B lists absorbed fractions for alpha emitters for cases in which the source and target organ are both in bone (ICRP, 1979). The values are assumed to be independent of age. For a source in a bone surface or bone volume compartment and a target consisting either of *Bone Surface* or *Red Marrow*, there is assumed to be no contribution to *SE* from alpha recoils.

Spontaneous fission

Spontaneous fission occurs in the decay of some isotopes of uranium, plutonium, curium, berkelium, californium, and einsteinium and results in the emission of photons, electrons, and neutrons, as well as fission fragments. Spontaneous fission products have not yet been incorporated into the internal dosimetry methodology. Therefore, radionuclides for which spontaneous fission is an important transformation process, including ^{244}Pu , ^{248}Cm , ^{250}Cm , ^{252}Cf , and ^{254}Cf , are not addressed in this report.

Computation of *SE*

Within the DCAL computational system (Eckerman et al., 1999), the *SEs* are computed by the module SEECAL (Cristy and Eckerman, 1993). These *SE* calculations are based on nuclear decay data files, libraries of specific absorbed fractions for non-penetrating radiations and photons,

and age-specific organ masses. The nuclear decay data files and specific absorbed fractions are those currently used by the ICRP (Cristy and Eckerman 1987, 1993). Organ masses for adults are taken from ICRP Publication 23 (1975). For children, age-specific organ masses are taken from the phantoms of Cristy and Eckerman (1987), which are based on data from ICRP Publication 23.

CHAPTER 6. DOSIMETRIC MODELS FOR EXTERNAL EXPOSURES

Three external exposure scenarios are considered in this report: submersion in a semi-infinite cloud, exposure to ground surface contamination, and exposure to soil contaminated to an infinite depth. Persons are assumed to be exposed throughout their lifetimes to a unit concentration of the radionuclide in air, on the ground surface, or in soil.

Dose rate coefficients from external exposure are taken from Federal Guidance Report No. 12 (EPA, 1993), which tabulates coefficients for external exposure to photons and electrons. The coefficients are based on state-of-the-art methods for calculating the energy and angular distribution of the radiations incident upon the body and the transport of these radiations within the body.

Tabulations in Federal Guidance Report No. 12 are for a reference adult, as defined in ICRP Publication 23 (1975). Calculations were based on the 70-kg phantom of Cristy (Cristy and Eckerman, 1987), with two modifications: the head region was made more realistic by including a neck and shortening the right elliptical cylinder comprising the lower portion of the head, and a model of the esophagus was added.

Although there is expected to be some age dependence in organ dose rates from external exposures, comprehensive tabulations of age-specific external dose coefficients are not yet available. Therefore, the tabulations for the reference adult in Federal Guidance Report No. 12 are applied to all age groups. As discussed in Appendix D to this report, the application of these external dose coefficients to other age groups appears to result in relatively small errors (usually <30%) in most cases. In extreme cases, such as for external irradiation of deep organs (e.g., ovaries or colon) of infants at energies less than 100 keV energies, 2- to 3-fold errors may arise. In applications of the derived risk coefficients, however, errors arising from application of age-independent external dose rates are likely to be negligible compared with errors associated with the simplified exposure scenarios used here (e.g., constant placement and position, no shielding, and infinite or semi-infinite source regions). Simplified exposure scenarios are used because it is not feasible to develop an external dosimetric methodology that applies to arbitrary distributions of contamination or to differences in life styles.

Interpretation of dose coefficients from Federal Guidance Report No. 12

Dose coefficients for external exposure relate the dose to organs and tissues of the body to the concentration of radionuclides in environmental media. The term “external exposure” is used

to indicate that the radiations originate outside the body. The radiations of concern are those that are sufficiently penetrating to traverse the overlying tissues of the body and thus are limited to photons, including bremsstrahlung, and electrons.

Because it is not feasible to develop an external dosimetric methodology that applies to arbitrary distributions of radionuclides in environmental media, it has become common practice to consider simplified and idealized exposure geometries. In particular, a semi-infinite source region generally is assumed for submersion in contaminated air, and an infinite source region generally is assumed for exposure to contaminated soil.

If one assumes an infinite or semi-infinite source region with a uniform concentration $C(t)$ of a radionuclide at time t , then the equivalent dose in tissue T , H_T , can be expressed as

$$H_T = h_T \int C(t) dt \quad (6.1)$$

where h_T denotes the time-independent dose coefficient for external exposure. The coefficient h_T represents the dose to tissue T of the body per unit time-integrated exposure (integrated concentration of the radionuclide). That is,

$$h_T = \frac{H_T}{\int C(t) dt} \quad (6.2)$$

Alternatively, one may interpret h_T as representing the instantaneous dose rate in organ T per unit activity concentration of the radionuclide in the environment. Furthermore, since only low-LET radiations are considered in the derivation of external dose coefficients, equivalent and absorbed doses are numerically equal.

In Federal Guidance Report No. 12, h_T is interpreted as the dose per unit time-integrated exposure. In this report, however, h_T is interpreted as a dose rate because dose rates are required as input into the radiation risk methodology applied here.

Nuclear data files used

The energies and intensities of the radiations emitted in spontaneous nuclear transformations of radionuclides have been reported in Publication 38 of the International Commission on Radiological Protection (ICRP, 1983). That publication is a report of the Task Group on Dose Calculations of ICRP Committee 2 and was assembled at Oak Ridge National Laboratory (ORNL)

during the preparation of ICRP Publication 30 (ICRP, 1979). The nuclear decay data of ICRP Publication 38 are based on the Evaluated Nuclear Structure Data Files (ENSDF) (Ewbank and Schmorak, 1978) of the Department of Energy's Nuclear Data Project as processed by the EDISTR code (Dillman, 1980). The processed data files retained in the ICRP/ORNL dosimetric data base include full tabulations of the average or unique energies and intensities of the radiations and also the beta spectra (Eckerman et al., 1994). The dose coefficients for external irradiation given in Federal Guidance Report No. 12 are based on these data files.

Radiations considered

For external exposures, the radiations of concern are those that are sufficiently penetrating to traverse the overlying tissues of the body and deposit ionizing energy in radiosensitive organs and tissues. Photons and electrons are the most important penetrating radiations produced by radionuclides in the environment.

Some radionuclides produce bremsstrahlung that is sufficiently penetrating to be of potential importance in the estimation of external dose. Bremsstrahlung, from the German for “braking radiation”, is produced when deceleration of electrons in a medium results in conversion of a small fraction of their initial kinetic energy into energy in the form of photons. Bremsstrahlung energy is distributed from zero up to the initial electron energy. The bremsstrahlung yield is small (about 0.5% at 1.0 MeV in tissue) but for pure beta emitters is sometimes the only source of radiation of sufficiently penetrating nature to irradiate some radiosensitive tissues.

The types of radiations considered in Federal Guidance Report No. 12 are photons, including bremsstrahlung, and electrons. The energy spectrum of emitted radiations can be characterized as either (1) discrete emissions of a unique energy (e.g, gamma radiation), and (2) continuous energy distribution of electrons as in the case of beta particles and bremsstrahlung. The beta spectra are used in Federal Guidance Report No. 12 to evaluate the contribution of the beta particles to the skin dose and to determine the yield of bremsstrahlung.

Spontaneous fission occurs in the decay of several radionuclides in the actinide series and results in the emission of photons, electrons, and neutrons, as well as fission fragments. However, spontaneous fission is an important decay mode for only a few radionuclides, including ^{244}Pu , ^{248}Cm , ^{250}Cm , ^{252}Cf , and ^{254}Cf . For these cases, the dose coefficients given in Federal Guidance Report No. 12 may underestimate true doses considerably due to neglect of the contribution to dose from spontaneous fission. These five radionuclides are not addressed in this report, either in the external or the internal exposure scenarios.

Effects of indoor residence

The dose coefficients for air submersion and exposure to contaminated soil are taken from Federal Guidance Report No. 12 (EPA, 1993). These dose coefficients assume that exposed individuals spend all of the time outdoors. Depending on such factors as photon energy, type of structure, fraction of time spent indoors, and degree of disequilibrium in the concentration of a radionuclide in indoor and outdoor air, there could be a substantial reduction in the equivalent dose from external exposures during indoor residence due to shielding by structures.

For noble-gas radionuclides, air submersion is the only external exposure mode of concern. The effects of indoor residence on equivalent doses to skin due to electrons should be negligible during chronic releases, unless the range of the emitted electrons in air is somewhat greater than the interior dimensions of building rooms, because the indoor and outdoor air concentrations for noble gases will be about the same.

A radionuclide-independent dose reduction factor is sometimes applied to external dose coefficients to account for the effects of indoor residence (e.g., NRC, 1977). However, the average reduction in external dose due to indoor residence depends on the radionuclide as well as other factors indicated above and generally cannot be quantified with much certainty. In the present document, the external dose coefficients given in Federal Guidance Report No. 12 are not reduced to account for the effects of indoor residence.

CHAPTER 7. RADIOGENIC CANCER RISK MODELS

Calculations of radiogenic risk are based on risk projection models for specific cancer sites. The age- and gender-specific radiation risk models used in this report are taken from a recent EPA report (EPA, 1994) that provides a methodology for calculation of radiogenic cancer risks based on a critical review of data on the Japanese atomic bomb survivors and other study groups. Parameter values in the models have been modified in some cases in the present report to reflect the use of updated vital statistics for the U.S. and to achieve greater consistency in the assumptions made for different age groups and genders. The following age-at-exposure groups are considered in the models: 0-9, 10-19, 20-29, 30-39, and 40+ y.

Types of risk projection models

One of two basic types of radiogenic cancer risk projection models is used for a given cancer site: an absolute risk model or a relative risk model. An absolute risk model is based on the assumption that the age-specific excess force of mortality or morbidity (that is, the mortality or morbidity rate for a given cancer type) due to a radiation dose is independent of cancer mortality or morbidity rates in the population. A relative risk model is based on the assumption that the age-specific excess force of mortality or morbidity due to a radiation dose is the product of an exposure-age-specific relative risk coefficient and baseline cancer mortality or morbidity rate. In this report, risk models for bone, skin, and thyroid cancer are based on an absolute risk hypothesis, and risk models for other sites are based on a relative risk hypothesis.

In the absolute risk models used in this report, the absolute risk $\epsilon(x, x_e)$ at age x due to a unit absorbed dose received at an earlier age x_e ($x_e < x$) is calculated as

$$\epsilon(x, x_e) = \alpha(x_e) \zeta(t), \quad (7.1)$$

where:

$\alpha(x_e)$ is a non-negative number, called a “risk model coefficient”, that depends on gender as well as age at exposure; and

$\zeta(t)$ is either 0 or 1, depending on the time since exposure, $t = x - x_e$.

The function α defines the potential level of risk of dying from or experiencing a given type of cancer at any given age (and hence time) after the dose is received, and ζ defines the plateau period, that is, the time period during which the risk is expressed.

In the relative risk models used in this report, $\epsilon(x, x_e)$ is calculated as $\epsilon(x, x_e) = \mu(x) \times \eta(x, x_e)$, where $\mu(x)$ is the baseline force of cancer mortality or morbidity at age x and $\eta(x, x_e)$ is the relative risk at age x due to a unit absorbed dose received at age x_e ($x_e < x$); $\eta(x, x_e)$ is calculated as

$$\eta(x, x_e) = \beta(x_e) \zeta(t, x_e), \quad (7.2)$$

where

$$t = x - x_e;$$

$\beta(x_e)$ is a non-negative number, called a “risk model coefficient”, that depends on gender as well as age at exposure; and

$\zeta(t, x_e)$ is the relative magnitude of the response at different times after exposure at age x_e .

For all cancers except leukemia, it is assumed that ζ is independent of the exposure age x_e and has a value of either 0 or 1, depending on the time since exposure, $t = x - x_e$. The time-since-exposure response function $\zeta(t, x_e)$ for either chronic granulocytic leukemia or for acute leukemia is given by $\zeta(t, x_e) = 0$ if $t \leq 2$ y and $\zeta(t, x_e) = \phi(t, \xi(x_e), \sigma^2)$ if $t > 2$ y, where

$$\phi(t, \xi(x_e), \sigma^2) = \frac{\exp(-0.5(\ln(t-2) - \xi(x_e))^2 / \sigma^2)}{(t-2)(2\pi\sigma^2)^{0.5}}. \quad (7.3)$$

In this expression, the function $\xi(x_e)$ and the value σ^2 depend on the type of leukemia. For chronic granulocytic leukemia, $\xi(x_e) = 2.68$ and $\sigma^2 = 1.51$. For acute leukemia, $\xi(x_e) = 1.61 + 0.015x_e + 0.0005x_e^2$ and $\sigma^2 = 0.65$ (EPA, 1994). The total leukemia time-since-response function is a weighted mean of the response function for chronic granulocytic leukemia, which is given a weight of 0.32, and the response function for acute leukemia, which is given a weight of 0.68 (EPA, 1994).

The function β in Eq. 7.2 times the baseline force of cancer mortality or morbidity, $\mu(x)$, at a given age defines the potential level of risk of dying from or experiencing a given type of cancer at that age, and ζ defines the period during which the risk is expressed and, in the case of leukemia, the changes in the level of response during that period. Because the time-since-response function for leukemia is scaled differently from the time-since-response functions for other cancers and has a maximum value much less than 1, the risk model coefficients (age- and gender-specific values of β) for leukemia are not directly comparable with the risk model coefficients for other cancers.

The term “risk coefficient” used in the EPA report on radiation risk models (EPA, 1994) has been replaced here with the term “risk model coefficient” to avoid confusion with the radionuclide risk coefficients tabulated in Chapter 2. The risk coefficients given in Chapter 2 refer to risk per unit intake or external exposure to a specific radionuclide in a specific environmental medium.

Epidemiological studies used in the development of risk models

The risk model coefficients given in the EPA report (EPA, 1994) were based in large part on information from the Radiation Effects Research Foundation (RERF) Life Span Study (LSS) cohort of Hiroshima and Nagasaki atomic bomb survivors (Shimizu et al., 1989, 1990). The LSS has the advantages that it includes a large, relatively healthy population at the time of exposure, a wide range of reasonably well established doses to individual subjects (although some important dosimetric issues remain), a large, well matched control group (that is, people who were present in Hiroshima or Nagasaki at the time of bombing but who received only small doses of radiation), and a detailed, long-term epidemiological follow-up. A statistically significant excess cancer mortality associated with radiation has been found among the bomb survivors for the following types of cancer: leukemia, esophagus, stomach, colon, liver, lung, breast, ovary, urinary tract, and multiple myeloma.

Results of other epidemiological studies on radiation-exposed populations were used for development of risk models for a few sites for which the A-bomb survivor do not appear to provide best available information on radiogenic risk. For example, risk models for the thyroid and breast were based primarily on results of epidemiological studies of medical exposures of these organs. For two other sites, bone and liver, low-LET risk estimates were extrapolated from results of epidemiological studies of humans exposed to ^{224}Ra and thorostrast, respectively (EPA, 1994), together with data on comparative biological effectiveness of alpha and low-LET radiations in laboratory animals. There are additional important epidemiological studies of persons exposed either to low-LET or high-LET radiation, but results of these additional studies were used mainly for comparison with results for the A-bomb survivors.

Modification of epidemiological data for application to low doses and dose rates

All of the epidemiological studies used in the development of the radiation risk models involve subjects who experienced high radiation doses delivered in a relatively short time. Available evidence indicates that the response per unit dose at low doses and low dose rates from low-LET

radiation may be overestimated if one extrapolates from observations made at high, acutely delivered doses (NCRP, 1980). The degree of overestimation is commonly expressed in terms of a dose and dose rate effectiveness factor (DDREF). For example, a DDREF of 2 means that the risk per unit dose observed at high acute doses should be divided by 2 before being applied to low doses or low dose rates. “Low dose” and “low dose rate” are defined here in terms of the range of applicability of a DDREF of 2; “low dose” is defined as <0.2 Gy and “low dose rate” is defined as <0.1 mGy min^{-1} (UNSCEAR, 1993; EPA, 1994). For comparison, the ICRP (1991) used a DDREF of 2 in the calculation of probability coefficients for all equivalent doses below 0.2 Gy and from higher doses resulting from absorbed dose rates less than 0.1 Gy h^{-1} (about 1.7 mGy min^{-1}).

In the EPA report on radiation risk models (EPA, 1994) and hence in the present report, low-LET radiogenic cancer risks for sites other than the breasts are assumed to be reduced by a DDREF of 2 at low doses and low dose rates compared to risks at high acute dose exposure conditions. The DDREF assumed for breast cancer is 1. Risks from high-LET (alpha particle) radiation are assumed to increase linearly with dose and to be independent of dose rate.

Relative biological effectiveness factors for alpha particles

Except for breast cancer and leukemia, the EPA has followed the ICRP’s recommendation (ICRP, 1991) and assumed that the relative biological effectiveness (RBE) for alpha particles is 20, in comparison to low-LET radiation at low doses and dose rates (EPA, 1994). For leukemia, an effective alpha particle RBE of 1 is used. For breast cancer, an alpha particle RBE of 10 is used.

Where comparison was made in the EPA report (EPA, 1994) against acute high doses of low-LET radiation, a value of 10 was assumed for the alpha particle RBE. This is consistent with the RBE of 20 relative to acute, low-dose, low-LET radiation, given the assumption of a DDREF of 2 for low-LET radiation at low doses and dose rates.

Risk model coefficients for specific organs

Age- and gender-specific risk model coefficients used in this report are summarized in Table 7.1 for cancers other than leukemia and in Table 7.2 for leukemia. Risk model coefficients for esophagus, stomach, colon, lung, ovary, bladder, leukemia, and “residual” are based on updated information on the Japanese atomic bomb survivors and are derived using a slightly modified version of a model of Land and Sinclair (1991). The risk model coefficients for these sites are obtained by taking the geometric mean of model coefficients derived from two equally plausible methods used

Table 7.1. Revised mortality risk model coefficients^{a,b} for cancers other than leukemia, based on the EPA radiation risk methodology (EPA, 1994).

Cancer type	Risk model type ^c	Age group (x_e)				
		0-9 y	10-19 y	20-29 y	30-39 y	40+ y
Male:						
Esophagus	R	0.2877	0.2877	0.2877	0.2877	0.2877
Stomach	R	1.223	1.972	2.044	0.3024	0.2745
Colon	R	2.290	2.290	0.2787	0.4395	0.08881
Liver	R	0.9877	0.9877	0.9877	0.9877	0.9877
Lung	R	0.4480	0.4480	0.0435	0.1315	0.1680
Bone	A	0.09387	0.09387	0.09387	0.09387	0.09387
Skin	A	0.06597	0.06597	0.06597	0.06597	0.06597
Breast	R	0.0	0.0	0.0	0.0	0.0
Ovary	R	0.0	0.0	0.0	0.0	0.0
Bladder	R	1.037	1.037	1.037	1.037	1.037
Kidney	R	0.2938	0.2938	0.2938	0.2938	0.2938
Thyroid	A	0.1667	0.1667	0.08333	0.08333	0.08333
Residual	R	0.5349	0.5349	0.6093	0.2114	0.04071
Female:						
Esophagus	R	1.805	1.805	1.805	1.805	1.805
Stomach	R	3.581	4.585	4.552	0.6309	0.5424
Colon	R	3.265	3.265	0.6183	0.8921	0.1921
Liver	R	0.9877	0.9877	0.9877	0.9877	0.9877
Lung	R	1.359	1.359	0.1620	0.4396	0.6047
Bone	A	0.09387	0.09387	0.09387	0.09387	0.09387
Skin	A	0.06597	0.06597	0.06597	0.06597	0.06597
Breast	R	0.7000	0.7000	0.3000	0.3000	0.1000
Ovary	R	0.7185	0.7185	0.7185	0.7185	0.7185
Bladder	R	1.049	1.049	1.049	1.049	1.049
Kidney	R	0.2938	0.2938	0.2938	0.2938	0.2938
Thyroid	A	0.3333	0.3333	0.1667	0.1667	0.1667
Residual	R	1.122	1.122	0.8854	0.3592	0.1175

^aThe tabulated risk model coefficients are the precise values derived from the epidemiological data and used in the calculations. The use of four significant digits should not be interpreted as indicating a low level of uncertainty in the risk model coefficients.

^bAge-specific risk model coefficients were used to derive composite risk coefficients representing averages over all ages. Application of these risk model coefficients to a specific age group is not recommended due to the high sampling variability in the underlying epidemiological data for some age groups.

^cA indicates that an absolute risk model is used (coefficient units, $10^{-4} \text{ Gy}^{-1} \text{ y}^{-1}$), and R indicates that a relative risk model is used (Gy^{-1}). $\alpha(x_e)$ is given for absolute risk model (Eq. 7.1) and $\beta(x_e)$ for a relative risk model (Eq. 7.2).

Table 7.2. Revised mortality risk model coefficients (Gy^{-1}) for leukemia, based on the EPA radiation risk methodology (EPA, 1994).^a

Gender	Age group (x_e)				
	0-9 y	10-19 y	20-29 y	30-39 y	40+ y
Male	982.3	311.3	416.6	264.4	143.6
Female:	1176	284.9	370.0	178.8	157.1

^aA relative risk model is used (coefficient units, Gy^{-1}). Risk model coefficients for leukemia are not directly comparable to those for other types of cancer (Table 7.1) due to differences in the scales of the time-since-exposure response functions for leukemia and other cancers (see the discussion following Eq. 7.2).

by Land and Sinclair for transporting risk from one population to another. Both methods assume a constant excess relative risk coefficient beginning 10 y after an exposure and continuing throughout the rest of life for each cancer site, excluding leukemia. One method (multiplicative) assumes that the relative risk estimator is the same across populations. The other (NIH, for National Institutes of Health) assumes that the relative risk model coefficients for the target population should yield the same risks as those calculated with the additive risk model coefficients from the original population over the period of epidemiological follow-up, excluding the minimal latency period. These excess relative risk model coefficients are then used to project the risk over the remaining years of life. The data considered in deriving risk model coefficients consisted of cancers observed 10-40 y after exposure for solid tumors and 5-40 y after exposure for leukemia.

As described below, some modifications in the method of calculation of the NIH model coefficients have been made to remove inconsistencies in the derived coefficients. Some but not all of these changes were made in the EPA report on radiation risk models (EPA, 1994); therefore, some of the risk coefficients in Tables 7.1 and 7.2 differ from values given in that report.

An examination of the coefficients for the additive and multiplicative models of Land and Sinclair (1991) reveals that in several instances data for exposures of two or more age groups were combined to calculate a single risk coefficient. In such cases, a single NIH model coefficient has been calculated for use in the present report by combining the risks calculated for the corresponding groups. This was done in the EPA report (EPA, 1994) for model coefficients for lung and colon cancer for two exposure age groups (0-9 y and 10-19 y), and the same principle has been extended in the present report to the coefficients for esophagus, ovary, and bladder cancer. For these three sites, the age-group-specific additive coefficients of Land and Sinclair were based on a single-coefficient multiplicative risk model. For the present report, an NIH model excess relative

risk coefficient has been calculated corresponding to the combined risk for exposure for all age-groups, expressed 10-40 years after exposure for the additive risk model.

EPA (1994) noted inconsistencies between ages and between genders in the additive and multiplicative risk models of Land and Sinclair (1991) with regard to coefficients for the residual site for age groups 0-9 y and 10-19 y. These inconsistencies may be the result of uncertain differences between the total observed excess cancers and the sum of those attributed to specific sites. In the EPA report (EPA, 1994), risk model coefficients for the residual site for age group 10-19 y were applied to age group 0-9 y. For the present report, the additive model risks for these two age groups have been combined to calculate gender-specific, single coefficients for the NIH risk model. Single risk coefficients equivalent to the risks projected by the multiplicative model for 10-40 y following exposure of those in this age group were also calculated. These values were used to calculate gender-specific risk model coefficients for these two age groups for the EPA risk model.

For kidney, the LSS data are suggestive of a radiogenic risk but the number of excess cancers is not statistically significant. The existence of a radiogenic kidney cancer risk is indicated by an epidemiological study of subjects receiving radiation treatments for cervical cancer (NAS, 1990; Boice et al., 1988). Given the importance of the kidney as a possible target organ for uranium and some other radionuclides, the EPA (1994) has developed a risk model for this site based on the LSS data. A constant relative risk model independent of age at exposure and sex is used, and a 10-y latency period is assumed.

Risk model coefficients for the liver are based on epidemiological data on patients injected with Thorotrast, an x-ray contrast medium containing isotopes of thorium (NAS, 1980, 1988). To develop risk model coefficients for high-dose, low-LET radiation, an RBE of 10 is assumed for alpha particles. A constant relative risk model independent of age at exposure and sex is used, and a 10-y latency period is assumed.

Estimates of skin cancer risks are highly uncertain, but the mortality risk is known to be relatively low. For acute exposures, the EPA has adopted the mortality risk estimate given in ICRP Publication 60 (1991) but, in contrast to ICRP, has applied a DDREF of 2 in estimating the skin cancer risk at low doses and dose rates. Non-fatal skin cancers, which represent perhaps 99.99% of basal cell carcinomas and about 99% of squamous cell carcinomas, are excluded from the risk model coefficients. A 10-y latency period is assumed.

Thyroid risk estimates are based on NCRP Report 80 (NCRP, 1985). The Nuclear Regulatory Commission (NRC) and the ICRP have also adopted this approach (NRC, 1991, 1993; ICRP, 1991). The mortality risk is assumed to be one-tenth the morbidity risk. The estimated morbidity and mortality risks are each reduced by a factor of 3 in the case of exposures to

iodine-125, -129, and -131. This reduction includes the effect of lowered dose rate on the risk, as well as other possible factors. Hence, the DDREF of 2 applied to organ specific risk estimates is not applied in the case of exposure to these radionuclides. A latency period of 5 y is assumed for radiogenic thyroid cancers.

As a basis for estimating radiation-induced bone sarcomas, the EPA has adopted BEIR IV's risk estimate based on alpha irradiation by ^{224}Ra (NAS, 1988). However, this risk estimate refers to *average skeletal dose* and has previously been applied incorrectly as endosteal cell dose. For example, bone cancer risk appears to be substantially overestimated in ICRP Publication 60 (1991) due to a confusion between endosteal and average skeletal doses (Puskin et al., 1992). Because the bone seeker ^{224}Ra decays quickly, the endosteal dose from injected ^{224}Ra is estimated to be an order of magnitude higher than the average skeletal dose. Thus, a risk model coefficient derived in terms of average skeletal dose, if applied to average endosteal dose, would overestimate the radiation-related risk of bone cancer. Risk model coefficients for high-dose, low-LET radiation are derived by dividing values based on alpha irradiation by a factor of 10 and reducing the risk model coefficients by another 30% to account for the fact that about 70% of bone sarcomas are fatal. Following BEIR III (NAS, 1980), a constant absolute risk model is used to project risk, with an expression period extending from 2 to 27 y after exposure.

For breast cancer, the EPA has adopted a model of Gilbert developed for the U.S. Nuclear Regulatory Commission (NRC, 1991, 1993) and based on data for persons receiving medical exposures to radiation. A major issue with regard to breast cancer is in the transport of risk from Japan to the U.S., where the baseline rates are much higher. The model of Gilbert for breast cancer avoids this problem because it is based on North American data.

Site-specific cancer mortality risk estimates from low-dose, low-LET uniform irradiation of the whole body, based on the risk model coefficients in Tables 7.1 and 7.2, are given in Table 7.3. These estimates are age-averaged values for the hypothetical stationary population described in Chapter 3. The method of computation is described in a later section.

Association of cancer type with dose location

The dose locations associated with the different cancer types are shown in Table 7.4. When more than one dose location is associated with a given cancer type, risks are calculated for a weighted mean of the doses at these locations using the weights shown in the table. For specific cancer types, the association of cancer type with dose location follows recommendations in ICRP

Table 7.3. Age-averaged site-specific cancer mortality risk estimates (cancer deaths per person-Gy) from low-dose, low-LET uniform irradiation of the body.

Site	Males	Females	Combined genders
Esophagus	7.30×10^{-4}	1.59×10^{-3}	1.17×10^{-3}
Stomach	3.25×10^{-3}	4.86×10^{-3}	4.07×10^{-3}
Colon	8.38×10^{-3}	1.24×10^{-2}	1.04×10^{-2}
Liver	1.84×10^{-3}	1.17×10^{-3}	1.50×10^{-3}
Lung	7.71×10^{-3}	1.19×10^{-2}	9.88×10^{-3}
Bone	9.40×10^{-5}	9.60×10^{-5}	9.50×10^{-5}
Skin	9.51×10^{-5}	1.05×10^{-4}	1.00×10^{-4}
Breast	—	9.90×10^{-3}	5.06×10^{-3}
Ovary	—	2.92×10^{-3}	1.49×10^{-3}
Bladder	3.28×10^{-3}	1.52×10^{-3}	2.38×10^{-3}
Kidney	6.43×10^{-4}	3.92×10^{-4}	5.15×10^{-4}
Thyroid	2.05×10^{-4}	4.38×10^{-4}	3.24×10^{-4}
Leukemia	6.48×10^{-3}	4.71×10^{-3}	5.57×10^{-3}
Residual ^a	1.35×10^{-2}	1.63×10^{-2}	1.49×10^{-2}
Total	4.62×10^{-2}	6.83×10^{-2}	5.75×10^{-2}

^aResidual is a composite of all radiogenic cancers that are not explicitly identified by site in the model.

Publication 60 (1991), except that the weights assigned to regions within the colon and lung are based on more recent recommendations in ICRP Publication 66 (1994a) and 67 (1993), respectively. The residual cancer category represents a composite of primary and secondary cancers that are not otherwise considered in the model. The three dose locations associated with these cancers (skeletal muscle, pancreas, and adrenals) were chosen to be generally representative of doses to soft tissues and are not considered to be the sites where all residual neoplasms originate.

Table 7.4. Dose regions associated with cancer types.

Cancer type	Dose region	Weighting factor
Esophagus	Esophagus ^a	1.0
Stomach	Stomach Wall	1.0
Colon	Upper Large Intestine Wall	0.568
	Lower Large Intestine Wall	0.432
Liver	Liver	1.0
Lung	Bronchial Region – Basal Cells	0.1667
	Bronchial Region – Secretory Cells	0.1667
	Bronchiolar Region – Secretory Cells	0.3333
	Alveolar-Interstitial Region	0.3333
Bone	Bone Surface	1.0
Skin	Skin	1.0
Breast	Breasts	1.0
Ovary	Ovaries	1.0
Bladder	Urinary Bladder Wall	1.0
Kidney	Kidney	1.0
Thyroid	Thyroid	1.0
Leukemia	Red Marrow	1.0
Residual	Muscle	0.3334
	Pancreas	0.3333
	Adrenals	0.3333

^aFor intakes of radionuclides, the estimated dose to the thymus is applied to the esophagus, which is not represented explicitly in the mathematical phantoms used for internal dosimetric calculations. The esophagus is represented explicitly in the phantom used for external dose calculations (EPA, 1993).

Relation between cancer mortality and morbidity

To obtain estimates of radiation-induced cancer morbidity, each site-specific mortality risk estimate is divided by its respective lethality fraction, that is, the fraction of radiogenic cancers at that site which are fatal. Aside from thyroid cancer, the lethality fraction is generally assumed to

Table 7.5. Lethality data for cancers by site in adults.^a

Cancer site	Lethality fraction <i>k</i>
Esophagus	0.95
Stomach	0.90
Colon	0.55
Liver	0.95
Lung	0.95
Bone	0.70
Skin ^b	0.002
Breast	0.50
Ovary	0.70
Bladder	0.50
Kidney	0.65
Thyroid	0.10
Leukemia (acute)	0.99
Residual	0.71

^aLethality fractions (mortality-to-morbidity ratios) are from Tables B-19 and B-20 of ICRP Publication 60 (ICRP, 1991).

^bAt least 83% of skin cancers are basal cell carcinomas (~0.01% lethality) and the remainder are squamous cell carcinomas (~1% lethality). The morbidity estimates for skin cancer given in this report reflect only fatal cases and omit the much larger number of nonfatal cases, most of which are easily curable and result in little trauma for the patient (ICRP, 1992). Left untreated, however, non-fatal skin cancers may require intensive medical treatment or be disfiguring.

be the same for radiogenic cancers as for the totality of other cancers at that site. A list of lethality fractions recommended in ICRP Publication 60 (1991) and adopted by the EPA (1994) is reproduced in Table 7.5.

Site-specific cancer morbidity risk estimates from low-dose, low-LET uniform irradiation of the whole body, based on the data in Tables 7.5, are given in Table 7.6. These estimates are age-

Table 7.6. Age-averaged site-specific cancer morbidity risk estimates (cancer cases per person-Gy) from low-dose, low-LET uniform irradiation of the body.

Site	Male	Female	Combined genders
Esophagus	7.69×10^{-4}	1.68×10^{-3}	1.23×10^{-3}
Stomach	3.61×10^{-3}	5.40×10^{-3}	4.53×10^{-3}
Colon	1.52×10^{-2}	2.25×10^{-2}	1.89×10^{-2}
Liver	1.94×10^{-3}	1.23×10^{-3}	1.58×10^{-3}
Lung	8.12×10^{-3}	1.26×10^{-2}	1.04×10^{-2}
Bone	1.34×10^{-4}	1.37×10^{-4}	1.36×10^{-4}
Skin ^a	9.51×10^{-5}	1.05×10^{-4}	1.00×10^{-4}
Breast	—	1.98×10^{-2}	1.01×10^{-2}
Ovary	—	4.17×10^{-3}	2.13×10^{-3}
Bladder	6.55×10^{-3}	3.04×10^{-3}	4.76×10^{-3}
Kidney	9.88×10^{-4}	6.03×10^{-4}	7.91×10^{-4}
Thyroid	2.05×10^{-3}	4.38×10^{-3}	3.24×10^{-3}
Leukemia	6.54×10^{-3}	4.75×10^{-3}	5.63×10^{-3}
Residual ^b	1.91×10^{-2}	2.29×10^{-2}	2.11×10^{-2}
Total	6.51×10^{-2}	1.03×10^{-1}	8.46×10^{-2}

^aSkin cancer morbidity risk coefficients include fatal cancer risks only. See text.

^bResidual is a composite of all radiogenic cancers that are not explicitly identified by site in the model.

averaged values for the hypothetical stationary population described in Chapter 3. The method of computation is described in a later section.

Based on the methods of this report, skin is projected to contribute most of the nonfatal cancers induced by uniform whole body irradiation. At least 83% of all skin cancers are basal cell carcinomas and the remainder are squamous cell carcinomas. Approximately 99.99% of the former and 99% of the latter are non-fatal. The morbidity estimates for skin cancer given in the present report reflect only fatal cases.

Treatment of discontinuities in risk model coefficients

The radiogenic cancer models described in the preceding sections are discontinuous at some times. For example, the function $\zeta(t)$ that describes the period of expression of risk for solid cancers typically has a value of zero for times between exposure and 10 y after exposure but suddenly jumps to a value of 1 starting at 10 y after exposure.

To calculate a risk coefficient for a given radionuclide and environmental medium, it is necessary to integrate functions that include such discontinuous risk model functions as factors. The integration is accomplished by fitting a smoothly varying spline function to the integrand and performing a straightforward integration of the spline function. The difficulty arises that the integral of the spline function may include unintended contributions to the risk. For example, suppose that the function to be integrated (the integrand) includes the function $\zeta(t)$ described above as a factor, and suppose the integrand is evaluated at one-year increments. Fitting a spline to the integrand provides a continuous transition from the value at 9 y to the value at 10 y but includes an unintended contribution from this interval. The problem is resolved by replacing the value of the discontinuous function at the discontinuity with the average of the values immediately above and below it. For this case, the value of the function $\zeta(t)$ at $t=10$ y is changed from 1 to $(0 + 1) / 2 = 0.5$.

Computation of radionuclide risk coefficients

The calculations of radiogenic risk in this report account for the possibility that an exposed person who may have eventually died from, or developed, a radiogenic cancer will die at an earlier age from a competing cause of death. It is assumed that the survival function is not significantly affected by the exposures being assessed, that is, that the number of radiogenic cancer deaths at any age is small compared with the number of deaths at that age from competing causes. Therefore, the risk coefficients tabulated in this document should not be applied to exposure levels that are sufficiently high to cause a substantial increase in the mortality rate at any age.

The age-specific cancer risk attributable to a unit intake of a radionuclide is calculated from the absorbed dose rate due to a unit intake of the radionuclide and the age-specific risk per unit dose model coefficients. The calculation is specific for each cancer and associated absorbed dose site in the risk model. The complete calculation may involve the sum of contributions from more than one target tissue and from both low- and high-LET absorbed doses.

The age-specific *lifetime risk coefficient (LRC)*, $r(x)$, is the risk per unit absorbed dose of a subsequent cancer death (Gy^{-1}) due to radiation received at age x . In the EPA report on radiation risk

models (EPA, 1994), $r(x)$ is referred to as an *attributable lifetime risk (ALR) coefficient*, but the terminology has been changed for use in this report because the term *attributable risk* is defined differently by different authors.

For an absolute risk model, the *LRC* for a given contribution is

$$r(x) = \frac{\int_0^{\infty} \alpha(x) \zeta(z-x) S(z) dz}{S(x)} \quad (7.4)$$

where α is the risk model coefficient in Eq. 7.1, ζ defines the plateau period (Eq. 7.1), and S is the survival function, that is, the fraction of live-born individuals in an unexposed population expected to survive to a given age. $S(0) = 1$, and S decreases monotonically for increasing values of x . $S(x)$ is obtained by a spline fit to decennial life table values to provide a continuous function of x .

Similarly, for a relative risk model,

$$r(x) = \frac{\int_0^{\infty} \eta(z,x) \mu(z) S(z) dz}{S(x)} \quad (7.5)$$

where $\eta(z,x)$ is the relative risk at age z due to a dose received at age x and $\mu(z)$ is the baseline force of mortality at age z for the given cancer type.

Following a unit intake of a radionuclide at age x_i , the absorbed dose rate $\dot{D}(x)$ to a given target tissue varies continuously with age $x \geq x_i$. The cancer risk $r_a(x_i)$ resulting from a unit intake of a radionuclide at age x_i is calculated from the continuously varying absorbed dose rate $\dot{D}(x)$ as follows:

$$r_a(x_i) = \frac{\int_{x_i}^{\infty} \dot{D}(x) r(x) S(x) dx}{S(x_i)} \quad (7.6)$$

where $r(x)$ is the cancer risk due to a unit absorbed dose (Gy^{-1}) at the site at age x . The absorbed dose rate is the absorbed dose rate for low-LET radiation, plus the product of the high-LET absorbed dose rate and the RBE applicable to the cancer type.

Age-specific male and female risk coefficients are combined by calculating a weighted mean:

$$r_a(x_i) = \frac{1.05 r_{ma}(x_i) u_m(x_i) S_m(x_i) + r_{fa}(x_i) u_f(x_i) S_f(x_i)}{1.05 S_m(x_i) u_m(x_i) + S_f(x_i) u_f(x_i)} \quad (7.7)$$

where

$r_a(x_i)$ is the combined cancer risk coefficient for a unit intake of activity at age x_i ,

1.05 is the presumed sex ratio at birth (male-to-female),

$r_{ma}(x_i)$ is the male risk per unit activity at age x_i ,

$r_{fa}(x_i)$ is the female risk per unit activity at age x_i ,

$S_m(x_i)$ is the male survival function at age x_i ,

$S_f(x_i)$ is the female survival function at age x_i , and

$u_m(x_i)$ and $u_f(x_i)$ are the usage rates (see Chapter 3) of the contaminated medium for males and females, respectively.

This formulation weights each sex-specific risk coefficient by the proportion of that sex in a stationary combined population at the desired age of intake.

The average lifetime risk coefficient for a radionuclide intake presumes that the intake rate is proportional to a constant environmental concentration (e.g., the radionuclide concentration in air). However, usage (e.g., the breathing rate) is also age and gender specific and therefore must be included in the averaging process. Defining the average lifetime risk as the quotient of the expected lifetime risk and the expected lifetime intake from exposure to a constant environmental concentration yields

$$\bar{r}_a = \frac{\int_0^{\infty} u(x) r_a(x) S(x) dx}{\int_0^{\infty} u(x) S(x) dx} \quad (7.8)$$

The radionuclide concentration in the environmental medium does not appear in the expression because it is a common factor in the numerator and denominator.

The above description applies to a stationary population that is subject to fixed gender-specific survival functions and fixed cancer mortality rates. In such a population, the age distribution of a given gender is proportional to the survival function for that gender. The derived risk coefficients may be interpreted either as risk per unit exposure to a typical member of the population exposed throughout life to a constant concentration of a radionuclide in an environmental medium, or as average risk per unit exposure to members of the population due to acute exposure to that radionuclide in that environmental medium. As discussed in Appendix E, a similar analysis may be applied to the case of acute exposure of a population with an arbitrary age distribution, if it is assumed that the exposed population is subject to fixed gender-specific survival functions and fixed cancer mortality rates at all times after the exposure. In this case, the survival function $S(x)$ in Eq. 7.8 is replaced by a function $P(x)$ representing the age distribution of the population at the time of acute exposure.

Lifetime risks for external radionuclide exposures are calculated in a manner similar to that for radionuclide intakes. Since the external exposure is not considered to be age dependent, the calculation is simpler. Given the age-specific cancer risk per unit dose, $r(x)$, and the corresponding dose per unit exposure coefficient, d_e , the lifetime risk is simply

$$r_e(x) = d_e r(x) \quad (7.9)$$

for an external exposure at age x . Age-specific male and female risk coefficients are combined by calculating a weighted mean as in Eq. 7.7, but with the usage rates $u_m(x_i)$ and $u_f(x_i)$ removed from that equation. For lifetime external exposure at a constant exposure rate, d_e , the average lifetime risk is

$$\bar{r}_e = \frac{\int_0^{\infty} r_e(x) S(x) dx}{\int_0^{\infty} S(x) dx} \quad (7.10)$$

where $r_e(x)$ is given in Eq. 7.9 and $S(x)$ is the gender-weighted survival function. This equation applies to a specific cancer site. The total risk is the sum over all cancer sites.

APPENDIX A. MODELS FOR MORTALITY RATES FOR ALL CAUSES AND FOR SPECIFIC CANCERS

The life tables used in this report are based on data prepared by the National Center for Health Statistics for the U.S. Decennial Life Tables for 1989-91 (NCHS, 1997). The data are given in terms of $q(x)$, the probability of death in the age interval beginning at age x (NCHS, 1997, Tables 2 and 3). For each gender, tabulations are for age intervals from 0-1, 1-7, 7-28, and 28-365 days, and from 0-1 through 109-110 y in one-year increments. For purposes of this report, these values of $q(x)$ were extended in one year intervals to ages 110 y and above using the same methods that had been used to calculate the values for ages 100 to 109 y (Bell et al., 1992). Briefly, it is assumed that for $x > 109$ y, $q(x)$ for males is the minimum of $1.05q(x-1)$ and 1.0, and $q(x)$ for females is the minimum of $1.06q(x-1)$ and the value $q(x)$ for males. The completed set of values of $q(x)$ were then used to calculate $S(x)$, the probability of survival to age x [that is, $S(x) = (1-q(x-1))S(x-1)$] and $e^{\circ}(x)$, the expected life time remaining at age x . Values of $S(x)$ and $e^{\circ}(x)$ for a combined population were calculated for a male-to-female live birth ratio of 1.050. The derived values of $S(x)$ and $e^{\circ}(x)$ are shown in Table A.1.

For consistency with the survival data, age- and gender-specific cancer mortality rates (force of mortality) were calculated using NCHS data for reported deaths during 1989-91 (NCHS, 1992, 1993a, 1993b). Because of the small numbers of deaths for specific cancer sites at some ages, reasonably smooth force of mortality curves cannot be obtained by simply fitting the death data in one-year intervals. The method used here combines the one-year interval death data, starting with the first age with at least one death, into intervals of one or more years that contain at least five deaths. Above age 95 y, the one-year intervals are combined into a single group ending at the last age with any reported deaths. Cumulative deaths, expressed as a fraction of the total number of deaths in the interval in a stationary population defined by the gender-specific survival functions, are calculated at the end of each age interval. A third-order hermite polynomial spline (Fritsch and Carlson, 1980) is then fitted to these values. The “force of mortality” associated with a given cancer site and age is calculated as the quotient of the first derivative (with respect to age) of the spline fit to the cumulative deaths and the value of the survival function at that age.

The force of mortality estimate at the maximum reported age is applied to subsequent ages, and a value of zero is applied to ages below the minimum reported age. Finally, the calculated force of mortality data are smoothed by convolution with a gaussian response function with a full-width-half-maximum value of 3 years. Although the reported death data are discrete values for one-year intervals, the derived forces of mortality are continuous functions of age.

Table A.1. Gender- and age-specific values for the survival function, $S(x)$, and the expected remaining lifetime, $e^o(x)$, used in this report.

Age (y)	$S(x)$			$e^o(x)$		
	Combined	Male	Female	Combined	Male	Female
0	1.0000	1.0000	1.0000	75.24	71.83	78.81
1	9.9064E-01	9.8961E-01	9.9173E-01	74.94	71.58	78.47
2	9.8992E-01	9.8884E-01	9.9106E-01	74.00	70.64	77.52
3	9.8944E-01	9.8830E-01	9.9064E-01	73.03	69.68	76.55
4	9.8908E-01	9.8789E-01	9.9033E-01	72.06	68.70	75.58
5	9.8878E-01	9.8754E-01	9.9008E-01	71.08	67.73	74.60
6	9.8851E-01	9.8723E-01	9.8984E-01	70.10	66.75	73.61
7	9.8826E-01	9.8696E-01	9.8963E-01	69.12	65.77	72.63
8	9.8804E-01	9.8670E-01	9.8944E-01	68.13	64.78	71.64
9	9.8784E-01	9.8647E-01	9.8928E-01	67.15	63.80	70.65
10	9.8766E-01	9.8628E-01	9.8912E-01	66.16	62.81	69.67
11	9.8750E-01	9.8611E-01	9.8897E-01	65.17	61.82	68.68
12	9.8735E-01	9.8594E-01	9.8882E-01	64.18	60.83	67.69
13	9.8713E-01	9.8570E-01	9.8864E-01	63.20	59.85	66.70
14	9.8682E-01	9.8528E-01	9.8843E-01	62.22	58.87	65.71
15	9.8636E-01	9.8465E-01	9.8815E-01	61.24	57.91	64.73
16	9.8574E-01	9.8377E-01	9.8780E-01	60.28	56.96	63.75
17	9.8498E-01	9.8267E-01	9.8740E-01	59.33	56.03	62.78
18	9.8410E-01	9.8140E-01	9.8694E-01	58.38	55.10	61.81
19	9.8315E-01	9.8000E-01	9.8646E-01	57.44	54.17	60.84
20	9.8217E-01	9.7855E-01	9.8597E-01	56.49	53.25	59.87
21	9.8114E-01	9.7703E-01	9.8545E-01	55.55	52.34	58.90
22	9.8008E-01	9.7546E-01	9.8492E-01	54.61	51.42	57.93
23	9.7897E-01	9.7383E-01	9.8437E-01	53.67	50.51	56.96
24	9.7785E-01	9.7218E-01	9.8381E-01	52.73	49.59	56.00
25	9.7671E-01	9.7050E-01	9.8324E-01	51.79	48.68	55.03
26	9.7556E-01	9.6881E-01	9.8266E-01	50.86	47.76	54.06
27	9.7440E-01	9.6710E-01	9.8207E-01	49.92	46.84	53.09
28	9.7321E-01	9.6536E-01	9.8146E-01	48.98	45.93	52.12
29	9.7197E-01	9.6356E-01	9.8081E-01	48.04	45.01	51.16
30	9.7067E-01	9.6167E-01	9.8013E-01	47.10	44.10	50.19
31	9.6930E-01	9.5970E-01	9.7939E-01	46.17	43.19	49.23
32	9.6786E-01	9.5763E-01	9.7861E-01	45.23	42.28	48.27
33	9.6636E-01	9.5549E-01	9.7778E-01	44.30	41.37	47.31
34	9.6479E-01	9.5325E-01	9.7690E-01	43.38	40.47	46.35
35	9.6314E-01	9.5092E-01	9.7597E-01	42.45	39.57	45.40
36	9.6140E-01	9.4847E-01	9.7498E-01	41.52	38.67	44.44
37	9.5958E-01	9.4591E-01	9.7394E-01	40.60	37.77	43.49
38	9.5767E-01	9.4324E-01	9.7282E-01	39.68	36.88	42.54
39	9.5567E-01	9.4048E-01	9.7162E-01	38.76	35.98	41.59
40	9.5358E-01	9.3762E-01	9.7034E-01	37.85	35.09	40.65
41	9.5140E-01	9.3467E-01	9.6896E-01	36.93	34.20	39.70
42	9.4910E-01	9.3160E-01	9.6748E-01	36.02	33.31	38.76
43	9.4668E-01	9.2840E-01	9.6587E-01	35.11	32.43	37.83
44	9.4409E-01	9.2501E-01	9.6413E-01	34.21	31.54	36.89
45	9.4132E-01	9.2140E-01	9.6223E-01	33.31	30.66	35.97
46	9.3831E-01	9.1752E-01	9.6013E-01	32.41	29.79	35.04
47	9.3502E-01	9.1333E-01	9.5780E-01	31.52	28.93	34.13
48	9.3145E-01	9.0880E-01	9.5524E-01	30.64	28.07	33.22
49	9.2758E-01	9.0392E-01	9.5242E-01	29.77	27.22	32.31
50	9.2339E-01	8.9868E-01	9.4933E-01	28.90	26.37	31.42
51	9.1884E-01	8.9301E-01	9.4595E-01	28.04	25.54	30.53
52	9.1387E-01	8.8686E-01	9.4223E-01	27.19	24.71	29.65
53	9.0844E-01	8.8017E-01	9.3814E-01	26.35	23.89	28.77
54	9.0253E-01	8.7288E-01	9.3367E-01	25.52	23.09	27.91
55	8.9610E-01	8.6494E-01	9.2882E-01	24.70	22.30	27.05
56	8.8913E-01	8.5634E-01	9.2356E-01	23.89	21.52	26.20
57	8.8157E-01	8.4701E-01	9.1785E-01	23.09	20.75	25.36
58	8.7334E-01	8.3687E-01	9.1164E-01	22.30	19.99	24.53
59	8.6437E-01	8.2583E-01	9.0485E-01	21.53	19.25	23.71
60	8.5460E-01	8.1381E-01	8.9744E-01	20.77	18.53	22.90

Table A.1, continued

Age (y)	S(x)			$\hat{e}(x)$		
	Combined	Male	Female	Combined	Male	Female
61	8.4405E-01	8.0086E-01	8.8940E-01	20.02	17.82	22.11
62	8.3274E-01	7.8701E-01	8.8076E-01	19.29	17.13	21.32
63	8.2064E-01	7.7224E-01	8.7147E-01	18.57	16.44	20.54
64	8.0770E-01	7.5649E-01	8.6148E-01	17.86	15.78	19.77
65	7.9390E-01	7.3974E-01	8.5076E-01	17.16	15.12	19.02
66	7.7922E-01	7.2201E-01	8.3930E-01	16.47	14.48	18.27
67	7.6370E-01	7.0334E-01	8.2708E-01	15.79	13.85	17.53
68	7.4729E-01	6.8369E-01	8.1406E-01	15.13	13.23	16.80
69	7.2989E-01	6.6298E-01	8.0014E-01	14.48	12.63	16.09
70	7.1140E-01	6.4109E-01	7.8522E-01	13.84	12.05	15.38
71	6.9173E-01	6.1797E-01	7.6919E-01	13.22	11.48	14.69
72	6.7085E-01	5.9359E-01	7.5197E-01	12.62	10.93	14.02
73	6.4873E-01	5.6801E-01	7.3349E-01	12.03	10.40	13.36
74	6.2547E-01	5.4137E-01	7.1377E-01	11.46	9.89	12.71
75	6.0118E-01	5.1387E-01	6.9286E-01	10.90	9.39	12.08
76	5.7598E-01	4.8565E-01	6.7082E-01	10.36	8.90	11.46
77	5.4988E-01	4.5679E-01	6.4764E-01	9.82	8.44	10.85
78	5.2292E-01	4.2742E-01	6.2321E-01	9.31	7.98	10.26
79	4.9505E-01	3.9763E-01	5.9734E-01	8.80	7.54	9.68
80	4.6622E-01	3.6750E-01	5.6987E-01	8.31	7.12	9.12
81	4.3643E-01	3.3706E-01	5.4077E-01	7.85	6.72	8.59
82	4.0583E-01	3.0647E-01	5.1017E-01	7.40	6.34	8.07
83	3.7468E-01	2.7609E-01	4.7821E-01	6.97	5.98	7.58
84	3.4339E-01	2.4650E-01	4.4512E-01	6.56	5.64	7.10
85	3.1230E-01	2.1816E-01	4.1115E-01	6.17	5.30	6.65
86	2.8153E-01	1.9116E-01	3.7643E-01	5.79	4.98	6.22
87	2.5117E-01	1.6550E-01	3.4113E-01	5.43	4.68	5.81
88	2.2156E-01	1.4140E-01	3.0573E-01	5.09	4.39	5.42
89	1.9307E-01	1.1910E-01	2.7074E-01	4.76	4.12	5.06
90	1.6604E-01	9.8784E-02	2.3666E-01	4.46	3.87	4.72
91	1.4063E-01	8.0549E-02	2.0372E-01	4.17	3.63	4.40
92	1.1706E-01	6.4441E-02	1.7231E-01	3.92	3.42	4.11
93	9.5685E-02	5.0524E-02	1.4310E-01	3.68	3.23	3.85
94	7.6820E-02	3.8824E-02	1.1672E-01	3.47	3.06	3.61
95	6.0582E-02	2.9266E-02	9.3463E-02	3.26	2.90	3.39
96	4.6893E-02	2.1656E-02	7.3392E-02	3.08	2.74	3.18
97	3.5553E-02	1.5693E-02	5.6407E-02	2.90	2.60	2.99
98	2.6410E-02	1.1151E-02	4.2432E-02	2.74	2.47	2.81
99	1.9215E-02	7.7620E-03	3.1241E-02	2.59	2.34	2.65
100	1.3686E-02	5.2851E-03	2.2507E-02	2.44	2.22	2.49
101	9.5253E-03	3.5144E-03	1.5837E-02	2.30	2.10	2.34
102	6.4653E-03	2.2780E-03	1.0862E-02	2.16	1.99	2.20
103	4.2700E-03	1.4365E-03	7.2452E-03	2.03	1.88	2.06
104	2.7372E-03	8.7932E-04	4.6879E-03	1.90	1.77	1.93
105	1.6982E-03	5.2121E-04	2.9340E-03	1.78	1.67	1.80
106	1.0164E-03	2.9833E-04	1.7705E-03	1.66	1.57	1.68
107	5.8477E-04	1.6438E-04	1.0262E-03	1.55	1.47	1.56
108	3.2202E-04	8.6882E-05	5.6892E-04	1.44	1.38	1.45
109	1.6891E-04	4.3873E-05	3.0020E-04	1.34	1.29	1.35
110	8.3912E-05	2.1069E-05	1.4990E-04	1.24	1.21	1.24
111	3.9216E-05	9.5701E-06	7.0343E-05	1.14	1.12	1.15
112	1.7103E-05	4.0859E-06	3.0771E-05	1.05	1.05	1.05
113	6.8928E-06	1.6274E-06	1.2422E-05	0.97	0.97	0.97
114	2.5380E-06	5.9920E-07	4.5737E-06	0.89	0.89	0.89
115	8.5432E-07	2.0170E-07	1.5396E-06	0.82	0.82	0.82
116	2.5924E-07	6.1205E-08	4.6717E-07	0.75	0.75	0.75
117	6.9636E-08	1.6441E-08	1.2549E-07	0.68	0.68	0.68
118	1.6159E-08	3.8150E-09	2.9120E-08	0.62	0.62	0.62
119	3.1292E-09	7.3878E-10	5.6391E-09	0.55	0.55	0.55
120	4.7981E-10	1.1328E-10	8.6466E-10	0.49	0.49	0.49

APPENDIX B. ADDITIONAL DETAILS OF THE DOSIMETRIC MODELS

Definitions of special source and target regions

The source region *Body Tissues* (formerly called *Whole Body*) consists of the entire body, minus the contents of the gastrointestinal (GI) tract, the urinary bladder, the gall bladder, and the heart. Thus, *Body Tissues* consists essentially of the "living tissues" of the body. The source region *Blood* is assumed to be uniformly distributed in *Body Tissues*.

The source region *Soft Tissues* represents *Body Tissues* minus cortical and trabecular bone. This source region is used to describe the distribution of some radionuclides that are distributed throughout the soft tissues of the body but have little deposition in mineral bone.

The target region historically referred to as *Bone Surface* represents radiosensitive endosteal tissue that actually is neither bone in its composition nor a surface of bone. This target region is defined as the volume of soft tissue within 10 μm of the endosteal surface of bone. The target region *Bone Surface* should not be confused with the source regions *Cortical Bone Surface* and *Trabecular Bone Surface*, which refer to radioactivity assumed to be associated with infinitely thin surfaces of cortical and trabecular bone, respectively.

Within mineral bone, activity may be distributed within the volume of cortical or trabecular bone as well as on the surfaces of mineral bone. The four source regions *Cortical Bone Surface*, *Cortical Bone Volume*, *Trabecular Bone Surface*, and *Trabecular Bone Volume* are not used as target regions because mineral bone is not radiosensitive.

Following long-term usage in radiation dosimetry, the source or target region *Red Marrow* is identified with the hematopoietically active marrow. The percentage of active marrow cells (cellularity) within a volume of marrow varies from site to site in the skeleton. The age-specific distribution of marrow within the body and relative cellularity at different sites have been taken into account in the dosimetry.

For a given biokinetic model, the source region *Other* consists of *Body Tissues*, minus the source organs identified explicitly in the biokinetic model. The contribution of radiations emitted in *Other* to the energy deposition in a target region *T* is derived by assuming that the radioactivity is distributed uniformly by mass in *Other*.

Only source regions that are regarded as "volume sources" (that is, that have non-zero volume) may be considered as part of *Other*. Because the source regions *Cortical Bone Surface* and *Trabecular Bone Surface* are considered as infinitely thin surfaces of bone, they are not volume

sources and hence cannot be part of *Other*. However, *Cortical Bone Volume* and *Trabecular Bone Volume* are volume sources and may be part of *Other*. If no source regions in the volume of mineral bone or on its surfaces are explicitly identified in the biokinetic model, then *Other* includes radioactivity uniformly distributed by mass in *Cortical Bone Volume* and *Trabecular Bone Volume*. If any source region in the volume or on the surfaces of mineral bone is explicitly identified in the biokinetic model, then *Other* does not include any activity in mineral bone, that is, neither *Cortical Bone Volume* nor *Trabecular Bone Volume*. The entire mineral bone (*Cortical Bone Volume* plus *Trabecular Bone Volume*) is either included in *Other* or the entire mineral bone is excluded. It is never separated. *Red Marrow* will always be part of *Other* unless it is explicitly identified as a source region in the biokinetic model.

The esophagus is a radiosensitive tissue but has not yet been incorporated explicitly into the mathematical phantom used for internal dosimetric calculations. At present, the dose calculated for the target region *Thymus* is used as a surrogate for the dose to the esophagus.

Age-dependent masses of source and target regions

Age-specific masses of source and target regions are given in Table B.1. With the exception of *Urinary Bladder Contents*, values for children are taken from the phantom series of Cristy and Eckerman (1987), and those for the adult male are taken from ICRP Publication 23 on Reference Man (ICRP, 1975). Masses of *Urinary Bladder Contents* are based on data assembled for the revision of Reference Man and represent average contents (Cristy and Eckerman, 1993).

For the adult female, regional masses are mostly reference values from ICRP Publication 23 (1975) but, where none are given, are scaled from those for the reference adult male. Masses for the target region *Bone Surface* or for source regions within mineral bone of the adult female are taken as 75% of the values for males. For *Urinary Bladder Contents* and *Urinary Bladder Wall*, values for the 15-y-old male are applied to the adult female.

Absorbed fractions for radiosensitive tissues in bone

For electrons, the radiation is usually assumed to be absorbed entirely in the source region. Exceptions are made for alpha and beta emitters when the source and target regions are parts of the skeleton. The absorbed fractions in Table B.2 are taken from ICRP Publication 30, Part 1 (1979), and are applied to all ages.

Table B.1. Age-specific masses (g) of source and target organs.

Organ	Newborn	1 y	5 y	10 y	15 y	Adult female ^a	Adult male ^a
Adrenals	5.83	3.52	5.27	7.22	10.5	14.0	14.0
Brain	35.2	88.4	1260	1360	1410	1200	1400
Breasts	0.107	0.732	1.51	2.60	360	360	a
Gallbladder Contents	2.12	4.81	19.7	38.5	49.0	50.0	62.0
Gallbladder Wall	0.408	0.910	3.73	7.28	9.27	8.00	10.0
Lower Large Intestine Contents	6.98	18.3	36.6	61.7	109	135	135
Lower Large Intestine Wall	7.96	20.6	41.4	70.0	127	160	160
Small Intestine Contents	20.3	53.1	106	179	322	375	400
Small Intestine Wall	32.6	84.9	169	286	516	600	640
Stomach Contents	10.6	36.2	75.1	133	195	230	250
Stomach Wall	6.41	21.8	49.1	85.1	118	140	150
Upper Large Intestine Contents	11.2	28.7	57.9	97.5	176	210	220
Upper Large Intestine Wall	10.5	27.8	55.2	93.4	168	200	210
Heart Contents	36.5	72.7	134	219	347	410	500
Heart Wall	25.4	50.6	92.8	151	241	240	330
Kidneys	22.9	62.9	116	173	248	275	310
Liver	121	292	584	887	1400	1400	1800
Muscle	760	2500	5000	11,000	22,000	17,000	28,000
Ovaries	0.328	0.741	1.73	3.13	11.0	11.0	a
Pancreas	2.80	10.3	23.6	30.0	64.9	85.0	100
Red Marrow	47.0	150	320	610	1050	1300	1500
Cortical Bone Volume	0.0	299	875	1580	3220	3000	4000
Trabecular Bone Volume	14.0	20.0	219	396	806	750	1000
Bone Surface	15.0	26.0	37.0	68.0	120	90.0	120
Skin	118	271	538	888	2150	1790	2600
Spleen	9.11	25.5	48.3	77.4	123	150	180
Testes	0.843	1.21	1.63	1.89	15.5	0.0	35.0
Thymus	11.3	22.9	29.6	31.4	28.4	20.0	20.0
Thyroid	1.29	1.78	3.45	7.93	12.4	17.0	20.0
Urinary Bladder Contents	10.4	26.0	67.6	78.0	88.4	88.4	120

Table B.1, continued

Organ	Newborn	1 y	5 y	10 y	15 y	Adult female ^a	Adult male ^a
Urinary Bladder Wall	2.88	7.70	14.5	23.2	35.9	35.9	45.0
Uterus	3.85	1.45	2.70	4.16	80.0	80.0	80.0
Body Tissues	3535.7	9543.1	19,458	32,620	55,825	56,912	68,831
Extrathoracic 1 - Basal Cells	0.00173	0.00413	0.00828	0.0126	0.0185	0.0170	0.0200
Extrathoracic 2 - Basal Cells	0.0389	0.0930	0.186	0.284	0.416	0.390	0.450
Lymph Nodes - Extrathoracic	0.701	2.05	4.11	6.78	11.7	12.3	15.0
Bronchial - Basal Cells	0.0938	0.155	0.234	0.311	0.408	0.390	0.432
Bronchial - Secretory Cells	0.187	0.310	0.469	0.622	0.816	0.780	0.864
Bronchiolar - Secretory Cells	0.385	0.596	0.946	1.30	1.76	1.90	1.94
Alveolar-Interstitial	51.4	151	301	497	859	904	1100
Lymph Nodes - Thoracic	0.701	2.05	4.11	6.78	11.7	12.3	15.0

^aIn this report, dosimetric calculations are not performed separately for adult males and females but are based on a reference adult formed by adding the breasts, ovaries, and uterus of the adult female phantom to the adult male phantom.

Table B.2. Absorbed fractions for alpha and beta emitters in bone (ICRP, 1979, 1980).

Source Region	Target Region	α -emitter	β -emitter, average energy < 0.2 MeV	β -emitter, average energy \geq 0.2 MeV
Cortical Bone Surface	Red Marrow	0.0	0.0	0.0
Cortical Bone Volume	Red Marrow	0.0	0.0	0.0
Trabecular Bone Surface	Red Marrow	0.5	0.5	0.5
Trabecular Bone Volume	Red Marrow	0.05	0.35	0.35
Cortical Bone Surface	Bone Surface	0.25	0.25	0.015
Cortical Bone Volume	Bone Surface	0.01	0.015	0.015
Trabecular Bone Surface	Bone Surface	0.25	0.25	0.025
Trabecular Bone Volume	Bone Surface	0.025	0.025	0.025
Red Marrow	Red Marrow	1	1	1
Red Marrow	Bone Surface	(fraction endosteal tissue associated with Red Marrow) • (mass of endosteal tissue) ÷ (mass of Red Marrow) ^a		

^aThis equation corresponds to the assumption that the specific absorbed fraction in endosteal tissue is the same as that in Red Marrow itself. The fraction of endosteal tissue in whole skeleton associated with Red Marrow is assumed to be 1.0, 0.83, 0.65, 0.65, 0.65, and 0.5 for ages newborn, 1-y, 5-y, 10-y, 15-y, and adult, respectively. Adult value is from ICRP Publication 30, and other values are from Cristy and Eckerman (1987).

APPENDIX C. AN ILLUSTRATION OF THE MODELS AND METHODS USED TO CALCULATE RISK COEFFICIENTS FOR INTERNAL EXPOSURE

This appendix provides a detailed example to illustrate the models and computational steps involved in the derivation of a risk coefficient for ingestion or inhalation of a radionuclide. A secondary purpose is to illustrate some recent changes in the ICRP's biokinetic and dosimetric models (ICRP, 1989, 1993, 1994a, 1995a, 1995b)

The radionuclide selected for detailed consideration is ^{232}Th because this radionuclide represents nearly all of the different types of changes that have been made recently in the ICRP's biokinetic and dosimetric models. For example, age-dependent f_I values have been introduced for thorium and the f_I value for the adult has been changed (ICRP, 1995a); a new, age-specific systemic biokinetic model has been adopted for thorium (ICRP, 1995a); the treatment of ingrowing radioactive progeny of ^{232}Th and other thorium isotopes has been revised (ICRP, 1995a); and a new model of the biokinetics of inhaled radionuclides, including ^{232}Th , has been adopted (ICRP, 1994a).

To keep the analysis to a reasonable length, the discussion focuses on estimating the risk, per unit intake of ^{232}Th , of dying from a single cancer type. Leukemia is considered because of the relatively high degree of sophistication and detail provided in the risk model for this type of cancer. Because radiogenic leukemia is assumed to arise from irradiation of the bone marrow, discussion of the dosimetric models focuses on this tissue.

Gastrointestinal tract model and f_I values

The ICRP's model for transit of material through the gastrointestinal tract is described in Chapter 4. This model has not been changed since its appearance in ICRP Publication 30 (1979). However, applications of the model have changed in recent ICRP publications in the following ways: the model is now applied to all age groups; some of the ICRP's updated systemic biokinetic models depict secretion of activity from the systemic tissues and fluids into compartments of the gastrointestinal tract model; new f_I values have been adopted for several elements, for application to environmental intakes by the adult; and age-specific f_I values have been adopted for several elements, for application to environmental intakes.

In ICRP Publication 69 (1995a), an f_I value of 5×10^{-4} is recommended for calculation of doses from ingestion of environmental thorium by persons of age ≥ 1 y. This f_I value, which is 2.5 times the value recommended in ICRP Publication 30 (1979) for consideration of occupational

exposures to thorium, is based on experimental data on gastrointestinal absorption of thorium, neptunium, plutonium, americium, and curium in human subjects. On the basis of experimental results indicating that gastrointestinal absorption of actinide elements typically is several times higher in newborn than adult animals, an f_i value of 5×10^{-3} is assigned to infants (ICRP, 1995a).

Respiratory tract model

The ICRP's new respiratory tract model is described in Chapter 4. The present discussion focuses on predictions of the model for three hypothetical forms (absorption types) of inhaled thorium, including the distribution of thorium in the respiratory tract, its absorption to blood, and its movement from the respiratory tract to excreta, as a function of time after inhalation.

Although the respiratory tract model was designed to allow consideration of compound-specific kinetics, parameter values have been developed for only a few general situations. In current applications of the model, a given compound of an element usually is assigned to one of three default absorption types: Type F, representing fast dissolution and a high level of absorption to blood; Type M, representing an intermediate rate of dissolution and an intermediate level of absorption to blood; and Type S, representing slow dissolution and a low level of absorption to blood. Ideally, the user bases an absorption type on data on the form of material expected to be encountered. In practice, the form of the inhaled material often cannot be characterized with much confidence.

Predictions of the fate of inhaled ^{232}Th of Type F, M, or S based on the ICRP's new respiratory tract model are shown on the left side of Fig. C.1. The assumed particle size is $1 \mu\text{m}$ (AMAD). Because it is assumed in the model that the behavior of material in the respiratory tract depends only on particle size and absorption type, the predictions apply to all long-lived radionuclides whose gastrointestinal absorption is negligible compared with the indicated levels of absorption from the respiratory tract to blood. For short-lived radionuclides, the curves for the *extrathoracic (ET)*, *alveolar-interstitial (AI)*, *bronchial (BB)*, and *bronchiole (bb)* regions may decline faster and those for *Gastrointestinal (GI) excretion*, *Nasal excretion*, and *Absorption* may have lower maximum values than the curves shown in Fig. C.1 due to radioactive decay in the respiratory tract. Here, *GI excretion* represents the cumulative activity transferred from the respiratory tract to the GI Tract, and *Nasal excretion* refers to removal of material from the *ET* region directly to the environment by such mechanisms as nose blowing.

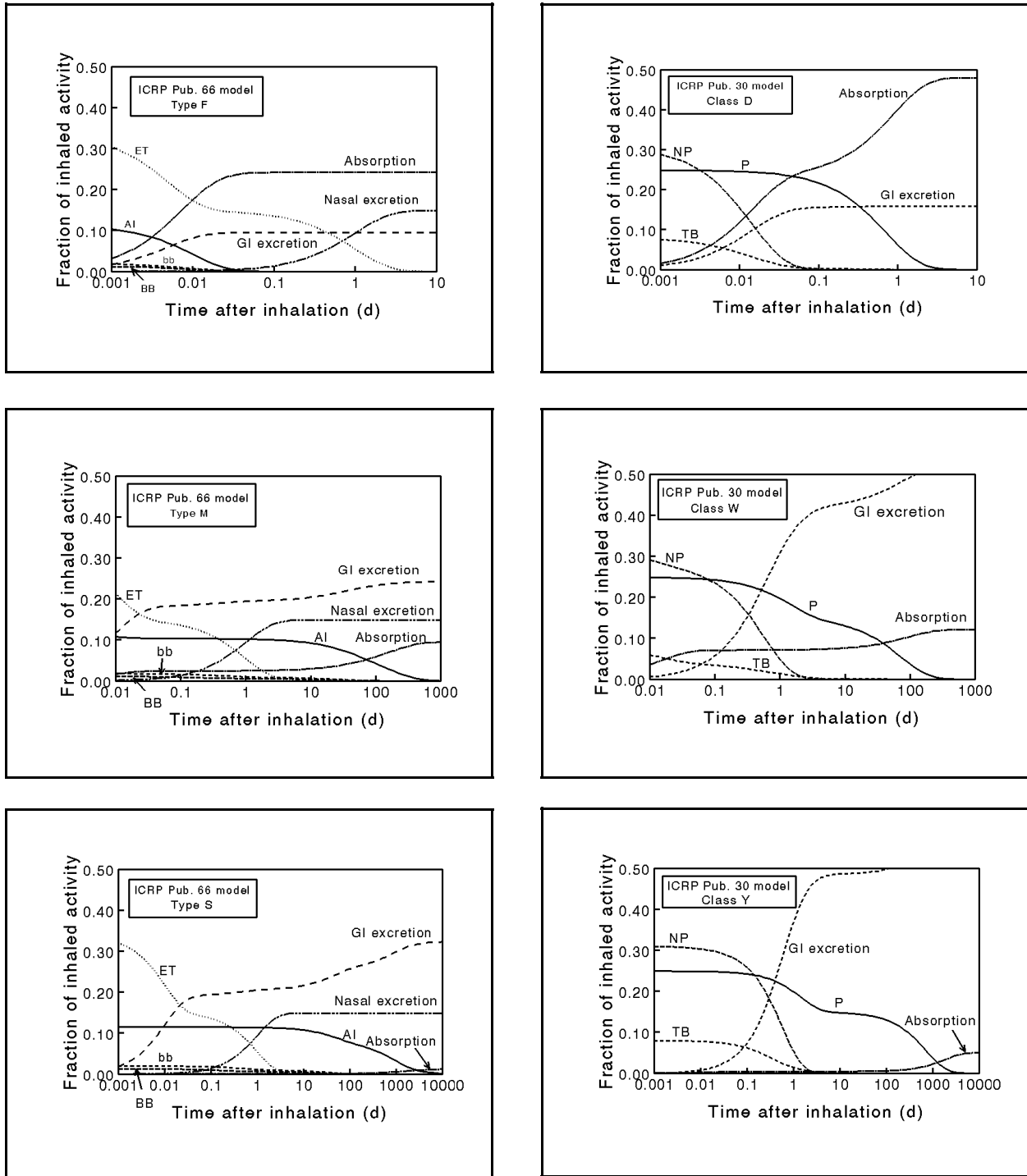


Fig. C.1. Predictions of the ICRP's updated (ICRP, 1994a) and previous (ICRP, 1979) respiratory tract models, for inhalation of ^{232}Th in soluble, moderately soluble, or insoluble 1- μm (AMAD) particles.

The three absorption types, F, M, and S, correspond roughly to the three lung clearance classes D (days), W (weeks), and Y (years) used in the ICRP's previous respiratory tract model (ICRP, 1979). Predictions of the previous model for inhaled ^{232}Th of particle size $1\ \mu\text{m}$ and clearance classes D, W, and Y are shown on the right side of Fig. C.1 for comparison with predictions of the new model. Although there is not an exact correspondence between the different regions of the two models, the *nasal-pharyngeal (NP)* region may be compared with the *ET* region, the *tracheobronchial (TB)* region with the *bronchi (BB)* plus *bronchioles (bb)*, and the *pulmonary (P)* region with the *alveolar-interstitial (AI)* region of the new model. Compared with the new model, the previous model predicts higher total deposition in the respiratory tract, greater deposition in the lower lungs, faster removal from the extrathoracic regions, and greater absorption to blood.

Biokinetics of absorbed thorium

Structure of the systemic biokinetic model for thorium

A new biokinetic model for thorium was introduced in ICRP Publication 69 (ICRP, 1995a). The model is developed within a generic model framework adopted by the ICRP for application to a class of "bone-surface-seeking" radionuclides (Fig. C.2). To this point, the generic model framework has been applied by the ICRP to thorium, plutonium, americium, curium, and neptunium.

While the model structure is generic, many of the transfer coefficients are not. Some transfer coefficients associated with compartments within the skeleton are expressed in terms of bone remodeling rates and thus are independent of the bone-surface seeker, but element-specific transfer coefficients are required for most of the paths shown in Fig. C.2.

The generic model structure divides systemic tissues and fluids into six main parts: *BLOOD*, *SKELETON*, *LIVER*, *KIDNEYS*, *GONADS*, and *OTHER SOFT TISSUES*. *BLOOD* and *GONADS* are treated as uniformly mixed pools, but each of the other major parts is further divided into a minimal number of compartments needed to explain available biokinetic data on thorium and chemically similar elements.

SKELETON is divided into cortical and trabecular fractions, and each of these is subdivided into fractions associated with bone surface, bone volume, and bone marrow. Activity entering *SKELETON* initially deposits in compartments of bone surface but is transferred gradually to bone marrow by bone resorption or to compartments of bone volume by bone formation. Activity in bone volume compartments is transferred gradually to bone marrow compartments by resorption. Activity

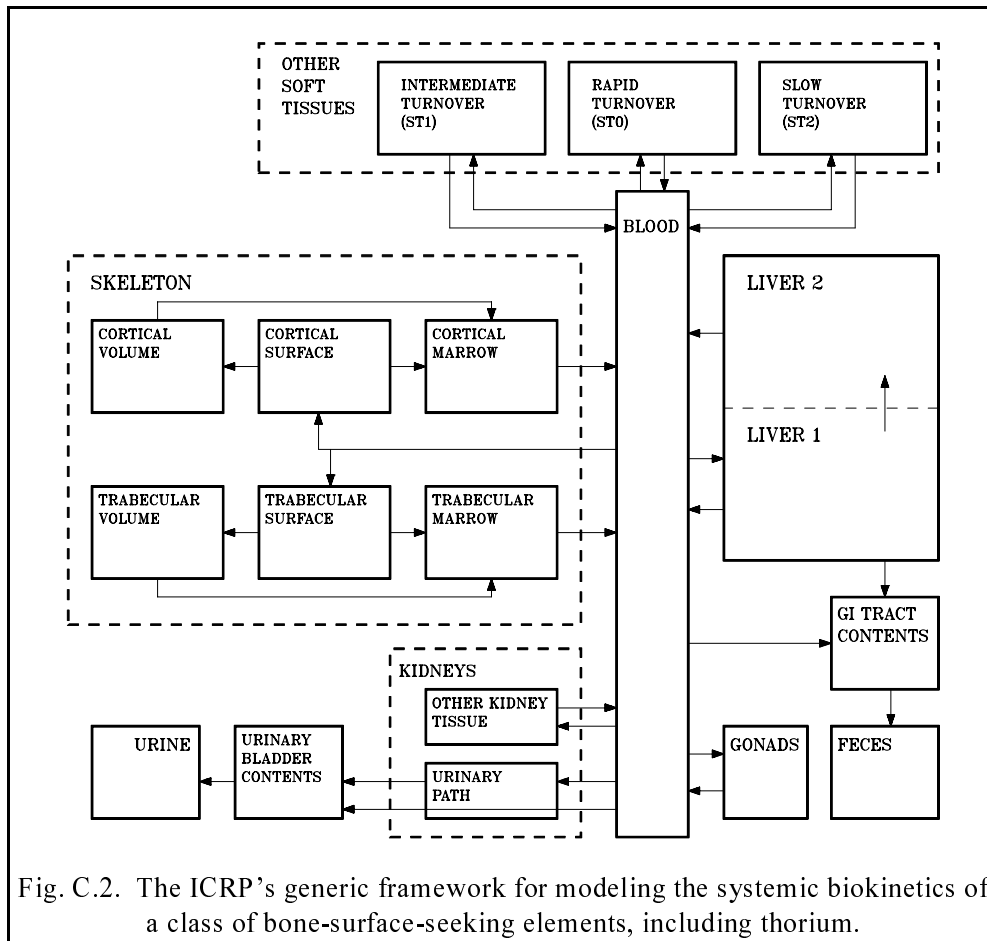


Fig. C.2. The ICRP's generic framework for modeling the systemic biokinetics of a class of bone-surface-seeking elements, including thorium.

moves from bone marrow compartments to *BLOOD* over a few months and is subsequently redistributed in the same pattern as the original input to blood.

LIVER is viewed as consisting of two compartments, called *LIVER 1* and *LIVER 2*. *LIVER 1* represents relatively short-term retention and *LIVER 2* represents relatively long-term retention in the liver. Activity entering the liver is assigned to *LIVER 1*. Activity removed from *LIVER 1* by biological processes is divided among blood, *LIVER 2*, and the contents of the GI tract. Activity leaving *LIVER 2* is assigned to blood.

KIDNEYS consists of two compartments, one that loses activity to urine and another that returns activity to blood. *URINARY BLADDER CONTENTS* is considered as a separate pool that receives all material destined for urinary excretion.

Compartment *ST0* is a soft-tissue pool that includes the extracellular fluids and exchanges material with blood over a period of hours or days. Soft-tissue compartments *ST1* and *ST2* represent intermediate-term retention (up to a few years) and tenacious retention (many years), respectively, in the massive soft tissues (for example, muscle, skin, and subcutaneous fat).

Parameter values for the systemic model for thorium

Movement of material in the body is depicted as a system of first-order processes. Parameter values are expressed as transfer coefficients (fractional transfer per day) between compartments. Age-specific transfer coefficients for thorium are listed in Table C.1 for the six ages considered in the ICRP series on age-dependent dosimetry (ICRP, 1989, 1993, 1995a, 1995b, 1996). Rates for intermediate ages are obtained by interpolating linearly with age between the listed values. For example, a given transfer coefficient for age 4 y is calculated as 0.25 times the rate given for age 1 y plus 0.75 times the rate given for age 5 y. For consideration of the biokinetics of thorium, the age of the mature adult is assumed to be ≥ 25 y.

Transfer coefficients for the adult were based largely on experimental, occupational, and environmental data on the behavior of thorium in humans, but it was necessary to use data on laboratory animals to fill gaps in the data base for man. For example, the model was required to be consistent with data on early retention, excretion, and blood clearance of thorium in healthy, elderly human subjects who received radiothorium by intravenous injection (Maletskos et al., 1966, 1969), but the early distribution of thorium in the body was based mainly on experimental data on the early distribution of thorium in beagles (Stover et al., 1960) in the absence of such information for human subjects. Parameter values controlling predictions of the long-term distribution and retention of thorium were developed mainly on the basis of bioassay or autopsy measurements on occupationally or environmentally exposed humans (Rundo, 1964; Newton et al., 1981; Wrenn et al., 1981; Singh et al., 1983; Ibrahim et al., 1983; Dang et al., 1992), together with consideration of bone restructuring rates in humans (ICRP, 1995c).

Due to the paucity of age-specific data on the biokinetics of thorium, default assumptions concerning the relative kinetics of bone seekers in children and adults were used in ICRP Publication 69 (1995a) to extend parameter values from adults to children. These assumptions are based on numerous observations of the age-specific biokinetics of various bone seekers in laboratory animals and, to a lesser extent, human subjects (Leggett, 1992a, 1992b; ICRP, 1993, 1995b). It is postulated that differences with age in the biokinetics of a bone-seeking radionuclide is determined largely by three factors: (1) increased fractional transfer from plasma to bone in children in association with

Table C.1. Age-specific transfer coefficients (d^{-1}) in the systemic biokinetic model for thorium (ICRP, 1995a).

Pathway ^a	Age (y)					
	Infant (100 d)	1 y	5 y	10 y	15 y	Adult
Blood to Liver 1	0.0647	0.0647	0.0647	0.0647	0.0647	0.0970
Blood to Cort Surf	0.7763	0.7763	0.7763	0.7763	0.7763	0.6793
Blood to Trab Surf	0.7763	0.7763	0.7763	0.7763	0.7763	0.6793
Blood to UBC	0.0711	0.0711	0.0711	0.0711	0.0711	0.1067
Blood to Urinary Path	0.0453	0.0453	0.0453	0.0453	0.0453	0.0679
Blood to OKT	0.0129	0.0129	0.0129	0.0129	0.0129	0.0194
Blood to LI Contents	0.00647	0.00647	0.00647	0.00647	0.00647	0.00970
Blood to Testes	0.000039	0.000058	0.000066	0.000077	0.00062	0.00068
Blood to Ovaries	0.000023	0.000030	0.000076	0.00013	0.00023	0.00021
Blood to ST0	0.832	0.832	0.832	0.832	0.832	0.832
Blood to ST1	0.162	0.162	0.162	0.162	0.162	0.243
Blood to ST2	0.0259	0.0259	0.0259	0.0259	0.0259	0.0388
ST0 to Blood	0.462	0.462	0.462	0.462	0.462	0.462
Urinary Path to UBC	0.0462	0.0462	0.0462	0.0462	0.0462	0.0462
OKT to Blood	0.00038	0.00038	0.00038	0.00038	0.00038	0.00038
ST1 to Blood	0.00095	0.00095	0.00095	0.00095	0.00095	0.00095
ST2 to Blood	0.000019	0.000019	0.000019	0.000019	0.000019	0.000019
Trab Surf to Trab Vol	0.00822	0.00288	0.00181	0.00132	0.000959	0.000247
Trab Surf to Bone Marrow	0.00822	0.00288	0.00181	0.00132	0.000959	0.000493
Cort Surf to Cort Vol	0.00822	0.00288	0.00153	0.000904	0.000521	0.0000411
Cort Surf to Bone Marrow	0.00822	0.00288	0.00153	0.000904	0.000521	0.0000821
Trab Vol to Bone Marrow	0.00822	0.00288	0.00181	0.00132	0.000959	0.000493
Cort Vol to Bone Marrow	0.00822	0.00288	0.00153	0.000904	0.000521	0.0000821
Bone Marrow to Blood	0.0076	0.0076	0.0076	0.0076	0.0076	0.0076
Liver 1 to Liver 2	0.00095	0.00095	0.00095	0.00095	0.00095	0.00095
Liver 1 to SI Contents	0.000475	0.000475	0.000475	0.000475	0.000475	0.000475
Liver 1 to Blood	0.000475	0.000475	0.000475	0.000475	0.000475	0.000475
Liver 2 to Blood	0.000211	0.000211	0.000211	0.000211	0.000211	0.000211
Testes/Ovaries to Blood	0.00019	0.00019	0.00019	0.00019	0.00019	0.00019

^aCort = Cortical, Trab = Trabecular, Surf = Surface, Vol = Volume, UBC = Urinary Bladder Contents, OKT = Other Kidney Tissue, LI = Large Intestine, SI = Small Intestine.

elevated bone formation rates in the maturing skeleton; (2) decreased fractional transfer from plasma to soft tissues and excreta in children due to relatively greater competition from immature bone; and (3) an elevated rate of transfer from bone to plasma in children due to an elevated rate of bone turnover. For actinide elements, the additional assumption is made that fractional deposition in the gonads at a given age depends on the mass of the gonads at that age. Except where there is evidence to the contrary, removal half-times from soft tissues, bone surfaces, and exchangeable bone volume are assumed to be independent of age.

In the model for thorium, the deposition fraction on all bone surfaces combined is set at 0.8 for ages ≤ 15 y compared with 0.7 for adults, and the deposition fractions in soft tissues and excretion pathways are reduced by one-third for application to ages ≤ 15 y to maintain mass balance. Of greater importance for dose estimates for thorium isotopes in children, however, is the generic assumption that the removal rate of thorium from bone surfaces, its rate of burial in bone volume, and its rate of removal from bone volume to blood (via bone marrow) are all directly related to the bone remodeling rate, which is estimated to be several-fold higher in children than in adults. For example, ICRP Publication 70 (1995c) gives reference values for the remodeling rate of trabecular bone of more than $100\% \text{ y}^{-1}$ for ages ≤ 1 y, $48\% \text{ y}^{-1}$ for age 10 y, and an average of $18\% \text{ y}^{-1}$ for ages ≥ 25 y.

Predicted differences with age in the systemic biokinetics of thorium

Predicted differences with age in the biokinetics of thorium are illustrated in Fig. C.3, which shows the estimated retention of ^{232}Th on trabecular surfaces as a function of time after intravenous injection at each of three injection ages: infancy (100 d), age 10 y, and age 25 y. The model predicts that there is greater deposition on trabecular surfaces in children than adults but that the bone surface activity declines at a considerably higher rate in children than in adults due to elevated bone turnover rates in children. Part of the activity removed from bone surfaces is assumed to be buried in bone volume. The remainder is assumed to be removed to bone marrow and then to blood, after which a small fraction is excreted and the remainder is recycled to bone surfaces and soft tissues. Activity in bone volume is also assumed to be recycled in the same manner after its gradual release due to bone remodeling.

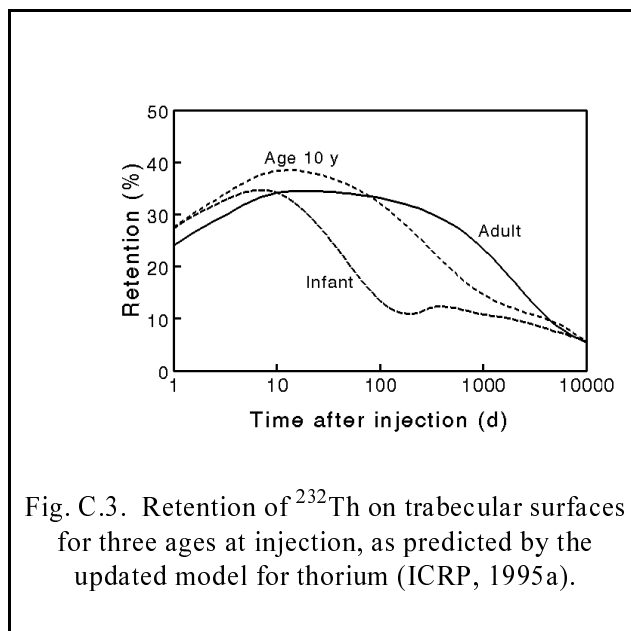


Fig. C.3. Retention of ^{232}Th on trabecular surfaces for three ages at injection, as predicted by the updated model for thorium (ICRP, 1995a).

Table C.2 gives model predictions of the 50-y integrated activity of ^{232}Th in different regions of the body after injection of a unit activity of ^{232}Th into blood at age 100 d (infant), 10 y, or 25 y. The indicated differences with age at injection result from some combination of three assumptions: elevated uptake of thorium by immature bone, an elevated rate of remodeling of immature bone, and

Table C.2. Predictions of 50-y integrated activity of ^{232}Th (nuclear transformations per Bq injected), following injection into blood at age 100 d, 10 y, or 25 y.

Compartment	Age at injection		
	100 d	10 y	25 y
Trabecular surfaces	9.8×10^7	1.2×10^8	1.4×10^8
Cortical surfaces	2.8×10^8	4.3×10^8	6.3×10^8
Trabecular volume	8.8×10^7	9.3×10^7	6.4×10^7
Cortical volume	1.8×10^8	2.7×10^8	1.6×10^8
Red marrow	3.1×10^7	2.0×10^7	1.3×10^7
Liver	5.7×10^7	4.2×10^7	3.8×10^7
Kidneys	1.1×10^7	8.4×10^6	7.5×10^6
Testes	2.9×10^5	4.3×10^5	4.6×10^5
Ovaries	1.5×10^5	1.8×10^5	1.4×10^5

an age-independent removal half-time for soft tissues. For example, cumulative activity in red marrow decreases with age at injection, mainly as a result of rapid recycling of activity from trabecular bone to red marrow in children and an age-independent removal half-time from bone marrow. For gonads, elevated feedback of activity from bone at younger ages is offset by relatively low deposition in the gonads, resulting in little change with age at injection in cumulative activity.

Treatment of ^{232}Th chain members produced in systemic tissues

In ICRP Publication 30 (1979), decay chain members produced in the body after intake of a parent radionuclide generally were assigned the biokinetic model of the parent; this is the so-called assumption of "shared kinetics" of decay chain members. In a subsequent critical review of experimental data on the fate of radionuclides formed *in vivo*, it was suggested that the following assumption of "independent kinetics" of chain members may be more realistic than the assumption of shared kinetics in most cases (Leggett et al., 1984): (1) a radionuclide born in soft tissues or on bone surfaces behaves as if taken into the body as a parent radionuclide; (2) a radionuclide born in bone volume has the same kinetics as the parent until removed from bone volume and then behaves as if taken into the body as a parent radionuclide.

There is some experimental evidence to support the assumption of independent kinetics for thorium chains (Leggett et al., 1984). For example, activity ratios $^{224}\text{Ra}/^{228}\text{Th}$ in tissues and excreta

of beagles injected with ^{228}Th are consistent with the assumption that ^{224}Ra born on bone surfaces migrated from ^{228}Th over a period of days and then behaved as if injected directly into blood (Van Dilla and Stover, 1956; Van Dilla et al., 1957; Stover et al., 1965a, 1965b). Time-dependent activity ratios of subsequent members of the ^{228}Th chain also suggest redistribution consistent with the characteristic biokinetic models of individual members, although the extent of migration of these chain members and hence the interpretation of the data are limited by the short half-lives of the chain members (Stover et al., 1965a, 1965b).

The assumption of independent kinetics was applied in ICRP Publication 69 (1995a) to chain members produced *in vivo* after absorption of thorium isotopes to blood, except that some simplifying assumptions were made in cases where there was little difference, in effect, between the assumptions of shared and independent kinetics. Parameter values for individual chain members can be found in Appendix C of ICRP Publication 71 (ICRP, 1995b). The models for members of various thorium chains are summarized in the following:

1. Radium isotopes formed *in vivo* are assumed to follow the model for radium as a parent (Leggett, 1992a; ICRP, 1993). This requires that the model structure for thorium (Fig. C.2) be expanded to include compartments that are in the radium model (see Chapter 4, Fig. 4.6) but not in the thorium model. For example, each bone volume compartment in the thorium model must be divided into exchangeable and nonexchangeable bone volume compartments to describe the behavior of radium after its movement from plasma to bone surfaces to bone volume. According to the radium model, bone contains about 30%, soft tissues about 15%, and excreta plus excretion pathways (mainly intestinal contents) about 55% of the injected amount at 1 d after injection of long-lived radium into blood of an adult. Most radium atoms entering bone or soft tissues return to plasma within a few days. By 100 d after injection, bone retains less than 5% and soft tissues less than 1% of the injected amount, the rest having been lost in excreta.
2. Radon produced in soft tissues or bone surfaces is assumed to be removed to plasma at a fractional rate of 100 d^{-1} . Radon produced in the exchangeable and nonexchangeable bone volume compartments is assumed to migrate to plasma at rates of 1.5 and 0.36 d^{-1} , respectively. Radon entering plasma is assumed to be removed from the body by exhalation at a fractional rate of 1 min^{-1} .
3. Lead isotopes formed *in vivo* are assumed to follow the model for lead as a parent (Leggett, 1993; ICRP, 1993). Therefore, the model structure used to address a thorium chain that includes lead as a daughter must include compartments such as red blood cells and exchangeable and nonexchangeable bone volume that are in the lead model (Fig. 4.6) but are

not identified separately in the thorium model. According to the lead model, the approximate contents of various regions at 1 d after injection of long-lived lead into blood of an adult are as follows: red blood cells, 59% (of the injected amount); bone, 15%; liver, 11%; kidneys, 5%; other soft tissues, 3%; and excreta plus excretion pathways, 7%. Over the next few weeks there is a gradual shift of lead from red blood cells to bone, soft tissues, and excreta. After 100 d, the predicted contents of the regions are as follows: red blood cells, 4% (of the injected amount); bone, 22%; liver, 5%; kidneys, 2%; other soft tissues, 5%; and excreta, 62%.

4. The model for polonium as a decay chain member is based on the non-recycling model for polonium as a parent given in ICRP Publication 67 (1993), but the latter model is converted into a recycling model to fit into the framework used for thorium, radium, and lead. Removal of polonium from all tissues except bone volume is assumed to occur at a fractional rate of 0.1 d^{-1} , with activity going to plasma. Removal from bone volume to plasma is assumed to occur at the rate of bone turnover. Of polonium reaching plasma, 10% goes to the gastrointestinal tract contents and subsequently to feces and 5% goes to the urinary bladder contents and then to urine. The unexcreted amount is divided as follows: 30% to liver, 10% to kidneys, 5% to spleen, 10% to red marrow, and 45% to other tissues.
5. Bismuth is assumed to be removed from all tissues except bone volume at a fractional rate of 0.035 d^{-1} , with activity going to plasma. From plasma, 35% goes to urine, 7% to feces via the intestines, 35% to the kidneys, 5% to the liver, and 18% to other tissues.
6. Isotopes of thallium appearing in important thorium chains are short-lived and are assumed to decay at their point of origin, and isotopes of actinium, protactinium, and thorium produced *in vivo* are assigned the model for thorium.

The treatment of decay chain members is a particularly important consideration in the internal dosimetry of ^{232}Th due to the fact that the radioactive progeny of ^{232}Th emit substantially more alpha energy than the parent over a period of a few years. The estimated alpha activity of the total chain is reduced substantially if it is assumed, as indicated by available experimental data, that ^{228}Ra and subsequent chain members migrate over a period of hours or days from sites of production on bone surfaces and in soft tissues and then behave as if injected directly into blood (Table C.3).

Comparison of updated and previous systemic models for thorium

The ICRP's new systemic biokinetic model for thorium differs substantially from its previous model (ICRP, 1979) with regard to basis, structure, and predictions. The previous model consists of three tissue compartments fed by a transfer compartment (Fig. C.4). On the basis of observations

Table C.3. Comparison of estimated 50-y integrated activities of ^{232}Th and its decay chain members, assuming (A) independent or (B) shared kinetics of decay chain members, for the case of injection of ^{232}Th into blood of an adult^a.

Radionuclide	Ratio of integrated activities, A:B						
	Cortical bone surface	Trabecular bone surface	Cortical bone volume	Trabecular bone volume	Red bone marrow	Liver	Testes, ovaries
^{232}Th	1.0	1.0	1.0	1.0	1.0	1.0	1.0
^{228}Ra , ^{228}Ac	0.001	0.003	0.9	0.7	0.08	0.04	0.05
^{228}Th	0.02	0.06	0.8	0.5	0.2	0.06	0.05
^{224}Ra through ^{208}Tl	~0.005	~0.02	~0.8	~0.5	~0.1	~0.05	~0.05

^aThe biokinetic model for thorium given in ICRP Publication 69 (ICRP, 1995a) is applied to ^{232}Th . For the case of independent kinetics, the models and assumptions of ICRP Publication 69 are applied to the radioactive progeny of ^{232}Th .

of the fate of ^{228}Th in beagles (Stover et al., 1960), it is assumed in that model that activity leaves the transfer compartment with a half-time of 0.5 d, with 70% depositing on bone surfaces, 4% depositing in the liver, 16% depositing in other soft tissues, and 10% lost in excreta. Thorium is assumed to be removed from bone surfaces to excretion with a biological half-time of 8000 d and from liver and other soft tissues to excretion with a biological half-time of 700 d. The assumption that skeletal deposits remain on bone surfaces until removed to excretion is generally applied in ICRP Publication 30 to actinide elements.

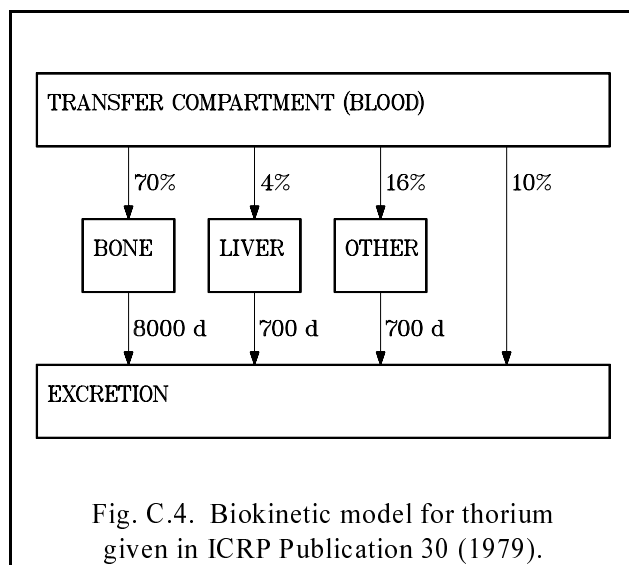


Fig. C.4. Biokinetic model for thorium given in ICRP Publication 30 (1979).

Compared with the model of ICRP Publication 30, the new model predicts considerably longer retention of thorium in the skeleton, liver, and other soft tissues, and consequently much longer retention in the total body of the adult. For example, the model of Publication 30 predicts that

about 75% of an amount injected into blood at time zero will be excreted in 10,000 days, compared with a prediction of about 30% based on the new model (Fig. C.5).

In the model of ICRP Publication 30, the time-dependent concentration of thorium in kidneys and gonads is assumed to be the same as that in all soft tissues other than liver. In the new model, the kidneys and gonads are addressed separately from other soft tissues and are depicted as relatively important repositories for thorium. This is demonstrated in Table C.4, where comparisons are made of the updated and previous models as predictors of the 50-y cumulative activity of ^{232}Th and ^{228}Ra in selected organs of an acutely exposed adult. Three types of acute intake are considered in this table: injection of ^{232}Th into blood, ingestion of ^{232}Th , and inhalation of a moderately soluble form of ^{232}Th (Type M or class W, respectively, in the updated and previous respiratory tract models). The assumption of independent kinetics of decay chain members is used in conjunction with the updated systemic model, and the assumption of shared kinetics is used with the systemic model of ICRP Publication 30.

Conversion of activity to estimates of dose rates to tissues

SE values

The dose rate to a target region T due to activity in a source region S depends on the amount of activity in S , the nature of the radiations emitted in the source region, the spatial relationships between the source and target regions, the nature of the tissues lying between the source and target regions, and the mass of T . As discussed in Chapter 5, the details of these considerations are embodied in a coefficient called the specific energy or SE .

The ICRP's updated SE values for the adult male generally do not differ substantially from those applied to Reference Man in ICRP Publication 30 (1979), but there are notable exceptions. The most important exception is for the lung as a target region. In ICRP Publication 30, the dose to the lung is an average dose over the entire lung tissue. In ICRP Publication 66 (1994a), the dose to the lung is redefined as a weighted average of doses to sensitive cells of the bronchi, bronchioles, and alveolar-interstitium, with the relatively small mass of cells of the bronchi and bronchioles receiving greater weight per unit mass than the relatively large mass of the alveolar-interstitium. The two definitions of lung dose can result in substantially different estimates for some radionuclides that emit mainly non-penetrating radiations. This is because the new definition assigns much greater importance to the generally small fraction of the total activity in the lungs that is associated with the radiosensitive cells of the bronchi and bronchioles. For example, for the case of acute inhalation of

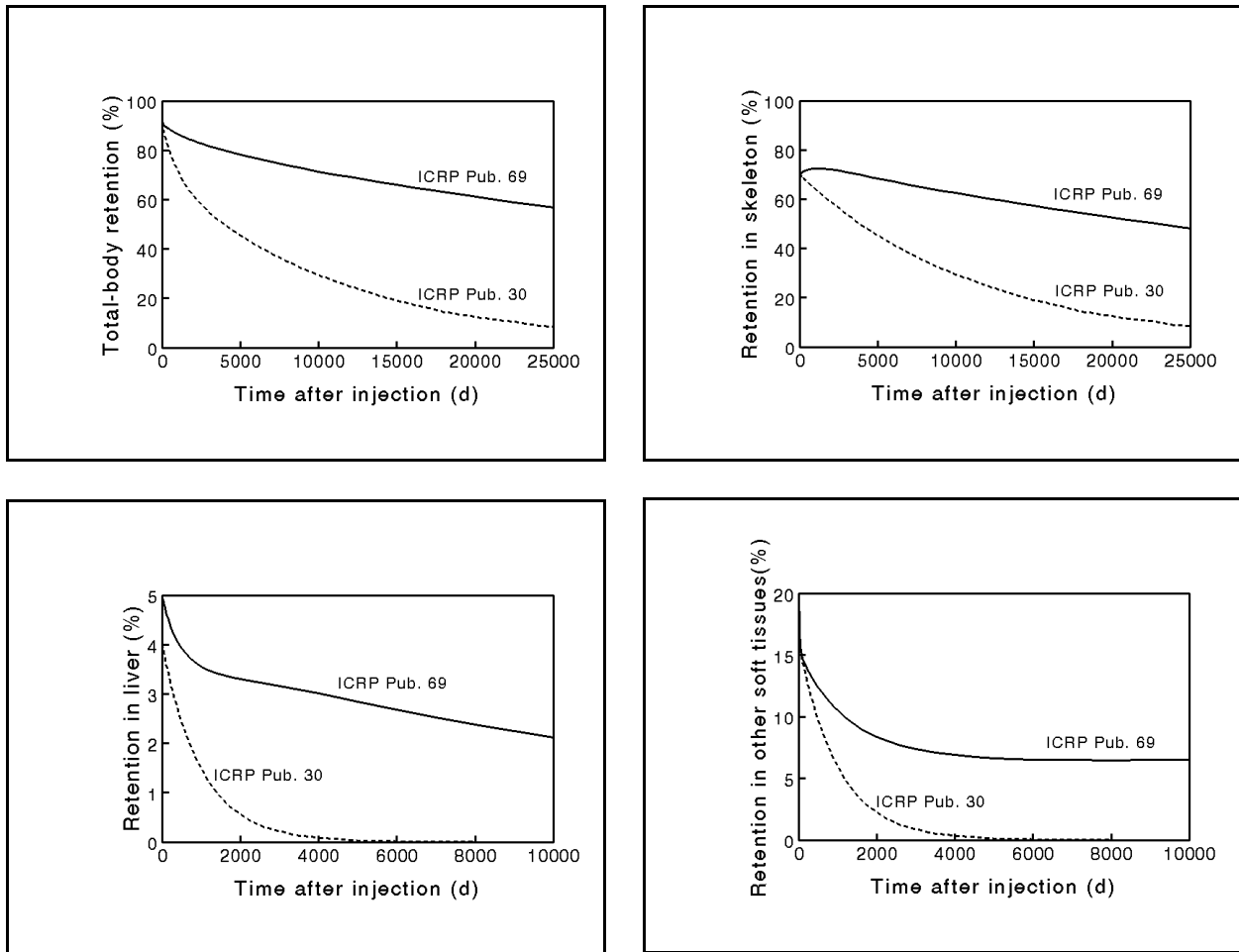


Fig. C.5. Comparison of predictions of ICRP's updated (ICRP, 1995a) and previous (ICRP, 1979) systemic biokinetic models for thorium.

a moderately soluble form of ^{232}Th (Type M) by an adult, the estimated activity of all chain members in the alveolar-interstitium (region *AI*) at 50 d after inhalation is about a factor of 40 greater than that in the bronchioles (region *bb*, Fig. 4.1). Yet the estimated dose rate to bronchiolar secretory cells from high-LET radiation at that time is nearly twice as great as that to *AI* as a result of the small mass assigned to the bronchiolar secretory cells.

For purposes of calculating radiogenic risk to members of the public, an important advance in internal dosimetry in recent years has been the introduction of age-specific *SE* values. *SE* values for most pairs of source and target organs vary substantially with age due to changes with age in the

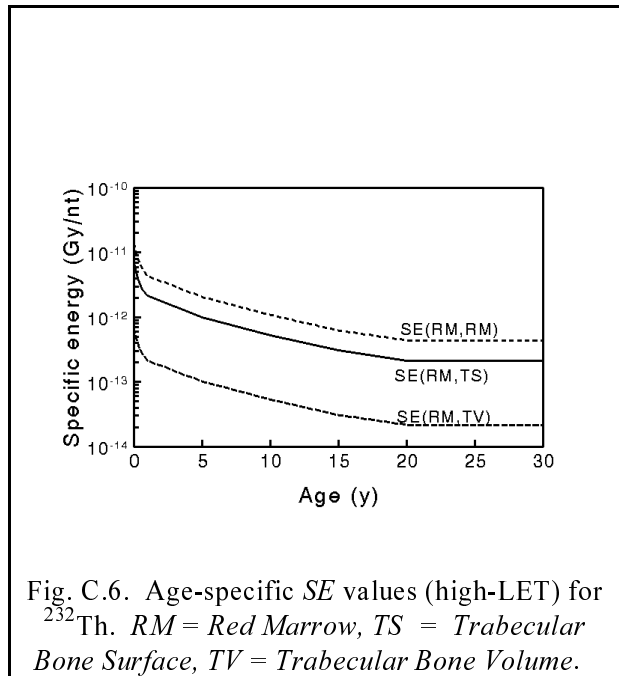
Table C.4. Comparison of ICRP's updated (ICRP, 1995a) and previous (ICRP, 1979) models as predictors of 50-y integrated activity after acute intake of ^{232}Th by an adult.

Compartment	Ratio of integrated activities (updated models : previous models)					
	Injection		Ingestion		Inhalation	
	^{232}Th	$^{228}\text{Ra}^a$	^{232}Th	$^{228}\text{Ra}^a$	^{232}Th	$^{228}\text{Ra}^a$
Trabecular surfaces	0.49	0.0014	1.2	0.0036	0.39	0.0011
Cortical surfaces	2.3	0.0026	5.7	0.0064	1.8	0.0020
Liver	11	1.4	27	3.5	8.4	1.0
Kidneys	110	9.0	280	23	86	7.0
Gonads	60	8.9	150	22	47	7.0
Other systemic activity	25	56	62	140	19	42

^aRefers to ^{228}Ra produced in the body after intake of ^{232}Th .

masses of target organs and, in some cases, in the relative geometries of the source and target organs during growth.

Changes with age in *SE* values for ^{232}Th are illustrated in Fig. C.6 for the red marrow as a target organ and for each of three source organs: *Trabecular Bone Surface (TS)*, *Red Marrow (RM)*, and *Trabecular Bone Volume (TV)*. In Fig. C.6, *SE(T,S)* indicates the *SE* value for target organ *T* and source organ *S*. The indicated *SE* values are for high-LET (alpha) radiation, which is the dominant radiation type for ^{232}Th . The decrease with age in the *SE* values result from an increase with age in the mass of *Red Marrow* (Fig. C.7).



Use of *SE* values to calculate dose rates

The calculation of dose rates is illustrated for the case of high-LET (alpha) irradiation of *Red Marrow* from internally deposited ^{232}Th . Due to the short range of the alpha particles, the contributing source organs in this case are those in intimate contact with *Red Marrow*, namely, *Red Marrow*, *Trabecular Bone Surface*, and *Trabecular Bone Volume*.

Recall that for a given type of radiation, the absorbed dose rate, $\dot{D}_T(t)$, at age t in target region T can be expressed as:

$$\dot{D}_T(t) = \sum_S \sum_j q_{S,j}(t) SE(T \leftarrow S; t)_j, \quad (\text{C.1})$$

where $q_{S,j}(t)$ is the activity of radionuclide j present in source region S at age t and $SE(T \leftarrow S; t)_j$ is the specific energy deposited in target region T per nuclear transformation of radionuclide j in source region S at age t . Therefore, the high-LET dose rate $\dot{D}_{RM}(t)$ to *Red Marrow* from ^{232}Th (excluding radioactive progeny) at age t due to intake of ^{232}Th at age t_0 is the sum

$$\begin{aligned} \dot{D}_{RM}(t) = & q_{RM}(t) SE(RM \leftarrow RM; t) + q_{TS}(t) SE(RM \leftarrow TS; t) \\ & + q_{TV}(t) SE(RM \leftarrow TV; t), \end{aligned} \quad (\text{C.2})$$

where the three *SE* values are as indicated (with shortened notation) in Fig. C.6. As predicted by the biokinetic and dosimetric models used here, the right side of Eq. C.2 usually is dominated by the term involving *Trabecular Bone Surface* as a source organ (second term). Although all alpha particles emitted in *Red Marrow* are assumed to be absorbed by *Red Marrow*, the contribution to $\dot{D}_{RM}(t)$ from *Red Marrow* typically is much smaller than the contribution from *Trabecular Bone Surface* for the case of ^{232}Th because the predicted number of thorium atoms contained in *Red*

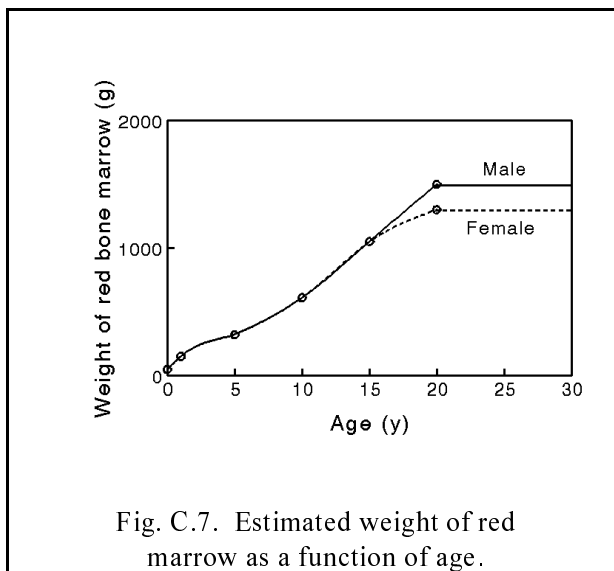


Fig. C.7. Estimated weight of red marrow as a function of age.

Marrow at a given time typically is much smaller than the number of thorium atoms in *Trabecular Bone Surface*. Although the predicted number of thorium atoms in *Trabecular Bone Volume* may be larger than that in *Trabecular Bone Surface* at some ages, the contribution to $\dot{D}_{RM}(t)$ from *Trabecular Bone Volume* (third term in Eq. C.2) typically is smaller than the contribution from *Trabecular Bone Surface* because $SE(RM-TV;t)$ is much smaller than $SE(RM-TS;t)$ (Fig. C.6). The relationship between the three terms on the right side of Eq. C.2 as a function of time after acute injection of ^{232}Th is illustrated in Fig. C.8 for the adult. It is emphasized that the curves in Fig. C.8 represent only the contribution of the parent, ^{232}Th , to the high-LET dose rate to *Red Marrow*. The total high-LET dose rate to *Red Marrow* will also include contributions from the radioactive progeny of ^{232}Th contained in the *Red Marrow*, *Trabecular Bone Surface*, and *Trabecular Bone Volume*.

Calculated high-LET dose rates to *Red Marrow* for the cases of acute ingestion and acute inhalation of 1 Bq of ^{232}Th are shown in Figs. C.9 and C.10, respectively, for three ages at intake: infancy (100 d), 10 y, and 25 y. The dose rates indicated in these figures include contributions from radioactive progeny of ^{232}Th as well as from the parent radionuclide. Due to migration of ^{228}Ra and subsequent chain members from the parent, however, ^{232}Th is the major contributor to the indicated dose rates.

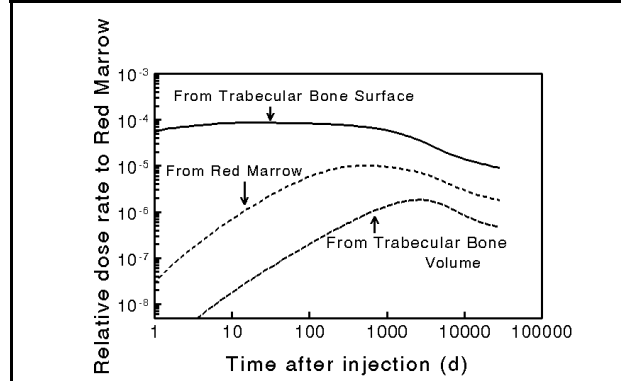


Fig. C.8. Contributions of ^{232}Th in *Trabecular Bone Surface*, *Trabecular Bone Volume*, and *Red Marrow* to the high-LET dose rate to *Red Marrow* in the adult.

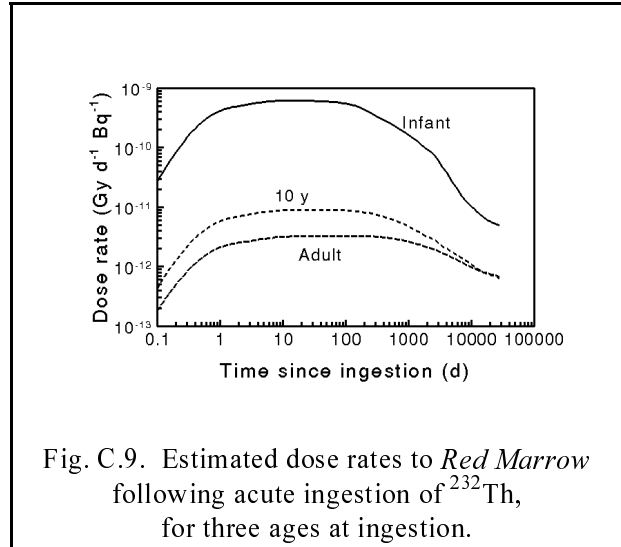


Fig. C.9. Estimated dose rates to *Red Marrow* following acute ingestion of ^{232}Th , for three ages at ingestion.

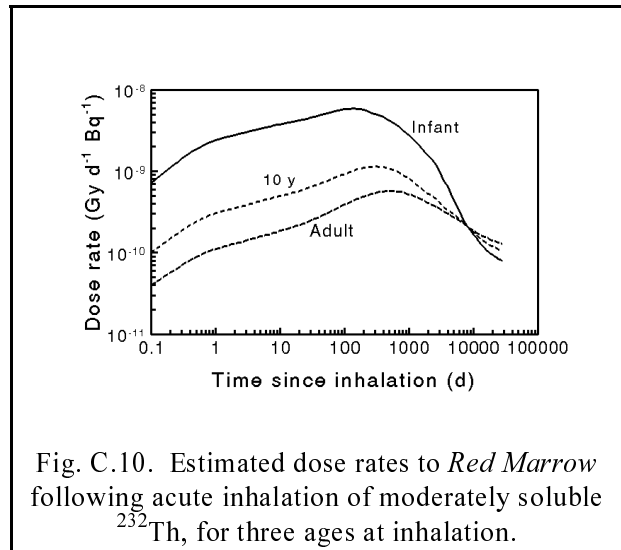


Fig. C.10. Estimated dose rates to *Red Marrow* following acute inhalation of moderately soluble ^{232}Th , for three ages at inhalation.

Conversion of dose rates to estimates of radiogenic cancers

The age-specific cancer risk attributable to a unit intake of a radionuclide is calculated from the absorbed dose rate due to a unit intake of the radionuclide and the age-specific risk per unit dose model coefficients. The calculation is specific for each cancer and associated absorbed dose site in the risk model. The complete calculation for each cancer and associated dose site may involve the sum of contributions from more than one target tissue and from both low- and high-LET absorbed doses.

In the following, attention is focused on the problem of estimating the risk of dying from radiogenic leukemia following intake of ^{232}Th . That is, the problem is one of deriving a mortality risk coefficient for leukemia for ingestion or inhalation of ^{232}Th . In this case, the target organ of interest is red marrow. The risk model used in this report for leukemia is a relative risk model, with age- and gender-specific risk model coefficients.

Recall that the age-specific *lifetime risk coefficient (LRC)*, $r(x)$, is the risk per unit dose of a subsequent cancer death (Gy^{-1}) due to radiation received at age x . For a relative risk model, the *LRC* for a given contribution is

$$r(x) = \frac{\int_x^{\infty} \eta(u,x) \mu(u) S(u) du}{S(x)} \quad (\text{C.3})$$

where $\eta(u,x)$ is the relative risk at age u due to a dose received at age x , $\mu(u)$ is the force of mortality at age u for the given cancer type, and $S(x)$ is the survival function. Because the *LRC* for a given cancer type is independent of the radionuclide and exposure scenario, the *LRCs* need not be recalculated in each derivation of a radionuclide risk coefficient but can be calculated once, stored, and used as input data in the calculation of all radionuclide risk coefficients.

The excess relative risk, $\eta(u,x)$, is the product of a risk model coefficient, $\beta(x)$, and a time-since-exposure response function, $\zeta(t,x)$, that defines the period during which the risk is expressed and, in the radiogenic risk model for leukemia, changes with time in the level of response during that period. The age- and gender-specific risk model coefficients $\beta(x)$ for leukemia are given in Table 7.2, and the time-since-exposure response function $\zeta(t,x)$ for leukemia is described in Eq. 7.3 and the text accompanying that equation.

Relative risk functions $\eta(u,x)$ for radiogenic leukemia in males are shown in Fig. C.11 for three ages at irradiation: infancy (100 d), 10 y, and 25 y. The functions for females are similar to those for males but are not identical because the risk model coefficients, $\beta(x)$, differ slightly for the two genders (Table 7.2).

The gender-specific force of mortality functions for leukemia are shown in Fig. C.12 (NCHS, 1992, 1993a, 1993b), and the gender-specific survival functions $S(x)$ (all causes of death) are shown in Fig. C.13 (NCHS, 1997). The *LRC* functions $r(x)$ for radiogenic leukemia in males and females, calculated by integrating the product of the functions $\eta(u,x)$, $\mu(u)$, and $S(x)$ from age x to infinity (age 120 y), are shown in Fig. C.14. The sharp changes in direction in the *LRC* functions at some ages stem mainly from jumps in the risk model coefficients $\beta(x)$ for leukemia at those ages (Table 7.2).

The *LRC* function $r(x)$ is based on a unit dose received at age x . Following intake of a radionuclide at age x_i , the absorbed dose rate $\dot{D}(x)$ to a given target tissue varies continuously with age $x \geq x_i$. The cancer risk $r_a(x_i)$ resulting from a unit intake of a radionuclide at age x_i is calculated from the continuously varying absorbed dose rate $\dot{D}(x)$ using the equation:

$$r_a(x_i) = \frac{\int_{x_i}^{\infty} \dot{D}(x) r(x) S(x) dx}{S(x_i)} \quad (\text{C.4})$$

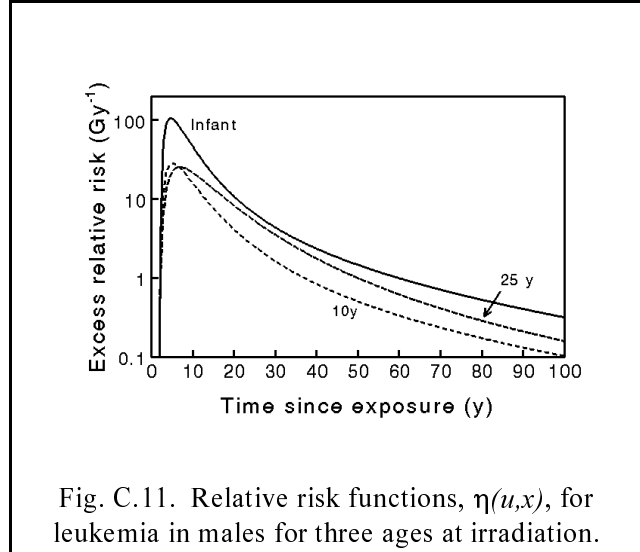


Fig. C.11. Relative risk functions, $\eta(u,x)$, for leukemia in males for three ages at irradiation.

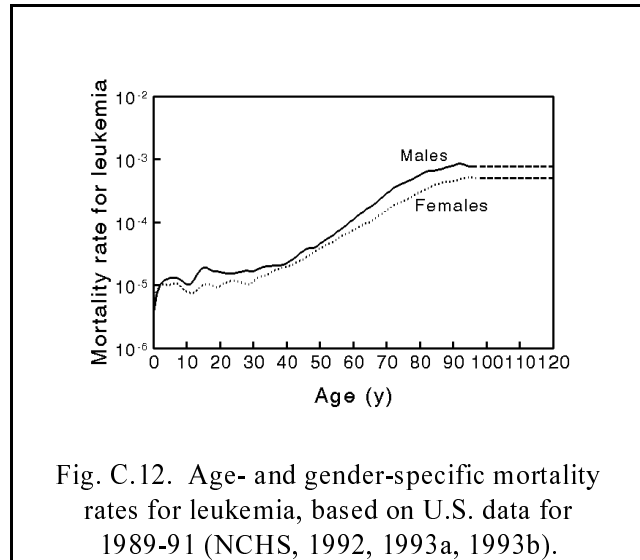


Fig. C.12. Age- and gender-specific mortality rates for leukemia, based on U.S. data for 1989-91 (NCHS, 1992, 1993a, 1993b).

where $r(x)$ is the cancer risk due to a unit absorbed dose (Gy^{-1}) at the site at age x . The functions $S(x)$ and $r(x)$ in the integrand are shown in Figs. C.13 and C.14, respectively. The dose rate function $\dot{D}(x)$ in the integrand is illustrated in Fig. C.9 for ingestion of ^{232}Th and in Fig. C.10 for inhalation of moderately soluble ^{232}Th at age 10 d, 10 y, or 25 y.

Derived gender-specific risks $r_a(x_i)$ of dying from radiogenic leukemia due to acute ingestion of ^{232}Th are shown in Fig. C.15 for ingestion ages from birth through old age. Model predictions for the case of acute inhalation of ^{232}Th are shown in Fig. C.16. The derived values $r_a(x_i)$ for males and females are combined into a risk estimate for the total population of age x_i by calculating a weighted mean that accounts for the proportion of each sex in a stationary combined population at the desired age of intake (see Chapter 7, Eq. 7.7).

For a given gender, the average lifetime leukemia risk coefficient for ingestion or inhalation of ^{232}Th is calculated from the derived age- and gender-specific values, $r_a(x)$. Because $r_a(x)$ is based on acute intake of 1 Bq of ^{232}Th at age x , $r_a(x)$ must be scaled by (that

is, multiplied by) the age-specific intake rate, $C u(x)$, where C is the constant radionuclide concentration in the environmental medium and $u(x)$ is the usage rate at age x as specified in the usage scenario. The product $u(x)r_a(x)$ must be further scaled by the value of the survival function at x , $S(x)$, to account for the possibility that the exposed person will die from a competing cause before reaching age x . Therefore, for a given gender, the estimated risk of dying from leukemia due to lifetime intake of ^{232}Th is the integral over age from birth to the maximum possible value of x (assumed here to be 120 y) of the product $C u(x) r_a(x) S(x)$. Because a risk coefficient is expressed as a risk per unit intake, the integral of $C u(x) r_a(x) S(x)$ must be divided by the probable lifetime

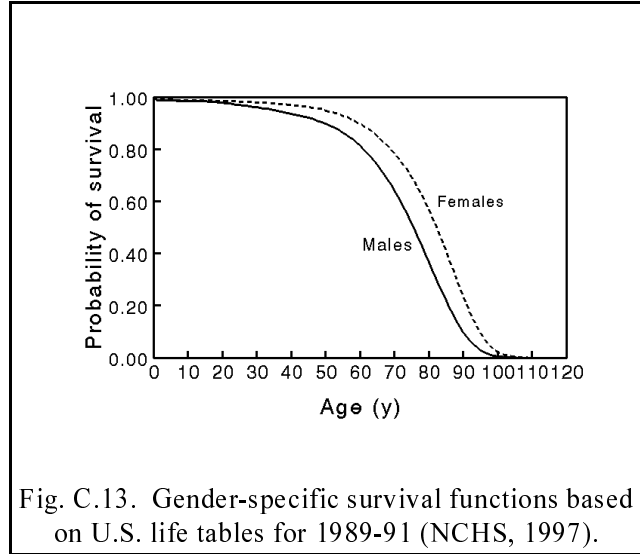


Fig. C.13. Gender-specific survival functions based on U.S. life tables for 1989-91 (NCHS, 1997).

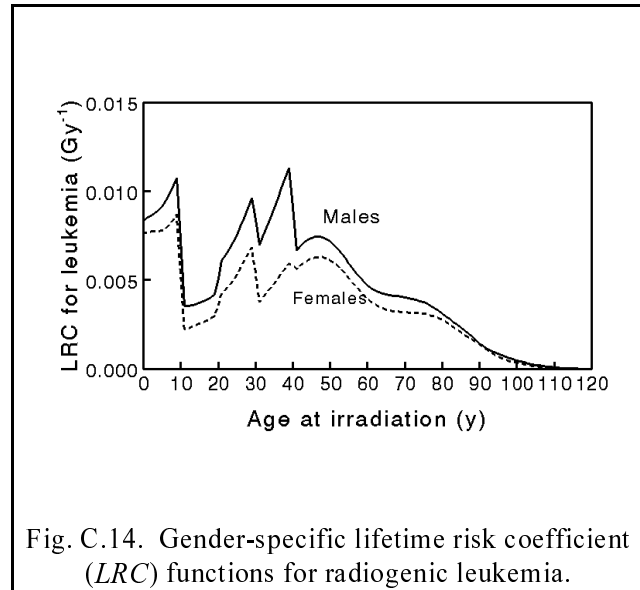


Fig. C.14. Gender-specific lifetime risk coefficient (LRC) functions for radiogenic leukemia.

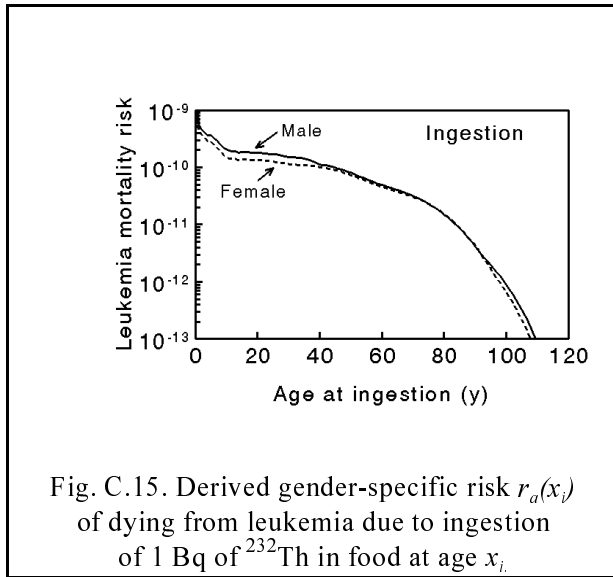


Fig. C.15. Derived gender-specific risk $r_a(x_i)$ of dying from leukemia due to ingestion of 1 Bq of ^{232}Th in food at age x_i .

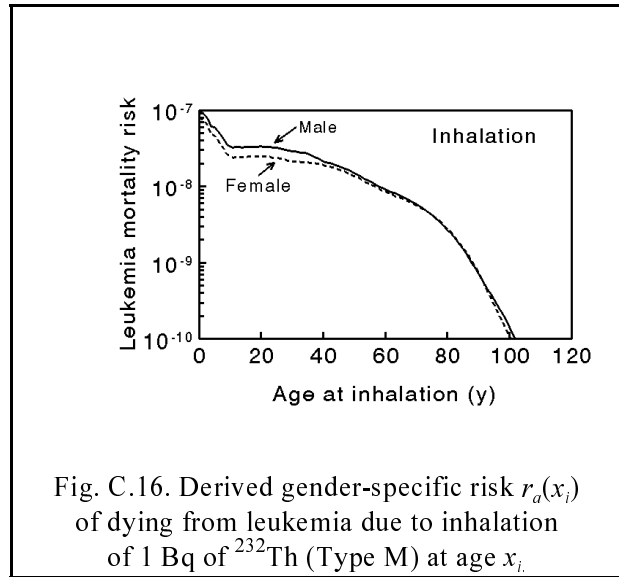


Fig. C.16. Derived gender-specific risk $r_a(x_i)$ of dying from leukemia due to inhalation of 1 Bq of ^{232}Th (Type M) at age x_i .

intake of ^{232}Th . Because the probable intake rate at age x is $Cu(x)$ times the probability $S(x)$ of surviving to age x , the probable lifetime intake of ^{232}Th is the integral over age of the product $Cu(x)S(x)$. Therefore, for a given gender, the average lifetime leukemia risk coefficient for ingestion or inhalation of ^{232}Th is given by:

$$\bar{r}_a = \frac{\int_0^{\infty} u(x) r_a(x) S(x) dx}{\int_0^{\infty} u(x) S(x) dx} \quad . \quad (\text{C.5})$$

The radionuclide concentration in the environmental medium, C , disappears from the equation because it is a factor in both numerator and denominator.

Gender-weighted average lifetime risk coefficients for ingestion of ^{232}Th are indicated in the bar graph in Fig. C.17, and risk coefficients for inhalation of a moderately soluble form of ^{232}Th are indicated in the bar graph in Fig. C.18. These two figures show the relative contributions of some cancer-specific risk coefficients, including that for leukemia, to the total combined risk coefficient for ingestion or inhalation of ^{232}Th . Shown for comparison are risk coefficients for ^{232}Th based on the risk methodology described in this report but using the biokinetic models and assumptions of ICRP Publication 30 (1979).

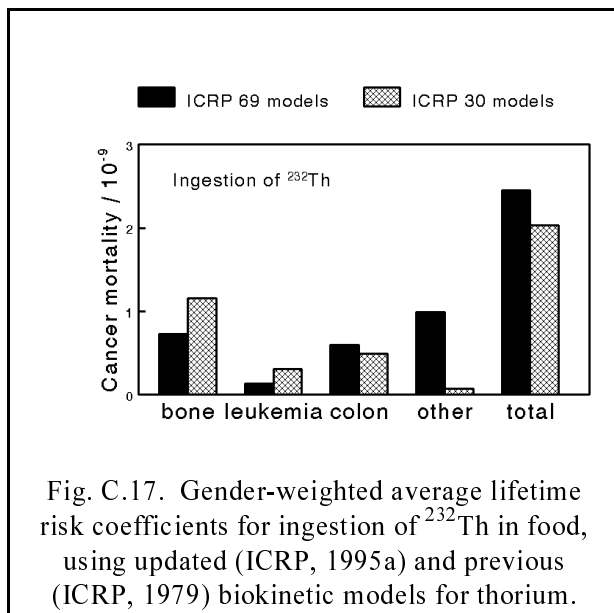


Fig. C.17. Gender-weighted average lifetime risk coefficients for ingestion of ²³²Th in food, using updated (ICRP, 1995a) and previous (ICRP, 1979) biokinetic models for thorium.

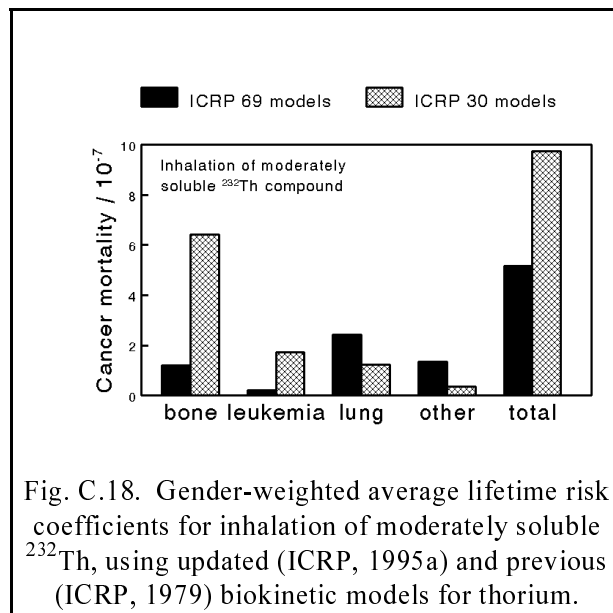


Fig. C.18. Gender-weighted average lifetime risk coefficients for inhalation of moderately soluble ²³²Th, using updated (ICRP, 1995a) and previous (ICRP, 1979) biokinetic models for thorium.

Comparison with risk estimates based on effective dose

As a measure of the risk from intake of radionuclides, the ICRP uses a quantity called the effective dose. The effective dose is a weighted sum of equivalent doses (that is, integrated equivalent dose rates) to radiosensitive tissues, with tissue weighting factors representing the relative contribution of each tissue to the total detriment for the case of uniform irradiation of the whole body. The effective dose is based on an integration period of 50 years for intake by adults and to age 70 years for intake by children.

The ICRP relates the effective dose to the probability of a fatal cancer through a multiplicative factor called a “nominal fatality probability coefficient”. This coefficient is referred to as “nominal” because of the uncertainties inherent in radiation risk estimates and because the ICRP’s estimated relation of effective dose and fatal cancers is based on an idealized population receiving a uniform equivalent dose over the whole body. A nominal fatality probability coefficient of 0.05 Sv⁻¹ is given in ICRP Publication 60 (1991) for all cancer types combined. According to ICRP Publication 60, “If the equivalent dose is fairly uniform over the whole body, it is possible to obtain the probability of fatal cancer associated with that effective dose from the nominal fatality probability coefficient. If the distribution of equivalent dose is non-uniform, this use of the nominal coefficient will be less accurate because the tissue weighting factors include allowances for non-fatal and hereditary conditions.” Another difficulty with the effective dose as a measure of risk is that

it cannot accurately reflect the contribution of competing risks for the many different temporal patterns of dose rates to tissues that occur for various long-lived, tenaciously retained radionuclides.

Despite such limitations in the effective dose, it is common practice to use the nominal fatality probability coefficient to convert effective doses from internally deposited radionuclides to estimates of fatal radiogenic cancers. The effective dose is taken by some analysts as the effective dose equivalent of ICRP Publication 30 (1979, 1980, 1981, 1988) as tabulated in Federal Guidance Report No. 11 (1988), and is taken by others from tabulations in the ICRP's recent series of documents on doses to the public from intake of radionuclides (see summary report, ICRP Publication 72, 1996). Because the latter documents provide the effective dose as a function of age at acute intake, the effective dose may be represented by a weighted average of age-specific effective doses, where the weights reflect assumed levels of intake at different ages. Because such weighted effective doses typically differ by <30% from the effective dose for intake by the adult, the latter is generally applied.

Cancer mortality risk for ingestion of ^{232}Th in food and for inhalation of a moderately soluble form (Type M) of ^{232}Th of particle size $1\ \mu\text{m}$ (AMAD), as derived by the methods of this report, are compared in Table C.5 with estimates derived from the effective dose, E (that is, as $e \times 0.05\ \text{Sv}^{-1}$). Two different estimates of effective dose are considered, one derived using the committed effective dose coefficient from Federal Guidance Report No. 11 (1988) and the other derived using the effective dose coefficient from ICRP Publication 72 (1996). The latter document is a compilation of age-dependent doses to members of the public based on the ICRP's most recent biokinetic and dosimetric models. Both estimates are based on an intake of 1 Bq. The two estimates are abbreviated as $0.05\ \text{Sv}^{-1} \times E(\text{FGR11})$ and $0.05\ \text{Sv}^{-1} \times E(\text{ICRP72})$, respectively. For simplicity, $E(\text{ICRP72})$ is taken to be the effective dose for intake by the adult.

For the case of ingestion of ^{232}Th in food, $0.05\ \text{Sv}^{-1} \times E(\text{FGR11})$ is about three-fold higher than $0.05\ \text{Sv}^{-1} \times E(\text{ICRP72})$, and 15-fold higher than the risk based on the coefficient derived here (Table C.5). The discrepancies between $0.05\ \text{Sv}^{-1} \times E(\text{FGR11})$ and $0.05\ \text{Sv}^{-1} \times E(\text{ICRP72})$ result in part from differences in the new and previous biokinetic models for thorium (discussed earlier), and in part from recent changes in the ICRP's tissue weighting factors (ICRP, 1991). The discrepancies between $0.05\ \text{Sv}^{-1} \times E(\text{ICRP72})$ and the risk coefficient are the net result of a variety of factors, including the limitations of the effective dose as a measure of risk for non-uniformly distributed radionuclides such as ^{232}Th and its radioactive progeny, differences between the high-LET RBEs for leukemia and breast cancer used in the present methodology and those used by the ICRP, and the failure of the effective dose to account adequately for competing risks when the organ doses are received over several decades.

Table C.5. Comparison of cancer mortality risk coefficients with risk estimates based on effective dose, for ingestion or inhalation of ^{232}Th .

Method	Ingestion of ^{232}Th		Inhalation of ^{232}Th , Type M, 1 μm	
	Cancer mortality risk (Bq^{-1})	Multiple of value derived in this report	Cancer mortality risk (Bq^{-1})	Multiple of value derived in this report
$0.05 \text{ Sv}^{-1} \times E(\text{FGR11})^{\text{a}}$	3.69E-08	15	2.22E-05	43
$0.05 \text{ Sv}^{-1} \times E(\text{ICRP72})^{\text{b}}$	1.15E-08	4.7	2.25E-06	4.3
This report	2.45E-09	–	5.18E-07	–

^a $E(\text{FGR11})$ is the effective dose given in Federal Guidance Report No. 11 (1988), which is based on models and methods of ICRP Publication 30 (1979).

^b $E(\text{ICRP72})$ is the effective dose for intake by the adult, based on models and methods of the ICRP's recent series of documents on age-dependent dosimetry (ICRP, 1989, 1993, 1995a, 1995b, 1996). Use of intake-weighted average of age-dependent effective doses typically yields <30% difference from indicated values for commonly used age-specific intake scenarios.

The discrepancies in the three methods of estimation of fatal cancers are even greater for the case of inhalation of moderately soluble ^{232}Th , for which $0.05 \text{ Sv}^{-1} \times E(\text{FGR11})$ is 10-fold higher than $0.05 \text{ Sv}^{-1} \times E(\text{ICRP72})$ and about 40-fold higher than the risk coefficient. The reasons for these discrepancies are essentially the same as those described above for the ingestion case. The main reason that relative differences between $0.05 \text{ Sv}^{-1} \times E(\text{FGR11})$ and the other two estimates are smaller in the ingestion case than in the inhalation case is that the new, higher f_i values for thorium offset part of the reduction in the estimate of effective dose for ingestion of ^{232}Th implied by other recent changes in the biokinetic models and tissue weighting factors. By contrast with model revisions concerning the level of absorption of ingested thorium, the new respiratory tract model predicts slightly lower absorption of inhaled material to blood than does the previous respiratory tract model.

APPENDIX D: UNCERTAINTIES IN ESTIMATES OF CANCER RISK FROM ENVIRONMENTAL EXPOSURE TO RADIONUCLIDES

Purposes of this appendix

Characterization of the uncertainties in estimates of cancer risk from environmental exposure to radionuclides is a complex problem that has received little attention in the literature. The problem is particularly complicated for internally deposited radionuclides because each radionuclide presents a unique combination of issues associated with deposition and retention in the respiratory tract, the rate and level of absorption from the respiratory or gastrointestinal tract to blood, the time-dependent distribution and retention of the parent radionuclide and any radioactive progeny in systemic tissues, and the types and energies of emitted radiations. Conclusions drawn for a given radionuclide may not apply to other radioisotopes of the same element due to differences in the types of radiation emitted and differences in radiological half-lives that may result in changes in the time-frame over which the dose is received. Conclusions drawn for intake of a certain chemical form of a radionuclide may not apply to other chemical forms due to differences in retention properties in the respiratory tract or in the level of absorption to blood from the respiratory or gastrointestinal tract.

For such reasons, a relatively complete and detailed characterization of the uncertainties in risk coefficients for a comprehensive set of radionuclides is not a feasible task. In fact, the “uncertainty in a risk coefficient” is not a well defined concept because the level of confidence that can be placed in a risk coefficient may vary considerably from one application to another. For example, the uncertainty associated with an inhalation risk coefficient for a radionuclide may depend strongly on the level of information concerning the physical and chemical form of the inhaled radionuclide because the dose to lungs and other radiosensitive tissues depends strongly on the form of the radionuclide. Also, a risk coefficient that is considered to be a reasonably reliable predictor for a relatively high, acute external exposure to a radionuclide may be appreciably less certain for a lower, prolonged exposure due to uncertainty in the shape of the dose-response curve at low doses.

The purposes of this appendix are to discuss the sources and extent of uncertainties in the biokinetic, dosimetric, and radiation risk models used in this report and to examine how these uncertainties may be propagated in the calculation of risk coefficients. A systematic procedure is proposed for determining nominal uncertainty intervals for risk coefficients. These intervals are referred to as nominal because they are intended to reflect only major uncertainties that are largely independent of the exposure scenario. They do not reflect uncertainties associated with the use of a linear, no-threshold model for radiogenic cancer (except for consideration of the differences in the

reported dose and dose-rate effectiveness factors), absorbed dose as a measure of radiogenic cancer risk, or idealized representations of the population and exposure. Essentially, a nominal uncertainty interval is intended to reflect the precision with which an estimate of radiogenic cancer mortality can be made for an ideal population and exposure scenario, assuming that the probability of inducing a radiogenic cancer is proportional to absorbed dose.

General sources of uncertainty in biokinetic estimates

Uncertainties associated with the structure of a biokinetic model

The confidence that can be placed in predictions of a biokinetic model for an element depends not only on uncertainties associated with parameter values of the model but also on uncertainties associated with the model structure. Such uncertainties may arise because the structure provides an oversimplified representation of the known processes, because unknown processes have been omitted from the model, or because part or all of the model formulation is based on mathematical convenience rather than consideration of processes. Some combination of these limitations in model structure is associated with each of the biokinetic models used in this document. These limitations hamper the assignment of meaningful uncertainty statements to the parameter values of a model because they cast doubt on the physical interpretation of the parameter values. For purposes of assessing the uncertainties associated with predictions of a biokinetic model for an element, it is often more illuminating to examine the range of values generated by a limited number of alternative modeling approaches than to produce large numbers of predictions based on variation of parameter values within a fixed but uncertain model structure.

Types of information used to construct biokinetic models for elements

Regardless of the model formulation or modeling approach, a biokinetic model for an element usually is based on some combination of the following sources of information:

- H1: direct information on humans, i.e., quantitative measurements of the element in human subjects;
- H2: observations of the behavior of chemically similar elements in human subjects;
- A1: observations of the behavior of the element in non-human species;
- A2: observations of the behavior of one or more chemically similar elements in non-human species.

Data types H2, A1, and A2 serve as surrogates for H1, which is the preferred type of information on which to base a biokinetic model.

The sources H1, H2, A1, and A2 are sometimes supplemented with various other types of information or constraints, such as quantitative physiological information (e.g., rates of bone restructuring); considerations of mass balance; predictions of theoretical models based on fundamental physical, chemical, and mathematical principles (e.g., a theoretical model of deposition of inhaled particles in the different segments of the lung); experimental data derived with anatomically realistic physical models (e.g., hollow casts of portions of the respiratory tract used to measure deposition of inhaled particles); and *in vitro* data (e.g., dissolution of compounds in simulated lung fluid). Among these supplemental sources of information, mass balance and quantitative physiological data (P) have particularly wide use.

Sources of uncertainty in applications of human data

Clearly it is desirable to base a biokinetic model for an element on observations of the time-dependent distribution and excretion of that element in human subjects ("H1 data"). Some degree of this type of direct information is available for most essential elements, as well as for some important non-essential elements, such as cesium, lead, radium, uranium, americium, and plutonium. Depending on the degree of biological realism in the model formulation, it may be possible to supplement element-specific information for human subjects with quantitative physiological information on the important processes controlling the biokinetics of the element of interest. For example, in ICRP Publication 67 (1993), 69 (1995a), and 71 (1995b), long-term removal of certain radionuclides from bone volume is identified with bone turnover.

Although it is the preferred type of information for purposes of model construction, H1 data often have one or more of the following limitations: small study groups, coupled with potentially large inter-subject variability in the biokinetics of an element; short observation periods, coupled with potentially large intra-subject variability; use of unhealthy subjects whose diseases may alter the biokinetics of the element; paucity of observations for women and children; collection of small, potentially non-representative samples of tissue; inaccuracies in measurement techniques; uncertainty in the pattern or level of intake of the element; atypical study conditions; and inconsistency in reported values. In some cases, inconsistency in reported values may provide some of the best evidence of the uncertain nature of the data.

An important tool in the development of biokinetic models for radionuclides has been the use of reference organ contents of stable elements, as estimated from autopsy measurements on

subjects chronically exposed at environmental levels or at elevated levels encountered in occupational exposures (ICRP, 1975). Such data are commonly used to adjust parameter values of biokinetic models or introduce new model components to achieve balance between reported values of intake, total-body content, and excretion of stable elements. Such balance considerations can provide useful constraints on model parameters, provided the data have been collected under carefully controlled conditions. However, such balance considerations often have been based on data from disparate sources of information and unreliable measurement techniques and in some cases may have led to erroneous models or parameter values.

A confidence statement based on H1 data would reflect a variety of factors, such as the reliability of the measurement technique(s), the number and state of health of the subjects, representativeness of the subjects and biological samples, consistency in data from different studies, knowledge concerning the level and pattern of intake, and the relevance of the information to the situation being modeled. For example, high confidence usually would not be placed in a parameter value based on H1 data for any one of the following study populations: several seriously ill subjects with known intakes, several healthy subjects with poorly characterized intakes, or one healthy subject with known intake.

Uncertainty in interspecies extrapolation of biokinetic data

Interspecies extrapolation of biokinetic data is based on the concept of a general biological regularity across the different species with regard to cellular structure, organ structure, and biochemistry. Mammalian species, with cell structure, organ structure, biochemistry, and body temperature regulation particularly close to those of man, are expected to provide better analogies to man than do non-mammalian species with regard to biokinetics of contaminants.

Despite the broad structural, functional, and biochemical similarities among mammalian species, interspecies extrapolation of biokinetic data has proven to be an uncertain process. Similarities across species often are more of a qualitative than quantitative nature, in that two species that handle an internally deposited radionuclide in the same qualitative manner may exhibit dissimilar kinetics with regard to that substance. Moreover, there are important structural, functional, and biochemical differences among the mammalian species, including differences in specialized organs, hepatic bile formation and composition, level of biliary secretion, urine volume and acidity, the amount of fat in the body, the magnitude of absorption or secretion in various regions of the digestive tract, types of bacteria in the digestive tract, and microstructure and patterns of remodeling of bones.

In general, the choice of an animal model will depend strongly on the processes and subsystems of the body thought to be most important in the biokinetics of the radionuclide in humans, because a given species may resemble humans with regard to certain processes and subsystems and not others. For example, data on monkeys or baboons may be given relatively high weight for purposes of modeling the distribution of a radionuclide in the skeleton due to the close similarities in the skeletons of non-human primates and humans. Data on dogs may be given relatively high weight for purposes of modeling the rate of loss of a radionuclide from the liver due to broad quantitative similarities between dogs and humans with regard to hepatic handling of many radionuclides. Because the skeleton of the dog shows many qualitative similarities to that of man, data for dogs might be given relatively high weight for purposes of modeling the biokinetics of radionuclides that show considerable exchange between the skeleton and liver.

A physiologically based model provides the proper setting in which to extrapolate data from laboratory animals to man, in that it helps to focus interspecies comparisons on specific physiological processes and specific subsystems of the body for which extrapolation may be valid, even if whole-body extrapolations are invalid. Depending on the process being modeled, it may be preferable to limit attention to data for a single species or small number of species, or to appeal to average or scaled data for a collection of species.

The degree of confidence that can be placed in a model value based on animal data depends on the quality and completeness of the data and the expected strength of the animal analogy for the given situation. Thus, one must consider potential experimental and statistical problems in the data as well as the logical basis for extrapolation of those particular data to humans. Relatively high confidence might be placed in a model value based on animal data if fairly extensive interspecies comparisons have been made and include observations on the species expected to be most human-like (usually non-human primates, dogs, and/or pigs, but this varies with the quantity of interest); these comparisons suggest a strong basis for interspecies extrapolation, either because the data are species-invariant or because the physiological processes governing the biokinetics of the element in different species have been reasonably well established; the model structure allows meaningful extrapolation to man, usually on the basis of physiological processes; and such processes have been well quantified in humans (i.e., the central value for humans has been reasonably well established). A fairly wide uncertainty interval is indicated if data are available only for species that frequently exhibit qualitative differences from man (e.g., if data were available only for rats) or if no meaningful basis for extrapolation to man has been established with regard to the quantity of interest. Whatever the quality of the animal data, the uncertainty interval should reflect the fact that some confidence in the predictive strength of the data is lost when the data are extrapolated across species.

Uncertainty in inter-element extrapolation of biokinetic data

Biokinetic models for elements often are constructed partly or wholly from data for chemically similar elements, on the basis of empirical evidence that chemical analogues often exhibit close physiological similarities. For example, the alkaline earth elements, calcium, strontium, barium, and radium, exhibit many physiological as well as chemical similarities (ICRP 1993, 1995a), and the alkali metals rubidium and cesium closely follow the movement of their chemical analogue, potassium.

There are, however, counterexamples to the premise that chemical analogues are also physiological analogues. For example, the alkali metals potassium and sodium share close physical and chemical similarities but exhibit diametrically opposite behaviors in the body, with potassium being primarily an intracellular element and sodium being primarily an extracellular element.

Moreover, chemically similar elements that behave in a qualitatively similar fashion in the body may exhibit quite different kinetics. For example, cesium appears to follow the behavior of potassium in the body in a qualitative sense but is distributed somewhat differently from potassium at early times after intake and exhibits a substantially longer whole-body retention time.

The level of confidence that can be placed in a model value based on human data for a chemically similar element depends on the quality and completeness of the data for the analogue, as well as the expected strength of the analogy for the given situation. Whatever the quality of the data for the chemical analogue, the confidence interval should reflect the fact that some confidence in the predictive strength of the data is lost when the data are extrapolated across elements.

The strength of the chemical analogy for a given element depends largely on the extent to which the chemically similar elements have also been found to be physiologically similar. That is, the analogy would be considered strong for a pair of elements if a relatively large set of experimental data indicate that these elements have essentially the same qualitative behavior in the body and their quantitative behavior either is similar or differs in a predictable fashion. In view of counterexamples to the premise that chemically similar elements are necessarily physiologically similar, the chemical analogy does not provide high confidence if the elements in question have not been compared in animals or man.

If a chemical analogue has been shown to be a good physiological analogue, then application of human data on the chemical analogue (H2 data) may be preferable to application of animal data on the element of interest (A1 data). For example, for purposes of constructing or evaluating a biokinetic model for americium in humans, use of quantitative human data on the physiological analogue curium seems preferable to use of the best quantitative animal data on americium. Similar

statements can be made for radium and barium, rubidium and potassium, or other pairs of close physiological analogues. On the other hand, if two chemically similar elements show only broad physiological similarities, the animal analogy may be preferred to the chemical analogy, particularly if element-specific data are available for a variety of animal species. In general, lower confidence would be placed in animal data for a chemical analogue than in animal data for the element of interest.

Uncertainty in central estimates stemming from variability in the population

In this report, “uncertainty” refers to lack of knowledge of a central value for a population, and “variability” refers to quantitative differences between different members of a population. Although uncertainty and variability are distinct concepts, the variability in biokinetic characteristics within a population is often an important factor contributing to the uncertainty in a central estimate of a biokinetic quantity. This is because such variability complicates the problem of identifying the central tendency of these characteristics in the population due to the small number of observations generally available and the fact that subjects usually are not randomly selected.

Variability in the biokinetics of radionuclides, pharmaceuticals, or chemicals in human populations appears to result from many different physiological factors or modulating host factors of an environmental nature, including age, gender, pregnancy, lactation, exercise, disease, stress, smoking, and diet. Large inter-individual biokinetic variations sometimes persist in the absence of appreciable environmental differences and suggest that these variations may be genetically controlled. In real-world situations, genetic and environmental factors may interact dynamically, producing sizable variations in the behavior of substances taken into the human body.

Examples of data sources for some specific biokinetic models

Model of the respiratory tract

The respiratory tract model used in this report is described in Chapter 4. The model depicts air intake (ventilation), deposition of airborne material in compartments within the extrathoracic (*ET*) and thoracic regions of the respiratory tract, and clearance of material from these compartments by mechanical processes and absorption to blood. The airways of the *ET* region are divided into the anterior nasal passages, in which deposits are removed by extrinsic means such as nose blowing, and the posterior nasal passages including the nasopharynx, oropharynx, and the larynx, from which

deposits are swallowed. The airways of the thorax include the bronchi, bronchioles, and alveolar region. Material deposited in the thoracic airways may be cleared into blood by absorption, to the gastrointestinal tract by mechanical processes (that is, transported upward and swallowed), and to the regional lymph nodes via lymphatic channels. The rates of movement by mechanical processes are based on different kinetic phases observed in humans or laboratory animals. The mechanical clearances are the same for all radionuclides, but the rate of absorption to blood depends on the dissolution rate of the inhaled material, which in turn depends on the chemical and physical form in which a radionuclide is inhaled. Although the model permits consideration of compound-specific dissolution rates, a particulate is generally assigned to one of three default absorption types: Type F (fast dissolution and high absorption to blood), Type M (an intermediate rate of dissolution and intermediate absorption to blood), and Type S (slow dissolution and low absorption to blood).

Most parameter values of the respiratory tract model are based on data from human studies, but data derived from laboratory animals and *in vitro* studies are often used to assign an absorption type to a given form of a radionuclide. Some of the parameter values of the respiratory tract model are independent of the chemical properties of the inhaled material (e.g., total and regional deposition fractions). In such cases, H2 data are as valuable as H1 data, and A2 data are as valuable as A1 data.

Uncertainties in the integrated activity of an inhaled radionuclide and the distribution of that activity in the respiratory tract arise from incomplete knowledge of the ventilation rate, total and regional deposition of inhaled material, the rate of mucociliary clearance of particles from the tracheobronchial region, the extent of long-term retention of material in the airway walls in the tracheobronchial region, the retention time for insoluble particles in the alveolar region, the rate of dissolution of particles and absorption of the radionuclide to blood, the rate of movement of material to the lymph nodes, and the retention time of material in the lymph nodes. Some of these quantities have been studied extensively in human subjects and are known within narrow bounds. For example, the average ventilation rate may be known within about 30-40%. Total deposition in the respiratory tract and in specific regions of the tract have not been determined with such high precision, although there are fairly extensive human data for some ranges of particles size (e.g., for particle sizes near 1 μm AMAD). With regard to estimates of dose or cancer risk, the uncertainty in total deposition in the respiratory tract tends to be more important than uncertainties in regional deposition fractions because the latter tend to offset one another to some extent in estimates of dose to the lungs or systemic organs. Knowledge of mechanical clearance rates varies with the region and time frame considered. For example, the authors of ICRP Publication 66 (1994a) concluded that the mean clearance rate from the alveolar-interstitial region up to 100 d may be known within about 20%, the rate at 200-300 d within a factor of 2, and the long-term removal rate from the alveolar

interstitium to the bronchioles (0.0001 d^{-1} , corresponding to a half-time of almost 7000 d) within a factor of 3. Particle clearance from the tracheobronchial region has not been characterized with much precision, but there is convincing evidence that most of the deposit will clear in several hours.

The lung dose is defined as a weighted average of the doses to three radiosensitive regions of the lungs: the bronchial region (BB), the bronchiolar region (bb), and the alveolar-interstitial (AI) region. The ICRP (1994a) recommends the use of equal weights, or detriment apportionment factors, for these three regions but points out the possibility, in view of the regional distribution of spontaneous lung cancers in the general non-smoking population, that uniform irradiation of the lungs may be more likely to lead to the induction of cancer in the bronchial region than in the alveolar and bronchiolar regions. Estimates of lung dose are relatively insensitive to the choice of regional apportionment factors for radionuclides that emit penetrating radiation because the three regions are in close proximity to one another, but estimates depend strongly on the choice of regional apportionment factors for some radionuclides that emit mainly alpha or low-energy beta particles.

In many cases, a major uncertainty in the estimated doses to lungs as well as systemic tissues is the rate of absorption to blood. This rate depends strongly on the physicochemical form of the radionuclide. The form of an airborne particulate usually is not known with much certainty and, if known, may not be unambiguously associated with a given absorption type (Type F, M, or S) on the basis of available studies. Even if there is sufficient information to assign the inhaled material to a general absorption type, each type represents a wide range of absorption rates to blood. According to recommendations of the ICRP (1995b), a material would be assigned to Type F if available information suggests that the rate of absorption to blood is 0.069 d^{-1} or greater, to Type S if the absorption rate is 0.001 d^{-1} or less, and to Type M if the absorption rate is between 0.069 d^{-1} and 0.001 d^{-1} . Depending on the half-life of the radionuclide, the range of absorption rates for any given absorption type could correspond to a wide range of potential doses to the lung or systemic organs. Although the ICRP recommends that material-specific rates of absorption should be applied whenever reliable data exist for human subjects or laboratory animals, such data seldom exist.

Gastrointestinal tract model and f_1 values

The ICRP's current model of transit of material through the segments of the gastrointestinal tract is described in Chapter 4. The model divides the contents of the gastrointestinal tract into four segments: stomach, small intestine, upper large intestine, and lower large intestine. Transit of material through the gastrointestinal tract and absorption to blood are described by first-order kinetics. Absorption is assumed to occur in the small intestine and is represented by an element-

specific uptake fraction, called an f_1 value, that is converted to a transfer coefficient from the small intestine contents to blood. The transfer coefficients for movement of intestinal contents are equal to the reciprocal of the mean residence times, taken to be 1 h for the stomach, 4 h for the small intestine, 13 h for the upper large intestine and 24 h for the lower large intestine. The model was originally intended for application to radiation workers but is broadly consistent with data for women and children (NCRP, 1998). Moreover, the transit times used in the ICRP's model seem reasonably consistent with newer data. It appears that incomplete knowledge of typical transit times through the gastrointestinal tract, or inaccurate representation of these transit times in the ICRP's model, do not contribute greatly to uncertainties in cancer risk estimates for intake of radionuclides.

The uncertainty in fractional uptake from the gastrointestinal tract to blood (f_1 value) varies considerably from one element to another. In a relative sense (that is, when expressed as a multiple of the ICRP's value), uncertainties in the f_1 values are smallest for elements that are known to be nearly completely absorbed, including hydrogen (as tritium), carbon, sodium, chlorine, potassium, bromine, rubidium, molybdenum, iodine, cesium, thallium, fluorine, sulfur, and germanium. Average uptake from the gastrointestinal tract is also reasonably well established for several frequently studied elements whose absorption is incomplete but represents at least a few percent of intake, such as copper, zinc, magnesium, technetium, arsenic, calcium, strontium, barium, radium, lead, iron, manganese, cobalt, and uranium. Relative uncertainties generally are greater for the remaining elements, usually due to some combination of the following problems: (1) there is little direct information on man (e.g., ruthenium, silver, aluminum); there are substantial inconsistencies in reported absorption fractions (e.g., beryllium, antimony, silicon); and (3) absorption is too low to be determined with much precision under most conditions (e.g., most actinide and lanthanide elements). Absorption of a few poorly absorbed elements such as thorium, plutonium, americium, and curium has been studied under controlled conditions in human subjects, and average uptake in the adult may be established within a factor of about 5 for these elements. Relative uncertainties may be greatest for several elements whose absorption has not been studied in man but for which A1 data or other indirect evidence indicates absorption on the order of at most a few hundredths of a percent, such as samarium, gadolinium, dysprosium, erbium, thulium, actinium, yttrium, and scandium. The f_1 values for these elements are, at best, order-of-magnitude estimates.

Systemic biokinetic models for parent radionuclides

The quantity and quality of information available to model the time-dependent distribution of an element after its absorption to blood varies considerably from one element to another. For

several essential elements and a few non-essential elements such as cesium and strontium, a reasonably detailed biokinetic data base has been derived from studies involving human subjects (H1). For some other elements, such as zirconium, hafnium, antimony, and cerium, development of a systemic biokinetic model must be based almost entirely on surrogate information such as A1 and A2 data. Information for most elements falls somewhere between these extremes, in that the systemic biokinetics has been studied to a limited extent in human subjects, and some supplementary information is available in the form of A1, H2, and/or A2 data.

The following paragraphs summarize available information on the systemic biokinetics of each of eleven elements: hydrogen (as tritiated water), cobalt, strontium, ruthenium, antimony, iodine, cesium, radium, thorium, uranium, and plutonium. These elements were chosen for consideration because of their environmental importance and because they illustrate different levels of knowledge of the systemic biokinetics of elements in the human body. The discussions of tritium, cobalt, strontium, ruthenium, antimony, cesium, radium, and thorium were taken from a paper by Leggett et al. (1998); the discussion of iodine was extracted from reviews by Dunning and Schwarz (1981) and ICRP (1989); and discussions of thorium and uranium were extracted from reviews by Leggett (1994, 1997).

Tritium, as tritiated water (HTO): There is a large data base on whole-body retention of tritium in adult humans exposed to HTO (H1 data), and there have been several detailed studies of the behavior of HTO in laboratory animals (A1 data). It has been established that tritium is fairly uniformly distributed in the body and that retention can be described as a sum of two or three exponential terms. The dominant, short-term component closely approximates the turnover of body water, and the longer-term components, accounting for only a small percentage of the cumulative activity, appear to represent other forms of molecularly bound tritium. The consistency in reported means of the short-term half-time in largely adult male study groups (Fig. D.1) indicate that the typical short-term half-time — and hence the typical cumulative activity — is reasonably well

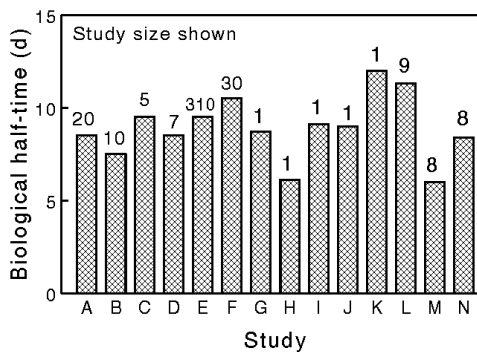


Fig. D.1. Reported half-times for the short-term retention component for tritium taken in mainly as HTO by adult humans (after Leggett et al. 1998).

established for this portion of the population. The equivalence of the short-term component with the turnover of body water, as supported by observations on adult male humans and laboratory animals of various ages, provides a means of extending the model to children and adult females with some confidence. Thus, a combination of three different types of data (H1, P, and A1) leads to reasonably high confidence in age- and gender-specific estimates of cumulative activity of tritium in the body after intake of HTO.

Cobalt: Whole-body retention of inorganic cobalt by the adult can be estimated with reasonably high confidence from H1 data, but considerable uncertainties remain with regard to the time-dependent distribution in the human body. Information on the internal distribution of cobalt comes mainly from studies on laboratory animals (A1 data), and these data cannot be extrapolated to humans with high confidence because of apparent species differences in the behavior of cobalt. For example, the long-term retention component is considerably larger in human subjects than other studied species, and the difference cannot be explained by metabolic rate or body size. Limited comparisons of data for man and laboratory animals suggest that the liver may be a more important long-term repository for cobalt in humans than in other studied species. Development of a biokinetic model is complicated by the fact that environmental cobalt may have substantially different biokinetic properties from the inorganic forms of cobalt generally used in experimental studies. Age-specific data for cobalt are available only for rats, which is not a preferred species for age-specific modeling.

Strontium: Relatively plentiful H1 data exist for strontium, but the heterogeneity of these data complicates the modeling process. A large data base related to the transfer of ^{90}Sr from food and milk to the human skeleton was developed in the 1950s and 1960s, but interpretation of these environmental H1 data is complicated by the facts that measured skeletal burdens were accumulated over an extended period and fractional uptake of ^{90}Sr from the gastrointestinal tract at a given age is not known with much precision. More easily interpreted age-specific H1 data on the systemic biokinetics are available from controlled H1 studies, but such data are limited for children. Age-specific data on retention of strontium in beagles (A1) help to clarify the behavior of strontium at early times after intake as well as relative patterns of buildup and decline of strontium in bone at different stages of bone development. Because strontium is a close physiological analogue of calcium, data from controlled studies of calcium in humans (H2) provide supporting information for selection of age-specific parameter values for strontium. The use of a biologically meaningful model framework allows the strontium data to be superimposed on information concerning addition and

turnover of skeletal calcium and restructuring of bone (type P data). The collective data provide high confidence in model predictions of cumulative activity in bone of adults and reasonably high confidence for children. Overall, the systemic biokinetics of strontium is reasonably well understood but cannot be estimated as accurately as that of cesium or tritium, for example.

Ruthenium: The systemic biokinetics of ruthenium is slightly less well understood than that of cobalt, for example. Knowledge of the systemic biokinetics of ruthenium comes mainly from A1 data, including studies on mice, rats, guinea pigs, rabbits, cats, dogs, and monkeys. Reported long-term retention half-times range from about 200 d to about 1600 d and show no trend with body mass. H1 data consist mainly of whole-body retention measurements on one healthy human subject who ingested different chemical forms of ^{103}Ru or ^{106}Ru on different occasions. The estimated long-term half-time in this subject is within the broad range of values indicated by the animal data. Data on the systemic distribution of ruthenium comes mainly from studies on rodents and suggest a somewhat uniform distribution, the main exception being an elevated concentration in the kidneys in the early weeks after injection. Information on age-related changes in the biokinetics of ruthenium is available only for rodents (A1).

Antimony: Despite the availability of A1 data for several species as well as some scattered H1 data, only order-of-magnitude estimates can be made for the cumulative activity of absorbed ^{125}Sb in most organs. A1 data are available from studies on mature mice, rats, hamsters, rabbits, cows, dogs, and monkeys, and some age-specific data are available for rats. H1 data come from measurements of excretion following accidental or controlled exposure to antimony and a few autopsy measurements in occupationally or environmentally exposed persons. Both the A1 and H1 data are complicated by a sizable variability with chemical form of antimony administered and with route of exposure. The A1 data are further weakened by a species dependence in the internal distribution of antimony. The H1 data are suspect due to the questionable reliability of reported measurements of low-level environmental antimony in food and human tissues. H2 data are of little use because the nearest neighbors in the periodic chart, arsenic and bismuth, do not appear to be close physiological analogues of antimony.

Iodine: The systemic biokinetics of iodine is well understood in a qualitative sense, but it is difficult to define “typical” systemic biokinetics of this element. There is a large body of age-specific data on uptake and retention of iodine by the human thyroid. Reported thyroidal uptake

Table D.1. Summary of reported data on uptake and retention of iodine by the human thyroid (Dunning and Schwarz, 1981).

Age (y)	Uptake by thyroid (%)				Apparent biological T _{1/2} (d)			
	N	Median	Mean	Range	N	Median	Mean	Range
Newborn	67	37	47	6-97	4	13	16	6-23
0.5-2	25	37	39	18-66	9	10	13	4-39
6-16	114	43	47	17-88	17	44	50	19-118
>18	565	17	19	8-46	47	72	85	21-372

fractions and biological half-times are highly variable, probably due in large part to a high inter-subject variability in the biokinetics of iodine resulting from a strong dependence on the level of stable iodine in the thyroid. The scatter in reported values is an important source of uncertainty in typical thyroidal uptake fractions and half-times for iodine because it complicates the problem of identifying the central tendency of these values in the population. In an investigation of the imprecision in age-specific estimates of dose to the thyroid from intake of ¹³¹I, Dunning and Schwarz (1981) examined the variation in reported age-specific values for uptake and retention of iodine by the thyroid. Medians and ranges of the collected values are summarized in Table D.1. For each age group, wide ranges of reported values were found for each parameter. Particularly extensive data were found for the biological half-time in the adults (18-fold difference between maximum and minimum values) and uptake in the newborn (16-fold difference). For ¹³¹I, uncertainty in the biological half-time in the thyroid is not an important source of uncertainty in the integrated activity in the thyroid, because the estimated lower bound of the retention time is long compared with the radiological half-life of ¹³¹I. A more important consideration is the level of thyroidal uptake of absorbed ¹³¹I, which may be increased substantially in persons with low intake of iodine in food.

Cesium: With regard to systemic biokinetics, cesium is among the best understood elements. There is an enormous literature on the biological behavior of cesium in human subjects exposed under natural or controlled conditions. These H1 data indicate that cesium is fairly uniformly distributed in the body and that whole-body retention can be approximated reasonably well by a single biological half-time, although one or two additional short-term half-times have been identified in several studies. The consistency of reported mean half-times for groups of healthy adult males

from different regions of the world leads to high confidence in a central estimate for this portion of the population (Fig. D.2). Comparative data for healthy adult males and females reveal that the mean half-time for females is consistently 15-30% lower than that for males. The pattern of change with age in the retention half-time during growth is also well established. Thus, there is sufficient high-quality H1 data on cesium to characterize typical whole-body retention of this element within narrow bounds, for children as well as for adults of both genders.

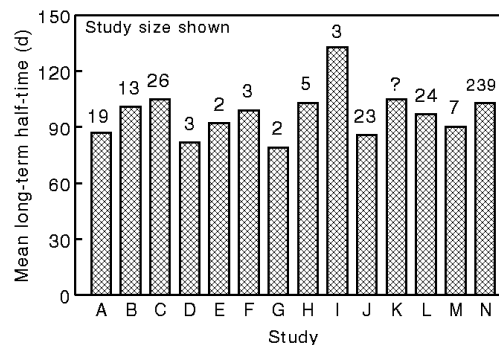


Fig. D.2. Reported biological half-times for cesium in adult male humans (from Leggett et al., 1998).

Radium: The systemic biokinetics of radium is slightly less well understood than that of strontium, for example. A relatively large but incomplete H1 data base for radium can be supplemented with various types of surrogate data for purposes of constructing a systemic biokinetic model. Measurements of whole-body retention of radium are available for many human subjects, but the data are scattered and many of the subjects were unhealthy, elderly, or received relatively high doses that may have affected the bone turnover rate. Whole-body retention data for radium can be supplemented with H2 data from controlled studies on its close chemical and physiological analogue, barium. The systemic distribution of radium at times soon after exposure has been determined in a few seriously ill human subjects and can also be estimated from A1 data, although species differences in endogenous fecal excretion of radium must be taken into account. Limited age-specific H1 data for radium indicate that retention at early times after injection is proportional to the rate of addition of calcium to the skeleton, and this is supported by A1 and H2 data. Available H1, H2, and A1 data for radium can be superimposed on a biologically meaningful model of calcium addition and turnover and bone restructuring (see Fig. 4.6 of the main text). The combined information can be used to characterize the biological behavior of radium in man in reasonable detail, although the surrogate information provides less confidence than equally detailed H1 data would provide.

Thorium: The biokinetics of thorium is reasonably well understood on the basis of extensive data on beagles and other laboratory animals (A1), together with limited data on human subjects (H1). For some of the most important isotopes of thorium, however, tissue doses are due

mainly to radioactive progeny produced in the body, and the biokinetics of ingrowing chain members is generally less well understood than the biokinetics of the thorium parent. Useful H1 data on thorium as a parent come from a controlled study involving elderly human subjects, long-term measurements of ^{227}Th or ^{228}Th in the bodies and excreta of occupationally exposed persons, and measurements of thorium isotopes in autopsy samples from non-occupationally exposed subjects. Additionally, there have also been several studies of the biokinetics of thorium isotopes in laboratory animals, including a particularly detailed study on dogs. The animal studies also provide some information on the migration of chain members from ^{228}Th or ^{232}Th , for example. The collective H1 and A1 data establish that thorium is cleared very slowly from the body and has a much higher affinity for bone than for other tissues. It is reasonably well established that thorium deposits on bone surfaces and is removed by bone restructuring processes over a period of years. There is little direct information on changes with age in the biokinetics of thorium, but it is expected that the turnover of skeletal thorium will be elevated at younger ages due to a high rate of bone restructuring. Results of studies on laboratory animals suggest that members of the ^{228}Th or ^{232}Th chains produced in soft tissues and on bone surfaces migrate from the parent and behave as if injected into blood.

Uranium: Collective H1 and A1 data provide a reasonably good picture of the behavior of uranium in the human body during the first few months after its entry into blood but cannot be used to characterize the long-term retention of uranium in bone and soft tissues with much certainty. The most direct information on the biokinetics of uranium, particularly its rate of urinary excretion as a function of time after injection, comes from three studies on human subjects who were intravenously injected with uranium isotopes and followed for periods varying from a few days to 1.5 y after injection. In one of these studies, several bone biopsy samples were taken during the first day or two after injection, and autopsy samples of bone and soft tissues were collected at times up to 1.5 y after injection, but the usefulness of these postmortem data is limited by the poor physical conditions of the subjects at the time of administration of uranium. Best available information on the long-term distribution of uranium in the human body comes from postmortem measurements of uranium in tissues of occupationally and environmentally exposed subjects, but the usefulness of these data is limited by the small numbers of subjects, the small samples of tissue collected in most cases, uncertain exposure histories, and technical difficulties in measuring the typically low concentrations of uranium in tissues of environmentally exposed subjects. Various aspects of the biokinetics of uranium have been examined in baboons, dogs, rabbits, rats, mice, monkeys, sheep, and other animal species (A1 data). The animal studies yield much information not provided by the human studies, including some indication of changes with age in the biokinetics of uranium.

Plutonium: Although there have been many studies of the biological behavior of plutonium in human subjects exposed either occupationally or under controlled conditions, these H1 data do not fully characterize the relatively complex behavior of plutonium in the body. The rate of urinary excretion of plutonium as a function of time after intake is now reasonably well established from H1 data, and there is some information on the time-dependent urinary-to-fecal excretion ratio. Recently reported injection data for healthy volunteers suggest a gender dependence in the rate of excretion of plutonium in adults. H1 as well as A1 data indicate that most of the body's plutonium is sequestered in skeleton and liver at all times after exposure. H1 data on the division between liver and skeleton soon after exposure are contradictory, with generally small samples of autopsy data from unhealthy subjects indicating that skeleton contains more than liver and external measurements on healthy subjects suggesting the opposite. Most but not all A1 data indicate greater initial uptake in the skeleton than the liver. The long-term division between liver and skeleton is reasonably well established by H1 data. The qualitative behavior of plutonium after deposition on bone surfaces, including burial in bone volume and removal to bone marrow or plasma, is understood from observations of plutonium and related elements in laboratory animals (A1, A2) and, to a lesser extent, humans (H1, H2). However, the rates of removal of plutonium from bone surfaces and burial in bone volume are not well established and are important sources of uncertainty in estimates of cumulative activity of isotopes of plutonium on bone surface. Predictions of uptake and retention of plutonium by the gonads must be based largely on A1 data. Information on changes with age in the biokinetics of plutonium and related elements comes from studies on dogs and other laboratory animals. These A1 and A2 data indicate that fractional deposition of actinide elements in the skeleton is much greater in immature than mature animals.

Models for radionuclides produced in the body by radioactive decay

Dose and risk estimates for ingestion or inhalation of a radionuclide are sometimes strongly influenced by assumptions concerning the biokinetics of radioactive chain members produced in the body. For example, risk coefficients for inhalation or ingestion of ^{60}Fe , ^{210}Pb , or ^{232}Th depend strongly on assumptions concerning the extent of migration of chain members from the parent, because the parent represents only a small portion of the total energy of the chain in each case. For ^{210}Pb , ^{232}Th , and several other important radionuclides, some information on the fate of ingrowing radioactive progeny is available from observations on laboratory animals and occupationally exposed subjects (Leggett et al., 1984). For ^{60}Fe and many other radionuclides, however, lack of information on the biological fate of radioactive progeny represents a major source of uncertainty in cancer risk

estimates. The ICRP's assumptions concerning the behavior of decay chain members produced in the body are discussed in Chapter 4 of this report.

Uncertainties in internal dosimetric models

Specific energy (*SE*) for photons

There are two principal computational procedures available for estimating specific absorbed fractions (SAF) for photon emissions: the Monte Carlo method of simulation of radiation transport and the point-source kernel method. Both of these methods may involve non-trivial errors, depending on the photon energy and the organs under consideration. An examination of the advantages and disadvantages of these two very different methods, together with a comparison of predictions of the two methods for various situations, provides insight into the uncertainties in *SEs* for photons and ways to minimize those uncertainties.

The Monte Carlo method is a computerized approach for estimating the probability of a photon interaction within target organ *T* after emission from source organ *S*. This method is carried out for all combinations of source and target organs and for several photon energies. The body is represented by an idealized phantom in which the internal organs are assigned masses, shapes, positions, and attenuation coefficients based on their chemical composition. Hypothetical interactions of numerous photons emanating in randomly chosen directions from points in the source organ are recorded as the photon travels through tissues and escapes from the body or loses its energy. This approach can produce significant statistical errors in situations where few interactions are expected to occur, such as cases involving low initial energies or target organs that are relatively small or remote from important sources of activity.

The second procedure for estimating specific absorbed fractions for photon emissions involves integration of a point-source kernel $\phi(x)$, where x is the distance from the point source. The function ϕ is composed of inverse-square and exponential attenuation factors that reflect the loss of energy from photon interactions and a buildup factor that reflects the contribution of scattered photons to dose. The point-source kernel method technically is valid only for a homogeneous, unbounded medium and may yield errors of a factor of two or more in cases involving significant variations in composition or density of body tissue or smaller errors (up to about 10%) in cases where target organs or important sources of activity lie near a boundary of the body.

Results of Cristy and Eckerman (1987) indicate that the specific absorbed fractions for photons vary substantially with age for some energies, source organs, and target organs. As a rule,

uncertainties in *SAFs* are greater for children than adults due to greater uncertainties concerning typical sizes and shapes of organs of children.

Maximal differences between the Monte Carlo and classical point-kernel methods are expected to occur for widely separated organ pairs and for large coefficients of variation for the Monte Carlo estimates. A comparison of the two methods was made for such situations in phantoms representing children of ages 1-15 y (Cristy and Eckerman, 1987). The results of this comparison indicate that the two approaches agree within a factor of two at all energies and within about 20% at energies greater than 500 keV. The largest differences between the methods occur at very low energies (10 keV or less) and at energies near 100 keV. The disagreement at 10 keV or less probably results from some combination of poor statistics for the Monte Carlo values and poor data underlying the point-source kernel at these energies. The disagreement at energy levels near 100 keV probably is due largely to the inability of the point-source kernel method to account properly for the effects of scattering. Comparisons of the Monte Carlo and point-kernel methods have been used to determine correction factors for values generated by the point-kernel method (Cristy and Eckerman, 1987). It appears that, for most situations, uncertainties associated with photon absorbed fractions can be minimized by applying a weighted average of the specific absorbed fraction $SAF(T,S)$ and the reciprocal $SAF(T,S)$ produced by the Monte Carlo method. In cases where the Monte Carlo values are statistically unreliable, however, it is preferable to apply the corrected point-kernel method.

SEs for beta particles and discrete electrons

Beta particles and discrete electrons usually are not sufficiently energetic to contribute significantly to cross-irradiation doses of targets separated from a source organ. Thus, for these radiation types it is generally assumed that $SAF(S,S)$ is the inverse of the mass of organ S , and if source S and target T are separated, $SAF(T,S) = 0$. Exceptions occur when the source and target are in close proximity, which can occur in the respiratory tract or in the skeleton.

In the respiratory tract, there are narrow layers of radiosensitive basal and secretory cells in the epithelium. These are irradiated to some extent by beta particles and discrete electrons emanating from nearby "source organs", including the gel layer, the sol layer, and other identified compartments within the epithelium.

The skeleton is generally represented as a uniform mixture of its component tissues: cortical bone, trabecular bone, fatty marrow, red marrow, and connective tissues. Tissues of interest for dosimetric purposes are the red marrow, which lies within the generally tiny cavities of trabecular

bone, and osteogenic cells adjacent to the surfaces of both cortical and trabecular bone. For the red marrow the pertinent dose is assumed to be the average dose to the marrow space within trabecular bone. For the osteogenic tissue, the ICRP recommends that the equivalent dose be calculated as an average over tissues up to a distance of 10 μm from the relevant bone surface.

In the vicinity of discontinuities in tissue compositions such as that between bone mineral and soft tissues, the assumption that the skeleton is a uniform mixture of its component tissues can lead to sizable errors in estimates of dose from beta particles and discrete electrons, as well as photons. For example, neglect of energy transferred to electrons by photon interactions in these regions can result in overestimates of dose to bone marrow by as much as 300-400% for photon energies less than 100 keV. Similarly, conventional methods for treating beta emissions in the skeleton may substantially overestimate the dose to soft tissues of the skeleton. With regard to the ICRP's *SE* values, this problem was recently addressed for photons (Cristy and Eckerman, 1993), but conventional methods are still used for treatment of beta emissions.

SEs for alpha particles

The energy of alpha particles and their associated recoil nuclei is generally assumed to be absorbed in the source organ. Therefore, for alpha particles, $SAF(S,S)$ is taken to be the inverse of the mass of the source organ S , and $SAF(T,S) = 0$ if S and T are separated.

If an alpha emitter is uniformly distributed on the surface of trabecular bone then, by simple geometric considerations, the absorbed fraction in the marrow space is 0.5. Lacking information on the location of the hematopoietic stem cells, the ICRP assumes that the cells are uniformly distributed within the marrow space. If the sensitive cells were located more than 10 μm from the bone mineral surface, the relevant absorbed fraction would be reduced to 0.23-0.34 for an alpha emitter with energy in the range 5-8 MeV.

For an alpha emitter uniformly distributed in the mineral of trabecular bone, the absorbed fraction in the red marrow depends on the energy of the alpha particle. Calculations for alpha emitters ranging in energy from 5 to 8 MeV indicate that the absorbed fraction in the marrow space ranges between 0.041 and 0.087, which bracket the value of 0.05 recommended by the ICRP. If the sensitive cells were located more than 10 μm from the bone mineral surface, the relevant absorbed fraction would be reduced to 0.015-0.055. Thus, dose estimates to skeletal tissues for alpha emitters are sensitive to assumptions regarding the spatial relationship between the source and target regions. It seems likely that the ICRP's nominal *SE* values for alpha emissions from bone surface or volume may overestimate the dose to red marrow by a factor of 2 or more in many cases.

For an alpha emitter uniformly distributed in bone mineral, estimates of the absorbed fraction in bone surface ranges from less than 0.02 to more than 0.03, depending on the energy of the alpha particle. The nominal value recommended by the ICRP is 0.025.

Special dosimetric problems presented by walled organs

The so-called "walled organs" of the body are the parts of the gastrointestinal tract and the bladder in which the radionuclide may be present in the contents of the organ. In the case of beta radiation, it is assumed that the dose to the wall of the organ is equivalent to the dose at the surface of the contents. For beta particles of low energy, this approach seems likely to overestimate the dose to the wall and to the cells associated with maintaining the epithelial lining of the wall (Poston et al. 1996a, 1996b). For alpha radiations the dose to the wall is taken as 1% of the dose at the surface of the contents. This value is not based on calculations of energy deposition but is a cautiously high value based on an acute toxicity study on rats (Sullivan et al., 1960). In that study, the LD₅₀ for ingested ⁹¹Y was estimated as about 12 Gy while a more than 100-fold greater dose to the mucosal surface from ²³⁹Pu had no effect. Although there may be essentially no dose to radiosensitive cells of walled organs from alpha particles in the organ contents, the cautious assumption indicated above continues to be used due to concerns that some radionuclides may be retained in the walls of these organs to a greater extent than commonly modeled. Also, for the intestines, considerable difficulties are encountered in defining the appropriate geometry of the convoluted wall and the contents of this organ.

Uncertainties in external dosimetric models

Transport of radiation from the environmental source to humans

In Federal Guidance Report No. 12 (EPA, 1993), the problem of estimating external dose rates from contaminated air, soil, or ground surfaces was divided into two steps: (1) the calculation of the radiation field incident on the surface of the body and (2) calculation of organ dose rates due to a body surface source. The uncertainties associated with the second step are essentially the same as those discussed above with regard to internal radiation sources.

The method of calculation of the external radiation field was checked as far as practical against other theoretical methods or experimentally determined values (EPA, 1993). The results of the comparisons suggest that the external radiation fields can be determined with reasonably high

accuracy, at least for the idealized geometries generally considered. For example, derived values for the case of a contaminated ground source were checked by comparing the energy and angular dependence of the air kerma above a 1.25-MeV plane source at the air-ground interface with calculations of Beck and de Plaque (1968) based on another method and with the calculations and measurements given in the Shielding Benchmark Problems report (Garrett, 1968). Agreement was within a few percent in both cases.

The greatest uncertainties in the modeled external radiation fields as predictors of real-world situations generally arise from oversimplifications in the exposure scenarios rather than from inadequacies in the dosimetric models *per se*. For example, there will often be considerable differences between the simplified, infinite exposure geometries and real, finite exposure geometries. An important example is exposure to contaminated ground surface, for which the source region is assumed to be a smooth plane. In the real world, external dose rates from sources on the ground surface generally are reduced by shielding provided by “ground roughness”, including irregularities in the terrain and surface vegetation. Dose-reduction factors for a photon spectrum representative of fallout following releases from nuclear reactors are given by Burson and Profio (1977). The recommended values range from essentially unity for paved areas to about 0.5 for a deeply plowed field, and a representative value is about 0.7. Such dose-reduction factors for ground roughness should overestimate equivalent doses due to external exposure to contaminated ground surfaces if the radionuclides emit mostly low-energy photons (Kocher, 1980).

The dose coefficients for air submersion and exposure to contaminated soil assume that exposed individuals spend all of the time outdoors and have no shielding from the radiation (EPA, 1993). For the typical adult male considered in Federal Guidance Report No. 12, one of the largest uncertainties in the external dose rates as applied in the present report is the question of whether a uniform reduction factor, or possibly radionuclide-specific reduction factors, should be used to account for shielding during indoor residence. In the present document, no reduction factors are applied. This approach may be appropriate for some radionuclides (e.g., for some radioisotopes of noble gases) but probably leads to a substantial overestimate of actual dose rates for external exposures in many cases. It is left to the user to decide whether a reduction factor is appropriate for a given application.

For acute releases of radionuclides into the atmosphere, the relationship between indoor and outdoor airborne concentrations of radionuclides will vary with time during and after a release and will also depend strongly on the air exchange rate inside a building (Wallace, 1996). For such releases, a fixed reduction of external dose rates to account for indoor residence would not appear to be appropriate.

Effects of age and gender

The dose coefficients tabulated in Federal Guidance Report No. 12 were calculated for an anthropomorphic model of the adult body derived by Cristy (Cristy and Eckerman, 1987) from ICRP Reference Man data (ICRP, 1975). For all calculations, the phantom is upright at the air-ground interface. The phantom is a hermaphrodite of design similar to that used in the dosimetric evaluation of ICRP Publication 30 (Part 1, 1979).

Age- and gender-specific aspects of external dose have been considered by Drexler et al. (1989) and Petoussi et al. (1991). Limited calculations indicate that the dose to organs of the body from external radiation increases with decreasing body size. This effect is more pronounced at low photon energy than at high energy and is also more pronounced for organs located deep in the body than for more shallow organs with less shielding by overlying tissues.

Calculated effects of age on the effective dose per unit photon fluence are indicated in Fig. D.3 for the case of photons uniformly distributed in angle (isotropic field). Estimates for intermediate ages fall between the curves for the adult and infant. Similar effects of age were calculated for the case of a broad parallel horizontal beam uniformly distributed about the phantom (rotational normal beam). The isotropic field corresponds to a photon source uniformly distributed in the air (submersion) and the rotational normal beam is similar to the situation in which the photon source is distributed on the ground surface. For both cases, the

dependence of the effective dose on age increases at low photon energies and exceeds a factor of two at energies less than about 0.050 MeV. It is for low photon energies that the reduction in dose by shielding by structures during indoor residence becomes increasingly effective. Uncertainties associated with the use of age-independent external dose rates appear to be overshadowed in most cases by uncertainties associated with shielding and exposure geometries.

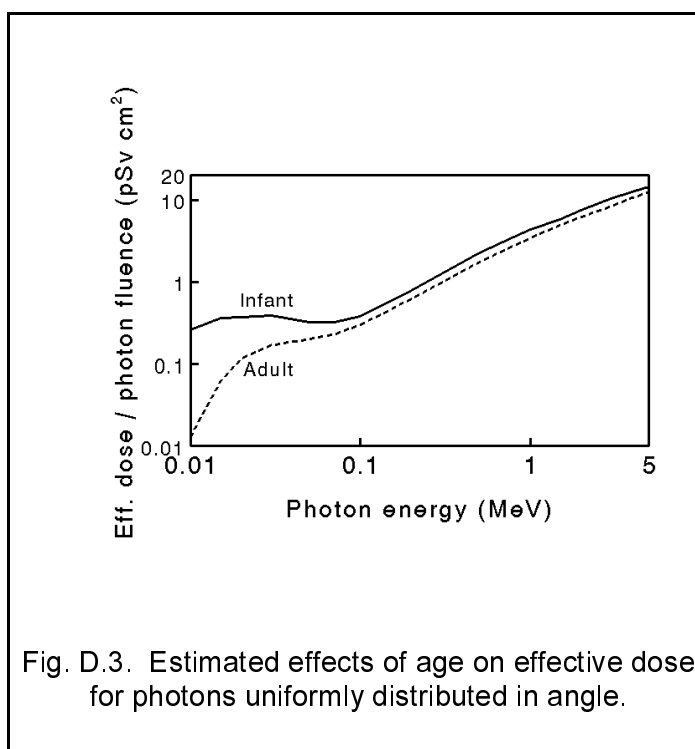


Fig. D.3. Estimated effects of age on effective dose for photons uniformly distributed in angle.

Uncertainties in risk model coefficients

Sampling variability

Epidemiologic data on an irradiated population generally can be organized and modeled in many different ways. For example, choices can be made regarding the grouping of cancer sites, the extent of division of the study population by age and gender, the mathematical form of the dose-response, and the general form of the age and temporal dependence. Although interesting features of the data may be revealed by considering small subgroups, there is a concomitant increase in statistical variability that may preclude any meaningful improvement in the model.

For the statistical analysis of the Life Span Study (LSS) data, the deaths and person-years of survival were aggregated by city, gender, six age groups, seven follow-up intervals, and 10 radiation dose intervals (Shimizu et al. 1989). Site-specific risk coefficients were calculated with a maximum likelihood estimation method that assumes that the numbers of deaths in each group are independent Poisson variates. Based on this analysis, Shimizu and coworkers derived excess relative risk estimates with associated 90% confidence intervals, (A,B) , for a number of cancer sites. Their analysis indicates that sampling variability could lead to sizable errors in estimates of excess relative risk, particularly for sites showing relatively small numbers of excess cancer deaths. For example, the analysis indicates a quotient B/A of about 3 for stomach or lung, 4 for breast, colon, or urinary tract, 8 for ovary, and 10 for esophagus. For leukemia and combined cancers excluding leukemia, B/A is about 1.9 and 1.6, respectively. The implications of the results of Shimizu and coworkers with regard to sampling errors are discussed in greater detail in a recent EPA report on uncertainties in estimates of radiogenic cancer risk (EPA, 1999).

Diagnostic misclassification

Two types of diagnostic misclassification of cancer can occur: classification of cancers as non-cancer cases (detection error) and erroneous classification of non-cancer cases as cancer (confirmation error). Detection errors lead to an underestimate of the excess absolute risk but do not affect the estimated excess relative risk. Confirmation errors lead to an underestimate of the excess relative risk but do not affect the excess absolute risk (NCRP, 1997; EPA, 1999).

Based on results from an RERF autopsy study, Sposto and coworkers (1992) estimated that, due to diagnostic misclassification between cancer and noncancer causes of death, the estimated excess relative risk of induced cancers in the LSS population should be corrected upward by 13%.

Following the approach outlined by Sposto and coworkers, Pierce et al. (1996) estimated that the excess absolute risk estimate should be adjusted upward by about 16% to reflect errors in diagnostic misclassification. However, misclassification errors vary considerably by cancer site, both with respect to proper identification of cancer as the cause of death and with respect to the primary site (EPA, 1999).

Errors in dosimetry

In epidemiological studies of irradiated populations, organ doses generally cannot be determined with high accuracy. For internally exposed subjects, the level or pattern of intake may not be well established, and there is always incomplete information concerning the time-dependent distribution and excretion of the internally deposited radionuclide(s) and any radioactive progeny of those radionuclides produced *in vivo*. For externally exposed subjects, uncertainties in organ doses may arise because the radiation source or the position, shielding, or exposure times of the subjects are not well established.

Random errors in the individual dose estimates for the atomic bomb survivor population have been estimated as 25-45% (Jablon, 1971; Pierce et al., 1990; Pierce and Vaeth, 1991). These random errors are likely to result in an overestimate of the average dose in the high dose groups and, assuming a linear dose response function, a slight underestimate of the dose response (Pierce et al., 1990; Pierce and Vaeth, 1991). More significantly, perhaps, the shape of the dose response will be distorted towards a convex (downward) curvature; hence, a true linear-quadratic dependence may be distorted to look linear (Pierce and Vaeth, 1991).

Measurements of neutron activation products in Hiroshima indicate that neutron doses for Hiroshima survivors may have been underestimated and that the relative magnitude of the error increased with distance from the epicenter (Straume et al., 1992). If neutron doses have been underestimated, then a larger fraction of the radiogenic cancers would be attributable to neutrons, and the estimate of risk from gamma rays should be reduced. Using the tentatively revised estimates of neutron flux derived by Straume and coworkers, Preston et al. (1993) have calculated that the estimated risk from gamma rays for all cancers other than leukemia could be as much as 25% too high, with the calculated overestimate depending on the neutron RBE assumed.

An NCRP committee identified three additional sources of uncertainty relating to the current dosimetry for the Japanese atomic bomb survivors: (1) bias in gamma ray estimates; (2) uncertainty in the characterization of radiation shielding by buildings; and (3) uncertainty in neutron RBE (NCRP, 1997). Altogether, the dosimetric uncertainties were judged to result in roughly a 15% overestimate of risk model coefficients for combined cancers other than leukemia.

Uncertainties in the effects of radiation at low dose and dose rate

For purposes of radiation protection, it is generally assumed that the probability of inducing radiogenic cancers in a human population is proportional to the radiation dose received, even for extremely low doses and dose rates. This “linear, no-threshold” model is a major source of uncertainty, and controversy, in radiogenic cancer risk estimation.

Carcinogenesis is understood to be a multistage process in which a single cell gives rise to a tumor, with mutation of DNA required in one or more of the steps leading to malignancy. Since cancer is a common disease, the background rates for each of these steps must be greater than zero, and any filtration mechanism for removing precancerous cells must be imperfect. Traversal of a single ionizing track through a cell appears to be capable of causing DNA damage that cannot always be faithfully repaired. Thus, it seems reasonable to assume that any exposure that increases the rate of mutation of DNA has a nonzero probability of causing cancer (EPA, 1999). On the other hand, scientific evidence does not rule out the possibility that the risk per unit dose is effectively zero at environmental exposure levels or that there may be a net beneficial effect of low dose radiation (Luckey 1990, Jaworowski 1995, Goldman 1996).

Arguments for and against the existence of an effective threshold for radiation effects have been made on the basis of epidemiological data, but conclusions appear to depend on the population and cancer type considered, the nature of the exposure, and the assumptions underlying the analysis. It is doubtful that human epidemiological data can be used to determine the existence or absence of a threshold for radiogenic cancer, due to the statistical uncertainties inherent in such data. Data for laboratory animals can furnish important information but cannot confirm or refute the existence of thresholds for radiogenic cancer in man.

Evidence that low dose radiation may induce or activate cellular DNA repair mechanisms through an adaptive response or some stimulatory mechanism has led to speculation that low doses may be protective against cancer. The stimulatory effects seen to date have been short term and may not provide a significant reduction in cancer risk (Puskin 1997). A detailed review of possible radiation induced adaptive responses can be found in the UNSCEAR (1994) report.

Primarily on the basis of laboratory studies of cells, plants, and animals, the authors of NCRP Report 64 (NCRP, 1980) advocated a linear-quadratic dose response for acute doses up to about 2.5-4 Gy, above which the dose response begins to turn over due to cell killing. At low doses, the quadratic term is negligible compared with the linear term.

A theoretical framework for the linear-quadratic dose response model has been developed by Kellerer and Rossi (1972). In this theory of "dual radiation action", events leading to "lesions" or permanent changes in cellular DNA require the formation of interacting pairs of "sublesions".

The interacting pairs can be produced by a single track (traversing particle) or by two tracks, giving rise, respectively, to a linear and a quadratic term in the dose response relationship. According to the theory, a sublesion may be repaired before it can interact to form a lesion, with the probability of such repair increasing with time. As the dose rate is reduced, the formation of lesions from sublesions caused by separate tracks becomes less important, and the magnitude of the quadratic term decreases. The theory predicts that at sufficiently low doses or dose rates, the response should be linear and, in either limit, should have the same slope.

The dual action theory has been challenged on experimental grounds, and observed variations in response with dose, dose rate, and LET can also be explained by other plausible theories. For example, the data are consistent with a mechanism involving only single lesions and a "saturable" repair process that decreases in effectiveness at high dose rates on the microscopic scale (Goodhead, 1982). One property of such a theory is that, in principle, the effectiveness of repair — and therefore the shape of the dose response curve — can vary widely with cell type, organ system, and species. Hence, results obtained on laboratory animals might not be entirely applicable to humans.

According to either the dual action theory or the saturable repair theory, the dose response should be linear at low doses or low dose rates, and with equal slopes. At higher doses and dose rates, multiple track events become important, and the dose response should bend upward. As a result, the response per unit dose at low doses and dose rates will be overestimated if one extrapolates linearly from observations made at high, acutely delivered doses (NCRP, 1980).

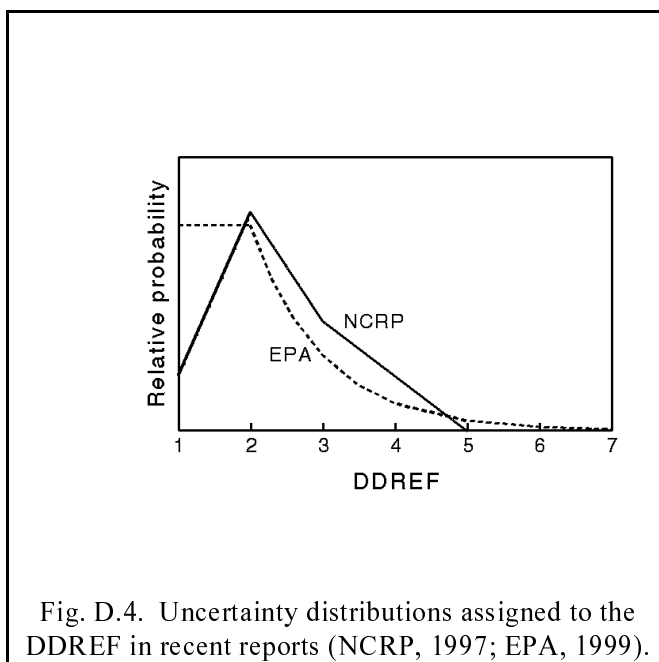
A linear dose response below about 0.2 Gy is consistent with an assumption of maximal DNA repair in that dose range. Repair of radiation-induced DNA damage has been found to be largely complete within a few hours of an acute exposure (Wheeler and Wierowski, 1983; Ullrich et al., 1987). This suggests that maximal repair persists at higher doses, provided the dose received within any time span of a few hours does not exceed 0.2 Gy. Further protraction should have little or no effect on the risk of cancer induction. Thus, the current mechanistic explanations suggest that the dose and dose-rate effectiveness factor (DDREF) is constant at any dose below about 0.2 Gy and for higher doses received at a low dose rate. EPA (1994) adopted the recommendation of UNSCEAR (1993) that an hourly averaged dose rate less than 0.1 mGy min^{-1} may be regarded as low in this context.

Until recently, it appeared that the LSS data could not be explained by a linear-quadratic model because there were inconsistencies for solid tumors or leukemia and also inconsistencies between models developed separately for Hiroshima and Nagasaki. With the revised "DS86" dosimetry, however, these inconsistencies were largely removed (Shimizu et al., 1990; NAS, 1990). The data from the two cities are now in reasonable agreement. The combined leukemia data can be fitted by a linear-quadratic dose response function, with the slope of the function at low doses being

about half that obtained by a linear fit to the data. On the other hand, the data for solid tumors are reasonably consistent with a linear dose response from low doses up to about 4 Gy. Using a linear-quadratic model to fit the data reduces the linear term by, at most, a factor of 2 compared to a simple linear model. Interpretation of these results on the basis of the model used in NCRP 64 (1980) indicates a best estimate of the DDREF of about 2 for leukemia and 1 for solid tumors, and an upper bound of about 2 for solid tumors. Errors in dose estimation may introduce a negative bias in the dose-squared dependence of the response. This has a relatively minor effect on the best estimate of the DDREF but could increase the upper bound to about 3 or 4. When compared with observed lung cancer risks in the atomic bomb survivors, results of clinical studies suggest that the DDREF could be large for lung cancer induction (Howe, 1995).

Results for solid tumors in humans differ from those obtained through laboratory studies, including studies of radiation-induced tumorigenesis in mice and rats. Most laboratory studies suggest a DDREF of about 2 or 3, and sometimes higher, depending on the end point.

Taken together, current scientific data are generally indicative of a DDREF between 1 and 3 for human cancer induction, except for a possibly higher value for lung. The authors of EPA (1994) concluded that a value of 2.0 provides a reasonable central estimate. The Agency's Radiation Advisory Committee agreed "that this choice is reasonable and ... consistent with current scientific judgment" (Loehr and Nygaard, 1992). A DDREF of 2 has recently been adopted by the ICRP (1991), as well as by other organizations (NCRP, 1993; CIRRPC, 1992). The authors of NCRP Report 126 (1997) assigned a piecewise linear uncertainty distribution to the DDREF by assuming that 2 is the most likely value, 1 is one-quarter as likely as 2, 3 is half as likely as 2, and a value less than 1 or greater than 5 is unlikely (Fig. D.4). The authors of a recent EPA report (EPA, 1999) made similar assumptions for values between 2 and 5 but placed more weight on values close to 1 and assigned a non-zero probability to all values greater than 5 (Fig. D.4).



Uncertainties in the RBE for alpha particles

Radiobiological data indicate that high-LET alpha radiation has a larger biological effect than an equal absorbed dose of low-LET radiation. However, ranges of estimated values for alpha particle RBE are wide, depending on both the biological system and the observed endpoint. The uncertainty in the RBE estimate from an individual study is also usually large, primarily due to the uncertainty in extrapolation of low-LET data to low doses. At relatively high doses, the effectiveness of alpha emitters has been found to be 15 to 50 times that of beta emitters for the induction of bone sarcomas, liver chromosome aberrations, and lung cancers (NCRP, 1990). Since the LET of secondary protons produced by fission neutrons in living tissue is comparable to that for alpha particles, data on the RBE of fission neutrons provides ancillary information relevant to the estimation of alpha particle RBE. Where the dose response data on carcinogenic endpoints are adequate to derive an estimate, fission neutrons have been found to have an RBE between 6 and 60 times that of low dose gamma rays (NCRP, 1990). Overall, experimental data for solid tumor induction with alpha particles and fission neutrons suggest a central value of about 10-30 and a range of roughly 5 to 60 for the RBE relative to low-dose, low-LET radiation (NCRP, 1990; NRC-CEC, 1997).

The data are generally suggestive of a linear no-threshold dose response for high-LET radiation, except for a possible fall-off in effectiveness at high doses. Under some conditions the effects of high-LET radiation appear to increase with fractionation or with a decrease in dose rate.

Site-specific cancer risk estimates for high-LET radiation (neutrons or alpha particles) are often calculated using human epidemiological data on low-LET radiation (e.g., from the LSS) and laboratory data on the relative biological effectiveness (RBE) of the high-LET radiation compared to a reference low-LET radiation (NCRP, 1990). Since the dose response relationship obtained for low-LET radiation typically is linear or concave upward while that for high-LET radiation is linear or concave downward, the RBE is dose dependent. The present report is concerned with risks at relatively low doses and dose rates, where the acute high dose risk for low-LET radiation is reduced by the DDREF. The dose responses for both low and high LET radiations are assumed to be linear in this range, and the RBE takes on a constant (maximum) value: RBE_M .

With the exception of radiation-induced breast cancer and leukemia, the authors of the EPA report (EPA, 1994) followed the ICRP's recommendation (ICRP 1991) and assumed that the RBE for alpha particles is 20, in comparison to low-LET radiation at low doses and dose rates. Where the comparison was made against acute high doses of low-LET radiation, however, a value of 10 was

assumed for the alpha particle RBE. Thus the low-LET radiation DDREF of 2 used for these cancers was incorporated implicitly into the RBE value for alpha radiation.

For breast cancer induction, a DDREF of 1 was adopted. It was assumed that the acute high dose RBE of 10 is also applicable to breast cancer at low doses and dose rates.

There is evidence that alpha particle leukemia risks estimated on the basis of an RBE of 20 are too high (EPA, 1991, 1999). For this reason, an alpha particle leukemia risk estimate of $5.0 \times 10^{-3} \text{ Gy}^{-1}$ was employed, consistent with the available high-LET epidemiological data (NAS, 1988; EPA, 1991). Quantitatively, this would correspond to an RBE of 1 for this site (relative to low dose, low-LET radiation). This should not be interpreted as implying that alpha radiation is no more carcinogenic than low-LET radiation in inducing leukemia. At least in part, the lower than expected leukemia risk produced by alpha emitters may result from a nonuniform distribution of dose within the bone marrow. That is, average doses to sensitive target cells of bone marrow may be substantially lower than calculated average marrow doses, to an extent that may vary from one alpha-emitting radionuclide to another. The RBE of 1 for alpha particles is regarded as an "effective RBE" that reflects factors other than just the relative biological sensitivity to high- and low-LET radiations.

Uncertainties in transporting risk estimates across populations

Baseline rates for specific cancer types vary from population to population and also vary over time within a population. For example, stomach cancer rates are substantially higher in Japan than in the U.S., while the reverse is true for lung, colon, and breast cancer. Moreover, the morbidity rates for lung and breast cancer have been increasing in both populations during recent years. Despite the observed rough proportionality between radiation risk and baseline cancer rates by age, it should not be inferred that excess relative risk will be the same as one goes from one population to another.

Information on how to transport risk estimates across populations is limited by the quality of data available on irradiated populations other than the atomic bomb survivors. Two cancer types for which comparative data exist are thyroid and breast. Data on the thyroid suggest that the risk increases with the baseline rate, but this does not appear to be true for breast. Some insight into the problem might be gained by looking at subgroups of an irradiated population. For example, lung cancer rates in Japanese males are several times higher than in Japanese females, presumably due in part to the higher smoking rate in males. Nevertheless, the excess absolute risk for lung cancer attributable to radiation does not differ significantly between the male and female bomb survivors. This suggests that, for lung cancer, absolute risk may be more transportable than relative risk.

Land and Sinclair (1991) present two relative risk models, differing in the method of transporting risk estimates from the LSS population to other populations. Both models assume a constant excess relative risk coefficient beginning 10 y after an exposure and continuing throughout the rest of life for each cancer site, excluding leukemia. One model (multiplicative) assumes that the relative risk coefficient is the same across populations. The other (NIH, for National Institutes of Health) assumes that the relative risk model coefficients for the target population should yield the same risks as those calculated with the additive risk model coefficients from the original population over the period of epidemiological follow-up, excluding the minimal latency period. These excess relative risk model coefficients are then used to project the risk over the remaining years of life. Projections made for the U.S. using the NIH model are much less sensitive to differences in site specific baseline rates between Japan and the U.S. than are those using the multiplicative model.

Data on North American women irradiated for medical purposes indicate about the same risk of radiogenic breast cancer per unit dose as the LSS data, despite the substantially higher breast cancer rates found in the U.S. or Canada, compared to Japan. For breast cancer, therefore, the NIH model projection agrees with observation better than the multiplicative model projection. Comparative data on other radiation-induced cancers are generally lacking or are too weak to draw any conclusions regarding the transportation of risk estimates from the LSS population to the U.S. population.

Both transportation models have a degree of biological plausibility. For example, the multiplicative model is consistent with the hypothesis that radiation acts as an “initiator” while the factors responsible for differences in baseline rates act as “promoters” of cancer. Alternatively, if both radiation and these factors act independently but at the same stage in the carcinogenesis process, their effects should be additive and radiation risks should be similar between populations despite differences in baseline rates. It seems likely that the actual situation is more complex than either of these alternatives and that some mixture of multiplicative and additive effects of radiation and non-radiogenic carcinogens may be involved.

Given the uncertainty in the transportation of risk across populations, the EPA recommends the use of geometric means of the age- and site-specific risk model coefficients derived from the multiplicative and NIH models of Land and Sinclair (EPA, 1994). The use of a geometric mean coefficient tends to de-emphasize extreme values that may reflect large extrapolations based on a few excess cancers observed among those exposed as children.

Uncertainties in age and time dependence of risk per unit dose

Information on the variation of risk of site-specific radiogenic cancers among the atomic bomb survivors with age and time is limited by sampling uncertainties and by the incomplete period of epidemiological follow-up. For a given age at time of the bomb, the excess solid tumor mortality has generally been found to increase with the age at death, roughly in proportion to the age-specific baseline rate for the site of interest. Consequently, models for most tumor sites are now generally framed in terms of relative risk.

For the period of epidemiological follow-up, the highest relative risks are found in the youngest exposure categories. However, the lifetime risks of solid tumors due to exposures before age 20 y remain highly uncertain. Individuals exposed as children are only now entering the years of life where the risk of cancer is concentrated, and the observed excess effects represent a small number of cancer deaths. Hence, the sampling error for most types of cancers is large for the younger age cohorts. Moreover, it is not known whether observed high relative risks will persist. Theoretical considerations, arising from carcinogenesis modeling, suggest that the relative risks may decrease over time. Recent epidemiological evidence indicates such a temporal fall-off in groups irradiated as children (UNSCEAR, 1988; Little et al., 1991).

In assigning uncertainties associated with temporal projection, three classes of cancer sites should be considered (EPA, 1999):

- (1) Sites for which follow-up is essentially complete, with relatively few additional radiation induced cancers expected. For this group, which might include bone sarcomas and leukemia, the uncertainty in lifetime risk associated with temporal projection outside the period of follow-up would be small.
- (2) Sites for which a constant relative risk model has been used to project risk beyond the period of follow-up, but for which the risk coefficients are dependent on the age at exposure. This group includes stomach, colon, lung, breast, thyroid, and residual cancers. Most of the projected lifetime risk for these sites is associated with exposures before age 20 y. The contribution of childhood exposures is highly uncertain in view of the statistical limitations and possible decreases in relative risk with time after exposure. For this group of sites, the model could overestimate cancer risk by as much as a factor of 2-2.5 but seems unlikely to underestimate risk.
- (3) Sites for which a constant relative risk projection has been used but for which the risk coefficient reflects a single age-averaged value. This group includes esophagus, liver, bladder, kidney, ovary, and skin. The data available on these sites are generally sketchy and

heavily weighted towards adult exposures. It is plausible that childhood exposures may convey a higher risk than adult exposures for these sites, as they appear to do for other sites. Consequently, the model used to project risk may tend to understate the population risk in this case. Typically, the relative risks for childhood exposures are found to be 2 to 3 times the average for adults (Shimizu et al. 1990). If risks for childhood exposures are similarly elevated for the sites in question, the population risks would be increased by roughly 50%. On the other hand, a fall-off of 20% or more in relative risk conceivably could occur for these sites even in the case of adult exposures.

Uncertainties in site-specific cancer morbidity risk estimates

The cancer lethality fractions used in this report (see Chapter 7) reflect only cancers appearing in adults. Even for adults, the selection of these values relied in part on subjective judgment because there is no completely reliable way to determine long-term survival based on current (or future) treatment modalities. Moreover, lethality fractions derived for adults may not always be appropriate for children.

It appears that leukemia is now often curable in children. However, most radiogenic leukemias in the atomic bomb survivors occurred before successful treatment became available. Hence, the leukemia mortality risks derived from the Japanese may more properly reflect morbidity than mortality for children.

Imprecision in risk model coefficients as indicated by differences in expert judgments

The U.S. NRC and the Commission of European Communities (CEC) recently conducted a joint study aimed at characterizing the uncertainties in predictions of the consequences of accidental releases of radionuclides into the environment (NRC-CEC, 1997, 1998). As part of the exercise, experts on health effects of radiation were asked to provide 5%, 50%, and 95% quantiles of subjective probability distributions for the total number of radiation-induced cancer deaths and for the numbers of tissue-specific cancer deaths over a lifetime in a typical population of 100 million persons, each receiving a whole body dose of 1 Gy low LET radiation at a uniform rate over 1 min.

Median values provided by the nine experts are given in Table D.2. Comparison of the conclusions of the different experts provides some indication of the precision with which risk model coefficients can be determined on the basis of current epidemiological and radiobiological information. Reasonably consistent central estimates were made by the nine experts for leukemia and colon, for example, but there was less agreement for liver, stomach, bone, skin, and thyroid.

Table D.2. Age-averaged site-specific cancer morbidity risk estimates (cancer cases per person-Gy $\times 10^{-2}$) from low-LET uniform irradiation of the body at high dose and dose rate, as estimated by nine experts on health effects of radiation (NRC-CEC, 1997).

Cancer site	Expert								
	A	B	C	D	E	F	G	H	I
Colon	0.72	0.92	1.1	0.886	0.92	0.7	1.5	1.1	0.92
Stomach	0.50	0.17	0.25	0.405	0.172	2.5	0.63	0.1	0.172
Liver	0.29	0.055	0.065	0.073	0.055	1.3	0.049	0.08	0.055
Lung	1.83	3.4	3.5	2.057	3.373	1.8	1.0	3.8	3.37
Bone	0.018	0.1	0.1	0.012	0.087	0.05	0.022	0.1	0.087
Skin	0.031	0.056	0.08	0.038	0.056	0.05	0.0025	0.055	0.056
Breast	0.37	1.1	1.1	0.994	1.135	0.62	0.34	1.4	0.568
Thyroid	0.19	0.041	0.05	0.024	0.041	0.19	0.092	0.06	0.041
Leukemia	0.81	1.0	1.1	0.851	1.001	1.05	0.66	1.5	1.0
All cancers	10.7	8.8	9.85	9.726	8.832	13.3	7.3	7.5	8.83

Proposed procedure for assigning nominal uncertainty intervals to risk coefficients

A standard method of assessing the uncertainty associated with a model prediction is to investigate the effect of propagation of uncertainties associated with components of the model that correspond to observable phenomena. It is difficult to apply such an approach to the computational model used in this report (see Chapter 7) because of its relatively complex formulation involving numerous parameters that depend on time, age, and gender. It is possible, however, to formulate a simpler model whose predictions are consistently close to the risk coefficients tabulated in Chapter 2 and whose components are easier to assess. For inhalation or ingestion of a radionuclide, the simpler model is

$$\text{Cancer Mortality Risk} = \sum (d_i / \text{DDREF}_i + D_i \times \text{RBE}_i) R_i \quad (\text{D.1})$$

where d_i and D_i are, respectively, low- and high-LET integrated absorbed doses for tissue i , assuming acute intake of the radionuclide by an average adult; R_i is the age- and gender-averaged site-specific cancer mortality risk estimate for tissue i for low-LET uniform irradiation of the body at high dose

and dose rate; $DDREF_i$ is the dose and dose rate effectiveness factor for tissue i ; and RBE_i is the high-LET relative biological effectiveness assumed for tissue i . The risk estimates R_i in Eq. D.1 have not been reduced by a $DDREF$, because the $DDREF$ is considered in this equation as a separate, uncertain component of the risk model. Thus, the high-LET RBE_i values in the equation are relative to a high dose and dose rate risk; that is, the nominal RBE values are 0.5 for leukemia and 10 for all other tissues including breast. An integration period of 20 y was chosen on the basis of empirical considerations, in that substantially shorter periods were found to underestimate risk coefficients for some tenaciously retained radionuclides and substantially longer periods were found to overestimate the cancer risk from doses received late in life. For external exposure scenarios, the right side of Eq. D.1 reduces to $\sum (d_i / DDREF_i) \times R_i$ because the dose is due entirely to low-LET radiation.

For the external exposure scenarios considered in this report, it can be shown that cancer risk estimates based on Eq. D.1 are nearly identical to the risk coefficients given in Chapter 2. As illustrated in Fig. D.5 for the case of intake of tap water, predictions of the simplistic model represented by Eq. D.1 provide a reasonable approximation to risk coefficients for intake of radionuclides, although some systematic differences may arise for a given mode of intake. In Fig. D.5, comparisons are in terms of the quotient A/B , where A is the cancer mortality risk for acute ingestion of a radionuclide by an average adult as predicted by Eq. D.1, and B is the risk coefficient for that radionuclide ingested in drinking water, as given in Table 2.2a.

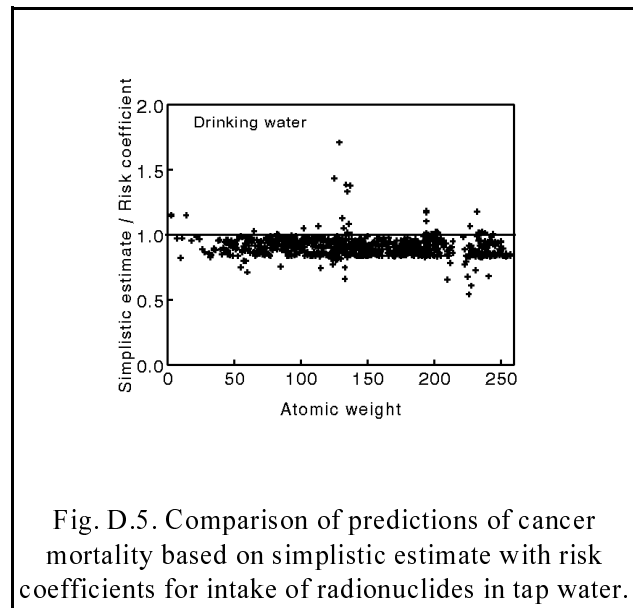


Fig. D.5. Comparison of predictions of cancer mortality based on simplistic estimate with risk coefficients for intake of radionuclides in tap water.

Due to the general agreement of predictions of Eq. D.1 and the computational model used to generate the risk coefficients in Chapter 2, the uncertainty analysis may be based on the simpler model represented by Eq. D.1. In theory, uncertainty distributions could be assigned to the parameter values R_i , RBE_i , $DDREF_i$, d_i , and D_i , and random simulation techniques could be applied to the model represented by Eq. D.1 to generate a range of possible values of each risk coefficient.

Even with this simpler model, a full-scale parameter uncertainty analysis for each of the risk coefficients tabulated in Chapter 2 is not a feasible task, due to the large number of radionuclides and exposure modes addressed and the lack of published expert judgments on uncertainties in tissue

dose estimates for radionuclides. It seems possible, however, to generate a nominal uncertainty interval for each risk coefficient tabulated in Chapter 2 on the basis of results of a systematic, computerized analysis of the sensitivity of predictions of Eq. D.1 to dominant uncertainties in the underlying biokinetic, dosimetric, and radiation risk models. Assignment of uncertainties to the values R_i could be based, for example, on a recent expert elicitation exercise described earlier (NRC-CEC, 1998); uncertainty distributions for the values $DDREF_i$ could be patterned after the tissue-independent uncertainty distribution for the $DDREF$ given in recent reports by the NCRP (1997) and EPA (1999) (see Fig. D.4); and uncertainties in the alpha RBEs could be assessed on the basis of the range of values determined in experimental and epidemiological studies, as summarized earlier in this appendix. The most difficult and time-consuming part of the exercise would be the characterization of uncertainties in the tissue-specific dose estimates d_i and D_i because these uncertainties depend strongly on the radionuclide as well as the exposure mode and because uncertainties in tissue dose estimates have rarely been addressed in the literature. Derivation of uncertainty intervals for the values d_i and D_i would require a separate sensitivity analysis in which the typically dominant components of the ICRP's dosimetric scheme are varied within plausible ranges of values, as determined by experts on the biokinetics and dosimetry of radionuclides.

In many cases, it would suffice to focus attention on a small number of the terms in Eq. D.1. This is because there is a small set of sites in the body that generally dominate cancer risk estimates due to their relatively high radiosensitivity and their importance as sites of deposition, transfer, or retention of radionuclides, and one or two of these sites often dominate the risk estimate as well as the uncertainty in that estimate for any given radionuclide. The typically dominant sites may be divided into two groups: "portal of entry" sites, meaning sites of deposition or transfer in the respiratory tract and gastrointestinal tract; and storage sites, meaning sites of relatively long-term retention.

The lung falls into both groups because it is a site of transfer of activity from the environment into the systemic circulation, and it may retain relatively insoluble forms of some radionuclides for months or years. Lung cancer is projected to be the dominant cancer type in a substantial portion of cases involving inhalation of radionuclides in moderately soluble or insoluble form. In terms of the default absorption types used by the ICRP, this would correspond to Type M or Type S material. For example, for inhalation of Type S material, lung cancer is projected to represent 50-99.9% of the total cancers for each of about five-sixths of the radionuclides addressed in Table 2.1. For radionuclides inhaled in relatively soluble form, the projected number of deaths from lung cancer is often substantially less than that for other types of cancer.

Colon cancer is projected to be the dominant cancer type for many ingested radionuclides. For example, for dietary intake, colon cancer represents 50-99.9% of the total projected cancer

mortality for nearly two-thirds of the radionuclides addressed in Table 2.2a. Colon cancer may also represent a substantial portion of the total projected cancers for radionuclides inhaled in relatively soluble form (Type F). Although there are various combinations of factors that result in a large number of decays in the colon compared with other tissues, this most often occurs for radionuclides with a low gastrointestinal absorption fraction and a half-life of a year or less.

Stomach cancer may represent a substantial portion of the total projected cancers for cases involving ingestion of radionuclides with half-lives of at most a few hours due to the relatively large portion of nuclear transformations in the body that occur in the stomach. For example, for dietary intake, stomach cancer represents at least half of the total projected cancer mortality for about one-sixth of the radionuclides addressed in Table 2.2a. However, these short-lived radionuclides generally are of limited importance with regard to environmental exposure assessments.

Certain systemic storage sites may represent a large portion of the total projected cancer risk for inhaled material of Type F or for ingested radionuclides that are readily absorbed from the gastrointestinal tract. For example, thyroid cancer is projected to be the dominant cancer type for inhalation or ingestion of many forms of radioiodine, and leukemia is projected to be the dominant cancer type for intake of some relatively well absorbed radionuclides that accumulate to a large extent in bone (for example, ^{45}Ca , ^{90}Sr) or bone marrow (for example, ^{55}Fe).

Systemic organs may also represent most of the projected cancer risk in cases in which an ingested radionuclide is poorly absorbed but is long-lived and tenaciously retained in systemic tissues. This occurs most often for actinide elements, for which liver and bone may be important cancer sites.

Exceptions to the above generalizations occur for several radionuclides that show both high absorption to blood and fairly uniform distribution among tissues (for example, ^3H or ^{137}Cs). For such cases, the projected cancer risk is fairly uniformly distributed among several tissues.

APPENDIX E. ADJUSTMENT OF RISK COEFFICIENTS FOR SHORT-TERM EXPOSURE OF THE CURRENT U.S. POPULATION

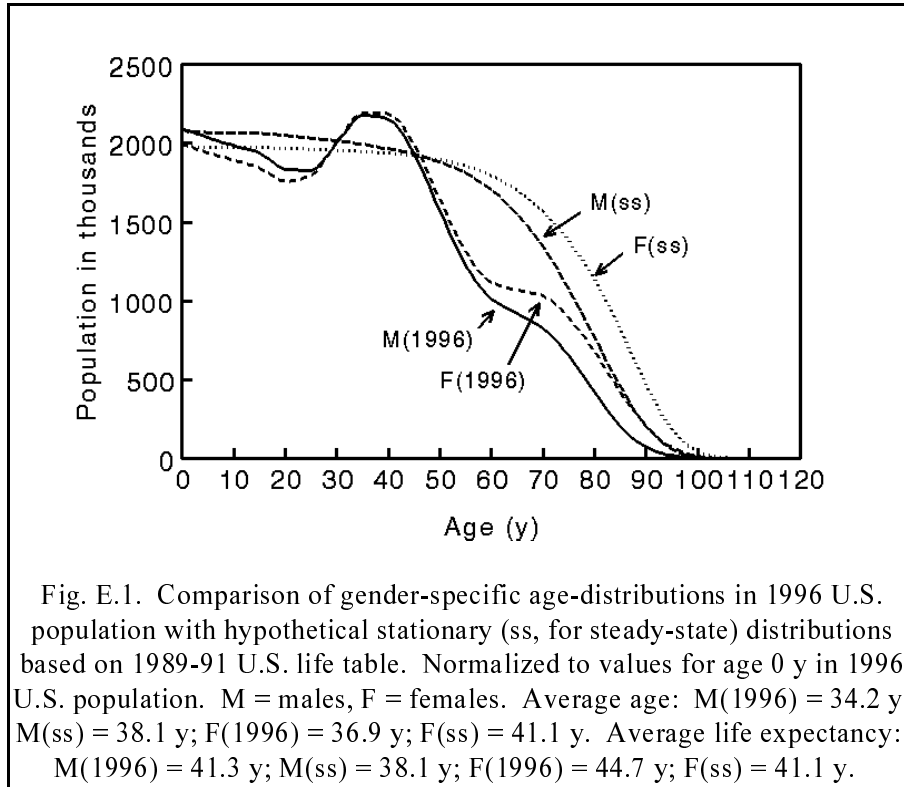
A risk coefficient given in Chapter 2 may be interpreted in terms of either chronic or acute (short-term) exposures. That is, a coefficient may be viewed as the average risk per unit exposure to persons exposed throughout life to a constant concentration of a radionuclide in an environmental medium, or as the average risk per unit exposure in populations exposed over a short period of time to the radionuclide in the environmental medium.

The assumed gender and age distributions in the exposed population are those that would eventually occur in a closed, steady-state population with male-to-female birth ratios characteristic of recent U.S. data and with time-invariant survival functions defined by the 1989-91 U.S. decennial life tables. Because of the uncertainty in the future composition of the U.S. population, the use of a stationary or steady-state population based on recent U.S. vital statistics is judged to be appropriate for consideration of long-term, chronic exposures to the U.S. population. However, these age distributions differ substantially from those of the current U.S. population (Fig. E.1). Hence, the question arises as to the applicability of the risk coefficients to short-term exposures of the U.S. population that might occur in the near future.

The purpose of this appendix is to compare the risk coefficients tabulated in Chapter 2 with coefficients derived for a short-term exposure of a hypothetical population with demographics based on the current U.S. population and, on the basis of this comparison, develop scaling factors for conversion of risk coefficients between the steady-state and current populations. As is the case for the stationary population considered in the main body of the report, total mortality rates in this hypothetical current population are defined by the 1989-91 U.S. decennial life table, and cancer mortality rates are defined by U.S. cancer mortality rates for the same period. In contrast to the stationary population, however, it is assumed that the gender-specific age distribution at the time of exposure is the same as that of the U.S. population of 1996 (U.S. Bureau of the Census, Population Division, 1997).

Computation of risk coefficients for the hypothetical current population

Short-term exposures are treated in the calculations as instantaneous exposures. For example, in the solution of the biokinetic models, ingestion or inhalation of a radionuclide is represented as an initial activity in the stomach compartment or in appropriate compartments of the



respiratory tract, respectively. However, the derived risk coefficients are applicable to any short-term exposure period (e.g., several days, weeks, or months) over which there are only small changes in the gender and age distributions in the population. The coefficients for the hypothetical current population should not be applied to exposure periods longer than a few years because of substantial changes in the age distribution over long periods.

As described in Chapter 7, the average lifetime risk coefficient, $\overline{r_a}$, for continuous intake of a radionuclide is calculated from the age- and gender-specific cancer risk coefficient, $r_a(x)$, by the equation:

$$\overline{r_a} = \frac{\int_0^{\infty} u(x) r_a(x) S(x) dx}{\int_0^{\infty} u(x) S(x) dx} \quad (\text{E.1})$$

where $u(x)$ is the gender-weighted usage rate, and $S(x)$ is the gender-weighted survival function. This equation was derived for a stationary population that is subject to fixed gender-specific survival functions and cancer mortality rates. In such a population, the age distribution of a given gender is proportional to the survival function $S(x)$ for that gender. The derived risk coefficients may be interpreted either in terms of lifetime exposure or acute exposure of this population to a radionuclide.

A similar analysis may be applied to the case of acute exposure of a population with an arbitrary age distribution, if it is assumed that the exposed population is subject to fixed gender-specific survival functions and fixed cancer mortality rates at all times after the exposure. In this case, the relative age distribution, $S(x)$, in Eq. E.1 is replaced by a function $P(x)$ representing the age distribution of the population at the time of acute exposure. This change is needed because usage of an environmental medium by members of age x in the hypothetical current population is proportional to $u(x)P(x)$ rather than $u(x)S(x)$. The equation for the current population corresponding to Eq. E.1 for the stationary population is then

$$\bar{r}_a = \frac{\int_0^{\infty} u(x) r_a(x) P(x) dx}{\int_0^{\infty} u(x) P(x) dx} \quad . \quad (E.2)$$

In applications of risk coefficients, it is sometimes necessary to estimate the average usage of environmental media by the population (see Appendix F). Average daily usage values for the hypothetical current population are given in Table E.1 for the four environmental media considered

Table E.1. Average daily usage of environmental media by the two hypothetical populations.

Medium	Males		Females		Combined	
	Stationary	Current	Stationary	Current	Stationary	Current
Air (m ³)	19.2	19.8	16.5	16.3	17.8	18.0
Tap water (L)	1.29	1.25	0.93	0.90	1.11	1.07
Diet (kcal)	2418	2450	1695	1717	2048	2075
Cow's milk (L)	0.282	0.292	0.207	0.214	0.243	0.252

in the internal exposure scenarios. Corresponding values for the stationary population are provided for comparison.

Lifetime risks for acute external exposures are calculated in a manner similar to that for radionuclide intakes. Since the external exposure is not considered to be age dependent, the calculation is simpler. As described in Chapter 7, the average lifetime risk, \overline{r}_e , to members of a stationary population from external exposure at a constant exposure rate can be calculated by removing the usage function from Eq. E.1. That is,

$$\overline{r}_e = \frac{\int_0^{\infty} r_e(x) S(x) dx}{\int_0^{\infty} S(x) dx} \quad (\text{E.3})$$

where $r_e(x)$ is the cancer risk coefficient at age x and $S(x)$ is the survival function and hence the relative age distribution in the stationary population. For the hypothetical current population, the relative age distribution, $S(x)$, is replaced by the function $P(x)$ representing the age distribution of the population at the time of acute exposure. This change is needed because the total exposure to members of the current population of age x is proportional to $P(x)$ rather than $S(x)$. The equation for the current population corresponding to Eq. E.3 for the stationary population is then

$$\overline{r}_e = \frac{\int_0^{\infty} r_e(x) P(x) dx}{\int_0^{\infty} P(x) dx} \quad (\text{E.4})$$

Comparison of coefficients for the current and stationary populations

For each type of exposure considered in the main text, risk coefficients for short-term exposure of the hypothetical current (1996) population were derived for more than 100 radionuclides representing a wide range of half-lives, radiation types, and energies. These coefficients were compared with the values tabulated in Chapter 2. Risk coefficients for the current population were consistently greater than the corresponding coefficients for the stationary population, with a

maximum difference of 16%. (Table E.2). For a given exposure scenario, the ratios of risk coefficients for the current and stationary populations did not depend strongly on the radionuclide. All ratios fell within 3%, and most fell within 1%, of the mean ratio (Table E.2).

Therefore, the risk coefficients for the stationary population appear to be reasonably good approximations of the corresponding risk coefficients for short-term exposure of the current population. A closer approximation may be obtained by scaling the coefficients for the stationary population by the exposure-specific mean ratio given in Table E.2. For example, for consideration of short-term inhalation of a radionuclide by the current population, the risk coefficient given in Table 2.1 should be multiplied by 1.11, the mean ratio of inhalation risk coefficients for the current and stationary populations (Table E.2).

Table E.2. Comparison of risk coefficients for the two hypothetical populations.

Environmental medium	Ratio of risk coefficients for acute exposure current population : stationary population		
	Mean	Standard deviation	Range
Air (inhalation)	1.11	0.008	1.08-1.13
Tap water (ingestion)	1.14	0.013	1.11-1.16
Food (ingestion)	1.10	0.008	1.08-1.11
Milk (ingestion of radioiodine)	1.09	0.006	1.08-1.10
External exposure by submersion in contaminated air	1.11	0.007	1.10-1.14
External exposure to contaminated ground plane	1.11	0.008	1.10-1.13
External exposure to soil contaminated to infinite depth	1.11	0.005	1.10-1.13

APPENDIX F. SAMPLE CALCULATIONS

This appendix provides several sample calculations that illustrate how the tabulated risk coefficients may be applied to different types of exposure. The simplistic exposure scenarios considered here were selected for didactic purposes and are not intended to suggest or endorse assumptions regarding the behavior of radionuclides in the environment.

The risk coefficients in this report represent estimated radiogenic cancer risk, either to a stationary population defined by the 1989-91 U.S. decennial life tables (see Chapter 3) or (when scaled as described in Appendix E) to a hypothetical current population with gender and age distributions based on the total U.S. population in 1996. Risk coefficients for the stationary population are intended mainly to apply to lifetime exposures to radionuclides but, as explained in Chapters 1 and 3, may also be interpreted in terms of acute exposures. Because risk coefficients for the hypothetical current population reflect actual age and gender distributions in the U.S. population in 1996, these coefficients may be appropriate for consideration of short-term exposures (1 y or less) to the current U.S. population or to a representative subpopulation.

For a selected exposure scenario, the computation of risk R involves multiplication of the applicable risk coefficient r by the *per capita* intake I or (external) exposure X for external exposure. That is, $R = r \cdot I$ for intake by inhalation or ingestion and $R = r \cdot X$ for external exposures, where I is the activity inhaled or ingested *per capita* and X is the time-integrated concentration of the radionuclide in air, on the ground surface, or within the soil. A risk coefficient r is specific to the radionuclide and the mode of exposure or intake. Usage rates for the examples in this appendix are taken from Table E.1.

Some radionuclides considered in this report form radioactive progeny, or daughter products, when undergoing radioactive decay. A series of radionuclides formed by successive radioactive decays is referred to as a decay chain, and the first member of the chain is referred to as the parent. A risk coefficient given in this document does not include the contribution to dose from exposure or intake of other radionuclides that might be present as daughter products in the environment. However, for each radionuclide considered in this document, separate risk coefficients are provided for all radioactive progeny that are considered to be of potential dosimetric significance. Thus, the user may combine risk coefficients for different members of a radionuclide chain to derive a risk coefficient that reflects growth of radioactive progeny in the environment over a user-selected time period.

For example, when considering external exposure to ^{137}Cs on the ground surface, it should be assumed that its short-lived radioactive daughter, $^{137\text{m}}\text{Ba}$ ($T_{1/2} = 2.552 \text{ m}$) is also present. Although the risk coefficient for external exposure to ^{137}Cs on the ground surface does not consider the presence of $^{137\text{m}}\text{Ba}$, a separate risk coefficient is provided for external exposure to $^{137\text{m}}\text{Ba}$ on the ground surface. As illustrated later in this appendix, an estimate of the risk from the mixture of ^{137}Cs and $^{137\text{m}}\text{Ba}$ present on the ground surface may be obtained as a linear combination of the separate risk coefficients for the two radionuclides.

For intake of a relatively long-lived radionuclide, the contribution to dose from intake of its short-lived radioactive progeny (defined here as radioactive progeny with a half-life shorter than 1 h) present in the environment usually is insignificant compared with the dose from the parent. For this reason, separate risk coefficients for ingestion and inhalation are not given for short-lived radioactive progeny of the radionuclides considered in the internal exposure scenarios. For example, risk coefficients are given for ingestion and inhalation of ^{137}Cs but not for ingestion or inhalation of $^{137\text{m}}\text{Ba}$.

On the other hand, after intake of a parent radionuclide, the production and decay of short-lived radioactive progeny in the body may contribute significantly to tissue doses. For this reason, risk coefficients for ingested or inhaled radionuclides include all contributions to dose from growth of chain members in the body.

Example 1. Suppose the concentration of ^{85}Kr in the atmosphere in the environs of a fuel reprocessing plant is 10^3 Bq m^{-3} . Compute the average cancer risk (mortality and morbidity) associated with lifetime external exposure to this level of airborne activity, assuming no shielding by structures.

From Table 2.3, the mortality and morbidity risk coefficients for external exposure to ^{85}Kr in air (submersion) are 7.23×10^{-18} and $1.00 \times 10^{-17} \text{ m}^3 \text{ Bq}^{-1} \text{ s}^{-1}$. The years of life lived (the life expectancy at birth) in the stationary population is about 75.2 y (Table A.1). The lifetime exposure resulting from this airborne concentration is

$$10^3 \frac{\text{Bq}}{\text{m}^3} \cdot 75.2 \text{ y} \cdot 3.15 \times 10^7 \frac{\text{s}}{\text{y}} = 2.37 \times 10^{12} \frac{\text{Bq} \cdot \text{s}}{\text{m}^3} .$$

Therefore, the estimated lifetime risks from the external exposure are

$$\text{Mortality: } 2.37 \times 10^{12} \frac{\text{Bq}^{-\text{s}}}{\text{m}^3} \cdot 7.23 \times 10^{-18} \frac{\text{m}^3}{\text{Bq}^{-\text{s}}} = 1.7 \times 10^{-5}$$

$$\text{Morbidity: } 2.37 \times 10^{12} \frac{\text{Bq}^{-\text{s}}}{\text{m}^3} \cdot 1.00 \times 10^{-17} \frac{\text{m}^3}{\text{Bq}^{-\text{s}}} = 2.4 \times 10^{-5} .$$

Example 2. As in Example 1, suppose the concentration of ^{85}Kr in the atmosphere in the environs of a fuel reprocessing plant is 10^3 Bq m^{-3} . Compute the average cancer risk (mortality and morbidity) associated with a one-year ($3.15 \times 10^7 \text{ s}$) external exposure to this level of airborne activity, assuming no shielding by structures and that the age distribution of the population is similar to that of the 1996 U.S. population.

Because the age distribution of the population is similar to that of the 1996 U.S. population, risk coefficients for the stationary population given in Table 2.3 will be scaled as indicated in Appendix E for application to the hypothetical current population. From Table 2.3 the mortality and morbidity risk coefficients for external exposure to ^{85}Kr in air are 7.23×10^{-18} and $1.00 \times 10^{-17} \text{ m}^3 \text{ Bq}^{-1} \text{ s}^{-1}$, respectively. From Table E.2, the scaling factor (mean ratio of risk coefficients for hypothetical current and stationary populations) for this exposure scenario is 1.11. The scaled mortality and morbidity risk coefficients for external exposure to ^{85}Kr in air are 8.03×10^{-18} and $1.11 \times 10^{-17} \text{ m}^3 \text{ Bq}^{-1} \text{ s}^{-1}$, respectively. The exposure (time-integrated concentration) is

$$10^3 \frac{\text{Bq}}{\text{m}^3} \cdot 3.15 \times 10^7 \text{ s} = 3.15 \times 10^{10} \frac{\text{Bq}^{-\text{s}}}{\text{m}^3} .$$

The estimated lifetime risks to the population as a consequence of the 1-y external exposure are

$$\text{Mortality: } 3.15 \times 10^{10} \frac{\text{Bq}^{-\text{s}}}{\text{m}^3} \cdot 8.03 \times 10^{-18} \frac{\text{m}^3}{\text{Bq}^{-\text{s}}} = 2.5 \times 10^{-7}$$

$$\text{Morbidity: } 3.15 \times 10^{10} \frac{\text{Bq}^{-\text{s}}}{\text{m}^3} \cdot 1.11 \times 10^{-17} \frac{\text{m}^3}{\text{Bq}^{-\text{s}}} = 3.5 \times 10^{-7} .$$

Example 3. Suppose the ground surface was uniformly contaminated at time zero with ^{137}Cs at a level of 2 Bq m^{-2} . Assume that radioactive decay is the only mechanism by which contamination is reduced. (Reduction of the time-integrated exposure due to weathering is ignored here for simplicity.) Compute the average lifetime cancer risk (mortality and morbidity) resulting from external exposures during the first year following the initial deposition, assuming no shielding and assuming that the age distribution of the exposed population is similar to that of the 1996 U.S. population.

Cesium-137 ($T_{1/2} = 30 \text{ y}$) forms $^{137\text{m}}\text{Ba}$ ($T_{1/2} = 2.552 \text{ m}$) in 94.6% of its decays (see Table G.1). Due to the short half-life of $^{137\text{m}}\text{Ba}$, the concentration of $^{137\text{m}}\text{Ba}$ on the ground surface will reach 1.89 Bq m^{-2} ($0.946 \cdot 2 \text{ Bq m}^{-2}$) within a half hour after time zero and will decline with the half-life of ^{137}Cs .

From Table 2.3 the mortality and morbidity risk coefficients for external exposure to ^{137}Cs distributed on the ground surface are 3.96×10^{-20} and $4.57 \times 10^{-20} \text{ m}^2 \text{ Bq}^{-1} \text{ s}^{-1}$. For $^{137\text{m}}\text{Ba}$ the corresponding coefficients are 3.12×10^{-17} and $4.60 \times 10^{-17} \text{ m}^2 \text{ Bq}^{-1} \text{ s}^{-1}$, respectively. From Table E.2, the scaling factor (mean ratio of risk coefficients for hypothetical current and stationary populations) for external exposure from ground surface contamination is 1.11. The scaled mortality and morbidity risk coefficients for ^{137}Cs are 4.40×10^{-20} and $5.07 \times 10^{-20} \text{ m}^2 \text{ Bq}^{-1} \text{ s}^{-1}$, respectively, and the scaled values for $^{137\text{m}}\text{Ba}$ are 3.46×10^{-17} and $5.11 \times 10^{-17} \text{ m}^2 \text{ Bq}^{-1} \text{ s}^{-1}$, respectively. The exposures (time-integrated concentration) for each radionuclide during the first year are

$$\text{Exposure} = A_0 \int_0^T e^{-\frac{\ln 2}{T_{1/2}} t} dt = \frac{A_0 T_{1/2}}{\ln 2} \left(1 - e^{-\frac{\ln 2}{T_{1/2}} T} \right)$$

$$\text{Cs-137: } \frac{2 \frac{\text{Bq}}{\text{m}^2} \cdot 30 \text{ y} \cdot 3.15 \times 10^7 \frac{\text{s}}{\text{y}}}{0.693} \left(1 - e^{-\frac{0.693}{30 \text{ y}} 1 \text{ y}} \right) = 6.23 \times 10^7 \frac{\text{Bq} \cdot \text{s}}{\text{m}^2}$$

$$\text{Ba-137m: } \frac{1.89 \frac{\text{Bq}}{\text{m}^2} \cdot 30 \text{ y} \cdot 3.15 \times 10^7 \frac{\text{s}}{\text{y}}}{0.693} \left(1 - e^{-\frac{0.693}{30 \text{ y}} 1 \text{ y}} \right) = 5.89 \times 10^7 \frac{\text{Bq} \cdot \text{s}}{\text{m}^2} .$$

The lifetime risks resulting from external exposures during the first year are

Mortality:

$$6.23 \times 10^7 \frac{\text{Bq} \cdot \text{s}}{\text{m}^2} \cdot 4.40 \times 10^{-20} \frac{\text{m}^2}{\text{Bq} \cdot \text{s}} \\ + 5.89 \times 10^7 \frac{\text{Bq} \cdot \text{s}}{\text{m}^2} \cdot 3.46 \times 10^{-17} \frac{\text{m}^2}{\text{Bq} \cdot \text{s}} = 2.0 \times 10^{-9}$$

Morbidity:

$$6.23 \times 10^7 \frac{\text{Bq} \cdot \text{s}}{\text{m}^2} \cdot 5.07 \times 10^{-20} \frac{\text{m}^2}{\text{Bq} \cdot \text{s}} \\ + 5.89 \times 10^7 \frac{\text{Bq} \cdot \text{s}}{\text{m}^2} \cdot 5.11 \times 10^{-17} \frac{\text{m}^2}{\text{Bq} \cdot \text{s}} = 3.0 \times 10^{-9}$$

The radiations emitted by $^{137\text{m}}\text{Ba}$ are the main contributors to risk.

Example 4. Assume that measurements of the photon radiation field indicate an average exposure rate of 4 $\mu\text{R}/\text{h}$ and that no information is available regarding the energy of the radiation or its origin. Compute the average lifetime risk to a population living in this radiation field, assuming no shielding by structures.

Although defined differently, the quantities exposure and air kerma may be considered to be equivalent for most practical purposes. That is, an exposure of 1 roentgen (R) corresponds to an air kerma of 0.01 Gy.

The relation between effective dose and air kerma depends on the environmental medium involved, the distribution of the radionuclide in the medium, and the age of the exposed individual. For naturally occurring radionuclides distributed uniformly in the soil, Saito et al. (1998) estimated effective dose per unit air kerma at 1 m for different age groups as tabulated below. For the purpose of estimating risk to a large population, it is reasonable to use their value for the adult, which is approximately 0.7 Sv Gy^{-1} . For infants and small children, reduced self-shielding of the body results in values closer to 1. In the absence of information on the exposure source, the value 0.7 Sv Gy^{-1} will be used here.

Age	Effective dose per air kerma (Sv Gy ⁻¹)		
	²³⁸ U series	²³² Th series	⁴⁰ K
Adult	0.672	0.695	0.709
Child	0.766	0.798	0.803
Infant	0.899	0.907	0.926

Table 7.3 gives a mortality risk of $5.75 \times 10^{-2} \text{ Gy}^{-1}$ for uniform irradiation of the body by low-LET radiation. Assuming the average lifetime is 75.2 y (Table A.1), the expected lifetime dose due to this radiation field is

$$4 \times 10^{-6} \frac{\text{R}}{\text{h}} \cdot 0.01 \frac{\text{Gy}}{\text{R}} \cdot 0.7 \frac{\text{Sv}}{\text{Gy}} \cdot 8.76 \times 10^3 \frac{\text{h}}{\text{y}} \cdot 75.2 \text{ y} \approx 1.84 \times 10^{-2} \text{ Gy}$$

and the mortality risk is estimated as

$$1.84 \times 10^{-2} \text{ Gy} \cdot 5.75 \times 10^{-2} \text{ Gy}^{-1} \approx 1.1 \times 10^{-3} .$$

Example 5. Calculate the average lifetime risk to the stationary population associated with ingestion of ²¹⁰Pb and its radioactive progeny, assuming that the *per capita* dietary intake rates of ²¹⁰Pb and ²¹⁰Po are 1.4 and 1.8 pCi d⁻¹, respectively.

Lead-210 decays to ²¹⁰Bi ($T_{1/2} = 5.012 \text{ d}$), which decays to ²¹⁰Po ($T_{1/2} = 138.8 \text{ d}$). Because of the relatively short half-life of ²¹⁰Bi, it is reasonable to assume that ²¹⁰Bi is in equilibrium with ²¹⁰Pb in diet.

From Table A.1, the average life expectancy is 27,448 d (75.2 y). Therefore, lifetime intakes of ²¹⁰Pb, ²¹⁰Bi, and ²¹⁰Po in the diet are estimated to be

$$\text{Pb-210/Bi-210: } 1.4 \frac{\text{pCi}}{\text{d}} \cdot 3.7 \times 10^{-2} \frac{\text{Bq}}{\text{pCi}} \cdot 27,448 \text{ d} = 1.4 \times 10^3 \text{ Bq}$$

$$\text{Po-210: } 1.8 \frac{\text{pCi}}{\text{d}} \cdot 3.7 \times 10^{-2} \frac{\text{Bq}}{\text{pCi}} \cdot 27,448 \text{ d} = 1.8 \times 10^3 \text{ Bq}$$

The following mortality and morbidity risk coefficients for ^{210}Pb , ^{210}Bi , and ^{210}Po in diet are taken from Table 2.2a: ^{210}Pb , 2.31×10^{-8} and 3.18×10^{-8} , respectively; ^{210}Bi , 1.95×10^{-10} and 3.52×10^{-10} , respectively; and ^{210}Po , 4.44×10^{-8} and 6.09×10^{-8} , respectively. The estimated risks are

$$\begin{aligned} \text{Mortality: } & 1.4 \times 10^3 \text{ Bq} \cdot 2.31 \times 10^{-8} \frac{1}{\text{Bq}} + \\ & 1.4 \times 10^3 \text{ Bq} \cdot 1.95 \times 10^{-10} \frac{1}{\text{Bq}} + \\ & 1.8 \times 10^3 \text{ Bq} \cdot 4.44 \times 10^{-8} \frac{1}{\text{Bq}} = 1.1 \times 10^{-4} \end{aligned}$$

$$\begin{aligned} \text{Morbidity: } & 1.4 \times 10^3 \text{ Bq} \cdot 3.18 \times 10^{-8} \frac{1}{\text{Bq}} + \\ & 1.4 \times 10^3 \text{ Bq} \cdot 3.52 \times 10^{-10} \frac{1}{\text{Bq}} + \\ & 1.8 \times 10^3 \text{ Bq} \cdot 6.09 \times 10^{-8} \frac{1}{\text{Bq}} = 1.5 \times 10^{-4} \end{aligned}$$

Note that ^{210}Bi makes an insignificant contribution to the total risk and that ^{210}Po accounts for about two-thirds of the risk.

Example 6. Assume a concentration of tritium in tap water of 10 pCi L^{-1} . Compute the average lifetime risk (mortality and morbidity) associated with use of tap water at this concentration, assuming that all tritium in tap water is in the form of tritiated water.

The average intake of tap water is 1.11 L d^{-1} (Table E.1), and the average life expectancy is 27,448 d (75.2 y, Table A.1), giving a lifetime intake of tap water of $3.0 \times 10^4 \text{ L}$. From Table 2.2a, the mortality and morbidity coefficients for ^3H (as tritiated water) in tap water are 9.44×10^{-13} and $1.37 \times 10^{-12} \text{ Bq}^{-1}$, respectively. Therefore, the estimated risks are

$$\text{Mortality: } 10 \frac{\text{pCi}}{\text{L}} \cdot 0.037 \frac{\text{Bq}}{\text{pCi}} \cdot 3.0 \times 10^4 \text{ L} \cdot 9.44 \times 10^{-13} \frac{1}{\text{Bq}} = 1.0 \times 10^{-8}$$

$$\text{Morbidity: } 10 \frac{\text{pCi}}{\text{L}} \cdot 0.037 \frac{\text{Bq}}{\text{pCi}} \cdot 3.0 \times 10^4 \text{ L} \cdot 1.37 \times 10^{-12} \frac{1}{\text{Bq}} = 1.5 \times 10^{-8}$$

Example 7. Suppose there is a short-term release of 40 mCi of ^{131}I as a vapor from a reactor and that observed atmospheric conditions indicate an atmospheric dispersion factor of about $1 \times 10^{-6} \text{ s m}^{-3}$ for a nearby population. Compute the risk associated with inhalation of ^{131}I as the cloud passes over the population, assuming that the age distribution of the population is similar to that of the stationary population considered in the main text.

The time integrated airborne concentration in the cloud is

$$40 \text{ mCi} \cdot 3.7 \times 10^7 \frac{\text{Bq}}{\text{mCi}} \cdot 1.0 \times 10^{-6} \frac{\text{s}}{\text{m}^3} = 1.48 \times 10^3 \frac{\text{Bq} \cdot \text{s}}{\text{m}^3} .$$

The average inhalation intake rate is $17.8 \text{ m}^3 \text{ d}^{-1}$ (Table E.1). The mortality and morbidity coefficients for inhalation of ^{131}I in vapor form are 1.48×10^{-10} and $1.36 \times 10^{-9} \text{ Bq}^{-1}$ (Table 2.1). Therefore, the estimated risks are

$$\text{Mortality: } 1.48 \times 10^3 \frac{\text{Bq} \cdot \text{s}}{\text{m}^3} \cdot 17.8 \frac{\text{m}^3}{\text{d}} \cdot \frac{1 \text{ d}}{8.64 \times 10^4 \text{ s}} \cdot 1.48 \times 10^{-10} \frac{1}{\text{Bq}} = 4.5 \times 10^{-11}$$

$$\text{Morbidity: } 1.48 \times 10^3 \frac{\text{Bq} \cdot \text{s}}{\text{m}^3} \cdot 17.8 \frac{\text{m}^3}{\text{d}} \cdot \frac{1 \text{ d}}{8.64 \times 10^4 \text{ s}} \cdot 1.36 \times 10^{-9} \frac{1}{\text{Bq}} = 4.1 \times 10^{-10} .$$

APPENDIX G. NUCLEAR DECAY DATA

The risk coefficients in Tables 2.1-2.3 are listed by radionuclide. In those tables, the entries in the column with the heading "Chain" indicate whether the radionuclide is in the same decay chain as other radionuclides addressed in the table. An entry "Y" (for "yes") under the subheading "P" (for "parent") indicates that the radionuclide is the parent of a decay chain containing at least one other radionuclide in the table. An entry "Y" under the subheading "D" (for "daughter") indicates that the radionuclide is formed in the decay chain of at least one other radionuclide in the table. In the compilation of this information, no consideration was given to the radiological significance of either the daughters or the possible parents of the radionuclide. This appendix provides a summary of information on the nuclear decay characteristics of each radionuclide and gives details of its decay chain when indicated. Table G.1 of this appendix was adapted from Appendix A of Federal Guidance Report No. 12 (EPA, 1993).

In some instances a radionuclide is not uniquely identified by its atomic number (or chemical symbol) and mass number. Nuclei of the same atomic and mass numbers, but with distinguishable nuclear properties, are referred to as isomers. Identification of an isomer requires reference to its physical half-life. The nuclide designations of Tables 2.1- 2.3 involve some nonstandard notation needed to reference isomers to data in Table G.1 of this appendix.

To differentiate isomers, when neither isomer has been designated as a metastable state, an "a" and "b" have been added to the chemical symbol and mass number notation. For example, the entry Nb-89a in Table G.1 indicates the isomer of ^{89}Nb with half-life 66 m. The "a" and "b" notations were arbitrarily assigned to the ^{89}Nb isomers. To identify multiple metastable states, the "m" notation of one isomer is shown as "n". For example, Sb-124m in Table G.1 refers to the metastable state with a half-life of 93 s, and Sb-124n refers to the state with half-life 20.2 m. Additional examples can be seen in entries of Tables 2.1- 2.3 and Table G.1 for indium (In), europium (Eu), terbium (Tb), rhenium (Re), iridium (Ir), and neptunium (Np).

Table G.1 contains the following information, intended to aid in the proper use of the risk coefficients tabulated in this report. The physical half-life of the radionuclides is given in the second column of the table. The time units are abbreviated as follows: y for year, d for day, h for hour, m for minute, s for second, ms for millisecond, and μs for microsecond. The modes of nuclear transformation applicable to the radionuclide are given in the column headed "Decay Mode". The modes are abbreviated as follows: B- for beta minus decay, B+ for beta plus decay, EC for electron capture, A for alpha decay, IT for isomeric transition, and SF for spontaneous fission. The nuclear

transformations of a radionuclide (the parent) may form a nucleus which is also radioactive (radioactive decay product). The entries in the columns headed by "Radioactive Decay Products and Fractional Yield" identify radioactive nuclei formed by nuclear transformations of the radionuclide and give the fraction of the parent's transformations forming each decay product (the branching fraction). No attempt is made to identify the radioactive nuclei formed by spontaneous fission. The notation "SF" simply indicates the accompanying branching fraction of spontaneous fission. The three columns on the extreme right give the *total energy per nuclear transformation* of emitted alpha particles, electrons, and photons². The entry for alpha particles represents the kinetic energy of the alpha particles and does not include the recoil energy of the newly formed nucleus. The entry for electrons includes the kinetic energy of all beta particles (negatron or positron), internal conversion electrons, and Auger electrons emitted in the nuclear transformations. Similarly, the photon entry encompasses gamma rays, x rays, and annihilation photons. If the nuclear transformations of the radionuclide do not result in emission of a particular radiation, then a dash, "-", is shown in the appropriate column. If radiations of a particular type are emitted, but the total energy per nuclear transformation is less than 1 keV, then the symbol "<" appears in the column.

The risk coefficients for intakes of radionuclides by inhalation and ingestion (Tables 2.1, 2.2a, and 2.2b) are based on the radiations emitted by the indicated radionuclide and all its decay products formed within the body following the intake. The risk coefficients for external exposure to radionuclides in the environment, Table 2.3, are based on the radiations emitted by the indicated radionuclide and do not include consideration of the radiations emitted by radioactive decay products. Radioactive decay products of a radionuclide are identified in Table G.1. For example, the entries for ¹⁴⁴Ce in Table G.1 indicate that ¹⁴⁴Ce has a half-life of 284.3 d and forms ¹⁴⁴Pr in 98.22% of its transformations and ^{144m}Pr in 1.78% of its transformations. The entries for ^{144m}Pr, which has a half-life of 7.2 m, indicate that it decays (in 99.9% of its transformations) by internal

²The total energy of radiation type R , $E_{T,R}$, is computed as

$$E_{T,R} = \sum_{i=1}^n y_{i,R} E_{i,R} ,$$

where $y_{i,R}$ is the mean number of radiations of type R emitted per nuclear transformation with unique or mean energy $E_{i,R}$. The quantity should not be confused with the mean energy of radiation type R , which is

$$\bar{E}_R = \frac{E_{T,R}}{\sum_{i=1}^n y_{i,R}} .$$

transition to ^{144}Pr ; the remaining transformations form the stable nucleus ^{144}Nd . Transformation of ^{144}Pr , which has a half-life of 17.28 m, also forms the stable nucleus ^{144}Nd . By repeated entry into Table G.1, one can follow the serial nuclear transformations (decay chain) associated with a radionuclide. For nuclides with multiple modes of nuclear transformation, the branch formed by each mode must be traced. In some instances the branches may converge. The branching fractions may not always add to one because only those branches leading to radioactive decay products are tabulated.

The serial transformation by radioactive decay of each member of a radioactive series is described by the Bateman equations (EPA, 1993). Assume that at time zero the activity of the parent nuclide is A_1^0 and that of all daughters is zero. The activity at time t of a chain member i , $i = 1, 2, \dots$, can be expressed as

$$A_i(t) = A_1^0 \prod_{j=1}^{i-1} f_{j,j+1} \lambda_j \sum_{j=1}^i \frac{e^{-\lambda_j t}}{\prod_{\substack{k=1 \\ k \neq j}}^i (\lambda_k - \lambda_j)} \quad (\text{G.1})$$

where

$$\prod_{i=1}^n a_i = \begin{cases} a_1 * a_2 * \dots * a_n, & \text{if } n \geq 1 \\ 1, & \text{if } n = 0 \end{cases} ,$$

$f_{j,j+1}$ denotes the fraction of the nuclear transformations of chain member j forming member $j+1$, and λ_i is the decay constant for nuclide i ($\lambda = 0.6931.../T_{1/2}$). If the parent is long-lived relative to the daughters, then at times t such that $\lambda_i t > 5$ the activity of the daughters ($i = 2$ to n) can be approximated as

$$A_i(t) = A_1(t) \prod_{j=1}^{i-1} f_{j,j+1} \quad . \quad (\text{G.2})$$

Under these conditions the activity of the decay products is in secular equilibrium with the parent's activity. For example, application of Eq. G.2 to ^{137}Cs and its daughter $^{137\text{m}}\text{Ba}$ indicates that the activity of $^{137\text{m}}\text{Ba}$ at time t is

$$A_{Ba-137\text{m}}(t) = 0.946 A_{Cs-137}(t) \quad ,$$

where 0.946 is the fraction of the ^{137}Cs nuclear transformations forming ^{137}Ba , as indicated in Table G.1. If a decay chain member is not short-lived relative to the parent, then it is necessary to apply Eq. G.1. In many instances, the mathematical models describing the fate of radionuclides in the environment (for example, their dispersion following release to the atmosphere) includes an evaluation of the growth of decay chain members. The information in Table G.1 should be useful to those implementing such models.

Table G.1. Summary information on the nuclear transformation of radionuclides

Nuclide	T _{1/2}	Decay Mode	Radioactive Decay Products and Fractional Yield						Energy (MeV nt ⁻¹)			
			Nuclide	Fraction	Nuclide	Fraction	Nuclide	Fraction	Alpha	Elect	Photon	
Hydrogen												
H-3	12.35y	B-								-	0.006	-
Beryllium												
Be-7	53.3d	EC								-	<	0.049
Be-10	1.6E6y	B-								-	0.252	-
Carbon												
C-11	20.38m	ECB+								-	0.385	1.020
C-14	5730y	B-								-	0.049	-
Nitrogen												
N-13	9.965m	ECB+								-	0.491	1.020
Oxygen												
O-15	122.24s	ECB+								-	0.734	1.021
Fluorine												
F-18	109.77m	ECB+								-	0.250	1.022
Neon												
Ne-19	17.22s	ECB+								-	0.963	1.022
Sodium												
Na-22	2.602y	ECB+								-	0.194	2.193
Na-24	15.00h	B-								-	0.554	4.121
Magnesium												
Mg-28	20.91h	B-	Al-28	1.000E+00						-	0.163	1.371
Aluminum												
Al-26	7.16E5y	ECB+								-	0.445	2.676
Al-28	2.240m	B-								-	1.242	1.779
Silicon												
Si-31	157.3m	B-								-	0.595	<
Si-32	450y	B-	P-32	1.000E+00						-	0.065	-
Phosphorus												
P-30	2.499m	ECB+								-	1.436	1.022
P-32	14.29d	B-								-	0.695	-
P-33	25.4d	B-								-	0.077	-
Sulfur												
S-35	87.44d	B-								-	0.049	-
Chlorine												
Cl-36	3.01E5y	ECB+B-								-	0.274	<
Cl-38	37.21m	B-								-	1.529	1.488
Cl-39	55.6m	B-	Ar-39	1.000E+00						-	0.823	1.438
Argon												
Ar-37	35.02d	EC								-	0.002	<
Ar-39	269y	B-								-	0.219	-
Ar-41	1.827h	B-								-	0.464	1.284
Potassium												
K-38	7.636m	ECB+								-	1.209	3.187
K-40	1.28E9y	B-EC								-	0.523	0.156
K-42	12.36h	B-								-	1.430	0.276
K-43	22.6h	B-								-	0.309	0.970
K-44	22.13m	B-								-	1.491	2.267
K-45	20m	B-	Ca-45	1.000E+00						-	0.984	1.866
Calcium												
Ca-41	1.4E5y	EC								-	0.002	<

Table G.1, continued

Nuclide	T _{1/2}	Decay Mode	Radioactive Decay Products and Fractional Yield				Energy (MeV nt ⁻¹)			
			Nuclide	Fraction	Nuclide	Fraction	Nuclide	Fraction	Alpha	Elect Photon
Calcium, continued										
Ca-45	163d	B-						-	0.077	<
Ca-47	4.53d	B-	Sc-47	1.000E+00				-	0.345	1.063
Ca-49	8.716m	B-	Sc-49	1.000E+00				-	0.870	3.165
Scandium										
Sc-43	3.891h	ECB+						-	0.313	1.096
Sc-44m	58.6h	ECIT	Sc-44	9.863E-01				-	0.033	0.280
Sc-44	3.927h	ECB+						-	0.597	2.137
Sc-46	83.83d	B-						-	0.112	2.009
Sc-47	3.351d	B-						-	0.163	0.108
Sc-48	43.7h	B-						-	0.229	3.349
Sc-49	57.4m	B-						-	0.822	0.001
Titanium										
Ti-44	47.3y	EC	Sc-44	1.000E+00				-	0.013	0.135
Ti-45	3.08h	ECB+						-	0.373	0.870
Vanadium										
V-47	32.6m	ECB+						-	0.803	0.995
V-48	16.238d	ECB+						-	0.149	2.914
V-49	330d	EC						-	0.004	<
Chromium										
Cr-48	22.96h	ECB+	V-48	1.000E+00				-	0.008	0.436
Cr-49	42.09m	ECB+	V-49	1.000E+00				-	0.602	1.055
Cr-51	27.704d	EC						-	0.004	0.033
Manganese										
Mn-51	46.2m	ECB+	Cr-51	1.000E+00				-	0.934	0.998
Mn-52m	21.1m	ECB+IT	Mn-52	1.750E-02				-	1.132	2.409
Mn-52	5.591d	ECB+						-	0.075	3.458
Mn-53	3.7E6y	EC						-	0.004	0.001
Mn-54	312.5d	EC						-	0.004	0.836
Mn-56	2.5785h	B-						-	0.830	1.692
Iron										
Fe-52	8.275h	ECB+	Mn-52m	1.000E+00				-	0.194	0.740
Fe-55	2.7y	EC						-	0.004	0.002
Fe-59	44.529d	B-						-	0.118	1.189
Fe-60	1E5y	B-	Co-60m	1.000E+00				-	0.049	-
Cobalt										
Co-55	17.54h	ECB+	Fe-55	1.000E+00				-	0.429	1.994
Co-56	78.76d	ECB+						-	0.124	3.580
Co-57	270.9d	EC						-	0.019	0.125
Co-58m	9.15h	IT	Co-58	1.000E+00				-	0.023	0.002
Co-58	70.80d	ECB+						-	0.034	0.976
Co-60m	10.47m	ITB-	Co-60	9.975E-01				-	0.058	0.007
Co-60	5.271y	B-						-	0.097	2.504
Co-61	1.65h	B-						-	0.463	0.091
Co-62m	13.91m	B-						-	1.051	2.698
Nickel										
Ni-56	6.10d	EC	Co-56	1.000E+00				-	0.007	1.721
Ni-57	36.08h	ECB+	Co-57	1.000E+00				-	0.143	1.922
Ni-59	7.5E4y	EC						-	0.005	0.002
Ni-63	96y	B-						-	0.017	-

Table G.1, continued

Nuclide	T _{1/2}	Decay Mode	Radioactive Decay Products and Fractional Yield						Energy (MeV nt ⁻¹)			
			Nuclide	Fraction	Nuclide	Fraction	Nuclide	Fraction	Alpha	Elect	Photon	
Nickel, continued												
Ni-65	2.520h	B-								-	0.632	0.549
Ni-66	54.6h	B-	Cu-66	1.000E+00						-	0.067	-
Copper												
Cu-60	23.2m	ECB+								-	0.895	3.898
Cu-61	3.408h	ECB+								-	0.311	0.829
Cu-62	9.74m	ECB+								-	1.285	1.007
Cu-64	12.701h	B-ECB+								-	0.123	0.191
Cu-66	5.10m	B-								-	1.068	0.085
Cu-67	61.86h	B-								-	0.155	0.115
Zinc												
Zn-62	9.26h	ECB+	Cu-62	1.000E+00						-	0.033	0.439
Zn-63	38.1m	ECB+								-	0.918	1.100
Zn-65	243.9d	ECB+								-	0.007	0.584
Zn-69m	13.76h	ITB-	Zn-69	9.997E-01						-	0.022	0.417
Zn-69	57m	B-								-	0.321	<
Zn-71m	3.92h	B-								-	0.548	1.552
Zn-72	46.5h	B-	Ga-72	1.000E+00						-	0.102	0.152
Gallium												
Ga-65	15.2m	ECB+	Zn-65	1.000E+00						-	0.831	1.176
Ga-66	9.40h	ECB+								-	0.970	2.473
Ga-67	78.26h	EC								-	0.036	0.158
Ga-68	68.0m	ECB+								-	0.739	0.951
Ga-70	21.15m	B-EC								-	0.644	0.008
Ga-72	14.1h	B-								-	0.497	2.711
Ga-73	4.91h	B-								-	0.494	0.316
Germanium												
Ge-66	2.27h	ECB+	Ga-66	1.000E+00						-	0.102	0.687
Ge-67	18.7m	ECB+	Ga-67	1.000E+00						-	1.297	1.406
Ge-68	288d	EC	Ga-68	1.000E+00						-	0.005	0.004
Ge-69	39.05h	ECB+								-	0.179	0.873
Ge-71	11.8d	EC								-	0.005	0.004
Ge-75	82.78m	B-								-	0.420	0.034
Ge-77	11.30h	B-	As-77	1.000E+00						-	0.648	1.086
Ge-78	87m	B-	As-78	1.000E+00						-	0.238	0.278
Arsenic												
As-69	15.2m	ECB+	Ge-69	1.000E+00						-	1.274	1.013
As-70	52.6m	ECB+								-	0.865	4.095
As-71	64.8h	ECB+	Ge-71	1.000E+00						-	0.119	0.574
As-72	26.0h	ECB+								-	1.026	1.794
As-73	80.30d	EC								-	0.060	0.016
As-74	17.76d	B-ECB+								-	0.268	0.759
As-76	26.32h	B-								-	1.064	0.430
As-77	38.8h	B-								-	0.229	0.009
As-78	90.7m	B-								-	1.356	1.252
Selenium												
Se-70	41.0m	ECB+	As-70	1.000E+00						-	0.489	0.999
Se-73m	39m	ECB+IT	As-73	2.700E-01	Se-73	7.300E-01				-	0.178	0.244
Se-73	7.15h	ECB+	As-73	1.000E+00						-	0.386	1.087
Se-75	119.8d	EC								-	0.015	0.394
Se-77m	17.45s	IT								-	0.072	0.088

Table G.1, continued

Nuclide	Decay $T_{1/2}$ Mode	Radioactive Decay Products and Fractional Yield						Energy (MeV nt ⁻¹)		
		Nuclide	Fraction	Nuclide	Fraction	Nuclide	Fraction	Alpha	Elect	Photon
Selenium, continued										
Se-79	65000y B-							-	0.056	-
Se-81m	57.25m ITB-	Se-81	1.000E+00					-	0.085	0.018
Se-81	18.5m B-							-	0.611	0.009
Se-83	22.5m B-	Br-83	1.000E+00					-	0.508	2.429
Bromine										
Br-74m	41.5m ECB+							-	1.412	4.082
Br-74	25.3m ECB+							-	1.115	4.549
Br-75	98m ECB+	Se-75	1.000E+00					-	0.524	1.216
Br-76	16.2h ECB+							-	0.691	2.633
Br-77	56h ECB+							-	0.009	0.321
Br-80m	4.42h IT	Br-80	1.000E+00					-	0.060	0.024
Br-80	17.4m B-ECB+							-	0.724	0.080
Br-82	35.30h B-							-	0.139	2.642
Br-83	2.39h B-	Kr-83m	1.000E+00					-	0.321	0.008
Br-84	31.80m B-							-	1.229	1.788
Krypton										
Kr-74	11.50m ECB+	Br-74	1.000E+00					-	0.792	1.169
Kr-76	14.8h EC	Br-76	1.000E+00					-	0.015	0.435
Kr-77	74.7m ECB+	Br-77	1.000E+00					-	0.642	1.016
Kr-79	35.04h ECB+							-	0.024	0.257
Kr-81m	13s IT	Kr-81	1.000E+00					-	0.059	0.131
Kr-81	2.1E5y EC							-	0.005	0.012
Kr-83m	1.83h IT							-	0.039	0.003
Kr-85m	4.48h ITB-	Kr-85	2.110E-01					-	0.255	0.158
Kr-85	10.72y B-							-	0.251	0.002
Kr-87	76.3m B-	Rb-87	1.000E+00					-	1.324	0.793
Kr-88	2.84h B-	Rb-88	1.000E+00					-	0.364	1.955
Rubidium										
Rb-79	22.9m ECB+	Kr-79	1.000E+00					-	0.820	1.358
Rb-80	34s ECB+							-	2.011	1.246
Rb-81m	32m IT	Rb-81	1.000E+00					-	0.074	0.010
Rb-81	4.58h ECB+	Kr-81	1.000E+00					-	0.197	0.623
Rb-82m	6.2h ECB+							-	0.095	2.910
Rb-82	1.3m ECB+							-	1.407	1.093
Rb-83	86.2d EC	Kr-83m	7.620E-01					-	0.015	0.504
Rb-84	32.77d ECB+B-							-	0.155	0.919
Rb-86	18.66d B-							-	0.668	0.095
Rb-87	4.7E10y B-							-	0.111	-
Rb-88	17.8m B-							-	2.066	0.629
Rb-89	15.2m B-	Sr-89	1.000E+00					-	1.013	2.071
Strontium										
Sr-80	100m EC	Rb-80	1.000E+00					-	0.005	0.008
Sr-81	25.5m ECB+	Rb-81	1.000E+00					-	1.000	1.386
Sr-82	25d EC	Rb-82	1.000E+00					-	0.005	0.008
Sr-83	32.4h ECB+	Rb-83	1.000E+00					-	0.149	0.801
Sr-85m	69.5m ITEC	Sr-85	8.790E-01					-	0.012	0.220
Sr-85	64.84d EC							-	0.009	0.512
Sr-87m	2.805h ECIT	Rb-87	3.000E-03					-	0.067	0.320
Sr-89	50.5d B-							-	0.583	<

Table G.1, continued

Nuclide	T _{1/2}	Decay Mode	Radioactive Decay Products and Fractional Yield						Energy (MeV nt ⁻¹)		
			Nuclide	Fraction	Nuclide	Fraction	Nuclide	Fraction	Alpha	Elect Photon	
Strontium, continued											
Sr-90	29.12y	B-	Y-90	1.000E+00					-	0.196	-
Sr-91	9.5h	B-	Y-91m	5.780E-01	Y-91	4.220E-01			-	0.656	0.697
Sr-92	2.71h	B-	Y-92	1.000E+00					-	0.196	1.339
Yttrium											
Y-86m	48m	ECB+IT	Y-86	9.931E-01					-	0.025	0.221
Y-86	14.74h	ECB+							-	0.226	3.589
Y-87	80.3h	ECB+	Sr-87m	9.990E-01					-	0.007	0.457
Y-88	106.64d	ECB+							-	0.007	2.692
Y-90m	3.19h	IT	Y-90	9.920E-01					-	0.047	0.629
Y-90	64.0h	B-							-	0.935	<
Y-91m	49.71m	IT	Y-91	1.000E+00					-	0.027	0.530
Y-91	58.51d	B-							-	0.602	0.004
Y-92	3.54h	B-							-	1.446	0.252
Y-93	10.1h	B-	Zr-93	1.000E+00					-	1.174	0.089
Y-94	19.1m	B-							-	1.675	1.110
Y-95	10.7m	B-	Zr-95	1.000E+00					-	1.528	0.894
Zirconium											
Zr-86	16.5h	EC	Y-86	1.000E+00					-	0.030	0.288
Zr-88	83.4d	EC	Y-88	1.000E+00					-	0.016	0.403
Zr-89	78.43h	ECB+							-	0.101	1.165
Zr-93	1.53E6y	B-	Nb-93m	1.000E+00					-	0.020	-
Zr-95	63.98d	B-	Nb-95m	7.000E-03	Nb-95	9.930E-01			-	0.116	0.739
Zr-97	16.90h	B-	Nb-97m	9.470E-01	Nb-97	5.300E-02			-	0.700	0.179
Niobium											
Nb-88	14.3m	ECB+	Zr-88	1.000E+00					-	1.237	4.126
Nb-89b	122m	ECB+	Zr-89	1.000E+00					-	1.115	1.391
Nb-89a	66m	ECB+	Zr-89	1.000E+00					-	0.834	1.925
Nb-90	14.60h	ECB+							-	0.403	4.224
Nb-93m	13.6y	IT							-	0.028	0.002
Nb-94	2.03E4y	B-							-	0.168	1.574
Nb-95m	86.6h	IT	Nb-95	1.000E+00					-	0.166	0.068
Nb-95	35.15d	B-							-	0.044	0.766
Nb-96	23.35h	B-							-	0.253	2.472
Nb-97m	60s	IT	Nb-97	1.000E+00					-	0.015	0.728
Nb-97	72.1m	B-							-	0.468	0.655
Nb-98	51.5m	B-							-	0.887	2.426
Molybdenum											
Mo-90	5.67h	ECB+	Nb-90	1.000E+00					-	0.204	0.827
Mo-93m	6.85h	IT	Mo-93	1.000E+00					-	0.097	2.250
Mo-93	3.5E3y	EC	Nb-93m	1.000E+00					-	0.006	0.011
Mo-99	66.0h	B-	Tc-99m	8.760E-01	Tc-99	1.240E-01			-	0.392	0.150
Mo-101	14.62m	B-	Tc-101	1.000E+00					-	0.589	1.368
Technetium											
Tc-93m	43.5m	ITEC	Mo-93	1.820E-01	Tc-93	8.180E-01			-	0.079	0.724
Tc-93	2.75h	EC	Mo-93	1.000E+00					-	0.006	1.459
Tc-94m	52m	ECB+							-	0.756	1.859
Tc-94	293m	ECB+							-	0.049	2.671
Tc-95m	61d	ECB+IT	Tc-95	4.000E-02					-	0.016	0.675
Tc-95	20h	EC							-	0.007	0.796
Tc-96m	51.5m	ITEC	Tc-96	9.800E-01					-	0.027	0.052

Table G.1, continued

Nuclide	Decay $T_{1/2}$	Mode	Radioactive Decay Products and Fractional Yield						Energy (MeV nt ⁻¹)			
			Nuclide	Fraction	Nuclide	Fraction	Nuclide	Fraction	Alpha	Elect	Photon	
Technetium, continued												
Tc-96	4.28d	EC								-	0.009	2.506
Tc-97m	87d	IT	Tc-97	1.000E+00						-	0.087	0.010
Tc-97	2.6E6y	EC								-	0.006	0.011
Tc-98	4.2E6y	B-								-	0.159	1.413
Tc-99m	6.02h	IT	Tc-99	1.000E+00						-	0.016	0.126
Tc-99	2.13E5y	B-								-	0.101	-
Tc-101	14.2m	B-								-	0.478	0.334
Tc-104	18.2m	B-								-	1.601	1.981
Ruthenium												
Ru-94	51.8m	EC	Tc-94m	1.000E+00						-	0.008	0.535
Ru-97	2.9d	EC	Tc-97m	7.550E-04	Tc-97	9.992E-01				-	0.013	0.240
Ru-103	39.28d	B-	Rh-103m	9.970E-01						-	0.075	0.469
Ru-105	4.44h	B-	Rh-105	1.000E+00						-	0.400	0.784
Ru-106	368.2d	B-	Rh-106	1.000E+00						-	0.010	-
Rhodium												
Rh-99m	4.7h	ECB+								-	0.032	0.685
Rh-99	16d	ECB+								-	0.042	0.608
Rh-100	20.8h	ECB+								-	0.070	2.767
Rh-101m	4.34d	ECIT	Rh-101	7.200E-02						-	0.020	0.307
Rh-101	3.2y	EC								-	0.032	0.269
Rh-102m	207d	ECB+ITB-	Rh-102	5.000E-02						-	0.168	0.486
Rh-102	2.9y	ECB+								-	0.012	2.140
Rh-103m	56.12m	IT								-	0.038	0.002
Rh-105	35.36h	B-								-	0.154	0.078
Rh-106m	132m	B-								-	0.313	2.915
Rh-106	29.9s	B-								-	1.413	0.205
Rh-107	21.7m	B-	Pd-107	1.000E+00						-	0.445	0.312
Palladium												
Pd-100	3.63d	EC	Rh-100	1.000E+00						-	0.044	0.129
Pd-101	8.27h	ECB+	Rh-101m	9.970E-01	Rh-101	3.000E-03				-	0.039	0.337
Pd-103	16.96d	EC	Rh-103m	1.000E+00						-	0.006	0.014
Pd-107	6.5E6y	B-								-	0.009	-
Pd-109	13.427h	B-								-	0.437	0.012
Silver												
Ag-102	12.9m	ECB+								-	0.819	3.353
Ag-103	65.7m	ECB+	Pd-103	1.000E+00						-	0.259	0.765
Ag-104m	33.5m	ECB+IT	Ag-104	3.300E-01						-	0.509	1.174
Ag-104	69.2m	ECB+								-	0.091	2.683
Ag-105	41.0d	ECB+								-	0.019	0.525
Ag-106m	8.41d	EC								-	0.013	2.822
Ag-106	23.96m	ECB+								-	0.508	0.711
Ag-108m	127y	ECIT	Ag-108	8.900E-02						-	0.016	1.627
Ag-108	2.37m	ECB+B-								-	0.610	0.018
Ag-109m	39.6s	IT								-	0.077	0.011
Ag-110m	249.9d	ITB-	Ag-110	1.330E-02						-	0.072	2.751
Ag-110	24.6s	B-EC								-	1.182	0.031
Ag-111	7.45d	B-								-	0.354	0.026
Ag-112	3.12h	B-								-	1.384	0.657
Ag-115	20.0m	B-	Cd-115m	6.600E-02	Cd-115	9.340E-01				-	1.042	0.707

Table G.1, continued

Nuclide	T _{1/2}	Decay Mode	Radioactive Decay Products and Fractional Yield						Energy (MeV nt ⁻¹)	
			Nuclide	Fraction	Nuclide	Fraction	Nuclide	Fraction	Alpha	Elect Photon
Cadmium										
Cd-104	57.7m	ECB+	Ag-104	1.000E+00					-	0.032 0.259
Cd-107	6.49h	ECB+							-	0.087 0.034
Cd-109	464d	EC							-	0.083 0.026
Cd-113m	13.6y	B-							-	0.185 -
Cd-113	9.3E15y	B-							-	0.093 -
Cd-115m	44.6d	B-	In-115	1.000E+00					-	0.607 0.022
Cd-115	53.46h	B-	In-115m	1.000E+00					-	0.303 0.233
Cd-117m	3.36h	B-	In-117m	1.000E-02	In-117	9.900E-01			-	0.229 2.044
Cd-117	2.49h	B-	In-117m	9.200E-01	In-117	8.000E-02			-	0.439 1.087
Indium										
In-109	4.2h	ECB+	Cd-109	1.000E+00					-	0.047 0.672
In-110b	4.9h	ECB+							-	0.012 3.049
In-110a	69.1m	ECB+							-	0.626 1.557
In-111	2.83d	EC							-	0.034 0.405
In-112	14.4m	B-ECB+							-	0.243 0.268
In-113m	1.658h	IT							-	0.134 0.258
In-114m	49.51d	ECIT	In-114	9.570E-01					-	0.143 0.094
In-114	71.9s	B-ECB+							-	0.771 0.003
In-115m	4.486h	ITB-	In-115	9.500E-01					-	0.172 0.161
In-115	5.1E15y	B-							-	0.152 -
In-116m	54.15m	B-							-	0.312 2.473
In-117m	116.5m	B-IT	In-117	4.710E-01					-	0.434 0.091
In-117	43.8m	B-	Sn-117m	3.200E-03					-	0.267 0.692
In-119m	18.0m	B-IT	In-119	2.500E-02					-	1.065 0.011
In-119	2.4m	B-	Sn-119m	1.090E-01					-	0.634 0.769
Tin										
Sn-110	4.0h	EC	In-110a	1.000E+00					-	0.014 0.301
Sn-111	35.3m	ECB+	In-111	1.000E+00					-	0.221 0.510
Sn-113	115.1d	EC	In-113m	1.000E+00					-	0.006 0.023
Sn-117m	13.61d	IT							-	0.161 0.158
Sn-119m	293.0d	IT							-	0.078 0.011
Sn-121m	55y	B-IT	Sn-121	7.760E-01					-	0.035 0.005
Sn-121	27.06h	B-							-	0.114 -
Sn-123m	40.08m	B-							-	0.475 0.140
Sn-123	129.2d	B-							-	0.520 0.007
Sn-125	9.64d	B-	Sb-125	1.000E+00					-	0.811 0.313
Sn-126	1.0E5y	B-	Sb-126m	1.000E+00					-	0.172 0.057
Sn-127	2.10h	B-	Sb-127	1.000E+00					-	0.534 1.910
Sn-128	59.1m	B-	Sb-128a	1.000E+00					-	0.255 0.666
Antimony										
Sb-115	31.8m	ECB+							-	0.238 0.909
Sb-116m	60.3m	ECB+							-	0.153 3.143
Sb-116	15.8m	ECB+							-	0.424 2.158
Sb-117	2.80h	ECB+							-	0.029 0.185
Sb-118m	5.00h	ECB+							-	0.040 2.585
Sb-119	38.1h	EC							-	0.026 0.023
Sb-120b	5.76d	EC							-	0.045 2.469
Sb-120a	15.89m	ECB+							-	0.308 0.452
Sb-122	2.70d	ECB-							-	0.565 0.441
Sb-124n	20.2m	IT	Sb-124m	1.000E+00					-	0.025 <

Table G.1, continued

Nuclide	Decay $T_{1/2}$ Mode	Radioactive Decay Products and Fractional Yield						Energy (MeV nt ⁻¹)	
		Nuclide	Fraction	Nuclide	Fraction	Nuclide	Fraction	Alpha	Elect Photon
Antimony, continued									
Sb-124m	93s	ITB-	Sb-124	8.000E-01				-	0.092 0.352
Sb-124	60.20d	B-						-	0.387 1.817
Sb-125	2.77y	B-	Te-125m	2.280E-01				-	0.100 0.431
Sb-126m	19.0m	ITB-	Sb-126	1.400E-01				-	0.591 1.548
Sb-126	12.4d	B-						-	0.283 2.834
Sb-127	3.85d	B-	Te-127m	1.760E-01	Te-127	8.240E-01		-	0.316 0.688
Sb-128b	9.01h	B-						-	0.438 3.093
Sb-128a	10.4m	B-						-	0.935 1.986
Sb-129	4.32h	B-	Te-129m	2.250E-01	Te-129	7.750E-01		-	0.408 1.437
Sb-130	40m	B-						-	0.722 3.264
Sb-131	23m	B-	Te-131m	9.930E-02	Te-131	9.007E-01		-	0.553 1.864
Tellurium									
Te-116	2.49h	EC	Sb-116	1.000E+00				-	0.053 0.073
Te-121m	154d	ECIT	Te-121	8.860E-01				-	0.080 0.217
Te-121	17d	EC						-	0.010 0.577
Te-123m	119.7d	IT	Te-123	1.000E+00				-	0.099 0.148
Te-123	1E13y	EC						-	0.006 0.020
Te-125m	58d	IT						-	0.109 0.036
Te-127m	109d	ITB-	Te-127	9.760E-01				-	0.082 0.011
Te-127	9.35h	B-						-	0.223 0.005
Te-129m	33.6d	ITB-	I-129	3.500E-01	Te-129	6.500E-01		-	0.260 0.038
Te-129	69.6m	B-	I-129	1.000E+00				-	0.544 0.059
Te-131m	30h	ITB-	I-131	7.780E-01	Te-131	2.220E-01		-	0.202 1.425
Te-131	25.0m	B-	I-131	1.000E+00				-	0.719 0.420
Te-132	78.2h	B-	I-132	1.000E+00				-	0.102 0.234
Te-133m	55.4m	ITB-	I-133	8.700E-01	Te-133	1.300E-01		-	0.705 2.313
Te-133	12.45m	B-	I-133	1.000E+00				-	0.819 0.929
Te-134	41.8m	B-	I-134	1.000E+00				-	0.300 0.886
Iodine									
I-120m	53m	ECB+						-	1.244 5.297
I-120	81.0m	ECB+						-	1.423 2.729
I-121	2.12h	ECB+	Te-121	1.000E+00				-	0.083 0.419
I-122	3.62m	ECB+						-	1.055 0.946
I-123	13.2h	EC	Te-123m	5.000E-05	Te-123	9.999E-01		-	0.028 0.172
I-124	4.18d	ECB+						-	0.194 1.098
I-125	60.14d	EC						-	0.019 0.042
I-126	13.02d	ECB+B-						-	0.157 0.455
I-128	24.99m	ECB+B-						-	0.748 0.085
I-129	1.57E7y	B-						-	0.064 0.025
I-130	12.36h	B-						-	0.297 2.139
I-131	8.04d	B-	Xe-131m	1.110E-02				-	0.192 0.382
I-132m	83.6m	ITB-	I-132	8.600E-01				-	0.159 0.322
I-132	2.30h	B-						-	0.495 2.280
I-133	20.8h	B-	Xe-133m	2.900E-02	Xe-133	9.710E-01		-	0.411 0.607
I-134	52.6m	B-						-	0.622 2.625
I-135	6.61h	B-	Xe-135m	1.540E-01	Xe-135	8.460E-01		-	0.367 1.576
Xenon									
Xe-120	40m	ECB+	I-120	1.000E+00				-	0.055 0.432
Xe-121	40.1m	ECB+	I-121	1.000E+00				-	0.569 1.815
Xe-122	20.1h	EC	I-122	1.000E+00				-	0.010 0.068

Table G.1, continued

Nuclide	T _{1/2}	Decay Mode	Radioactive Decay Products and Fractional Yield						Energy (MeV nt ⁻¹)	
			Nuclide	Fraction	Nuclide	Fraction	Nuclide	Fraction	Alpha	Elect Photon
Xenon, continued										
Xe-123	2.08h	ECB+	I-123	1.000E+00					-	0.184 0.634
Xe-125	17.0h	ECB+	I-125	1.000E+00					-	0.034 0.271
Xe-127	36.41d	EC							-	0.033 0.280
Xe-129m	8.0d	IT							-	0.185 0.051
Xe-131m	11.9d	IT							-	0.144 0.020
Xe-133m	2.188d	IT	Xe-133	1.000E+00					-	0.192 0.041
Xe-133	5.245d	B-							-	0.136 0.046
Xe-135m	15.29m	ITB-	Cs-135	4.500E-05	Xe-135	9.999E-01			-	0.098 0.429
Xe-135	9.09h	B-	Cs-135	1.000E+00					-	0.317 0.249
Xe-138	14.17m	B-	Cs-138	1.000E+00					-	0.673 1.125
Cesium										
Cs-125	45m	ECB+	Xe-125	1.000E+00					-	0.347 0.678
Cs-126	1.64m	ECB+							-	1.464 1.086
Cs-127	6.25h	ECB+	Xe-127	1.000E+00					-	0.029 0.420
Cs-128	3.9m	ECB+							-	0.846 0.900
Cs-129	32.06h	ECB+							-	0.018 0.282
Cs-130	29.9m	ECB+							-	0.401 0.517
Cs-131	9.69d	EC							-	0.007 0.023
Cs-132	6.475d	ECB+B-							-	0.014 0.705
Cs-134m	2.90h	IT	Cs-134	1.000E+00					-	0.112 0.027
Cs-134	2.062y	ECB-							-	0.164 1.555
Cs-135m	53m	IT	Cs-135	1.000E+00					-	0.036 1.586
Cs-135	2.3E6y	B-							-	0.067 -
Cs-136	13.1d	B-							-	0.139 2.166
Cs-137	30.0y	B-	Ba-137m	9.460E-01					-	0.187 -
Cs-138	32.2m	B-							-	1.207 2.361
Barium										
Ba-126	96.5m	ECB+	Cs-126	1.000E+00					-	0.020 0.163
Ba-128	2.43d	EC	Cs-128	1.000E+00					-	0.009 0.076
Ba-131m	14.6m	IT	Ba-131	1.000E+00					-	0.109 0.077
Ba-131	11.8d	ECB+	Cs-131	1.000E+00					-	0.046 0.459
Ba-133m	38.9h	IT	Ba-133	1.000E+00					-	0.221 0.067
Ba-133	10.74y	EC							-	0.054 0.402
Ba-135m	28.7h	IT							-	0.208 0.060
Ba-137m	2.552m	IT							-	0.065 0.597
Ba-139	82.7m	B-							-	0.898 0.043
Ba-140	12.74d	B-	La-140	1.000E+00					-	0.313 0.183
Ba-141	18.27m	B-	La-141	1.000E+00					-	0.901 0.845
Ba-142	10.6m	B-	La-142	1.000E+00					-	0.440 1.047
Lanthanum										
La-131	59m	ECB+	Ba-131	1.000E+00					-	0.208 0.671
La-132	4.8h	ECB+							-	0.522 2.011
La-134	6.67m	ECB+							-	0.739 0.698
La-135	19.5h	ECB+							-	0.007 0.036
La-137	6E4y	EC							-	0.007 0.024
La-138	1.35E11y	B-EC							-	0.037 1.236
La-140	40.272h	B-							-	0.537 2.315
La-141	3.93h	B-	Ce-141	1.000E+00					-	0.948 0.043
La-142	92.5m	B-							-	0.846 2.753
La-143	14.23m	B-	Ce-143	1.000E+00					-	1.324 0.094

Table G.1, continued

Nuclide	T _{1/2}	Decay Mode	Radioactive Decay Products and Fractional Yield						Energy (MeV nt ⁻¹)	
			Nuclide	Fraction	Nuclide	Fraction	Nuclide	Fraction	Alpha	Elect Photon
Cerium										
Ce-134	72.0h	EC	La-134	1.000E+00					-	0.007 0.026
Ce-135	17.6h	ECB+	La-135	1.000E+00					-	0.244 1.776
Ce-137m	34.4h	ECIT	La-137	5.900E-03	Ce-137	9.941E-01			-	0.203 0.053
Ce-137	9.0h	EC	La-137	1.000E+00					-	0.017 0.036
Ce-139	137.66d	EC							-	0.036 0.160
Ce-141	32.501d	B-							-	0.171 0.076
Ce-143	33.0h	B-	Pr-143	1.000E+00					-	0.433 0.282
Ce-144	284.3d	B-	Pr-144m	1.780E-02	Pr-144	9.822E-01			-	0.092 0.021
Praseodymium										
Pr-136	13.1m	ECB+							-	0.743 2.101
Pr-137	76.6m	ECB+	Ce-137	1.000E+00					-	0.198 0.501
Pr-138m	2.1h	ECB+							-	0.224 2.478
Pr-138	1.45m	ECB+							-	1.159 0.813
Pr-139	4.51h	ECB+	Ce-139	1.000E+00					-	0.046 0.122
Pr-142m	14.6m	IT	Pr-142	1.000E+00					-	0.004 <
Pr-142	19.13h	B-EC							-	0.808 0.058
Pr-143	13.56d	B-							-	0.314 <
Pr-144m	7.2m	ITB-	Pr-144	9.990E-01					-	0.047 0.013
Pr-144	17.28m	B-							-	1.208 0.032
Pr-145	5.98h	B-							-	0.677 0.013
Pr-147	13.6m	B-	Nd-147	1.000E+00					-	0.807 0.863
Neodymium										
Nd-136	50.65m	ECB+	Pr-136	1.000E+00					-	0.093 0.293
Nd-138	5.04h	EC	Pr-138	1.000E+00					-	0.008 0.043
Nd-139m	5.5h	ECB+IT	Pr-139	8.800E-01	Nd-139	1.200E-01			-	0.111 1.572
Nd-139	29.7m	ECB+	Pr-139	1.000E+00					-	0.201 0.406
Nd-141m	62.4s	ECIT	Nd-141	9.996E-01					-	0.068 0.759
Nd-141	2.49h	ECB+							-	0.016 0.075
Nd-147	10.98d	B-	Pm-147	1.000E+00					-	0.270 0.140
Nd-149	1.73h	B-	Pm-149	1.000E+00					-	0.506 0.384
Nd-151	12.44m	B-	Pm-151	1.000E+00					-	0.649 0.916
Promethium										
Pm-141	20.90m	ECB+	Nd-141m	9.680E-04	Nd-141	9.990E-01			-	0.632 0.744
Pm-142	40.5s	ECB+							-	1.365 0.868
Pm-143	265d	EC							-	0.008 0.315
Pm-144	363d	EC							-	0.017 1.563
Pm-145	17.7y	EC							-	0.014 0.031
Pm-146	2020d	B-EC	Sm-146	3.590E-01					-	0.097 0.753
Pm-147	2.6234y	B-	Sm-147	1.000E+00					-	0.062 <
Pm-148m	41.3d	B-IT	Pm-148	4.600E-02					-	0.170 2.000
Pm-148	5.37d	B-							-	0.724 0.575
Pm-149	53.08h	B-							-	0.366 0.011
Pm-150	2.68h	B-							-	0.807 1.431
Pm-151	28.40h	B-	Sm-151	1.000E+00					-	0.306 0.321
Samarium										
Sm-141m	22.6m	ITECB+	Pm-141	9.969E-01	Sm-141	3.100E-03			-	0.435 1.984
Sm-141	10.2m	ECB+	Pm-141	1.000E+00					-	0.706 1.405
Sm-142	72.49m	ECB+	Pm-142	1.000E+00					-	0.034 0.094
Sm-145	340d	EC	Pm-145	1.000E+00					-	0.032 0.065
Sm-146	1.03E8y	A							2.474	- -

Table G.1, continued

Nuclide	T _{1/2}	Decay Mode	Radioactive Decay Products and Fractional Yield				Energy (MeV nt ⁻¹)			
			Nuclide	Fraction	Nuclide	Fraction	Nuclide	Fraction	Alpha	Elect
Samarium, continued										
Sm-147	1.06E11y	A						2.248	-	-
Sm-151	90y	B-						-	0.020	<
Sm-153	46.7h	B-						-	0.273	0.062
Sm-155	22.1m	B-	Eu-155	1.000E+00				-	0.566	0.103
Sm-156	9.4h	B-	Eu-156	1.000E+00				-	0.206	0.121
Europium										
Eu-145	5.94d	ECB+	Sm-145	1.000E+00				-	0.029	1.458
Eu-146	4.61d	ECB+	Sm-146	1.000E+00				-	0.048	2.504
Eu-147	24d	A ECB+	Pm-143	2.200E-05	Sm-147	1.000E+00		<	0.042	0.497
Eu-148	54.5d	A ECB+	Pm-144	9.400E-09				<	0.023	2.177
Eu-149	93.1d	EC						-	0.011	0.063
Eu-150b	34.2y	EC						-	0.044	1.496
Eu-150a	12.62h	B-ECB+						-	0.312	0.047
Eu-152m	9.32h	ECB+B-	Gd-152	7.200E-01				-	0.507	0.293
Eu-152	13.33y	B-ECB+	Gd-152	2.792E-01				-	0.139	1.155
Eu-154	8.8y	ECB-						-	0.292	1.242
Eu-155	4.96y	B-						-	0.063	0.061
Eu-156	15.19d	B-						-	0.423	1.329
Eu-157	15.15h	B-						-	0.395	0.262
Eu-158	45.9m	B-						-	0.963	1.057
Gadolinium										
Gd-145	22.9m	ECB+	Eu-145	1.000E+00				-	0.549	2.257
Gd-146	48.3d	EC	Eu-146	1.000E+00				-	0.130	0.250
Gd-147	38.1h	ECB+	Eu-147	1.000E+00				-	0.060	1.337
Gd-148	93y	A						3.183	-	-
Gd-149	9.4d	EC	Eu-149	1.000E+00				-	0.059	0.420
Gd-151	120d	A EC	Sm-147	8.000E-09				<	0.034	0.064
Gd-152	1.08E14y	A						2.148	-	-
Gd-153	242d	EC						-	0.044	0.106
Gd-159	18.56h	B-						-	0.304	0.050
Terbium										
Tb-147	1.65h	ECB+	Gd-147	1.000E+00				-	0.564	1.590
Tb-149	4.15h	ECB+A	Eu-145	2.000E-01	Gd-149	8.000E-01		0.793	0.186	1.614
Tb-150	3.27h	ECB+						-	0.546	1.679
Tb-151	17.6h	ECB+A	Eu-147	9.500E-05	Gd-151	1.000E+00		<	0.080	0.892
Tb-153	2.34d	ECB+	Gd-153	1.000E+00				-	0.049	0.229
Tb-154	21.4h	ECB+						-	0.081	2.352
Tb-155	5.32d	EC						-	0.034	0.140
Tb-156m	24.4h	IT	Tb-156	1.000E+00				-	0.024	0.025
Tb-156n	5.0h	IT	Tb-156	1.000E+00				-	0.084	0.004
Tb-156	5.34d	EC						-	0.103	1.826
Tb-157	150y	EC						-	0.005	0.003
Tb-158	150y	B-EC						-	0.116	0.798
Tb-160	72.3d	B-						-	0.257	1.124
Tb-161	6.91d	B-						-	0.197	0.035
Dysprosium										
Dy-155	10.0h	ECB+	Tb-155	1.000E+00				-	0.028	0.582
Dy-157	8.1h	EC	Tb-157	1.000E+00				-	0.013	0.357
Dy-159	144.4d	EC						-	0.013	0.045
Dy-165	2.334h	B-						-	0.449	0.026
Dy-166	81.6h	B-	Ho-166	1.000E+00				-	0.159	0.040

Table G.1, continued

Nuclide	Decay $T_{1/2}$ Mode	Radioactive Decay Products and Fractional Yield						Energy (MeV nt ⁻¹)	
		Nuclide	Fraction	Nuclide	Fraction	Nuclide	Fraction	Alpha	Elect Photon
Holmium									
Ho-155	48m ECB+	Dy-155	1.000E+00					-	0.241 0.387
Ho-157	12.6m ECB+	Dy-157	1.000E+00					-	0.081 0.493
Ho-159	33m ECB+	Dy-159	1.000E+00					-	0.052 0.366
Ho-161	2.5h EC							-	0.033 0.062
Ho-162m	68m ITEC	Ho-162	6.100E-01					-	0.078 0.576
Ho-162	15m ECB+							-	0.062 0.168
Ho-164m	37.5m IT	Ho-164	1.000E+00					-	0.092 0.047
Ho-164	29m ECB-							-	0.148 0.030
Ho-166m	1.20E3y B-							-	0.132 1.747
Ho-166	26.80h B-							-	0.695 0.029
Ho-167	3.1h B-							-	0.219 0.365
Erbium									
Er-161	3.24h ECB+	Ho-161	1.000E+00					-	0.051 0.914
Er-165	10.36h EC							-	0.008 0.038
Er-169	9.3d B-							-	0.104 <
Er-171	7.52h B-	Tm-171	1.000E+00					-	0.422 0.381
Er-172	49.3h B-	Tm-172	1.000E+00					-	0.129 0.522
Thulium									
Tm-162	21.7m ECB+							-	0.370 1.781
Tm-166	7.70h ECB+							-	0.103 1.870
Tm-167	9.24d EC							-	0.128 0.146
Tm-170	128.6d ECB-							-	0.331 0.005
Tm-171	1.92y B-							-	0.026 <
Tm-172	63.6h B-							-	0.530 0.477
Tm-173	8.24h B-							-	0.319 0.388
Tm-175	15.2m B-	Yb-175	1.000E+00					-	0.555 1.053
Ytterbium									
Yb-162	18.9m EC	Tm-162	1.000E+00					-	0.031 0.137
Yb-166	56.7h EC	Tm-166	1.000E+00					-	0.042 0.086
Yb-167	17.5m ECB+	Tm-167	1.000E+00					-	0.092 0.267
Yb-169	32.01d EC							-	0.125 0.310
Yb-175	4.19d B-							-	0.130 0.040
Yb-177	1.9h B-	Lu-177	1.000E+00					-	0.430 0.187
Yb-178	74m B-	Lu-178	1.000E+00					-	0.191 0.035
Lutetium									
Lu-169	34.06h ECB+	Yb-169	1.000E+00					-	0.054 1.041
Lu-170	2.00d ECB+							-	0.094 2.484
Lu-171	8.22d EC							-	0.084 0.697
Lu-172	6.70d ECB+							-	0.119 1.888
Lu-173	1.37y EC							-	0.036 0.130
Lu-174m	142d ECIT	Lu-174	9.930E-01					-	0.116 0.063
Lu-174	3.31y ECB+							-	0.042 0.126
Lu-176m	3.68h B-							-	0.477 0.014
Lu-176	3.60E10y B-							-	0.296 0.491
Lu-177m	160.9d B-IT	Lu-177	2.100E-01					-	0.272 1.003
Lu-177	6.71d B-							-	0.148 0.035
Lu-178m	22.7m B-							-	0.591 1.109
Lu-178	28.4m B-							-	0.773 0.140
Lu-179	4.59h B-							-	0.464 0.031

Table G.1, continued

Nuclide	T _{1/2}	Decay Mode	Radioactive Decay Products and Fractional Yield						Energy (MeV nt ⁻¹)		
			Nuclide	Fraction	Nuclide	Fraction	Nuclide	Fraction	Alpha	Elect Photon	
Hafnium											
Hf-170	16.01h	EC	Lu-170	1.000E+00					-	0.091	0.549
Hf-172	1.87y	EC	Lu-172	1.000E+00					-	0.118	0.118
Hf-173	24.0h	ECB+	Lu-173	1.000E+00					-	0.053	0.408
Hf-175	70d	EC							-	0.046	0.369
Hf-177m	51.4m	IT							-	0.500	2.252
Hf-178m	31y	IT							-	0.297	2.358
Hf-179m	25.1d	IT							-	0.188	0.901
Hf-180m	5.5h	IT							-	0.139	1.008
Hf-181	42.4d	B-							-	0.203	0.555
Hf-182m	61.5m	ITB-	Ta-182	5.400E-01	Hf-182	4.600E-01			-	0.235	0.933
Hf-182	9E6y	B-	Ta-182	1.000E+00					-	0.083	0.239
Hf-183	64m	B-	Ta-183	1.000E+00					-	0.451	0.752
Hf-184	4.12h	B-	Ta-184	1.000E+00					-	0.477	0.251
Tantalum											
Ta-172	36.8m	ECB+	Hf-172	1.000E+00					-	0.505	1.550
Ta-173	3.65h	ECB+	Hf-173	1.000E+00					-	0.358	0.585
Ta-174	1.2h	ECB+							-	0.367	0.627
Ta-175	10.5h	ECB+	Hf-175	1.000E+00					-	0.064	0.933
Ta-176	8.08h	ECB+							-	0.104	2.145
Ta-177	56.6h	EC							-	0.024	0.067
Ta-178b	2.2h	EC							-	0.155	1.023
Ta-178a	9.31m	EC							-	0.034	0.109
Ta-179	664.9d	EC							-	0.008	0.032
Ta-180m	8.1h	ECB-							-	0.055	0.049
Ta-180	1.0E13y	EC							-	0.123	0.560
Ta-182m	15.84m	IT	Ta-182	1.000E+00					-	0.251	0.252
Ta-182	115.0d	B-							-	0.217	1.294
Ta-183	5.1d	B-							-	0.345	0.293
Ta-184	8.7h	B-							-	0.547	1.612
Ta-185	49m	B-	W-185	1.000E+00					-	0.725	0.193
Ta-186	10.5m	B-							-	0.992	1.560
Tungsten											
W-176	2.3h	EC	Ta-176	1.000E+00					-	0.073	0.177
W-177	135m	ECB+	Ta-177	1.000E+00					-	0.104	0.903
W-178	21.7d	EC	Ta-178a	1.000E+00					-	0.007	0.014
W-179	37.5m	EC	Ta-179	1.000E+00					-	0.027	0.060
W-181	121.2d	EC							-	0.011	0.040
W-185	75.1d	B-							-	0.127	<
W-187	23.9h	B-	Re-187	1.000E+00					-	0.312	0.481
W-188	69.4d	B-	Re-188	1.000E+00					-	0.100	0.002
Rhenium											
Re-177	14.0m	ECB+	W-177	1.000E+00					-	0.361	0.620
Re-178	13.2m	ECB+	W-178	1.000E+00					-	0.578	1.218
Re-180	2.43m	ECB+							-	0.156	1.183
Re-181	20h	ECB+	W-181	1.000E+00					-	0.137	0.771
Re-182b	64.0h	EC							-	0.213	1.886
Re-182a	12.7h	ECB+							-	0.088	1.179
Re-184m	165d	ITEC	Re-184	7.470E-01					-	0.141	0.390
Re-184	38.0d	EC							-	0.056	0.891
Re-186m	2.0E5y	IT	Re-186	1.000E+00					-	0.124	0.019

Table G.1, continued

Nuclide	T _{1/2}	Decay Mode	Radioactive Decay Products and Fractional Yield						Energy (MeV nt ⁻¹)		
			Nuclide	Fraction	Nuclide	Fraction	Nuclide	Fraction	Alpha	Elect	Photon
Rhenium, continued											
Re-186	90.64h	B-EC							-	0.345	0.021
Re-187	5E10y	B-							-	<	-
Re-188m	18.6m	IT	Re-188	1.000E+00					-	0.098	0.080
Re-188	16.98h	B-							-	0.780	0.058
Re-189	24.3h	B-	Os-189m	2.410E-01					-	0.340	0.069
Osmium											
Os-180	22m	ECB+	Re-180	1.000E+00					-	0.028	0.065
Os-181	105m	ECB+	Re-181	1.000E+00					-	0.108	1.222
Os-182	22h	EC	Re-182a	1.000E+00					-	0.056	0.435
Os-185	94d	EC							-	0.019	0.719
Os-189m	6.0h	IT							-	0.029	0.002
Os-190m	9.9m	IT							-	0.116	1.588
Os-191m	13.03h	IT	Os-191	1.000E+00					-	0.065	0.009
Os-191	15.4d	B-							-	0.135	0.080
Os-193	30.0h	B-							-	0.373	0.073
Os-194	6.0y	B-	Ir-194	1.000E+00					-	0.034	0.002
Iridium											
Ir-182	15m	ECB+	Os-182	1.000E+00					-	0.935	1.340
Ir-184	3.02h	ECB+							-	0.279	1.908
Ir-185	14.0h	ECB+	Os-185	1.000E+00					-	0.115	0.601
Ir-186a	15.8h	ECB+							-	0.113	1.641
Ir-186b	1.75h	ECB+							-	0.203	0.964
Ir-187	10.5h	EC							-	0.060	0.363
Ir-188	41.5h	ECB+							-	0.058	1.584
Ir-189	13.3d	EC	Os-189m	8.300E-02					-	0.049	0.081
Ir-190n	3.1h	ITEC	Ir-190m	5.000E-02					-	0.126	1.555
Ir-190m	1.2h	IT	Ir-190	1.000E+00					-	0.024	0.002
Ir-190	12.1d	EC							-	0.129	1.443
Ir-191m	4.94s	IT							-	0.096	0.075
Ir-192m	241y	IT	Ir-192	1.000E+00					-	-	0.161
Ir-192	74.02d	B-EC							-	0.217	0.818
Ir-194m	171d	B-							-	0.156	2.335
Ir-194	19.15h	B-							-	0.812	0.090
Ir-195m	3.8h	ITB-	Ir-195	4.000E-02					-	0.480	0.432
Ir-195	2.5h	B-							-	0.380	0.059
Platinum											
Pt-186	2.0h	A EC	Os-182	1.400E-06	Ir-186b	1.000E+00			<	0.012	0.740
Pt-188	10.2d	EC	Ir-188	1.000E+00					-	0.080	0.202
Pt-189	10.87h	ECB+	Ir-189	1.000E+00					-	0.055	0.325
Pt-191	2.8d	EC							-	0.064	0.304
Pt-193m	4.33d	IT	Pt-193	1.000E+00					-	0.137	0.013
Pt-193	50y	EC							-	0.007	0.002
Pt-195m	4.02d	IT							-	0.183	0.076
Pt-197m	94.4m	B-IT	Pt-197	9.670E-01					-	0.324	0.083
Pt-197	18.3h	B-							-	0.254	0.025
Pt-199	30.8m	B-	Au-199	1.000E+00					-	0.535	0.202
Pt-200	12.5h	B-	Au-200	1.000E+00					-	0.243	0.061
Gold											
Au-193	17.65h	EC	Pt-193	1.000E+00					-	0.064	0.160
Au-194	39.5h	ECB+							-	0.043	1.067

Table G.1, continued

Nuclide	T _{1/2}	Decay Mode	Radioactive Decay Products and Fractional Yield						Energy (MeV nt ⁻¹)		
			Nuclide	Fraction	Nuclide	Fraction	Nuclide	Fraction	Alpha	Elect Photon	
Gold, continued											
Au-195m	30.5s	IT	Au-195	1.000E+00					-	0.117	0.201
Au-195	183d	EC							-	0.051	0.085
Au-198m	2.30d	IT	Au-198	1.000E+00					-	0.289	0.577
Au-198	2.696d	B-							-	0.327	0.405
Au-199	3.139d	B-							-	0.143	0.089
Au-200m	18.7h	B-IT	Au-200	1.800E-01					-	0.276	2.087
Au-200	48.4m	B-							-	0.740	0.272
Au-201	26.4m	B-							-	0.422	0.053
Mercury											
Hg-193m	11.1h	ECB+IT	Au-193	9.200E-01	Hg-193	8.000E-02			-	0.139	1.046
Hg-193	3.5h	ECB+	Au-193	1.000E+00					-	0.125	0.203
Hg-194	260y	EC	Au-194	1.000E+00					-	0.007	0.003
Hg-195m	41.6h	ITEC	Au-195	4.580E-01	Hg-195	5.420E-01			-	0.150	0.214
Hg-195	9.9h	EC	Au-195	1.000E+00					-	0.065	0.204
Hg-197m	23.8h	ECIT	Hg-197	9.300E-01					-	0.215	0.094
Hg-197	64.1h	EC							-	0.066	0.070
Hg-199m	42.6m	IT							-	0.352	0.186
Hg-203	46.60d	B-							-	0.099	0.238
Thallium											
Tl-194m	32.8m	ECB+	Hg-194	1.000E+00					-	0.342	2.319
Tl-194	33m	EC	Hg-194	1.000E+00					-	0.030	0.779
Tl-195	1.16h	ECB+	Hg-195	1.000E+00					-	0.096	1.271
Tl-197	2.84h	ECB+	Hg-197	1.000E+00					-	0.061	0.409
Tl-198m	1.87h	ECB+IT	Tl-198	4.700E-01					-	0.201	1.195
Tl-198	5.3h	ECB+							-	0.041	2.006
Tl-199	7.42h	ECB+							-	0.056	0.249
Tl-200	26.1h	ECB+							-	0.040	1.311
Tl-201	3.044d	EC							-	0.043	0.093
Tl-202	12.23d	ECB+							-	0.023	0.468
Tl-204	3.779y	ECB-							-	0.238	0.001
Tl-206	4.20m	B-							-	0.537	<
Tl-207	4.77m	B-							-	0.493	0.002
Tl-208	3.07m	B-							-	0.598	3.375
Tl-209	2.20m	B-	Pb-209	1.000E+00					-	0.688	2.032
Lead											
Pb-195m	15.8m	ECB+	Tl-195	1.000E+00					-	0.302	1.599
Pb-198	2.4h	EC	Tl-198	1.000E+00					-	0.079	0.439
Pb-199	90m	ECB+	Tl-199	1.000E+00					-	0.054	1.476
Pb-200	21.5h	EC	Tl-200	1.000E+00					-	0.099	0.209
Pb-201	9.4h	ECB+	Tl-201	1.000E+00					-	0.058	0.758
Pb-202m	3.62h	ITEC	Tl-202	9.500E-02	Pb-202	9.050E-01			-	0.076	2.043
Pb-202	3E5y	EC	Tl-202	1.000E+00					-	0.006	0.002
Pb-203	52.05h	EC							-	0.052	0.312
Pb-205	1.43E7y	EC							-	0.007	0.002
Pb-209	3.253h	B-							-	0.198	-
Pb-210	22.3y	B-	Bi-210	1.000E+00					-	0.038	0.005
Pb-211	36.1m	B-	Bi-211	1.000E+00					-	0.456	0.051
Pb-212	10.64h	B-	Bi-212	1.000E+00					-	0.176	0.148
Pb-214	26.8m	B-	Bi-214	1.000E+00					-	0.293	0.250

Table G.1, continued

Nuclide	Decay $T_{1/2}$ Mode	Radioactive Decay Products and Fractional Yield						Energy (MeV nt ⁻¹)		
		Nuclide	Fraction	Nuclide	Fraction	Nuclide	Fraction	Alpha	Elect	Photon
Bismuth										
Bi-200	36.4m	ECB+	Pb-200	1.000E+00				-	0.190	2.393
Bi-201	108m	EC	Pb-201	1.000E+00				-	0.258	1.339
Bi-202	1.67h	ECB+	Pb-202m	2.500E-03	Pb-202	9.975E-01		-	0.109	2.713
Bi-203	11.76h	ECB+	Pb-203	1.000E+00				-	0.080	2.384
Bi-205	15.31d	ECB+	Pb-205	1.000E+00				-	0.034	1.690
Bi-206	6.243d	EC						-	0.136	3.278
Bi-207	38y	ECB+						-	0.117	1.540
Bi-210m	3.0E6y	A	Tl-206	1.000E+00				4.913	0.047	0.257
Bi-210	5.012d	B-	Po-210	1.000E+00				-	0.389	-
Bi-211	2.14m	A B-	Tl-207	9.972E-01	Po-211	2.800E-03		6.550	0.010	0.047
Bi-212	60.55m	B-A	Tl-208	3.593E-01	Po-212	6.407E-01		2.174	0.472	0.186
Bi-213	45.65m	B-A	Tl-209	2.160E-02	Po-213	9.784E-01		0.126	0.442	0.133
Bi-214	19.9m	B-	Po-214	9.998E-01				-	0.659	1.508
Polonium										
Po-203	36.7m	ECB+	Bi-203	9.989E-01				-	0.164	1.644
Po-205	1.80h	A ECB+	Pb-201	1.400E-03	Bi-205	9.986E-01		0.007	0.060	1.581
Po-207	350m	ECB+	Bi-207	1.000E+00				-	0.052	1.331
Po-210	138.38d	A						5.297	<	<
Po-211	0.516s	A						7.442	<	0.008
Po-212	0.305 μ s	A						8.785	-	-
Po-213	4.2 μ s	A	Pb-209	1.000E+00				8.376	-	-
Po-214	164.3 μ s	A	Pb-210	1.000E+00				7.687	<	<
Po-215	0.00178s	A	Pb-211	1.000E+00				7.386	<	<
Po-216	0.15s	A	Pb-212	1.000E+00				6.779	<	<
Po-218	3.05m	A B-	Pb-214	9.998E-01	At-218	2.000E-04		6.001	<	<
Astatine										
At-207	1.80h	ECA	Bi-203	1.000E-01	Po-207	9.000E-01		0.576	0.080	1.325
At-211	7.214h	ECA	Bi-207	4.170E-01	Po-211	5.830E-01		2.446	0.006	0.039
At-215	0.10ms	A	Bi-211	1.000E+00				8.026	<	<
At-216	0.30ms	A	Bi-212	1.000E+00				7.799	<	0.002
At-217	0.0323s	A	Bi-213	1.000E+00				7.067	<	<
At-218	2s	A	Bi-214	9.990E-01				6.697	0.040	0.007
Radon										
Rn-218	35ms	A	Po-214	1.000E+00				7.132	<	<
Rn-219	3.96s	A	Po-215	1.000E+00				6.757	0.006	0.056
Rn-220	55.6s	A	Po-216	1.000E+00				6.288	<	<
Rn-222	3.8235d	A	Po-218	1.000E+00				5.489	<	<
Francium										
Fr-219	21ms	A	At-215	1.000E+00				7.313	<	0.003
Fr-220	27.4s	A	At-216	1.000E+00				6.637	0.028	0.012
Fr-221	4.8m	A	At-217	1.000E+00				6.304	0.010	0.031
Fr-222	14.4m	B-	Ra-222	1.000E+00				-	0.731	-
Fr-223	21.8m	B-	Ra-223	9.999E-01				-	0.400	0.059
Radium										
Ra-222	38.0s	A	Rn-218	1.000E+00				6.546	<	0.009
Ra-223	11.434d	A	Rn-219	1.000E+00				5.667	0.076	0.134
Ra-224	3.66d	A	Rn-220	1.000E+00				5.674	0.002	0.010
Ra-225	14.8d	B-	Ac-225	1.000E+00				-	0.107	0.014
Ra-226	1600y	A	Rn-222	1.000E+00				4.774	0.004	0.007

Table G.1, continued

Nuclide	Decay $T_{1/2}$	Mode	Radioactive Decay Products and Fractional Yield						Energy (MeV nt ⁻¹)		
			Nuclide	Fraction	Nuclide	Fraction	Nuclide	Fraction	Alpha	Elect	Photon
Radium, continued											
Ra-227	42.2m	B-	Ac-227	1.000E+00					-	0.439	0.167
Ra-228	5.75y	B-	Ac-228	1.000E+00					-	0.017	<
Actinium											
Ac-223	2.2m	A	Fr-219	1.000E+00					6.553	0.015	0.006
Ac-224	2.9h	A EC	Fr-220	1.000E-01	Ra-224	9.000E-01			0.611	0.040	0.200
Ac-225	10.0d	A	Fr-221	1.000E+00					5.787	0.022	0.018
Ac-226	29h	A B-EC	Th-226	8.280E-01	Ra-226	1.720E-01	Fr-222	6.000E-05	<	0.289	0.130
Ac-227	21.773y	B-A	Fr-223	1.380E-02	Th-227	9.862E-01			0.068	0.016	<
Ac-228	6.13h	B-	Th-228	1.000E+00					-	0.475	0.971
Thorium											
Th-226	30.9m	A	Ra-222	1.000E+00					6.308	0.021	0.009
Th-227	18.718d	A	Ra-223	1.000E+00					5.884	0.053	0.110
Th-228	1.9131y	A	Ra-224	1.000E+00					5.400	0.021	0.003
Th-229	7340y	A	Ra-225	1.000E+00					4.873	0.116	0.096
Th-230	7.7E4y	A	Ra-226	1.000E+00					4.671	0.015	0.002
Th-231	25.52h	B-	Pa-231	1.000E+00					-	0.165	0.026
Th-232	1.405E10y	A	Ra-228	1.000E+00					3.996	0.012	0.001
Th-234	24.10d	B-	Pa-234m	9.980E-01	Pa-234	2.000E-03			-	0.060	0.009
Protactinium											
Pa-227	38.3m	ECA	Ac-223	8.500E-01	Th-227	1.500E-01			5.468	0.016	0.022
Pa-228	22h	A ECB+	Ac-224	2.000E-02	Th-228	9.800E-01			0.120	0.165	1.141
Pa-230	17.4d	A ECB-	U-230	9.500E-02	Th-230	9.050E-01	Ac-226	3.200E-05	<	0.068	0.652
Pa-231	3.276E4y	A	Ac-227	1.000E+00					4.969	0.065	0.048
Pa-232	1.31d	B-	U-232	1.000E+00					-	0.175	0.939
Pa-233	27.0d	B-	U-233	1.000E+00					-	0.196	0.204
Pa-234m	1.17m	B-IT	U-234	9.987E-01	Pa-234	1.300E-03			-	0.822	0.012
Pa-234	6.70h	B-	U-234	1.000E+00					-	0.494	1.919
Uranium											
U-230	20.8d	A	Th-226	1.000E+00					5.864	0.022	0.003
U-231	4.2d	ECA	Th-227	5.500E-05	Pa-231	1.000E+00			<	0.071	0.082
U-232	72y	A	Th-228	1.000E+00					5.302	0.017	0.002
U-233	1.585E5y	A	Th-229	1.000E+00					4.817	0.006	0.001
U-234	2.445E5y	A	Th-230	1.000E+00					4.758	0.013	0.002
U-235	703.8E6y	A	Th-231	1.000E+00					4.396	0.049	0.156
U-236	2.3415E7y	A	Th-232	1.000E+00					4.505	0.011	0.002
U-237	6.75d	B-	Np-237	1.000E+00					-	0.196	0.143
U-238	4.468E9y	SFA	Th-234	1.000E+00	SF	5.400E-05			4.187	0.010	0.001
U-239	23.54m	B-	Np-239	1.000E+00					-	0.412	0.053
U-240	14.1h	B-	Np-240m	1.000E+00					-	0.138	0.008
Neptunium											
Np-232	14.7m	ECB+	U-232	1.000E+00					-	0.106	1.203
Np-233	36.2m	EC	U-233	1.000E+00					-	0.014	0.091
Np-234	4.4d	ECB+	U-234	1.000E+00					-	0.069	1.442
Np-235	396.1d	ECA	Pa-231	1.400E-05	U-235	9.999E-01			<	0.010	0.007
Np-236a	115E3y	ECB-	Pu-236	8.900E-02	U-236	9.110E-01			-	0.208	0.136
Np-236b	22.5h	B-EC	Pu-236	4.800E-01	U-236	5.200E-01			-	0.087	0.051
Np-237	2.14E6y	A	Pa-233	1.000E+00					4.769	0.070	0.035
Np-238	2.117d	B-	Pu-238	1.000E+00					-	0.264	0.553
Np-239	2.355d	B-	Pu-239	1.000E+00					-	0.260	0.173

Table G.1, continued

Nuclide	Decay $T_{1/2}$	Mode	Radioactive Decay Products and Fractional Yield						Energy (MeV nt ⁻¹)		
			Nuclide	Fraction	Nuclide	Fraction	Nuclide	Fraction	Alpha	Elect	Photon
Neptunium, continued											
Np-240m	7.4m	B-	Pu-240	9.989E-01					-	0.683	0.337
Np-240	65m	B-	Pu-240	1.000E+00					-	0.528	1.313
Plutonium											
Pu-234	8.8h	A EC	U-230	6.000E-02	Np-234	9.400E-01			0.371	0.011	0.069
Pu-235	25.3m	ECA	U-231	2.700E-05	Np-235	1.000E+00			<	0.021	0.095
Pu-236	2.851y	SFA	U-232	1.000E+00	SF	8.100E-10			5.753	0.013	0.002
Pu-237	45.3d	A EC	U-233	5.000E-05	Np-237	1.000E+00			<	0.016	0.052
Pu-238	87.74y	SFA	U-234	1.000E+00	SF	1.840E-09			5.487	0.011	0.002
Pu-239	24065y	A	U-235	1.000E+00					5.148	0.007	<
Pu-240	6537y	SFA	U-236	1.000E+00	SF	4.950E-08			5.156	0.011	0.002
Pu-241	14.4y	A B-	U-237	2.450E-05	Am-241	1.000E+00			<	0.005	<
Pu-242	3.763E5y	SFA	U-238	1.000E+00	SF	5.500E-06			4.891	0.009	0.001
Pu-243	4.956h	B-	Am-243	1.000E+00					-	0.173	0.026
Pu-244	8.26E7y	SFA	U-240	1.000E+00	SF	1.250E-03			4.575	0.007	0.001
Pu-245	10.5h	B-	Am-245	1.000E+00					-	0.350	0.417
Pu-246	10.85d	B-	Am-246m	1.000E+00					-	0.125	0.140
Americium											
Am-237	73.0m	A EC	Np-233	2.500E-04	Pu-237	9.997E-01			0.002	0.077	0.370
Am-238	98m	ECA	Np-234	1.000E-06	Pu-238	1.000E+00			<	0.052	0.891
Am-239	11.9h	A EC	Np-235	1.000E-04	Pu-239	9.999E-01			<	0.168	0.239
Am-240	50.8h	A EC	Np-236b	1.900E-06	Pu-240	1.000E+00			<	0.075	1.029
Am-241	432.2y	A	Np-237	1.000E+00					5.479	0.052	0.033
Am-242m	152y	A IT	Np-238	4.800E-03	Am-242	9.952E-01			0.025	0.044	0.005
Am-242	16.02h	ECB-	Cm-242	8.270E-01	Pu-242	1.730E-01			-	0.179	0.018
Am-243	7380y	A	Np-239	1.000E+00					5.270	0.022	0.056
Am-244m	26m	B-	Cm-244	1.000E+00					-	0.509	0.002
Am-244	10.1h	B-	Cm-244	1.000E+00					-	0.342	0.807
Am-245	2.05h	B-	Cm-245	1.000E+00					-	0.288	0.032
Am-246m	25.0m	B-	Cm-246	1.000E+00					-	0.498	1.018
Am-246	39m	B-	Cm-246	1.000E+00					-	0.655	0.699
Curium											
Cm-238	2.4h	ECA	Pu-234	1.000E-01	Am-238	9.000E-01			0.652	0.010	0.077
Cm-240	27d	A	Pu-236	1.000E+00					6.247	0.011	0.002
Cm-241	32.8d	A EC	Pu-237	1.000E-02	Am-241	9.900E-01			0.059	0.133	0.502
Cm-242	162.8d	SFA	Pu-238	1.000E+00	SF	6.800E-08			6.102	0.010	0.002
Cm-243	28.5y	A EC	Pu-239	9.980E-01	Am-243	2.400E-03			5.797	0.138	0.134
Cm-244	18.11y	SFA	Pu-240	1.000E+00	SF	1.350E-06			5.795	0.009	0.002
Cm-245	8500y	A	Pu-241	1.000E+00					5.363	0.065	0.096
Cm-246	4730y	SFA	Pu-242	9.997E-01	SF	2.610E-04			5.376	0.008	0.002
Cm-247	1.56E7y	A	Pu-243	1.000E+00					4.949	0.021	0.316
Cm-248	3.39E5y	SFA	Pu-244	9.174E-01	SF	8.260E-02			4.651	0.006	0.001
Cm-249	64.15m	B-	Bk-249	1.000E+00					-	0.284	0.019
Cm-250	6900y	SFA B-	Pu-246	2.500E-01	Bk-250	1.400E-01	SF	6.100E-01	1.296	0.002	-
Berkelium											
Bk-245	4.94d	A EC	Am-241	1.200E-03	Cm-245	9.988E-01			0.007	0.133	0.234
Bk-246	1.83d	EC	Cm-246	1.000E+00					-	0.054	0.951
Bk-247	1380y	A	Am-243	1.000E+00					5.610	0.061	0.105
Bk-249	320d	SFB-A	Am-245	1.450E-05	Cf-249	1.000E+00	SF	4.700E-10	<	0.033	<
Bk-250	3.222h	B-	Cf-250	1.000E+00					-	0.293	0.887

Table G.1, continued

Nuclide	T _{1/2}	Decay Mode	Radioactive Decay Products and Fractional Yield						Energy (MeV nt ⁻¹)			
			Nuclide	Fraction	Nuclide	Fraction	Nuclide	Fraction	Alpha	Elect	Photon	
Californium												
Cf-244	19.4m	A	Cm-240	1.000E+00						7.200	0.009	0.002
Cf-246	35.7h	SFA	Cm-242	9.997E-01	SF	2.000E-06				6.747	0.006	0.001
Cf-248	333.5d	SFA	Cm-244	1.000E+00	SF	2.900E-05				6.253	0.006	0.001
Cf-249	350.6y	A SF	Cm-245	1.000E+00	SF	5.200E-09				5.831	0.044	0.335
Cf-250	13.08y	SFA	Cm-246	9.992E-01	SF	7.700E-04				6.019	0.006	0.001
Cf-251	898y	A	Cm-247	1.000E+00						5.784	0.198	0.132
Cf-252	2.638y	SFA	Cm-248	9.691E-01	SF	3.092E-02				5.922	0.006	0.001
Cf-253	17.81d	B-A	Cm-249	3.100E-03	Es-253	9.969E-01				0.019	0.079	<
Cf-254	60.5d	SFA	Cm-250	3.100E-03	SF	9.969E-01				0.018	<	<
Einsteinium												
Es-250	2.1h	EC	Cf-250	1.000E+00						-	0.022	0.397
Es-251	33h	ECA	Bk-247	5.000E-03	Cf-251	9.950E-01				0.032	0.052	0.098
Es-253	20.47d	SFA	Bk-249	1.000E+00	SF	8.700E-08				6.628	0.004	0.001
Es-254m	39.3h	A B-	Bk-250	3.200E-03	Fm-254	9.800E-01				0.020	0.256	0.470
Es-254	275.7d	A	Bk-250	1.000E+00						6.423	0.071	0.019
Fermium												
Fm-252	22.7h	A	Cf-248	1.000E+00						7.034	0.005	0.001
Fm-253	3.00d	ECA	Cf-249	1.200E-01	Es-253	8.800E-01				0.822	0.022	0.083
Fm-254	3.240h	A	Cf-250	1.000E+00						7.182	0.006	0.001
Fm-255	20.07h	A	Cf-251	1.000E+00						7.019	0.098	0.014
Fm-257	100.5d	A	Cf-253	9.979E-01						6.511	0.121	0.111
Mendelevium												
Md-257	5.2h	A EC	Es-253	1.000E-01	Fm-257	9.000E-01				0.707	0.015	0.114
Md-258	55d	A	Es-254	1.000E+00						7.232	0.047	0.006

GLOSSARY

Absolute risk hypothesis: The assumption that the excess risk from radiation exposure adds to the underlying (baseline) risk by an increment dependent on dose but independent of the underlying risk.

Absorbed dose (*D*): The microscopic quantity is the differential $d\bar{\epsilon}/dm$, where $d\bar{\epsilon}$ is the mean energy imparted by ionizing radiation to matter of mass dm . The macroscopic quantity used in internal dosimetry is tissue-averaged; that is, the absorbed dose to a tissue is the total energy absorbed by the tissue, divided by the mass of the tissue. The special name for the SI unit of absorbed dose (J kg^{-1}) is gray (Gy). The conventional unit of absorbed dose is the rad. $1 \text{ rad} = 0.01 \text{ Gy}$.

Absorption type: In the ICRP's respiratory tract model introduced in 1994, a classification scheme for inhaled material according to its rate of absorption from the deep lungs to blood. Three main absorption types are considered: Type F (fast rate), Type M (moderate rate), and Type S (slow rate).

Absorbed fraction (*AF*): The fraction of energy emitted as a specified radiation type in a specified source region that is absorbed in a specified target region.

Activity: The quantity of a radioactive nuclide present at a particular time, expressed in terms of the mean rate of nuclear transformations. The special name for the SI unit of activity (s^{-1}) is becquerel (Bq). The conventional unit of activity is the curie (Ci). $1 \text{ Ci} = 3.7 \times 10^{10} \text{ Bq}$.

Activity Median Aerodynamic Diameter (AMAD): The diameter of a unit density sphere with the same terminal settling velocity in air as that of an aerosol particle whose activity is the median for the entire aerosol.

Acute exposure: For purposes of computing risk coefficients, an instantaneous exposure. For practical applications of risk coefficients, any relatively short-term exposure period over which there are numerically trivial changes in the body mass, biokinetic parameters, usage functions, and mortality rates of all, or nearly all, members of the population.

Air kerma-rate constant: For a radionuclide emitting photons, the air kerma rate at 1 m in vacuum from a point source of the nuclide of unit activity. The unit is $\text{m}^2 \text{ Gy (Bq s)}^{-1}$.

Alpha particle: Two neutrons and two protons bound as a single particle (helium nucleus), emitted from the nucleus of certain radionuclides during nuclear transformations.

Baseline cancer rate: The observed cancer mortality (or morbidity) rate in a population in the absence of the specific radiation exposure being studied.

Becquerel (Bq): The special name for the SI unit of activity. $1 \text{ Bq} = 1 \text{ s}^{-1}$.

Beta particle: A particle having the charge and mass of an electron, emitted from the nucleus of certain radionuclides.

Biokinetic model: A mathematical description of the time-dependent distribution and translocation of a substance in the body.

Body Tissues (BT): The entire body, minus the contents of the gastrointestinal tract, the urinary bladder, the gall bladder, and the heart. Formerly called Whole Body (WB).

Bone Surface: The soft tissues within $10 \mu\text{m}$ of the endosteal (interior) surfaces of bone.

Bremsstrahlung: Electromagnetic radiation produced when deceleration of electrons in a medium results in conversion of a fraction of their initial kinetic energy into photons.

Chain members: The sequence of radionuclides formed by successive nuclear transformations, beginning with a radionuclide referred to as the parent.

Chronic exposure: In this report, protracted exposure to a constant concentration of a radionuclide in a given environmental medium.

Committed equivalent dose: The time integral of the equivalent dose rate.

Committed effective dose: Sometimes shortened to “effective dose”; the time integral of the effective dose rate.

Competing cause of death: Any cause of death other than radiogenic cancers attributed to the radionuclide intake or external radiation exposure under consideration.

Cortical bone, compact bone: Bone with a surface-to-volume ratio less than $60 \text{ cm}^2 \text{ cm}^{-3}$.

Curie (Ci): The conventional unit of activity. $1 \text{ Ci} = 3.7 \times 10^{10} \text{ Bq}$.

Daughter radionuclide: A radionuclide formed by the nuclear transformation of another radionuclide referred to, in this context, as its parent.

DCAL: Acronym for DOSE CALCULATION System, the software used to compute the risk coefficients tabulated in this document.

DDREF: A factor used to account for an apparent decrease of the risk of cancer per unit dose at low doses or low dose rates for most cancer sites compared with observations made at high, acutely delivered doses.

Dose coefficient, dose factor: The committed equivalent dose to a tissue, or the committed effective dose, per unit intake of a radionuclide.

DOE: U.S. Department of Energy.

Effective dose (E): The sum over specified tissues of the products of the equivalent dose in a tissue or organ (T) and the weighting factor for that tissue, w_T , that is, $E = \sum w_T H_T$. Lower-case e is used in ICRP documents to denote an effective dose coefficient, that is, effective dose per unit intake of a radionuclide at a given age. The special name for the SI unit of effective dose (J kg^{-1}) is sievert (Sv). The conventional unit of effective dose is the rem. $1 \text{ rem} = 0.01 \text{ Sv}$.

EPA: U.S. Environmental Protection Agency.

Equivalent dose (H): The product of the absorbed dose (D) and the radiation weighting factor (w_R). Lower-case h is used in ICRP documents to denote a dose coefficient, that is, a committed equivalent dose per unit intake of a radionuclide at a given age. The special name for the SI unit of equivalent dose (J kg^{-1}) is sievert (Sv). The conventional unit of equivalent dose is the rem. $1 \text{ rem} = 0.01 \text{ Sv}$.

External exposure: Exposure to radiations emitted by radionuclides outside the body.

f_I : The fraction of a radionuclide reaching the stomach that would be absorbed to blood during passage through the gastrointestinal tract without radiological decay.

Federal Guidance: Principles, policies, and numerical primary guides, approved by the President upon recommendation of the Administrator of EPA, for use by Federal agencies as the basis for developing and implementing regulatory standards.

Force of mortality: The age- and gender-specific mortality (or hazard) rate coefficient, μ (y^{-1}), for a cause of death. The probability that an individual alive at age x will die of that cause before attaining age $x + dx$ is equal to μdx .

FRC: The former U.S. Federal Radiation Council, whose functions now reside with the Administrator of EPA.

Gamma radiation, gamma rays: Short wavelength electromagnetic radiation of nuclear origin, similar to x rays but usually of higher energy.

Gastrointestinal tract model: A model of the translocation of swallowed material through the stomach and intestines.

Gray (Gy): The special name for the SI unit of absorbed dose. $1 \text{ Gy} = 1 \text{ J kg}^{-1}$.

Half-time, biological: Time required for the quantity of a radionuclide in a compartment representing all or a portion of the body to diminish by 50% without radiological decay or any additional input to the compartment.

Half-life, radioactive: Time required for a radionuclide to lose 50% of its activity by spontaneous nuclear transformations (radiological decay).

HTO: Tritiated water.

ICRP: International Commission on Radiological Protection.

Independent kinetics of decay chain members: The assumption that each decay chain member produced in the body may have biokinetic behavior that is different from that of the radionuclide taken into the body.

Internal exposure: Exposure to radiations emitted by radionuclides distributed within the body.

Ionizing radiation: Any radiation capable of removing electrons from atoms or molecules, thereby producing ions.

***In utero* exposure:** Radiation exposure received in the womb, that is, before birth.

***In vivo*:** In the living organism.

I-S: Inorganic sulfur.

Isotopes: Nuclides that have the same number of protons in their nuclei and hence the same atomic number but differ in the number of neutrons and therefore in mass number.

Kerma: The kinetic energy transferred to charged particles per unit mass of irradiated medium when indirectly ionizing (uncharged) particles such as photons or neutrons traverse the medium. The special name for the SI unit of kerma (J kg^{-1}) is gray (Gy).

LET: Average amount of energy lost per unit track length of an ionizing charged particle. *Low LET* refers to radiation characteristic of light charged particles such as electrons produced by x rays and gamma rays where the distance between ionizing events is large on the scale of a cellular nucleus. *High LET* refers to radiation characteristic of heavy charged particles such as protons and alpha particles where the distance between ionizing events is small on the scale of a cellular nucleus.

Lethality fraction: The fraction of radiogenic cancers of a given type that are fatal.

Life Table: A table showing the number of persons who, for a given number of live born, survive to successively higher ages.

Lifetime risk coefficient (LRC): The risk per unit dose of a subsequent cancer death due to radiation received at a given age.

Linear model, Linear dose-effect relationship: A model describing a radiogenic effect as a linear function of dose.

Linear-quadratic model, Linear-quadratic dose-effect relationship: A model describing a radiogenic effect as a quadratic function of dose, D (that is, as $a \cdot D + b \cdot D^2$, where a and b are constants).

Low dose rate: In this report, an hourly averaged absorbed dose rate less than 0.1 mGy min^{-1} .

Low dose: In this report, an acute absorbed dose less than 0.2 Gy .

Minimal latency period: The minimal time following a radiation dose before expression of a radiogenic cancer.

Mortality rate: The age- and gender-specific or total rate at which people die from a specified cause of death, or all causes combined.

MIRD: Medical Internal Radiation Dose; a committee of the Society of Nuclear Medicine.

Morbidity: The age- and gender-specific or total incidence of a specified disease in the population.

Multiplicative transport model: The assumption that the excess relative risk coefficient for a radiogenic cancer is the same across populations.

NCHS: U.S. National Center for Health Statistics.

NCRP: U.S. National Council on Radiation Protection and Measurements.

Neutron: Uncharged subatomic particle capable of producing ionization in matter by collision with protons and through nuclear reactions.

NHANES III: A national dietary, health, and nutrition survey conducted by the National Center for Health Statistics (NCHS) during the period 1988-1994.

NIH: U. S. National Institutes of Health.

NIH transport model: The assumption that the relative risk model coefficients for the target population should yield the same risks as those calculated with the additive risk model coefficients from the original population over the period of epidemiological follow-up, excluding the minimal latency period.

Nominal uncertainty: A lower bound on the uncertainty in a given quantity, based on consideration of selected sources of uncertainty. As applied in this document to the uncertainty associated with a risk coefficient, the term “nominal” reflects the fact that the statement of uncertainty is based on an idealized population and exposure scenario and does not include the uncertainty associated with the assumption that the probability of inducing a radiogenic cancer is proportional to absorbed dose.

NRC: U.S. Nuclear Regulatory Commission.

Nuclear transformation: The spontaneous transformation of one radionuclide into a different nuclide or into a different energy state of the same nuclide.

OBT: Organically bound tritium.

OBS: Organically bound sulfur.

Other: In internal radiation dosimetry, an implicit source region, defined as the complement of the set of explicitly identified regions, that is, *Body Tissues* minus the explicit source organs identified in the biokinetic model.

Parent radionuclide: The first member of a chain of radionuclides. In an internal exposure scenario, the radionuclide assumed to be taken into the body.

Per capita: Averaged over the population.

Phantom: A mathematical model of the human body, used in radiation dosimetry to derive specific absorbed fractions for penetrating radiations.

Plateau period: The time period following a radiation dose during which radiogenic cancers are likely to occur.

Probability coefficient (for radiological risk): A multiplicative factor used to convert a measure of cumulative dose to a probability of a detrimental effect of radiation. As used by the ICRP, an estimate of the radiation risk per unit effective dose. A probability coefficient is generally based on an idealized population receiving a uniform dose over the whole body.

Rad: The conventional unit for absorbed dose of ionizing radiation. 1 rad = 0.01 Gy.

Radiation risk model: A mathematical model used to estimate the probability of experiencing a radiogenic cancer as a function of time after a radiation dose is received.

Radiation weighting factor (w_R): The principal modifying factor employed in deriving equivalent dose, H , from absorbed dose, D ; chosen to account for the relative biological effectiveness (RBE) of the radiation in question, but to be independent of the tissue or organ under consideration, and of the biological endpoint.

Radioisotope: A radioactive atomic species of an element with the same atomic number and usually identical chemical properties.

Radionuclide: A radioactive species of atom characterized by the number of protons and neutrons in its nucleus.

RBE: The relative biological effectiveness of a given type of radiation in producing a specified biological effect, compared with 200-kV x rays.

Reference Man: A hypothetical average adult person with the anatomical and physiological characteristics defined in the report of the ICRP Task Group on Reference Man (ICRP Publication 23).

Relative risk hypothesis: The assumption that the age-specific force of mortality or morbidity due to a radiation dose is the product of an exposure-age-specific excess relative risk coefficient and the corresponding baseline cancer mortality or morbidity rate.

Rem: The conventional unit of equivalent dose. $1 \text{ rem} = 0.01 \text{ Sv}$.

RERF: Radiation Effects Research Foundation; a bi-nationally funded Japanese foundation chartered by the Japanese Welfare Ministry under an agreement between the U.S. and Japan.

Residual cancers: A composite of all primary and secondary cancers not explicitly identified in a radiogenic risk model.

Respiratory tract model: A model of the deposition, retention, and translocation of particles in the respiratory tract.

Risk model coefficient: An age- and gender-specific multiplicative factor appearing in a radiogenic risk model and indicating the magnitude of the risk of dying from or experiencing a given type of cancer at any given time after the dose is received.

Risk coefficient: For a given radionuclide, environmental medium, and mode of exposure, the estimated probability of radiogenic cancer mortality or morbidity, per unit activity intake for internal exposures or per unit exposure for external exposures.

SEECAL: A computer code used to calculate age-dependent specific energies based on standard nuclear decay data files, libraries of specific absorbed fractions for photons and non-penetrating radiations, and organ masses of reference humans of different ages.

Shared kinetics of decay chain members: The assumption that decay chain members produced in the body have the same biokinetic behavior as the radionuclide taken into the body.

Shielding: Material between a radiation source and a potentially exposed person that reduces the radiation field incident on the exposed person.

Short-lived radionuclide: In this report, a radionuclide having a half-life less than 1 h.

Sievert (Sv): The special name for the SI unit of equivalent dose. $1 \text{ Sv} = 1 \text{ J kg}^{-1}$.

Soft Tissues: Body Tissues minus cortical and trabecular bone.

Source organ, source region, source tissue (S): Any tissue or organ of the body, or the contents of any organ, which contains a sufficient amount of a radionuclide to irradiate a target tissue (T) significantly.

Specific energy $SE(T-S)_R$: The energy per unit mass of target tissue (T), deposited in that tissue as a consequence of the emission of a specified radiation (R) per nuclear transformation of a specified radionuclide occurring in a source tissue (S).

Stationary population, Steady-state population: A hypothetical closed population whose gender-specific birth rates and survival functions remain invariant over time.

Submersion: External exposure to a radionuclide uniformly distributed in the air surrounding the exposed person.

Surface-seeking radionuclides: Radionuclides that deposit on and remain for a considerable period on the surface of bone structure.

Survival function: The fraction $S(x)$ of live-born individuals in an unexposed population expected to survive to age x .

Systemic biokinetic model: A model describing the distribution and translocation of a substance after its absorption or injection into the systemic circulation.

Tap water: Drinking water, water added to beverages, and water added to foods during preparation but not including water intrinsic in food as purchased.

Target organ, target region, target tissue (T): Any tissue or organ of the body in which radiation is absorbed.

Threshold hypothesis: The assumption that no radiation injury occurs below a specified dose.

Time-since-exposure (TSE) function: A function that defines the period during which radiogenic risk is expressed and any changes in the level of response during that period.

Tissue (organ) weighting factor (w_T): A factor indicating the relative level of risk of cancer induction or heredity defects from irradiation of a given tissue or organ; used in calculation of effective dose and committed effective dose.

Trabecular bone, cancellous bone: Bone with a surface-to-volume ratio greater than $60 \text{ cm}^2 \text{ cm}^{-3}$.

Transportation of risk estimates: Extrapolation of radiogenic dose-response data from one population to another.

Transfer coefficient: In the context of a compartmental model, fractional flow per unit time from one compartment to another.

Time-since-response function: A function describing the likely pattern of response as a function of time after irradiation of a large population.

Usage rate: The age- and gender-specific average intake rate of a specified environmental medium (air, food energy, tap water, or milk).

Volume-seeking radionuclides: Radionuclides that enter bone and exchange with bone mineral over the entire mass of bone.

Volume source: Relative to a given biokinetic model, a source region that has non-zero volume.

x radiation, x rays: Penetrating electromagnetic radiation, usually produced by bombarding a metallic target with fast electrons in a high vacuum, or emitted during rearrangement of the electrons about the nucleus following nuclear transformation of a radionuclide.

REFERENCES

- H. Beck and G. de Planque (1968). *The Radiation Field in Air Due to Distributed Gamma-Ray Sources in the Ground*, HASL-195 (Health and Safety Laboratory, NY).
- F. C. Bell, A. H. Wade, and S. C. Goss (1992). *Life Tables for the United States Social Security Area 1900-2080, Actuarial Study No.107*, SSA Pub. No. 11-11536 (U.S. Department of Health and Human Services, Social Security Administration, Office of the Actuary, Room 700, Altmeyer Bldg., Baltimore, MD 21235).
- J. D. Boice, Jr., G. Engholm, R. A. Kleinerman, M. Blettner, M. Stovall, H. Lisco, W. C. Moloney, D. F. Austin, A. Bosch, D. L. Cookfair, E. T. Krentz, H. B. Latourette, J. A. Merrill, L. J. Peters, M. D. Schulz, H. H. Storm, E. Bjorkholm, F. Pettersson, C. M. J. Bell, M. P. Coleman, P. Fraser, F. E. Neal, P. Prior, N. W. Choi, T. G. Hislop, M. Koch, N. Kreiger, D. Robb, D. Tobson, D. H. Thomson, H. Lochmuller, D. V. Fournier, R. Frischkorn, K. E. Kjorstad, A. Rimpela, M. H. Pejovic, V. P. Kim, H. Stankusova, F. Berrino, K. Soigurdsson, G. B. Hutchison, and B. MacMahon (1988). "Radiation dose and second cancer risk in patients treated for cancer of the cervix", *Radiat. Res.* 116, 3-55.
- Z. G. Burson and A. E. Profio (1977). "Structure Shielding in Reactor Accidents", *Health Phys.* 33, 287-299.
- CIRRPC (1992). Committee on Interagency Radiation Research and Policy Coordination; Office of Science and Technology Policy, "Use of BEIR V and UNSCEAR 1988 in Radiation Risk Assessment", (Available as ORAU 92/F-64 through NTIS, Springfield, VA 22161).
- M. Cristy and K. F. Eckerman (1987). *Specific Absorbed Fractions of Energy at Various Ages from Internal Photon Sources*, ORNL/TM-8381/V1-7 (Oak Ridge National Laboratory, Oak Ridge, TN).
- M. Cristy and K. F. Eckerman (1993). *SEECAL: Program to Calculate Age-Dependent Specific Effective Energies*, ORNL/TM-12351 (Oak Ridge National Laboratory, Oak Ridge, TN).

H. S. Dang, D. D. Jaiswal, K. B. S. Murthy, R. C. Sharma, P. P. V. J. Nambiar, and C. M. Sunta (1992). “Relevance of ICRP Metabolic Model of Thorium in Bio-Assay Monitoring”, *J. Radioanal. Nucl. Chem. Articles* 156, 55-64.

L. T. Dillman (1980). *EDISTR—A Computer Program to Obtain a Nuclear Decay Data Base for Radiation Dosimetry*. ORNL/TM-6689 (Oak Ridge National Laboratory, Oak Ridge, TN).

G. Drexler, H. Eckerl, and M. Zankl (1989). “On the Influence of the Exposure Model on Organ Doses”, *Radiat. Prot. Dosim.* 28, 181-191.

D. E. Dunning and G. Schwarz (1981). “Variability of human thyroid characteristics and estimates of dose from ingested ^{131}I ”, *Health Phys.* 40, 661-675.

P. W. Durbin (1960). “Metabolic Characteristics Within a Chemical Family”, *Health Phys.* 2, 225-238.

K. F. Eckerman, R. W. Leggett, and M. Cristy (1999). *User Guide to the DCAL System*. ORNL/TM report. To be published.

K. F. Eckerman, R. J. Westfall, J. C. Ryman, and M. Cristy (1994). “Availability of Nuclear Decay Data in Electronic Form, Including Beta Spectra Not Previously Published”, *Health Phys.* 67, 338-345.

EPA (1984a). *The Radioactivity Concentration Guides*, Federal Guidance Report No. 10, EPA 520/1-84-005 (Oak Ridge National Laboratory, Oak Ridge, TN; U. S. Environmental Protection Agency, Washington, DC).

EPA (1984b). *An Estimation of the Daily Average Food Intake by Age and Sex for Use in Assessing the Radionuclide Intake of Individuals in the General Population*, EPA 520/1-84-021 (U. S. Environmental Protection Agency, Washington, DC).

EPA (1987). U.S. Environmental Protection Agency, “Radiation Protection Guidance to Federal Agencies for Occupational Exposure; Approval of Environmental Protection Agency

Recommendations”, in the *Federal Register* 52, 2822-2834, Tuesday, January 27, 1987 (Office of the Federal Register, National Archives and Record Administration, Washington, DC 20408). [Corrections published in the *Federal Register* of Friday, January 30 and Wednesday, February 4, 1987.]

EPA (1988). *Limiting Values of Radionuclide Intake and Air Concentration and Dose Conversion Factors for Inhalation, Submersion, and Ingestion*, Federal Guidance Report No. 11, EPA-520/1-88-020 (Oak Ridge National Laboratory, Oak Ridge, TN; U. S. Environmental Protection Agency, Washington, DC).

EPA (1991). “Final Draft for the Drinking Water Criteria Document on Radium”, NTIS: PB 91225631 (Prepared by Life Systems, Inc., for the Environmental Protection Agency, Washington, DC).

EPA (1993). *External Exposure to Radionuclides in Air, Water, and Soil*, Federal Guidance Report No. 12, EPA-402-R-93-081 (Oak Ridge National Laboratory, Oak Ridge, TN; U. S. Environmental Protection Agency, Washington, DC).

EPA (1994). *Estimating Radiogenic Cancer Risks*, EPA 402-R-93-076 (U. S. Environmental Protection Agency, Washington, DC).

EPA (1998). *Health Risks from Low-Level Environmental Exposure to Radionuclides*, Federal Guidance Report No. 13 — Part 1, Interim Version, EPA-402/R-97-014 (Oak Ridge National Laboratory, Oak Ridge, TN; U. S. Environmental Protection Agency, Washington, DC).

EPA (1999). *Estimating Radiogenic Cancer Risks, Addendum: Uncertainty Analysis*, EPA 402-R-99-003 (U. S. Environmental Protection Agency, Washington, DC).

A. G. Ershow and K. P. Cantor (1989). *Total Water and Tap water Intake in the United States: Population-Based Estimates of Quantities and Sources*, Order No. 263-MD-810264 (National Cancer Institute, Bethesda, MD).

W. B. Ewbank and M. R. Schmorak (1978). *Evaluated Nuclear Structure Data File. A Manual for Preparation of Data Sets*, ORNL-5054/R1 (Oak Ridge National Laboratory, Oak Ridge, TN).

C. W. Garrett (1968). “Shielding Benchmark Problem No. 4.0. Gamma-Ray Dose above a Plane Source of ^{60}Co on an Air/Ground Interface”, *Shielding Benchmark Problems* (A. E. Profio, ed.), ORNL-RSIC-25 (Oak Ridge National Laboratory, Oak Ridge, TN).

M. Goldman (1996). “Cancer Risk at Low-level Exposure”, *Science* 271, 1821-1822.

D. T. Goodhead (1982). “An Assessment of the Role of Microdosimetry in Radiobiology”, *Radiat. Res.* 91, 45-76.

F. N. Fritsch and R. E. Carlson (1980). “Monotone Piecewise Cubic Interpolation”, *SIAM J. Numer. Anal.* 17, 238-246.

G. R. Howe (1995). “Lung Cancer Mortality between 1950 and 1987 after Exposure to Fractionated Moderate-Dose-Rate Ionizing Radiation in the Canadian Fluoroscopy Cohort Study and a Comparison with Lung Cancer Mortality in the Atomic Bomb Survivors Study”, *Radiat. Res.* 142, 295-304.

S. A. Ibrahim, M. E. Wrenn, N. P. Singh, N. Cohen, and G. Saccomanno (1983). “Thorium Concentration in Human Tissues from Two U.S. Populations”, *Health Phys.* 44, Suppl. 1, 213-220.

ICRP (1975). International Commission on Radiological Protection, “Report of the Task Group on Reference Man”, ICRP Publication 23 (Pergamon Press, Oxford).

ICRP (1979). International Commission on Radiological Protection, “Limits for Intakes by Workers”, ICRP Publication 30, Part 1 (Pergamon Press, Oxford).

ICRP (1980). International Commission on Radiological Protection, “Limits for Intakes by Workers”, ICRP Publication 30, Part 2 (Pergamon Press, Oxford).

ICRP (1981). International Commission on Radiological Protection, “Limits for Intakes by Workers”, ICRP Publication 30, Part 3 (Pergamon Press, Oxford).

ICRP (1983). International Commission on Radiological Protection, “Radionuclide Transformations Energy and Intensity of Emissions”, ICRP Publication 38 (Pergamon Press, Oxford).

ICRP (1988). International Commission on Radiological Protection, "Limits for Intakes by Workers: An Addendum", ICRP Publication 30, Part 4 (Pergamon Press, Oxford).

ICRP (1989). International Commission on Radiological Protection, "Age-Dependent Doses to Members of the Public from Intake of Radionuclides, Part 1", ICRP Publication 56 (Pergamon Press, Oxford).

ICRP (1991). International Commission on Radiological Protection, "1990 Recommendations of the International Commission on Radiological Protection", ICRP Publication 60 (Pergamon Press, Oxford).

ICRP (1992). International Commission on Radiological Protection, "The Biological Basis for Dose Limitation in the Skin", ICRP Publication 59 (Pergamon Press, Oxford).

ICRP (1993). International Commission on Radiological Protection, "Age-Dependent Doses to Members of the Public from Intake of Radionuclides, Part 2", ICRP Publication 67 (Pergamon Press, Oxford).

ICRP (1994a). International Commission on Radiological Protection, "Human Respiratory Tract Model for Radiological Protection", ICRP Publication 66 (Pergamon Press, Oxford).

ICRP (1994b). International Commission on Radiological Protection, "Dose Coefficients for Intakes of Radionuclides by Workers", ICRP Publication 68 (Pergamon Press, Oxford).

ICRP (1995a). International Commission on Radiological Protection, "Age-Dependent Doses to Members of the Public from Intake of Radionuclides, Part 3", ICRP Publication 69 (Pergamon Press, Oxford).

ICRP (1995b). International Commission on Radiological Protection, "Age-Dependent Doses to Members of the Public from Intake of Radionuclides, Part 4", ICRP Publication 71 (Pergamon Press, Oxford).

ICRP (1995c). International Commission on Radiological Protection, "Basic Anatomical and Physiological Data for Use in Radiological Protection: The Skeleton", ICRP Publication 70 (Pergamon Press, Oxford).

ICRP (1996). International Commission on Radiological Protection, "Age-Dependent Doses to Members of the Public from Intake of Radionuclides, Part 5. Compilation of Ingestion and Inhalation Dose Coefficients", ICRP Publication 72 (Pergamon Press, Oxford).

S. Jablon (1971). "Atomic Bomb Radiation Dose at ABCC,," TR 23-71 (Atomic Bomb Casualty Commission, Hiroshima).

Z. Jaworowski (1995). "Stimulating Effects of Ionizing Radiation: New Issue for Regulatory Policy", *Regul. Toxicol. and Pharmacol.* 22, 172-179.

A. M. Kellerer and H. M. Rossi (1972). "The Theory of Dual Radiation Action", *Curr. Top. Radiat. Res. Quart.* 8, 85-158.

D. C. Kocher (1980). "Effects of Indoor Residence on Radiation Doses from Routine Releases of Radionuclides to the Atmosphere", *Nucl. Technol.* 48, 171-181.

C. E. Land and W. K. Sinclair (1991). "The Relative Contributions of Different Organ Sites to the Total Cancer Mortality Associated with Low-Dose Radiation Exposure", pp. 31-57 of *Risks Associated with Ionising Radiations*", *Annals of the ICRP* 22, No. 1 (Pergamon Press, Oxford).

D. W. Layton (1993). "Metabolically Consistent Breathing Rates for Use in Dose Assessments", *Health Phys.* 64, 23-36.

R. W. Leggett (1992a). "A Generic Age-Specific Biokinetic Model for Calcium-Like Elements", *Radiat. Prot. Dosim.* 41, 183-198.

R. W. Leggett (1992b). "A Retention-Excretion Model for Americium in Humans", *Health Phys.* 62, 288-310.

R. W. Leggett (1997). "Basis and implications of the ICRP's new biokinetic model for thorium", *Health Phys.* 73, 587-600.

R. W. Leggett (1994). "Basis for the ICRP's age-specific biokinetic model for uranium", *Health Phys.* 67, 589-610.

R. W. Leggett, A. Bouville, and K. F. Eckerman (1998). “Reliability of the ICRP’s Systemic Biokinetic Models”, *Radiat. Prot. Dosim.* 79, 335-342.

R. W. Leggett, D. E. Dunning, Jr., and K. F. Eckerman (1984). “Modelling the Behaviour of Chains of Radionuclides Inside the Body”, *Radiat. Prot. Dosim.* 9, 77-91.

R. W. Leggett, K. F. Eckerman, and L. R. Williams (1993). “An Elementary Method for Implementing Complex Biokinetic Models”, *Health Phys.* 64, 260-278.

M. P. Little, M. M. Hawkins, R. E. Shore, M. W. Charles, and N. G. Hildreth (1991). “Time Variations in the Risk of Cancer Following Irradiation in Childhood”, *Radiat. Res.* 126, 304-316.

R. C. Loehr and O. E. Nygaard (1992). “Evaluation of EPA's Proposed Methodology for Estimating Radiogenic Cancer Risks”, Letter to William K. Reilly, EPA Administrator.

R. Loevinger, T. F. Budinger, and E. E. Watson (1988). *MIRD Primer for Absorbed Dose Calculations* (Society of Nuclear Medicine, New York, NY).

T. D. Luckey (1990). *Radiation Hormesis* (CRC Press, Boca Raton, FL).

C. J. Maletskos, A. T. Keane, N. C. Telles, and R. D. Evans (1966). “The Metabolism of Intravenously Administered Radium and Thorium in Human Beings and the Relative Absorption from the Human Gastrointestinal Tract of Radium and Thorium in Simulated Radium Dial Paints”, pp. 202-317 of *Radium and Mesothorium Poisoning and Dosimetry and Instrumentation Techniques in Applied Radioactivity*, MIT-952-3 (Massachusetts Institute of Technology, Cambridge, MA).

C. J. Maletskos, A. T. Keane, N. C. Telles, and R. D. Evans (1969). “Retention and Absorption of ^{224}Ra and ^{234}Th and Some Dosimetric Considerations of ^{224}Ra in Human Beings.” pp. 29-49 of *Delayed Effects of Bone-Seeking Radionuclides* (C. W. Mays; W. S. S. Jee; R. D. Lloyd; B. J. Stover; J. H. Dougherty; G. N. Taylor, eds.) (University of Utah Press, Salt Lake City, UT).

M. A. McDowell, R. D. Briefel, K. Alaimo, A. M. Bischof, C. R. Caughman, M. D. Carroll, C. M. Loria, and C. L. Johnson (1994). *Energy and Macronutrient Intakes of Persons Ages 2 Months and Over in the United States: Third National Health and Nutrition Examination Survey, Phase 1, 1989-91*, Advance Data 255 (U. S. Dept. of Health and Human Services).

NAS (1980). *The Effects on Populations of Exposure to Low Levels of Ionizing Radiation (BEIR III)* (National Academy of Sciences, National Academy Press, Washington, DC).

NAS (1988). *Health Risks of Radon and Other Internally Deposited Alpha-Emitters (BEIR IV)* (National Academy of Sciences, National Academy Press, Washington, DC).

NAS (1990). *Health Effects of Exposure to Low Levels of Ionizing Radiation (BEIR V)* (National Academy of Sciences, National Academy Press, Washington, DC).

NCHS (1992). *Vital Statistics Mortality Data, Detail, 1989*, NTIS order number for datafile tapes: PB92-504554 (U. S. Department of Health and Human Services, Public Health Service, National Center for Health Statistics, Hyattsville, MD).

NCHS (1993a). *Vital Statistics Mortality Data, Detail, 1990*, NTIS order number for datafile tapes: PB93-504777 (U. S. Department of Health and Human Services, Public Health Service, National Center for Health Statistics, Hyattsville, MD).

NCHS (1993b). *Vital Statistics Mortality Data, Detail, 1991*, NTIS order number for datafile tapes: PB93-506889 (U. S. Department of Health and Human Services, Public Health Service, National Center for Health Statistics, Hyattsville, MD).

NCHS (1997). *U. S. Decennial Life Tables for 1989-91*, Vol. 1, No. 1. DHHS, PHS-98-1150-1 (National Center for Health Statistics: United States Life Tables. Public Health Service, Washington, DC). October, 1997.

NCRP (1980). *Influence of Dose and Its Distribution in Time on Dose-Response Relationships for Low-LET Radiations*, NCRP Report 64 (National Council on Radiation Protection and Measurements, Bethesda, MD).

NCRP (1985). *Induction of Thyroid Cancer by Ionizing Radiation*, NCRP Report 80 (National Council on Radiation Protection and Measurements, Bethesda, MD).

NCRP (1990). *The Relative Biological Effectiveness of Radiations of Different Quality*, NCRP Report No. 104 (National Council on Radiation Protection and Measurements, Bethesda, MD).

NCRP (1993). *Risk Estimates for Radiation Protection*, NCRP Report No. 115 (National Council on Radiation Protection and Measurements, Bethesda, MD).

NCRP (1997). *Uncertainties in Fatal Cancer Risk Estimates Used in Radiation Protection*, NCRP Report No. 126 (National Council on Radiation Protection and Measurements, Bethesda, MD).

NCRP (1998). *Evaluating the Reliability of Biokinetic and Dosimetric Models and Parameters Used to Assess Individual Doses for Risk Assessment Purposes*, NCRP Commentary No. 15 (National Council on Radiation Protection and Measurements, Bethesda, MD).

D. Newton and D. A. Brown (1974). "The Long-Term Retention of Systemic Protactinium-231 and Actinium-227", *Health Phys.* 27, 459-467.

D. Newton, J. Rundo, and J. D. Eakins (1981). "Long-Term Retention of ²²⁸Th Following Accidental Intake", *Health Phys.* 40, 291-298.

NRC (1977). "*Regulatory Guide 1.109, Calculation of Annual Doses to Man from Routine Releases of Reactor Effluents for the Purpose of Evaluating Compliance with 10 CFR Part 50, Appendix I* (U. S. Nuclear Regulatory Commission, Washington, DC).

NRC (1991). "Chapter 3: Late Somatic Effects", In: S. Abrahamson, M. A. Bender, B. B. Boecker, E. S. Gilbert, and B. R. Scott. *Health Effects Models for Nuclear Power Plant Accident Consequence Analysis. Modifications of Models Resulting from Recent Reports on Health Effects of Ionizing Radiation, Low LET Radiation, Part II: Scientific Bases for Health Effects Models*, NUREG/CR-4214, Rev. 1, Part II, Addendum 1, LMF-132, (U. S. Nuclear Regulatory Commission, Washington, DC).

NRC (1993). "Chapter 3: Late Somatic Effects." In: S. Abrahamson, M. A. Bender, B. B. Boecker, E. S. Gilbert, and B. R. Scott. *Health Effects Models for Nuclear Power Plant Accident Consequence Analysis. Modification of Models Resulting from Addition of Effects of Exposure to Alpha-Emitting Radionuclides, Part II: Scientific Bases for Health Effects Models*, NUREG/CR-4214, Rev. 1, Part II, Addendum 2, LMF-136, (U. S. Nuclear Regulatory Commission, Washington, DC).

NRC-CEC (1997). *Probabilistic Accident Consequence Uncertainty Analysis. Late Health Effects Uncertainty Assessment*, NUREG/CR-6555; EUR 16774; SAND97-2322 (U.S. Nuclear Regulatory Commission, Washington, DC; Office for Publications of the European Communities, Luxembourg).

NRC-CEC (1998). *Probabilistic Accident Consequence Uncertainty Analysis. Uncertainty Assessment for Internal Dosimetry*, NUREG/CR-6571; EUR 16773; SAND98-0119 (U.S. Nuclear Regulatory Commission, Washington, DC; Office for Publications of the European Communities, Luxembourg).

NRPB (1993). National Radiological Protection Board. Estimates of Late Radiation Risks to the UK Population, *Documents of the NRPB* 4(4), (National Radiological Protection Board, Chilton, Didcot, UK).

N. Petoussi, P. Jacob, M. Zankl, and K. Saito (1991). "Organ Doses for Foetuses, Babies, Children and Adults from Environmental Gamma Rays", *Radiat. Protect. Dosim.* 37, 31-41.

D. A. Pierce, D. O. Stram, and M. Vaeth (1990). "Allowing for Random Errors in Radiation Exposure Estimates for the Atomic Bomb Survivor Data", *Radiat. Res.* 123, 275-284.

D. A. Pierce and M. Vaeth (1991). "The Shape of the Cancer Mortality Dose-response Curve for the A-bomb Survivors", *Radiat. Res.* 126, 36-42.

D. A. Pierce Y. Shimizu, D. L. Preston, M. Vaeth, and K. Mabuchi (1996). "Studies of the Mortality of Atomic Bomb Survivors, Report 12, Part I. Cancer: 1950-1990", *Radiat. Res.* 146, 1-27.

J. W. Poston, Jr., K.A. Kodimer, W.E. Bolch, and J.W. Poston, Sr. (1996a). "Calculation of Absorbed Energy in the Gastrointestinal Tract", *Health Phys.* 71, 300-306.

J. W. Poston, Jr., K.A. Kodimer, W.E. Bolch, and J.W. Poston, Sr. (1996b). "A Revised Model for the Calculation of Absorbed Energy in the Gastrointestinal Tract", *Health Phys.* 71, 307-314.

D.L. Preston, D. Pierce, and M. Vaeth (1993). "Neutrons and Radiation Risk: a Commentary", *RERF Update* 4, 5.

J. S. Puskin (1997). "Are Low Doses of Radiation Protective?", pp. 211-213 of *Health Effects of Low Dose Radiation. Challenges of the 21st Century*, (British Nuclear Energy Society, London).

J. S. Puskin, N. S. Nelson, and C. B. Nelson (1992). "Bone Cancer Risk Estimates", *Health Phys.* 63, 579-580.

L. G. Ralston, N. Cohen, M. H. Bhattacharyya, R. P. Larsen, L. Ayres, R. D. Oldham, and E. S. Moretti (1985). "The Metabolism and Gastrointestinal Absorption of Neptunium and Protactinium in Adult Baboons", *Speciation of Fission and Activation Products in the Environment* (R. A. Bulman and J. R. Cooper, eds.), (Elsevier Applied Science Publishers, London).

J. Rundo (1964). "Two Cases of Chronic Occupational Exposure to Radioactive Materials", pp. 291-306 of *Assessment of Radioactivity in Man, Vol. II* (IAEA, Vienna).

K. Saito, N. Petoussi-Henss, and M. Zankel (1998). "Calculation of the Effective Dose and its Variation from Environmental Gamma Ray Sources", *Health Phys.* 74(6), 698-706.

Y. Shimizu, H. Kato, W. J. Schull, D. L. Preston, S. Fujita, and D. A. Pierce (1989). "Studies of the Mortality of A-Bomb Survivors: 9. Mortality, 1950-1985: Comparison of Risk Coefficients for Site-Specific Cancer Mortality Based on the DS86 and T65DR Shielded Kerma and Organ Doses", *Radiat. Res.* 118, 502-524.

Y. Shimizu, H. Kato, and W. J. Schull (1990). "Studies of the Mortality of A-Bomb Survivors: 9. Mortality, 1950-1985: Part 2. Cancer Mortality Based on the Revised Doses (DS86)", *Radiat. Res.* 121, 120-141.

N. P. Singh, M. E. Wrenn, and S. A. Ibrahim (1983). "Plutonium Concentration in Human Tissues: Comparison to Thorium", *Health Phys.* 44, *Suppl. 1*, 469-476.

R. Sposto, D. L. Preston, Y. Shimizu, and K. Mabuchi (1992). "The Effect of Diagnostic Misclassification on Non-Cancer and Cancer Mortality Dose Response in A-Bomb Survivors", *Biometrics* 48, 605-617.

B. J. Stover, D. R. Atherton, N. Keller, and D. S. Buster (1960). "Metabolism of the Th-228 Decay Series in Adult Beagle Dogs", *Radiat. Res.* 12, 657-671.

B. J. Stover, D. R. Atherton, D. S. Buster, and F. W. Bruenger (1965a). “The Th-228 Decay Series in Adult Beagles: Ra-224, Pb-212, and Bi-212 in Selected Bones and Soft Tissues”, *Radiat. Res.* 26, 132-145.

B. J. Stover, D. R. Atherton, D. S. Buster, and N. Keller (1965b). “The Th-228 Decay Series in Adult Beagles: Ra-224, Pb-212, and Bi-212 in Blood and Excreta”, *Radiat. Res.* 26, 226-243.

T. Straume, S. D. Egbert, W. A. Woolson, R. C. Finkel, P. W. Kubik, H. E. Gove, P. Sharma, and M. Hoshi (1992). “Neutron Discrepancies in the DS86 Hiroshima Dosimetry System”, *Health Phys.* 63, 421-426.

M. F. Sullivan, P. L. Hackett, L. A. George, and R. C. Thompson (1960). “Irradiation of the Intestine by Radioisotopes”, *Radiat. Res.* 13, 343-355.

D. M. Taylor (1970). “The Metabolism of Actinium in the Rat”, *Health Phys.* 19, 411-418.

R. L. Ullrich, M. C. Jernigan, L. C. Satterfield, and N. D. Bowles (1987). “Radiation Carcinogenesis: Time-Dose Relationships”, *Radiat. Res.* 111, 179-184.

UNSCEAR (1982). *Ionizing Radiation: Sources and Biological Effects*, United Nations Scientific Committee on the Effects of Atomic Radiation (United Nations, NY).

UNSCEAR (1988). *Sources, Effects and Risks of Ionizing Radiation*, United Nations Scientific Committee on the Effects of Atomic Radiation (United Nations, NY).

UNSCEAR (1993). United Nations Scientific Committee on the Effects of Atomic Radiation, *Sources and Effects of Ionizing Radiation. 1993 Report to the General Assembly, with Scientific Annexes* (United Nations, NY).

UNSCEAR (1994). United Nations Scientific Committee on the Effects of Atomic Radiation, *Sources and Effects of Ionizing Radiation. 1994 Report to the General Assembly, with Scientific Annexes* (United Nations, NY).

U. S. Bureau of the Census Population Division (1997). *Release PPL-41, United States Population Estimates, by Age, Sex, Race, and Hispanic Origin, 1990 to 1995, with Associated Updated Tables*

for Recent Months, (Population Division, U. S. Bureau of the Census, Washington D. C. 20233). Available on www at: <http://www.census.gov/population/estimate-extract/nation/intfile2-1.txt>.

M. A. Van Dilla and B. J. Stover (1956). “On the Role of Radiothorium (Th-228) in Radium Poisoning”, *Radiology* 66, 400-401.

M. A. Van Dilla, B. J. Stover, and J. S. Arnold (1957). “On the Retention and Translocation of Ra-224 (ThX) in Dogs”, *Am. J. Roentgenol. Radiat. Ther. Nucl. Med.* 77, 503-510.

L. Wallace (1996). “Indoor Particles: A Review”, *J. Air & Waste Manage. Assoc.* 46, 98-126.

D. A. Weber, K. F. Eckerman, L. T. Dillman, and J. C. Ryman (1989). *MIRD: Radionuclide Data and Decay Schemes* (Society of Nuclear Medicine, New York, NY).

K. T. Wheeler and J. D. Wierowski (1983). “DNA Repair Kinetics in Irradiated Undifferentiated and Terminally Differentiated Cells”, *Radiat. Environ. Biophys.* 22, 3-19.

J. W. Wilson, C. W. Enns, J. D. Goldman, K. S. Tippet, S. J. Mickle, L. E. Cleveland, and P. S. Chahil (1997). *Data Tables: Combined Results from USDA’s 1994 and 1995 Continuing Survey of Food Intakes by Individuals and 1994 and 1995 Diet and Health Knowledge Survey* (U.S. Department of Agriculture).

M. E. Wrenn, P. W. Durbin, B. Howard, J. Lipsztein, J. Rundo, E. T. Still, and D. L. Willis (1985). “Metabolism of Ingested U and Ra”, *Health Phys.* 48, 601-633.

M. E. Wrenn, N. P. Singh, N. Cohen, S. A. Ibrahim, and G. Saccomanno (1981). *Thorium in Human Tissues*, NUREG/CR-1227 (New York University Medical Center).

A. Zapletal, M. Samanek, and T. Paul (1987). “Lung Function in Children and Adolescents”, *Methods, Reference Values* (Karger, Basel, Switzerland).